NOTICE: When government or other drawings, specifications or other data are used for any purpose other than in connection with a definitely related government procurement operation, the U. S. Government thereby incurs no responsibility, nor any obligation whatsoever; and the fact that the Government may have formulated, furnished, or in any way supplied the said drawings, specifications, or other data is not to be regarded by implication or otherwise as in any manner licensing the holder or any other person or corporation, or conveying any rights or permission to manufacture, use or sell any patented invention that may in any way be related thereto.

REPORT NO. R-245-025

ROUGH TERRAIN LANDING GEAR

M-245

FAIRCHILD AIRCRAFT & MISSILES DIVISION

HAGERSTOWN 10, MARYLAND

TREC 60-39

DESIGN, FABRICATION, AND TEST OF HIGH-FLOTATION TIRES AND RELATED VALVING MECHANISM FOR ROUGH TERRAIN LANDING GEAR.

REPORT NUMBER R-245-025
PROJECT M-245
BY
FAIRCHILD AIRCRAFT & MISSILES DIVISION
HAGERSTOWN 10, MARYLAND

UNITED STATES ARMY
TRANSPORTATION RESEARCH COMMAND
Fort Eustis, Virginia

Contract No. DA 44-177-TC-446 Project No. 9R38-01-017-47

" THE FINDINGS AND RECOMMENDATIONS CONTAINED IN THIS REPORT ARE THOSE OF THE FAIRCHILD AIRCRAFT AND MISSILES DIVISION AND DO NOT NECESSARILY REFLECT THE VIEWS OF THE CHIEF OF TRANSPORTATION, UNITED STATES ARMY."

FAIRCHILD AIRCRAFT AND MISSILES DIVISION

HAGERSTOWN 10, MARYLAND

SUBJECT DESIGN, FABRICATION, AND TEST OF HIGH-FLOTATION TIRES AND RELATED VALVING MECHANISM FOR ROUGH TERRAIN LANDING GEAR

PREPARED BY V. Frisby — V. Frisby

CHECKED BY

APPROVED BY N. M. Stefano — N. M. Stefano

APPROVED BY A. J. Thieblot — A. J. Thieblot

APPROVED BY

REPORT NO. R245-025

MODEL M-245B

COPY NO.

NO. OF PAGES 23 plus Appendices 1-6

DATE May 27, 1960

REVISIONS

REVISION DATE	PAGES AFFECTED	APPROVED

NS-800-69B

TABLE OF CONTENTS

LIST OF FIGURES

1. INTRODUCTION

a. This report covers the results of experiments directed toward the design, development, and testing of a laboratory-model, rough-terrain landing gear system using foldable high-flotation tires built by a novel continuously-wound-cord method and using venting-hub shock absorption. The contemplated end use of such a system is for STOL aircraft operated from rough, unprepared fields. The tires, due to their relatively light weight, low inflation pressures, and economical methods of production, can also be ideally adapted to land vehicles for off-road use, offering improved cross-country trafficability with lessoned tare weight. This prototype development project was preceded by analytical studies which indicated feasibility and which were reported upon by Fairchild Aircraft Division Reports Number R245-004I, R245-004II, and R245-004III, entitled, "Analytical Study of High Flotation Tires for Aircraft."

b. Early in this program it was recognized that development of the capability of operating aircraft from rough unpaved fields would require revolutionary advances in tire design and manufacturing techniques in order to achieve low inflation pressures and to minimize weight penalties. In addition, the size of low pressure tires posed problems of stowage space; and the ability to envelop rigid obstacles, rather than rolling over them, demanded higher deflections in the tires than was available from tires built by conventional methods. This latter aspect led to exploration of pneumatic shock absorption methods in order to overcome the rebound inherent during landing from the undamped spring rate of low-pressure tires with high deflection. There were three problem areas: weight, size, and rebound.

c. Details of the work in these problem areas are presented in the appendices to this report which are, in themselves, complete reports of the work in question. The main body of the report summarizes the findings and conclusions of the reports appended hereto. No extensive discussions are contained in this main body.

2. SUMMARIES

As would be concluded from a perusal of the appendices, workable solutions have been found for the problems cited in the above introduction. Feasibility of the novel, continuously-wound-cord, high-flotation, foldable tires has been demonstrated. Considerable research must still be conducted, however, before minimum weights and maximum service life are attained. Likewise, shock absorption and damping of the rebound of the high deflection, low pressure tires have been demonstrated. And, finally, folding of these tires in a slipstream at 95 knots was achieved. Summaries of the results of the work in each problem area - tire building, shock absorption, and folding - are presented in the following lettered sub-paragraphs:

a. Continuously-Wound-Cord Tires

(1) As reported in detail by Appendix 1, Development of Techniques for Building High-Flotation Tires of Continuously-Wound-Cord, R245-015, feasibility of production of foldable, high-flotation tires by the novel, continuously-wound-cord process has been demonstrated and a number of successful tires have been built by this method. The basic process can be deduced from examination of Figure 1, a photograph of the specially-built winding equipment. Briefly, tire cord, freshly coated with green, uncured carcass-stock rubber is passed through the hollow spindle of the winding arm, over fair leads on the arm and is wound into position on the mandrel on which has been applied a sheet of liner stock rubber. The winding arm rotates clockwise viewed from the left side of Figure 1 and the mandrel rotates counterclockwise viewed from the front of the figure. It may be noticed that the winding position of the hubs is outboard on the spindle of the mandrel at the distance from the mandrel which provides the desired tension in the cord when the hubs are pushed into the curing position in the recesses on each side of the mandrel. Varying the rotational velocities of the winding arm and mandrel varies the cord pattern across the tread areas of the tire. By varying these velocities, the shape of the mandrel, the size of the hubs, and the clearance between the end of the winding arm and the mandrel,

Figure 1

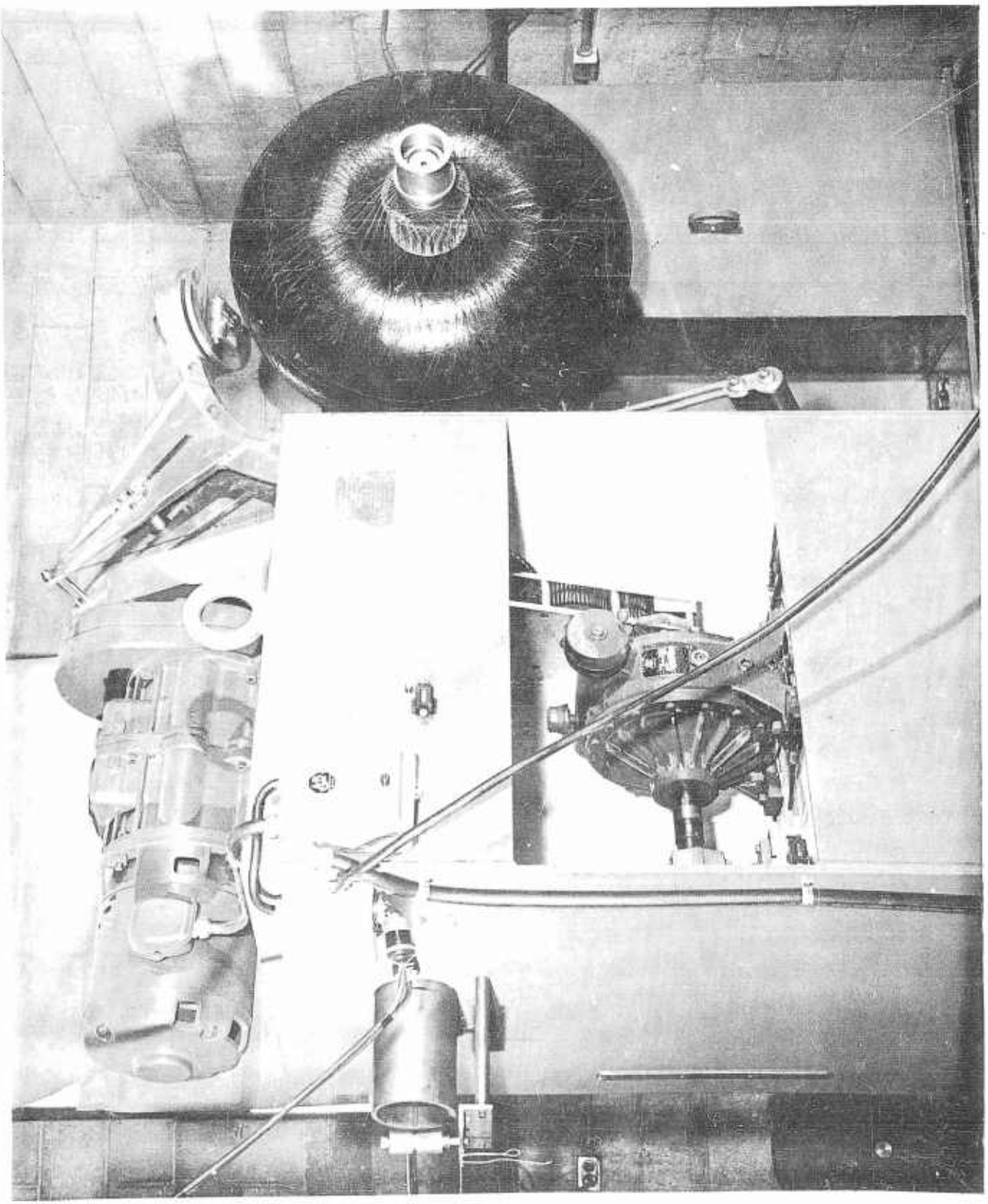

2. SUMMARIES (Continued)

a. Continuously-Wound-Cord Tires (Continued)

any reasonable cord pattern can be achieved in the tire. Since the cord pattern determines the inflated shape, and this in turn affects stress distribution in the tire when in service, this basic method permits remarkably close control of tire characteristics. In other words, the method gives precise control of the density and direction of the tire cord, throughout the carcass, in the cured tire.

(2) After the required amount of cord is wound into place on the mandrel, another thin sheet of carcass stock rubber is applied over the cord, the desired tread stock is applied over the tread area of the tire, the mandrel is removed from its spindle, the hubs jacked toward each other into the curing position, special curing flanges are place concentric to each hub, the whole assembly is covered with a pressure barrier of plastic film, and the assembly placed in an autoclave for cure. During the curing process, a vacuum is maintained on the inside of the tire to assure that curing tank pressure is maintained on the carcass. This positive pressure coupled with the vacuum assures that air trapped in the carcass during winding is removed from the tire during the cure and that any volatile material in the uncured rubber is likewise removed. Figure 2 shows a 34-inch tire in the curing autoclave.

(3) Additional conclusions from Appendix 1 are as follows:

(a) The techniques presently available for the continuous-cord tire-building need to be refined and the process simplified before production of continuously-wound tires is programmed.

(b) Analysis of the presently available techniques points clearly towards the path to follow during the evolution of satisfactory manufacturing processes.

Figure 2

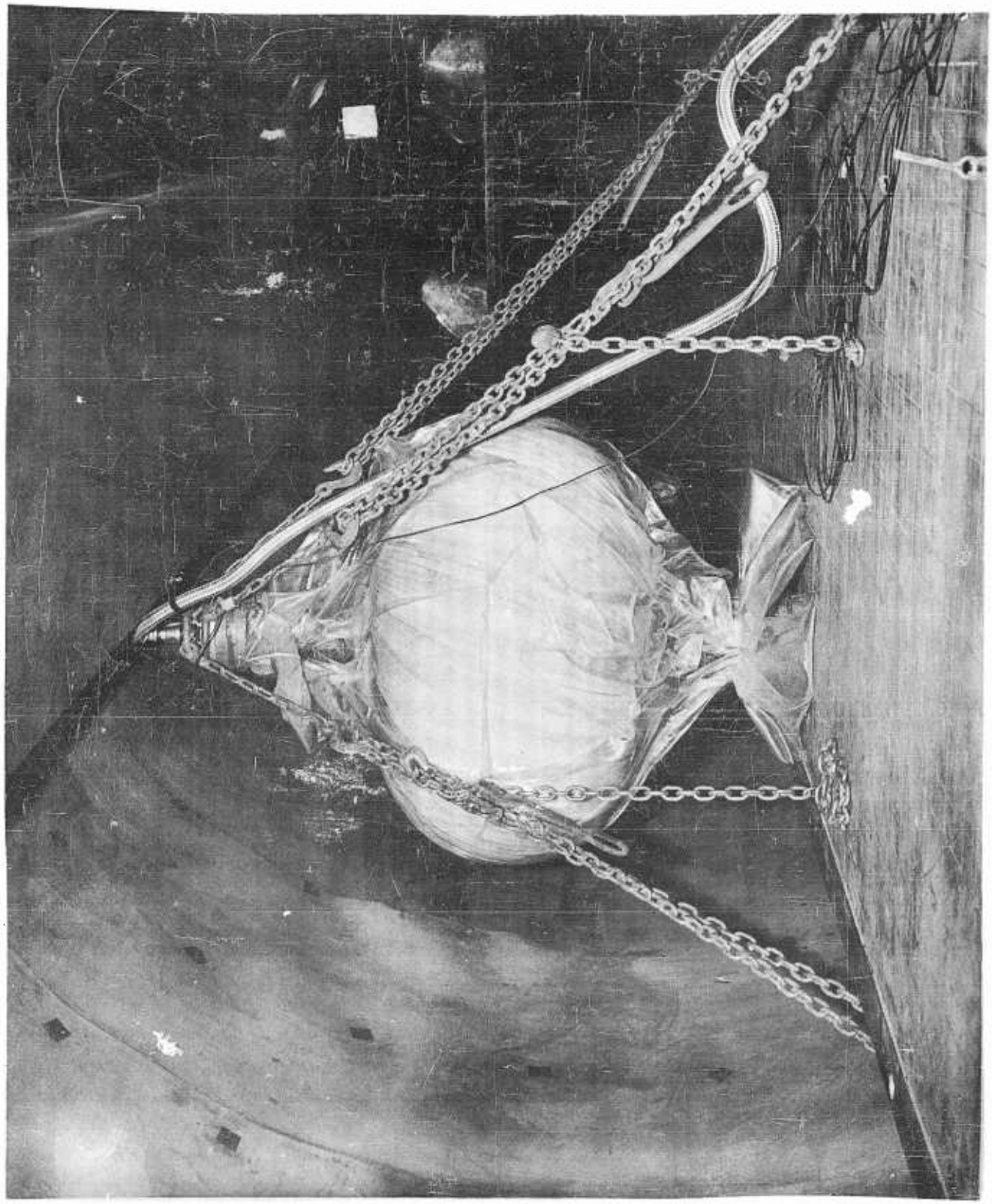

2. SUMMARIES (Continued)

a. Continuously-Wound-Cord Tires (Continued)

(3) (c) Uncertainty in the stress distribution in a high-flotation tire carcass when severely deformed under load indicates that it will be necessary to use empirical methods in the refinement of the design of continuously-wound-cord tires.

b. Characteristics of High-Flotation, Foldable Tires

(1) When the tire building experiments had progressed sufficiently so that several successful laboratory-model tires had been produced and future success could be logically predicted, it was decided to flight test the system. Preliminary to design of the flight-test, venting hub system, the test model tires were submitted to exhaustive tests to determine their load carrying ability and their reaction to encountering rigid obstacles and crossing pot-holes. Static tests on a specially design test rig produced the load deflection curves of Figure 3. The test rig is shown by Figure 4. These curves and other data obtained from the static tests are contained in Appendix 2. These other data include side and drag loads developed on the tire just prior to skidding for various vertical loads at several inflation pressures.

(2) The static tests were followed by dynamic tests to determine rolling resistance, cornering forces developed when the tire was steered and the reactions to encountering rigid obstacles and crossing ditches, all at several vertical loads and inflation pressures and at several speeds. These rolling tests were made with the same rig (Figure 4) operated as a semi-trailer. The dynamometer column on this rig was instrumented to secure simultaneous readings of the three perpendicular forces along the primary axes and the three moments about these axes. Typical results of these tests are presented by Figures 5 through 9. Details of the dynamic, or rolling test program, are contained in Appendix 3.

Figure 3

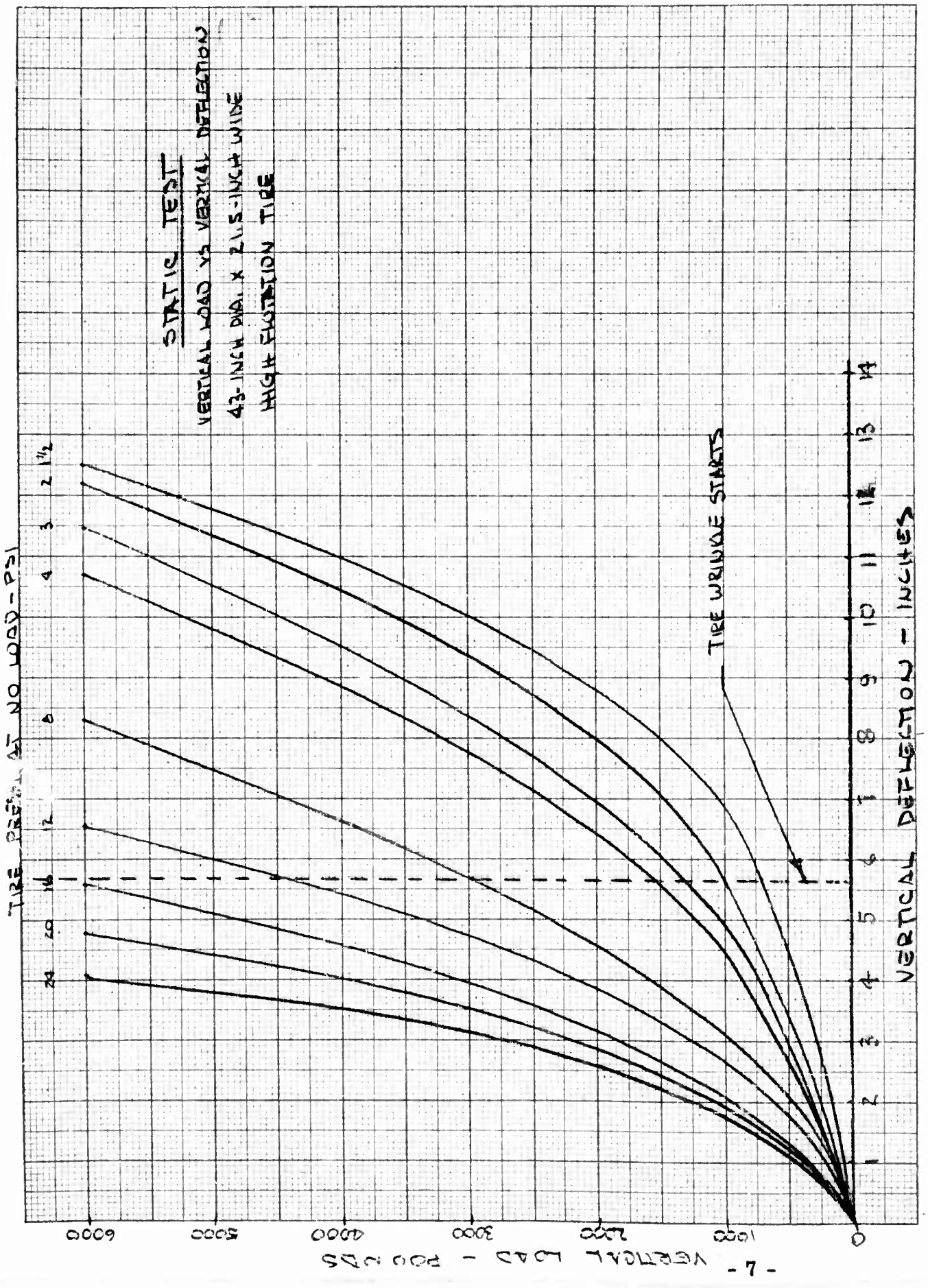

Figure 4

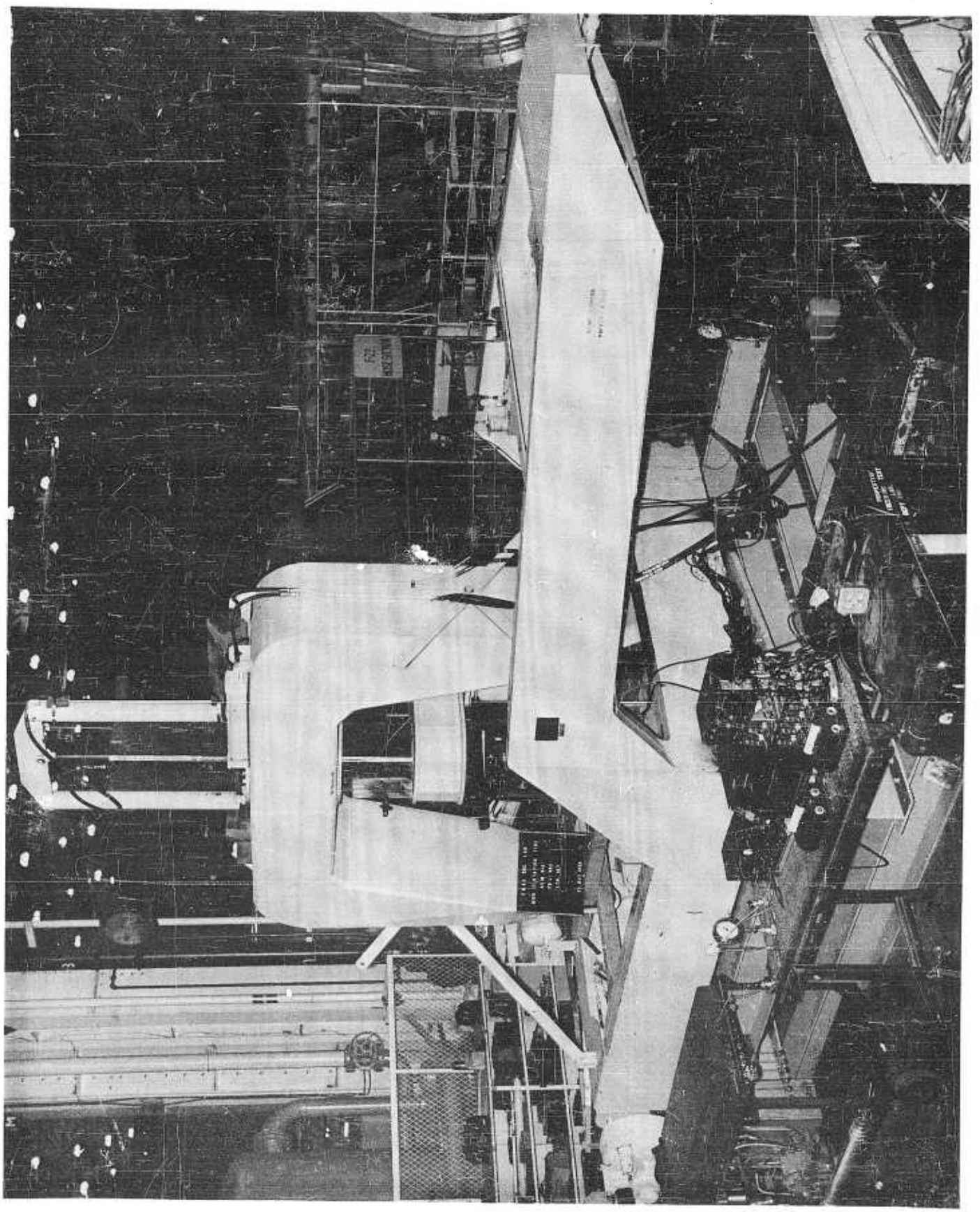

Figure 5

High Flotation Tire - Obstacle Test

Record No.	Obstacle Height	Tire Pressure (P.S.I.)	Static Vert. Load (Lbs.)	*Actual Vertical Load (Lbs.)	Peak Loads Occuring at Obstacles: Vert. Load (Lbs.)	Drag Load (Lbs.)	Side Moment In. (Lbs.)	Wheel Speed (m.p.h.)
12192	2"	4	1500	2400	3800	336 -895	-5285	28.6
12195	2"	4	1500	2800	4660	496 -870	-5285	40.1
12246	2"	4	3000	5470	8542	315 -1347	-2610	30.5
12247	2"	4	3000	5470	8817	516 -1081	-2610	19.5
12203	2"	8	1500	2870	5897	280 -1036	-5285	40.1
12204	2"	12	1500	2200	5292	336 -730	-7926	19.6
12206	2"	12	1500	3070	5065	392 -440	-10570	43.0
12218	2"	12	3000	5200	8392	590 -810	-2610	19.1
12219	2"	12	3000	5670	9148	560 -560	-2610	39.1
12207	2"	12	1500	2270	5443	390 -924	-7925	19.1
12208	2"	12	1500	3000	6274	365 -645	-13210	43.0
12220	2"	12	3000	5670	8921	812 -980	+2610	19.8
12201	2"	4	1500	2670	5443	364 -616	+2642	39.6
12209	2"	12	1500	2530	5821	420 -644	-18494	19.1
12210	2"	12	1500	1270	4460	476 -644	-15852	44.4
12248	2"	12	3000	3330	5373	-744	-18270	19.1
12250	2"	12	4500	3070	6338	1005 -1405	-23490	19.1
12249	2"	12	3000	2270	5373	485 -1060	-23490	38.7
12251	2"	12	4500	2600	5857	716 -1115	-26100	40.6
12253	2"	16	1500	270	4684	945 -1175	-36540	33.9
12254	2"	24	1500	4930	10540	746 -831	-41760	19.1
12255	2"	24	3000	8600	14329	532 -945	-41760	20.5
12256	2"	24	4500	9130	15018	831 -1261	-39150	21.5

*Just prior to impact.

Figure 6

High Flotation Tire - Obstacle Test

Record No.	Obstacle Height	Tire Pressure (P.S.I.)	Static Vert. Load (Lbs.)	*Actual Vertical Load (Lbs.)	Peak Loads Occuring at Obstacles: Vert. Load (Lbs.)	Drag Load (Lbs.)	Side Moment In. (Lbs.)	Wheel Speed (m.p.h.)
12274	4"	4	1500	1730	4800	-960	10440	20.5
12263	4"	24	1500	4400	11573	-1980	23490	16.0
12282	6"	12	1500	1800	8200	620 -1525	18270	20.0
12285	6"	24	1500	1930	11939	1551 -2115	33930	19.6
12280	6"	12	3000	3130	10800	790 -1380	18270	20.2
12281	6"	12	4000	3750	11601	902 -1890	23490	19.6
12372	6"	4	1500	2130	6067	365 -1410	13050	27.9
12276	6"	12	1500	1800	9067	620 -1551	15660	20.2
12277	6"	12	3000	3400	11467	565 -1380	15660	19.3
12278	6"	12	4000	3330	10533	790 -1580	15660	18.6
12433	8"	3	1200	270	3067	620 -935	10760	6.9
12436	8"	3	1200	330	3000	900 -1020	5380	11.5
12428	4" deep	4	1500	1330	800	680 -535	18830	10.5
12437	4" deep	12	1500	3670	133	735 -650	8070	16.0
12431	8" deep	4	1500	1400	933	765 -735	18830	16.0
12432	12"deep	4	1500	3670	1067	765 -1045	10760	*
12440	12"deep	24	1500	1530	400	850 -480	5380	12.9
12241	12"deep	24	3000	2400	400	595 -170	8070	13.2
12442	12"deep	24	4500	3400	133	790 -510	64550	14.8

* Just prior to impact.

Figure 7

High Flotation Tire - Rolling Tests
Drag versus Vertical Load at Various Tire Press.

Record Number	Vert. Load	Drag Load	Tire Pressure					
12198	2670#	501#	4 PSI					
12245	5130#	1512#	4 PSI					
12247	5470#	1395#	4 PSI					
12204	2200#	639#	12 PSI					
12218	5200#	1037#	12 PSI					
12250	3070#	1686#	12 PSI					
12254	4930#	1512#	24 PSI					
12255	8600#	1366#	24 PSI					
12256	9130#	1221#	24 PSI					

NOTE: THESE READINGS WERE TAKEN AT THE SAME POINT - JUST BEFORE THE TIRE HIT THE OBSTACLES DURING ROUGH TERRAIN TESTS.

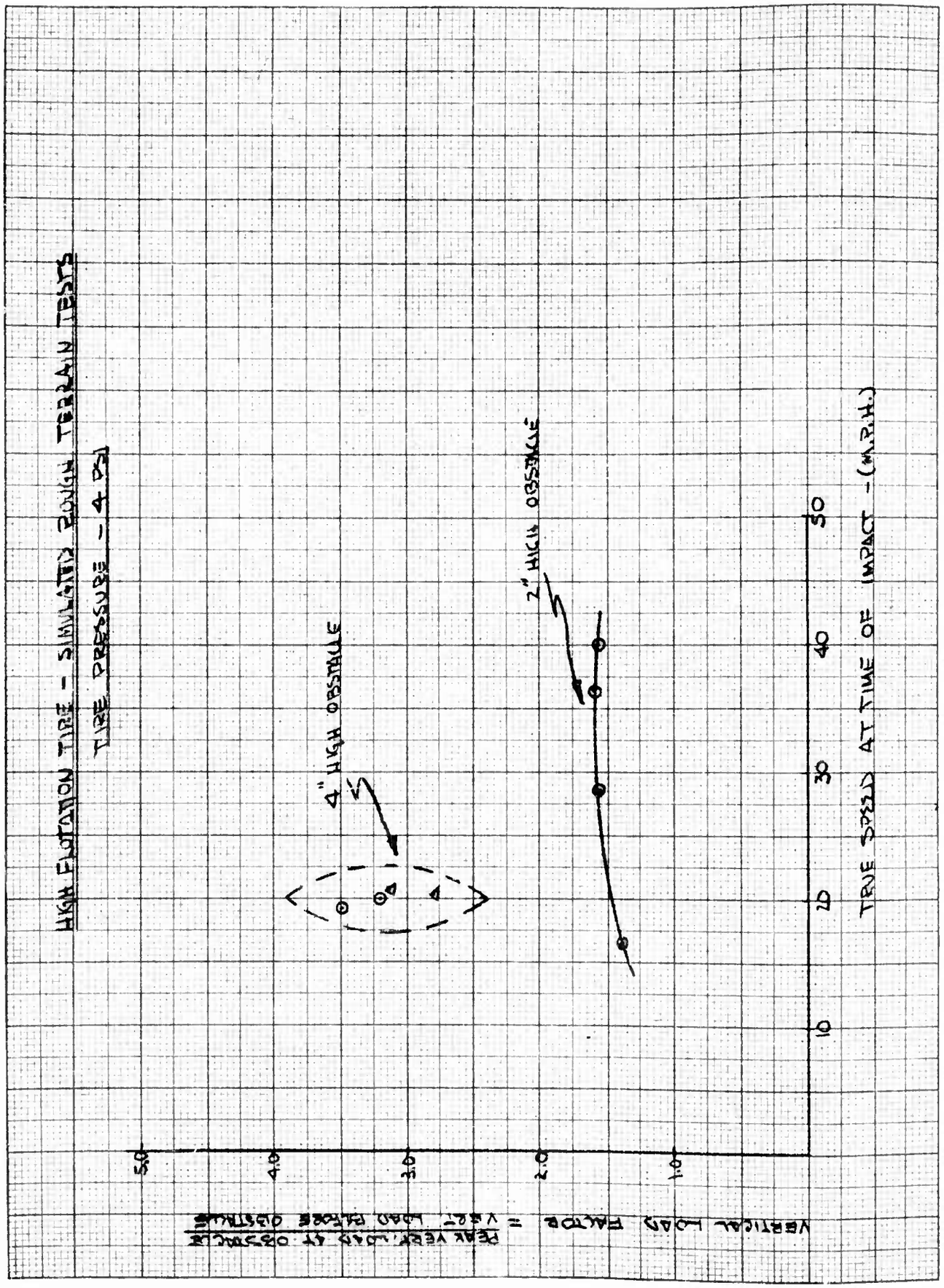

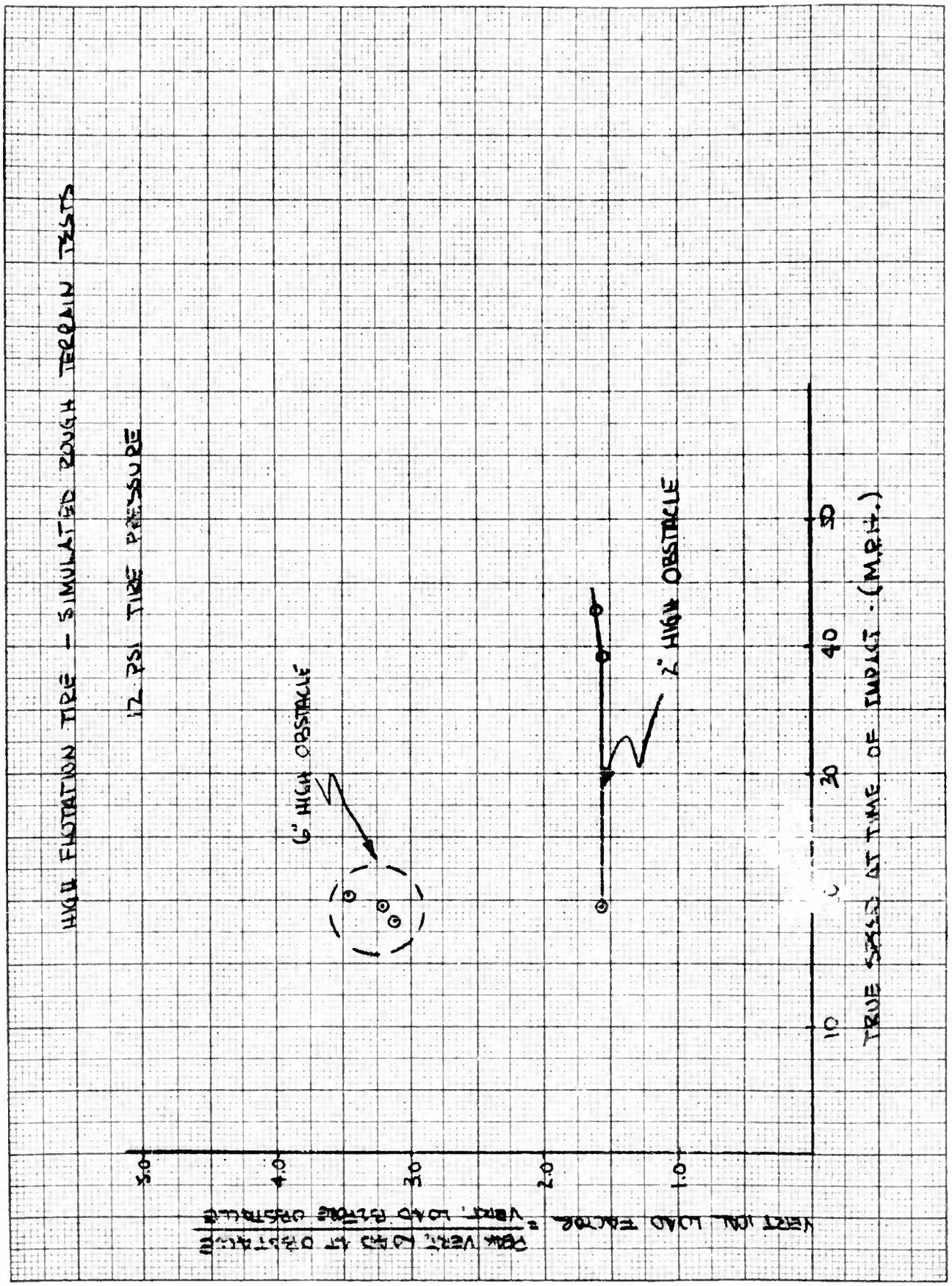

2. SUMMARIES (Continued)

b. Characteristics of High-Flotation, Foldable Tires (Continued)

(3) The general conclusion drawn from these static and rolling tests was that this model tire would carry successfully all loads which could be improved upon them by landings and taxiing of an L-19 type aircraft unless the structural limitations of the aircraft were exceeded. Therefore, it was also concluded that this model tire was structurally adequate for flight tests on the L-19 and four such tires were built for this purpose.

c. Venting-Hub Shock Absorption

(1) With the results of the preparatory analytical studies as a starting point, a 750-pound, laboratory model, venting-hub, shock absorption system was built and tested. This work is described by Appendix 4, The Design and Development of Laboratory Models to Study the Feasibility of High-Flotation Tires for Aircraft, R245-012. This prototype system made touchdown at relatively high pressure, sensed the vertical load, and opened the vent valve proportionally to the instantaneous load. At a programmed pressure at or near the optimum run-out pressure, the valve actuating mechanism was disconnected and the vent valve closed by spring action. The valves remained closed throughout the remainder of the landing run. To preclude cocking and consequent possibility of initiating an undesired venting upon encounter of an obstacle while taxiing, the system was arranged to be re-cocked only (1) when airborne i.e. there was no vertical load upon the tires and (2) when the tires have been inflated to a pressure just short of that to which they are normally inflated for touchdown. This, incidentally, permits a relatively high taxiing pressure which minimizes rolling resistance and tire wear on smooth pavements. Reliability of the mechanisms was established by approximately 3000 drop tests without spin-up and some 350 additional drop tests with spin-up to touchdown velocity. Landing gear efficiencies comparable to conventional oleo-shock struts were achieved.

2. SUMMARIES (Continued)

c. Venting-Hub Shock Absorption (Continued)

(2) Success with this laboratory model, 750-pound, capacity system led to a decision to adapt a partially designed 1500-pound capacity system to flight tests on an L-19 aircraft test bed. Details of the development of these flight-test venting-hubs are presented by Appendix 5, FAMD Report Number R245-014, "Design and Development of Laboratory and Flight-Test Models of Landing Gear for Aircraft to be Operated from Rough Unprepared Fields." The purpose of the flight tests was to determine the behavior of the tires and venting-hubs under actual landing conditions. These flight tests were made during the winter of 1959-1960 and the summer of 1960. Remarkably close agreement was obtained between the drop tests and the flight tests with respect to sinking speeds versus landing load factors. Details of the flight test program are contained in Appendix 6, FAMD Report Number FT 245-1, Initial Flight Tests, High Flotation Landing Gear. Figure 10 shows a plot of sinking speed versus load factor for both drop and flight tests.

(3) In general, the flight tests confirmed the results of the drop tests and demonstrated the feasibility of suppressing landing rebound of highly deflectable, high-flotation tires by the venting hub technique. The test bed used did not permit installation of a high-flotation tire on the tail gear because of limitations of gross weight and funding. Thus it was not practical to use this test bed for exploration of the capabilities of the system by landings and take-offs from rough, unprepared fields. It was considered that the small, high-pressure tail wheel, mounted on an undamped spring, would have presented a high probability of serious accident under these conditions.

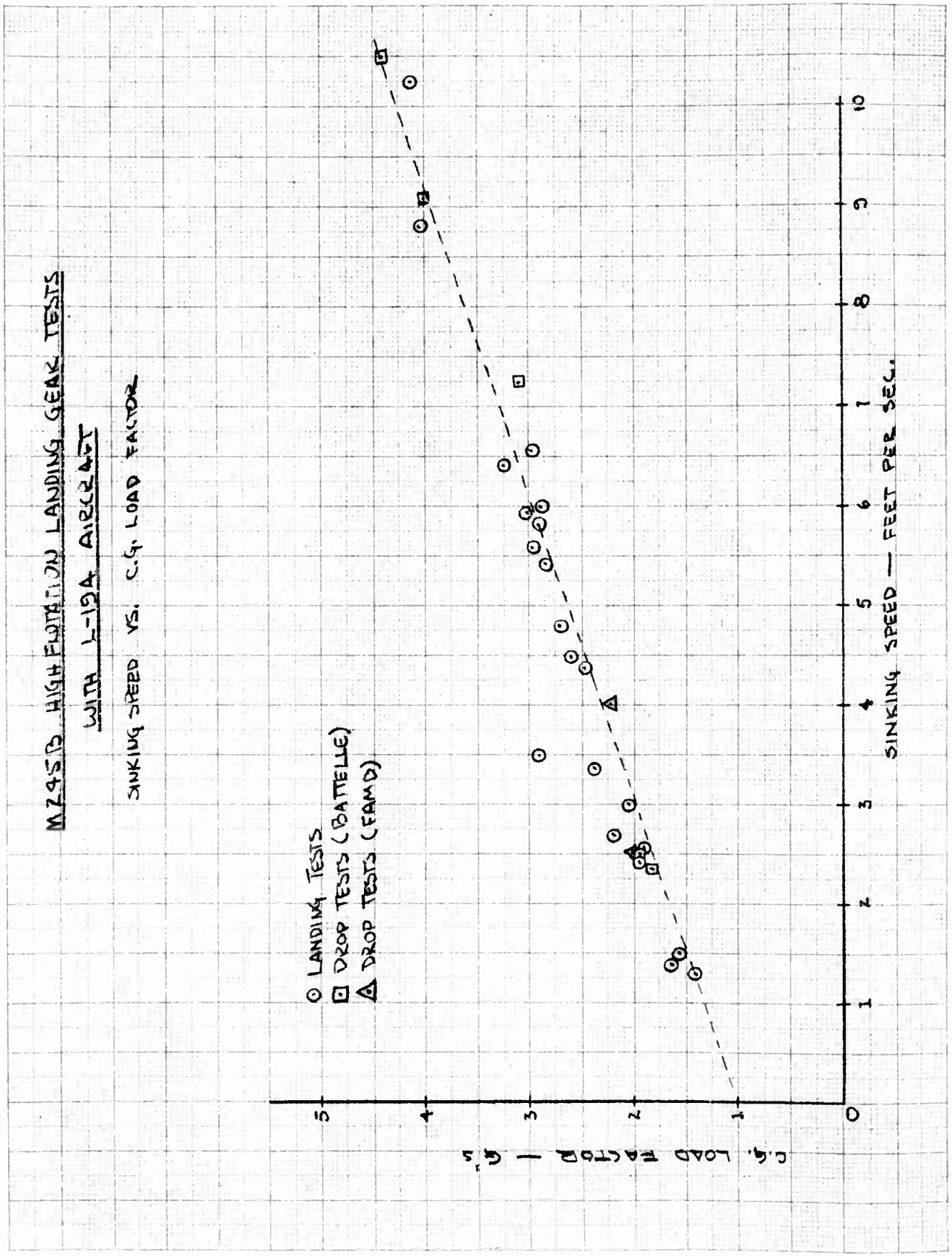
NZ4STB HIGH FLOTATION LANDING GEAR TESTS
WITH L-19A AIRCRAFT
SINKING SPEED VS. C.G. LOAD FACTOR
LANDING TESTS
DROP TESTS (BATTELLE)
DROP TESTS (FAMD)
C.G. LOAD FACTOR — Gs
SINKING SPEED — FEET PER SEC.
0
1
2
3
4
5
6
7
8
9
10

2. SUMMARIES (Continued)

d. Tire Folding in a Slip Stream

(1) With analytically predicted success, experiments were conducted with a helical bellows tire-folding scheme. The carcass of a 43-inch flight-test tire was stiffened by cemented-on V-belts in circles concentric to each hub and in a symmetric array across the tread area of the tire between the circles. The path of these semi-circular stiffening ribs can be seen from the long transverse scars on the surface of the inflated tire shown by Figure 11. Their path was skewed to the axis of the tire about 10 degrees. When a vacuum is applied to a thin-walled, continuously-wound-cord tire stiffened in this manner, the tire creases inwardly between the transverse stiffening ribs, developing a helical pattern of folds. As these folds progress, they exert opposite torque on the hubs, and one hub is permitted to rotate. This initial movement causes a progressive reduction in diameter of the tire as the helical bellows are formed. After about a quarter of a turn, the outward component of force on the free hub is reduced relative to the rotating force and atmospheric pressure forces the hub toward its mate. The tire is now committed to symmetric folding and, when completed, the effective width is reduced to approximately three-eights or slightly less of the inflated width and the diameter to slightly more than the inflated diameter. With a tire of a cross-section represented by two circles tangent to each other at the rolling axis, ten transverse stiffening ribs will permit a reduction in diameter to approximately one-half. With a greater number of transverse stiffening ribs it may be deduced that the folded diameter can be reduced to less than one-half.

(2) When tested in a slip stream at about 100 knots, it was found that cemented-on V-belts did not provide sufficient stiffening to preclude collapse of the leading edge of the tire against the axle when a vacuum was applied. In addition, study of moving pictures of the folding sequence conducted in the laboratory led to the conclusion that the permanent stiffness provided by V-belts (or molded on ribs) would interfere with folding to a minimum package. Accordingly, experiments were

2. SUMMARIES (Continued)

d. Tire Folding in a Slip Stream (Continued)

conducted with an array of pneumatically inflated tubes inside the tire in the same pattern as described above for the cemented-on V-belts. Control of the inflation pressure, and consequently of the stiffness of these inflatable stiffening devices, was independent of the inflation pressure of the tire. This system was tested at approximately 95 knots extended below the belly of a C-119 type aircraft and successful folding was achieved. The folded package was of the same dimensions and symmetry as achieved in the laboratory. Figures 11 through 14 are photographs of the first airborne folding sequence with the stiffening tubes inflated initially to approximately 25 pounds per square inch. Later tests at higher initial pressure in the stiffening tubes resulted in less partial collapse of the tubes on the forward side of the tire and slightly faster folding. It was deduced that higher pressures in the stiffening tubes would permit symmetric folding at higher aircraft speeds and probably would reduce folding time. This successful demonstration of airborne folding in a slip stream concluded the testing.

Figure 11

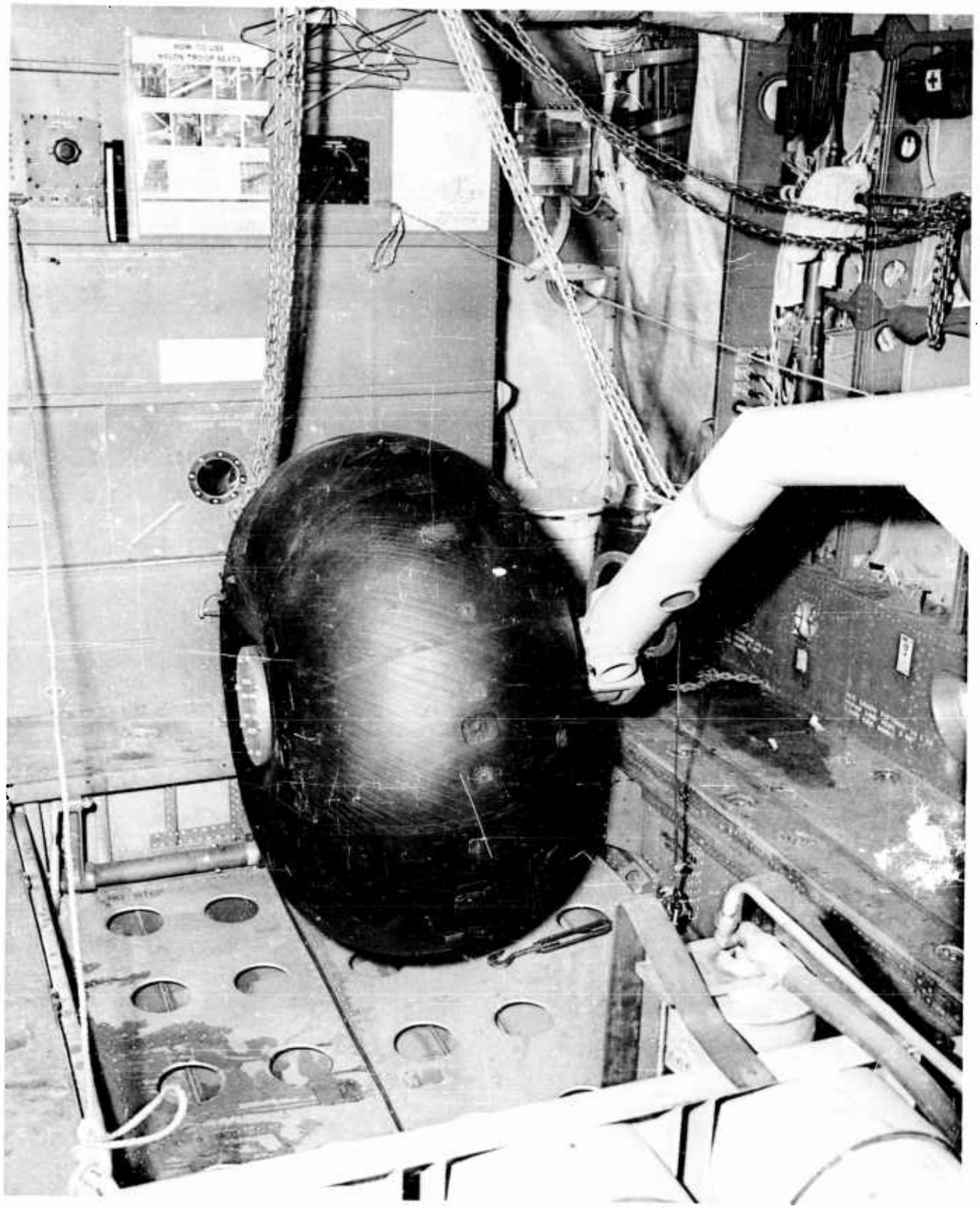

Figure 12

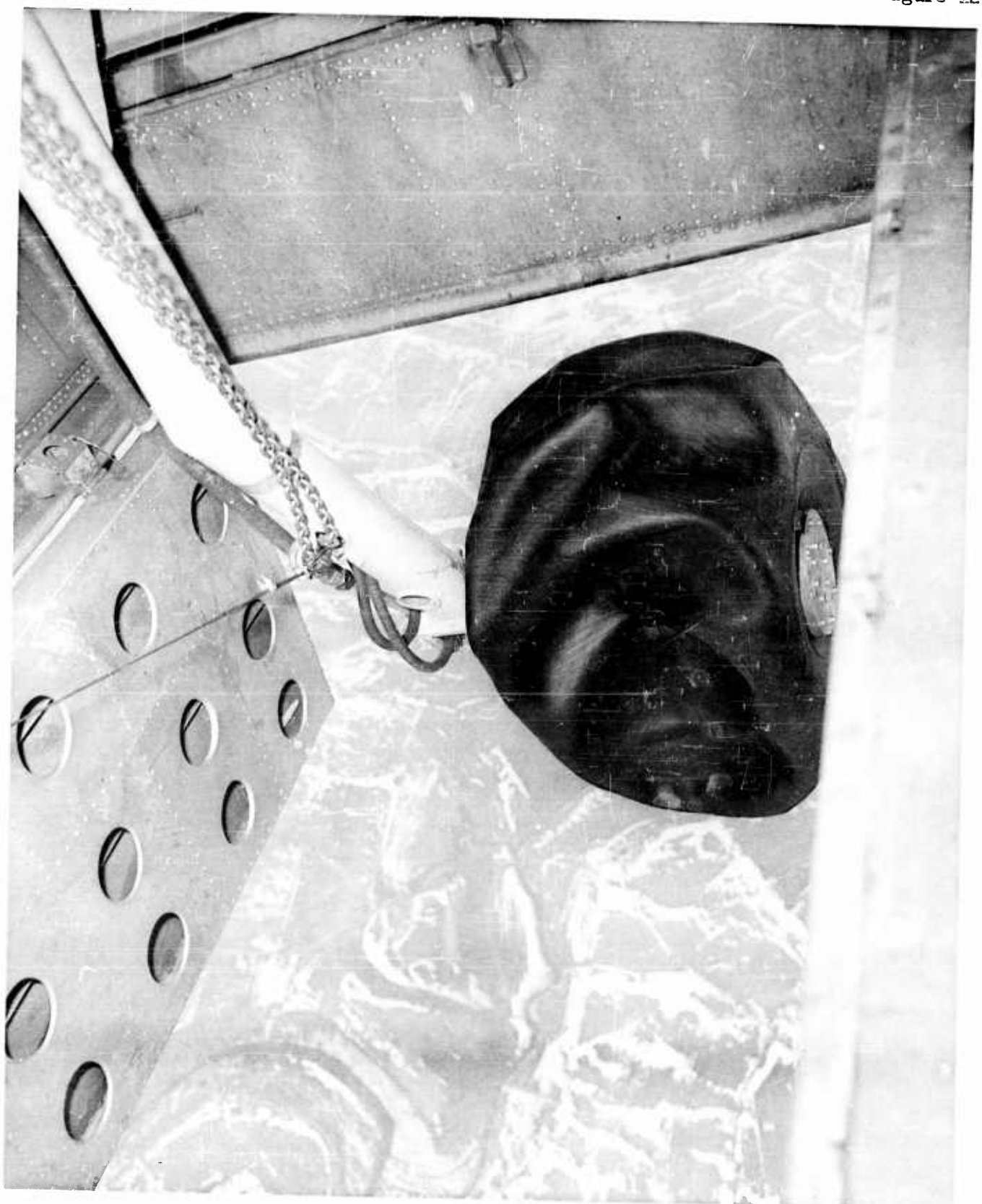

Figure 13

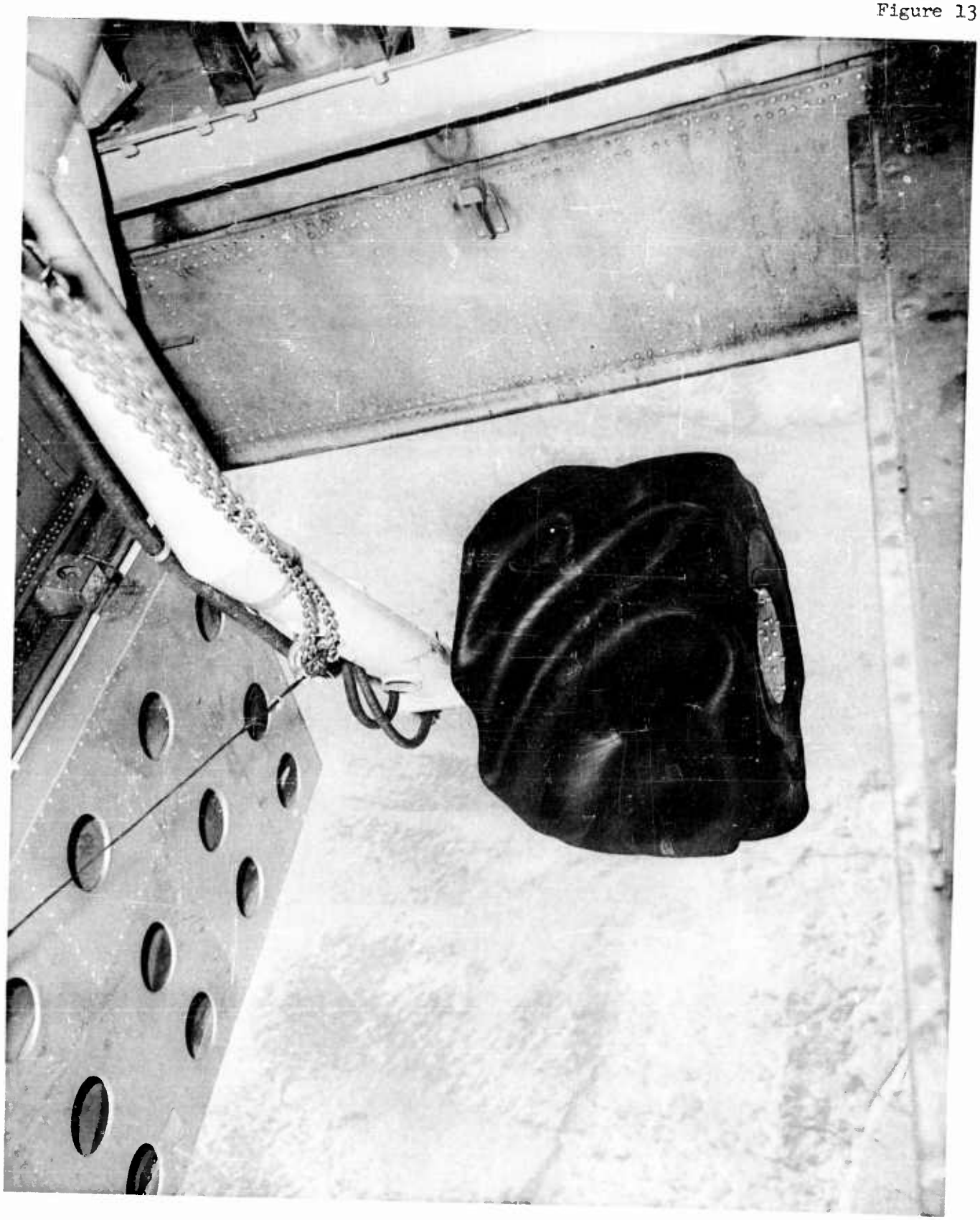

Figure 14

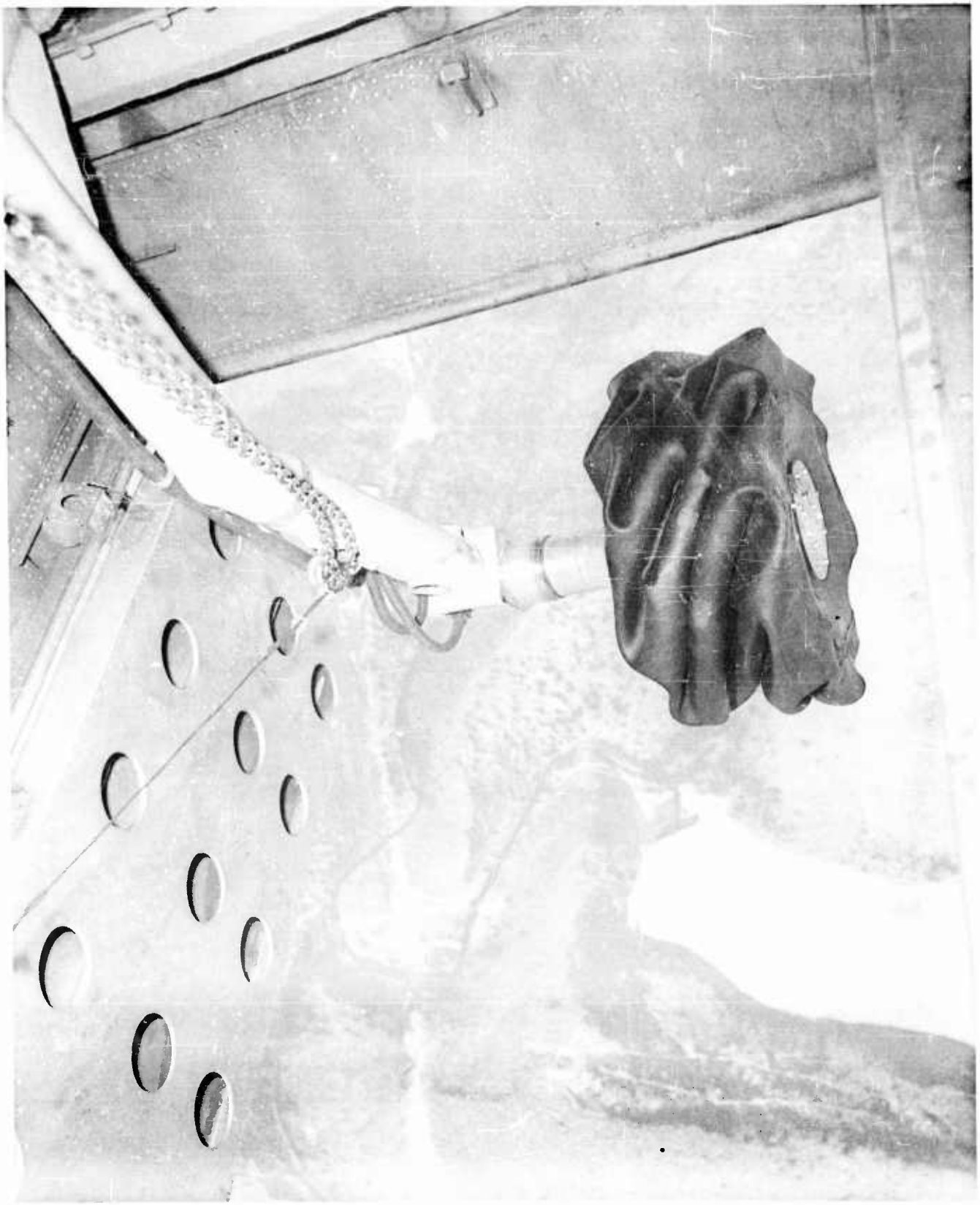

3. CONCLUSIONS AND RECOMMENDATIONS

It is concluded that rough field landing gear can be developed based on foldable, low-pressure tires and it is recommended that the exploratory work reported upon herein be followed by experimental research with a suitably large flying test bed and preferably of operational status.

FAIRCHILD AIRCRAFT AND MISSILES DIVISION

HAGERSTOWN 10, MARYLAND

SUBJECT DEVELOPMENT OF CONTINUOUSLY-WOUND-CORD TIRE-BUILDING TECHNIQUES

PREPARED BY V. Frisby — REPORT NO. R245.015

CHECKED BY _____ — MODEL M-245B

APPROVED BY S. W. Smith — COPY NO. _____

APPROVED BY _____ — NO. OF PAGES 65

APPROVED BY _____ — DATE 23 September 1959

REVISIONS

REVISION DATE	PAGES AFFECTED	APPROVED

NS-800-698

CONTENTS

SUMMARY

Feasibility of production of high-flotation tires by the continuously-wound-cord process has been demonstrated by the work reported on herein.

The techniques presently available for the continuous-cord tire-building need to be refined and the process simplified before production of continuously-wound-tires is programmed.

Analysis of the presently available techniques points clearly towards the path to follow during the evolution of satisfactory manufacturing processes.

Uncertainty in the stress distribution in a high-flotation tire carcass when severely deformed under load, indicates that it will be necessary to use empirical methods in the refinement of high-flotation tire design.

INTRODUCTION

This report presents the results of experiments to date directed towards development of techniques for the building of high-flotation tires of continuously-wound-cord. The contemplated end use of such tires is for STOL aircraft intended to be operated from rough unprepared fields, thus minimum tire weight is of great significance. Feasibility of the continuously-wound-cord method was predicted by the referenced reports of the Battelle Memorial Institute. At the writing a total of 24 tires have been built by the continuously-wound-cord method.

The main body of this report will be focused on the techniques used for the production of high-flotation tires No. 9 through 24. This main body presents the present state-of-the-art. It consists of a chart showing the sequence of steps in the tire-building operation followed by a series of photographs of the specially-developed equipment and descriptions of its use. During the production of these last 16 tires substantially no changes were made in the techniques employed.

Appendix A contains a description of the experimental work of building tires 1 through 8. This work resulted in the techniques employed for building the last 16 tires. During the building of tires 1 through 8, the major problems of techniques were recognized and interim, workable solutions found to overcome them. These solutions are considered interim because they are based on minimum equipment and require maximum hand work and thus tires built by these methods are relatively expensive. Analysis of these methods indicates that the bulk of the hand work could be eliminated by use of more refined equipment and techniques and that production costs using such methods would be equivalent to, or less than, costs of conventional tires of comparable size. Besides demonstrating that it is possible to build light-weight, foldable tires by the continuous-cord method, the work to date has also resulted in guidance for the development of more economical techniques.

The primary purpose of temporarily freezing technique development with tire No. 8 was to produce test lots of tires. At no time has it been concluded that the interim techniques would be suitable for production since the unit cost of tires built by these laboratory methods are too great. During the evolution of these interim techniques, and during building of tires No. 9 through 24, however, considerable thought was given to simplification and streamlining of the processes with view of reduction of manhours

and other costs of the continuously-wound-cord, tire-building process. The results of this thought are summarized at the end of Appendix A.

Appendix B is a summary of background information and discussion of present criteria for design of continuously-wound tires. Due to the uncertainty of the tensile stresses in a high-flotation tire carcass when deformed severely during service, the most significant conclusion which may be drawn concerning the continuously-wound-cord tire design at this writing is that the optimum design can be determined only by extensive testing of the tires under service conditions.

Appendix C is a tabulation of the design features of tires No. 10 through 24, included here for guidance of future tire-building technique development.

Appendix D tabulates the references. In general, material contained in the references is not repeated in this report so that fullest understanding of this report is enhanced by prior reading of the references.

SCHEMATIC TIRE-BUILDING

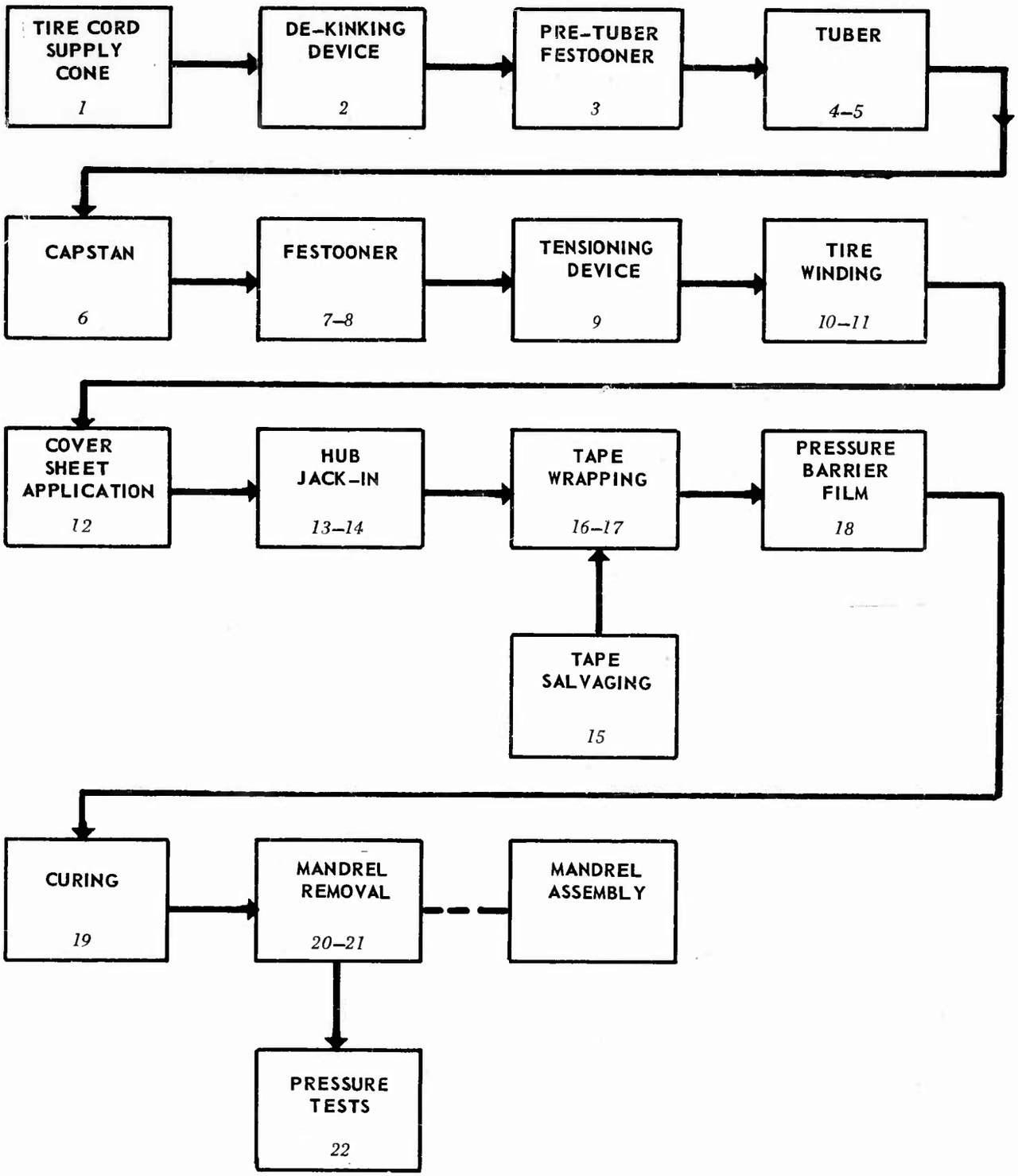

SCHEMATIC TIRE-BUILDING

The arrows on the chart on the facing page trace the path of tire cord from the supply cone, through the various steps in the continuously-wound-cord, tire-building process, to the cured tire. At the bottom is the box representing the pressure testing conducted on the cured tires as the first step in proving tire worth and included here as a matter of convenience.

The numbers at the bottom of each box refer to the like-numbered photographs which follow in the same sequence.

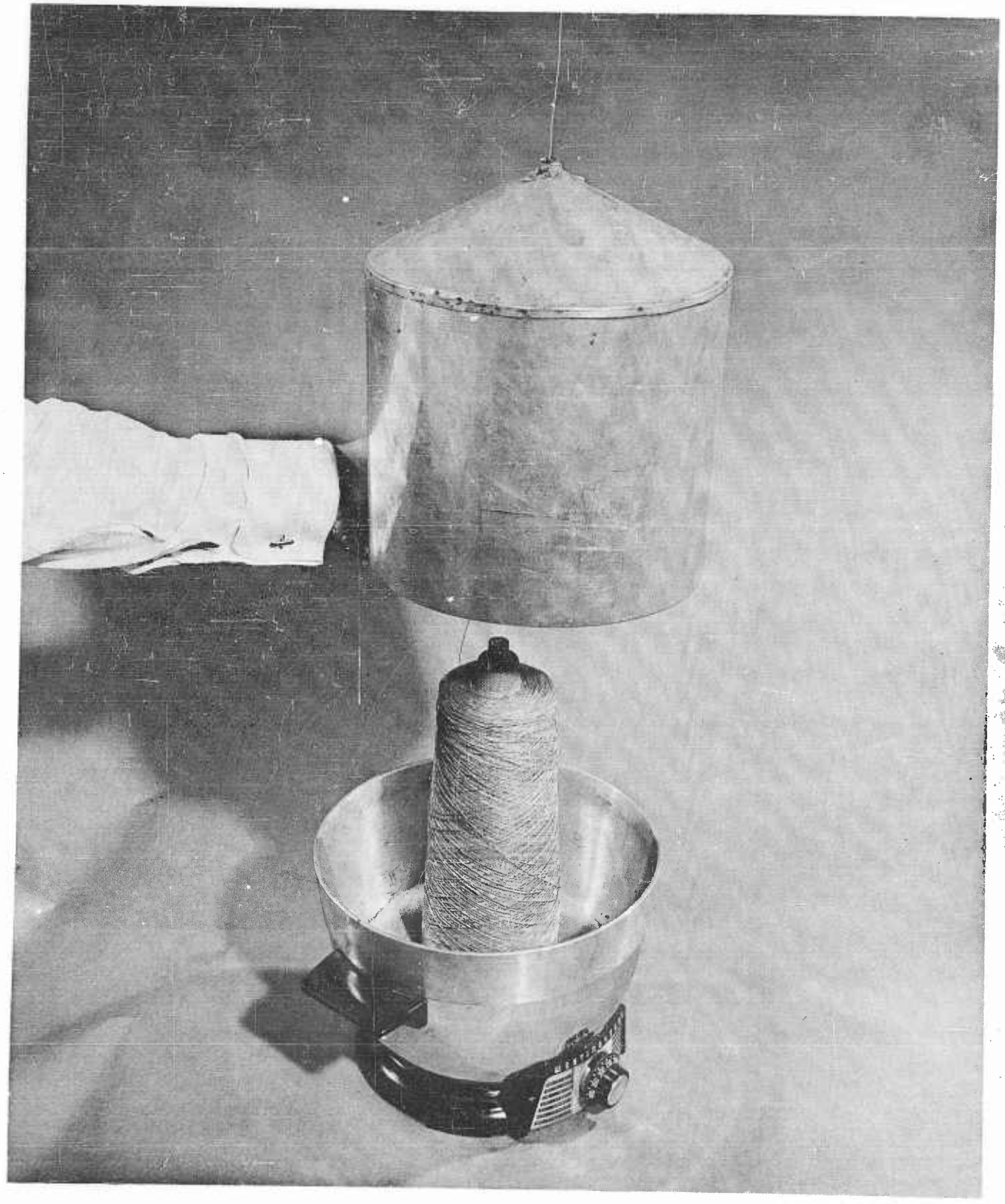

Photo No. 1

Tire Cord Supply

TIRE CORD SUPPLY

This photograph shows a cone of nylon tire cord as supplied by the textile industry. The supplier has coated the cord with a resin which promotes adhesion of the nylon to natural rubber. The cone is supported in its upright position by a tightly-fitting metal rod passing axially through the stiff cardboard reel upon which the cord is wound. The base of the cone fits snugly against a sheet of lamb's wool to prevent the cord from being drawn under the base of the cone as it pays off the upper end of the cone and out through the loose-fitting bushing at the top of the sheet-metal cover. The base is an off-the-shelf deep-fat-fryer used to control the temperature of the cord.

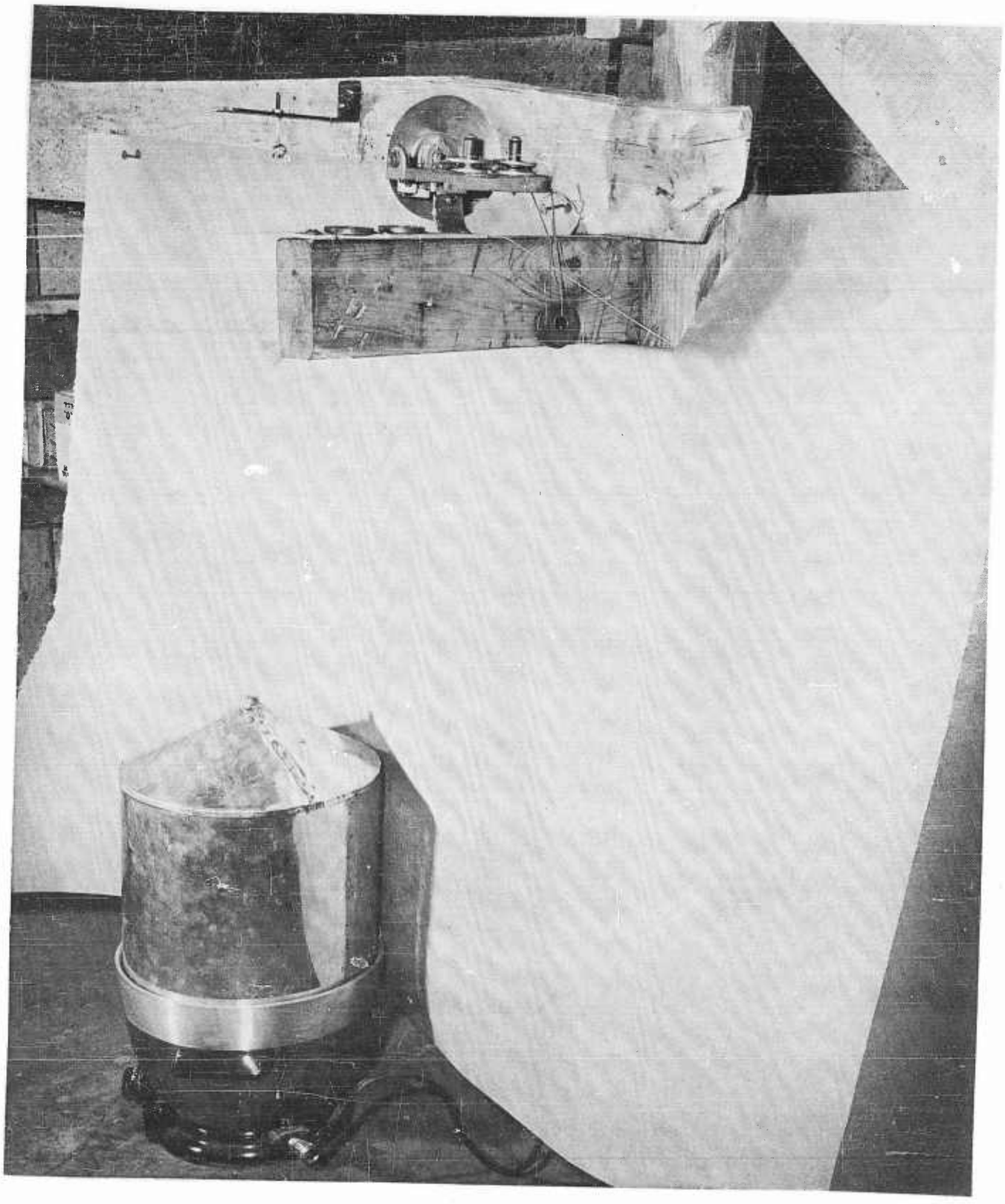

Photo No. 2

De-Kinker

DE-KINKER

In this view the sheet-metal cover has been replaced over the cone of tire cord. The cord passes upward through the bushing in the top of the cover, through the eye supported by the bracket, thence to the right and through the de-kinker and finally out of the picture to the left. The de-kinker is a device which smoothes out any kinks which may form in the cord as it pays off the cone at a rate up to 500 feet per minute. In the de-kinker the cord passes alternately around two vertical, hardened steel pins and between two, polished, rounded-edged bushings supported by each pin. These bushings can be loaded with washers to control the minimum tension in the cord between the de-kinker and the supply cone.

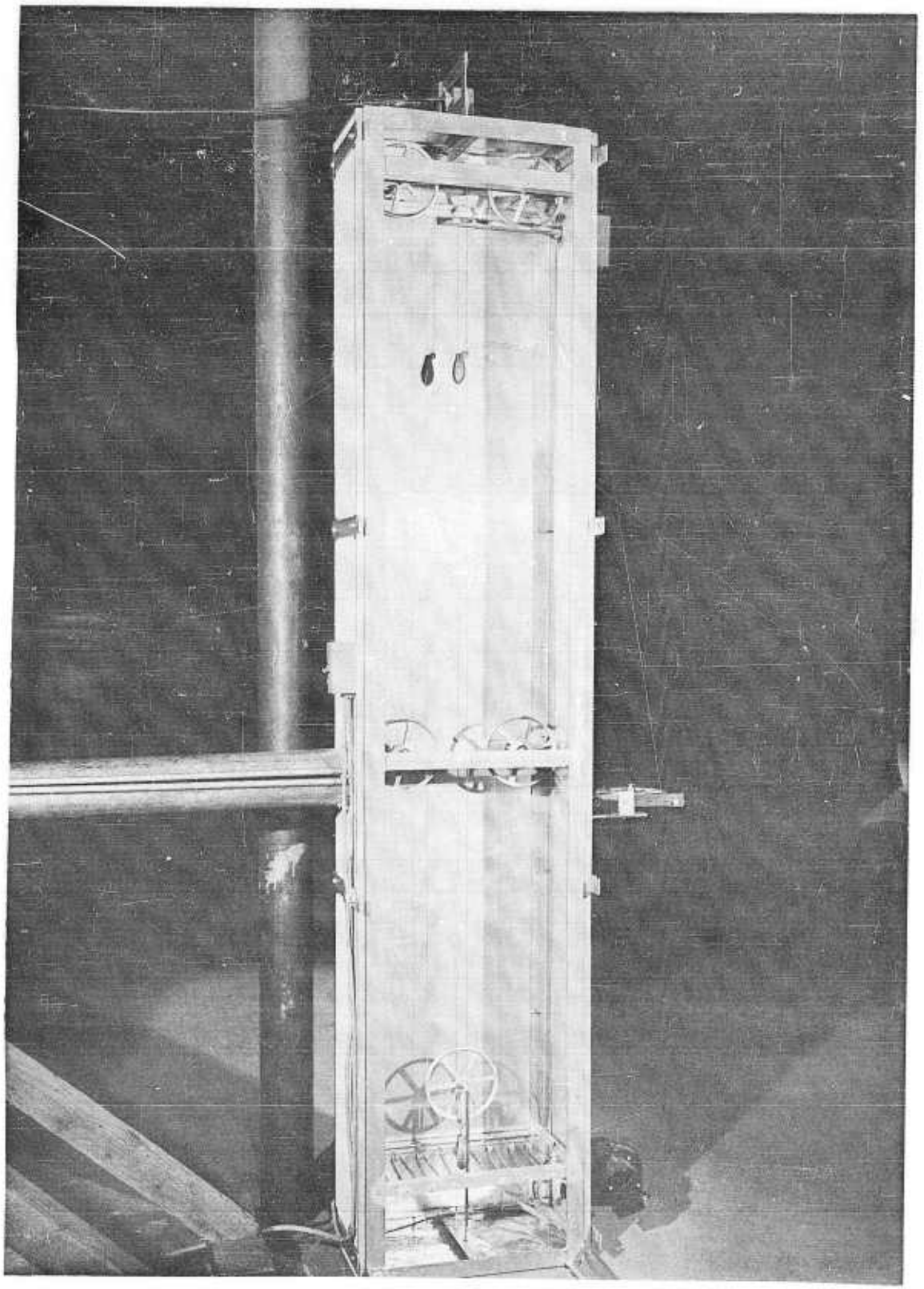

Photo No. 3

Pre-Tuber Festooner

PRE-TUBER FESTOONER

This device, shown with the front cover removed, performs two functions. Primarily, it heats the tire cord just prior to its passage through the extruder (hereafter called "tuber" in consonance with jargon of the rubber industry) in order to secure maximum adhesion of the rubber to the cord. The heat is provided by resistance elements at the bottom of the cabinet. The temperature is controlled by a thermostat at the top. The cord is further exposed to the heated air after it leaves the cabinet by the draft from a blower with intake at lower right. The heated air exhausts through the tube at the left which leads to a point near the entrance die of the tuber.

Secondarily, this machine avoids a prolonged suspension of tire-winding caused by knots or kinks attempting to pass through the entrance die of the tuber and a consequent breaking and unreeving of the cord. This is achieved as follows. The cord enters the cabinet after passing through a slot bushing at the right side and around a vertical-axis pulley; thence it passes under the fixed pulley at mid-height on the right; over the fixed pulley at upper right; then down and under the weighted, moveable pulley at the bottom, thence over the fixed pulley at upper left; and finally, after passing under the fixed pulley at mid-height on the left, passes to the tuber through the tube extending to the left of the cabinet. When a knot or kink is caught by the slot bushing, the weighted, moveable pulley at the bottom is caused to rise upward on its guide wires. When this moveable pulley lifts the weight shown suspended on one of the guide wires near the top of the cabinet, a micro-switch opens and all power is shut off, stopping the movement of the cord and preventing a break. A simple kink can then be straightened out and winding resumed. A knot can be cut out of the cord and the cord rethreaded through the tuber without unreeving any of the pulleys.

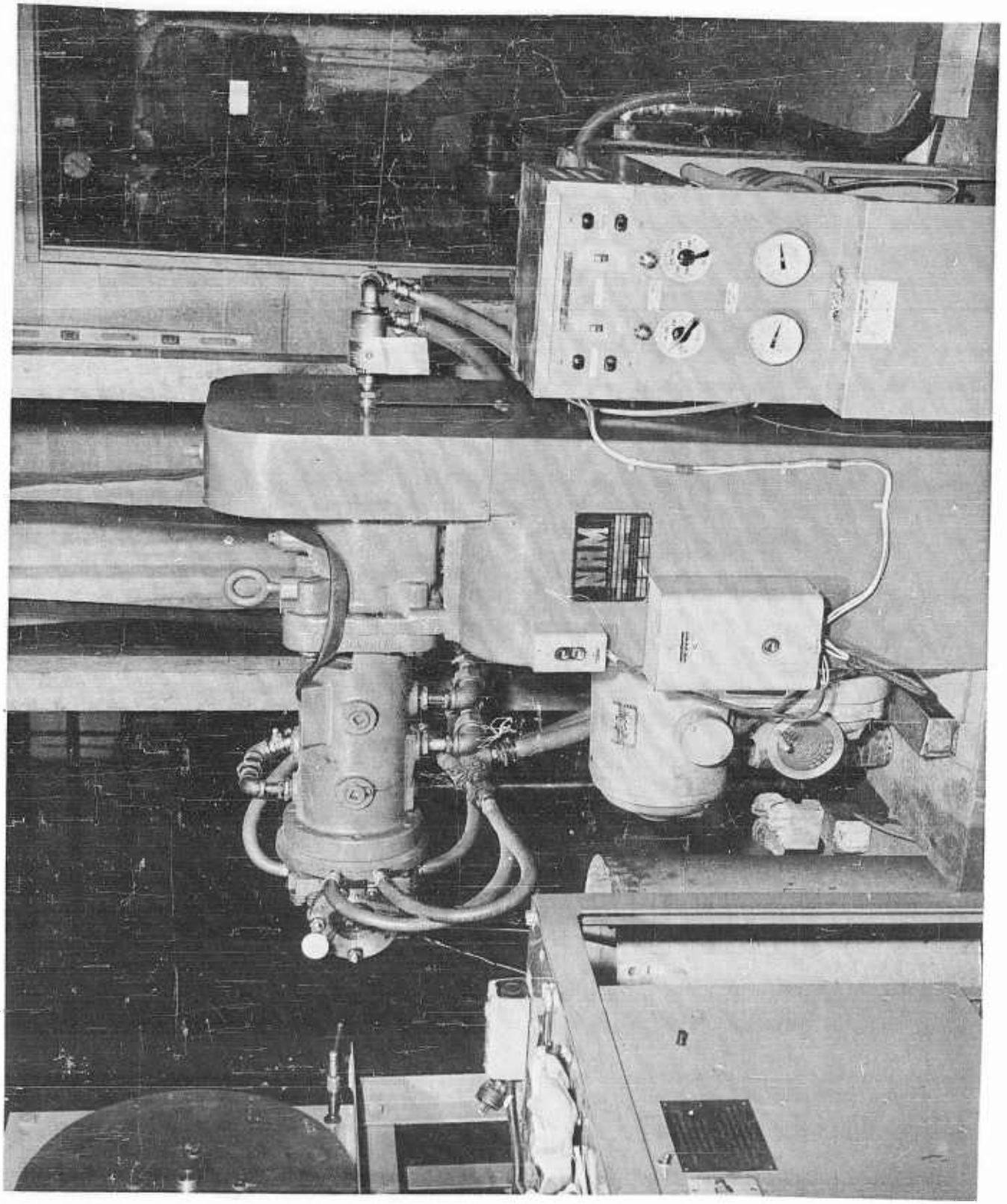

Photo No. 4

Tuber

TUBER

This view shows both the tuber (identified by the NRM nameplate) and its temperature control unit to the right. This equipment coats the tire cord with fresh, green, tacky, uncured, carcass-stock rubber. Prior to operation, the temperature of the barrel of the tuber must be raised to approximately 85°F, in order to prevent overloading of the masticating worm in the barrel. Rubber stock of about one inch of cross section area can then be fed into the barrel through the loading port just to the left of the lifting eye of the top of the tuber. When the tuber starts grinding the rubber, considerable heat is produced and the temperature control unit maintains the pre-set barrel temperature by cooling the barrel with cold water from the domestic service mains, wasting a small trickle of heated water. Simultaneously the temperature of the cross-head of the tuber is maintained at a pre-set temperature. A cross-head temperature of 200 - 210°F was found to be optimum with the natural-rubber carcass stock used in these experiments. The geometry and operation of the cross-head will be described in the next view. The tuber must be tended continuously during tire winding.

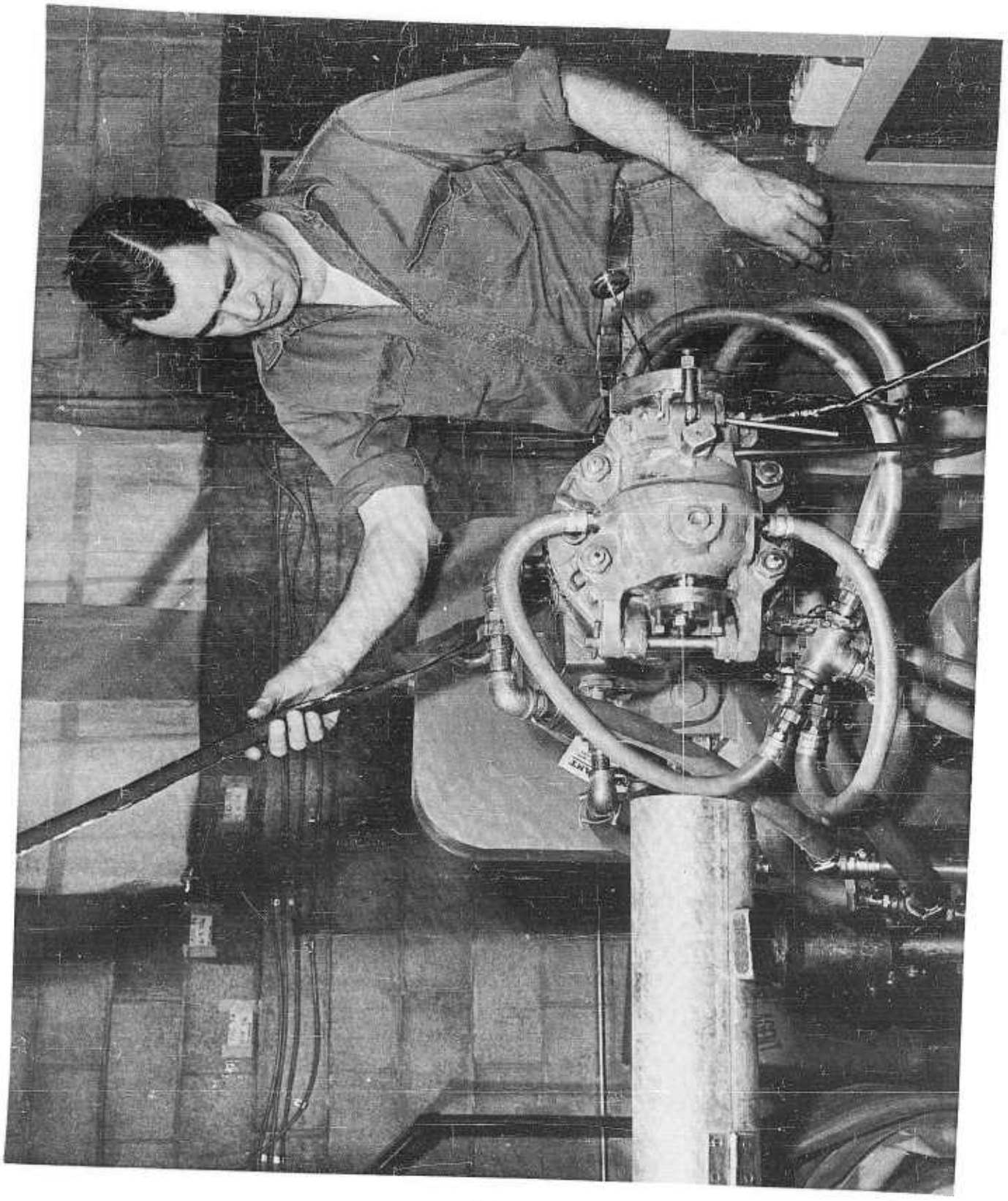

Photo No. 5

Tuber Cross-Head

TUBER CROSS-HEAD

This view shows the cross-head of the tuber. In it the pre-heated tire cord is coated with carcass-stock rubber. The cord is shown entering from the end of the tube at the left uncoated and departing coated at the right. The maximum cord velocity successfully coated and wound into a tire was approximately 450 feet per minute. The entrance die of the tuber is cone shaped on its outer surface, the apex of the cone pointing toward the direction of cord movement. The diameter of the axial hole in the entrance die should not be more than 10 or 12 thousandths of an inch greater than the nominal diameter of the cord, otherwise there may be a slow rearward flow of rubber through the die and this may cause the cord to jam in the die, breaking the cord. The exit die has a conical recess matching the cone of the entrance die. An axial distance between the two dies of approximately 3/16th of an inch gives optimum coating. Uncured rubber must be fed to the tuber at much greater rate than is actually coated to the cord; otherwise the rubber will remain at the elevated temperature of the cross-head long enough for partial cure. Therefore, provision is made for continuous passage of the semi-liquid rubber through the cross-head perpendicular to the cord movement. This flow is regulated by the pressure exerted by the worm in the barrel and by a valve at the over-flow port. The highest pressure attainable, consistent with uniform cord coating, is desired in order to secure thorough impregnation of the cord.

The rubber which passes through the over-flow port may be cooled down and re-fed to the tuber, thus eventually all being coated on the cord. Since the normal distance between the dies is only about one tenth of an inch, due to the conical shape of the space, there is a very rapid flow of rubber toward the cord at the small end of this conical shaped space. Any foreign matter, such as particles of sand, tend to collect at the exit die and if too large to pass through between the cord and the die, either prevents symmetrical coating or causes the cord to break. Since natural rubber is more likely to have foreign bodies present than synthetic rubber, it may be concluded that synthetic rubbers are more appropriate for use in a tuber than is natural rubber. The cross-section of the rubber coated to the cord should be equal to, or slightly less than, the nominal cross-section of the cord. This amount is probably the minimum necessary for complete impregnation of a tire and thus will minimize weight and thickness of the tire. In the limited number of continuous-cord tire-building experiments conducted to date, precise control of the rubber coated to the cord was never achieved. The amount coated was always greater than desired. A more rapid winding rate or a smaller exit bushing or both might have achieved a thinner coating. The experiments were suspended before these possibilities could be fully explored.

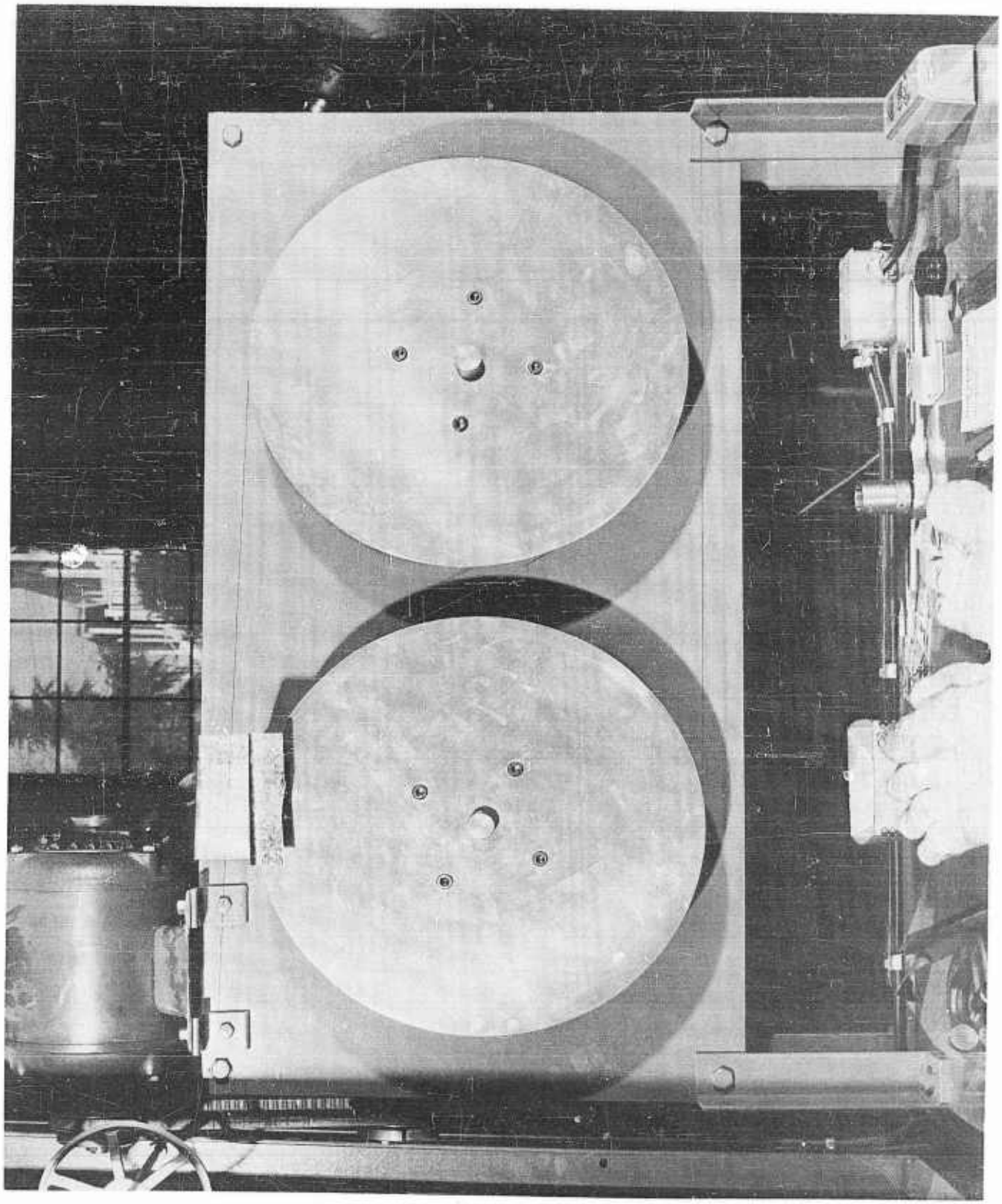

Photo No. 6 - 16 - Capstan

CAPSTAN

The coated cord is pulled through the tuber at a tension of up to 8 or 10 pounds by this capstan, passing clockwise around the left drum, down between them and counter-clockwise around the right drum. The drums are grooved to prevent the cord from running off and are driven by the direct current motor mounted above and to the left through a non-slip, toothed, rubber belt, a so-called timing belt. The speed of the motor is controlled by the demand at the winding machine in a manner explained opposite the next photograph.

Photo No. 7

Festooner

FESTOONER

This device provides for synchronization of the winding machine with the capstan, allowing sufficient dynamic storage to permit smooth acceleration of the speed of the winding operation. The cord passes under the pulley at the lower right, thence over the upper pulleys and under the three gang pulleys of the floating array, alternately, and finally down and out of the picture to the left. When the winding machine is speeded up the increased demand causes the floating array to be drawn upward. This causes the rotation of a master selsyn motor and in turn a slave selsyn operates to increase the speed of the direct current motor which drives the capstan and vise-versa. The floating gang pulleys travel up and down on piano wire with negligible friction. This device could be improved by the addition of fair leads for each stationary pulley and by deeper grooves on the sheaves, both improvements tending to inhibit accidental unreeving.

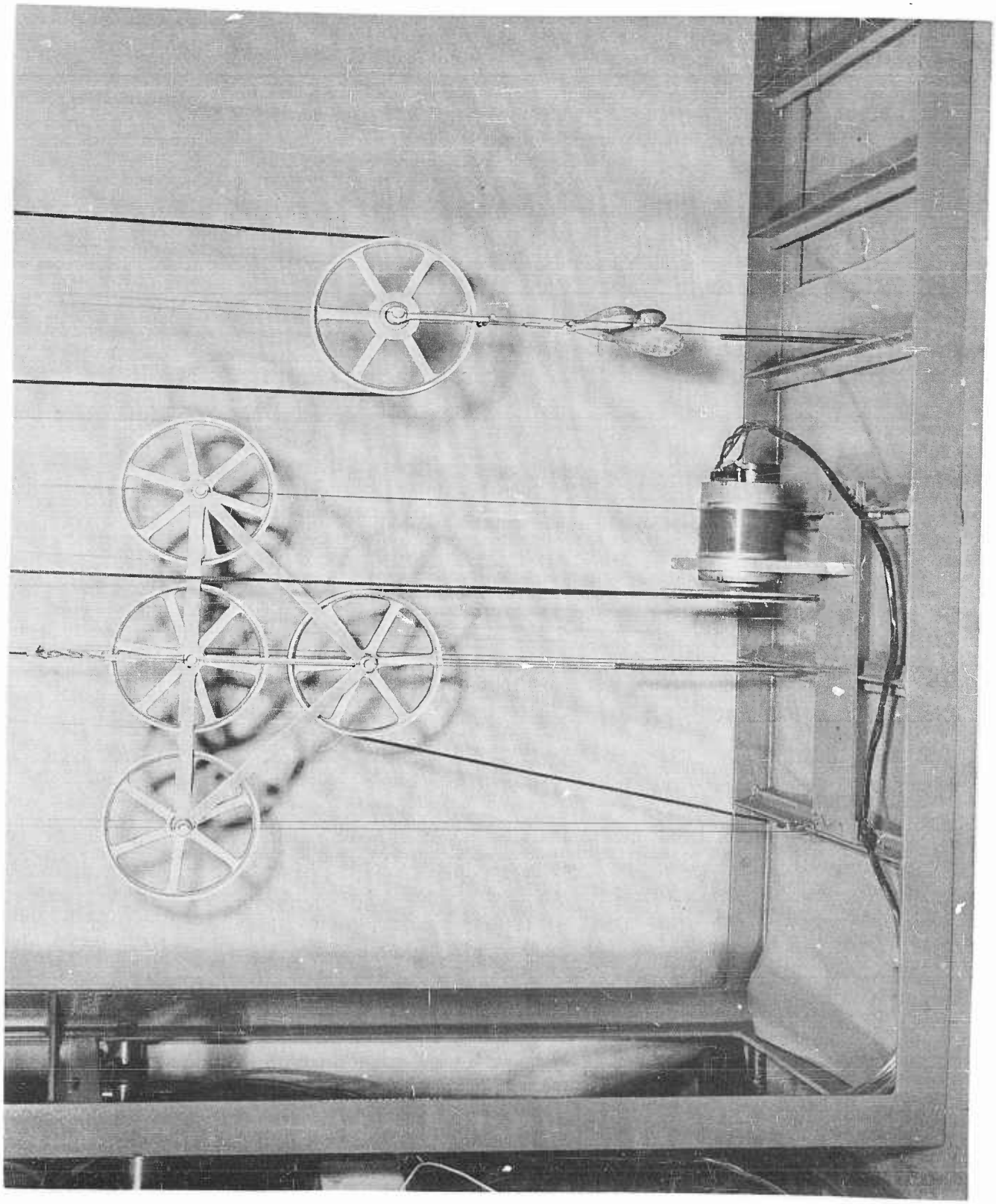

Photo No. 8

Master Selsyn Motor

MASTER SELSYN MOTOR

Cord tension in the festooner is controlled by the weights attached to the single floating pulley shown at the right. The heavy black cord which passes under this pulley passes over an idler pulley at the top of the frame, thence down and around the pulley on the shaft of the master selsyn motor and then over the lower pulley on the floating gang. Thus an upward or downward movement of the gang pulley causes a rotation of the selsyn motor.

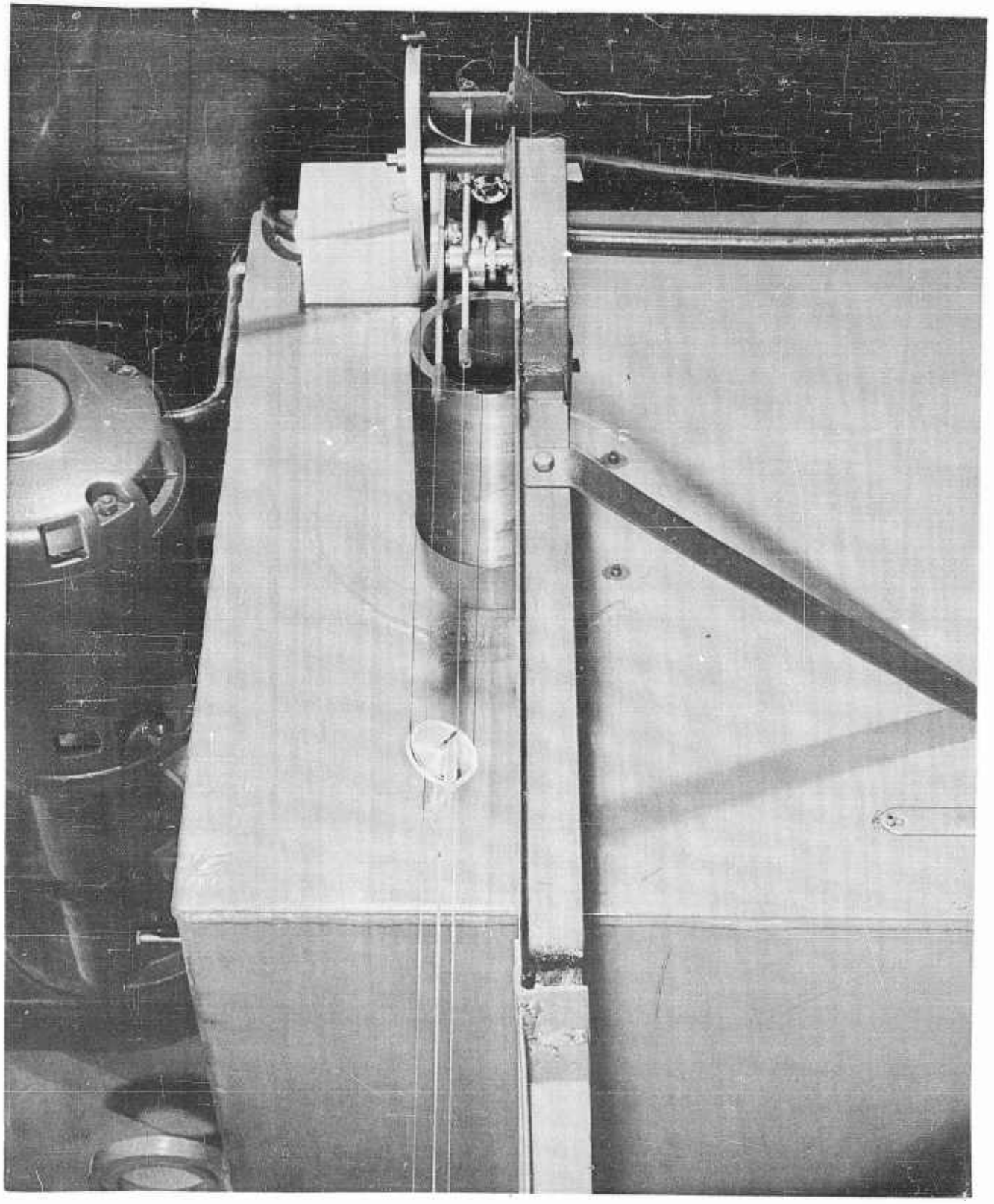

Photo No. 9

Final Tensioning Device

FINAL TENSIONING DEVICE

In the winding plane, the surfaces upon which the cord is wound are non-circular. Therefore, with uniform speed of rotation of the winding arm, there is varying velocity in the speed of the cord as it passes the fair loads at the end of the winding arm. If allowed to be transmitted back to the festooner, this varying velocity of the cord causes a cyclic up and down motion of the floating gang pulley and this limits the winding-arm rotational speed to an unacceptably low value. The device shown here smooths out the changes of velocity of the cord at the festooner and maintains a suitably low tension in the cord at the tire. The cord coming from the festooner passes around the vertical-axis pulley at the right, thence around the small, very light-weight, floating pulley in the center, and thence around another vertical-axis pulley and into the hollow axle of the winding arm. The floating pulley is held to the left by a long strand of rubber of the sort used to power model airplanes. Thus the six to ten inch travel of this pulley to and fro, twice for each revolution of the winding arm, causes a negligible change in tension of the cord.

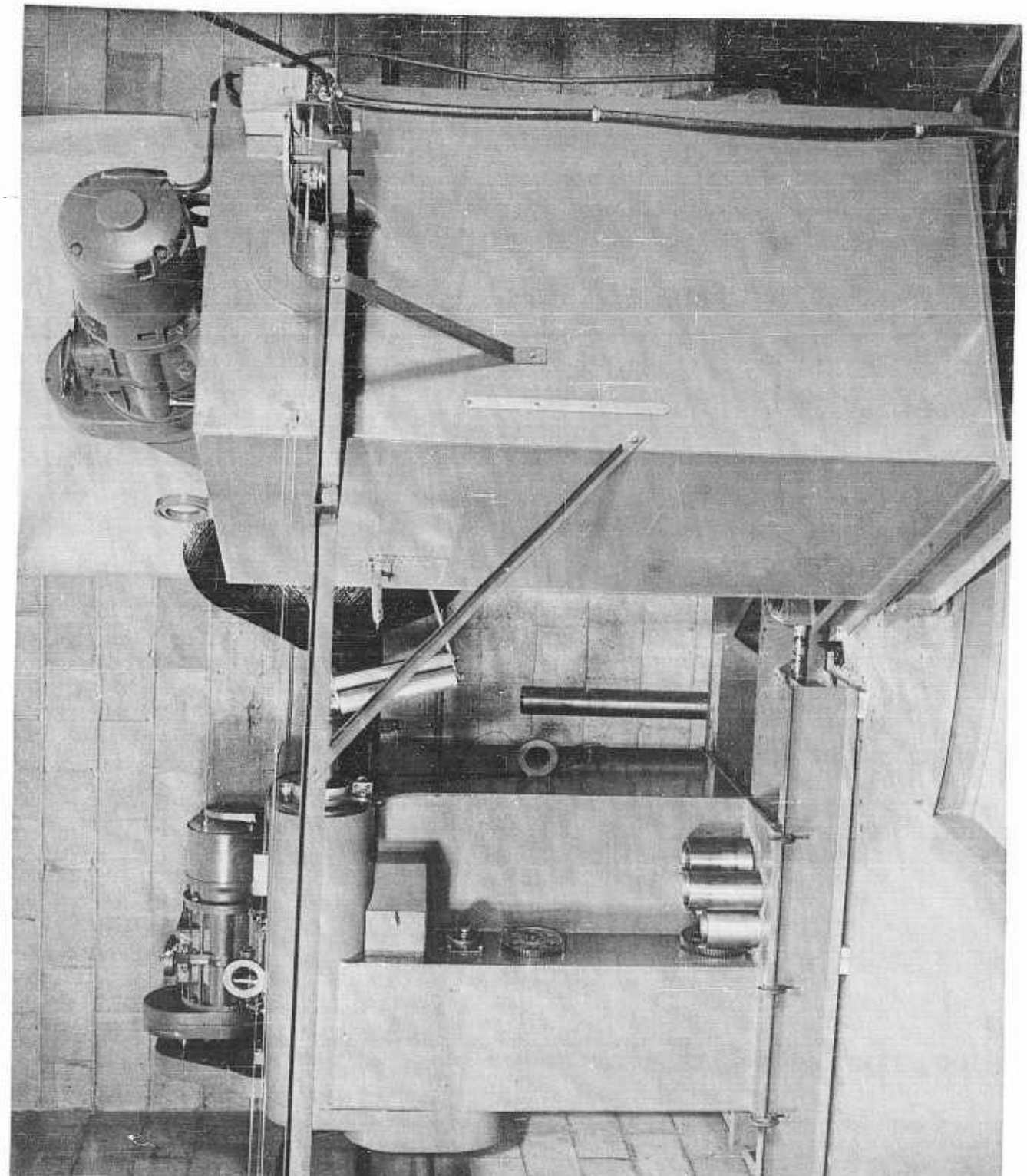

Photo No. 10

 Winding Machine -1

WINDING MACHINE - 1

From this view the set-out position of the tire hubs during winding can be observed as well as the shape of the non-circular surface upon which the tire cord is wound. Note also that the angle between the axis of the mandrel and the axis of the winding arm can be varied to accommodate variation in mandrel cross-section, hub diameter or relative speeds of rotation of winding arm and mandrel, all of which will cause a change in the angle between the plane swept by the winding arm and the axis of the mandrel. The correct angle between the axis of the mandrel and the axis of the winding arm can most easily be found by trial. In general, the winding plane should be set so that the cord is tangent to the axle at the hub during winding.

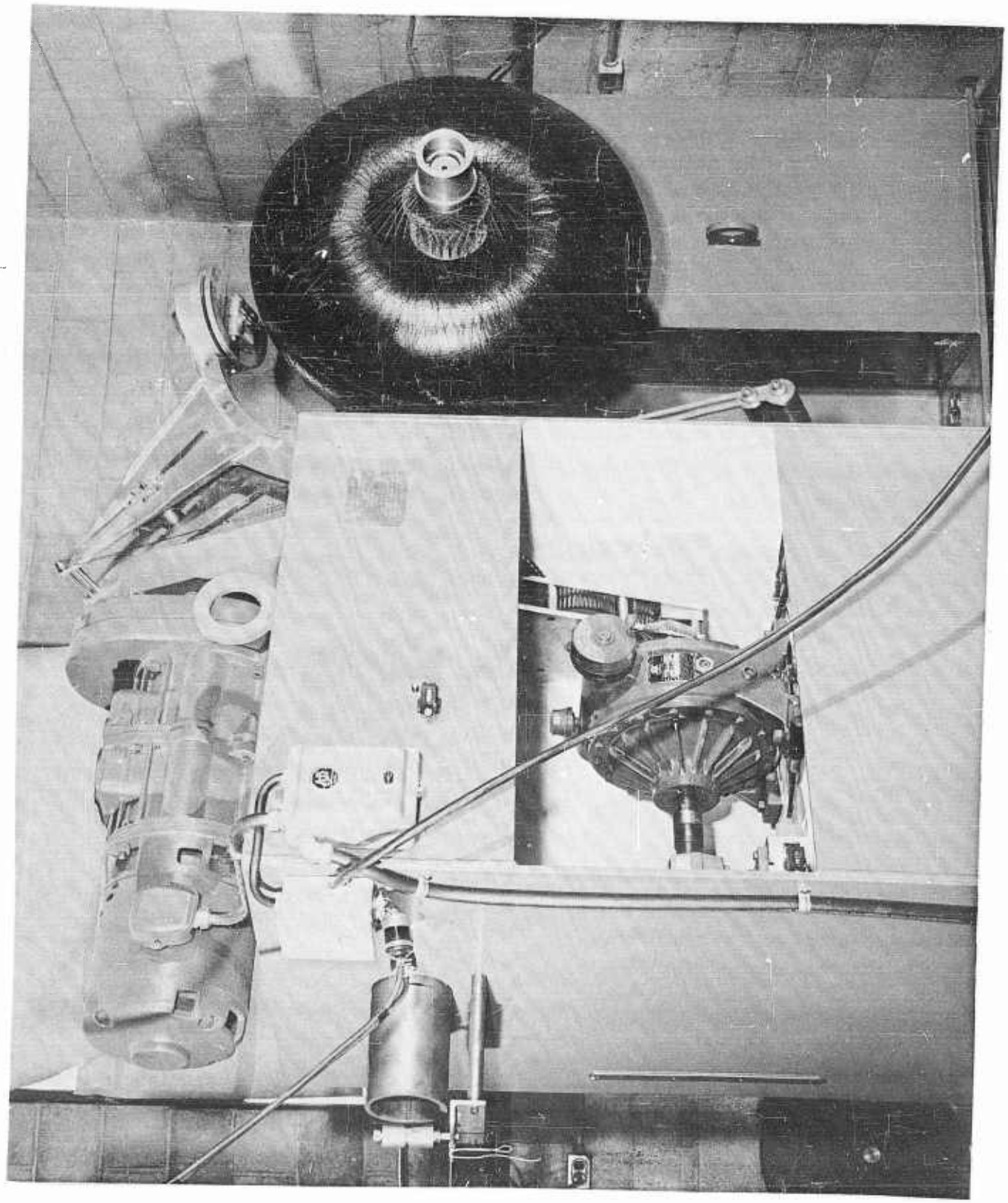

Photo No. 11

Winding Machine -2

WINDING MACHINE - 2

This view of the winding machine shows a tire with only a few dozen turns of cord wound into place. A thin sheet of rubber called a liner has been placed on the mandrel. The liner stock is compounded for minimum permeability to flow of gasses. Notice the set-out position of the hub and the recess in the mandrel which receives the hub prior to cure of the tire. The curved path of the tire cord across the tread area of the tire can also be observed in the upper portion of the tire. This curve can be varied in shape by increasing the clearance of the winding arm above and below the center-line of the tread of the tire, by varying the relative speed of rotation of the mandrel and winding arm, and by varying the angle between the axis of the mandrel and the winding plane. The shape of the curve of the tire cord on the mandrel surface will affect the inflated shape of the cured tire.

As winding progresses there will be a build-up of tire cord on the hub due to its wrapping around the hub while the winding arm rotates with the cord in contact with the hub but not in contact with the mandrel. This build-up will cause a change in tension of the cords of the completed tire unless accommodated for by a small movement of the hubs inward as winding progresses. The amount of movement inward required is determined by tire-cord diameter, total number of turns wound, depth of rubber coated on the cord, and the amount of wrap around on each hub for each turn. While winding a tire, all rotary power is furnished by the electric motor and variable speed drive mounted above the winding arm support. The rotation of the winding arm is carried through idler gears to the shaft of the variable speed drive mechanism shown mounted directly under the hollow axle of the winding arm. From here the power is carried by shafting downward to spur gears, thence parallel to the winding arm axis to a point directly under the center of symmetry of the mandrel where it changes direction to parallel the mandrel axis and thence upward through idlers to the mandrel axis. Once a tire design is standardized, the speed variator mounted under the axle of the winding arm could be changed for fixed gearing, thus removing one possible cause of trouble due to slippage in the friction drive of the speed variator.

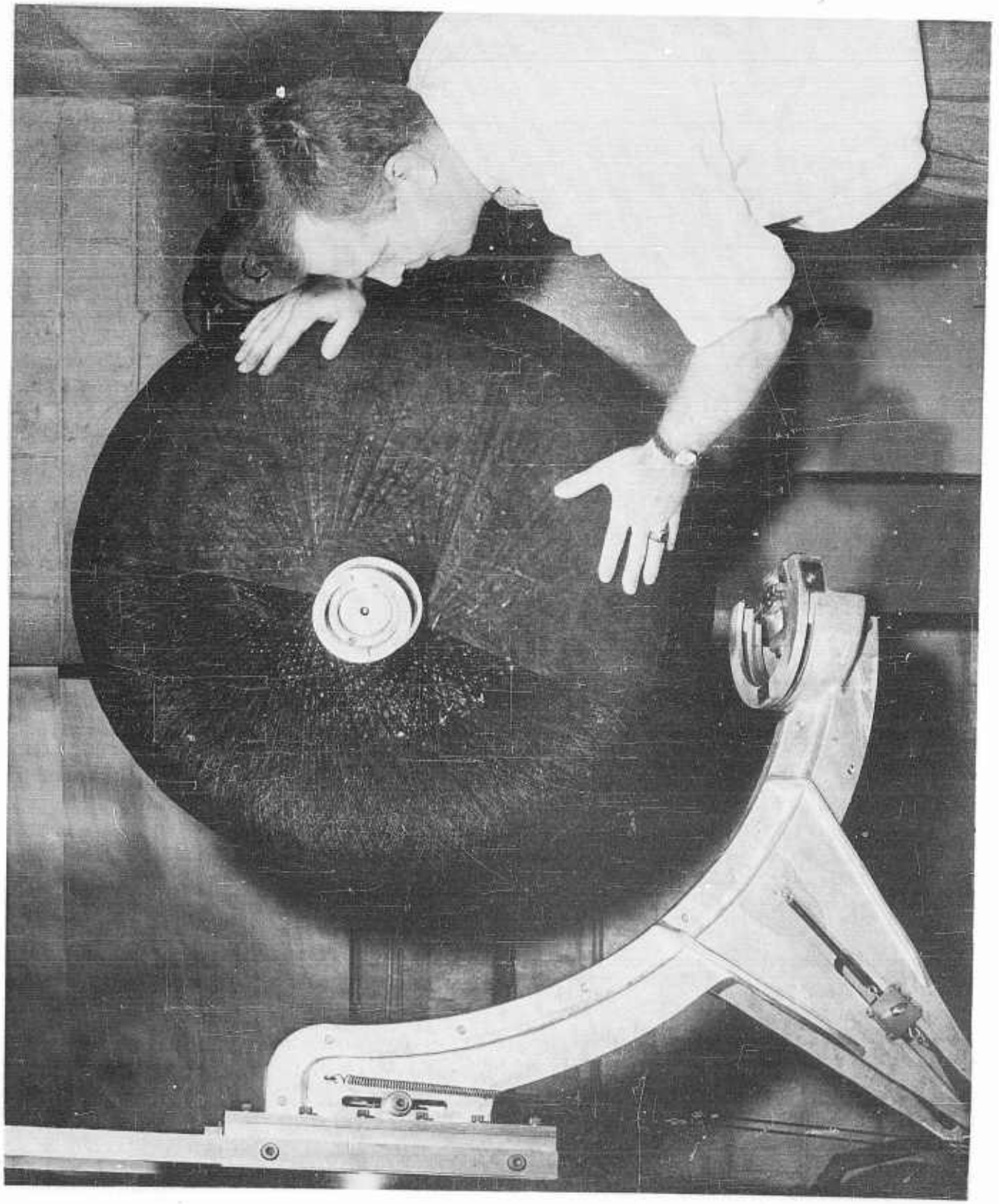

Photo No. 12

Cover Sheet Application

COVER SHEET APPLICATION

To provide protection against abrasion a cover sheet of carcass stock rubber, approximately 0.020 inches thick, is applied over the entire surface of the tire after winding is complete. This completes the structure of the tire. Wearing surface or tread is then applied as required by the service life desired.

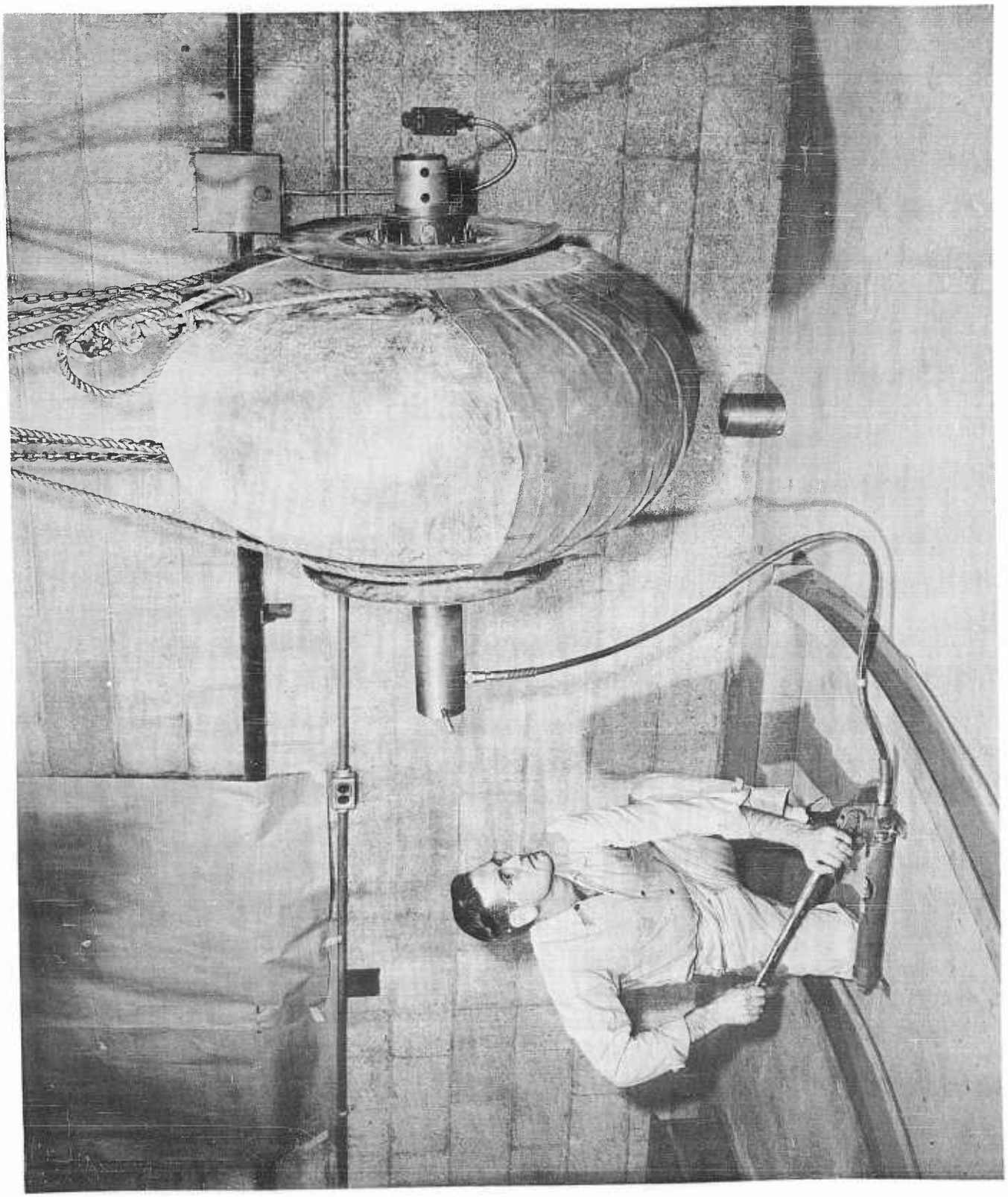

Photo No. 13

Jacking In The Hubs

JACKING IN THE HUBS

In this tire, winding and cover sheet application have been completed and the tire dusted with talc to prevent adhesion of the tire to the sling. The hubs are being jacked into curing position by a hydraulic jack inside the hollow axle.

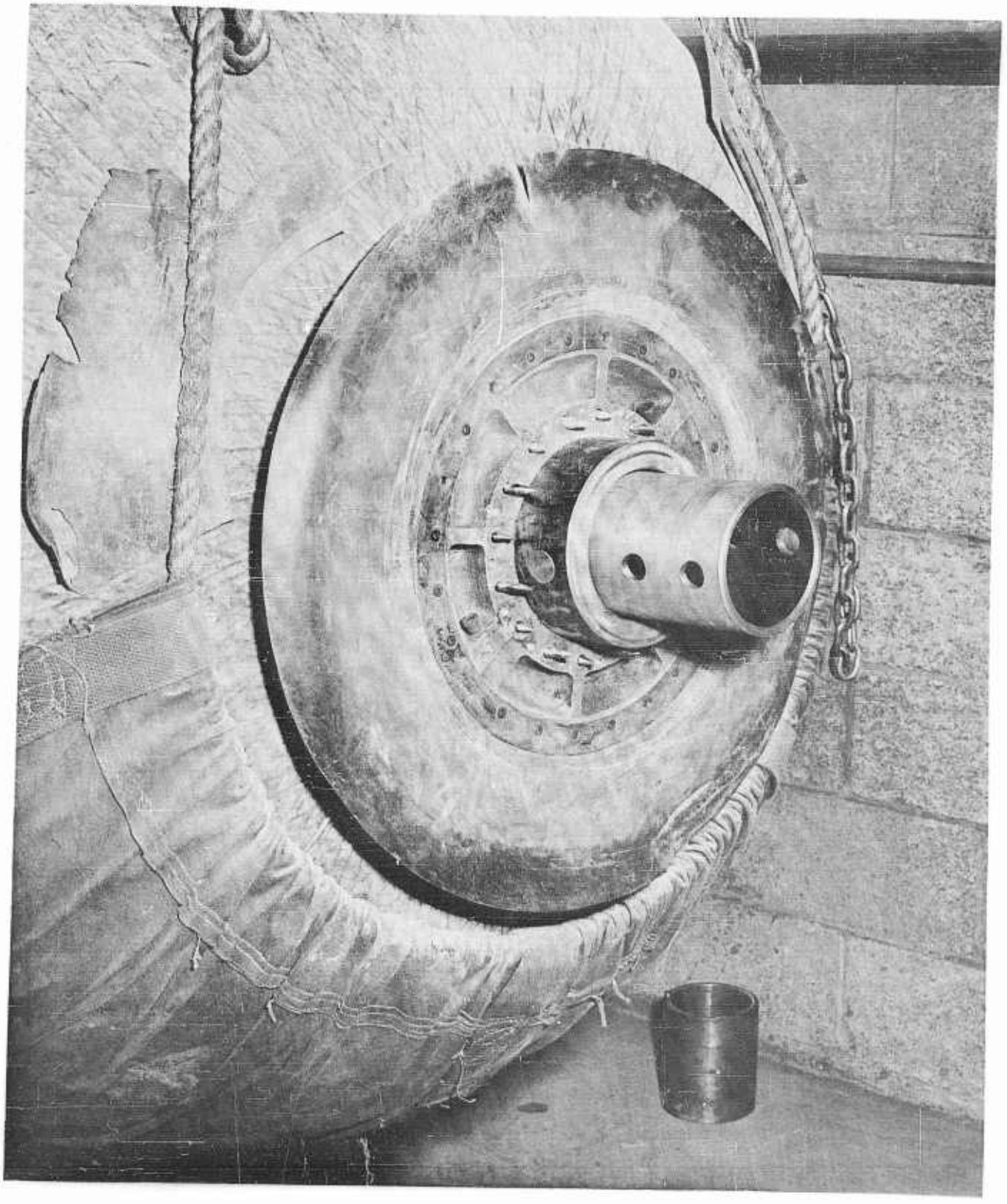

Photo No. 14 - 32 - Hub Detail

HUB DETAIL

This close-up of a hub being jacked into curing position shows the ends of the pointed rods which form the ring of flange bolt holes concentric to each hub. In the winding position the ends of these rods project just far enough into each hub to prevent the hubs from rotating on the mandrel spindle but not far enough to interfere with symmetric placement of the cord. Notice also that the curing flange has a metal center and a concentric rubber extension which fairs to zero at the shoulder, the widest part of the tire. The inside of the central metal portion of the curing flange is machined on the inside to the contours of the outside of the bead of the tire. Considerable force is needed to squeeze all the air out of the tire near the hub and to compress this bead area into the desired shape. This compression is begun during the preparation for cure and completed while the rubber is softened during the curing process. After the hubs are jacked in as far as practical at this stage, the pointed ends of the rods are unscrewed and replaced by nuts and washers holding the hubs in the jacked-in position.

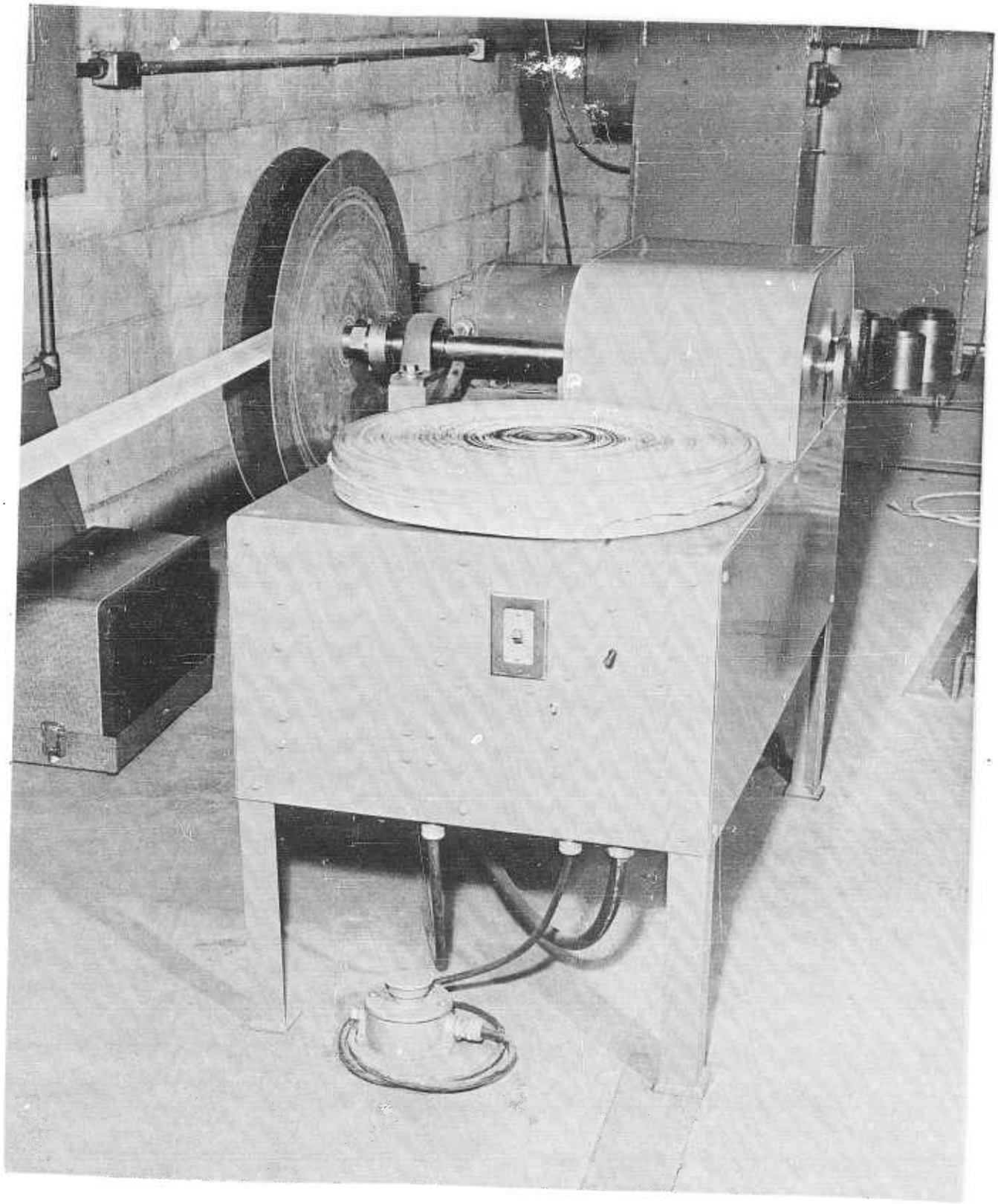

Photo No. 15

CURING TAPE, PREPARATION FOR USE

This view shows the machine developed for re-winding nylon curing tape after it has been pulled at high tension through a series of rollers submerged in hot water containing a silicone, mold-release compound. After use the nylon tape is set to a serpentine shape and must be softened by heat and stretched and moistened before re-use. A roll of tape ready for use is shown lying on the top of the re-winding machine.

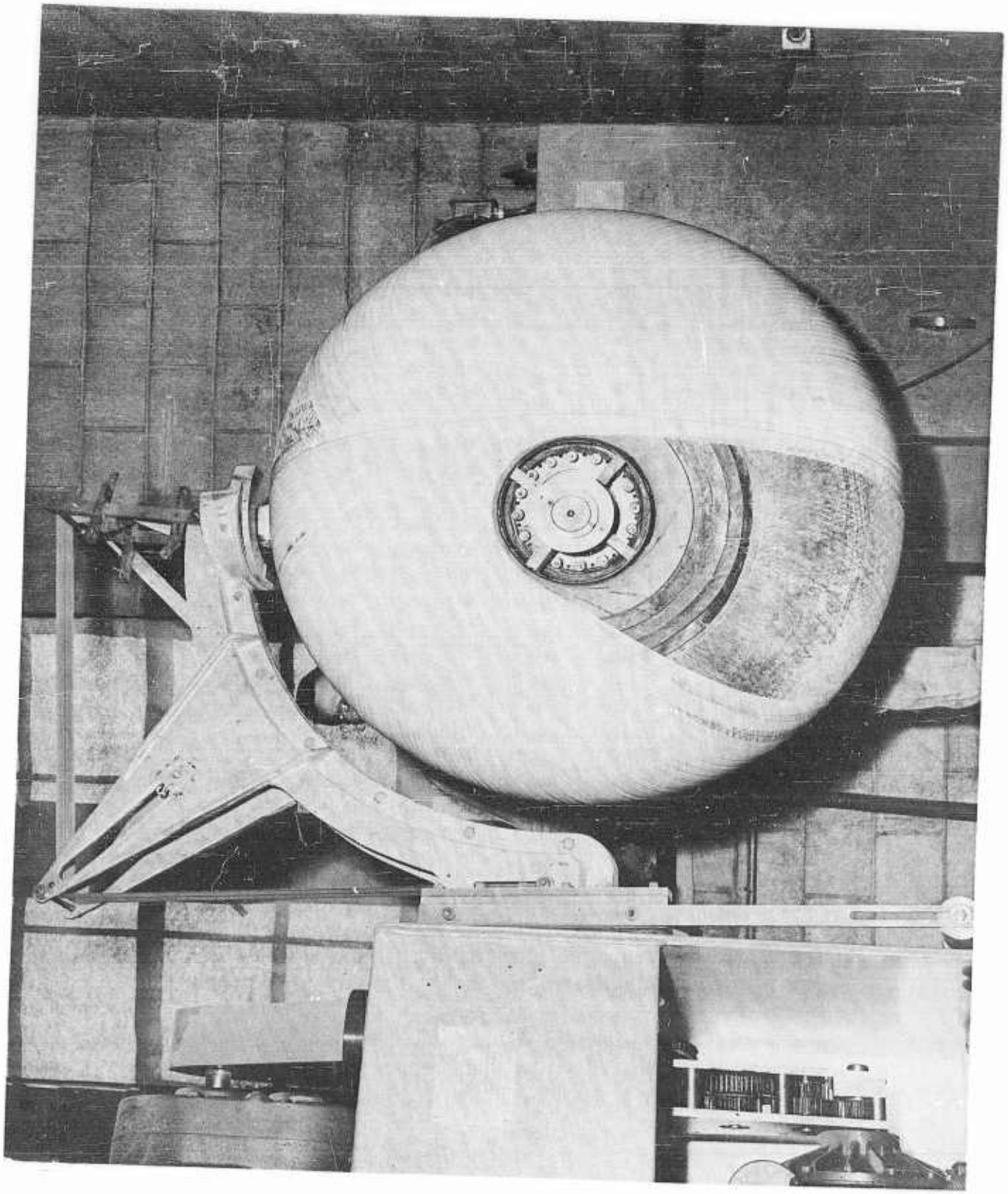

Photo No. 16

Nylon Tape Wrapping

NYLON TAPE WRAPPING

After the hubs are jacked-in, and secured by nuts set up on the flange-bolt-hole-forming rods, the assembly is remounted on the winding machine. Flat, flexible, copper washers are placed over the curing flanges concentric to the spindle. These washers cover the inner, metal portion of the curing flanges and extend outward in steps partially covering the flexible, rubber portion. These washers assist in securing a uniform pressure on the tire in the region of the hub during cure. A short length of steel cylinder is shown wedged by wooden blocks concentric to each hub with the inner end bearing against the metal portion of the curing flange. The angle between this stubby cylinder and the curing flange is filleted by an aluminum casting. The assembly is now wrapped with several hundred turns of thin nylon tape about three inches wide and moistened to reduce slipperiness. During this wrapping, the mandrel spindle and winding arm are driven independently at relative speeds which cause about a two thirds overlap of successive layers of tape. This tape, as with all nylon, has the property of shrinking with rising temperature up to the melting point of the nylon and this assures high pressure between the shoulders over the tread area of the tire during cure. The result is sound, dense rubber in this region after cure.

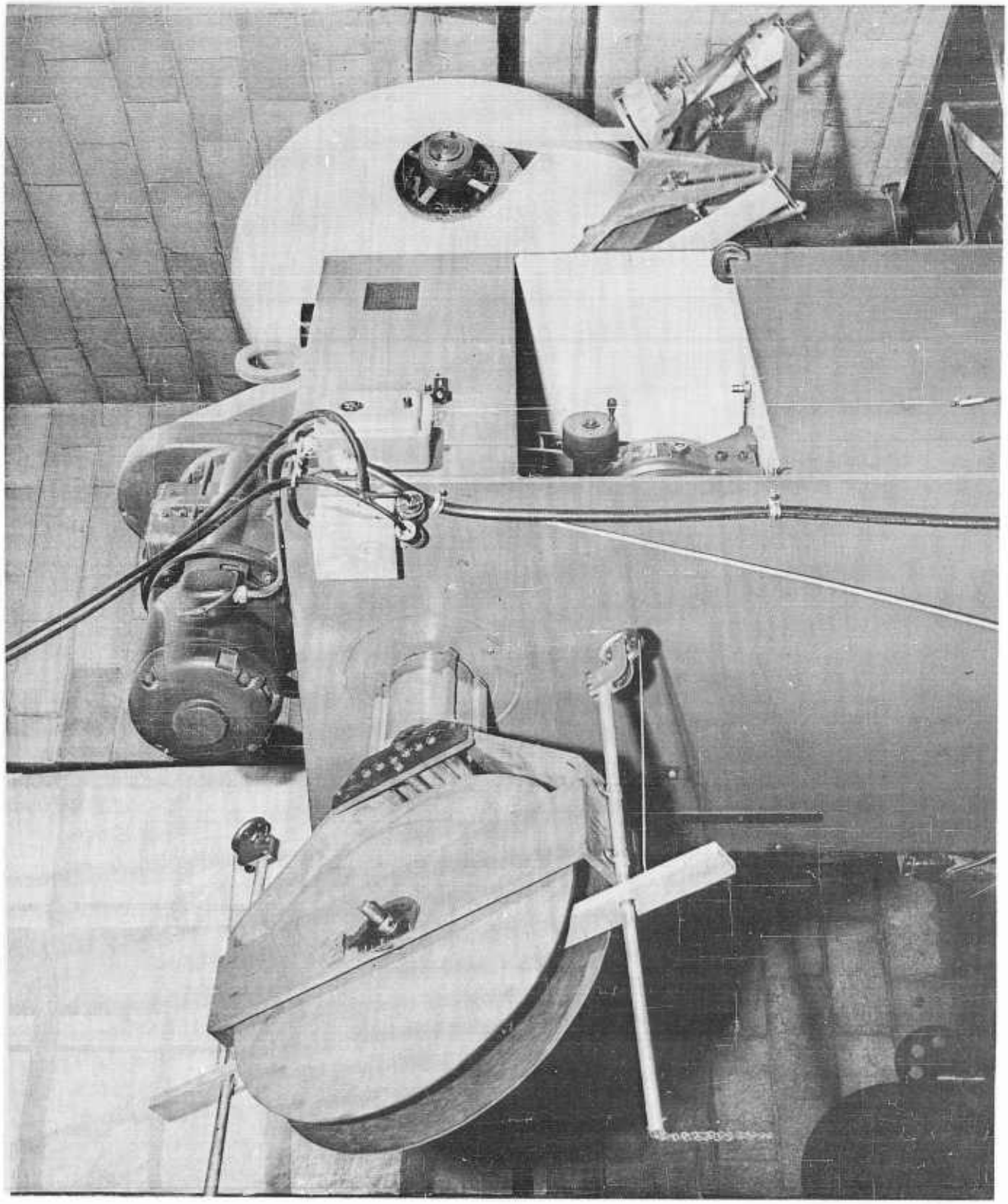

Photo No. 17

- 38 - Nylon Tape Wrapping, General Arrangement

NYLON TAPE WRAPPING, GENERAL ARRANGEMENT

This view shows the general arrangement of the winding machine adapted for tape wrapping. Notice that the reel of tape rotates with the axle of the winding arm avoiding twisting (or cabling) during wrapping and that the tension on the tape can be controlled by varying the load on the wooden slat which bears against the tape in the reel. In this view, the first complete layer of overlapping tape is almost wound into place.

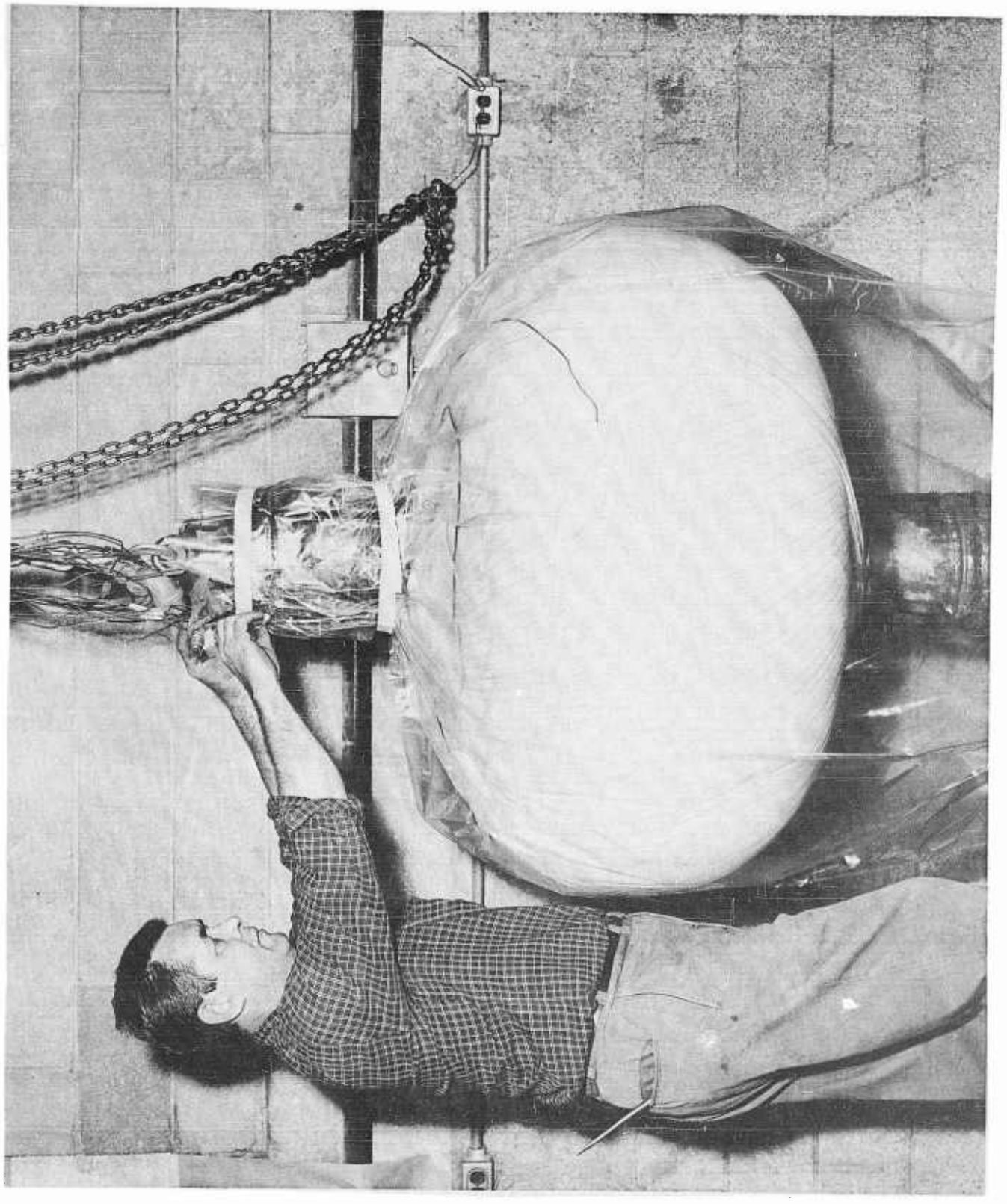

Photo No. 18

 Plastic Film Pressure Barrier

PLASTIC FILM PRESSURE BARRIER

After all the curing tape is wrapped into place, the stubby cylinders concentric to each hub are extended by capped cylinders held in place by a spring loaded rod passing through the hollow axle of the mandrel. An open ended sleeve of heat resistant plastic film is shown being sealed about the upper of the two capped cylinders. The bead area of the tire is further compressed during cure by inward movement of the capped cylinders caused by the curing tank pressure. This pressure is augmented by a partial vacuum maintained inside the pressure barrier provided by the plastic film. Maintenance of this vacuum assures pressure on the tire during cure; whereas loss of the vacuum indicates a break in the film and a curing failure unless the break is promptly repaired. Shown also in this view are thermocouple wires placed under the film in order to control curing temperatures.

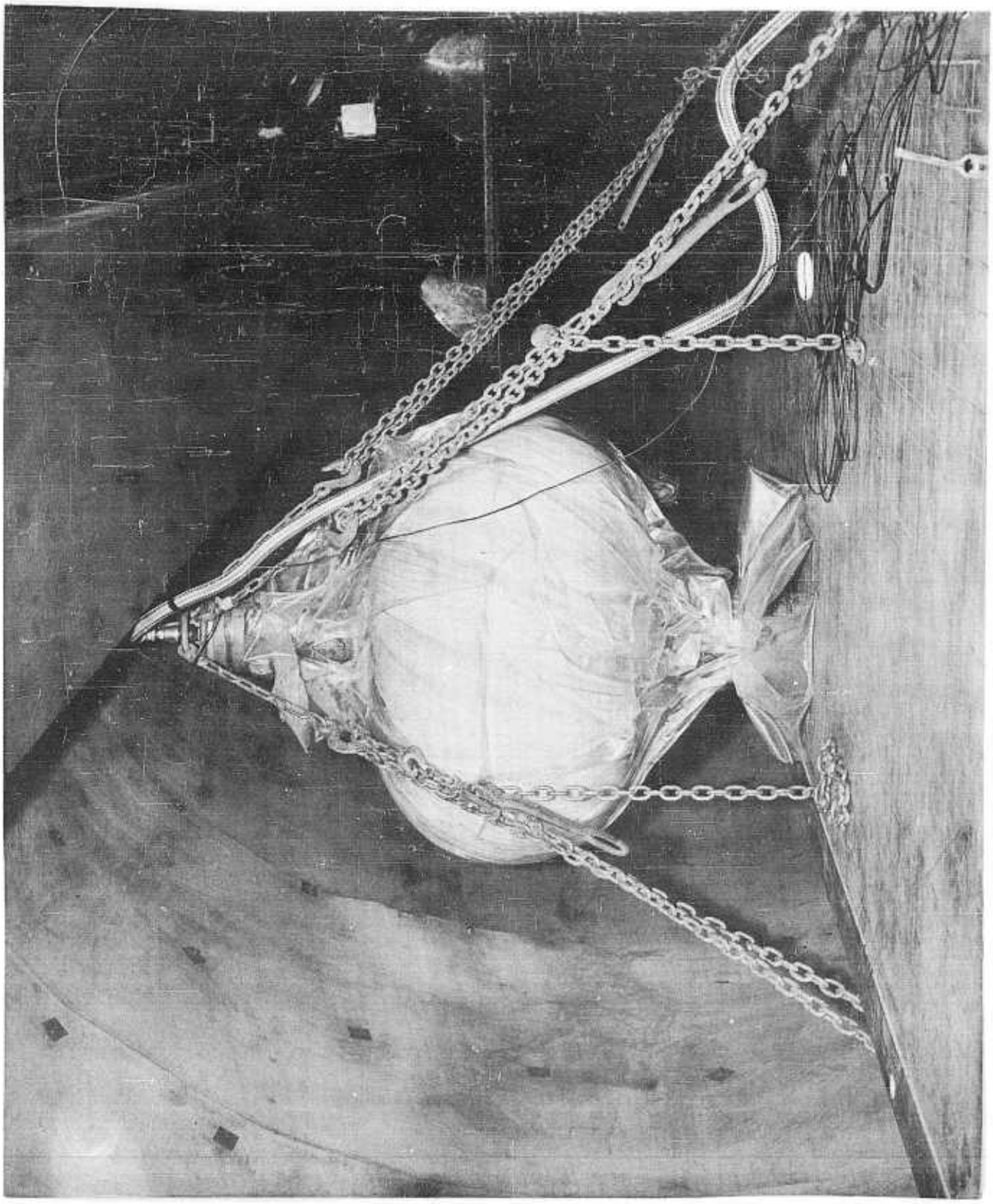

Photo No. 19 - 42 - Curing

CURING

This view shows a 34-inch tire in a curing tank with a partial vacuum on the assembly as indicated by the shrinking of the film against the tape wrapped tire. In later cures the sharp re-entrant angle in axial cross-section between the capped cylinders and the nylon tape near the beads of the tire was faired by filleting with heat-resistant rubber. This reduced the possibility of rupture of the pressure barrier film.

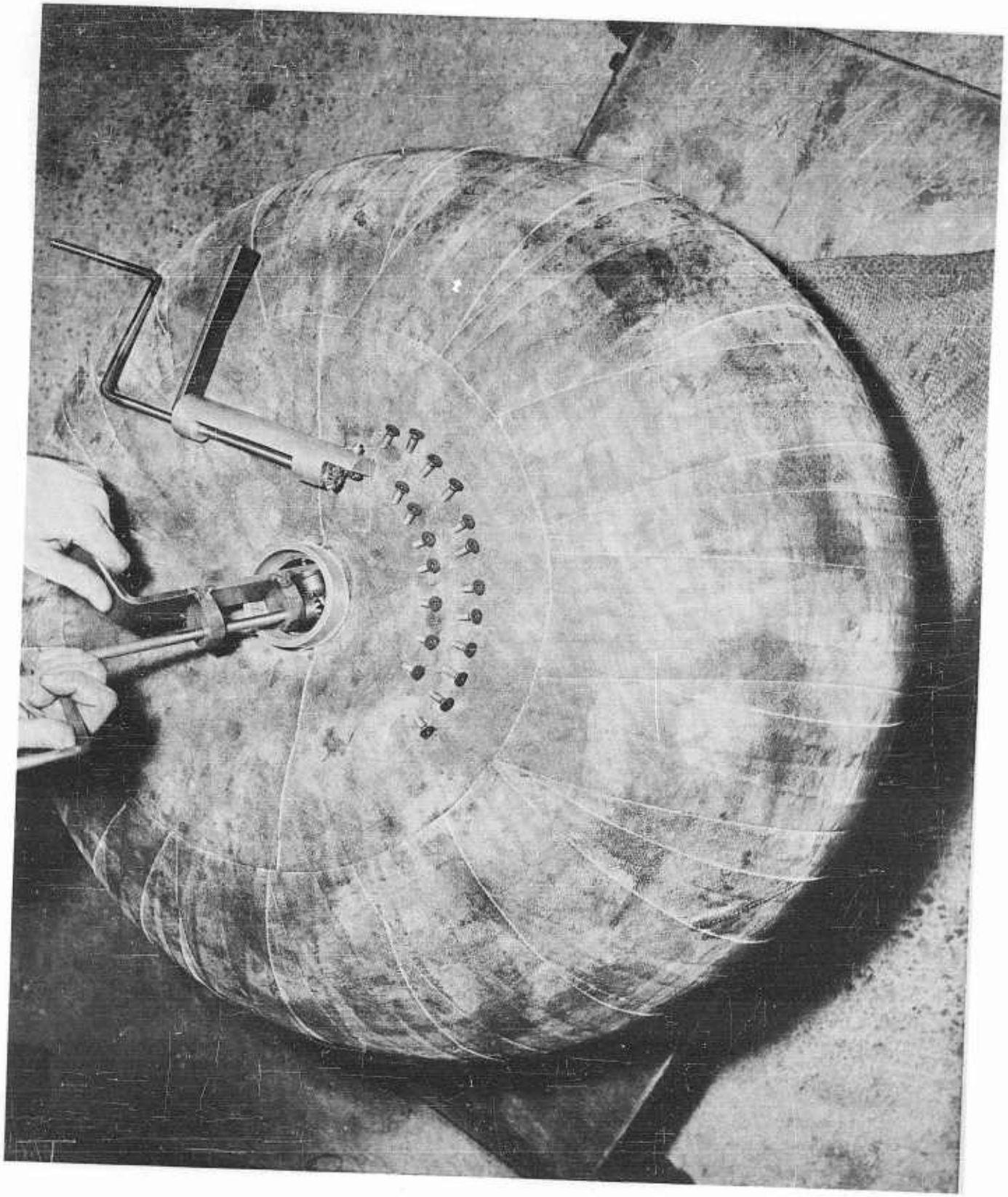

Photo No. 20

Removing The Mandrel

REMOVING THE MANDREL

After removal of the plastic film, the thermocouples, the capped cylinders, the nylon tape, the stub cylinders, the copper washers, and the nuts on the hub-flange, bolt-hole-forming rods, a plate is bolted over the central opening of each curing flange. One of these plates has an air hose fitting and the tire is inflated to approximately fifty (50) pounds per square inch pressure through this fitting. This pressure is sufficient to expand the tire and break its partial bond to the mandrel. The curing flanges are now removed and the hub-flange-bolt-hole-forming rods are unscrewed from their tapped holes in the inner mandrel segments. The sleeve which holds the inner mandrei segments in their assembled position is now freed for removal by extracting the flat-head machine screws which pass through the sleeve, radially outward, and screw into tapped holes in each of the inner mandrel segments. The special tool developed for this extraction is shown in use in the photograph. This photograph was taken during a test of disassembly of the 34-inch mandrel and extraction of the segments through the 3-inch hub holes of a simulated tire built by lay up of rubberized fabric. After the sleeve is freed by extraction of the radial screws, it may be removed by sliding it out axially. The keystone segment is then freed by loosening its toggle clamps and extracted. Thereafter, the remaining segments are unclamped and handed out through the opposite hub holes. Small hands are required for disassembly of the 34-inch mandrel with its 3-inch hub hole.

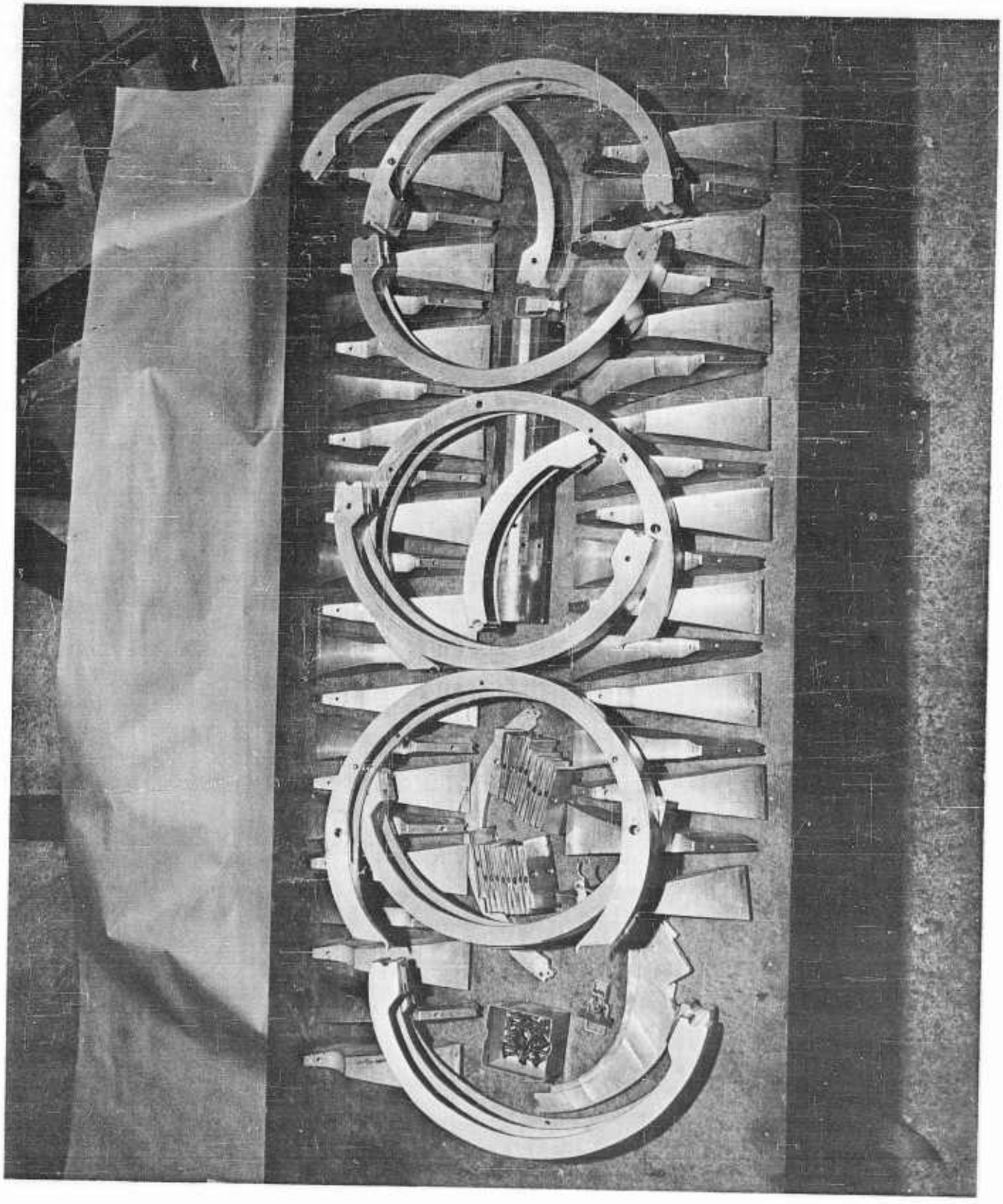

Photo No. 21 - 46 - Mandrel Components

MANDREL COMPONENTS

This shows a lay-out of part of the components of the 34-inch mandrel. The axial sleeve is underneath at right center. The inner segments which bolt to the axial sleeve are the tapered pieces on the bottom. The larger pieces on top span across the tread area of the tire between the inner segments. The parallel-sided, keystone segment is shown adjacent to the box of inner-segment screws at the left.

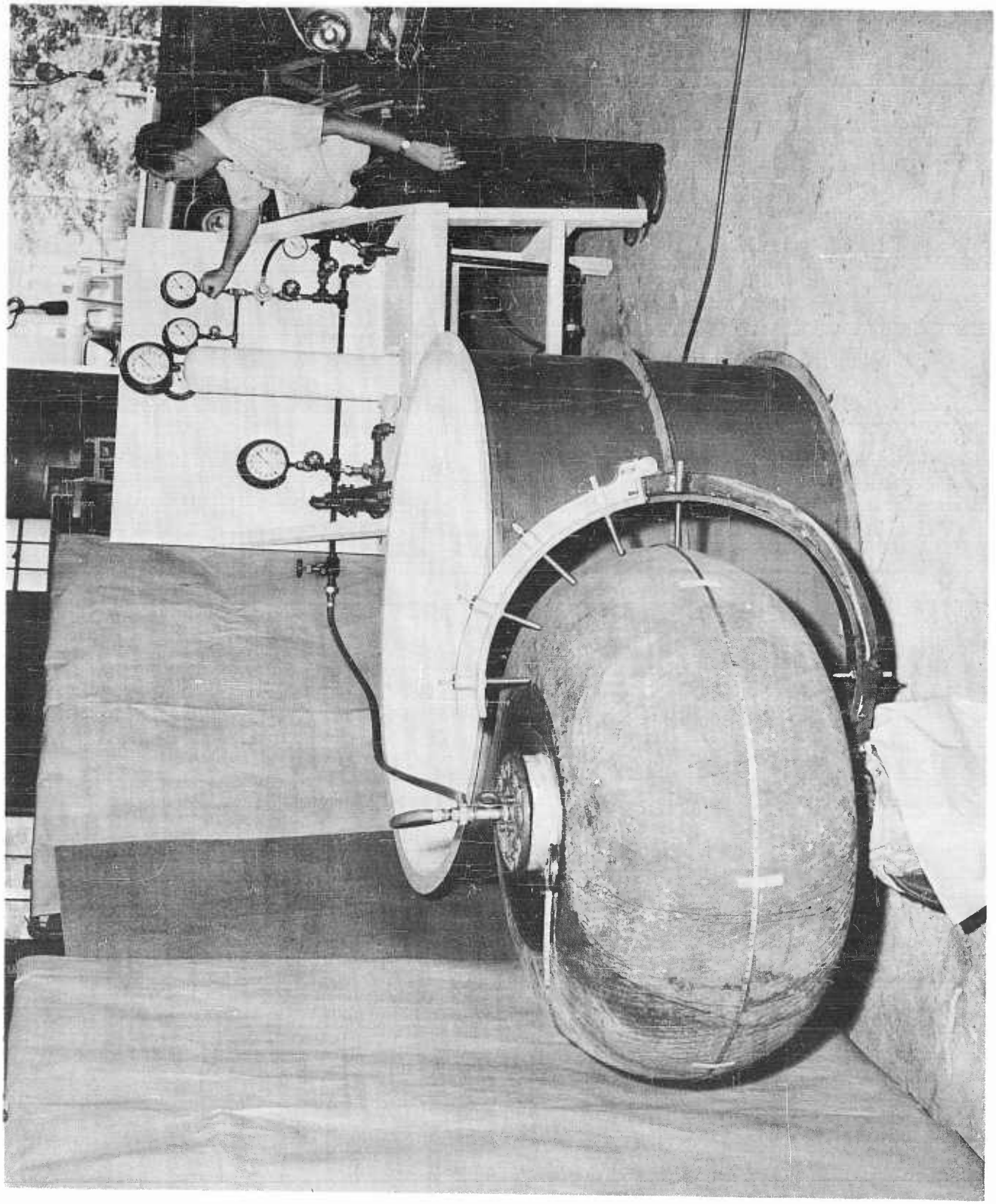

Photo No. 22 - 48 - Pressure Test Apparatus

PRESSURE TEST APPARATUS

This view shows the developed apparatus for conducting pressure tests. In the background are the gauges, the manually operated water pump, and the receiver tank which provides precise control of water pressure. When testing for the bursting pressure of a tire, it is inflated with water under water, thus eliminating probability of serious accident which might occur if a tire were to explode while inflated with air and also relieving the test tire from carrying the weight of the inclosed water as would be the case if the test tire were inflated with water in air. During burst tests, the tire is first filled with water and pressurized up to the pressure of the service main. The pressure is then gradually increased by alternately pumping up the receiver tank and bleeding it down into the tire, thus avoiding subjecting the test tire to the transient peak pressures developed with each stroke of the pump and permitting an accurate reading of the pressure at the instant of bursting. The gauge for reading water pressure is mounted on the top of the receiver tank. When inflating with air the water system is isolated by closing the valve with inclined stem at the right front edge of the stand. Air is then admitted to the tire through the pressure regulator shown just below the right hand of the technician. Note also the valve just below the regulator which isolates the air gauges when inflating a tire with water. Three air gauges are provided, each with its isolating valve. This arrangement permits a more accurate reading of pressure below 10 pounds per square inch than is possible if only one gauge with reading of 0 to 100 pounds were provided.

In the foreground is shown the apparatus used for measuring the cross-sectional change of shape of test tires with change of inflation pressure. The pointed rods with tips shown bearing against the tire are screwed outward just before each increase in pressure and then, when the desired pressure has been reached and is being maintained constant by the regulator (to overcome any loss by seepage through the temporary seal at the cast aluminum hub), the pointers are screwed into grazing contact and the distance between the tire surface and the rod support bracket is measured by reading calibrations on the rods. The tank in the center is used for submerging the tire while conducting a burst test.

DEVELOPMENT OF PRESENT TECHNIQUES FOR BUILDING TIRES OF CONTINUOUSLY-WOUND CORD

Eight experimental, high-flotation tires were fabricated prior to 1 May 1958, all by the continuous-cord process. The first four were defective in one respect or another and all had many leaks. The last four were considered successful in that they held air, were symmetrical when inflated and had been inflated to a higher pressure than intended in service. Further testing was required, of course, to prove service life and other requisite characteristics.

All eight were wound by the same basic process but with additions to the original machinery and techniques, the equipment being added to after each tire was built in order to solve problems which had caused difficulty with earlier experiments.

The first seven tires were wound of conventional tire cord from cones containing a variable and indeterminate number of knots. These knots were usually in only one strand of the cabled cord and thus, by custom of the industry, the cord was labeled "knotless" by the supplier. After special effort, the supplier eventually was persuaded to use techniques in cord processing which produced cones of truly knotless cord. This cord was used for tire No. 8. The lesson learned was that, when dealing with unfamiliar technical jargon, one must remember that semantic difficulties can occur. Knots in the cord precluded its passage through the rubber extruder, which coated the cord just before placement in the tire carcass, since only a few thousandths of an inch clearance was allowable at the entrance die of the extruder. Up to one and one-half hour delay occurred when a knot was encountered, the delay being the time necessary to cool down the extruder, open up and clean out the cross-head chamber, re-thread the cord through both the entrance and exit bushings, and close and warm up the extruder.

For tires No. 5 through 7, an extruder-threading device was available. This device, specially developed, consisted of a four-foot length of 0.025 music wire with a loop of 0.006" wire soldered to a ground-down section on one end. This four-foot length of wire could be pushed through both dies in the cross-head and then a faired-down cord end could be doubled back through the loop of fine music wire and pulled through the hot rubber. With this method, only five to ten minutes delay was caused by each knot. Such a delay was satisfactory for an experimental technique but was recognized as unsuitable for production. Efforts to secure truly knotless cord were continued with eventual success, as reported above.

For tires 1 through 3, erratic rubber coating by the extruder was encountered. This difficulty had not been anticipated and it caused much trouble. Eventually, two steps were found necessary and adequate to correct the condition. First, a heating cabinet was provided between the supply cone and the rubber extruder. This step was suggested because it was known that the rubber would adhere to hot cord more readily than to cold. The other step consisted of providing supplementary spillway ports for the rubber, concentric to the exit bushing of the extruder. This step was suggested after observation of partial cure of the rubber in the extruder when it had been opened for cleanout during re-threading occasioned by knots.

Another unanticipated problem was caused by the force of 8 to 10 pounds needed to pull the cord through the extruder. The resulting tension in the cord at the winding arm caused the cord to slide along the surface of the partially wound tire, in the region of the shoulders. This sliding resulted in a bunching and generally non-symmetric cord array which became increasingly severe as more and more turns of cord were wound into place. The low shear strength of the green, uncured rubber was not sufficient to hold the cord where wound. Several steps were taken to correct this condition and related problems. The first was to provide a servo-controlled, powered capstan and "festooner"(or temporary cord-holding device) between the rubber extruder and the winding machine. This unit reduced the tension in the cord at the mandrel to a pound or so and provided synchronization between winding machine and capstan. It produced a decided improvement, but not good enough, because even at this tension the cord had a tendency to slip on the shoulders of the mandrel and produce a non-symmetric pattern.

At about this time a related problem was appreciated. The surface of the mandrel, upon which the cord is wound, is not circular in the winding plane. As a result, a cyclic variation in the speed of the cord through the fair leads at the end of the winding arm is caused. This variation in speed produced a jiggling of the lower, or floating gang pulley of the festooner at all winding speeds except dead slow. Eventually this jiggling would cause the cord to become unreeved from one or more pulleys, with a consequent jamming and probable breakage. Winding would have to be stopped and the cord re-reeved. The cure was the provision of a tensioning device consisting of a horizontally sliding pulley held by a spring of several feet of thin rubber ribbon (salvaged from a golf ball initially). In addition, all pulleys between this spring-tensioner device and the fair leads at the end of the winding arm were replaced by very light weight ones of aluminum.

While experimenting with the tensioning devices and lightweight pulleys discussed above, it was found that more symmetrical winding could be secured if a thin sheet of carcass stock rubber were placed on the partially wound tire in order to provide a winding surface tacky enough to hold the cord in place. Several successful tires were built with these supplementary sheets of rubber, but this technique was abandoned when it was learned that erratic cord coating was being caused by foreign material in the carcass stock being fed to the extruder. When consistently good cord coating was secured with clean extruder stock and when the final tensioning device was in operation, it was found that symmetrical winding could be attained without applying the extra sheets of rubber.

It had been planned originally to provide pressure for the cure of the first few dozen tires by wrapping them with nylon tape, utilizing the shrinkage of nylon at rubber curing temperatures to provide the required curing pressure. Tires 1 through 4 had a good cure from one shoulder across the tread area to the other shoulder. As might perhaps have been expected from considerations of angle and normal force, the cure was poor in the sidewall portion of the tires between the shoulder and the metal curing flange bolted to the hubs and concentric thereto. For tires 3 and 4, an attempt was made to increase the pressure in the areas between the shoulders and the hubs by placing a small aircraft tire inner tube concentric to the hubs on each side and under the last half of the turns of curing tape and inflating these tubes before placing the wrapped tire in the curing autoclave. These attempts were failures, probably because the inner tubes failed by blowout sometime during the curing cycle. Adequate pressure concentric to the hubs was achieved in tires 5 through 8 by covering the whole assembly with a sleeve of either polyvinyl alcohol or polyvinyl fluoride and sealing this sleeve at each end to a capped metal tube, caps outward, held concentric to the axis of the tire. This arrangement provided adequate pressure for good cure throughout the whole tire carcass for these last four tires and assurance of continuous pressure was attained by keeping a vacuum on the inside of the tire during the curing cycle.

Another problem incident to tire winding was recognized. There is considerable build-up of tire cord around the hub, the amount varying with the relative velocities of rotation of the winding arms and mandrel and with the angle between the two axes of rotation. During experimental tire building to date, this build-up has been corrected by varying the angle slightly between the axes of rotation, during the winding of a tire. Admittedly this solution is only temporary measure because any change in this angle results in a change in the cross-over angle at the centerline of the tread, and consequently causes a change in the structural properties of the tire. This is a problem which needs more study.

It is expected that the proper angle between the two axes will be found only after a number of tires have been wound, with the same relative velocities of rotation but with the angle varied, and the results have been studied.

Related to the problem cited above is another one brought about by the geometry of the situation. The set-out position of the hubs on the winding spindle is that point which causes the length of cord from tangency on the mandrel to tangency at the hub to be equal to the same length along the surface of the mandrel when the hub has been moved into its recess in the mandrel after completion of winding. As the winding progresses, the build-up of cord at the hub disturbs these critical relationships. In tires wound to date, this difficulty has been corrected by an arbitrary set-in of the hubs at intervals during winding, in an attempt to have all the cords in the completely wound tire at the same tension. This problem also needs an experimental solution.

In the early planning stages of the overall program, it was recognized that a successfully wound tire would require a rigid mandrel. The tires built to date have been wound upon a segmented mandrel of cast aluminum, all parts of which will pass through a 3-inch hub opening for the 34-inch tire and through a 5-inch opening for the 43-inch tire. These mandrels require several man-hours for assembly and several more for disassembly after a tire has been cured upon them. Despite the use of mold-release compounds on the mandrels, all tires to date have had a tendency to stick to the mandrels. It has been learned that inflation of the tire prior to removal of the mandrel will cause separation of the tire carcass from the mandrel segments and permit relatively easy removal of the segments through the hubs. This inflation saves a few man-hours, but use of the segmented metal mandrel is recognized as satisfactory only during the development phase. Even with inflation of the tire prior to the disassembly of the mandrel, its use is too time consuming for a production process. Development must be continued on this part of the process.

The machine built for experimental tire winding has several features not required in a production machine. For instance, there is almost complete flexibility in relative speeds of rotation of mandrel and winding arm, and the angle between the axis of rotation of the two can be varied at will from 0^{o} through 90^{o}. Thus the machine can wind any cord pattern possible to achieve with a continuous cord process on a torroidal mandrel. A simpler machine with less flexibility would be more appropriate for production. Fixed gear ratios, rather than variable-speed drives, would be one advantageous feature possible in a production machine. Before fixed gear ratios can be specified, however, the optimum cord pattern must be determined with more certainty than

at present. It is the present belief that optimum gear ratios will be known only after extensive service testing of high-flotation tires.

The high-flotation tires built to date have been fabricated of conventional tire cord and natural rubber. Because of slippage in the shoulder region of the tires during winding, there is reason to believe that winding a ribbon of several, perhaps even as many as fifty, parallel cords each of very small diameter might result in a more accurate, consistent and controllable placement of the tension-carrying material in the tire carcass; in addition, using the method may produce a lighter, more flexible tire because of reduction of percentage of rubber by weight. Resolution of these points will require extensive experimentation because the critical factors are not known and thus this problem will not respond to analysis.

Some of the recent developments in synthetic rubbers, particularly neoprene and urethane rubbers, offer promise of greater utility in high-flotation tires than natural rubber. In particular, properties such as improved abrasion resistance and indifference to attack by ozone or hydrocarbons are very promising in the urethane rubbers. Considerable experimentation will be required before urethane rubbers or other rubber-like materials can be exploited.

Winding a high-flotation tire of one continuous cord is time consuming, at best. The present experimental winding machine has separate spindles for the mandrel and winding arm, thus limiting winding to one cord. If both rotational motions were achieved with one vertical axis, it would be possible to feed in any reasonable number of cords (or ribbons of parallel cords) simultaneously in a horizontal winding plane, thus reducing the time of winding a tire by a marked degree. It is believed that production winding machines should be based upon the principle of simultaneous winding of a number of cords (or ribbons of cords).

RECAPITULATION - PROBLEM AREAS

The remaining unsolved problems suggested by the above are presented again in the form of research and development objectives as follows:

1. Detailed design and construction of a high-flotation tire winding machine capable of simultaneous winding of more than one cord or ribbon of continuous cord; such a machine should have sufficient flexibility to permit winding of all cord patterns practical for any torus-shaped high-flotation tire but not necessarily capble of an infinite variation of cord-crossing angle at the centerline of the tread; the machine should be capable of winding tires of a maximum diameter of about seven feet. Adjustment of the angle between the axis of the mandrel and major axis of rotation and adjustment of position of hubs on mandrel axis shall be possible during high-flotation tire winding without cessation of winding.

2. The investigation of all tension-carrying and impregnating materials suitable for use in building high-flotation tires with particular emphasis on feasibility, light weight, abrasion resistance, immunity to attack by atmospheric oxygen and other chemical agents likely to be encountered in service, and retention of desirable properties at both low and high temperatures. This work should begin with reconnaissance of available fibers and rubber-like materials and progress through laboratory development of processes and auxiliary apparatus needed for use by high-flotation tire winding machines. In particular, possibilities of ribbon-shaped tension carrying materials should be fully explored.

3. Conduct such analytical and experimental work as is required to determine optimum shape and cord pattern for high-flotation tires as regards supported load versus foot print area and shape, ability to roll over obstacles, and maximum deflection to decelerate the sinking speed of a landing aircraft, all toward the end of minimum weight consistent with adequate performance and service life. This work should begin with an analytical reconnaissance of available shapes including cross-sections both of intersecting and non-intersecting circles, and the production of a test lot (approximately 8) of high-flotation

tires of a cross-section of intersecting circles of at least four cord patterns. Later phases should include exploration of other possible shapes and cord patterns and will utilize the mandrels developed by the work in that problem area. Basic tire behavior data should be gathered by the existing rolling test rig. Service life and performance of these experimental high-flotation tires will be determined by the tests performed under the subject service tests.

4. Investigate all available inflatable, fusible, dissolvable, or friable materials or combinations thereof which may be adapted to use as mandrels for high-flotation tire winding with the overall objective of reduction of man-hours and costs in the production of high-flotation tires. This work should begin with reconnaissance and small-scale laboratory experimentation. Later phases should include full scale experimentation and adaptation of the most promising materials to experimental high-flotation tire building.

5. Design and produce clam-shell-type, female, tire curing molds for all sizes of high-flotation tires. These molds should incorporate provisions for changing the tread pattern and for obtaining optimum pressure and temperature during curing cycles. Emphasis should be on sound tires and simplicity of equipment with complete control of the process rather than upon automation.

6. Determine relative merits of new high-flotation tire materials and configurations by service life tests conducted by ground vehicles. Initially, several designs of the 34-inch size should be tested to develop information on:

a. the ability to encompass obstacles,

b. the ability to transmit driving and braking torque,

c. heat produced while rolling,

d. fatigue failure of tire carcass due to severe flexing,

and e. abrasion and penetration resistance.

These tests under simulated service conditions will supplement but not duplicate the static and rolling tests conducted to determine optimum high-flotation tire configurations.

CONTINUOUSLY-WOUND-CORD TIRE DESIGN

A torroidal-shaped, inflated structure with a central hole small in relation to the overall diameter has a wide variation in the tensile stress pattern throughout the structure, especially if the pattern is interrupted by restraint as at the bead area of a tire. If the structure is stressed only by the inflation pressure and restraint at the bead, the stress pattern is essentially symmetrical about the major axis of symmetry and on each side of the plane of the centerline of the tread, but the intensity of the maximum stress varies greatly from the centerline of the tread toward the bead. For an inflated but unloaded tire of small bead diameter relative to the overall diameter and which inflates to essentially circular cross sections on both sides of the major axis, there is much evidence pointing toward maximum and minimum stress in the ratio of three to two at the centerline of the tread. At any point on this centerline, the minimum stress lies in the plane of the centerline of the tread (circumferential) and the maximum stress (radial) is perpendicular to it lying in a plane which contains the major axis. Moving toward the bead in a plane containing the major axis, the circumferential stress, which is perpendicular to the plane of the section, remains about constant but the radial stress increases. A perfectly balanced tire design should take account of this variation in the stress pattern and place the tension-carrying material in the density and direction which achieves equal stressing throughout the structure. Such ideal conditions are, of course, impossible to achieve with restraint at the bead, but a minimum weight structure will be the closest practical approximation. Placement of the tension carrying materials, the cords, in a properly-designed, continuously-wound tire can achieve this approximation to a remarkable degree.

Analytical determination of the stress at any particular point on a continuous-cord tire is very difficult, probably impossible at reasonable cost, when the structure is inflated and deformed by loading through the bead as is normal for tires when in use. Therefore, empirical methods have been used in the past for design of conventional tires and probably should be used for continuously-wound-cord tires. The development of the experience data upon which empirical design should be based will require the fabrication and testing (under service conditions) of a large number of tires because there are a number of variables which should be explored. Cord size, tire cross-section shape, quantity, type and placement of impregnating rubber, the shape of the curved portions of the cord paths in the tread area of the tire, and tread requirements are probably the most important of these variables. These factors are probably interrelated but the relationships are not known since experience gained with conventional tires is not directly applicable in most cases.

At the centerline of the tread, symmetry permits approximate analysis of the stress pattern for the inflated but unloaded tire. Let us assume the cross-section through the major axis is represented by two tangent circles. Let the radius of the centerline of the tread be R. Then the radius of the shoulder of the tire (the widest portion) about the major axis is $\frac{R}{2}$. For a given inflation pressure Δp, the total load across the centerline of the tread imposed by this pressure equals $\Delta p \pi R^2$ minus $\Delta p \pi \left(\frac{R}{2}\right)^2$. The circumference equals $2\pi R$. Dividing the total load by the distance along which it is applied, we get the load per unit length, the stress. This reduces to $3/8 \Delta p R$. It is the maximum stress (radial) at any point on the centerline of the tread for the inflated but unloaded tire.

The minimum stress (circumferential) at all points on the centerline of the tread is perpendicular to the planes passing through the major axis. The total load on any sections taken through the major axis resulting from the inflation pressure Δp is equal to $\frac{\Delta p \pi R^2}{2}$. The distance along which this load is applied equals $2\pi R$. Therefore the stress or load per unit length equals $\frac{\Delta p R}{4}$. (This analysis is not so rigorous as the analysis of the radial stress because symmetry does not necessarily require a uniform loading along the cross-section).

Assuming that the circumferential tension does equal $\frac{\Delta p R}{4}$, let us now determine the cord-crossing angle at the centerline of the tread which will produce a balanced design.

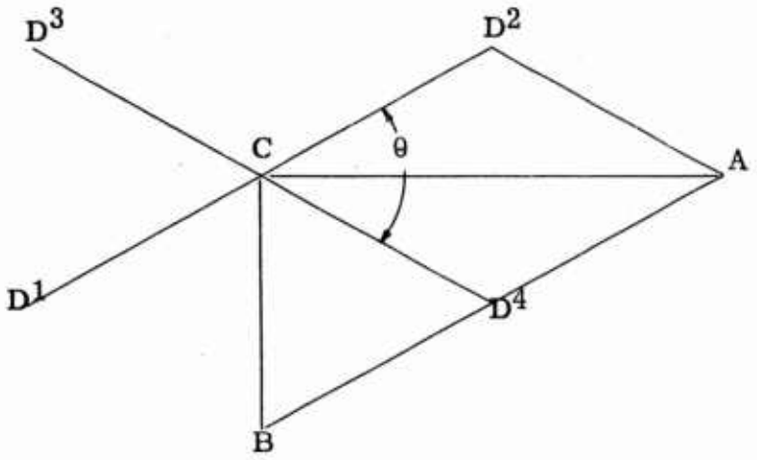

In the foregoing diagram let the line C B represent a portion of the centerline of the tread. Let D^1 - D^2 and D^3 D^4 represent two cords which cross at C. Let the angle D^2 C D^4 be known as the cord crossing angle Θ. Let T = tension in any one cord at C.

Then $2\,T \cos \frac{\theta}{2}$ = Stress in direction C A (radial)

and $2\,T \sin \frac{\theta}{2}$ = Stress in direction C B (circumferential)

If Radial Stress at C = three halves the circumferential stress at the same point,

then: $\cos \frac{\theta}{2} = 3/2 \sin \frac{\theta}{2}$

$$\tan \frac{\theta}{2} = 0.667$$

$$\frac{\theta}{2} = 33.7^{o}$$

$$\theta = 67^{o} \text{ (approximately)}$$

It may be concluded that a cord-crossing angle, as defined above, of approximately 67^{o} would provide the optimum stress pattern for the inflated but unloaded tire at the centerline of the tread. This means that along the centerline of the tread the inflated but unloaded tire carcass is strained to the same degree in all directions so long as the cross-section is essentially circular. Thus the forces tending to separate the cord from the impregnating rubber are minimized and it is probably safe to conclude also that the heat generated by change of stress intensity as the tire rolls along is also minimized. In other words, optimum design is achieved at the centerline of the tread when the cross-over angle at this point is about 67^{o} for an inflated but unloaded tire which inflates to a circular cross section. Since such a tire in service is essentially circular in cross section every place except in the areas in contact with or near the ground, this is probably very close to the optimum cross-over angle for the center line of the tread for a tire in service despite the disturbance to the stress pattern brought about by the restraint at the bead and the deformation caused by contact with the ground.

Because of the uncertainty of the theoretical distribution of the circumferential stress between the centerline of the tread and the

bead, with the inflated but unloaded tire, the foregoing analysis was not deemed adequate for the design of the tires to be used in flight tests of the venting-hub rough field landing gear system. Since available funding permitted the building and testing of only a very limited number of tires, it was decided to check this theory by building tires of three different designs and determine their inflated shape by direct measurements. It was considered that the design which inflated most nearly to circular cross sections and which would change shape most nearly symmetrically with increasing inflation pressure, would be selected as the most nearly balanced design and subjected to further tests for load-carrying ability, etc. before being mounted on the flying test-bed aircraft. Accordingly, tires with cross-over angles of 90^{o}, 60^{o}, and a combination of one-half 90^{o} and one-half 60^{o} were built. This latter design was selected as being equivalent to a design with a cross-over angle of 75^{o} with the further possible advantage of checking the affect, if any, of multiple cord directions, this latter being a moot question.

The three tires were then inflated to pressures of 5, 15, 30, 40 and 50 pounds per square inch and the cross-section shape measured and plotted full scale for each inflation pressure. The 90^{o} cross-over angle design appeared to "grow" more rapidly between the shoulders than in overall diameter as if the tire had more restraint than necessary to stress in the circumferential direction at the centerline of the tread. The 60^{o} tire appeared to "grow" with increasing inflation pressure slightly more in overall diameter than in width, but in general the inflated shape was more nearly circular than either of the other tire designs. The combination design appeared to "grow" more in width than in diameter, similarly to the 90^{o} design but to less extent. The 60^{o} design was selected for further testing because this design most nearly met the test objectives and because this design has less "wrap-around" of the hub and thus a tire built to it would have slightly less weight than for either of the others. In addition, the slight departure from a circular cross-section exhibited by the 60^{o} design in favor of slightly increased overall diameter appeared to be advantageous in that it provided a small amount of additional deflection, (or increased rolling radius) in the tire.

In view of the limited scope of these inflation tests, it is not believed that any conclusions should be drawn concerning the validity of the assumption that the maximum stress is 150% of the minimum stress at the centerline of the tread. The most that can be said with confidence is that the results of these tests are consistent with this assumption.

A continuous-cord tire designed with cross-over angle of about 67^{o} would, of course, not necessarily have the optimum cord pattern except at the centerline of the tread, because the bead diameter and the clearance of fair leads at the end of the winding arm as it crosses the plane of the centerline of the tread both affect the pattern of the cords over the tread area of the tire between the centerline and the point where the cord leaves or touches the surface of the mandrel during winding. Of these two variables, the bead diameter is usually established by considerations of axle size or vent port area requirements so that only the clearance of the winding-arm fair lead remains as a factor which may be varied in a program of empirical determination of optimum design, so long as the mandrel cross-section is based on two tangent circles.

The basic cross-sectional shape of the tire may also be varied, of course. If this cross-section is based on two intersecting circles, less distortion in the shape is needed to cause the carcass to conform to the ground when in contact; thus there may be less disturbance to the stress pattern in the portions of the tire not in contact with the ground. If this is true, this shape should have less reversal or change in stress while rolling and consequently less production of heat with a resulting increase in service life.

If the optimum cord-crossing angles, between the centerline of the tread and the circle where the cord leaves or returns to the surface of the mandrel during winding, cannot be attained with mandrels based on circular cross-sections, there are possibilities that elliptical or spiral cross-sections may achieve the desired results. Tires wound on such mandrels should probably be cured to a circular cross-section to avoid residual stress in the impregnating rubber, and thus experiments with non-circular mandrels should be conducted only after techniques of curing in conventional female molds are worked out.

There remains possibilities of restraining the contour of the tire in a manner which causes the inflated cross-section to become an approximation of a cylinder with segments of circles connecting the ends of the cylinder to the hubs. This cross-section can be wound by the same method employed for tires of intersecting or tangent circle cross-sections and in addition may have the advantage of even less disturbance of stress pattern for a loaded, rolling tire than is the case for the cross-section of intersecting circles. If this is true, and only empirical methods can determine its validity, minimum weight and maximum service life may be possessed by this design. The central portions of the tread area of such a tire would be reinforced with cords wound parallel to the plane of the centerline of the tread. These reinforcing cords would serve to restrain the inflated contour of the tread area of the tire to the desired cylindrical shape.

Minimum weight will be achieved with minimum but adequate tread. The restrained contour design may be the basic design which promotes minimum weight because the weight of the cord necessary to restrain the contour is a small percentage of the total weight of cord needed for a tire and this design may minimize tread wear (and required tread thickness) by reducing scrubbing of the rolling tire on the ground.

As regards cord, minimum diameter cord means minimum impregnating rubber, minimum tire weight and minimum thickness. Practical considerations set the minimum cord diameter if single cords are wound, but if a ribbon of parallel cords is wound, each cord may be very small in diameter without occassioning an unpractically large number of total winding turns in a tire. In addition, the flat surface of a ribbon will promote adhesion of the ribbon to the turns previously wound and reduce drift of the ribbon sidewise along the shoulder of the tire during winding thus permitting greater tension in the ribbon than in a single cord. Ribbons may be wound from a spool or reel which rotates with the winding arm axle without cabling the ribbon. It should be noted also that if the winding machine is arranged so that the mandrel axle rotates about an axis passing through the center of symmetry of the mandrel and perpendicular to the winding plane, a number of ribbons (or cords) may be wound in a horizontal winding plane, simultaneously, without cabling. It is believed that production winding machines should be based on this latter concept.

For continuous-cord tires which do not require folding, it is possible that steel wire may be a more useful "cord" material than nylon or other more conventional fibers. Since there is no problem of end anchorage in the continuous-cord method, and since steel wire possesses greater tensile strength for a given diameter, thus reducing the quantity of impregnating rubber needed, and since heat is carried away more rapidly by steel than conventional cord material, reducing local build-up of temperature, possibilities of use of steel wire should be explored.

CONTINUOUS CORD T

SPECIFICATIONS -

Hi - Flo TIRE

	TIRE NUMBER	10	11	12	
	SIZE	43"	43"	43"	
	TOTAL TURNS	7750	7700	7700	77
	CORD ANGLE	90°	60°	90°	90°
Materials -					
Rubber, Inner Carcass Cover, Ga. (Schenuit = S; Carlisle = C; Gates = G)		S-#5160 .020 1 Pc	S-5160 .020 1 Pc	S-#5160 .020 1 Pc	S-# .02
Intermediate, Cover, Ga.		S-#9059 .020 1 Pc	S-#9059 .020 1 Pc	S-#9059 .020 1 Pc	S-# .02
Outer Cover, Ga. Amount		S-#9059 .020 1 Pc	S-#9059 .020 1 Pc	S-#9059 .020 1 Pc	S-# .02
Ring, Around Hub, Ga. Amount		None	None	None	.02
Tread, Amount, Ga.					
Cord Insulation		S #9059	S #9059	S #9059	S #9
Cord, Type (Nylon 420/2)		420/2	420/2	← Cord	sticks
Hubs, Type(Inner Rubber Curing Flanges Used Tin Foil Between Hub and Flange)		Regular	Regular	Regular	Regu
Pre-Heater (Incl. Sheep's Wool Base, Pole for Cone) Temp.		150°	150°	150° to Room Temp.	150° Room
De-Kinker, Wt. Units, Heavy Washer (H) = 1.25 oz. Per Pole (2 Poles per unit), Light Washer (L) = .25 oz. Per Pole		1.25	1.50	1.50	1.50
Slot Bushing (.022" Opening)		.022" ←			
Pre-Festooner - Weights (1402 Constant) +		11	11	11	15
Temperature F°		250°	250°	250°	250°
Tuber					
Die Space - Male and Female, Inches		3/8	3/16 3/8 5/16	5/16 3/16	5/16
Exit Die, Inches, Type		.035 Al.	.035 Al.&Stl.	.050 Al.	.050
Barrel Temperature, F°		150°	150°	100 - 75°	75
Head Temperature, F°		200°	200°	200°	200°
Die Temperature, F°		200°	200°	200°	200
Exhaust Opening (Varies during Run) Screw Speed (R.P.M.)		3 to 5	5 to 6½	6½	6½
Capstan (2 pulleys - Heat Lamps)		2 Lights	2 Lights Varied	2 Lights	2 Lig V ari
Festooner - Counter Wts. oz. (Constant +)		12	12	17	17
Selsyn Wts. 12 oz. Constant +		12	12	20	20
Final Tensioning Device (Approx. 3' Rubber)		Golf Ball	No Good	Model Air- ←	

1

D T F E WINDING DATA

CONTINUOUS CORD TI

APPENDIX C

	13	14	15	16	17	18	19	20	21	
"	43"	34"	43"	43"	43"	43"	43"	34"	43"	
	7700	6000	7700	7700	7700	7700	7700	4500	7700	
°	90° - 60°	60°	60°	60°	60°	60°	60°	60°	60°	
60	S-#5160	S-#5160	S-#5160	S-#5160	C-#8233 Neop	C-#8233	C-#8233	C-#8233	C-#8233	C-
1 Pc	.020 1 Pc	.020 1 Pc	.020 2 Pcs	.020 1 Pc	.040 1 Pc	.040 1 Pc	.040 1 Pc.	.040 1 Pc	.040 1 Pc	.0
59	S-#9059	S-#9059	None	None	None	None	None	None	None	
1 Pc	.020 1 Pc	.020 1 Pc								
59	S-#9059	S-#9059	S-#9059	S-#9059	C-#8233	C-#8233	C-#8233	C-#8233	C-#8233	C-
1 Pc	.020 1 Pc	.020 1 Pc	.020 2 Pcs	.020 2 Pcs	.040 1 Pc	.040 1 Pc	.040 1 Pc	.040 1 Pc	.040 1 Pc	.0
	.020 1 Pc	None	.020 1 Pc	.020 1 Pc.	None	.040 1 Pc	.040 1 Pc	.040 1 Pc	.040 1 Pc	.0
		.020 8" #9059			S-#3001 .060 18" & 8"	S-#3001 .060 18" + 10"	S-#3001 .060 18"+10"	S-#3001 .060 10"	S-#3001 .060 18"+10"	S-
59	S #9059	S #9059	S #9059	S #9059 ¼ of tire used Sheet stock (Good)	C-#625	C-#625	C-#625	C-#625	C-#625	C-
ord	sticks on	spools →	420/2	420/2 Rewound ←						
r	Regular	Regular	Regular	Battelle	Regular	Regular (Try Ply'd) ←	Battelle	Regular	Battelle	Re
t. Temp.	150° to Room Temp 1.50	150° to Room Temp 1.50	150° 1.50	Room Temp .25	Room Temp .25	Room Temp .25	Room Temp .25	Room Temp .25	Room Temp No Cover .25 (1 only)	Ro No
	15 250°	19 250°	19 250°	0 250°	0 250°	0 250°	8 to 0 250°	0 to 8 250°	14 250°	
3/16	5/16 3/16	3/16	3/16	3/16	3/16"	3/16	3/16"	3/16"	3/16"	3/
l.	.050 Al.	.050 Al.	.050 Al.	.050 Al.	.050 Al.	.035 Stl.	.030 Stl.	.025 Stl. (STRIPPED @ TIMES)	.025 Stl.	.0
75°	75°	75°	75°	85°	75	90°	85	100	100	10
	200°	200°	200°	200°	200	205°	210	200	200	2
	200°	200°	200°	200°	200	190°	180	170	170	17
	6½	6½	6½	6½	6½	6½ (Replaced)	6½	6 3/8	6 3/8	
ts	2 Lights Varied	Varied	Varied	2 Lights	2 Lights	2 Lights	2 Lights	2 Lights	2 Lights	2
	17 20	17 20	17 20	12 12	12 to 6 12 to 6	6 0	6 0	6 0	6 0	
Air-	←									

DATA

CONTINUOUS CORD TIRE WINDING DATA

APPENDIX C

	16	17	18	19	20	21	22	23	24
	43"	43"	43"	43"	34"	43"	34"	43"	34"
	7700	7700	7700	7700	4500	7700	4500	7700	4500
	60°	60°	60°	60°	60°	60°	60°	60°	60°
Pcs	S-#5160 .020 1 Pc None	C-#8233 N_o P .040 1 Pc None	C-#8233 .040 1 Pc None	C-#8233 .040 1 Pc. None	C-#8233 .040 1 Pc None	C-#8233 .040 1 Pc None	C-#8233 .040 1 Pc None	C-#8233 .040 1 Pc None (Patches)	G-E-6 Neop. .020 1 Pc None
Pcs Pc	S-#9059 .020 2 Pcs .020 1 Pc.	C-#8233 .040 1 Pc None	C-#8233 .040 1 Pc	C-#8233 .040 1 Pc	C-#8233 .040 1 Pc	C-#8233 .040 1 Pc	C-#8233 .040 1 Pc	S-#5160 .020 2 Pcs .020 1 Pc	G-E-6 .020 2 Pcs. G-E-6 .020 1 Pc.
	S #9059 ¼ of tire used Sheet stock (Good)	S-#3001 .060 18" & 8" C-#625	S-#3001 .060 18" + 10" C-#625	S-#3001 .060 18"+10" C-#625	S-#3001 .060 10" C-#625	S-#3001 .060 18"+10" C-#625	S-#3001 .060 10" C-#625	S-#3001 .060 18"+10" C-#625	G-E-7 Neop. .050 10"+8" C-#625
	420/2 Rewound Battelle	Regular	Regular (Try Ply'd)	Battelle	Regular	Battelle	Regular	Battelle	420/2 Rewound Regular (Try-Ply'd)
	Room Temp .25	Room Temp .25	Room Temp .25	Room Temp .25	Room Temp .25	Room Temp No Cover .25 (1 only)	Room Temp No Cover .25	Room Temp No Cover .25	Room Temp No Cover .25
	0 250°	0 250°	0 250°	8 to 0 250°	0 to 8 250°	14 250°	14 250°	14 250° (New Male Die)	.022" 14 250°
	3/16	3/16"	3/16	3/16"	3/16"	3/16"	3/16"	5/16"-3/16"	3/16"
l.	.050 Al.	.050 Al.	.035 Stl.	.030 Stl.	.025 Stl. (STRIPPED @ Times)	.025 Stl.	.025 Stl.	.025 Stl. (CH4 @ 6800 h .030)	.030 Stl.
	85	75	80°	85	100	100	100 to 85	85	85
	200°	200	205°	210	200	200	200	200	200
	200°	200	190°	180	170	170	170-190	180	180-190
	6½	6½	6½ (Replaced)	6½	6 3/8	6 3/8	6½	6½	6½
	2 Lights	2 Lights	2 Lights	2 Lights	2 Lights	2 Lights	2 Lights	2 Lights	2 Lights
	12 12	12 to 6 12 to 6	6 0	6 0	6 0	6 0	6 0	6 0	6 → 0 0

	Rubber	3 Strands	pl
Winding Arm - R.P.M. Average *	9 to 25	25	
Setting From Mark	42¼"	33 11/16"	42
From Mandrel	3/8"	3/8"	3
Worm Gear Ratio	30 - 1 ←		
Speed Variator Setting	12.6	5.0	12
Hubs, Bolts - Length	7¼	7¼	
Setting at Start From Mandrel	5 5/8	5 5/8	5
Amount Turned in @ 1/4, 1/2 & 3/4 Mark	1/8"	1/8"	1/
Pulling In Hubs	Manual	Hydro-Jack	Ja
Type Curing Flanges	Schenuit 1 use only	Schenuit 1 use only	Sc 1
Wrapping			
Number of Tape Turns	260	265	
Overlap	50%	50%	
Curing			
Type - Curing Bag	R-20 ←		
- Thermocouples	#1	#1	#
- Vacuum Test	O.K.	O.K.	O.
Actual Cure	Good	Bag Broke Replaced	Fa
Average Vacuum	26	15	1
Finished Tire			
Description	O.K. Thin Around S/W.	O.K. Thin	O. Th
Weight - Pounds	Never Weighed ←		

* Each Turn on 43" = 10' Approx.
Each Turn on 24" = 8' Approx.

4

rands	plane 1/8" wide								
	20	25	30	25	25	30	30	30	30
1/16"	42~~t~~	42~~t~~ & 33 11/16"	33 11/16"	33 11/16"	33 11/16"	33 11/16 to 34 3/16		34 3/16"	34 3/16
"	3/8"	3/8"	3 5/8"	3/8"	3/8"	3/8	3/8"	3/8"	3 5/8"
	12.6	12.6 to 5.0	5	5	5 to 5.005	5 to 5.25	5 (-.005)	5.00	5.00
	7"	7"	7"	7" 2 ea Too Long	7 (Pickl'd)	7	7	7	7
8	5 5/8	5 5/8	6"	5 5/8	5 5/8	5 5/8	5 5/8	5 5/8	6"
	1/8	1/8"	3/16"	1/8 (100 turns past 3/4 mark)	1/8	1/8"	1/8	1/8	3/16"
o-	Jack	Jack	Manual	Jack	Jack	Jack	Jack	Jack	Jack
muit e only	Schenuit 1 use only	Schenuit 1 use only	Schenuit Used again	Schemuit 1 use only	Schenuit 1 use only	Belko - Sample → Too hard & too small to fit →		Belko - Fits perfect. Can be used over - New build-up (rubber stock)	Schenuit Use Over
5	250	260	312	215	212	312	335	280	178
%	50%	50%	50%	80%	80%	80	80	80	80
Broke laced	#1 O.K. Fair	#1 O.K. Good	#1 O.K Good	#1 O.K. Good	#2 O.K. Fair	#1 O.K. Bad @ S/W Due to Flange →	#1 O.K.	#1 O.K. Good	#1 O.K. Good
5	19	22	24	22	23 (Lost During Cure Repaired)	21	19	19	24
K. in	O.K. Thin	O.K. S/W Best	O.K.	O.K. Good Tire Used On TestRig	Good Tire sent to Battelle	N/G	Fair - Leaks air on S/W	O.K. Looks Good	O.K. Good
→	Never Weighed		28½	57	49.5	Never Weighed ←		47	24.5

5

25	30	30	30	30	30	35	30	30
33 11/16"	33 11/16 to 34 3/16		34 3/16"	34 3/16	34 3/16	34 3/16"	33 11/16 - 34 3/16	33 11/16
3/8"	3/8	3/8"	3/8"	3 5/8"	3/8"	3 5/8"	3/8"	30 - 1
5 to 5.005	5 to 5.25	5 (-.005)	5.00	5.00	5.00	5→-.015	5 - .005	5.00
7 (Pickl'd)	7	7	7	7	7	7	7 2 en. 7½	7
5 5/8	5 5/8	5 5/8	5 5/8	6"	5 5/8	6"	5 5/8	6"
1/8	1/8"	1/8	1/8	3/16"	1/8"	3/16"	1/8	3/16" Inner Rubber Curing Flange Jammed 1 Side
Jack	Jack	Jack	Jack	Jack	Jack	Jack	Jack	Jack
Schenuit 1 use only	Belko - Sample → Too hard → Too small to fit →		Belko - Fits perfect, can be used over - New build-up (rubber stock)	Schenuit Use Over	Belko Re-Use. New build-up (rubber)	Schenuit Re-Use	Belko Re-Use New build-up (rubber)	Schenuit Re-Use
212	312	335	280	178	225	211	286	200
80%	80	80	80	80	80	80	80	80
								R-20
#2 O.K. Fair	#1 O.K. Bad @ S/W Due to Flange →	#1 O.K.	#1 O.K. Good	#1 O.K. Good	#1 O.K. Good	#2 O.K. Good	#2 O.K. Good	#2 O.K. Good
23	21	19	19	24	16	24	23	25
(Lost During Cure Repaired) Good Tire sent to Battelle	N/G	Fair - Leaks air on S/W	O.K. Looks Good	O.K. Good	Looks Good	Good	Good	
49.5	Never Weighed ← →		47	24.5	49.5	21.5	43	26.5

6

REFERENCES

RR 45 - A Progress Report on the Development of Landing Gear for Use by STOL Aircraft Operating From Rough Unprepared Fields --- Fairchild Aircraft, Division of Fairchild Engine and Airplane Corporation, Hagerstown, Maryland, 1 August 1957.

R245-004 I - An Analytical Study of High-Flotation Tires for Aircraft --- The Battelle Memorial Institute, Columbus, Ohio. Phase I, 26 October 1956. Phase II, 15 March 1957. Phase III, 1 April 1957.

Monthly Technical Progress Reports, numbers 1 through 26, beginning with Report No. 1 for the period 21 May through 30 June 1957, for Fairchild Aircraft and Missiles Division, Project M-245B, Contract Number DA 44-176-TC-446, to The Commanding Officer, Transportation Research and Engineering Command, Fort Eustis, Virginia.

R245-010 - Static Test, High-Flotation Tire, Fairchild Aircraft and Missiles Division, 19 February 1959.

R245-011 - Rolling Tests, High-Flotation Tire, Fairchild Aircraft and Missiles Division, 17 April 1959.

ENGINEERING REPORT NO.

R245-010

SUBJECT

STATIC TEST

HIGH-FLOTATION TIRE.

MODEL: M245-B

Fairchild Aircraft

DIVISION OF
FAIRCHILD ENGINE & AIRPLANE CORPORATION
HAGERSTOWN 10, MARYLAND

Date of Test: 10-21-58 to 12-18-58

Tested by: W. J. Sawyer
W.J. Sawyer

DATE: 19 February 1959

NO. PAGES: 34

PREPARED BY: W. J. Sawyer
W.J. Sawyer

APPROVED BY: J. N. Marsden
J.N. Marsden
Supervisor, Engineering Lab.

CHECKED BY: R R Enterline
R.R. Enterline

APPROVED: R.C. Smith
R.C. Smith
Chief, Technical Engineering

APPROVED: V. Frisby
Project: V. Frisby

REVISIONS

DATE	PAGES AFFECTED	BY	REMARKS

FA-800-69A

FAIRCHILD AIRCRAFT AND MISSILES DIVISION

Report Number R245-010

Model M-245 B

STATIC TEST - HIGH FLOTATION TIRE

CONTRACT NUMBER DA 44-177-TC-446

"The findings and recommendations contained in this report are those of the Fairchild Aircraft and Missiles Division, and do not necessarily reflect the views of the Chief of Transportation."

ADMINISTRATIVE DATA

PURPOSE:

As specifically authorized by Contract DA 44-177-TC-446, the purpose of the static testing of a high-flotation tire reported upon herein was as follows:

(a) Determination of stress distribution by measurement of strain in the tire carcass of one flight test model tire at full range of deflection from the inflated but unloaded tire to the fully bottomed condition in appropriate steps with the initial inflation pressure equivalent to the maximum touchdown pressure in service.

(b) Determination of footprint area through the full range of deflection.

(c) Determination of pressure variation through the full range of deflection.

(d) Determination of supported load versus deflection for the full range of deflection.

In addition a secondary objective was the calibration of the test rig which was subsequently to be used in rolling tests of the same tire.

MANUFACTURER:

Fairchild Aircraft and Missiles Division
Hagerstown, Maryland

MANUFACTURER'S TYPE OR MODEL NO.:

High-Flotation tire #15 rated at 1500# - 43" diameter, 60° cross-over angle of cord-winding.

DRAWINGS, SPECIFICATIONS, EXHIBITS:

Engineering Laboratory Folder No. LTM-187
Wilson, Nuttall, Raimond Drawing No. 41-9
FAMD Drawing No. TM-296

QUANTITY OF ITEMS TESTED:

One

SECURITY CLASSIFICATION:

Unclassified

ADMINISTRATIVE DATA (continued)

DATE TEST COMPLETED:

18 December 1958

TEST CONDUCTED BY:

W.J. Sawyer, FAMD Engineering Laboratory

DISPOSITION OF SPECIMEN:

Held for use in rolling tests.

ABSTRACT:

Static tests were conducted on a 43" diameter 60° cross-over high flotation tire developed by FAMD under contract DA 44-177-TC-446 with TRECOM. The tire, rated at 1500# was subjected to vertical, side, drag, and torque load tests. Oscillograph records of all test runs were made to calibrate the Wilson-Nuttall-Raimond designed dynamometer.

The vertical load phase of the tests consisted of applying a 6000# load through the axle and tire against a reaction platen at each of the initial tire pressures of $1\frac{1}{2}$, 2, 3, 4, 8, 12, 16, 20, and 24 PSI. Footprint areas with the tire depressed to 6000# vertical load and at initial tire pressures of 4, 8, 12, 16, 20, and 24 PSI were measured and recorded.

Side load tests were accomplished by holding a constant side load on the platen while vertical load at the tire was first increased to 6000# and then reduced until skidding occurred between the platen and the tire. These side load tests were run at 5% increments of a 3200# side load for each of the initial tire pressures of 2, 4, 8, 12, 16, and 20 PSI.

Drag and torque load tests were accomplished in a similar manner to the side load test. Drag load tests were done for initial tire pressures of 4, 8, 12, 16, and 20 PSI. The drag load was applied in steps of 320# with a maximum value of 2880# applied at 20 PSI initial tire pressure. Torque load tests were done for initial tire pressures of 2, 4, 8, 12, 16, and 20 PSI. Torque load was applied to the platen in increments of 4,480 inch pounds with a maximum value of 44,800 inch pounds applied at 4 PSI initial tire pressure.

Oscillograph records were forwarded to Battelle Memorial Institute, Columbus, Ohio for tabulation of the data and plotting of the curves presented in the Appendix of this report.

SUBJECT:- Static Test - High Flotation Tire.

FACTUAL DATA

DESCRIPTION OF TEST APPARATUS:

The test apparatus used in the static test of the high-flotation tire consisted of a heavy steel truck trailer type rig designed by Wilson, Nuttall, and Raimond and manufactured by Thompson Equipment Machine Co. The rig was supported at its front end by a steel tube stand and at the rear by two calibrated load cells which were mounted on a series of steel support beams. The test set-up is illustrated in photograph no. 38382 in the Appendix.

The rig consisted of an open rectangular base mounted on truck wheels, for use in rolling tests, located at the rear of the base, and a raised platform at the front or tow end suitable for mounting equipment for rolling tests. A large U- shaped yoke was mounted vertically on the longitudinal center line of the trailer which supported an air cylinder, rated at 750 PSI. This jack was used for applying vertical load. The test specimen, a 43" diameter 60° cross-over High-Flotation tire, was mounted on a rotating axle and brake assembly which had for its supporting strut a 6-component dynamometer designed by Wilson, Nuttall, Raimond, This dynamometer and tire axle acting as a strut assembly were mounted in the yoke so that the jack could apply vertical loads to the tire.

The dynamometer was of such design that all extraneous loads felt by the strut under a given loading condition would be cancelled out, and the dynamometer reading recorded for each of the 6 components would be only the loads or moments existing at the center-line of the test tire.

The wooden loading platen under the tire was supported on steel balls rolling between ground steel plates to allow free movement in the horizontal plane. Jacks mounted on the steel beams supporting the rig were attached to sides of the platen so that side, drag, and torque loads could be applied to the platen independently with the tire depressed under the vertical load. Sandpaper was glued to the platen surface to provide a high friction surface for the side, drag, and torque tests.

Tire radius and tire width changes were measured by standard laboratory deflection pick-ups (Ref. drawings TM280 and TM281). Vertical deflections were measured by helipots (Ref. drawing TM-315). Standard deflection pick-ups were monnted on the jig base and connected to the platen, for side, drag and torque tests, to measure movement of the platen under these loads. All of the deflection measuring devices, the 6 channel dynamometer, the 2 vertical load cells and hydraulic jack load cells when used, were recorded on a C.E.C. Oscillograph.

SUBJECT:- Static Test - High Flotation Tire.

FACTUAL DATA (continued)

DESCRIPTION OF TEST APPARATUS: (continued)

Stress distribution by measurement of strain in the tire carcass was not accomplished as no satisfactory method of measuring strain over a short gage length could be determined.

The vertical jack, the dynamometer and strut assembly, tire reaction platen, and deflection measuring devices are shown in photographs 38383 and 38384, and detailed in drawings TM-296 (FAMD) and Wilson, Nuttall, Raimond drawing No. 41-9.

TEST PROCEDURE:

VERTICAL LOAD TEST.

At an initial tire pressure of 4 PSI, a vertical load of 6000# was slowly applied to the tire by depressing it against the platen, and then the load was slowly removed. An oscillograph record of the load cells and dynamometer during the load application and removal was made. A pip was recorded on the oscillograph at the time at which the tire began to wrinkle under load. This procedure was repeated at 8, 12, 16, 20, 24, 3, 2, and 1½ PSI initial tire pressures. Following this test, stamp pad ink was brushed onto the tire surface and a large piece of paper was placed on the platen. A 6000# vertical load was applied depressing the tire onto the paper. Tire footprints were made in this manner at initial tire pressures of 4, 8, 12, 16, 20 and 24 PSI and 6000# vertical load. The footprint areas were measured and are presented in the data section of the appendix. A plot of vertical deflection vs vertical load for each initial tire pressure was plotted from data obtained in this phase of the test as well as a calibration curve for dynamometer vertical load.

SIDE LOAD TEST.

Side load tests were conducted by applying a sufficient vertical load to hold the platen steady while a side load was applied by separate hydraulic jacks. Holding this side load constant, the vertical load was increased to 6000# and slowly reduced until the platen skidded from under the tire. Using this procedure, oscillograph records were taken in 5% increments of a 3200# side load at 2, 4, 8, 12, 16 and 20 PSI. The point at which the skid occurred was observed visually and recorded as a blip on the oscillograph. A plot of vertical deflection vs. vertical load for each increment of side load was plotted from data obtained. Separate curves were plotted in this manner for each initial tire pressure. A calibration curve for the dynamometer side load was also plotted.

FACTUAL DATA (continued)

TEST PROCEDURE: (continued)

DRAG LOAD TESTS.

Drag load tests were done in the same manner as the side load except braking action of the tire was required for this test. This necessitated the use of a locking plate to restrain the tire from rotating when the brake installed for that purpose failed to hold. Similar curves were also plotted.

TORQUE LOAD TESTS.

Torque load tests were conducted in a like manner to those above and curves of the same type were plotted.

Comparison curves of vertical load vs side load and vertical load vs drag load at skid point were also plotted and appear in the Appendix.

RESULTS OF TEST:

The dynamometer readings were found to be consistent for given loads and the high flotation tire withstood all loading phases of the test with no measureable permanent distortion. Some wearing of the tire's surface occurred as a result of the frictional pull and twist encountered in the side, drag, and torque load phases of the test. The lack of tread-stock on this test tire is responsible for this result.

Vertical load test curves of vertical load versus vertical deflection at varying initial tire pressures indicate wrinkling of the tire at $1\frac{1}{2}$ PSI under a load as small as 750#, and very small or no wrinkling at all at 16, 20, and 24 PSI under full 6000# load.

Curves plotted from side, drag, and torque load test data show a 1.51 ratio of vertical load to side load at skid, a 1.45 ratio of vertical load to drag load at skid, and .117 pounds of vertical load per inch pound of torque at skid. Curves of vertical deflection versus vertical load plotted for side, drag, and torque loads show only a small variation of vertical deflection resulting from high and low, side, drag or torque loads. The maximum vertical deflection variation being approximately 2 inches for drag loads under 6000# vertical load and 4 PSI initial tire pressure. The general trend was for maximum variation of deflection at low initial tire pressures and then diminishing with increased tire pressures.

FACTUAL DATA (continued)

RESULTS OF TEST:(continued)

Pressure variation under 6000# vertical load ranges from almost double the initial tire pressure at 4 PSI to a negligible change at 24 PSI.

TEST DATA:

Submitted in the Appendix.

CONCLUSIONS:

The test specimen withstood a maximum of 6000# vertical load, a maximum of 2880# side load in combination with a 6000# vertical load, a maximum drag load of 2880# in combination with a 6000# vertical load, and a maximum torque of 44,800"# in combination with a 6000# vertical load. The test tire showed no signs of undue stress under repeated loading combinations at varying initial tire pressures. It is thus concluded that the test tire has load carrying capabilities well in excess of its design values.

RECOMMENDATIONS:

It is recommended that the tire be subjected to a Rolling Test program to determine dynamic stability prior to flight tests. In the opinion of the FAMD Engineering Laboratory, the tire should prove completely satisfactory for flight testing.

APPENDIX

CONTENTS OF APPENDIX

SUBJECT:- Static Test - High-Flotation Tire.

APPENDIX

LIST OF PHOTOGRAPHS:

Number	Title
38382	Test Fixture Rig
38383	Close-up of Tire & Dynamometer
38384	Close-up of Tire and Dynamometer

LOG OF TEST:

Date	
10-10-58	Received test tire.
10-31-58	Started static test runs.
11-25-58	Vertical load phase of test completed.
12-1-58	Side load phase of test completed.
12-12-58	Drag load phase of test completed.
12-18-58	Torque load phase of test completed.

STATIC TEST LABORATORY DATA SHEET

FAIRCHILD AIRCRAFT DIVISION

PAGE _____ OF _____

PROJECT: HIGH FLOTATION TIRE TEST DATE _____

MODEL: _____ CONDITION: TIRE FOOTPRINT AREAS

TEST NO. _____ TESTED BY: _____

STRESS WITNESS: _____ CUSTOMER INSPECTION: _____

	1		2		3		4	
	TIRE PRESS. NO LOAD PSI		TIRE PRESS. 6000 # VERT. LOAD PSI		AREA OF TIRE FOOTPRINT SQ. INCHES		COLUMN 2 X COLUMN 3 POUNDS	
	4		7.83		674.1		5278	
	8		10.18		532.9		5425	
	12		13.31		411.0		5470	
	16		16.98		338.9		5755	
	20		20.76		280.8		5829	
	24		24.44		240.0		5866	

FA-800-22

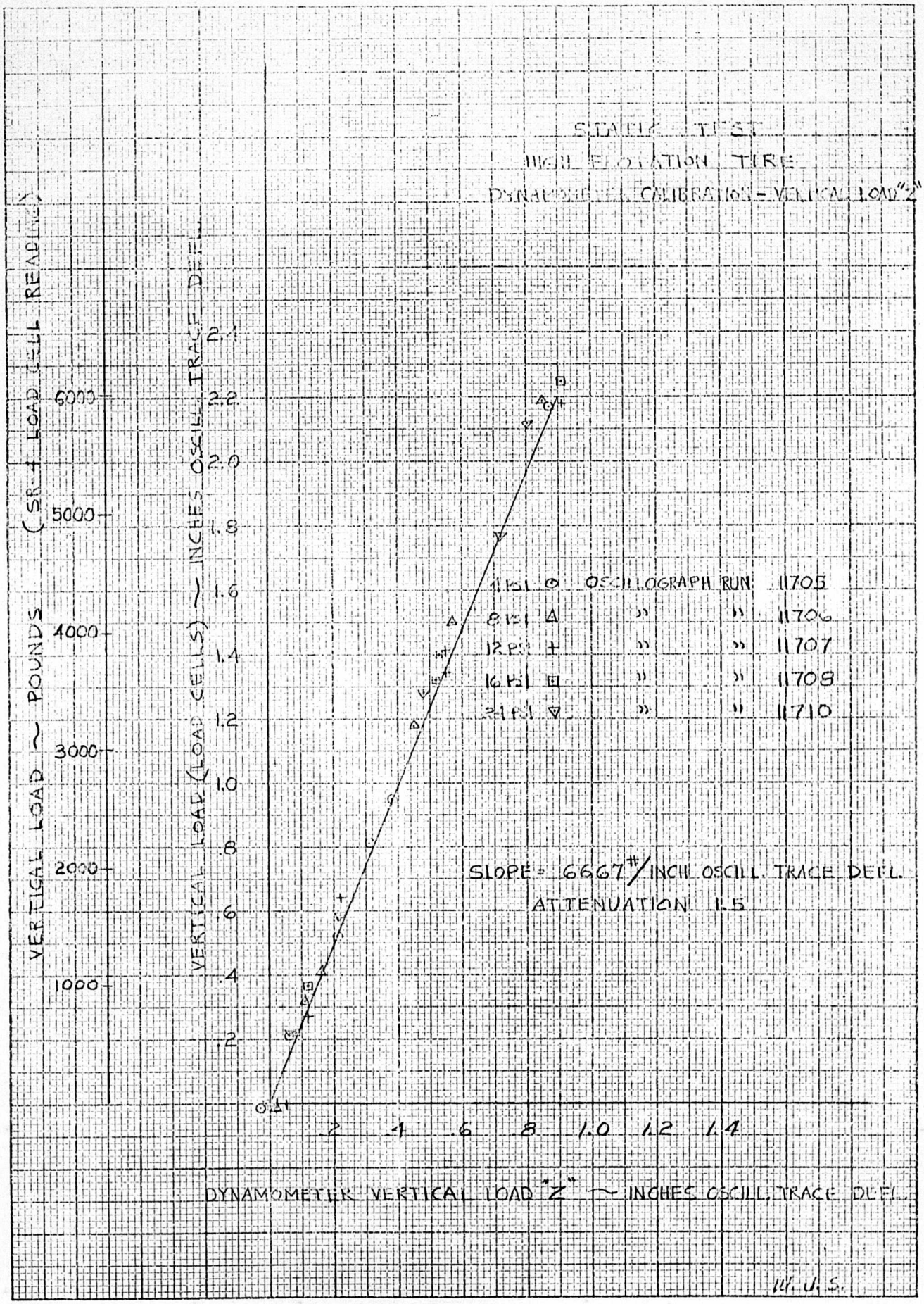
STATIC TEST
NACELLE ELEVATION TUBE
DYNAMOMETER CALIBRATION - VERTICAL LOAD "Z"
VERTICAL LOAD ~ POUNDS (SR-4 LOAD CELL READING)
VERTICAL LOAD (LOAD CELLS) ~ INCHES OSCILL. TRACE DEFL.
6000
5000
4000
3000
2000
1000
2.2
2.0
1.8
1.6
1.4
1.2
1.0
.8
.6
.4
.2
OSCILLOGRAPH RUN 1705
" " 1706
" " 1707
" " 1708
" " 1710
SLOPE = 6667#/INCH OSCILL. TRACE DEFL.
ATTENUATION 1.5
.2
.4
.6
.8
1.0
1.2
1.4
DYNAMOMETER VERTICAL LOAD "Z" ~ INCHES OSCILL. TRACE DEFL.
W. J. S.

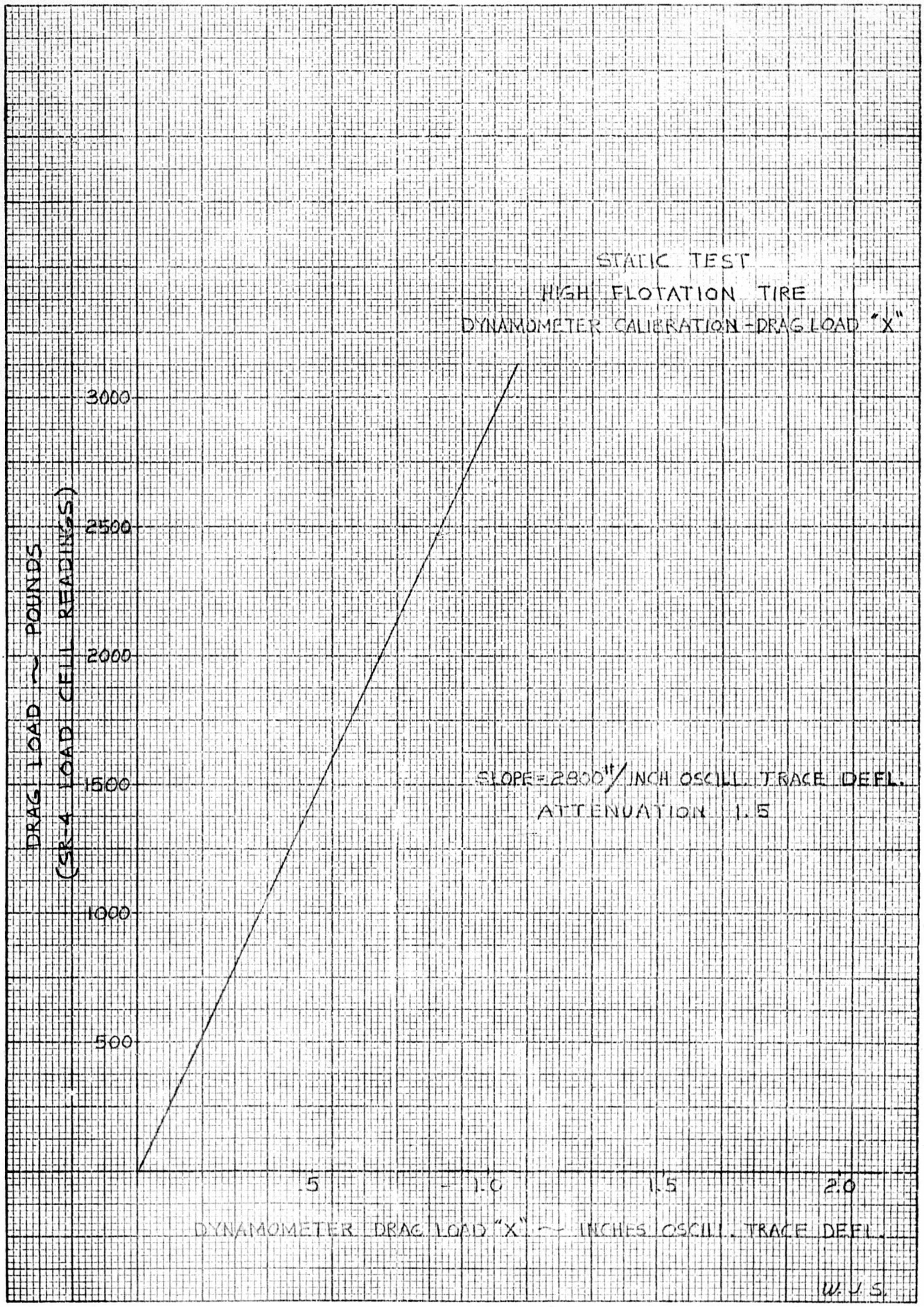
STATIC TEST
HIGH FLOTATION TIRE
DYNAMOMETER CALIBRATION - DRAG LOAD "X"
DRAG LOAD ~ POUNDS
(SR-4 LOAD CELL READINGS)
3000
2500
2000
1500
1000
500
SLOPE = 2800 #/INCH OSCILL. TRACE DEFL.
ATTENUATION 1.5
.5
1.0
1.5
2.0
DYNAMOMETER DRAG LOAD "X" ~ INCHES OSCILL. TRACE DEFL.
W. J. S.

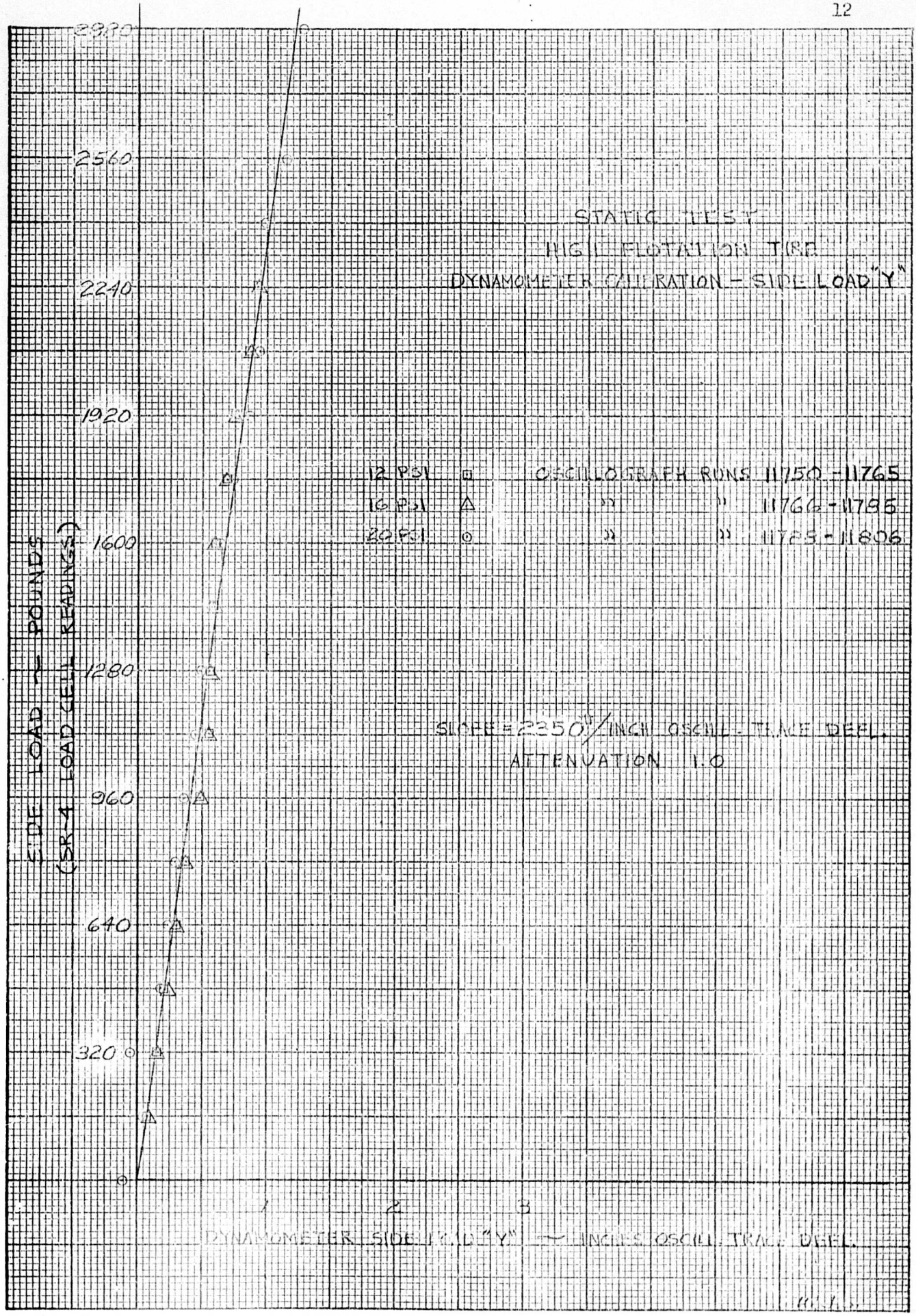
STATIC TEST
HIGH FLOTATION TIRE
DYNAMOMETER CALIBRATION – SIDE LOAD "Y"
12 PSI
16 PSI
20 PSI
OSCILLOGRAPH RUNS 11750 - 11765
" 11766 - 11795
" 11725 - 11806
SLOPE = 2250 #/INCH OSCILLOGRAPH DEFL.
ATTENUATION 1.0
SIDE LOAD – POUNDS
(SR-4 LOAD CELL READINGS)
2880
2560
2240
1920
1600
1280
960
640
320
1
2
3
DYNAMOMETER SIDE LOAD "Y" – INCHES OSCILLOGRAPH DEFL.

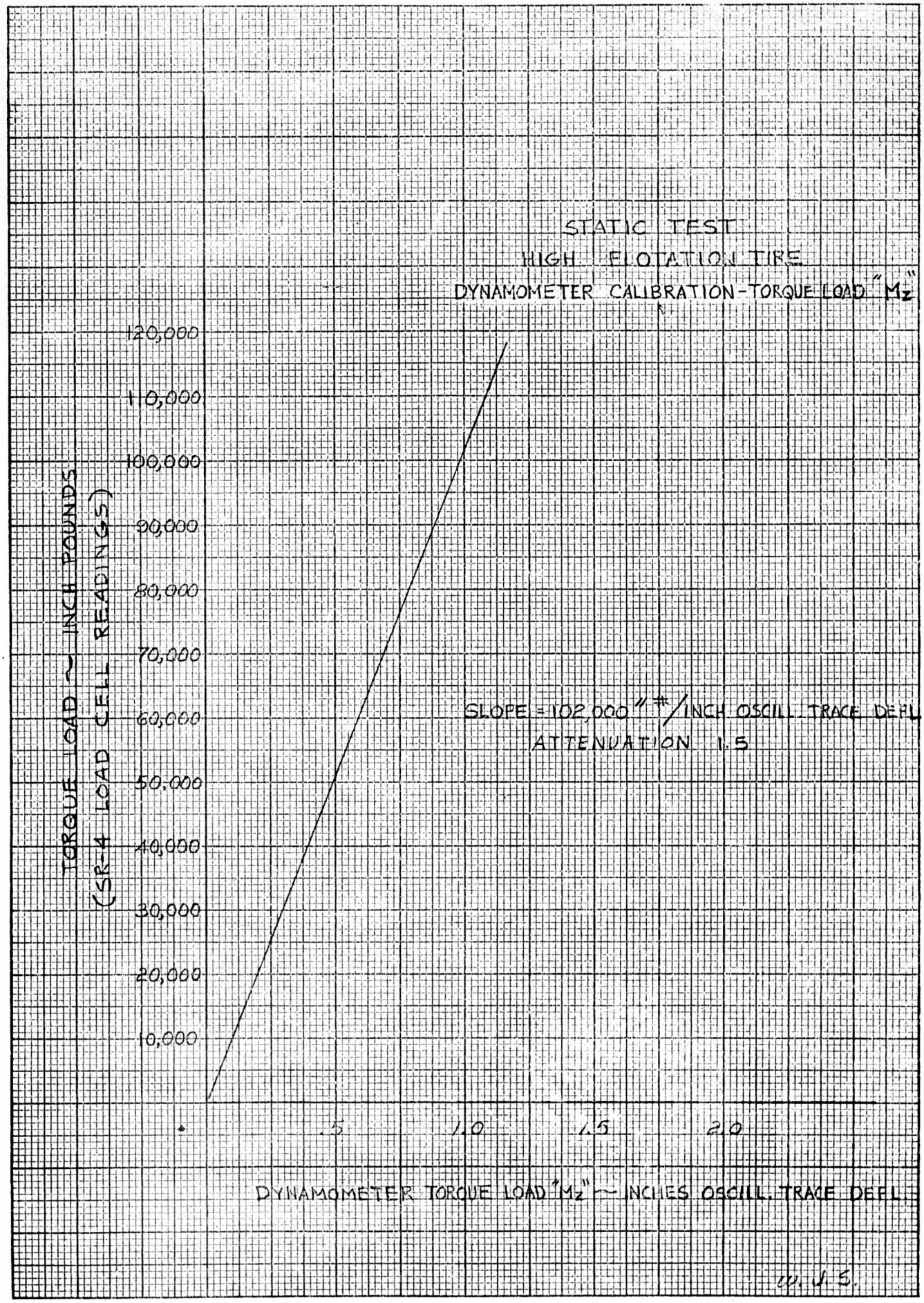
STATIC TEST
HIGH FLOTATION TIRE
DYNAMOMETER CALIBRATION - TORQUE LOAD "Mz"
TORQUE LOAD ~ INCH POUNDS
(SR-4 LOAD CELL READINGS)
120,000
110,000
100,000
90,000
80,000
70,000
60,000
50,000
40,000
30,000
20,000
10,000
SLOPE = 102,000 "#/INCH OSCILL. TRACE DEFL.
ATTENUATION 1.5
.5
1.0
1.5
2.0
DYNAMOMETER TORQUE LOAD "Mz" ~ INCHES OSCILL. TRACE DEFL.
W. J. S.

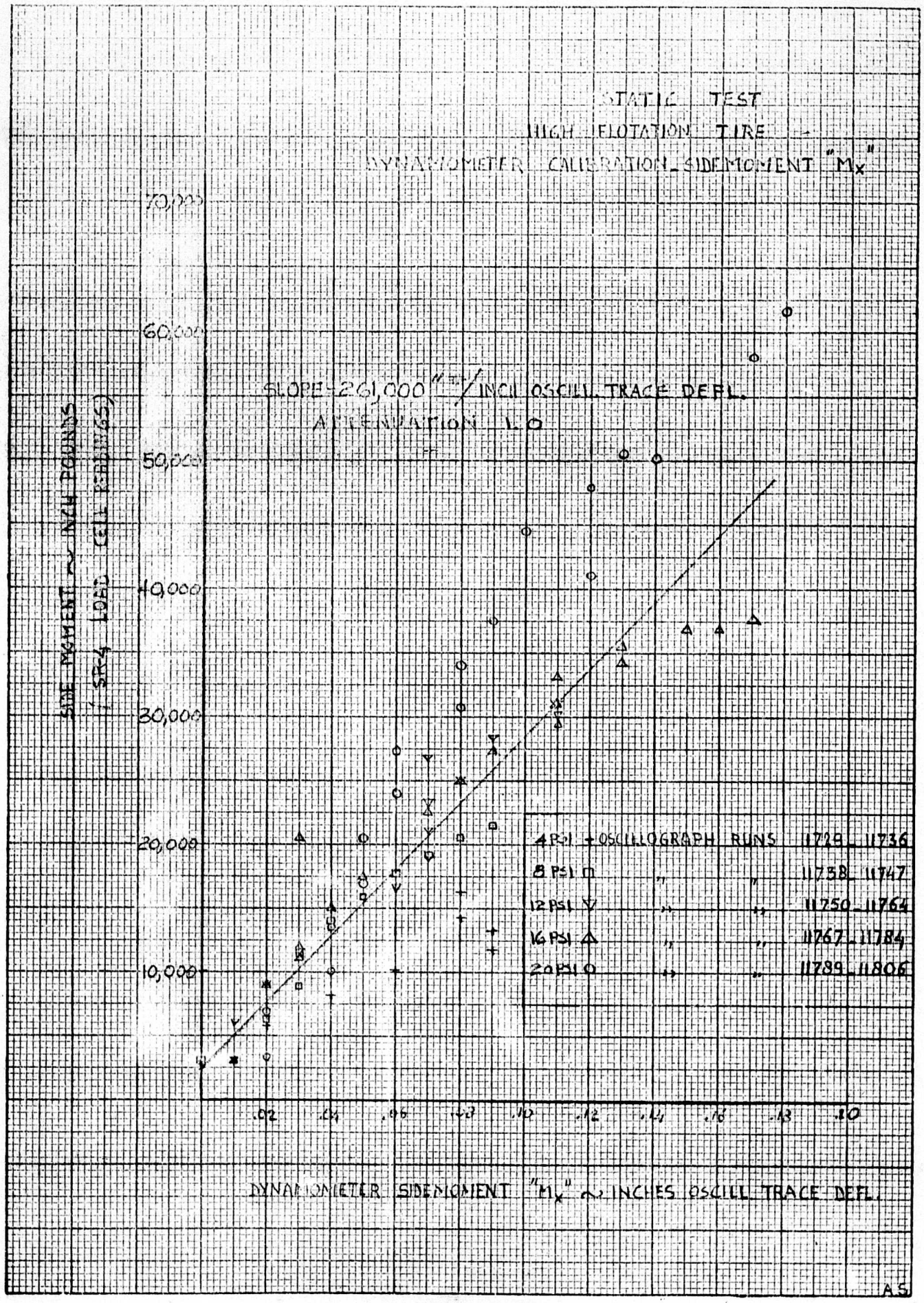
STATIC TEST
HIGH FLOTATION TIRE
DYNAMOMETER CALIBRATION - SIDEMOMENT "Mx"
SLOPE = 261,000 "-#"/INCH OSCILL TRACE DEFL.
ATTENUATION 1.0
SIDE MOMENT ~ INCH POUNDS
("SR4 LOAD CELL READINGS)
70,000
60,000
50,000
40,000
30,000
20,000
10,000
4 PSI + OSCILLOGRAPH RUNS 11729 - 11736
8 PSI □ " " 11738 - 11747
12 PSI ▽ " " 11750 - 11764
16 PSI △ " " 11767 - 11784
20 PSI ○ " " 11789 - 11806
.02
.04
.06
.08
.10
.12
.14
.16
.18
.20
DYNAMOMETER SIDEMOMENT "Mx" ~ INCHES OSCILL TRACE DEFL.
A.S.

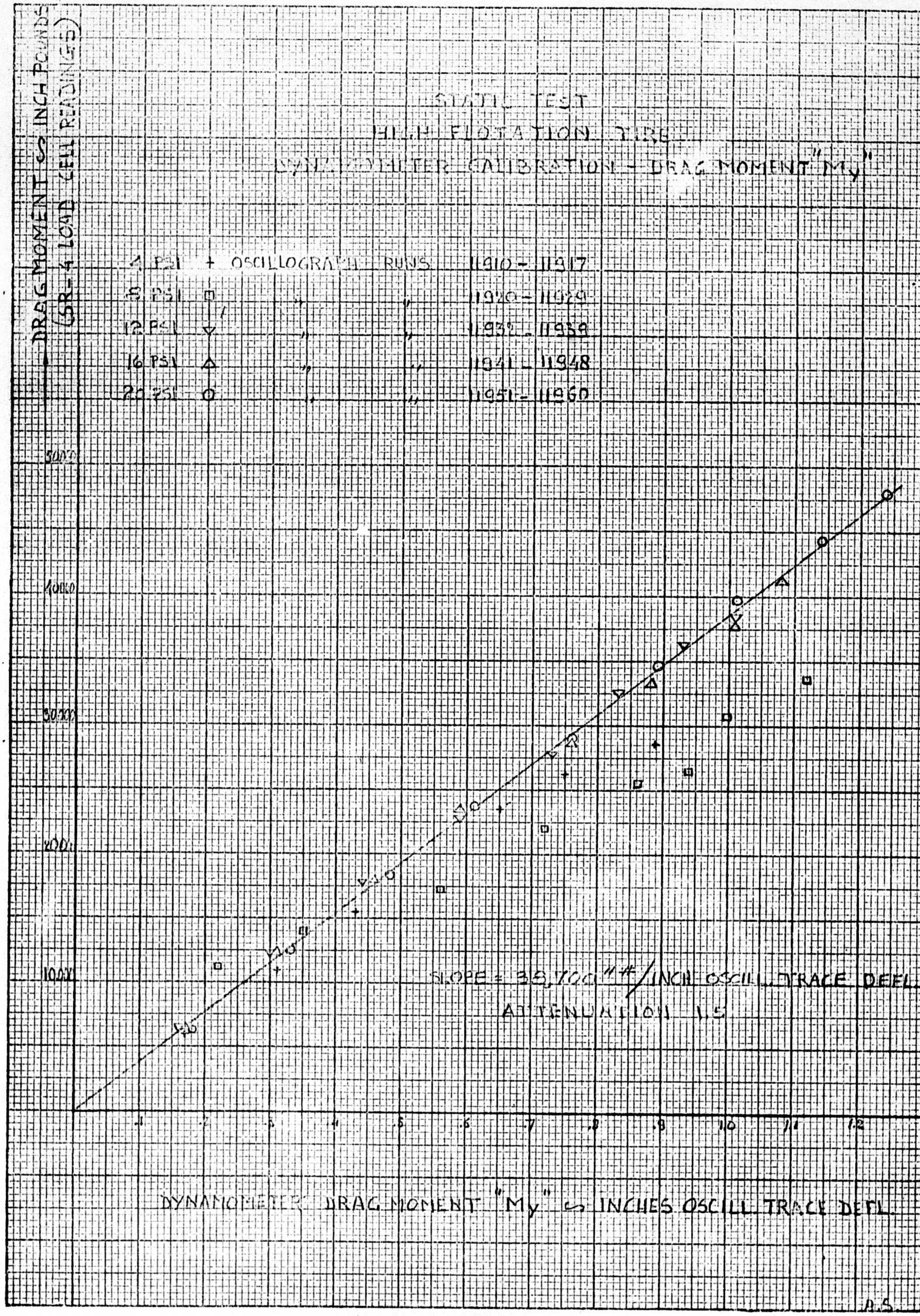
STATIC TEST
HIGH FLOTATION TIRE
DYNAMOMETER CALIBRATION - DRAG MOMENT "My"
4 PSI + OSCILLOGRAPH RUNS 11910 - 11917
8 PSI □ " " 11920 - 11929
12 PSI ▽ " " 11932 - 11939
16 PSI △ " " 11941 - 11948
20 PSI ○ " " 11951 - 11960
DRAG MOMENT ~ INCH POUNDS
(SR-4 LOAD CELL READINGS)
SLOPE = 38,700 "#/INCH OSCILL TRACE DEFL
ATTENUATION 1.5
DYNAMOMETER DRAG MOMENT "My" ~ INCHES OSCILL TRACE DEFL.
D.S.

REPORT NO.	FAIRCHILD AIRCRAFT DIVISION OF FAIRCHILD ENGINE & AIRPLANE CORPORATION		PAGES	PAGE
MODEL	PREPARED BY	CHECKED BY	APPROVED BY	

SUBJECT:- _____

DATE _____

REVISED _____

FA-800-23A

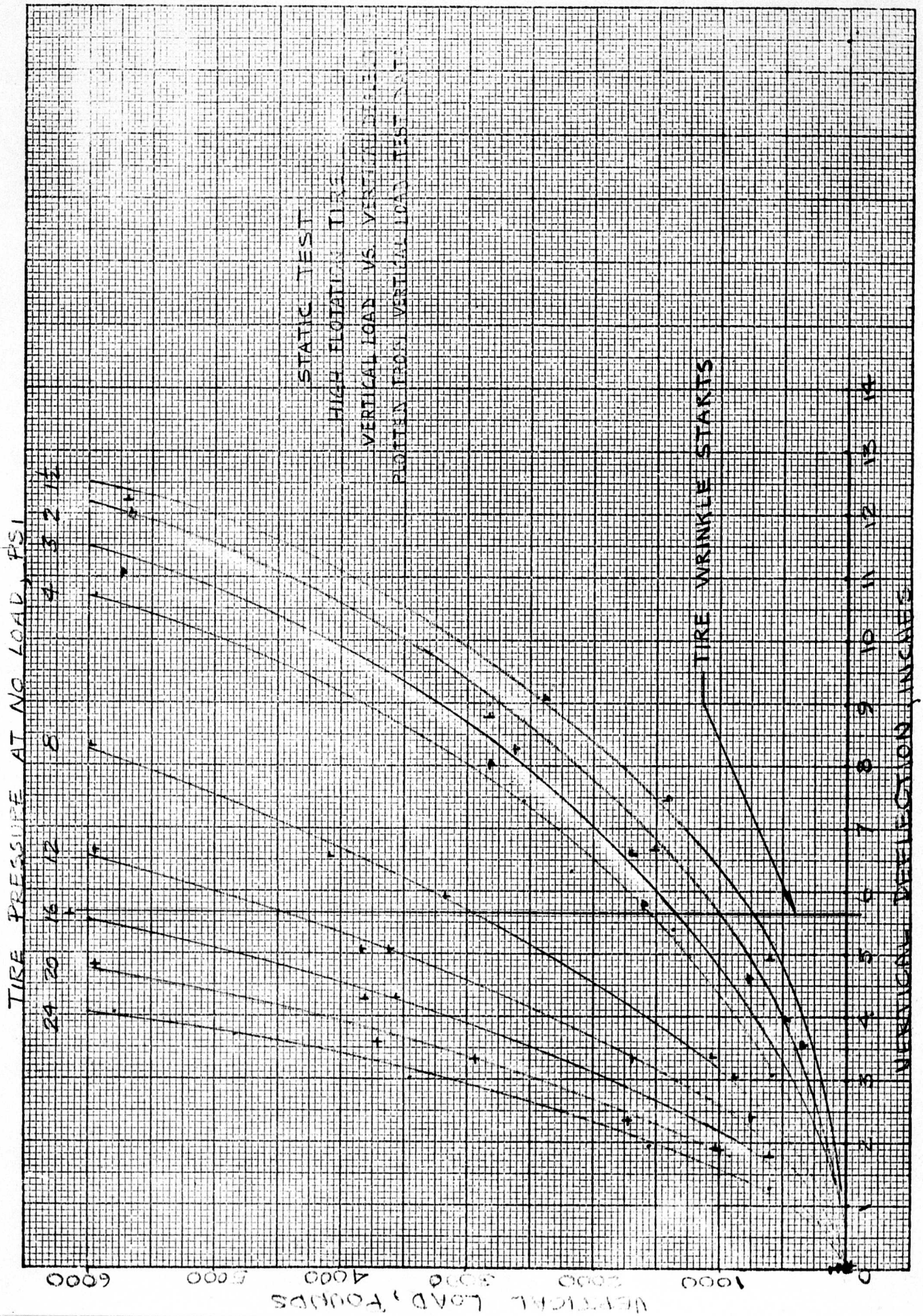
STATIC TEST
HIGH FLOTATION TIRE
VERTICAL LOAD VS VERTICAL DEFLECTION
PLOTTED FROM VERTICAL LOAD TEST
TIRE PRESSURE AT NO LOAD, PSI
TIRE WRINKLE STARTS
VERTICAL DEFLECTION, INCHES
VERTICAL LOAD, POUNDS
0
1000
2000
3000
4000
5000
6000
1
2
3
4
5
6
7
8
9
10
11
12
13
14
4
6
8
10
12
16
20
24

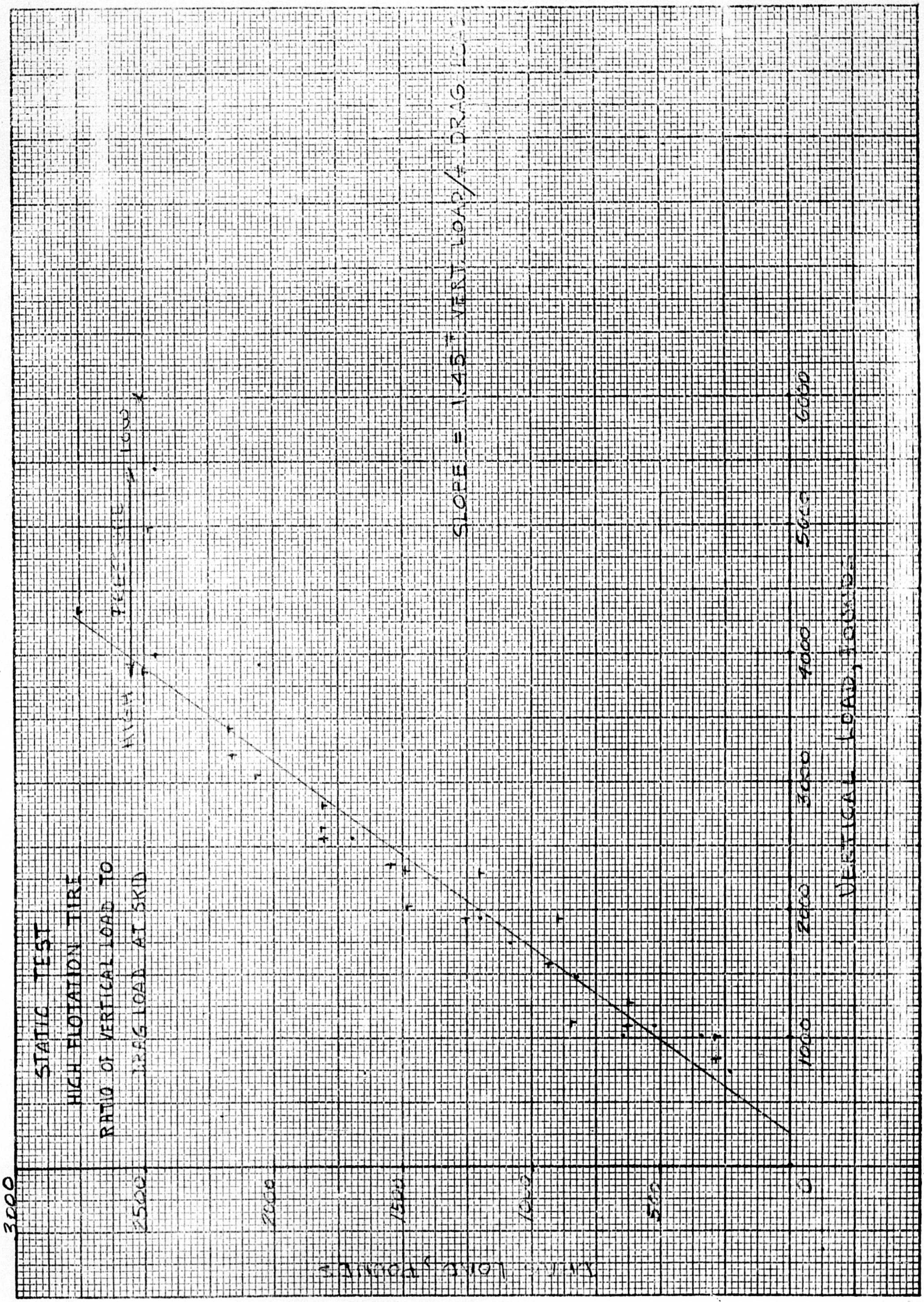
STATIC TEST
HIGH FLOTATION TIRE
RATIO OF VERTICAL LOAD TO
DRAG LOAD AT SKID
SLOPE = 1.45# VERT LOAD/# DRAG
HIGH
LOW
VERTICAL LOAD, POUNDS
0
1000
2000
3000
4000
5000
6000
500
1000
1500
2000
2500
3000

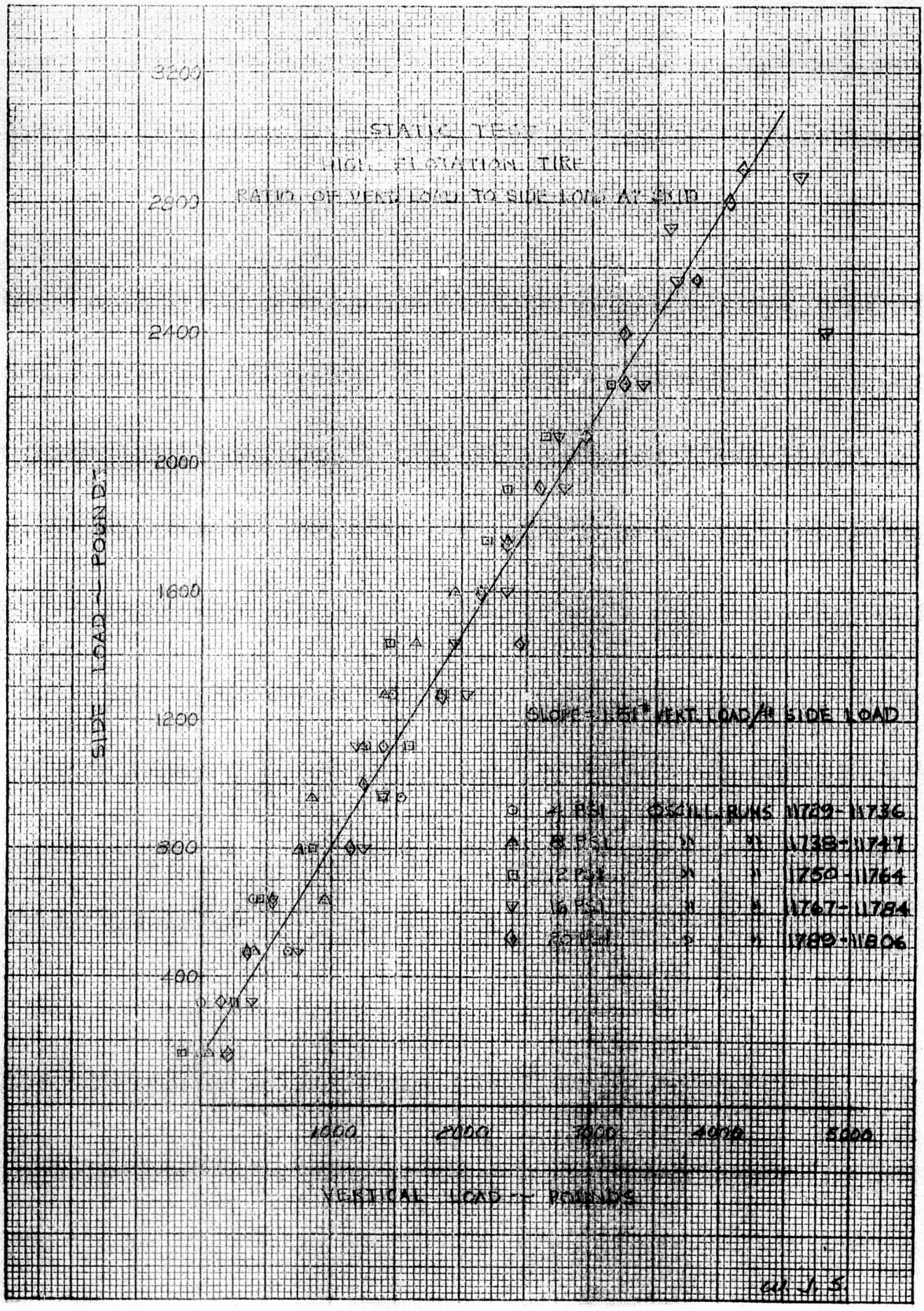
STATIC TEST
HIGH FLOTATION TIRE
RATIO OF VERT. LOAD TO SIDE LOAD AT SKID
SIDE LOAD -- POUNDS
VERTICAL LOAD -- POUNDS
3200
2800
2400
2000
1600
1200
800
400
1000
2000
3000
4000
5000
SLOPE = 1.51* VERT. LOAD/# SIDE LOAD
4 PSI OSCILL. RUNS 11729-11736
8 PSI " " 11738-11747
12 PSI " " 11750-11764
16 PSI " " 11767-11784
20 PSI " " 11789-11806

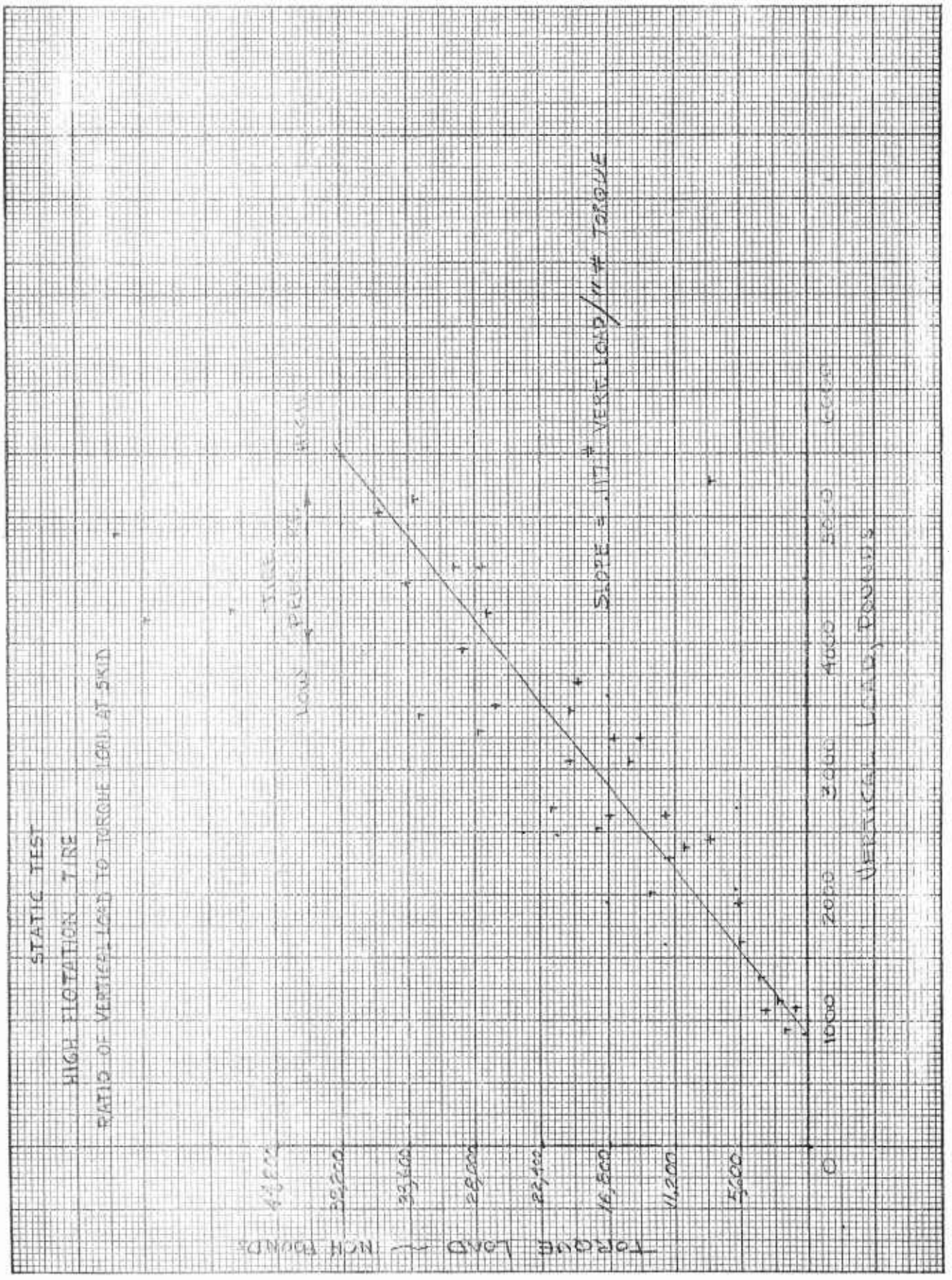
STATIC TEST
HIGH FLOTATION TIRE
RATIO OF VERTICAL LOAD TO TORQUE 100 AT SKID
SLOPE = .117 # VERTICAL LOAD/1# TORQUE
VERTICAL LOAD, POUNDS
TORQUE LOAD - INCH POUNDS
0
1000
2000
3000
4000
5000
6000
39,200
33,600
28,000
22,400
16,800
11,200
5,600

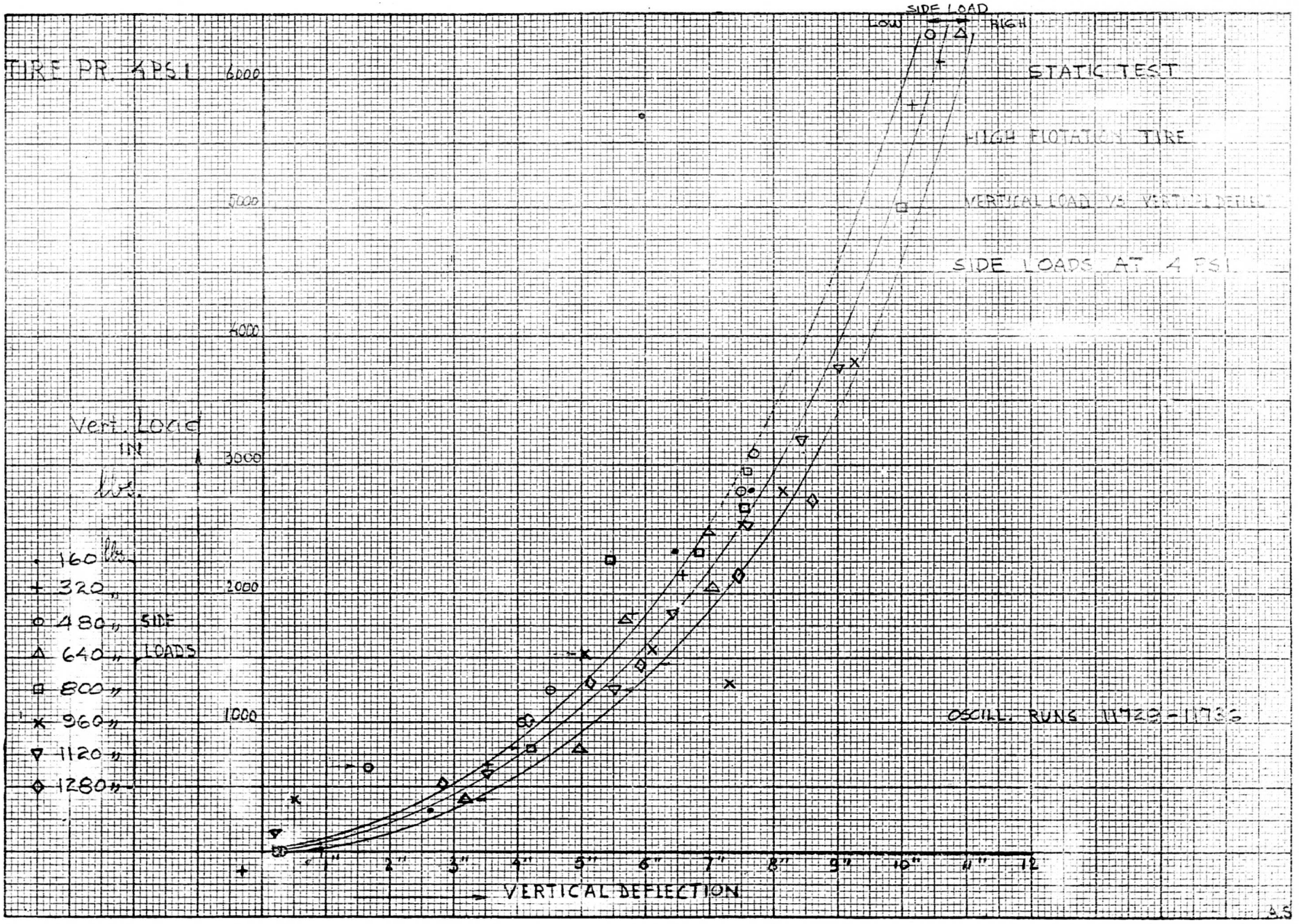
TIRE PR 4 PSI
6000
5000
4000
3000
2000
1000
Vert. Load
lbs.
160 lbs
320 "
480 "
640 "
800 "
960 "
1120 "
1280 "
SIDE LOADS
SIDE LOAD
LOW
HIGH
STATIC TEST
HIGH FLOTATION TIRE
VERTICAL LOAD VS VERTICAL DEFLECTION
SIDE LOADS AT 4 PSI
OSCILL. RUNS 11725-11736
1"
2"
3"
4"
5"
6"
7"
8"
9"
10"
11"
12
VERTICAL DEFLECTION
A.S

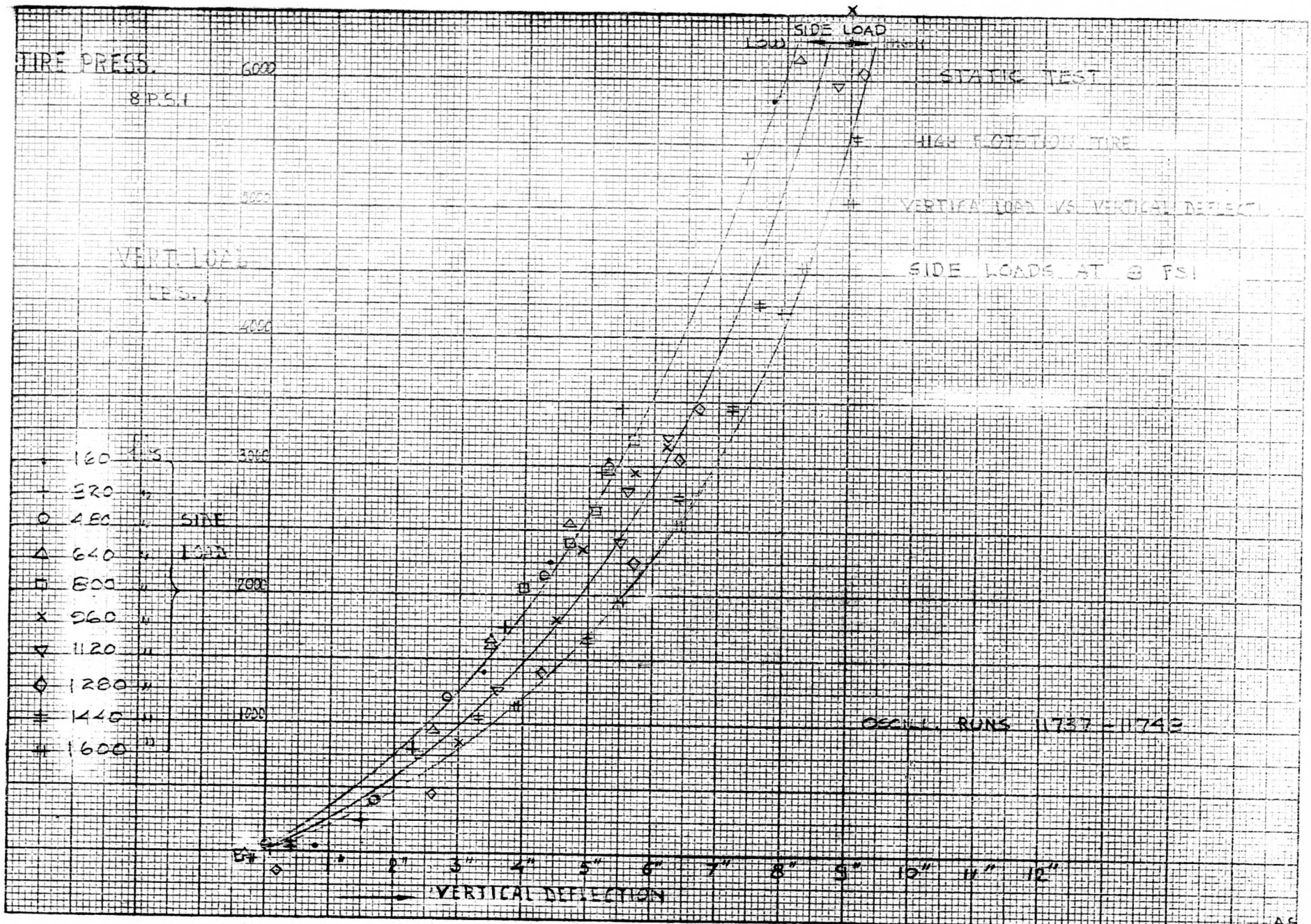
TIRE PRESS.
8 PSI
STATIC TEST
HIGH FLOTATION TIRE
VERTICAL LOAD VS VERTICAL DEFLECTION
SIDE LOADS AT 8 PSI
SIDE LOAD
VERT. LOAD
LBS.
6000
4000
2000
1000
160 LBS
320 "
480 "
640 "
800 "
960 "
1120 "
1280 "
1440 "
1600 "
SIDE LOAD
OSCILL. RUNS 1737 - 1742
2"
3"
4"
5"
6"
7"
8"
9"
10"
11"
12"
VERTICAL DEFLECTION
A.S.

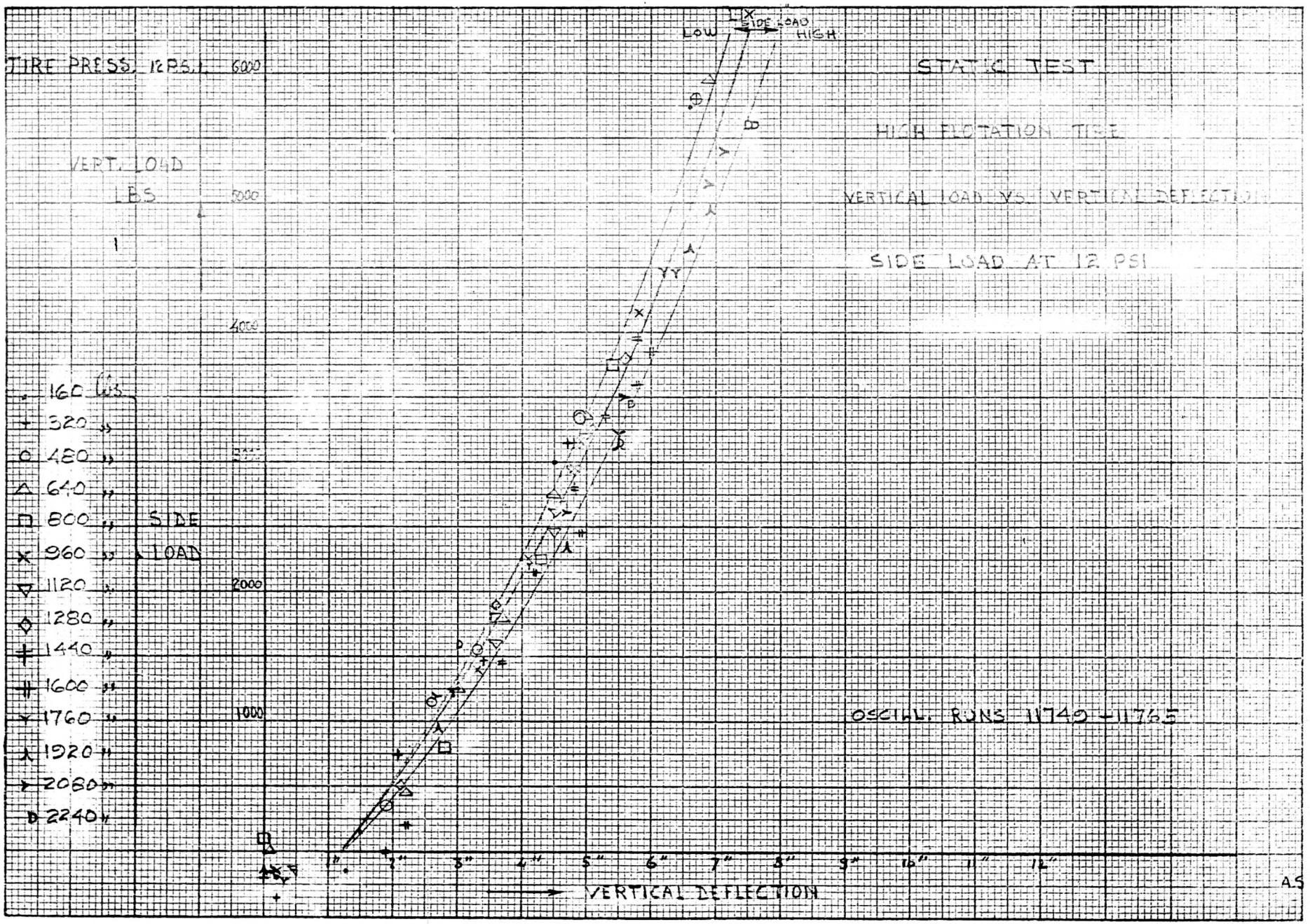
TIRE PRESS. 12 P.S.I.
STATIC TEST
HIGH FLOTATION TIRE
VERTICAL LOAD VS. VERTICAL DEFLECTION
SIDE LOAD AT 12 PSI
OSCILL. RUNS 11740 - 11765
VERT. LOAD LBS
6000
4000
2000
1000
LOW
SIDE LOAD
HIGH
160 LBS
320 "
480 "
640 "
800 "
960 "
1120 "
1280 "
1440 "
1600 "
1760 "
1920 "
2080 "
2240 "
SIDE LOAD
1"
2"
3"
4"
5"
6"
7"
8"
9"
10"
11"
12"
VERTICAL DEFLECTION

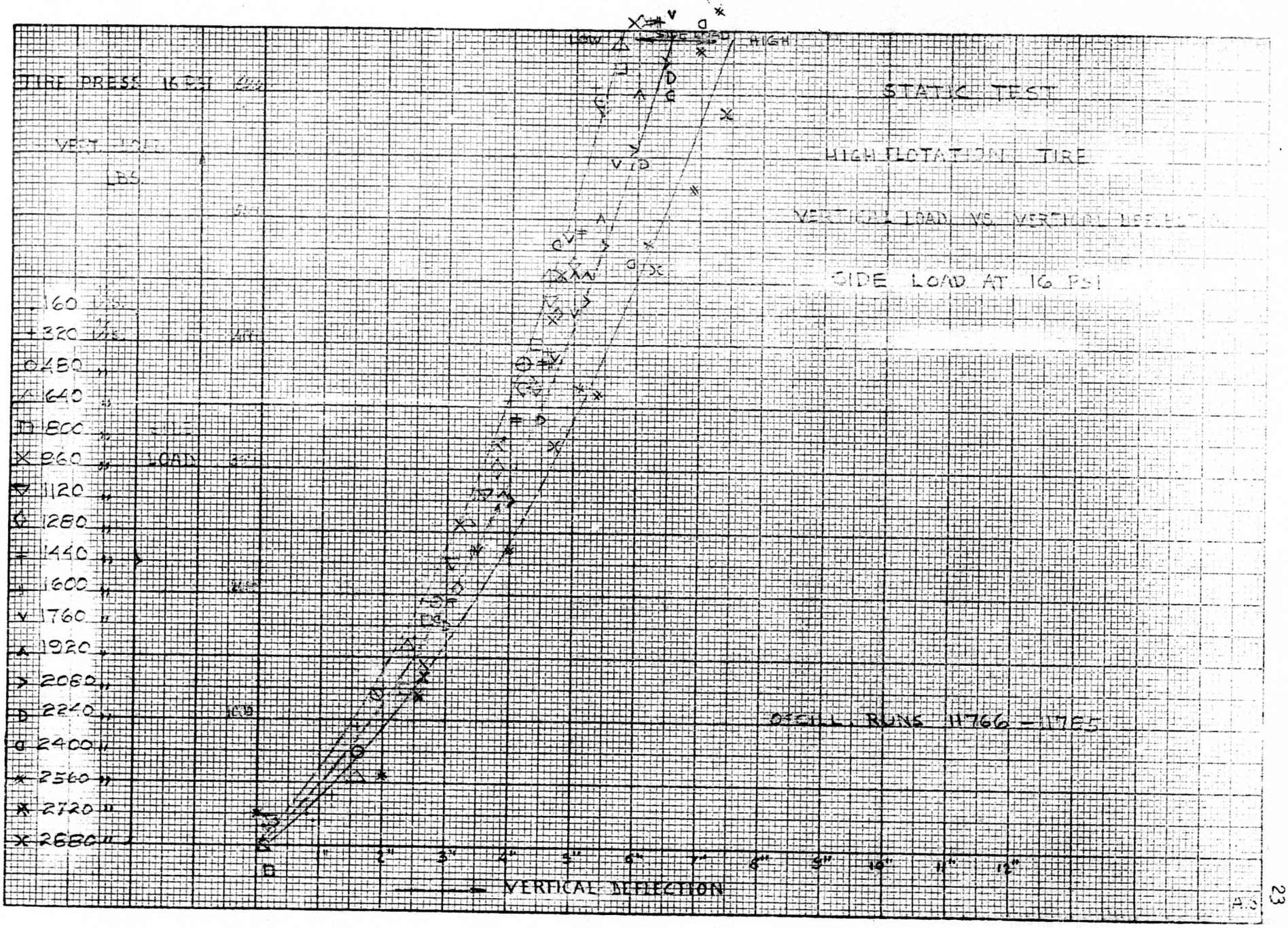
STATIC TEST
HIGH FLOTATION TIRE
VERTICAL LOAD VS VERTICAL DEFLECTION
SIDE LOAD AT 16 PSI
TIRE PRESS 16 PSI
VERT LOAD
LBS
LOW
SIDE LOAD
HIGH
160 LBS
320 "
480 "
640 "
800 "
960 "
1120 "
1280 "
1440 "
1600 "
1760 "
1920 "
2080 "
2240 "
2400 "
2560 "
2720 "
2880 "
1"
2"
3"
4"
5"
6"
7"
8"
9"
10"
11"
12"
VERTICAL DEFLECTION
OSCILL. RUNS 11766 - 17E5

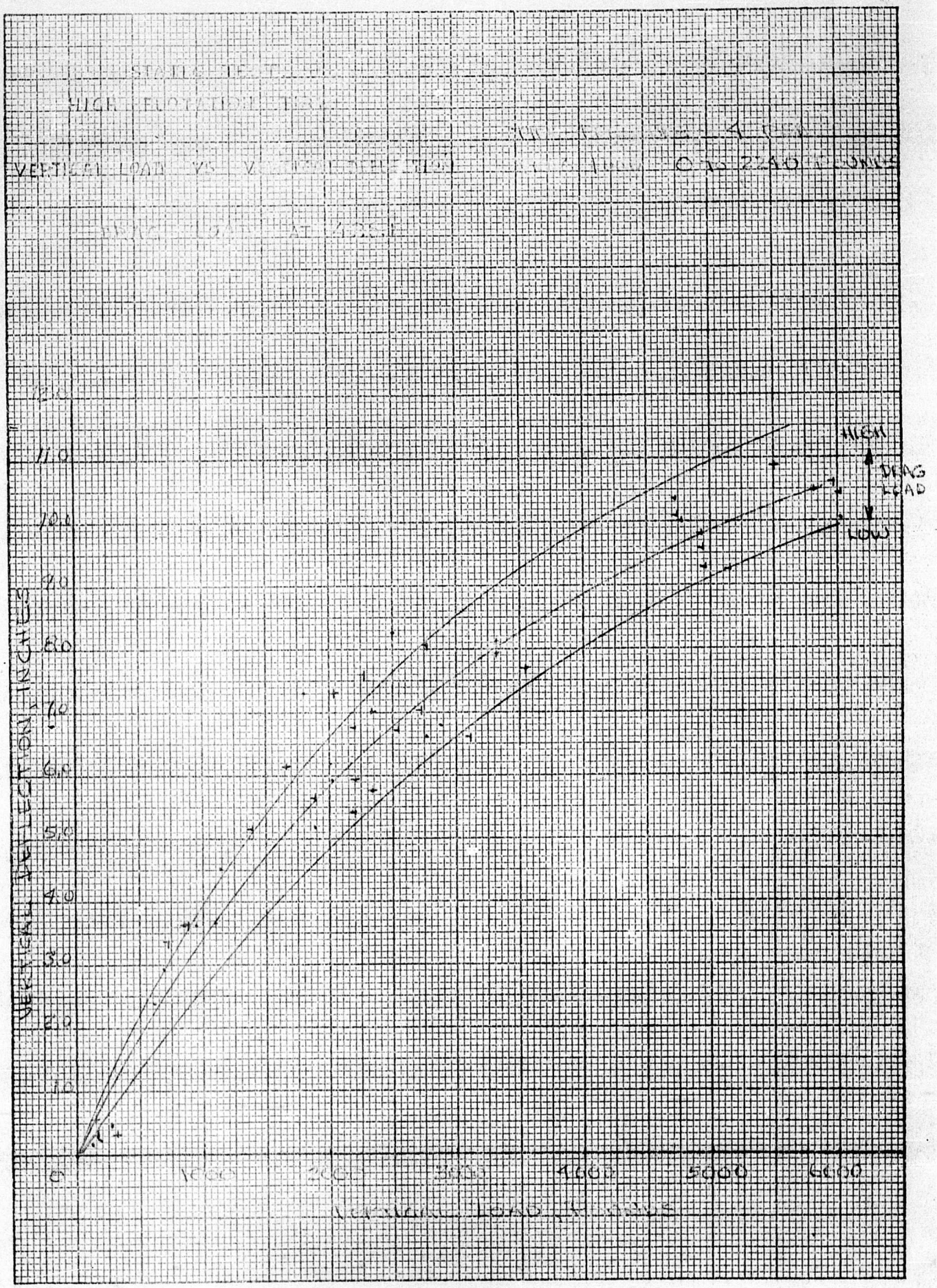
HIGH
DRAG LOAD
LOW
DEFLECTION IN INCHES
5000
6000

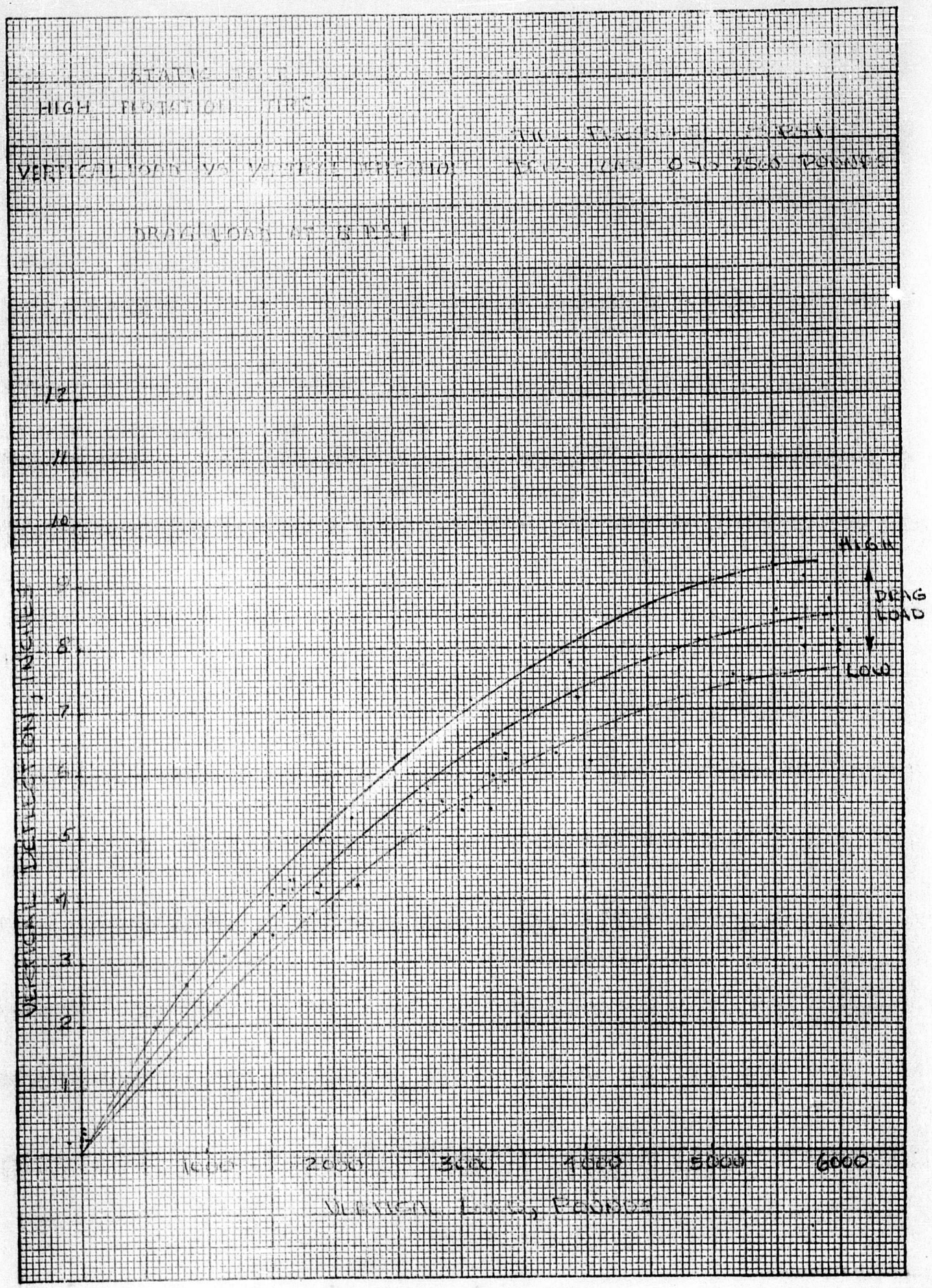
HIGH
DRAG LOAD
LOAD
12
11
10
9
8
7
6
5
4
3
2
1
2000
3000
4000
5000
6000

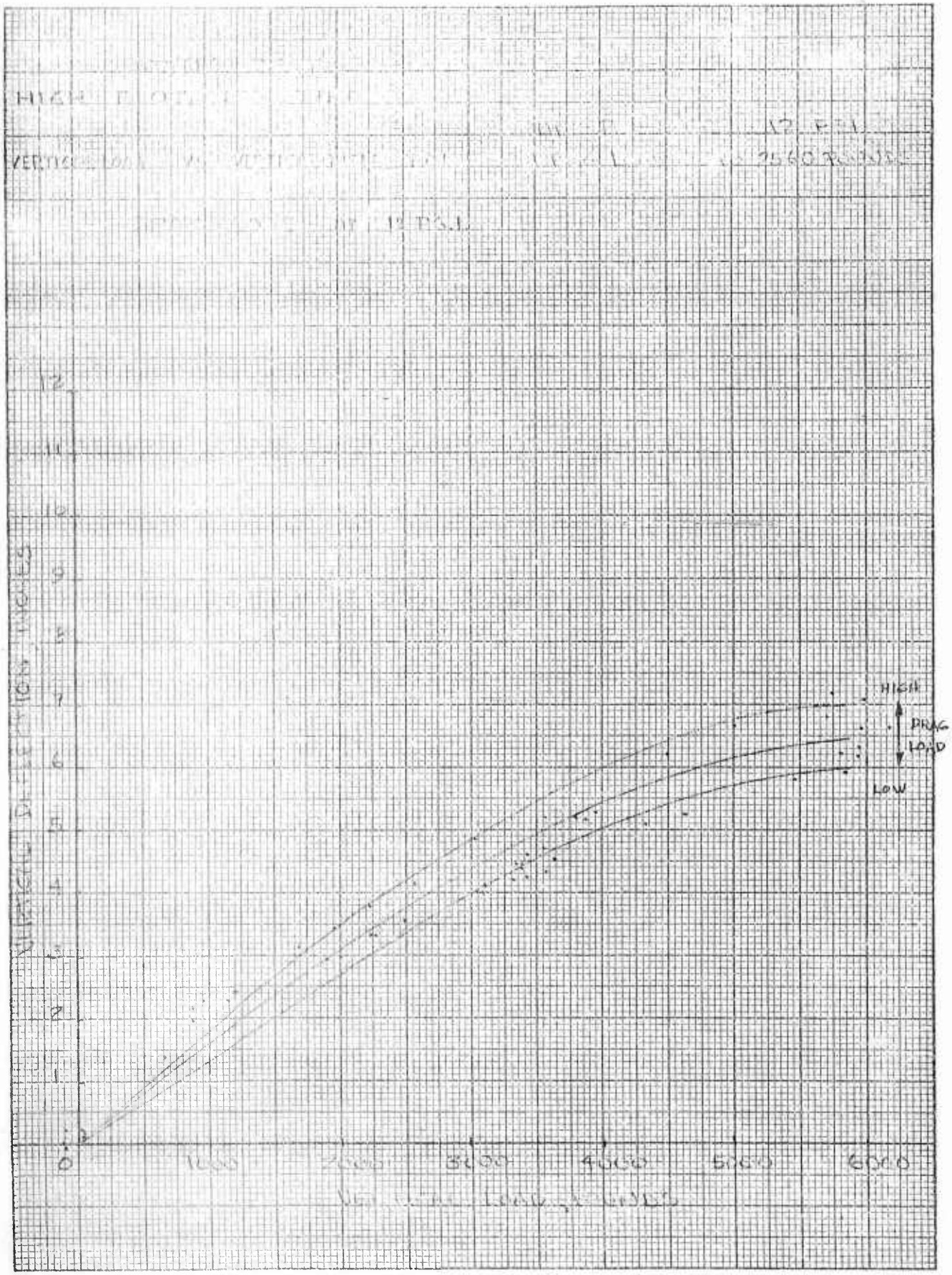
HIGH
DRAG
LOAD
LOW

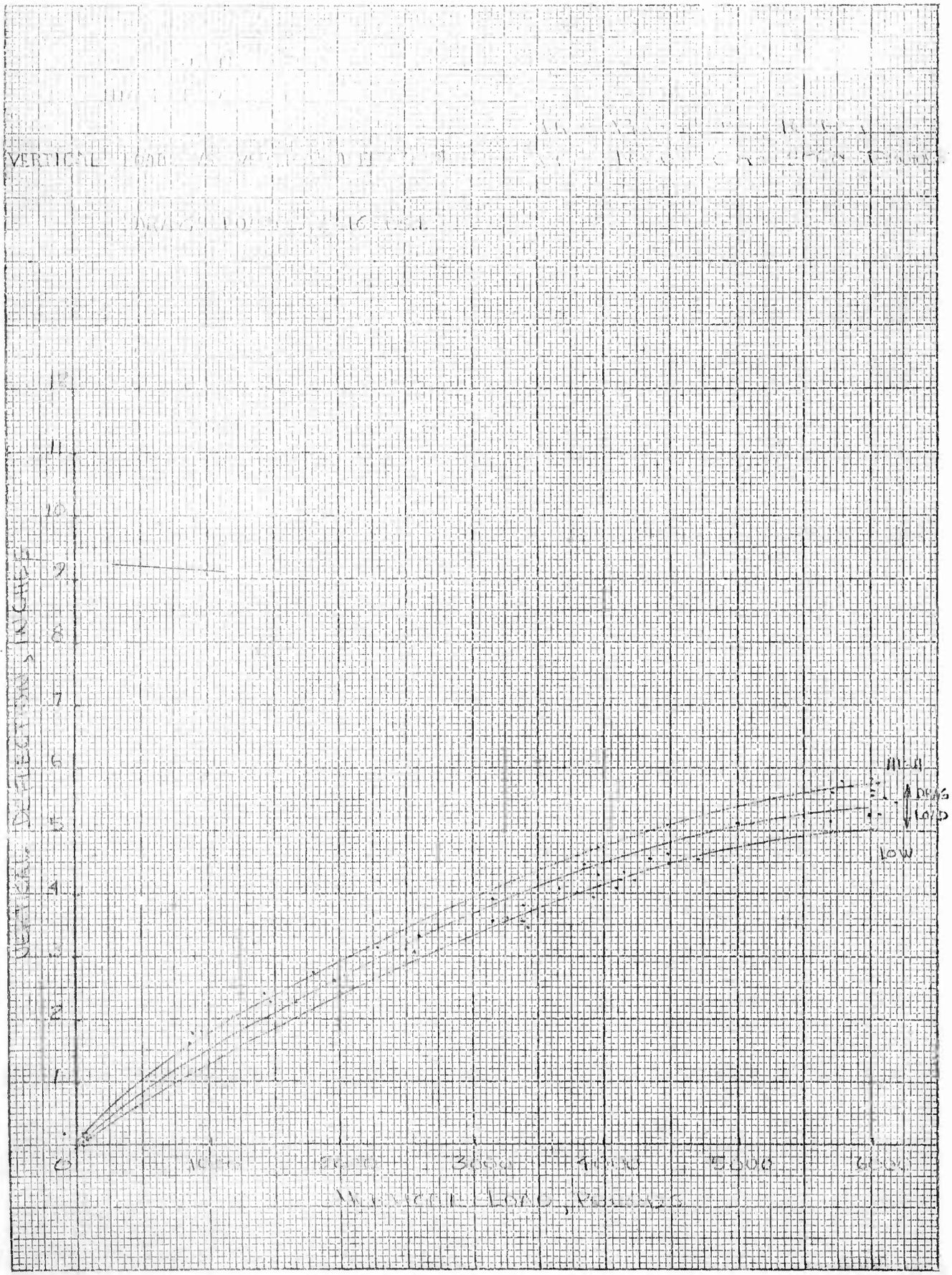
VERTICAL LOAD
DEFLECTION
HIGH
LOW

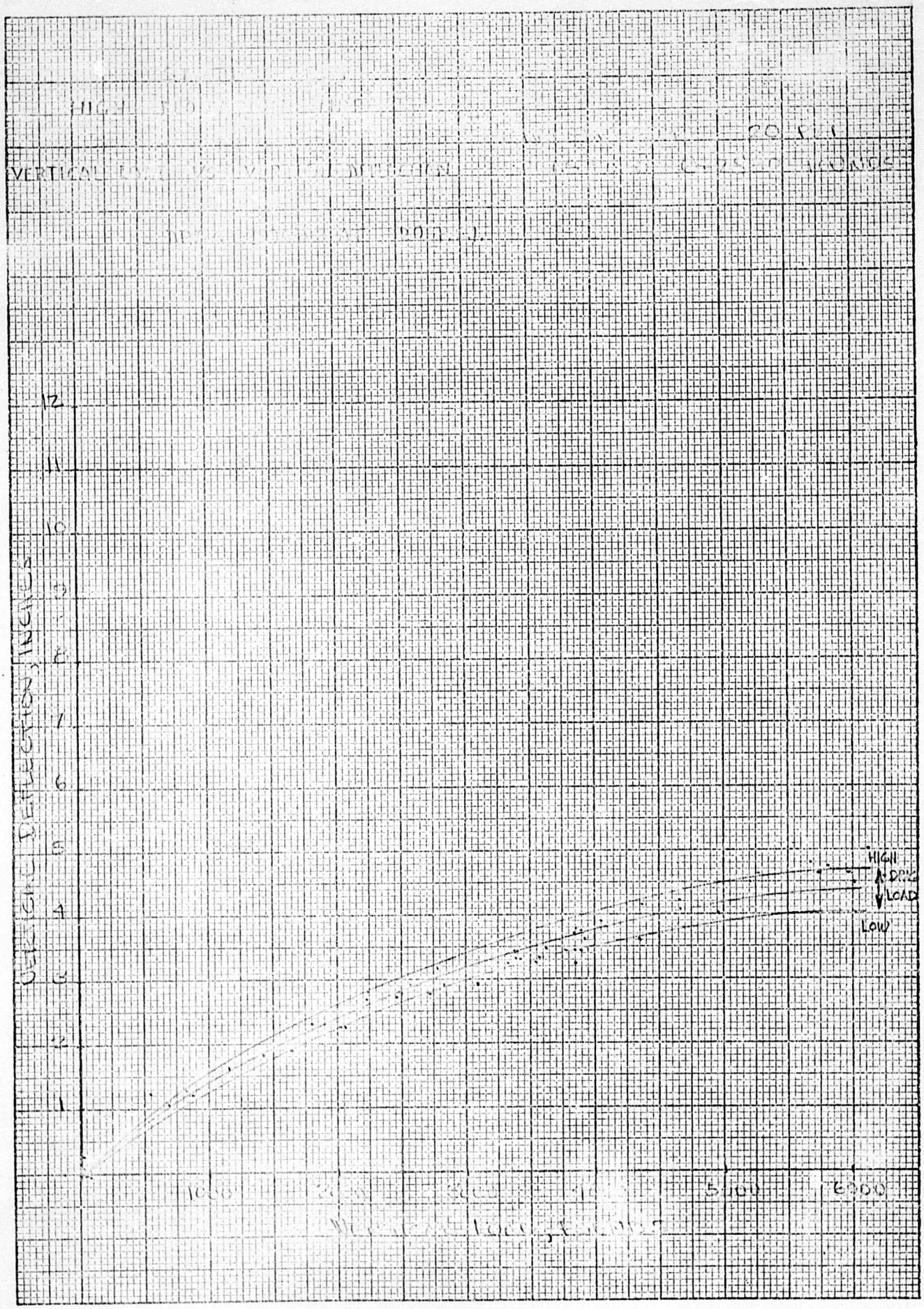
SETTLEMENT, INCHES
12
11
10
9
8
7
6
5
4
3
2
1
HIGH
DRIVE
LOAD
LOW
5000
6000

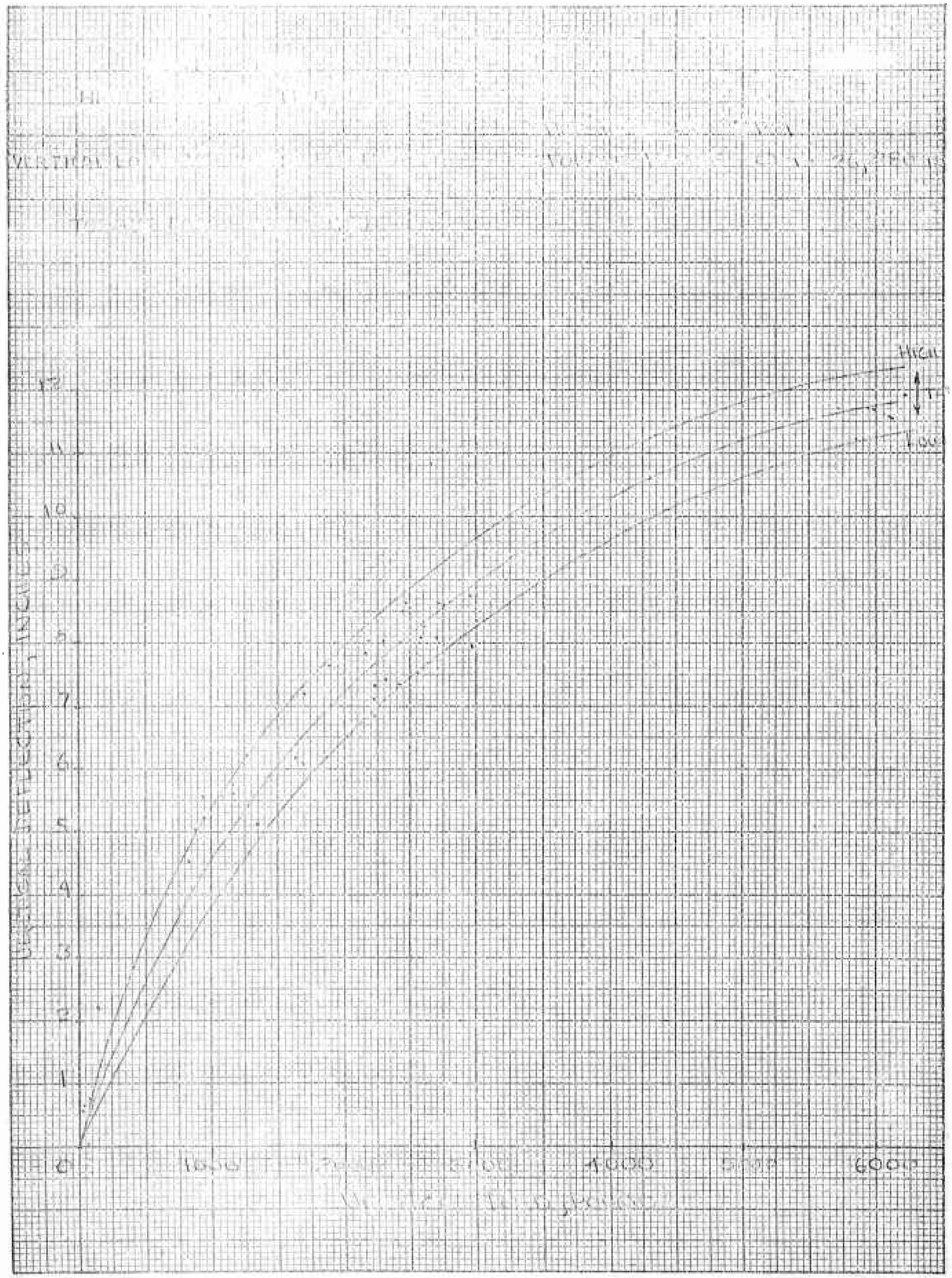
HIGH
LOW
VERTICAL DEFLECTION, INCHES
12
11
10
9
8
7
6
5
4
3
2
1
0
1000
2000
3000
4000
5000
6000

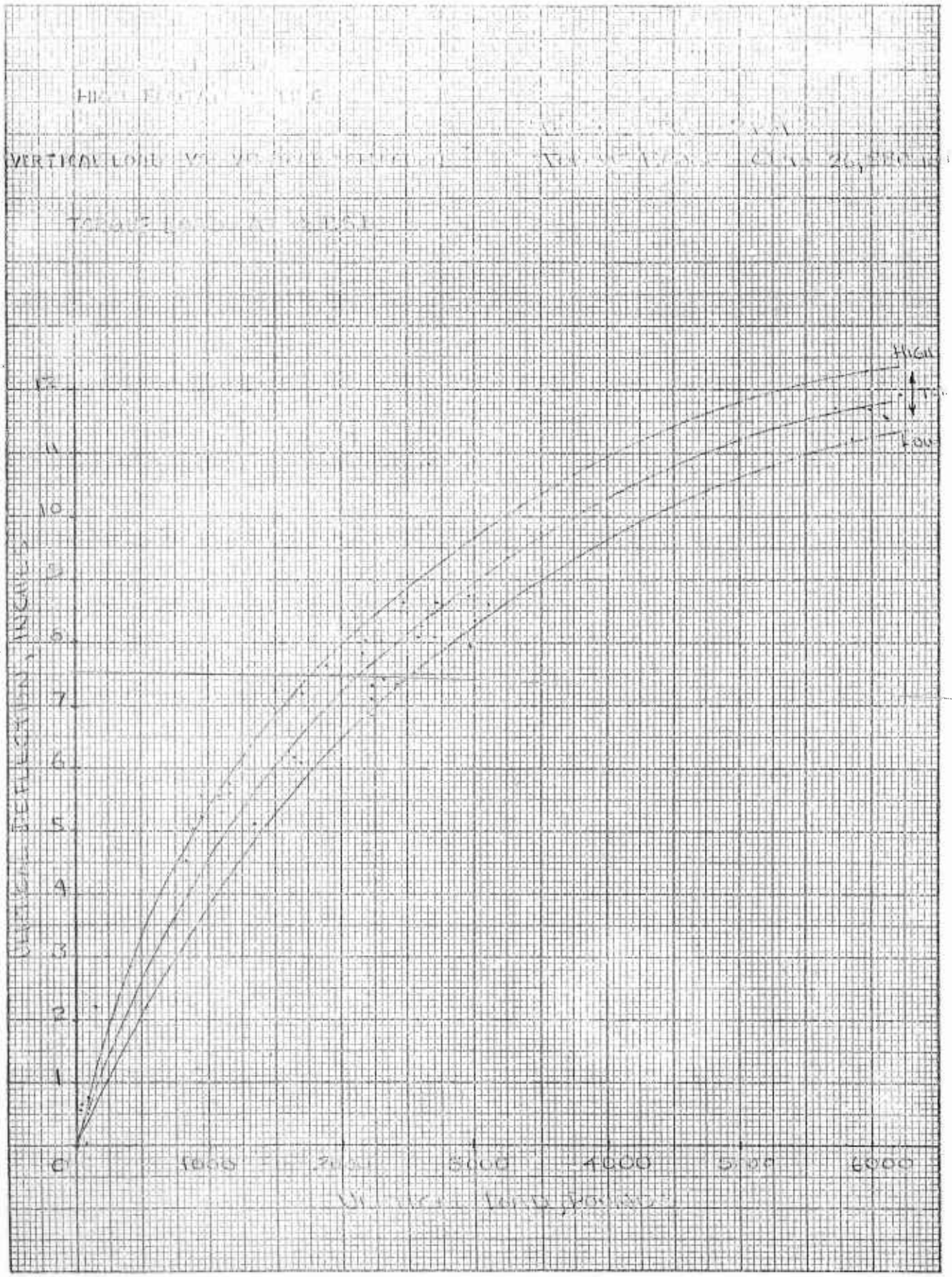
HIGH
LOW
12
11
10
9
8
7
6
5
4
3
2
1
0
1000
5000
6000

STATIC TEST

HIGH ELOTATION TIRE

VERTICAL LOAD VS VERTICAL DEFLECTION

TORQUE LOAD AT 4 P.S.I

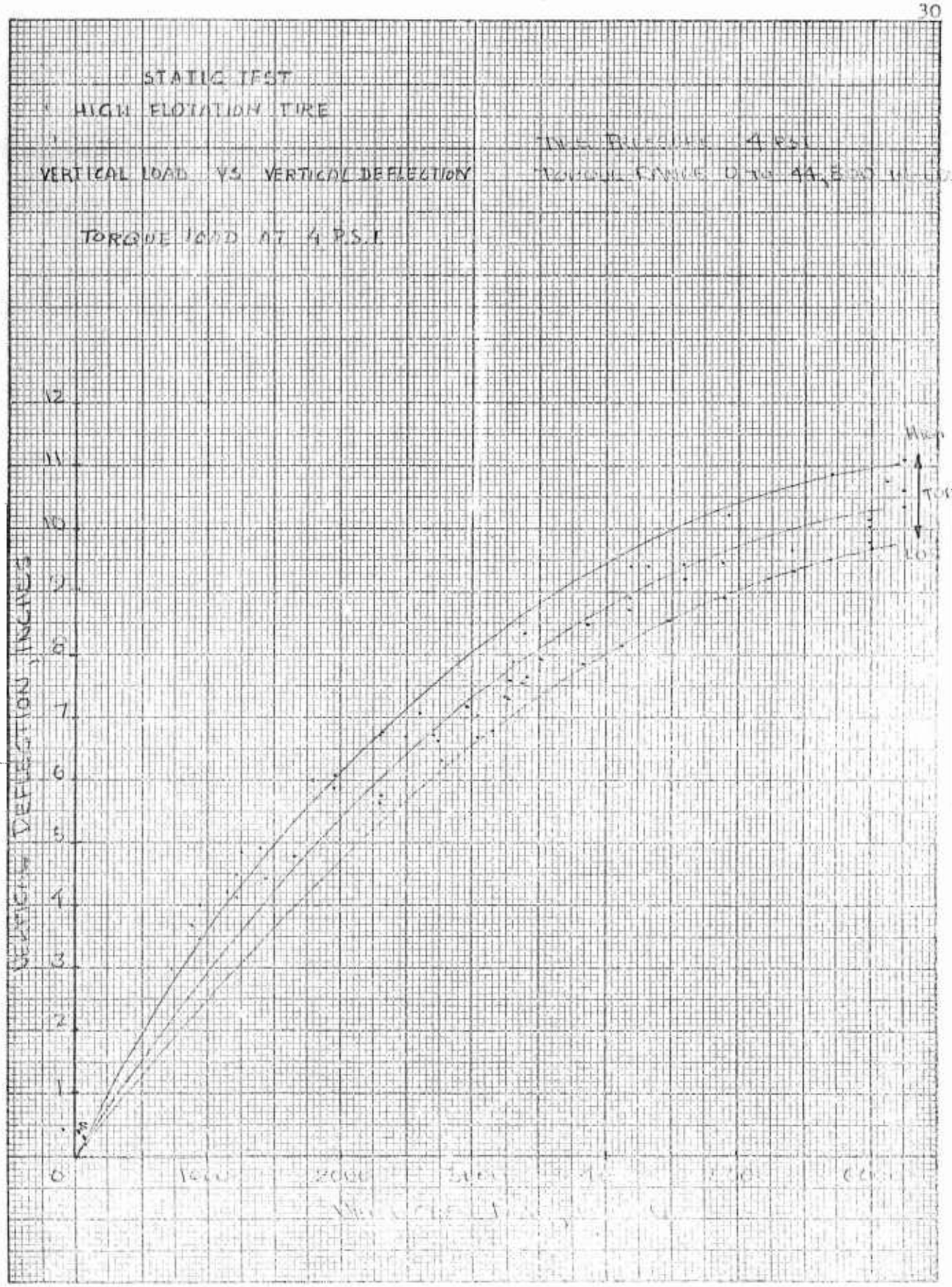

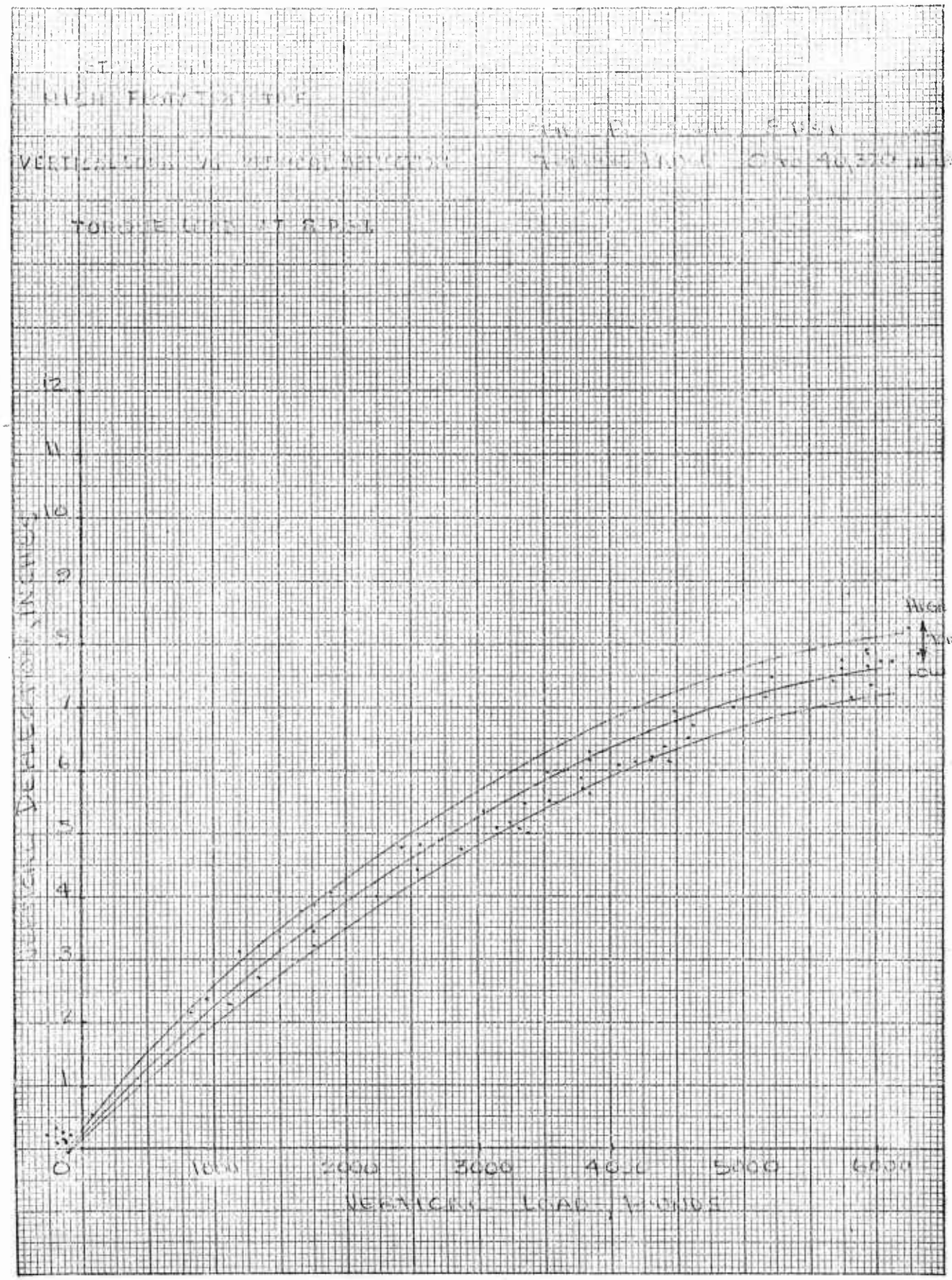
DEFLECTION, INCHES
0
1
2
3
4
5
6
7
8
9
10
11
12
1000
2000
3000
4000
5000
6000
VERTICAL LOAD, POUNDS

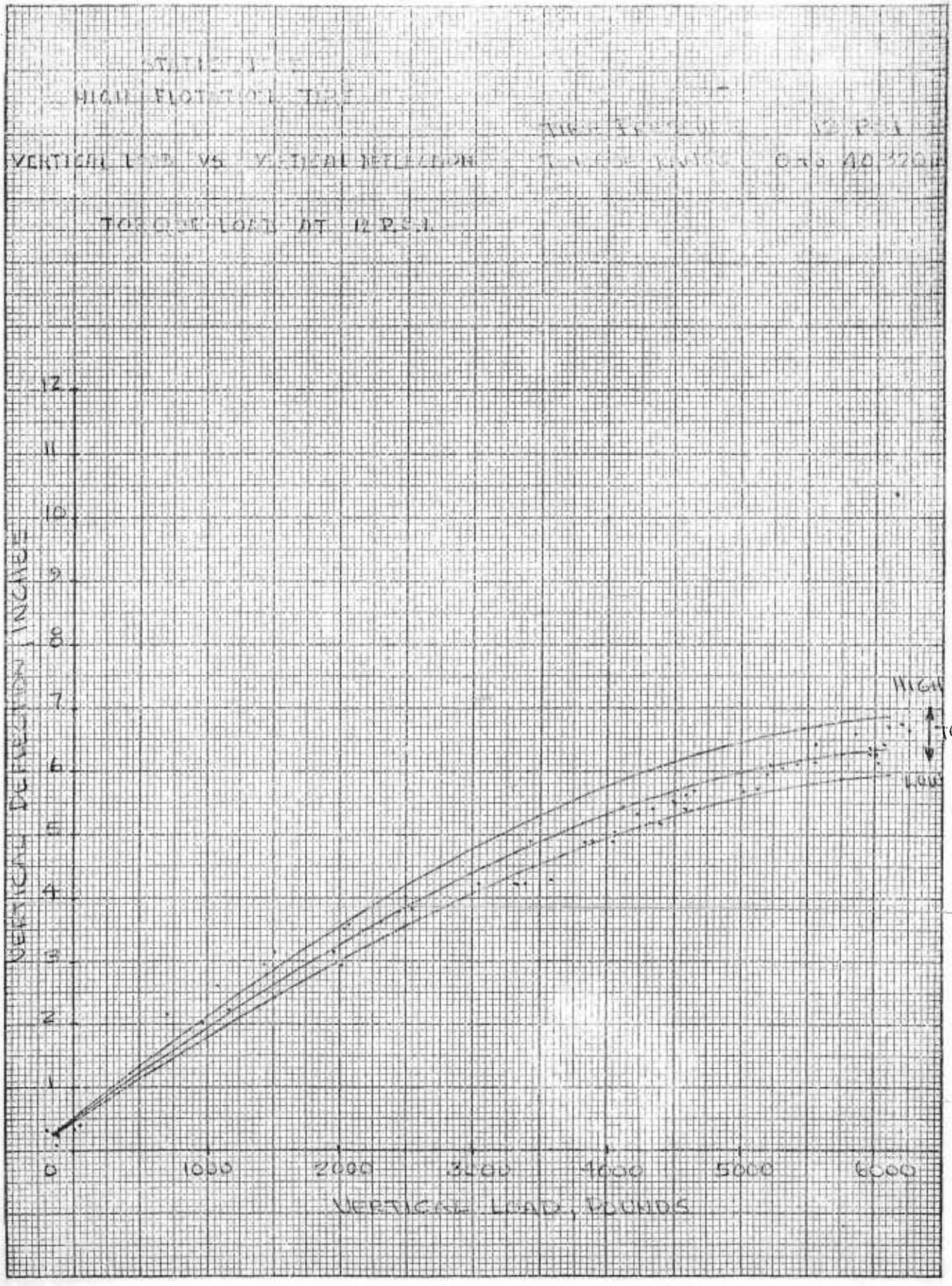
VERTICAL DEFLECTION, INCHES
VERTICAL LOAD, POUNDS
0
1000
2000
3000
4000
5000
6000
1
2
3
4
5
6
7
8
9
10
11
12
HIGH
TORQUE
LOW

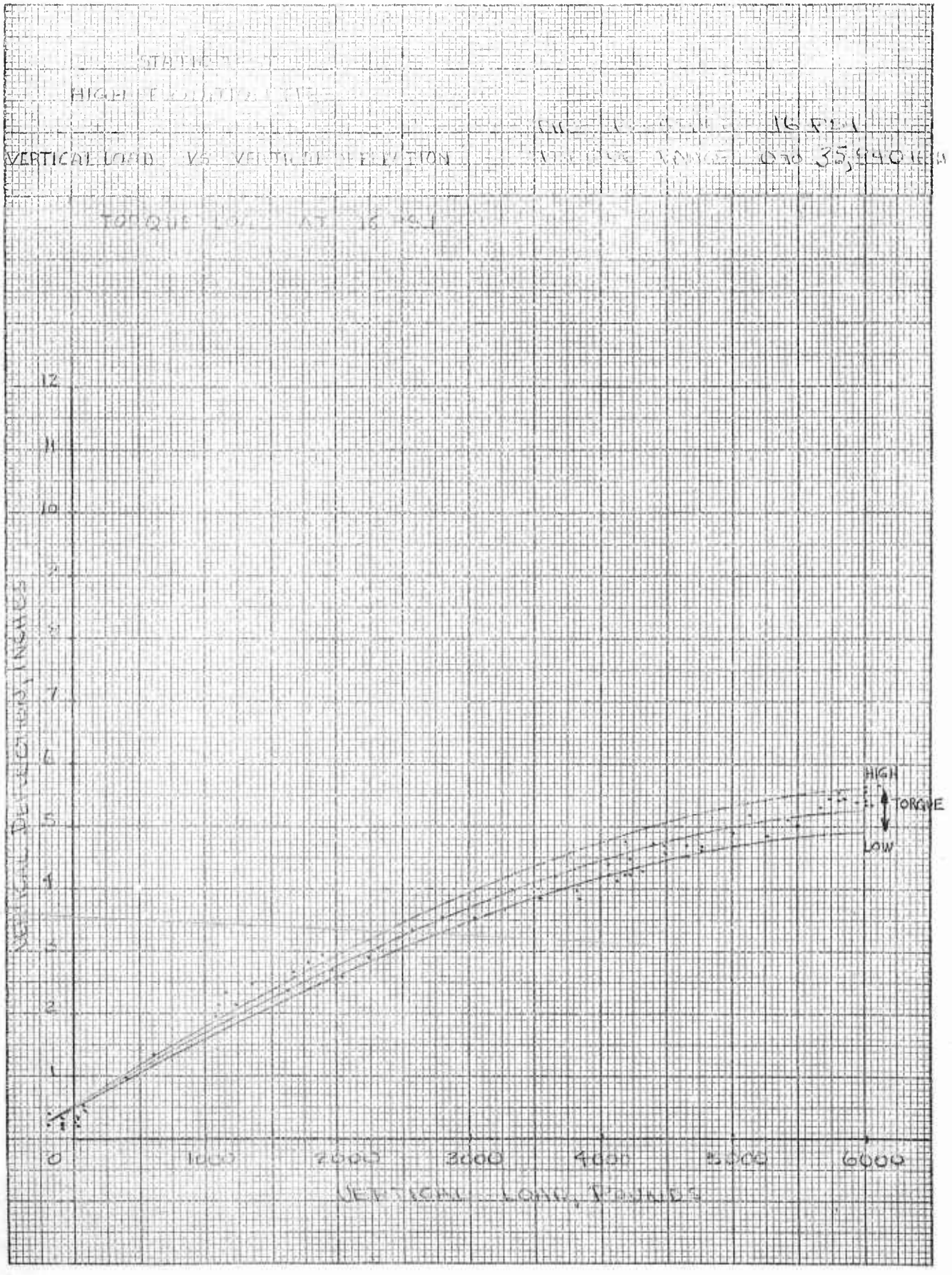
HIGH
TORQUE
LOW
12
11
10
9
8
7
6
5
4
3
2
1
0
1000
2000
3000
4000
5000
6000

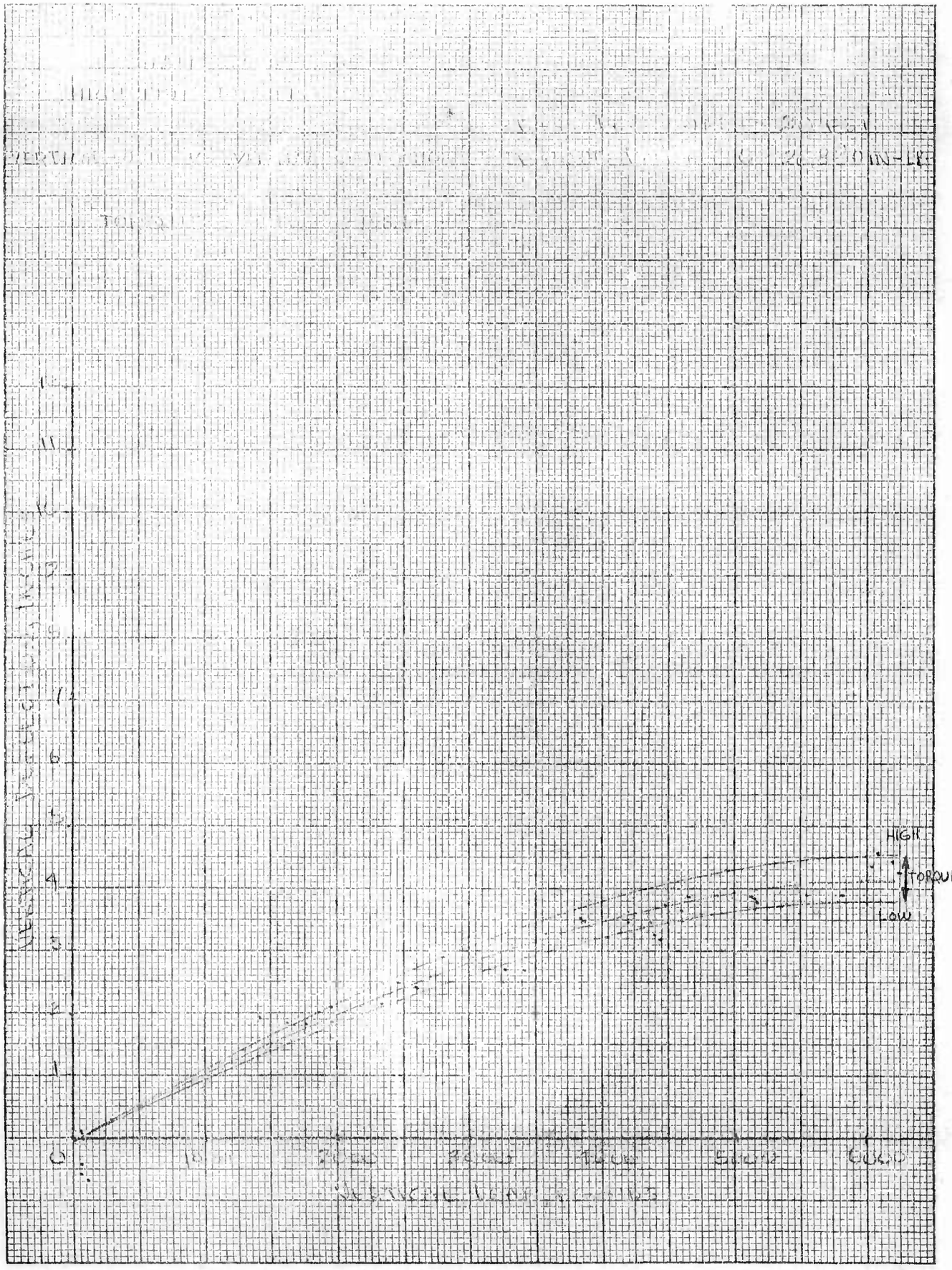
HIGH
TORQUE
LOW

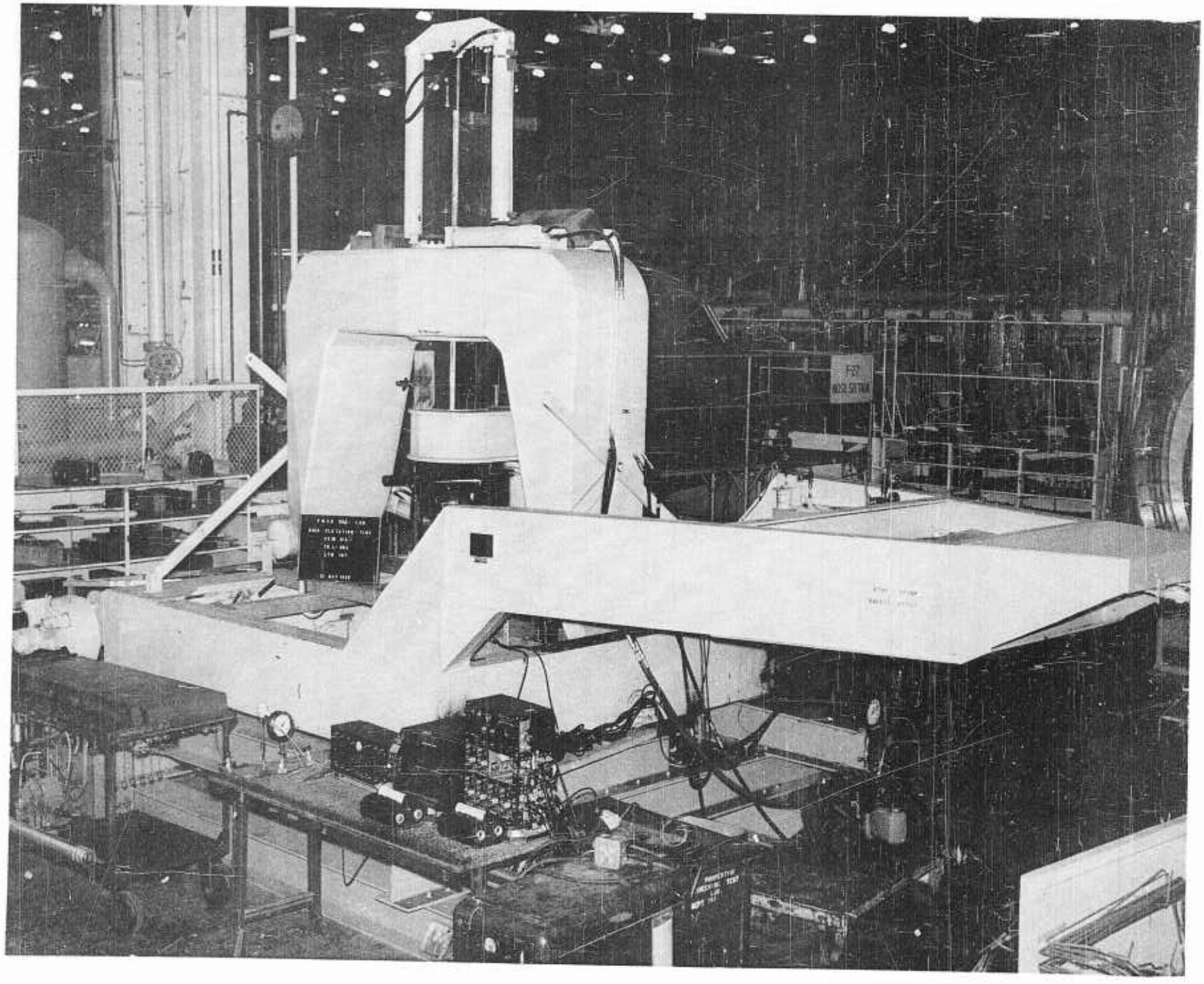

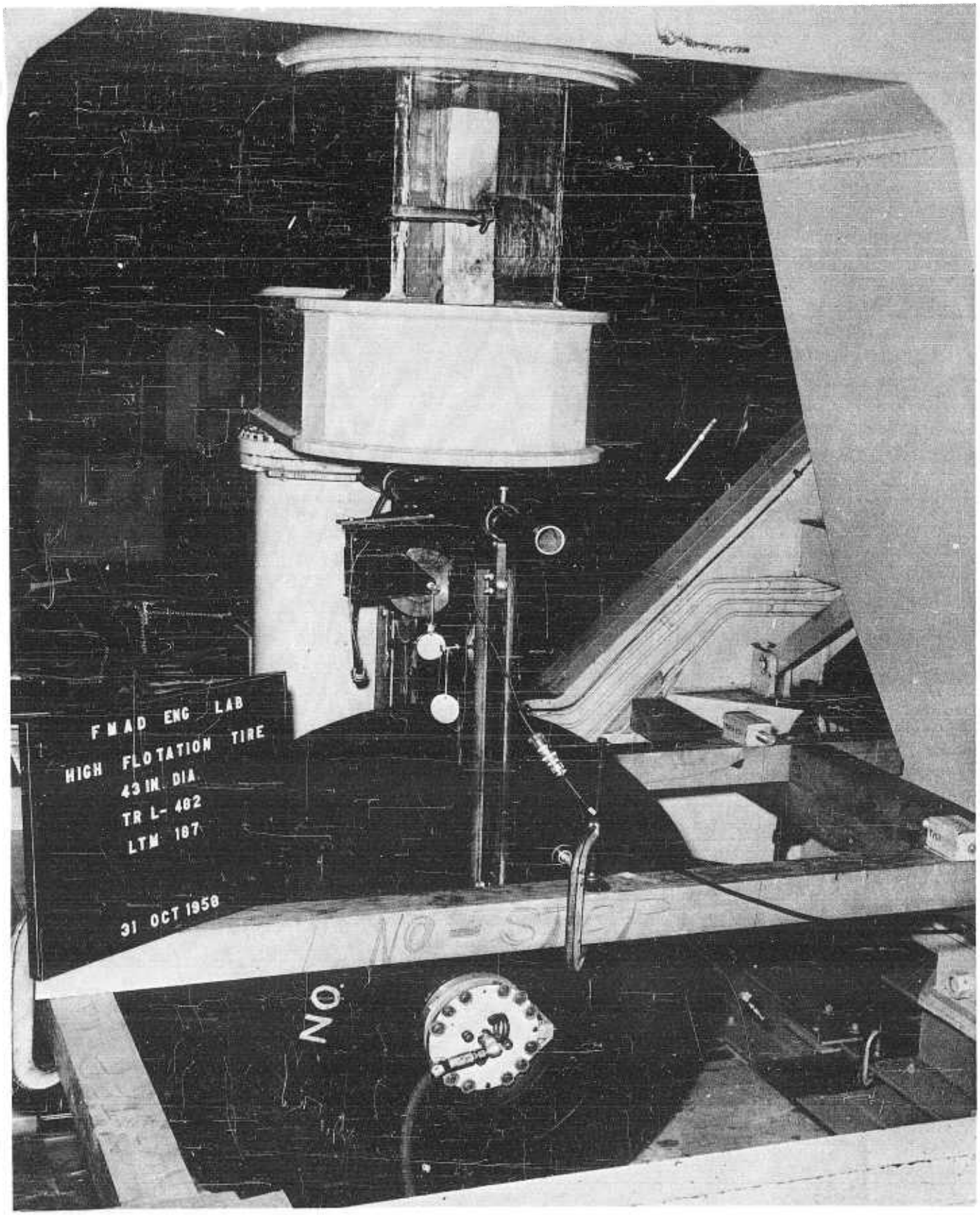
F M A D ENG LAB
HIGH FLOTATION TIRE
43 IN. DIA
TR L- 482
LTM 187
31 OCT 1958
NO STEP
NO.

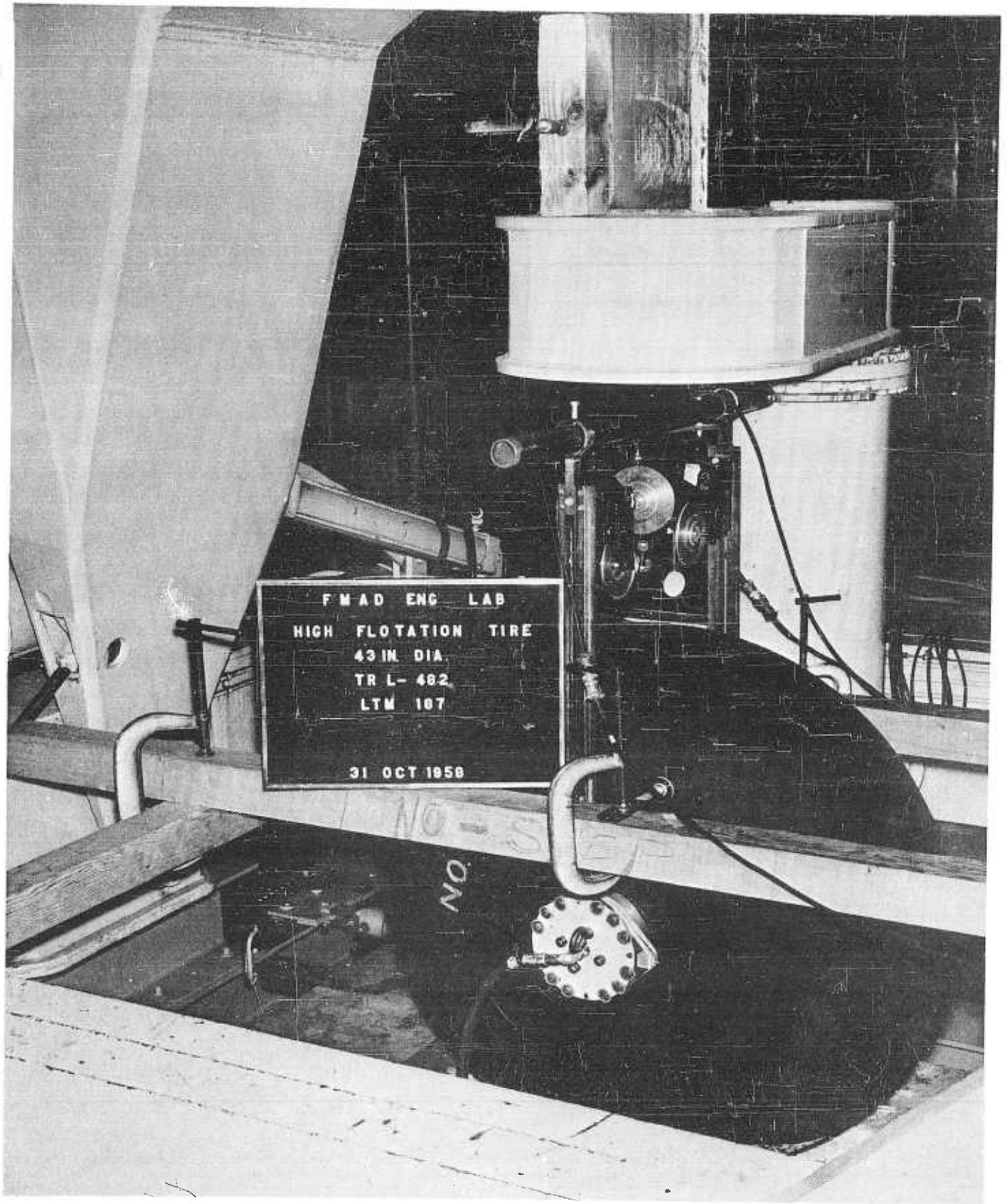
FMAD ENG LAB
HIGH FLOTATION TIRE
43 IN DIA
TR L- 482
LTM 187
31 OCT 1958

ENGINEERING REPORT NO.

R245-011

SUBJECT

ROLLING TESTS

HIGH-FLOTATION TIRE

MODEL: M-245

Fairchild Aircraft

DIVISION OF
FAIRCHILD ENGINE & AIRPLANE CORPORATION
HAGERSTOWN 10, MARYLAND

Date of Test: 1-22-59 to 3-9-59

Tested by: B.R. Klein

DATE: April 17, 1959

NO. PAGES: 46

PREPARED BY: B.R. Klein
B.R. Klein

APPROVED BY: J.N. Marsden
J.N. Marsden
Assistant Manager, Tech. Testing

CHECKED BY: R.R. Enterline
R.R. Enterline

APPROVED BY: E.E. Morton
E.E. Morton
Manager, Tech. Design & Analysis

APPROVED: Project - V. Frisby
V. Frisby

REVISIONS

DATE	PAGES AFFECTED	BY	REMARKS
4/21/59	Pg.9 Revised, Pg. 9a added.	R.Enterline	

FA-800-69A

REPORT NO. R245-011 FAIRCHILD AIRCRAFT DIVISION OF FAIRCHILD ENGINE & AIRPLANE CORPORATION			PAGES | PAGE 1
MODEL M-245	PREPARED BY D.H. Klein	CHECKED BY R.P. Rutledge	APPROVED BY Swen/Norton/Frisby

SUBJECT:- Rolling Test - High Flotation Tire.

DATE April 13, 1959

REVISED

ABSTRACT

Rolling tests were conducted on a tire to determine rolling resistance on smooth pavement, reaction to simulated rough terrain, cornering, camber angle, braking, lateral stability, and shimmying tendencies. The test specimen was a 43" diameter high flotation tire, rated at 1500#, with 60° cord cross-over developed by FAMD under contract with TRECOM. Oscillograph records were made of all tests and moving pictures were taken of some runs at each phase of testing.

The test rig consisted of an open rectangular base mounted on truck wheels, located at the rear of the base, and a raised platform at the front or tow end on which was mounted a three sided instrumentation and personnel shelter. This rig was towed by a highway type tractor. The basic rig was the same as used for the static tests and described in FAMD Report No. R245-010.

The rolling resistance phase of the tests consisted of applying a 1500# vertical load through the axle and tire at each of the initial tire pressures of 4, 8, 12, 16 and 24 psi., and making runs up to 40 MPH on smooth pavement.

The simulated rough terrain phase of the tests consisted of rolling, at various speeds, over obstacles and across a ditch which simulated ruts, bumps, and pot holes respectively. The height and spacing of obstacles and depth of the ditch were changed for different tests. Vertical loads of 1500#, 3000#, and 4500# were applied at initial tire pressures of 4, 12 and 24 psi.

The smooth pavement cornering phase of the tests consisted of setting the axle at a 15° caster angle and making a 0-15 MPH run on smooth pavement. Loads of 1000# and 1500# were applied at initial tire pressures of 4 and 24 psi.

The camber angle phase of the tests consisted of setting the normally vertical axis of the strut at a 15° angle from the vertical and making a run of 0-40-0 MPH on smooth pavement. Runs were made with 1500#, 3000#, and 4500# loads applied at initial tire pressures of 12, 20 and 24 psi.

The last phase of testing was the braking, lateral stability, and shimmying tendencies on smooth pavement tests. This consisted of making 0-40-0 MPH runs on smooth pavement and 'steering' the tire so as to try to induce shimmy. The high flotation tire brake was applied on the deceleration part of these tests.

Oscillograph records were made of every run and the tabulated data and graphs are presented in the Appendix of this report.

The tire withstood all phases of testing with no apparent damage except in the cornering tests when the lack of tread-stock on this tire resulted in surface-wear exposing the cording.

SUBJECT:- Rolling Test - High Flotation Tire.

ADMINISTRATIVE DATA

PURPOSE:

As specifically authorized by contract DA44-177-TC-446, the purpose of this test on a high-flotation tire was as follows:

(a) Determination of rolling resistance of the high-flotation, prototype flight test model tire on smooth pavement through the practical range of inflation pressures and ranges of deflection for speeds from 0 to the limits imposed by the available test vehicle, but not to exceed 115 feet per second.

(b) Determination of behavior of flight test model tires at 100, 200, 300 per centum rated load as regards cornering, braking, lateral stability and shimmying tendencies, while rolling upon smooth pavements at speeds from 0 to the limits imposed by the available test vehicles, but not to exceed 115 feet per second.

(c) Determination of behavior of flight test model tires, to include reaction forces generated from encountering various ruts, bumps, potholes, etc., at speeds from 0 to limits imposed by the available test vehicle, but not to exceed 115 feet per second and with supported loads up to 300 percent rated load or as limited by bottoming or tire wrinkling.

MANUFACTURER:

Fairchild Aircraft and Missiles Division
Hagerstown, Maryland

MANUFACTURER'S TYPE OR MODEL NO.:

High-Flotation Tire Serial No. 15 rated at 1500# - 43" diameter, 60° cross-over angle of cord winding.

DRAWINGS, SPECIFICATIONS, EXHIBITS:

Contract No. DA44-177-TC-446
FAMD Report R245-010
Wilson Nuttall Raimond Drawing No. 41-9
(Copies may be obtained on request to FAMD)

QUANTITY OF ITEMS TESTED:

One

SUBJECT:- Rolling Test - High Flotation Tire.

ADMINISTRATIVE DATA (continued)

SECURITY CLASSIFICATION OF ITEM:

Unclassified

DATE TEST COMPLETED:

March 9, 1959

TEST CONDUCTED BY:

B.R. Klein
FAMD, Engineering Laboratory

DISPOSITION OF SPECIMEN:

Held pending disposition notice from TRECOM.

MODEL M-245 | PREPARED BY B.R. Klein | CHECKED BY R.R. Fotheringe | APPROVED BY Patton/Frisby

DATE April 13, 1959

REVISED

SUBJECT:- Rolling Test - High Flotation Tire.

FACTUAL DATA

DESCRIPTION OF TEST APPARATUS:

The test apparatus used in the rolling tests of the high-flotation tire consisted of a heavy steel truck trailer type rig designed by Wilson, Nuttall and Raimond (reference drawing No. 41-9) and manufactured by Thompson Equipment Machine Company. This rig was towed by a highway type truck tractor. The set-up is illustrated in photographs no. 38948 39013 and 39011 in the Appendix.

This rig was basically the same as used on the static test and described in FAMD Report R245-010. A three sided instrumentation and personnel shelter was mounted on the raised platform at the front or tow end of the rig. A multichannel C.E.C. oscillograph and amplifiers were mounted in this shelter.

Electrical power was supplied by an engine-driven generator, 28 volt D.C. 70 amp. capacity. A moving picture camera was mounted a few feet in front of the tire to obtain regular and slow motion pictures of the tire during testing. Seats were installed in the shelter for an oscillograph operator and an observer.

A foot brake system for the high flotation tire was installed under the instrument table, and was operated by the oscillograph operator when braking data was desired. A wheel was installed at the rear of the rig which was instrumented to record the direction and speed of the rig on the oscillograph. Compressed air bottles were mounted on the side of the rig for changing the tire pressure and operating the vertical-load cylinder. However, after about two thirds of the test program was completed, excessive air leakage in the cylinder prompted a change to oil operation.

Deflection and turning of the strut were measured by helipots, reference photograph no. 39012 in the Appendix. All of the deflection measuring devices, the 6 channel strut dynamometer and the helipots, were recorded on the C.E.C. oscillograph. Strain gages had been installed and calibrated on the dynamometer during the static test program using laboratory load cells.

The obstacles used in the rough terrain tests were as follows: obstacles simulating ruts and bumps were installed singly and in series at spacings of 4 to 16 feet. A 2 x 10 board was anchored to the runway and other boards fastened to it to change the obstacle height. These obstacles may be seen in photograph 38971. A pothole was simulated by making a ditch with plywood sides to prevent crumbling of the edges. The ditch was 24 inches wide by 40 inches long. The depth of the ditch was varied from 12 to 4 inches by adding or removing boards. The ditch is shown in photograph no. 38970.

SUBJECT:- Rolling Test - High Flotation Tire.

FACTUAL DATA (continued)

TEST PROCEDURE:

ROLLING RESISTANCE TESTS-

At an initial tire pressure of 4 psi, a vertical load of 1500# was applied to the tire and a run made from 0-40-0 MPH. An oscillograph record was taken during the entire run. This procedure was repeated at 8, 12, 16 and 24 psi initial tire pressures. The high flotation tire brake was applied during the deceleration of some of these runs.

SMOOTH PAVEMENT, BRAKING, LATERAL STABILITY & SHIMMYING TENDENCIES TESTS-

These tests were conducted by "Steering" the tire from neutral to 5 or 10 degrees in each direction during a 0-40-0 MPH run. This was done to try to induce shimmy. The brake on the high flotation tire was applied during deceleration on those runs. Tests were run at 4, 12 and 24 psi tire pressure. At 4 psi, loads of 1000# and 1500# were applied at 12 and 24 psi, loads of 1000#, 1500#, 3000# and 4500# were applied. Oscillograph records were taken during all runs.

SIMULATED ROUGH TERRAIN TESTS (RUTS AND BUMPS)-

These tests were conducted by running the tire over wooden obstacles simulating bumps. Two obstacles were used, varying in height from 2" to 10" and in spacing from 4 to 16 feet. Tests were run at 4 psi initial tire pressure with 1500# vertical load applied and at 12 and 24 psi with loads of 1500#, 3000# and 4500#. The height of the obstacles was increased at each tire pressure and load until it was considered unsafe for the tire or for axle clearance. Oscillograph records were taken and a blip was put on the record as the tire hit the obstacles.

SIMULATED ROUGH TERRAIN (DITCH)-

These tests were conducted by running the tire over the ditch at the various loads and tire pressures. Three different ditch depths were used, 4, 8 and 12 inches, until it was concluded that the depth had little or no effect on the tire. This was due to the fact that oil, used to raise and power the vertical load cylinder, hydraulically locked the cylinder in place, thus preventing the tire from dropping into the ditch. It should be noted here that the cylinder did not move vertically, even when air was used in the system while conducting the tests over obstacles and therefore the change to oil had little effect on the results of this test.

SUBJECT:- Rolling Test - High Flotation Tire.

FACTUAL DATA (continued)

TEST PROCEDURE:

SIMULATED ROUGH TERRAIN (DITCH)- (continued)

Tests were run at the identical tire pressures and loads used in the tests over the obstacles simulating ruts and bumps. Oscillograph records were taken during each run.

CAMBER ANGLE TESTS-

These tests were conducted by rotating the large U-shaped yoke on the rig to the desired camber angle. The first angle tried was 25°. However, it was found after one run, that at this angle the friction in the cylinder and excessive leakage past the piston prevented raising the tire. It was also found that there was interference at this angle between the brake drum and the side of the rig at the higher loads. Therefore all of these tests were run at 15° camber angle. Since at this angle the tire wrinkled to excess at any appreciable load at 4 psi tire pressure, tests were run only at 12, 20 and 24 psi tire pressure. At 12 psi, loads of 1500# and 3000# were applied and at 20 and 24 psi initial tire pressure, loads of 1500#, 3000# and 4500# were applied. The test consisted of a 0-40-0 MPH run on smooth pavement. Oscillograph records were taken.

SMOOTH PAVEMENT CORNERING-

These tests were conducted by rotating the axle to a 15° caster angle and making a run on smooth pavement at a speed considered safe for the tire. In this case the runs were made at speeds up to 15 MPH. Due to the large amount of rubber taken off the tire in these tests, runs were made only at 1000# and 1500# at tire pressures of 4 and 24 psi. Oscillograph records were made during entire run.

In every phase of testing, a representative number of moving pictures were taken, at different tire pressures, loads and test conditions.

SUBJECT:- Rolling Test - High Flotation Tire

FACTUAL DATA (continued)

RESULTS OF TEST:

Dynamometer cross channel response was determined by investigating static test calibration runs. It was determined that the only loading condition that affected other channels was vertical loading which caused some response in the side, drag moment, and torque bridges. The amount of this response is tabulated on page 12.

Overall calibration accuracy of the dynamometer was within ± 2% of full range. The oscillograph records can be read to within ± 1% accuracy for 1 inch of trace deflection. Before each group of test runs, calibration runs were corrected for any change in voltage that occurred.

It is estimated that the overall accuracy of the plotted data are within ± 4%.

The high flotation tire withstood all phases of testing with no noticeable permanent distortion. Considerable wearing of the tire surface occured during the caster angle and the "steering" tests. The condition of the tire after this type of test may be seen in photo. no. 38911. The lack of tread-stock on this tire is primarily responsible for this result.

Curves plotted from all tests, except the rough terrain tests, show that speed had no effect on any of the reactions. The brake was applied on the deceleration part of some of these runs but the brake was inadequate for this system and therefore the data for this phase were inadequate.

On some of the curves negative drag was indicated. This may be explained by the fact that the top of the dynamometer was slightly aft of its theoretically vertical position due to the position of the rig when attached to the tractor. This was reduced later in the test program by changing the rear axle height of the rig.

Curves plotted from rolling resistance tests on smooth pavement show that there was a maximum drag load of 0.5% of the vertical load and the maximum indicated side load was 30% of the vertical. Part of this side load reading was caused by the dynamometer cross channel influence (see pg.12) and the fact that the wheel position was found to be $\frac{1}{2}^{o}$ off the true fore and aft position.

Efforts to induce shimmy in the tire by "steering" were unsuccessful. All the runs in this phase were run while steering the tire from 0^{o} to 10^{o} in each direction and vertical, drag, and drag moment loads increased or decreased in unison with the side loads and the steering angle as can be seen on the plotted curves of these tests.

SUBJECT:- Rolling Test - High Flotation Tire

FACTUAL DATA (continued)

RESULTS OF TEST:

Tabulations were made to show the effect of tire pressure on drag versus vertical loads and may be found on page 15. Curves were plotted to show the effect of obstacle height and tire pressure on vertical loads during rough terrain tests, and may be found on pages 16 - 18.

Curves plotted from camber angle tests show a negative drag load at all vertical loads. However, these loads are very close to the instrumentation accuracy and can therefore be considered negligible. The side load varied from 25% of vertical load to 70% of vertical load.

Curves plotted from caster angle tests show that drag load can again be considered negligible. During these runs the ratio of side load to vertical load reached a maximum of approximately four times the vertical load.

Variation in vertical load during an individual run was due to unevenness of the pavement on the runway on which the tests were made.

TEST DATA:

Data submitted in the Appendix.

RECOMMENDATIONS:

It is recommended that if any additional testing is to be done with this rig the friction in the vertical strut should be reduced in order to permit vertical motion and thereby simulate actual reactions during rough terrain tests. Ideally, this action should be provided by an "A" frame parallelogram mounting.

It is further recommended that this type of tire be approved for tests on aircraft up to its rated load of 1500#, as it completed all phases of this testing with no difficulty or signs of failure.

SUBJECT:- Rolling Test - High Flotation Tire.

APPENDIX

CONTENTS OF APPENDIX

APPENDIX (continued)

ITEM | PAGE

Graphs (continued)

SUBJECT:- Rolling Test - High Flotation Tire.

APPENDIX

LIST OF PHOTOGRAPHS:

Number	Title
38911	Condition of tire after steering test.
38948	Test rig and tractor.
38970	Ditch simulating pot hole.
38971	Obstacles simulating ruts and bumps.
39011	Control Panel.
39012	Turn Indicator Helipot.
39013	Tire and Strut.

SUBJECT:- Rolling Test - High Flotation Tire.

APPENDIX

LOG OF TEST:

Date	
12-22-58	Received test request and folder.
1-13-59	Completed FAMD Drawing TM-327
1-16-59	Completed test procedure.
1-22-59	Made two smooth pavement runs.
2-2-59	Made two smooth pavement runs. Axle seized tight. Discovered damaged spacer on axle. Spacer removed and hub relocated with set screws.
2-5-59	Made two smooth pavement runs and 17 runs over obstacles.
2-6-59	Made three runs over obstacles. Axle started to work out of hub. Added additional set screw with locating hole in axle.
2-12-59	Made fifteen runs - smooth pavement and obstacle.
2-13-59	Made fourteen runs over obstacles.
2-17-59	Made three runs over obstacles. Truck hit obstacles on third run - broke obstacles.
2-19-59	Made one run on smooth pavement at 25° camber angle. Couldn't raise the tire after run with side of rig. Reduced angle to 15° for future runs.
2-24-59	Made eight runs at 15° camber angle at 0-40-0 MPH.
2-25-59	Made ten runs "steering" the tire.
3-2-59	Made thirteen runs over ditch and two runs over 8" obstacle for film purposes.
3-3-59	Made five runs steering the tire and two runs at 15° caster angle.
3-9-59	Made two runs on dirt and made three smooth pavement runs at 15° caster angle.

MODEL | PREPARED BY | CHECKED BY | APPROVED BY

SUBJECT:- High Flotation Tire - Rolling Tests.

DATE

REVISED

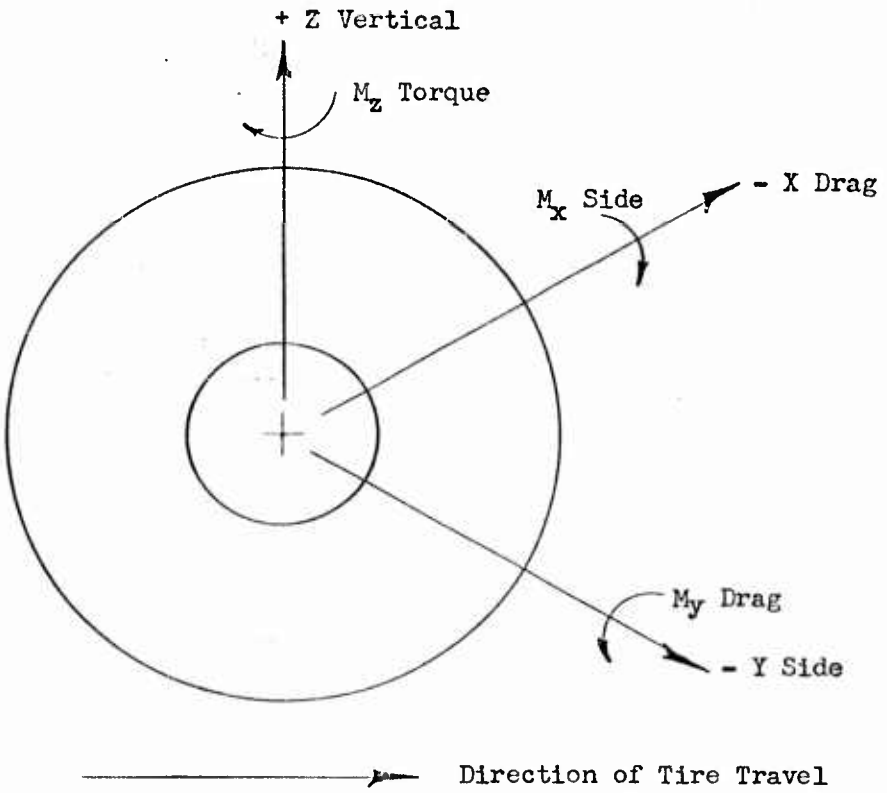

DYNAMOMETER CROSS CHANNEL RESPONSE

Applied Load	Vertical	Side	Drag	M_y (Drag)	M_x (Side)	M_z (Torque)
Vertical	1.0	-41#/1000#	0	-270"#/1000#	0	+590"#/1000#
Side	0	1.0	0	0	0	0
Drag	0	0	1.0	0	0	0
M_y (Drag)	0	0	0	1.0	0	0
M_x (Side)	0	0	0	0	0*	0
M_z (Torque)	0	0	0	0	0	1.0
Accuracy of Readings	± 70#	± 30#	± 30#	± 400"#		± 1000"#

* The side moment bridge is so insensitive that no readings were ever noted for this reaction.

STATIC TEST LABORATORY DATA SHEET

FAIRCHILD AIRCRAFT DIVISION

PAGE _____ OF _____

PROJECT: High Flotation Tire DATE _____

MODEL: _____ CONDITION: Obstacle Test

TEST NO. _____ TESTED BY: _____

STRESS WITNESS: _____ CUSTOMER INSPECTION: _____

Record No.					Peak Loads Occuring at Obstacles			
	Obstacle Height	Tire Pressure	Vert. Load Lbs.	Act. Vertical Load	Vert. Load Lbs.	Drag Load Lbs.	Side Moment In. Lbs.	Wheel Speed
12192	2"	4	1500	2400	3800	336 -895	-5285	28.6
12195	2"	4	1500	2800	4660	496 -870	-5285	40.1
12246	2"	4	3000	5470	8542	315 -1347	-2610	30.5
12247	2"	4	3000	5470	8817	516 -1081	-2610	19.5
12203	2"	8	1500	2870	5897	280 -1036	-5285	40.1
12204	2"	12	1500	2200	5292	336 -730	-7926	19.6
12206	2"	12	1500	3070	5065	392 -440	-10570	43.0
12218	2"	12	3000	5200	8392	590 -810	-2610	19.1
12219	2"	12	3000	5670	9148	560 -560	-2610	39.1
12207	2"	12	1500	2270	5443	390 -924	-7925	19.1
12208	2"	12	1500	3000	6274	365 -645	-13210	43.0
12220	2"	12	3000	5670	8921	812 -980	+2610	19.8
12201	2"	4	1500	2670	5443	364 -616	+2642	39.6
12209	2"	12	1500	2530	5821	420 -644	-18494	19.1
12210	2"	12	1500	1270	4460	476 -644	-15852	44.4
12248	2"	12	3000	3330	5373	-744	-18270	19.1
12250	2"	12	4500	3070	6338	1005 -1405	-23490	19.1
12249	2"	12	3000	2270	5373	485 -1060	-23490	38.7
12251	2"	12	4500	2600	5857	716 -1115	-26100	40.6
12253	2"	16	1500	270	4684	945 -1175	-36540	33.9
12254	2"	24	1500	4930	10540	746 -831	-41760	19.1

STATIC TEST LABORATORY DATA SHEET

FAIRCHILD AIRCRAFT DIVISION

PAGE _____ OF _____

PROJECT: High Flotation Tire DATE _____

MODEL: _____ CONDITION: Obstacle Test

TEST NO. _____ TESTED BY: _____

STRESS WITNESS: _____ CUSTOMER INSPECTION: _____

Record No.					Peak Loads Occuring at Obstacles			
	Obstacle Height	Tire Pressure	Vert. Load Lbs.	Act. Vertical Load	Vert. Load Lbs.	Drag Load Lbs.	Side Moment In.Lbs.	Wheel Speed
12255	2"	24	3000	8600	14329	532 -945	-41760	20.5
12256	2"	24	4500	9130	15018	831 -1261	-39150	21.5
12274	4"	4	1500	1730	4800	-960	10440	20.5
12263	4"	24	1500	4400	11573	-1980	23490	16.0
12282	6"	12	1500	1800	8200	620 -1525	18270	20.0
12285	6"	24	1500	1930	11939	1551 -2115	33930	19.6
12280	6"	12	3000	3130	10800	790 -1380	18270	20.2
12281	6"	12	4000	3750	11601	902 -1890	23490	19.6
12372	6"	4	1500	2130	6067	365 -1410	13050	27.9
12276	6"	12	1500	1800	9067	620 -1551	15660	20.2
12277	6"	12	3000	3400	11467	565 -1380	15660	19.3
12278	6"	12	4000	3330	10533	790 -1580	15660	18.6
12433	8"	3	1200	270	3067	620 -935	10760	6.9
12436	8"	3	1200	330	3000	900 -1020	5380	11.5
12428	4"deep	4	1500	1330	800	680 -535	18830	10.5
12437	4"deep	12	1500	3670	133	735 -650	8070	16.0
12431	8"deep	4	1500	1400	933	765 -735	18830	16.0
12432	12"deep	4	1500	3670	1067	765 -1045	10760	*
12440	12"deep	24	1500	1530	400	850 -480	5380	12.9
12241	12"deep	24	3000	2400	400	595 -170	8070	13.2
12442	12"deep	24	4500	3400	133	790 -510	64550	14.8

STATIC TEST LABORATORY DATA SHEET

FAIRCHILD AIRCRAFT DIVISION

PAGE _____ OF _____

PROJECT: High Flotation Tire - Rolling Tests DATE _____

MODEL: M-245 CONDITION: Drag versus Vertical Load at Various Tire Press.

TEST NO. _____ TESTED BY: _____

STRESS WITNESS: _____ CUSTOMER INSPECTION: _____

Record Number	Vert. Load	Drag Load	Tire Pressure					
12198	2670#	501#	4 PSI					
12245	5130#	1512#	4 PSI					
12247	5470#	1395#	4 PSI					
12204	2200#	639#	12 PSI					
12218	5200#	1037#	12 PSI					
12250	3070#	1686#	12 PSI					
12254	4930#	1512#	24 PSI					
12255	8600#	1366#	24 PSI					
12256	9130#	1221#	24 PSI					
	NOTE: THESE READINGS WERE TAKEN AT THE SAME POINT -							
	JUST BEFORE THE TIRE HIT THE OBSTACLES DURING ROUGH							
	TERRAIN TESTS.							

FA-800-22

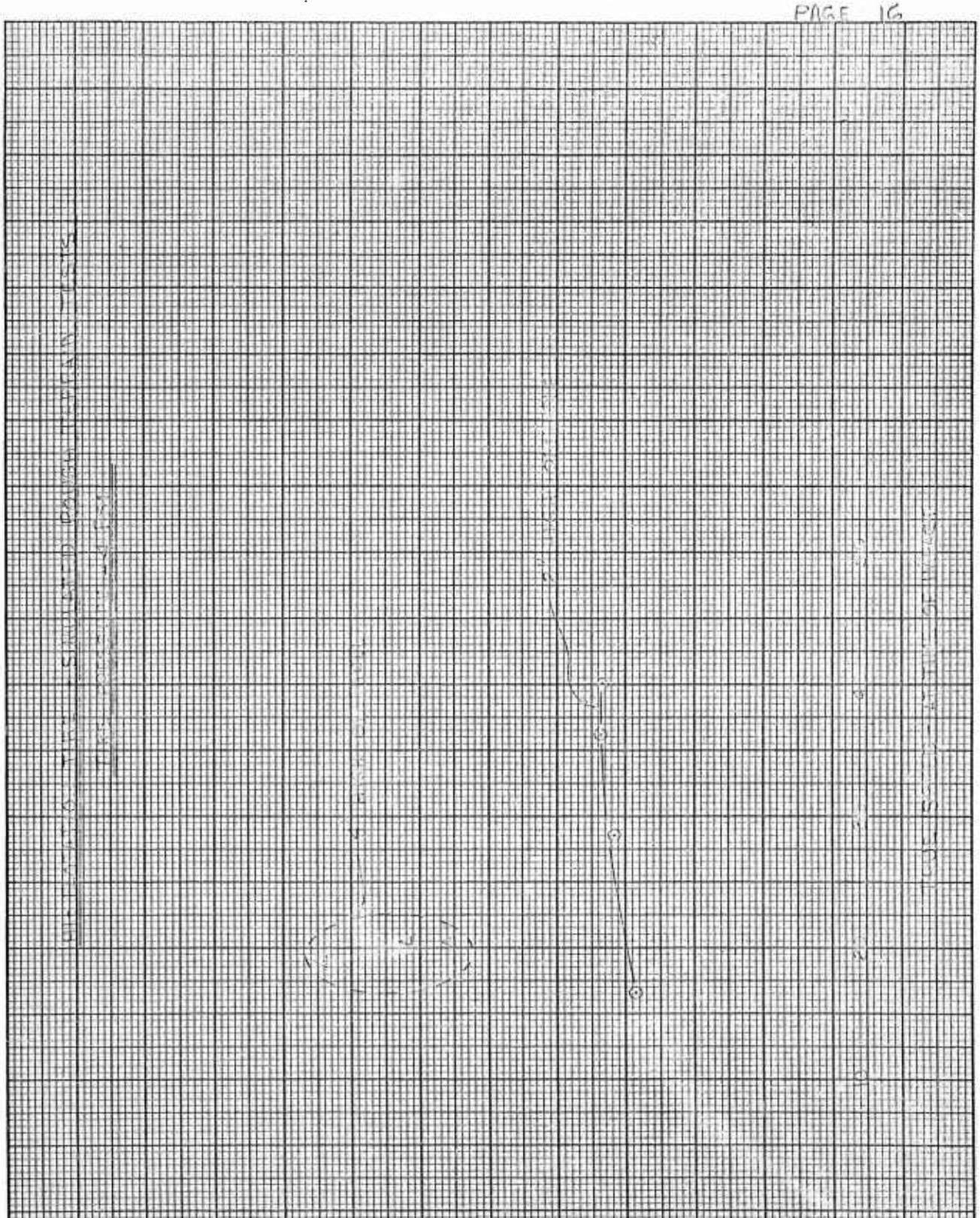

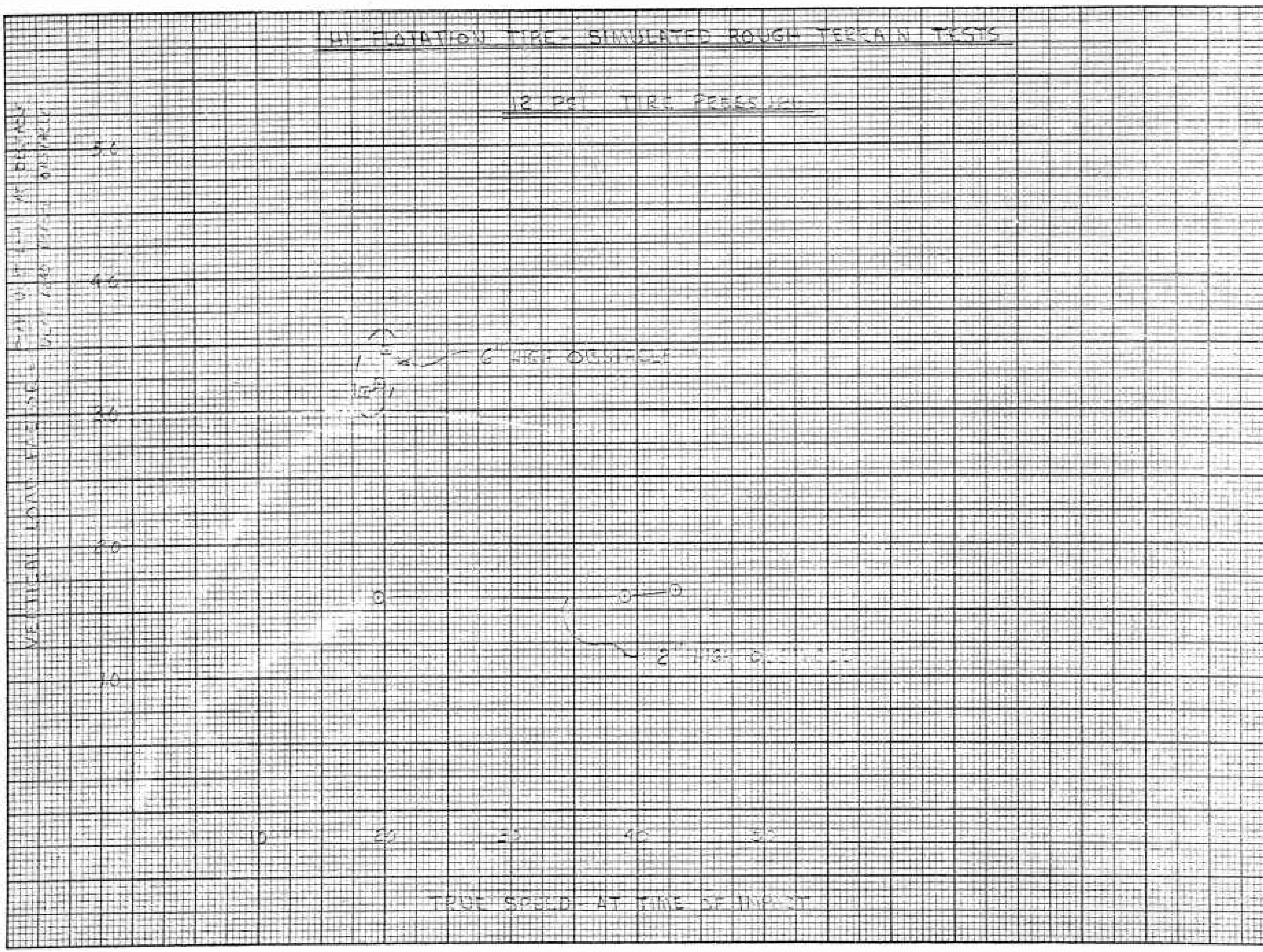
HI-FLOTATION TIRE - SIMULATED ROUGH TERRAIN TESTS
12 PSI TIRE PRESSURE
6" HIGH OBSTACLE
2" HIGH OBSTACLE
10
20
30
40
50
TRUE SPEED AT TIME OF IMPACT

B.E.K. 4-16-??

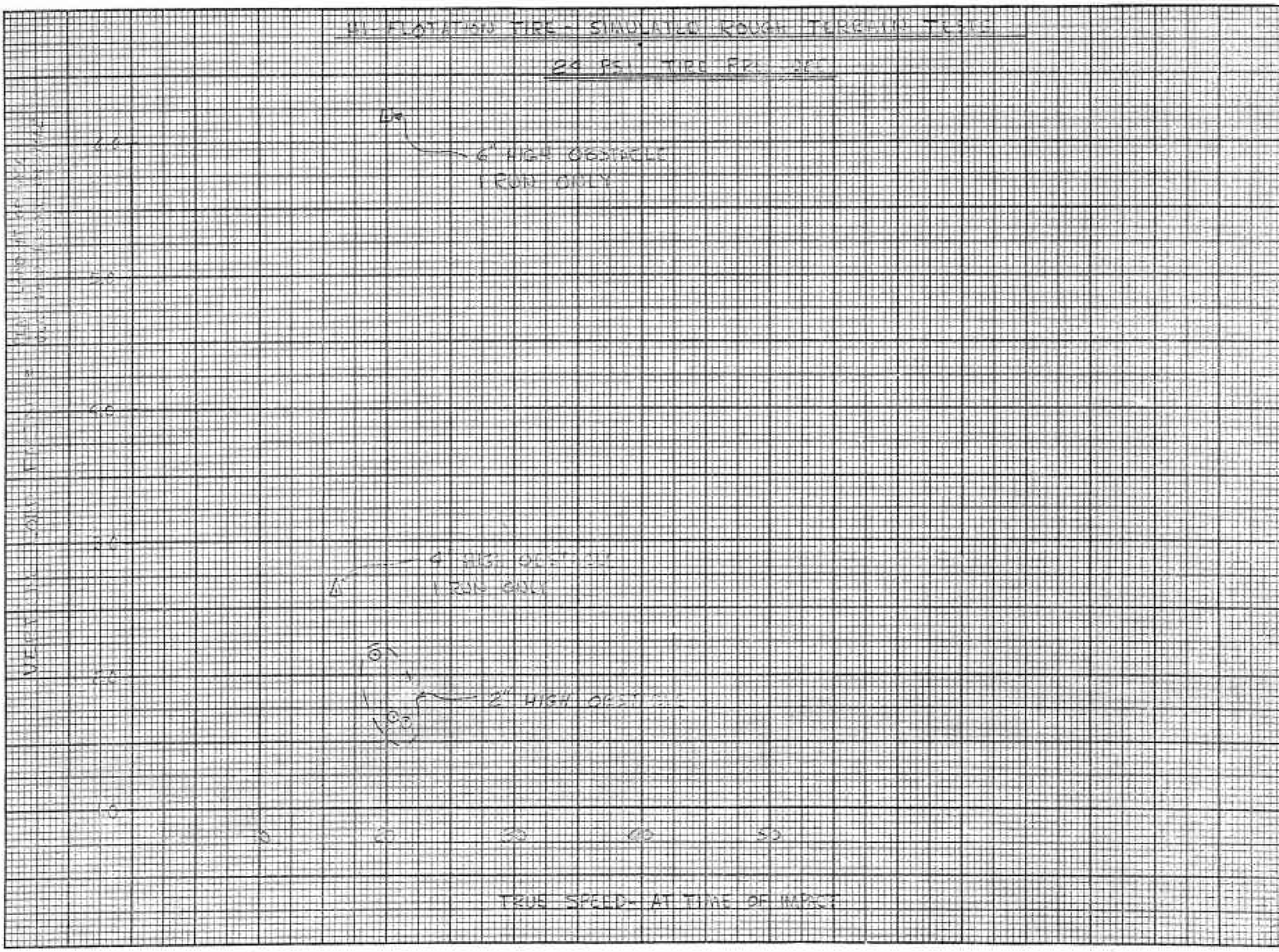
FLOTATION TIRE - SIMULATED ROUGH TERRAIN TESTS
24 PSI TIRE
6" HIGH OBSTACLE
1 RUN ONLY
4" HIGH OBSTACLE
1 RUN ONLY
2" HIGH OBSTACLE
5.0
4.0
3.0
2.0
1.0
10
20
30
40
50
TRUE SPEED - AT TIME OF IMPACT

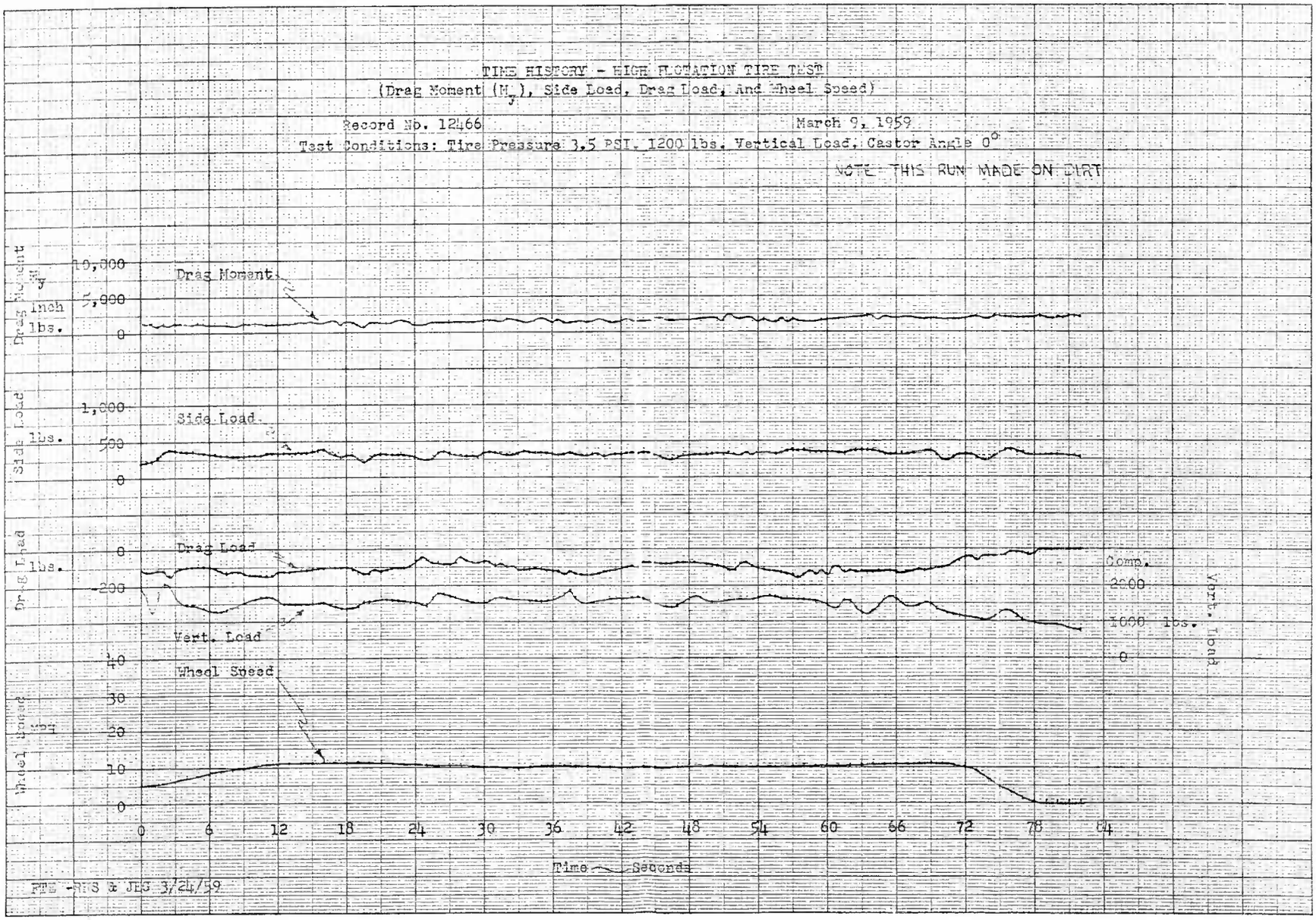
TIME HISTORY - HIGH FLOTATION TIRE TEST
(Drag Moment (M_y), Side Load, Drag Load, And Wheel Speed)
Record No. 12466
March 9, 1959
Test Conditions: Tire Pressure 3.5 PSI, 1200 lbs. Vertical Load, Castor Angle 0°
NOTE: THIS RUN MADE ON DIRT
Drag Moment
Side Load
Drag Load
Vert. Load
Wheel Speed
Drag Moment M_y Inch lbs.
10,000
5,000
0
Side Load lbs.
1,000
500
0
Drag Load lbs.
0
-200
Comp.
2000
1600 lbs.
0
Vert. Load
Wheel Speed MPH
40
30
20
10
0
0 6 12 18 24 30 36 42 48 54 60 66 72 78 84
Time — Seconds
FTE - HS & JES 3/24/59

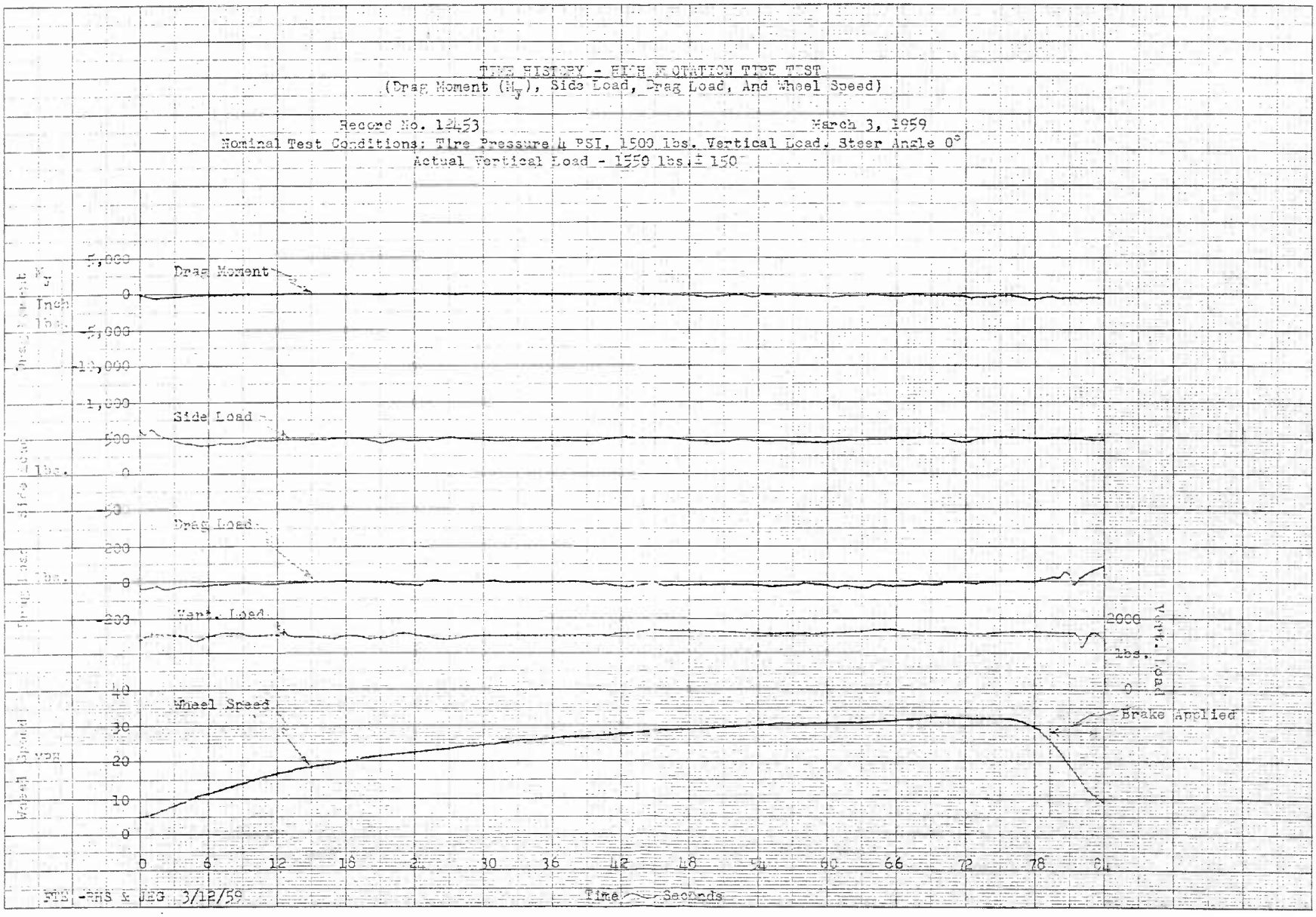
TIME HISTORY - HIGH ROTATION TIRE TEST
(Drag Moment (M_y), Side Load, Drag Load, And Wheel Speed)
Record No. 1243
March 3, 1959
Nominal Test Conditions: Tire Pressure 4 PSI, 1500 lbs. Vertical Load, Steer Angle 0°
Actual Vertical Load - 1550 lbs. ± 150
Drag Moment
Side Load
Drag Load
Wheel Load
Wheel Speed
Brake Applied
Vertical Load
2000 lbs.
0
5,000
0
-5,000
-10,000
1,000
500
0
-500
200
0
-200
40
30
20
10
0
0
6
12
18
24
30
36
42
48
54
60
66
72
78
84
Time — Seconds
FTE -RHS & JEG 3/12/59

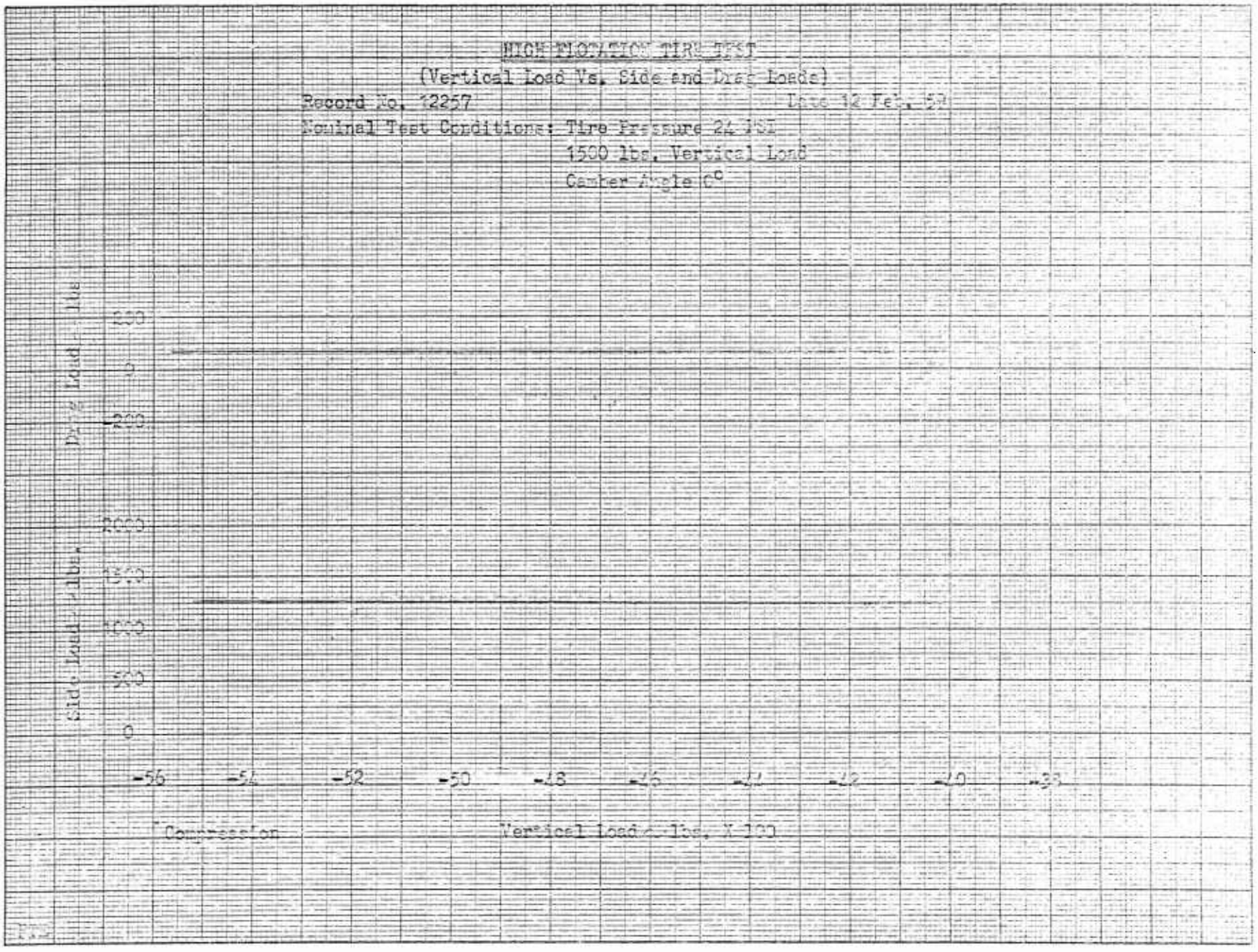
HIGH ELEVATION TIRE TEST
(Vertical Load Vs. Side and Drag Loads)
Record No. 12257
Date 12 Feb. 52
Nominal Test Conditions: Tire Pressure 24 PSI
1500 lbs. Vertical Load
Camber Angle 0°
Side Load - Lbs.
Drag Load - Lbs.
600
0
-600
2000
1500
1000
500
0
-56
-54
-52
-50
-48
-46
-44
-42
-40
-38
Compression
Vertical Load - Lbs. X 100

Page 21

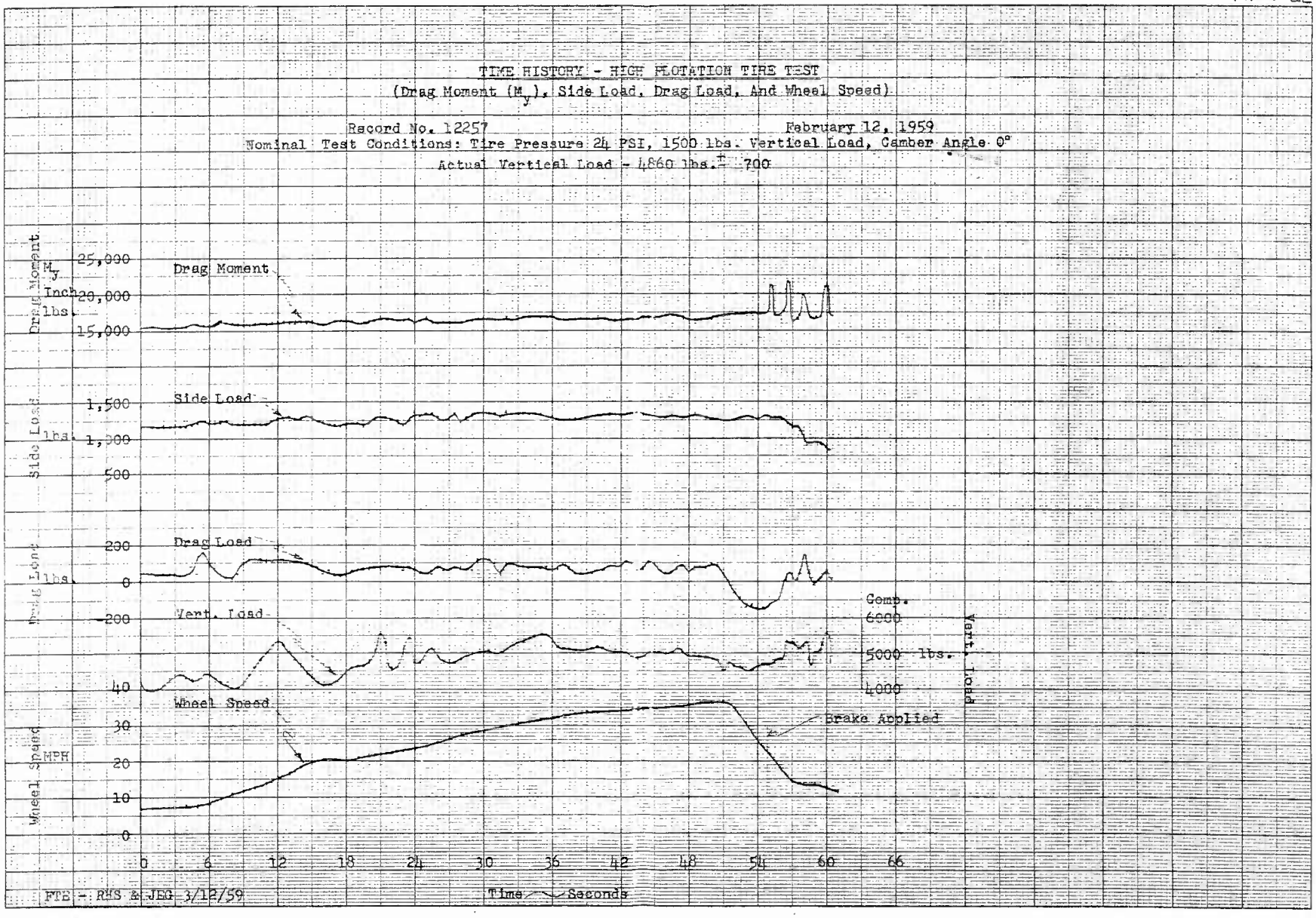
TIME HISTORY - HIGH FLOTATION TIRE TEST
(Drag Moment (M_y), Side Load, Drag Load, And Wheel Speed)
Record No. 12257
February 12, 1959
Nominal Test Conditions: Tire Pressure 24 PSI, 1500 lbs. Vertical Load, Camber Angle 0°
Actual Vertical Load - 4860 lbs. ± 700
Drag Moment M_y Inch lbs.
25,000
20,000
15,000
Drag Moment
Side Load lbs.
1,500
1,000
500
Side Load
Drag Load lbs.
200
0
-200
Drag Load
Vert. Load
Comp.
6000
5000 lbs.
4000
Vert. Load
40
30
20
10
0
Wheel Speed MPH
Wheel Speed
Brake Applied
0
6
12
18
24
30
36
42
48
54
60
66
Time — Seconds
FTE - RHS & JEG 3/12/59

TIME HISTORY - HIGH FLOTATION TIRE TEST

(Drag Moment (M_y), Side Load, Drag Load, And Wheel Speed)

Record No. 12451 March 3, 1959

Nominal Test Conditions: Tire Pressure 4 PSI, 1000 lbs. Vertical Load, Steer Angle 10°R-0-10°L

Actual Vertical Load - 1000 lbs. ± 200

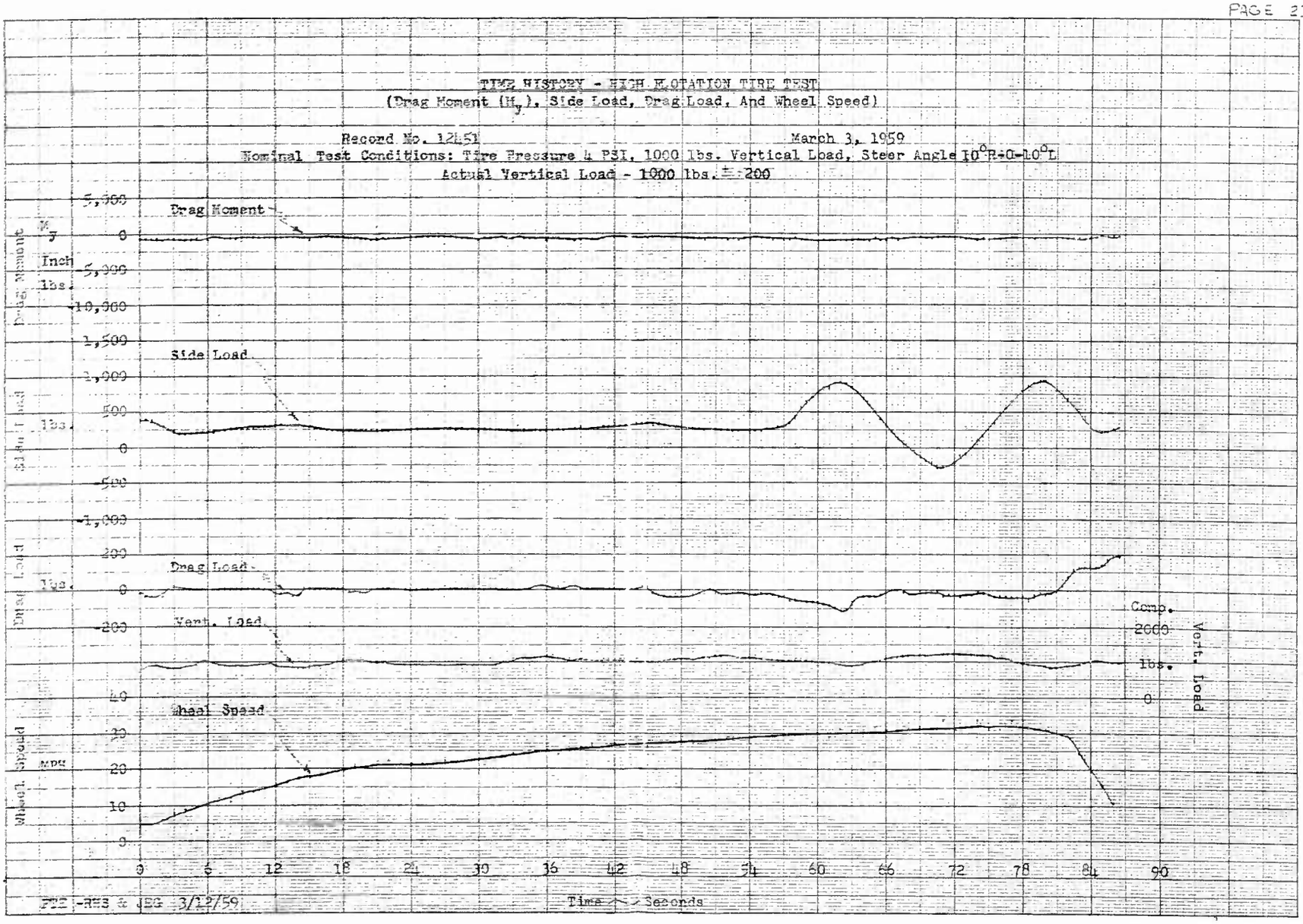

TIME HISTORY - HIGH FLOTATION TIRE TEST
(Drag Moment (M_y), Side Load, Drag Load, And Wheel Speed)

Record No. 12452 March 3, 1959

Nominal Test Conditions: Tire Pressure 4 PSI, 1500 lbs. Vertical Load, Steer Angle 10°R-0-10°L

Actual Vertical Load - 1500 lbs. ± 200

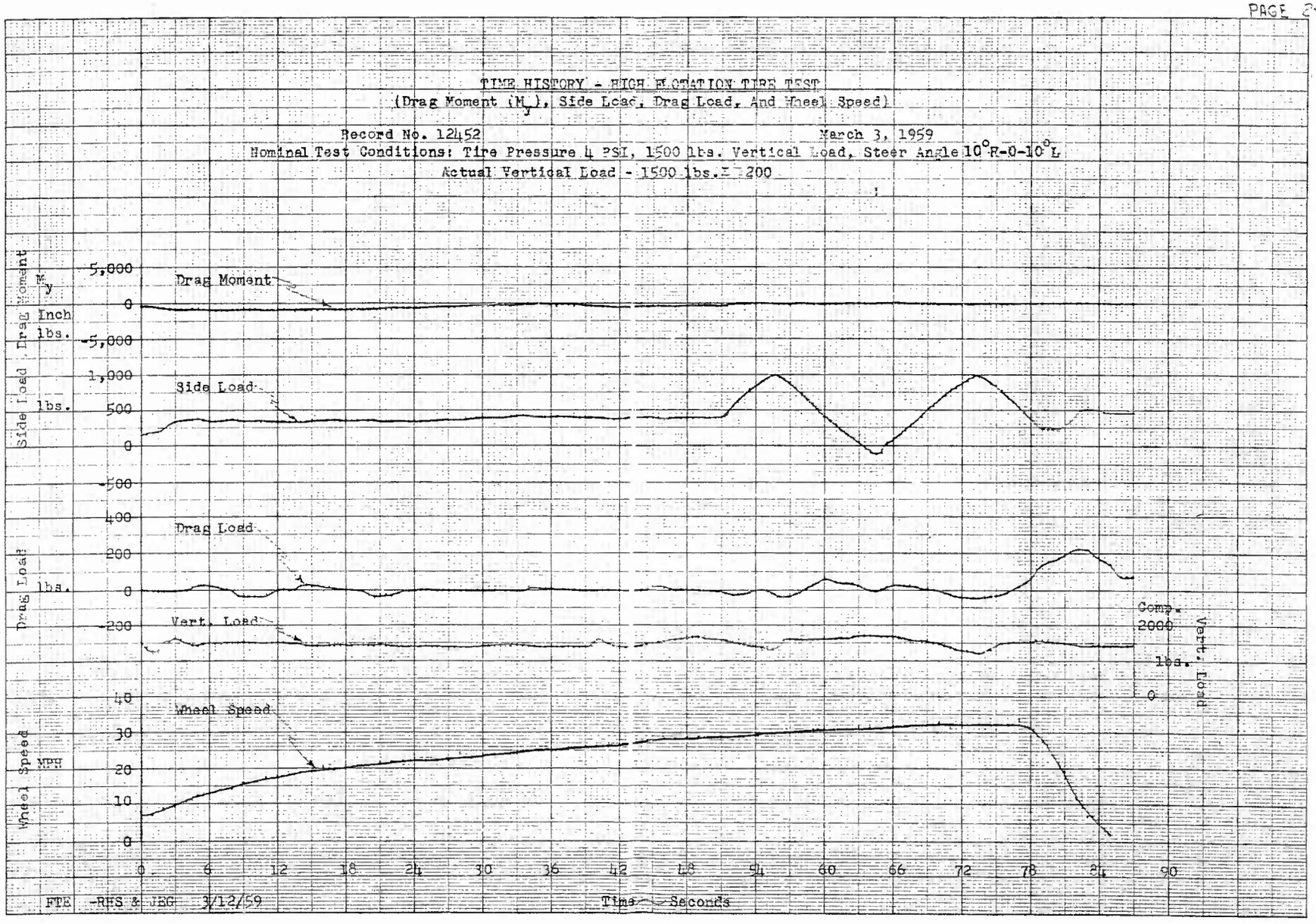

FTE -RHS & JBG 3/12/59

TIME HISTORY - HIGH FLOTATION TIRE TEST

(Drag Moment (My), Side Load, Drag Load, And Wheel Speed)

Record No. 1240$ February 25, 1959

Nominal Test Conditions: Tire Pressure 12 PSI, 1000 lbs. Vertical Load, Steer Angle 10°R-0-10°L

Actual Vertical Load - 1000 lbs. [illegible]

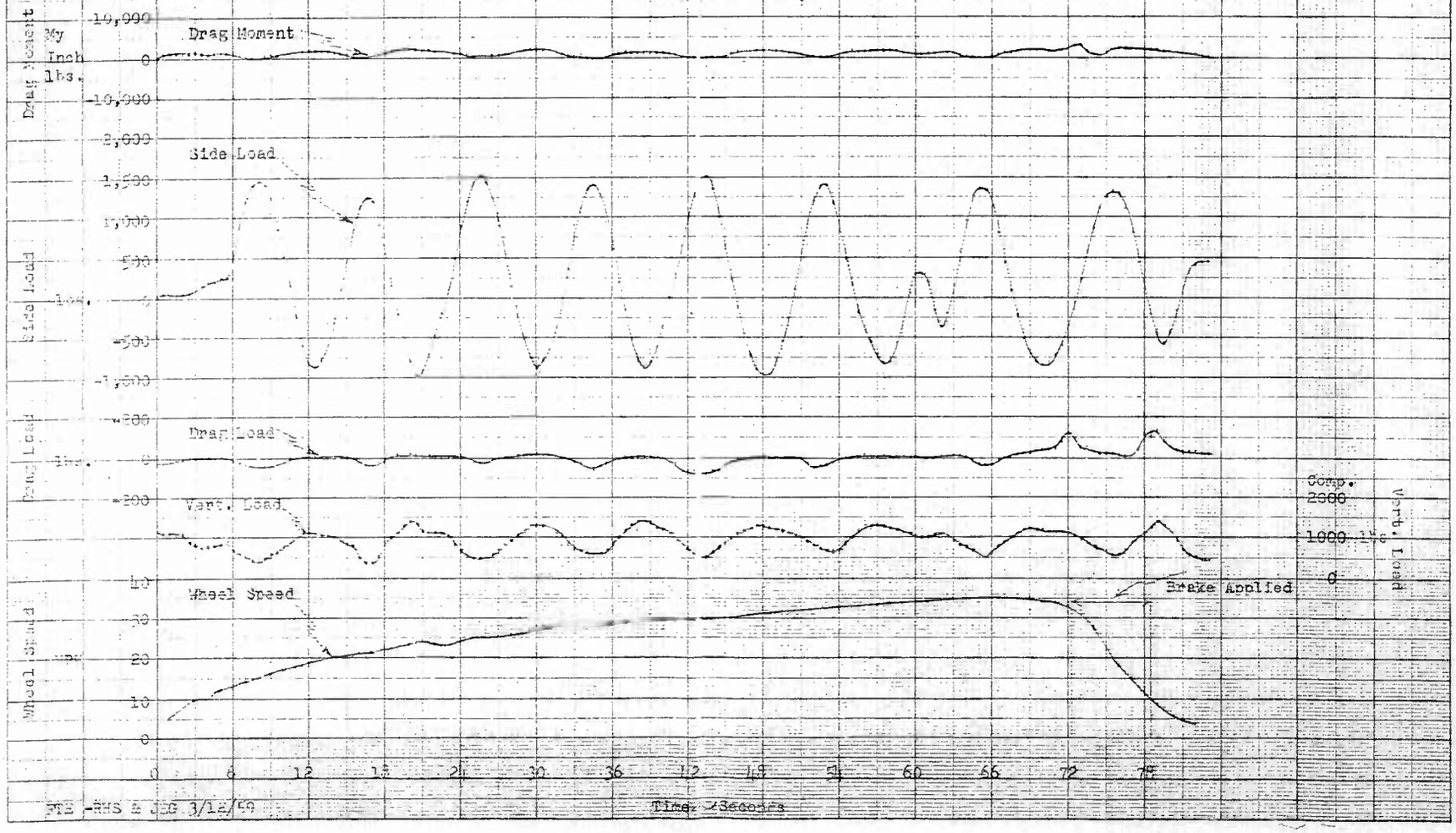

FTE -RHS & JCG 3/12/59

TIME HISTORY - HIGH FLOTATION TIRE TEST
(Drag Moment (My), Side Load, Drag Load, And Wheel Speed)

Record No. 12409 February 25, 1959
Nominal Test Conditions: Tire Pressure 12 PSI, 1500 lbs. Vertical Load, Steer Angle 10°R-0-10°L
Actual Vertical Load - 2000 lbs. ± 500

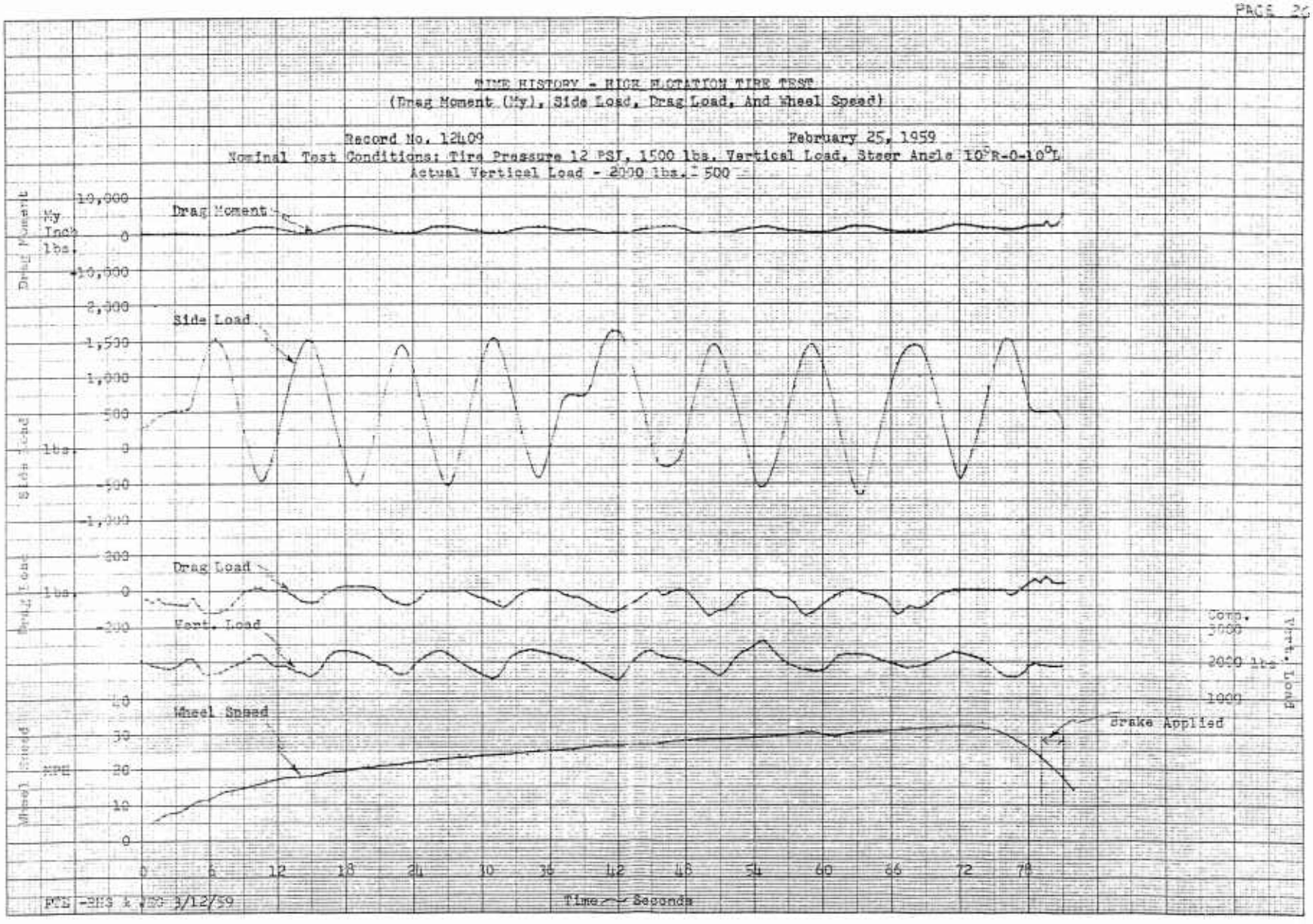

TIME HISTORY- HIGH ELEVATION TIRE TEST

(Drag Moment (My), Side Load, Drag Load, And Wheel Speed)

Record No. 12412 February 25, 1959

Nominal Test Conditions: Tire Pressure 12 PSI, 3000 lbs. Vertical Load, Steer Angle 10°R-C-10°L

Actual Vertical Load = 2500 lbs. ± 500

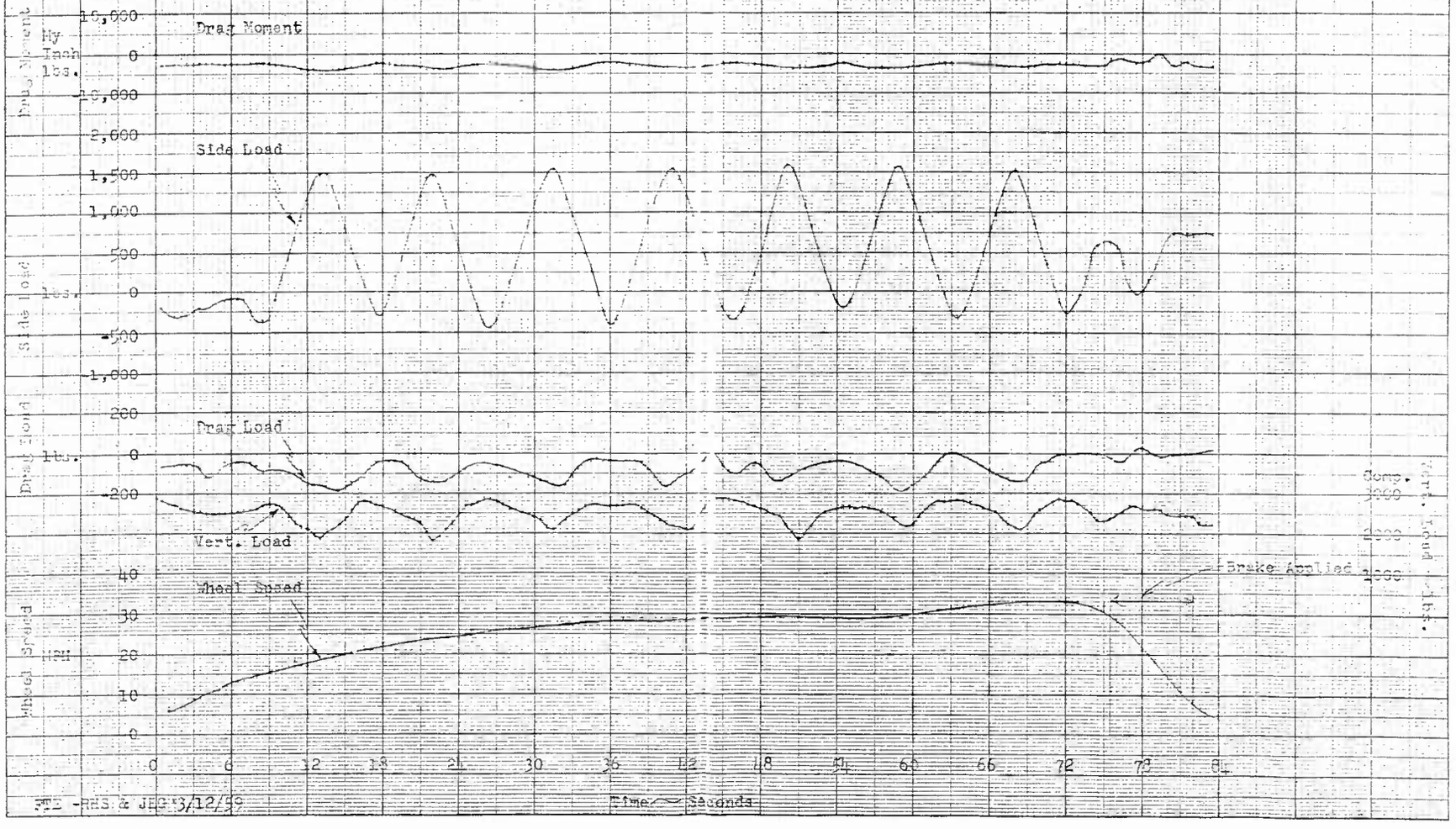

FTD -RHS & JEC 3/12/59

TIME HISTORY - HIGH FLOTATION TIRE TEST
(Drag Moment (My), Side Load, Drag Load, And Wheel Speed)

Record No. 12413 February 25, 1959
Nominal Test Conditions: Tire Pressure 12 PSI, 4500 lbs. Vertical Load, Steer Angle 10°R-0-10°L
Actual Vertical Load - 4200 lbs. ± 500

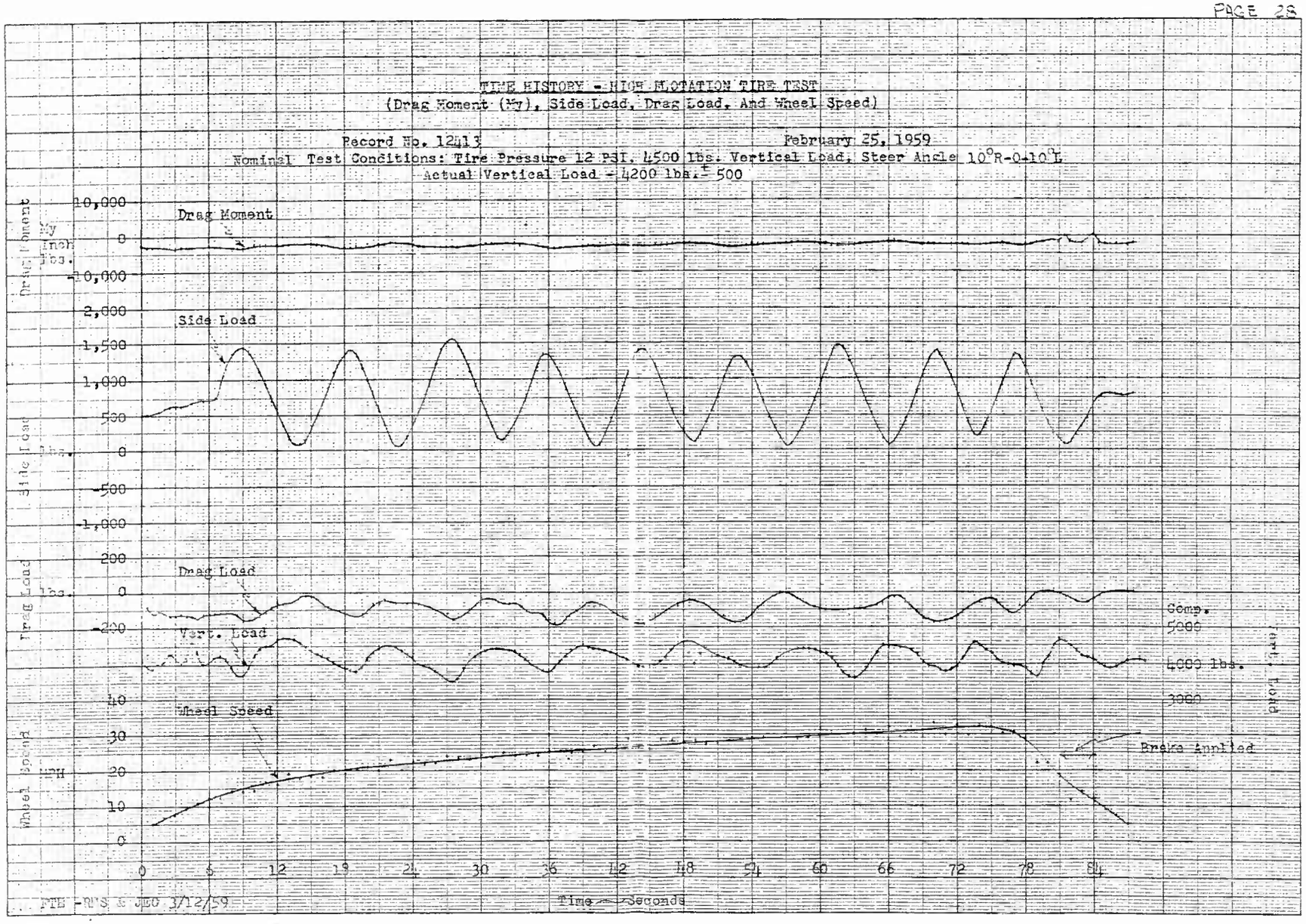

PTE-RWS & JEO 3/12/59

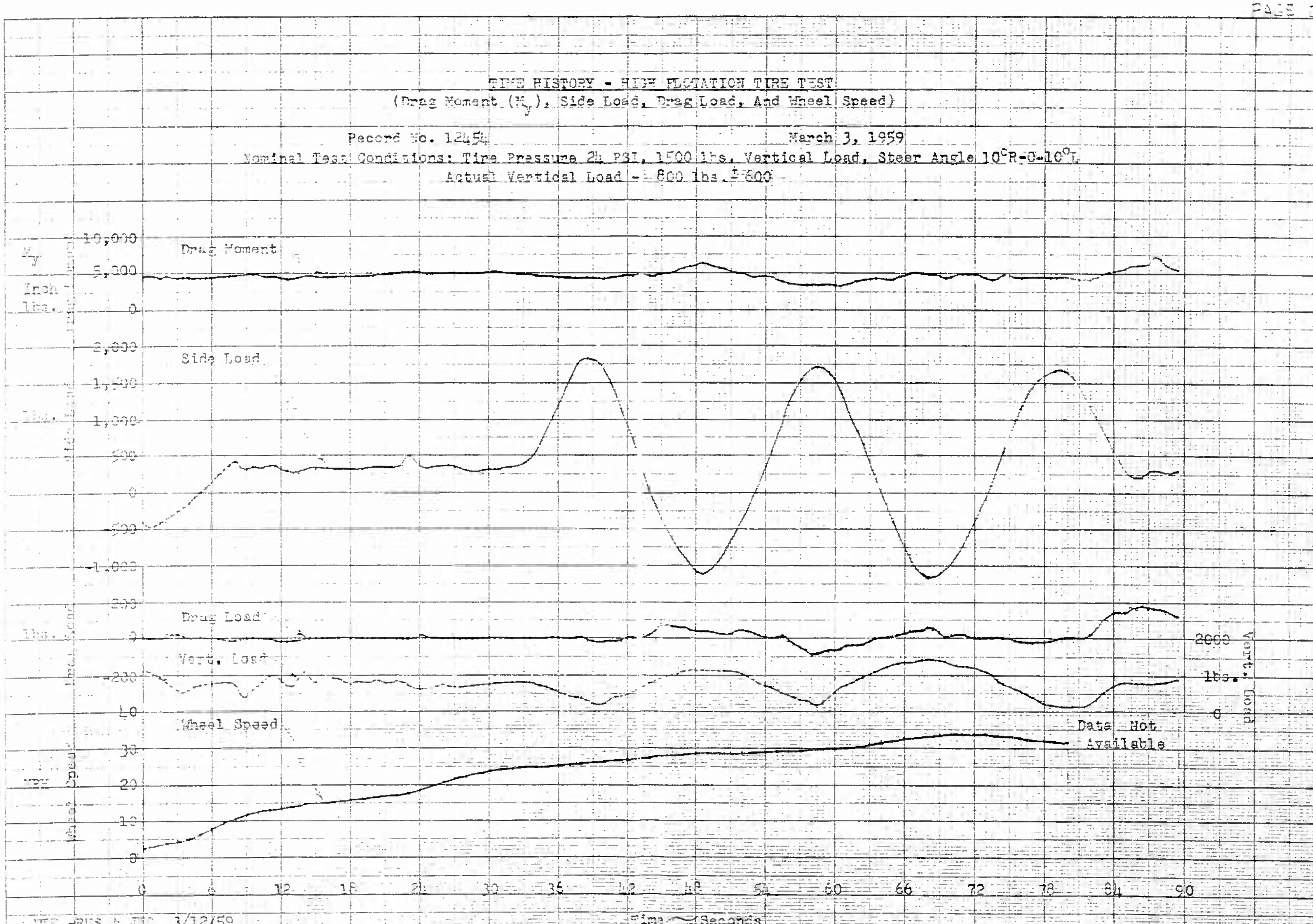
TIME HISTORY - HIGH FLOTATION TIRE TEST
(Drag Moment (M_y), Side Load, Drag Load, And Wheel Speed)
Record No. 12454
March 3, 1959
Nominal Test Conditions: Tire Pressure 24 PSI, 1500 lbs. Vertical Load, Steer Angle 10°R-0-10°L
Actual Vertical Load - 800 lbs. ± 600
M_y
Inch - lbs.
10,000
5,000
0
Drag Moment
Side Load
2,000
1,500
1,000
500
0
-500
-1,000
lbs.
Drag Load
200
0
-200
Vert. Load
Vert. Load
2000
lbs.
0
Wheel Speed
MPH
40
30
20
10
0
Data Not Available
0
6
12
18
24
30
36
42
48
54
60
66
72
78
84
90
Time ~ Seconds
RHS & JHD 3/12/59

TIME HISTORY - HIGH FLOTATION TIRE TEST
(Drag Moment (My), Side Load, Drag Load, And Wheel Speed)

Record No. 12417 February 25, 1959
Nominal Test Conditions: Tire Pressure 24 PSI, 3000 lbs. Vertical Load, Steer Angle 10°R-0-10°L
Actual Vertical Load - 1500 ~~lbs.~~ F 1000

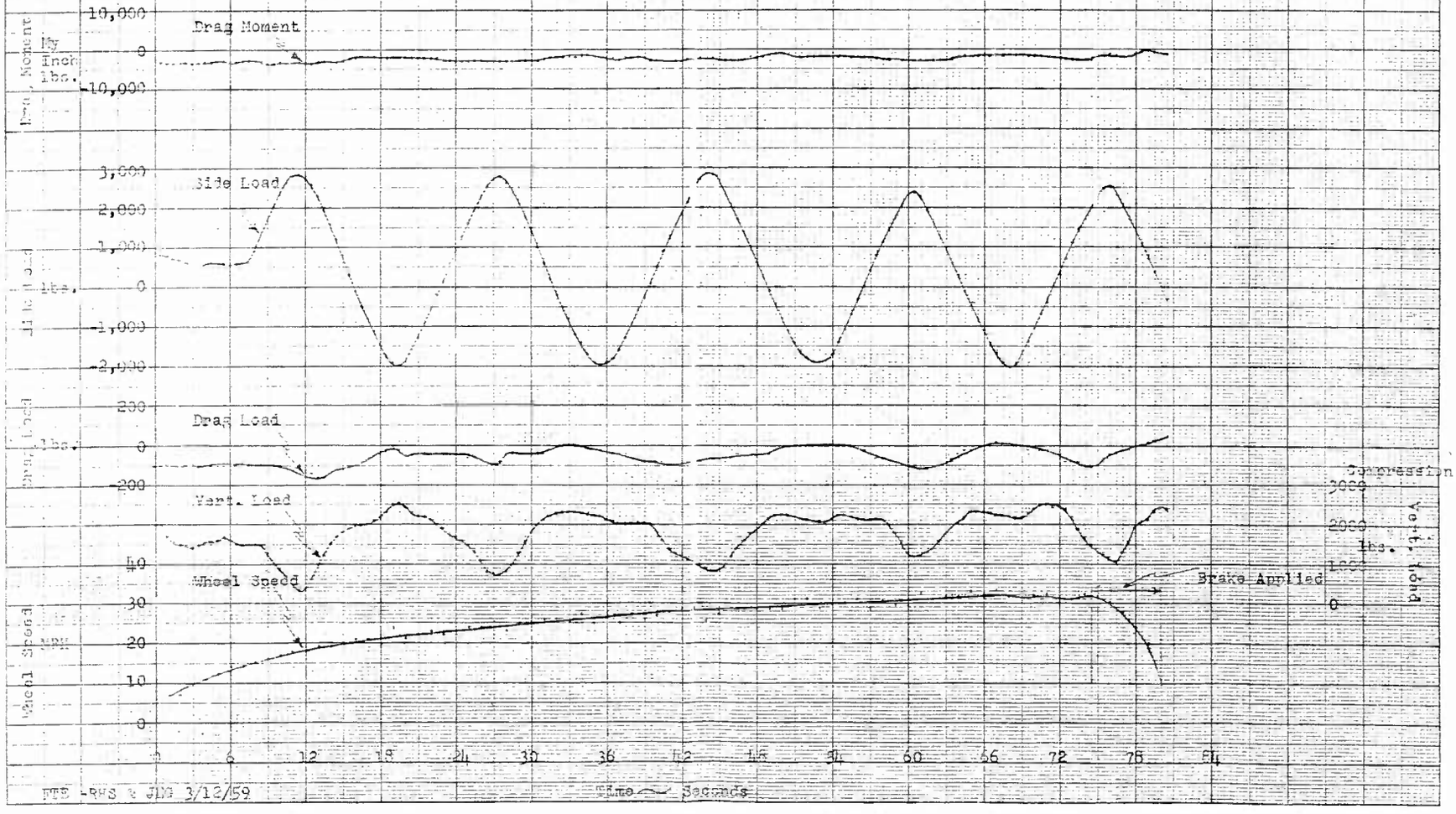

PTE -RHS & JDG 3/12/59

TIME HISTORY - HIGH ROTATION TIRE TEST
(Drag Moment (M_y), Side Load, Drag Load, And Wheel Speed)

Record No. 12455 March 3, 1959

Nominal Test Conditions: Tire Pressure 24 PSI, 4500 lbs. Vertical Load, Steer Angle 10°R-0-10°L

Actual Vertical Load - 3500 lbs. - 500

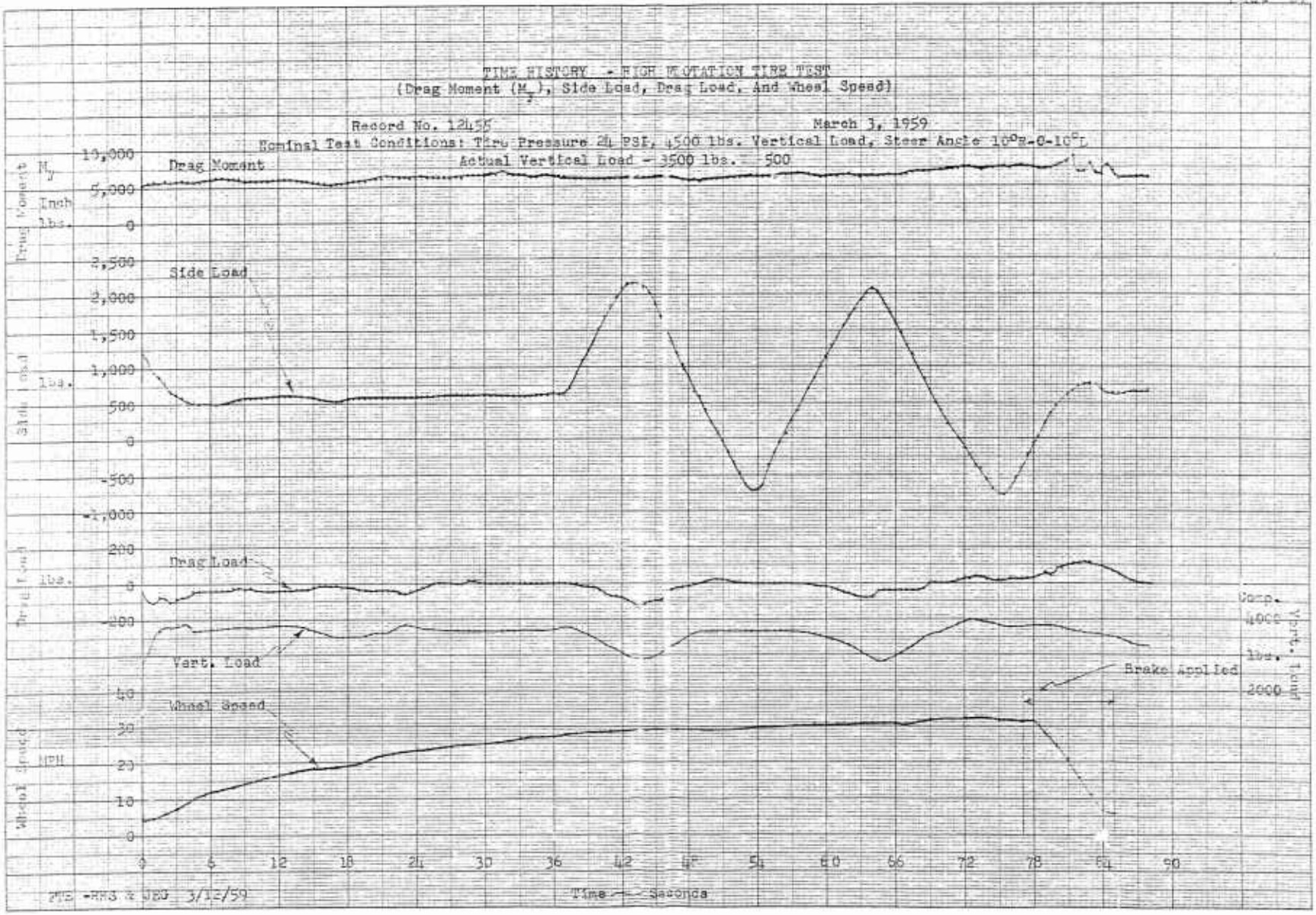

TIRE HISTORY - HIGH FLOTATION TIRE TEST
(Drag Moment (M_y), Side Load, Drag Load, And Wheel Speed)

Record No. 12382 February 19, 1959

Nominal Test Conditions: Tire Pressure 12 PSI, 1500 lbs. Vertical Load, Camber Angle 25°
Actual Vertical Load - 1750 lbs. ± 300

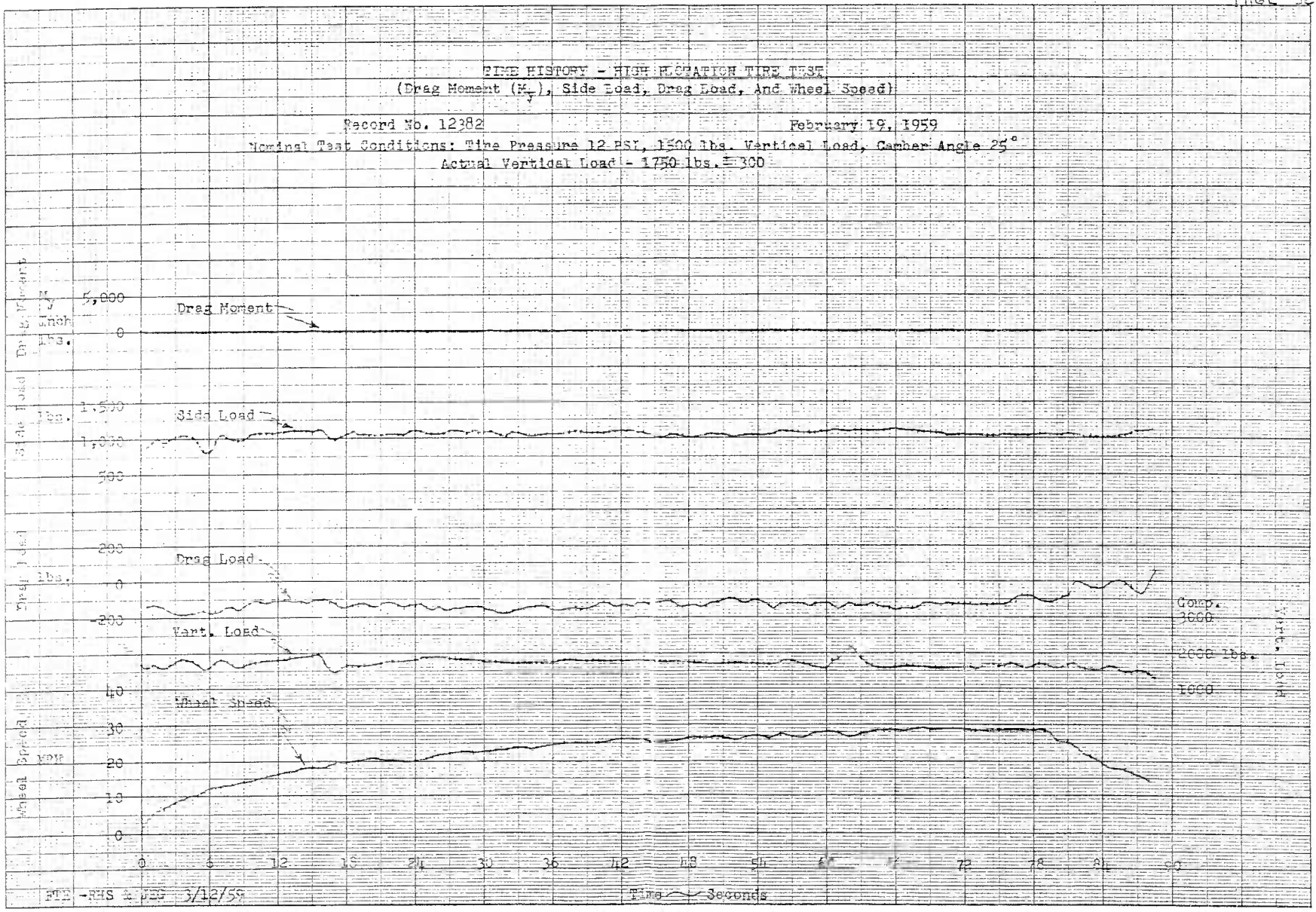

HIGH FLOTATION TIRE TEST

(Vertical Load Vs.Side and Drag Loads)

Record No. 12391 Date 25 Feb. 59

Nominal Test Conditions: Tire Pressure 12 PSI
1500 lbs. Vertical Load
Camber Angle 15°

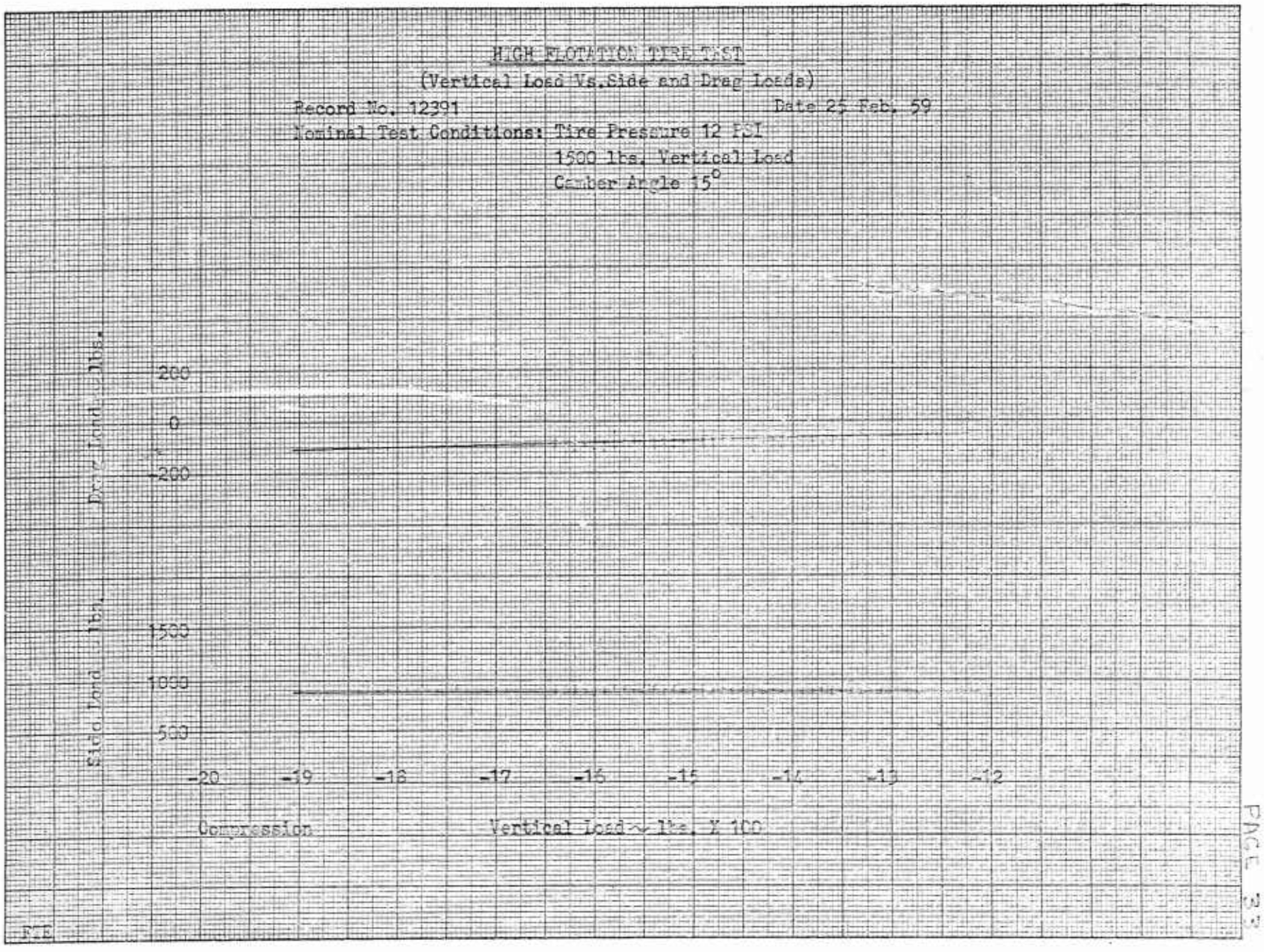

FIE

TIME HISTORY - HIGH FLOTATION TIRE TEST
(Drag Moment (M_y), Side Load, Drag Load, And Wheel Speed)

Record No. 12391 February 25, 1959
Nominal Test Conditions: Tire Pressure 12 PSI, 1500 lbs. Vertical Load, Camber Angle 15°
Actual Vertical Load - 1500 lbs. ±300

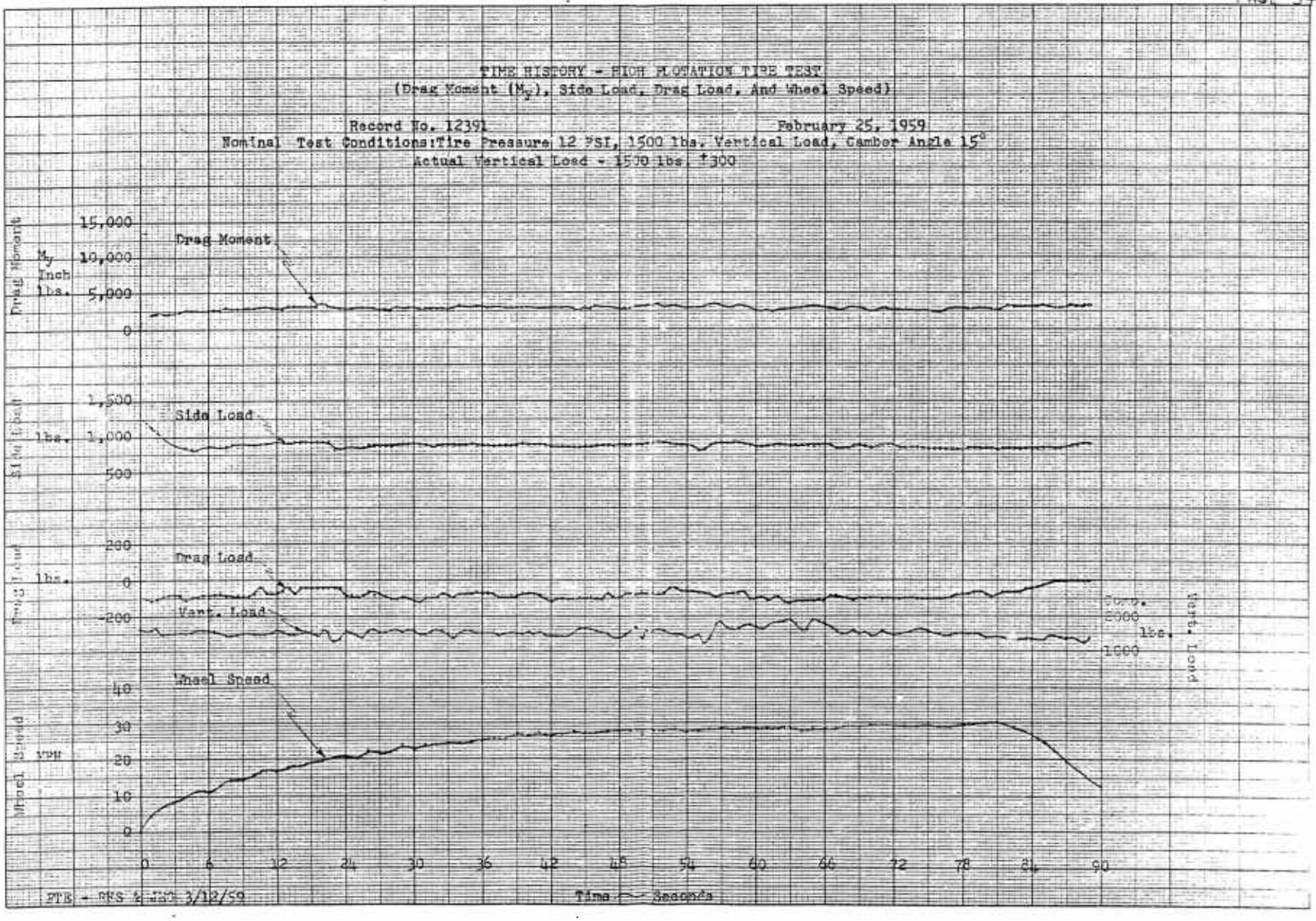

HIGH FLOTATION TIRE TEST

(Vertical Load Vs. Side and Drag Loads)

Record No. 12392 Date 25 Feb. 59

Nominal Test Conditions: Tire Pressure 12 PSI
3000 lbs. Vertical Load
Camber Angle 15°

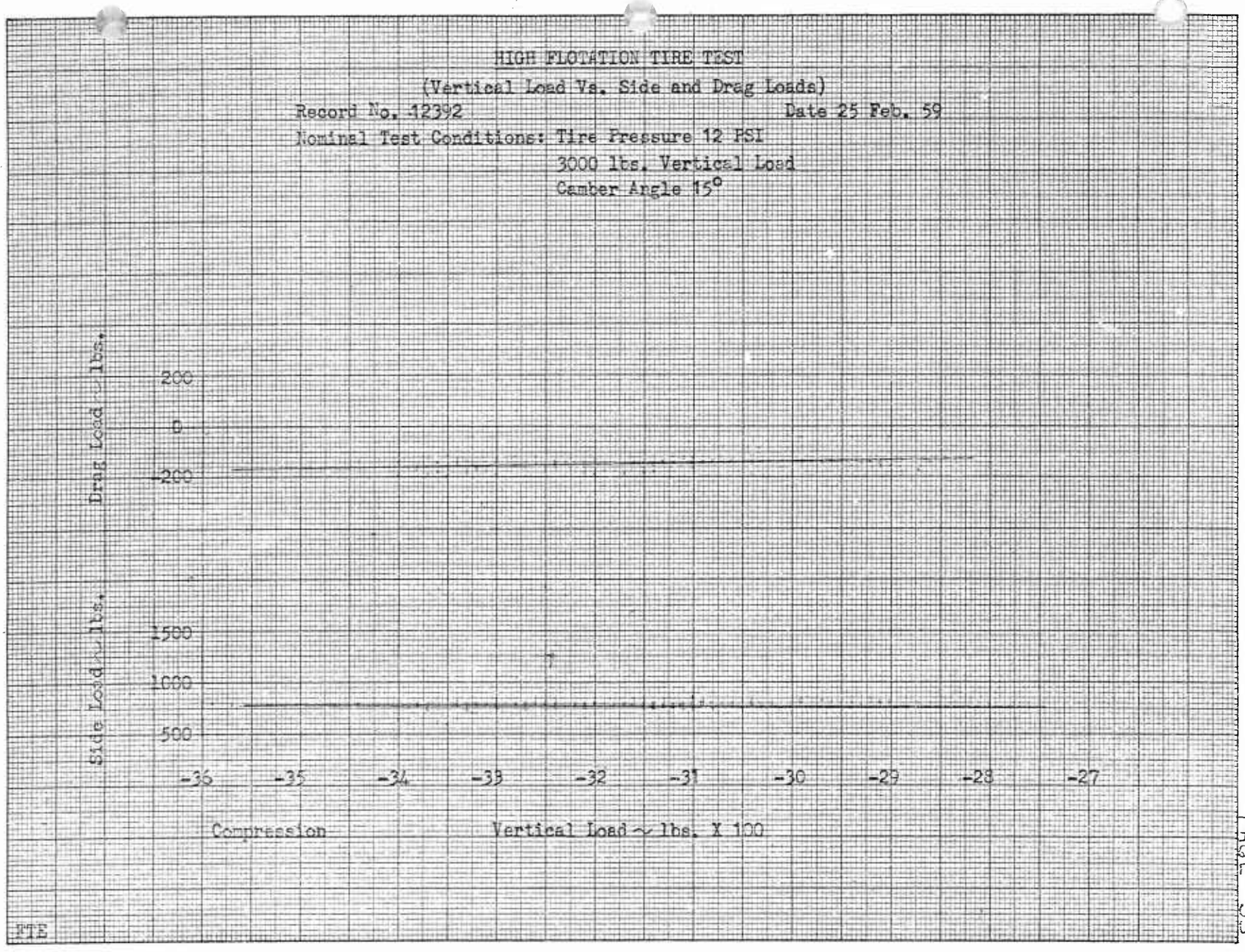

FTE

TIME HISTORY - HIGH ROTATION TIRE TEST
(Drag Moment (M_y), Side Load, Drag Load, And Wheel Speed)

Record No. 12392 February 25, 1959
Nominal Test Conditions: Tire Pressure 12 PSI, 3000 lbs. Vertical Load, Camber Angle 15°
Actual Vertical Load = 3200 lbs. ±400

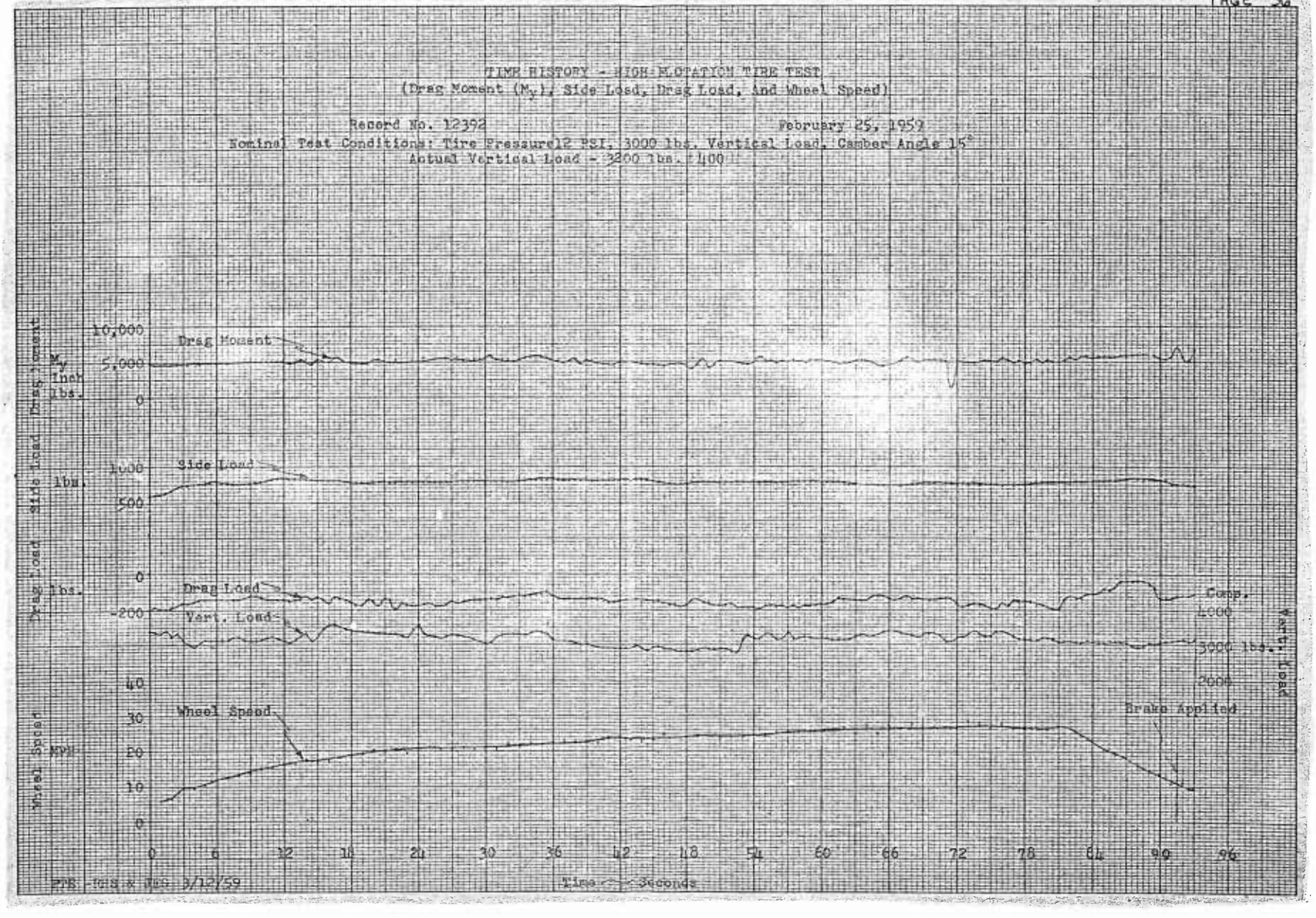

TIME HISTORY - HIGH ROTATION TIRE TEST

(Drag Moment (M_y), Side Load, Drag Load, And Wheel Speed)

Record No. 12393 February 25, 1959

Nominal Test Conditions: Tire Pressure 20 PSI, 1500 lbs. Vertical Load, Camber Angle 15°

Actual Vertical Load - 1400 lbs. - 30°

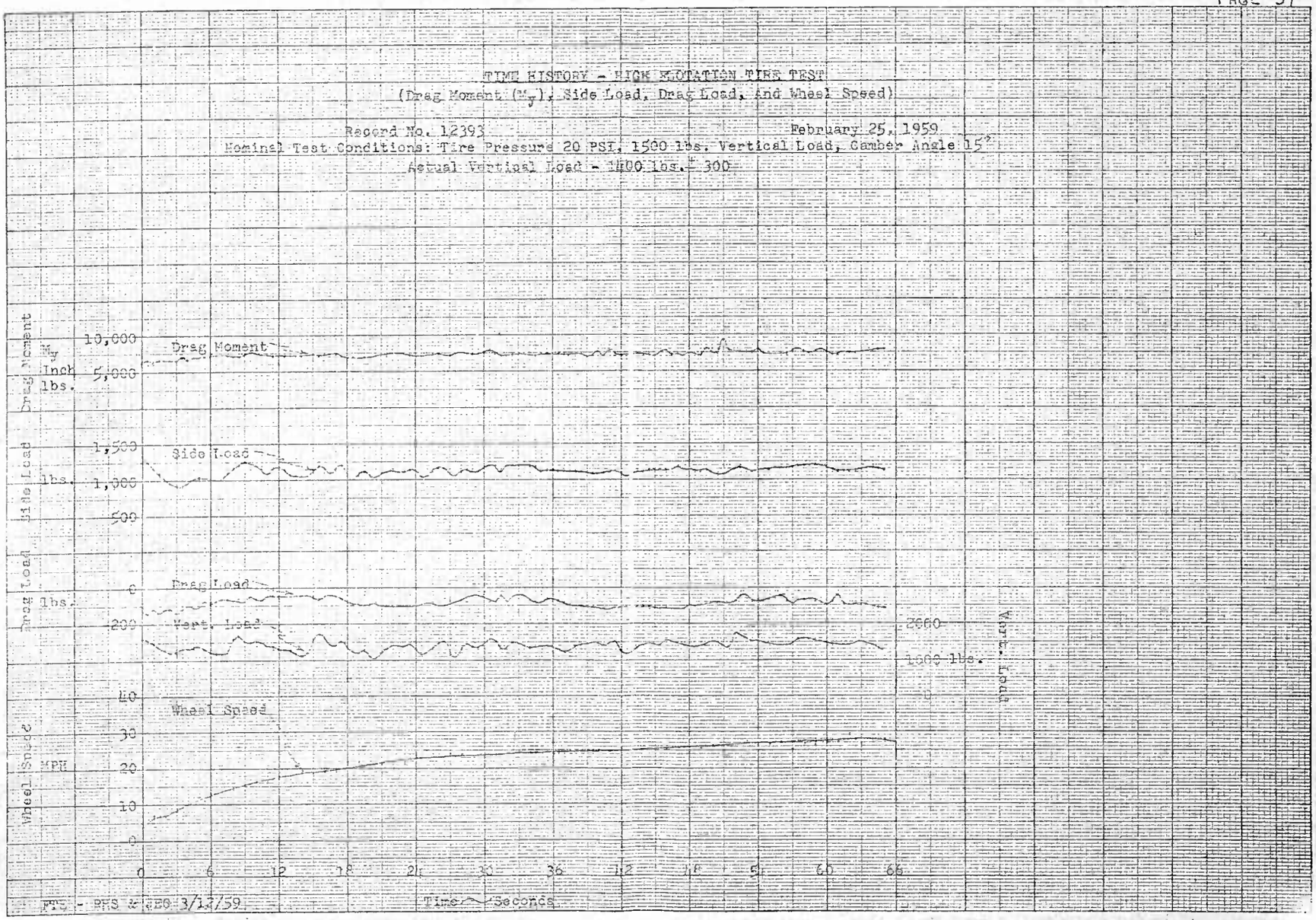

TIME HISTORY - HIGH FLOTATION TIRE TEST

(Drag Moment (M_y), Side Load, Drag Load, And Wheel Speed)

Record No. 12394 February 25, 1959

Nominal Test Conditions: Tire Pressure 20 PSI, 3000 lbs. Vertical Load, Camber Angle 15°

Actual Vertical Load - 3450 lbs. ± 400

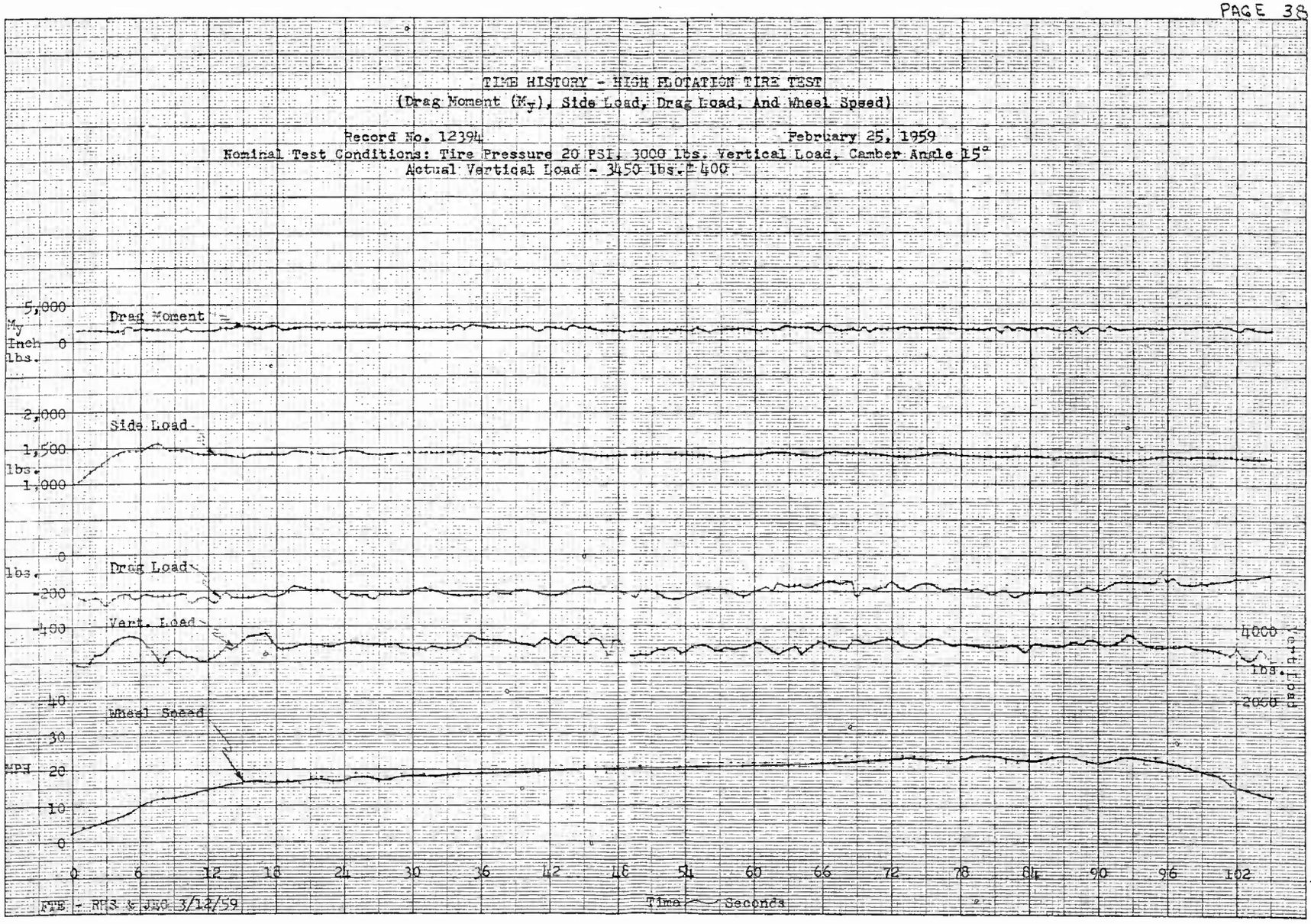

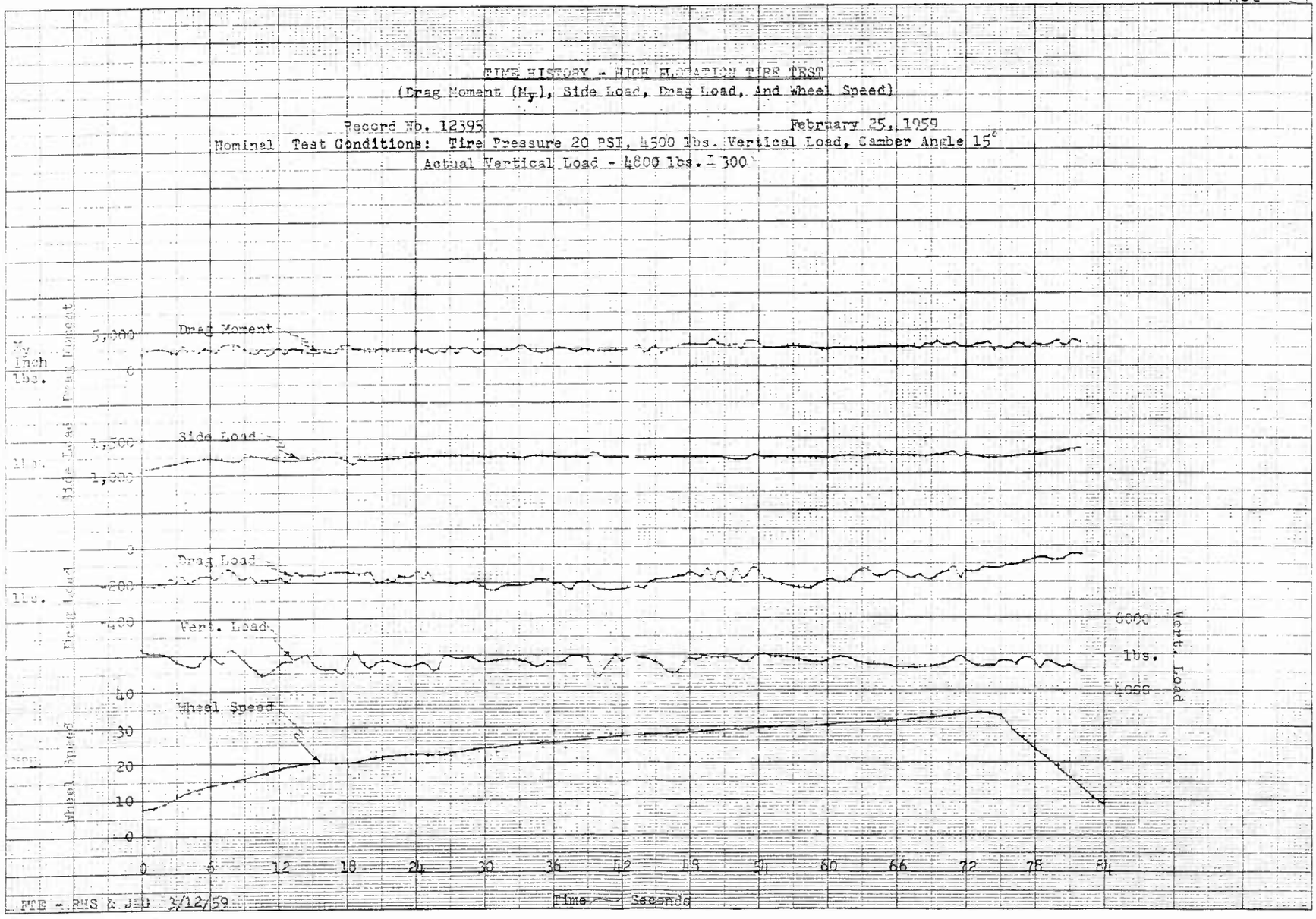
TIME HISTORY - HIGH ELEVATION TIRE TEST
(Drag Moment (M_y), Side Load, Drag Load, and Wheel Speed)
Record No. 12395
February 25, 1959
Nominal Test Conditions: Tire Pressure 20 PSI, 4500 lbs. Vertical Load, Camber Angle 15°
Actual Vertical Load - 4800 lbs. ± 300
Drag Moment
My Inch lbs.
5,000
0
Side Load
1,500
1,000
Drag Load
0
-200
-400
lbs.
Vert. Load
6000
lbs.
Loss
Vert. Load
Wheel Speed
40
30
20
10
0
MPH
0
6
12
18
24
30
36
42
48
54
60
66
72
78
84
Time — Seconds
FTE - RHS & JEG 3/12/59

TIME HISTORY - HIGH FLOTATION TIRE TEST

(Drag Moment (M_y), Side Load, Drag Load, And Wheel Speed)

Record No. 12396 February 25, 1959

Nominal Test Conditions: Tire Pressure 24 PSI, 1500 lbs. Vertical Load, Camber Angle 15°

Actual Vertical Load - 2000 lbs. ± 500

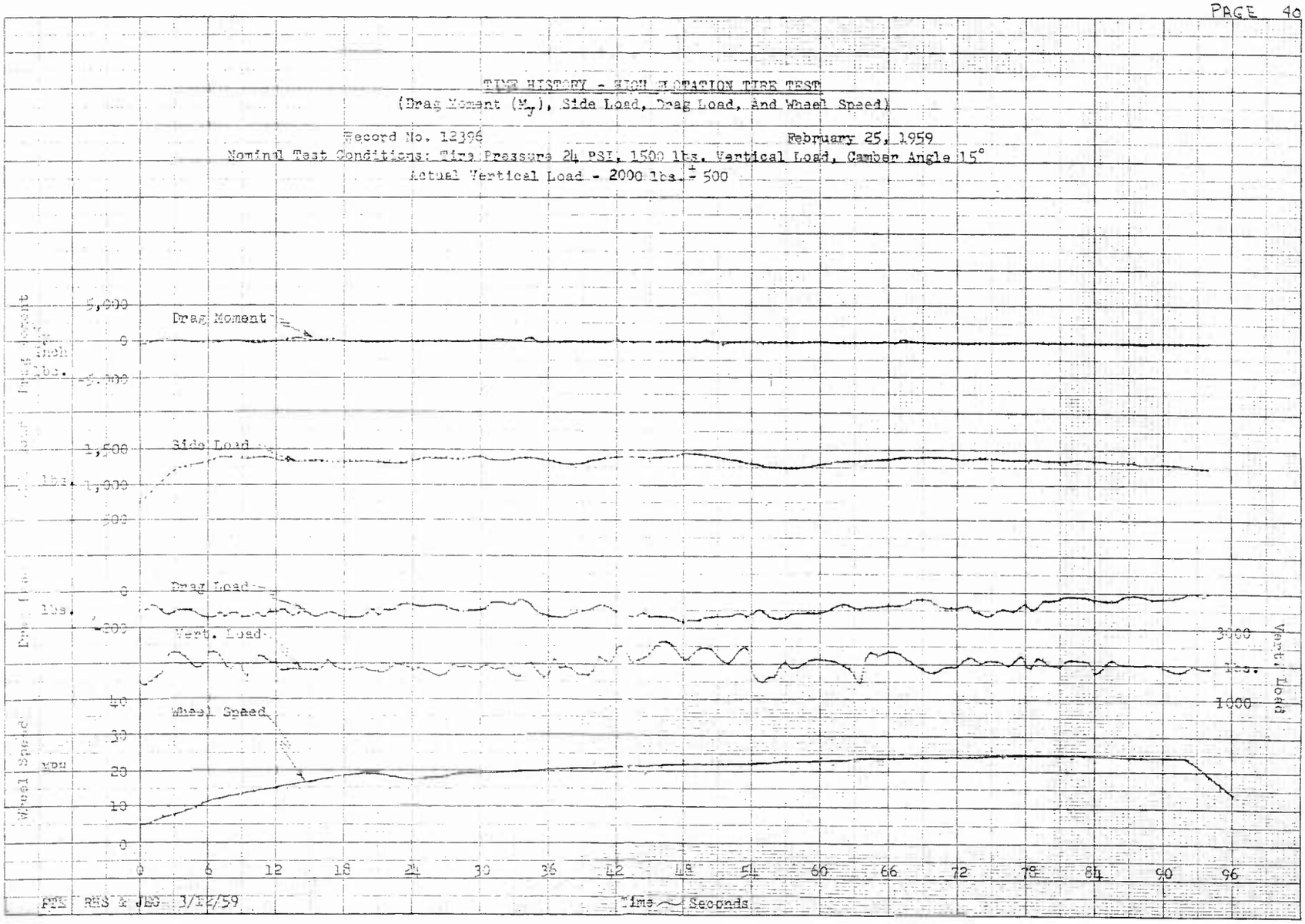

TIME HISTORY - HIGH FLOTATION TIRE TEST

(Drag Moment (M_y), Side Load, Drag Load, And Wheel Speed)

Record No. 12397 February 25, 1959

Nominal Test Conditions: Tire Pressure 24 PSI, 3000 lbs. Vertical Load, Camber Angle 15°

Actual Vertical Load - 3100 lbs. ± 300

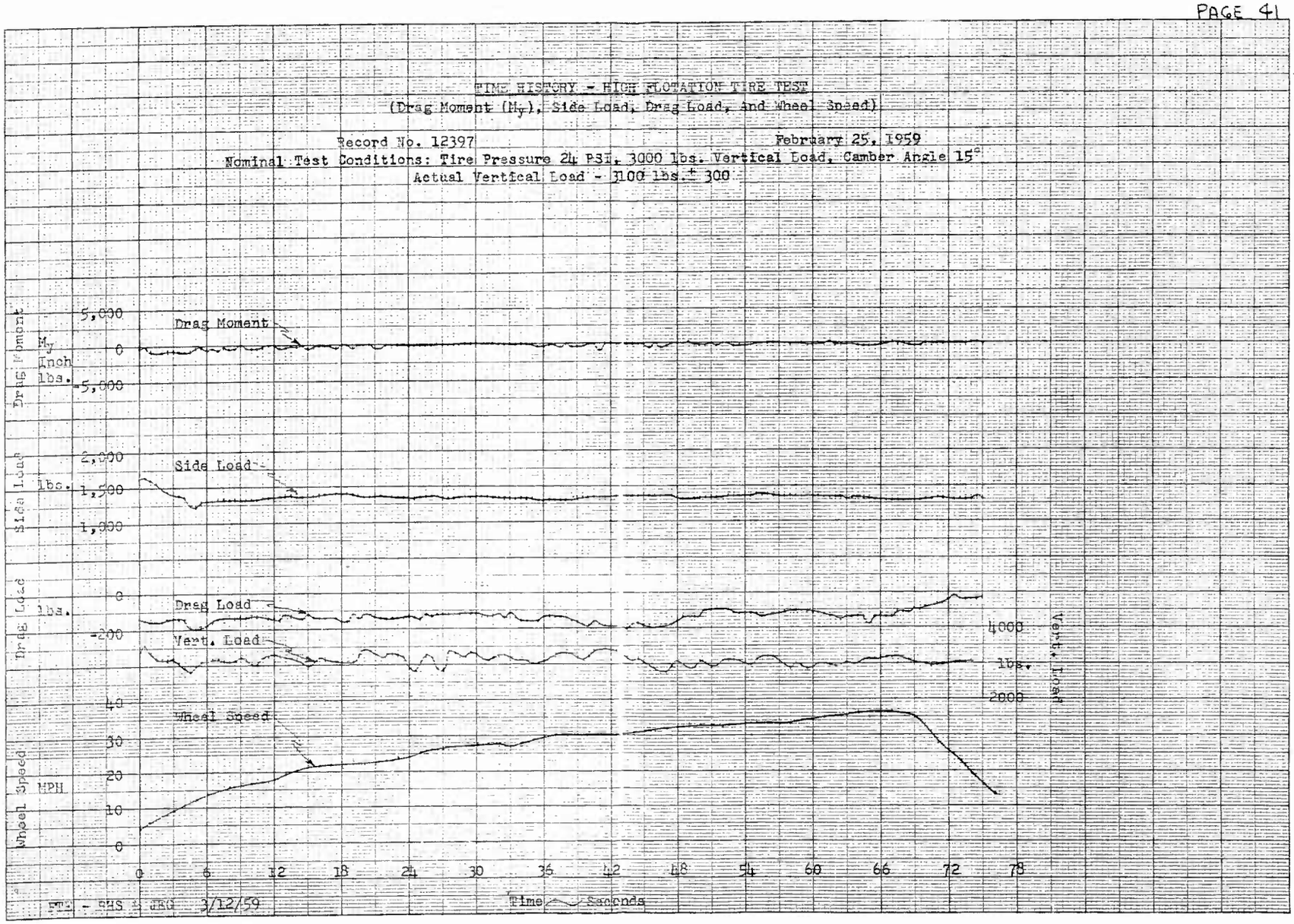

FTS - SHS - JMG 3/12/59

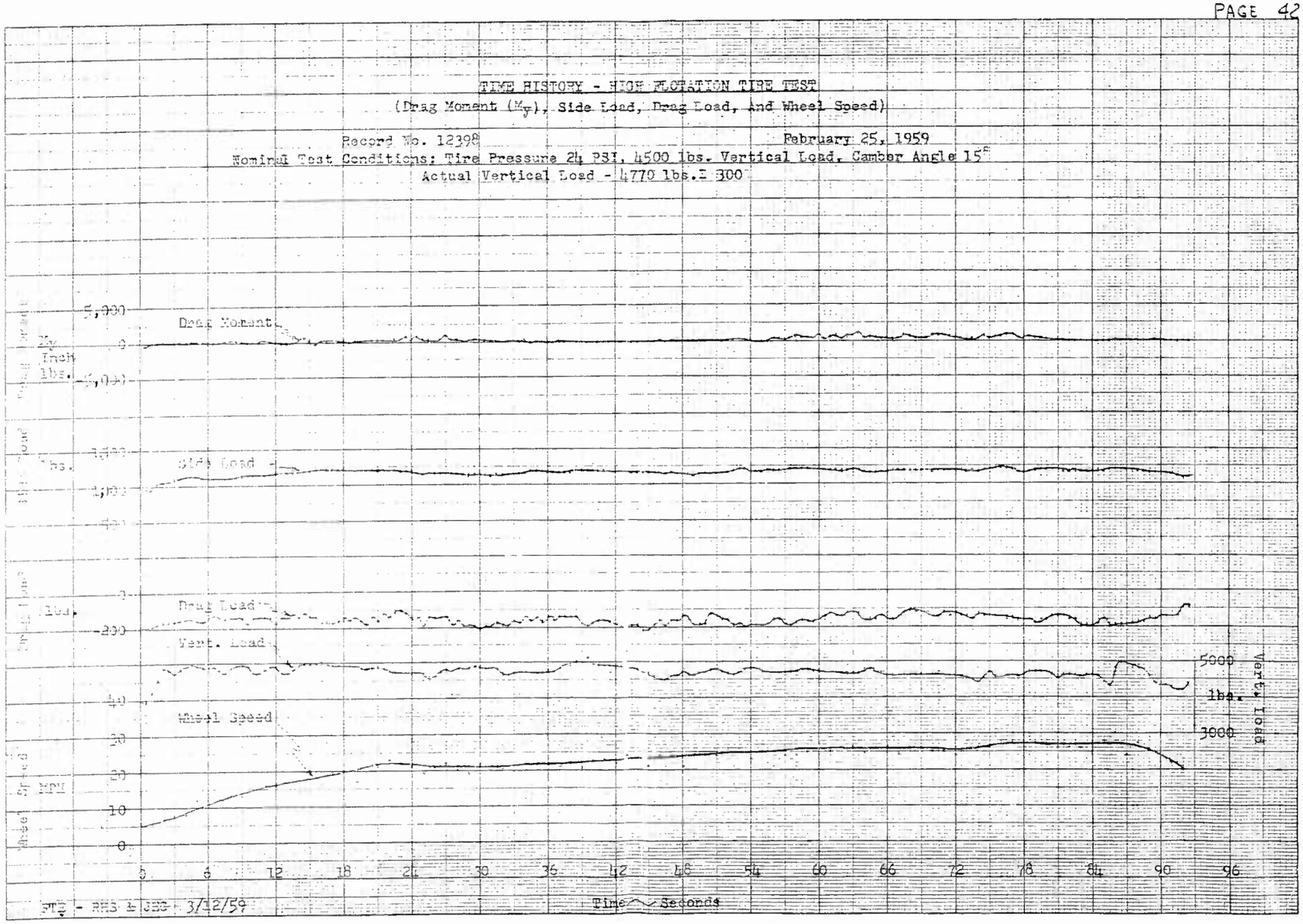
TIRE HISTORY - HIGH FLOTATION TIRE TEST
(Drag Moment (M_y), Side Load, Drag Load, And Wheel Speed)
Record No. 12398
February 25, 1959
Nominal Test Conditions: Tire Pressure 24 PSI, 4500 lbs. Vertical Load, Camber Angle 15°
Actual Vertical Load - 4770 lbs.± 300
Drag Moment
Side Load
Drag Load
Vert. Load
Wheel Speed
Vert. Load
5000
lbs.
3000
Time - Seconds
FTD - RHS & JBC - 3/12/59

TIME HISTORY - HIGH FLOTATION TIRE TEST

(Drag Moment (M_y), Side Load, Drag Load, And Wheel Speed)

Record No. 12470 March 9, 1959

Test Conditions: Tire Pressure 3.5 PSI, 800 lbs. Vertical Load, Castor Angle 15°

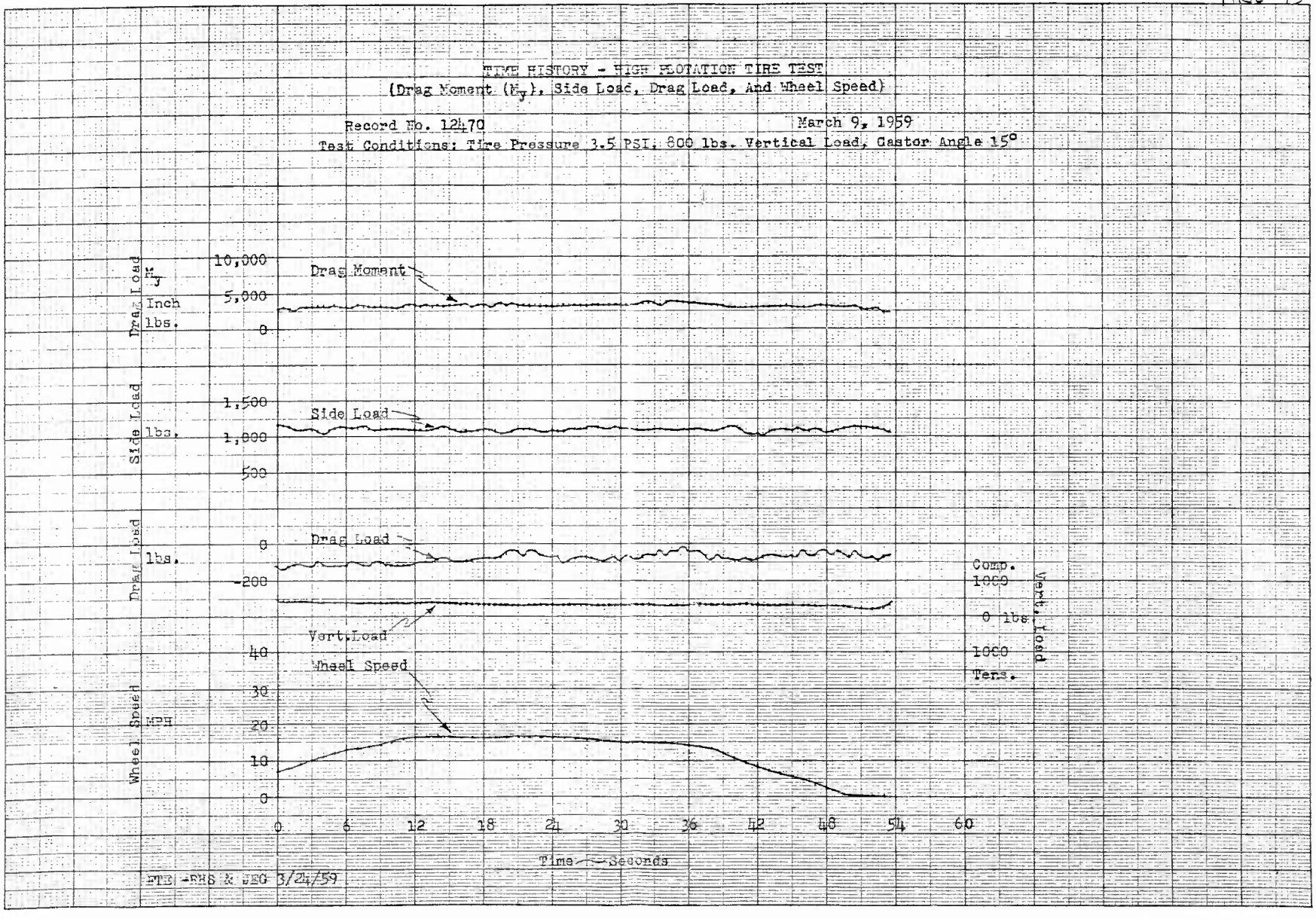

FTE -FHS & JEG 3/24/59

TIME HISTORY - HIGH FLOTATION TIRE TEST
(Drag Moment (M_y), Side Load, Drag Load, And Wheel Speed)

Record No. 12471 March 9, 1959
Test Conditions: Tire Pressure 4 PSI, 1000 lbs. Vertical Load, Caster Angle 15°

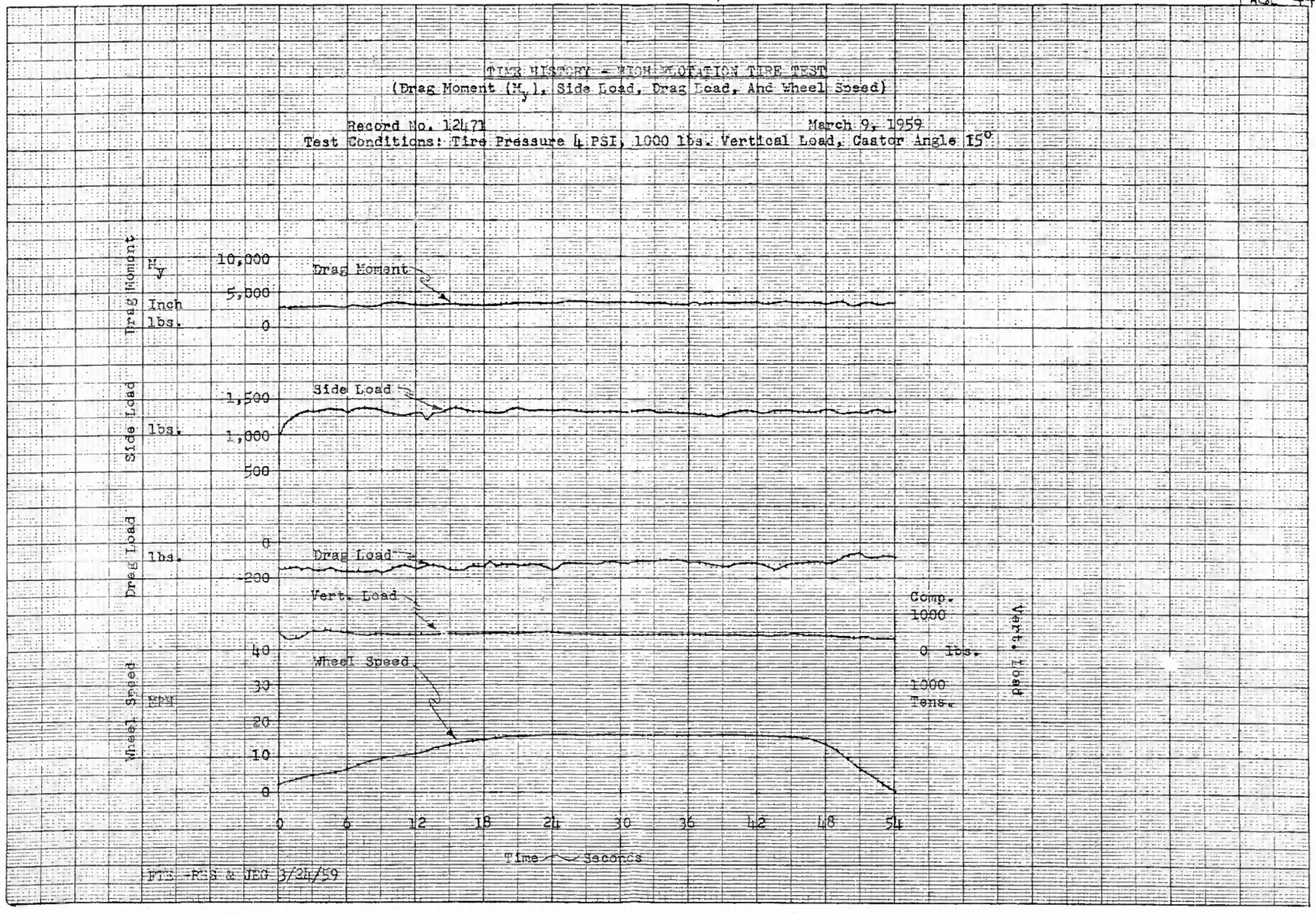

PTR - RHS & JEG 3/24/59

HIGH FLOTATION TIRE TEST

(Vertical Load Vs. Side and Drag Loads)

Record No. 12457 Date 3 Mar. 59

Nominal Test Conditions: Tire Pressure 24 PSI

1500 lbs. Vertical Load

Caster Angle 15°

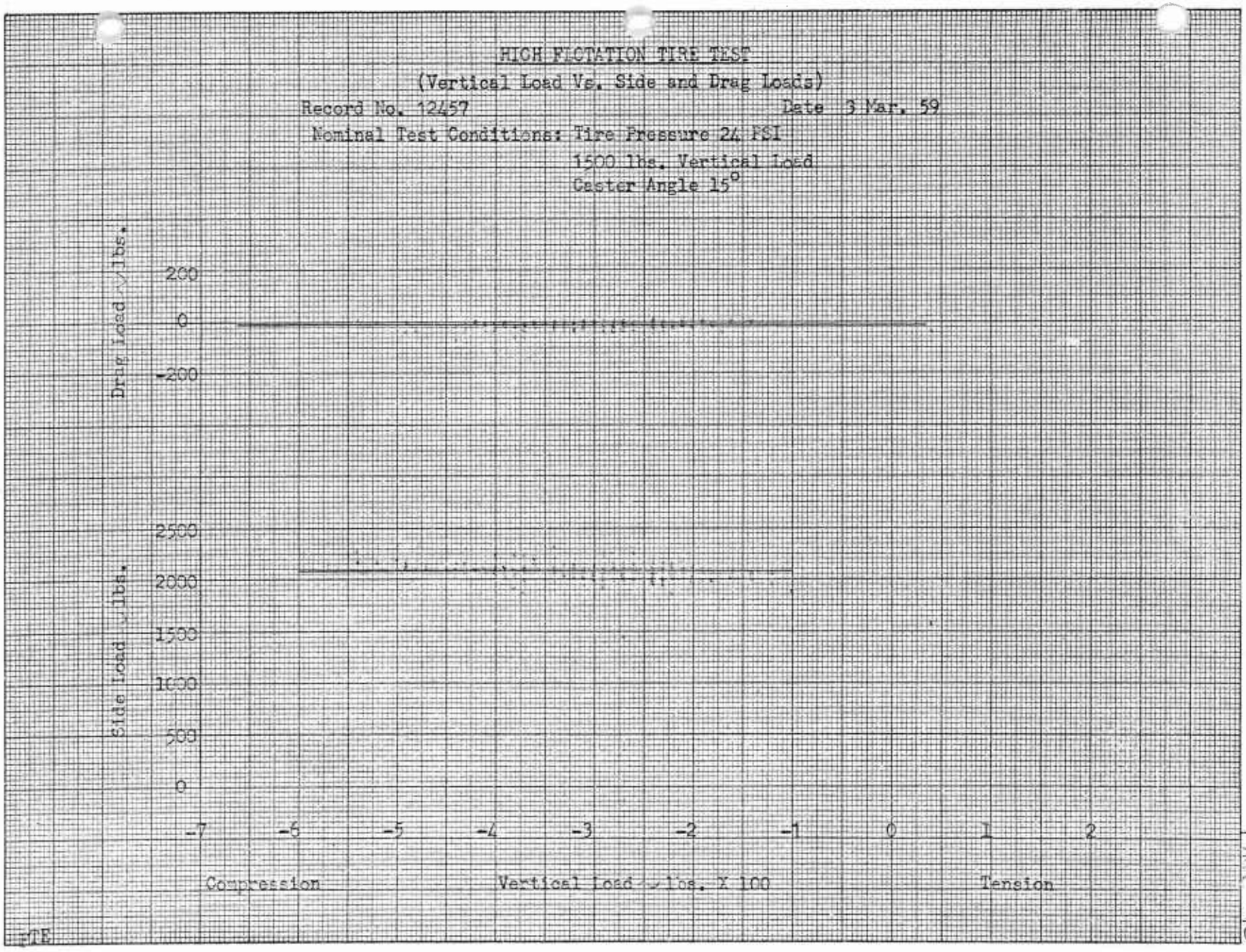

FTE

TIME HISTORY - HIGH FLOTATION TIRE TEST

(Drag Moment (M_y), Side Load, Drag Load, And Wheel Speed)

Record No. 12457 March 3, 1959

Nominal Test Conditions: Tire Pressure 24 PSI, 1500 lbs. Vertical Load, Caster Angle 15°

Actual Vertical Load = 300 lbs. = 200

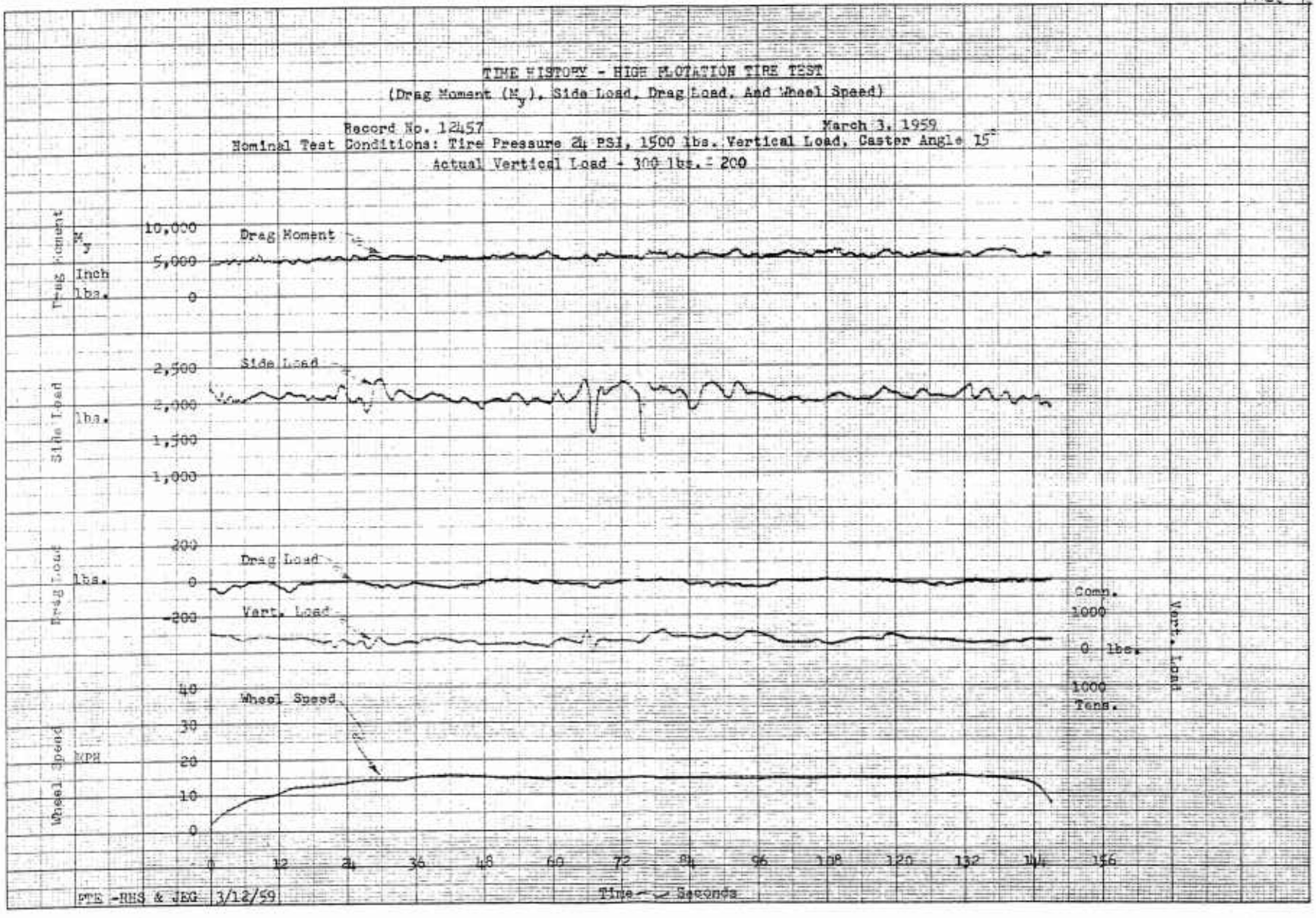

PTE -RHS & JEG 3/12/59


FAMD ENGR. LAB
HIGH FLOTATION TIRE
ROLLING TEST 43 IN DIA
TR-L-605
CONDITION OF TIRE
AFTER STEERING TESTS
26 FEB. 59

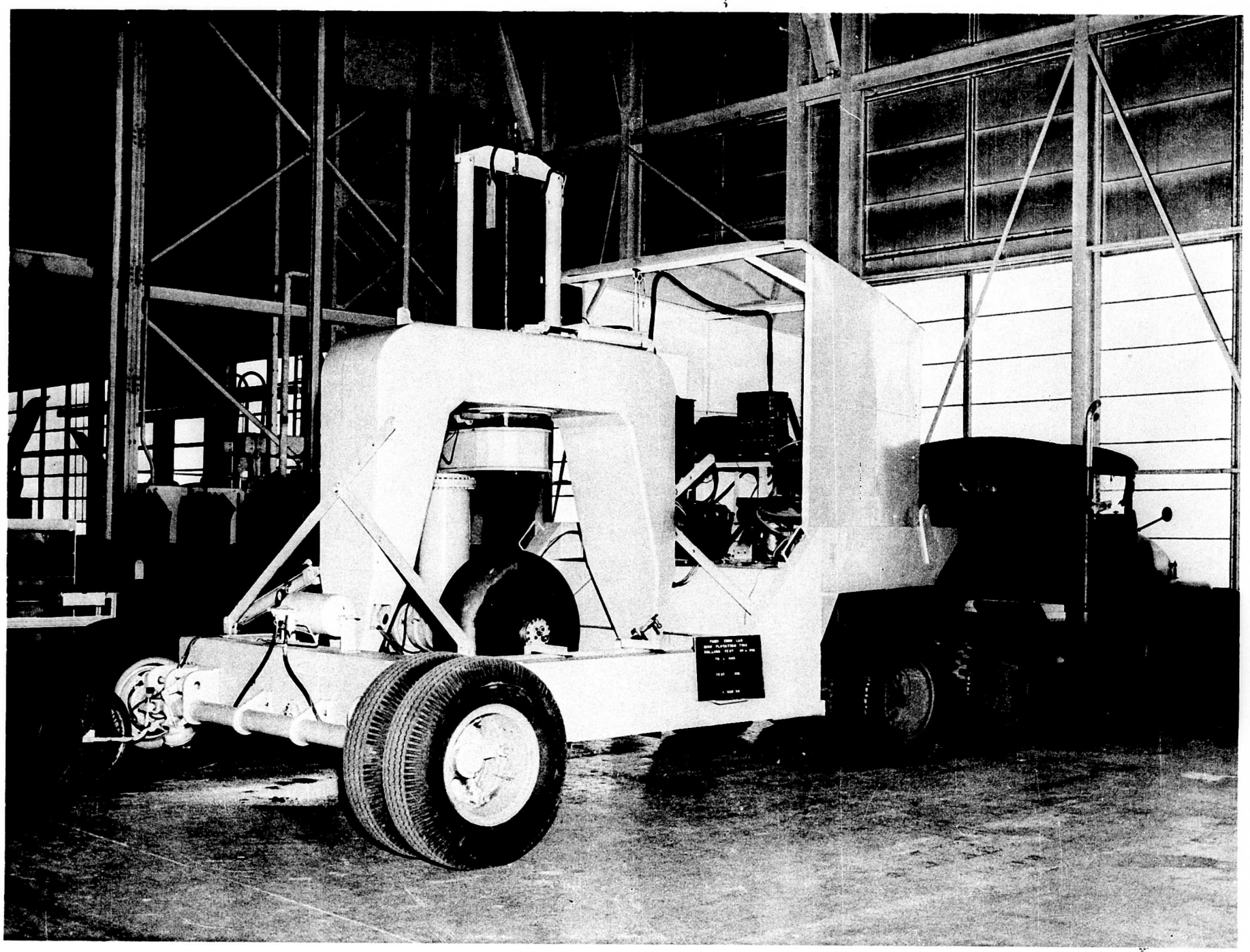

DITCH SIMULATING
POT HOLES.

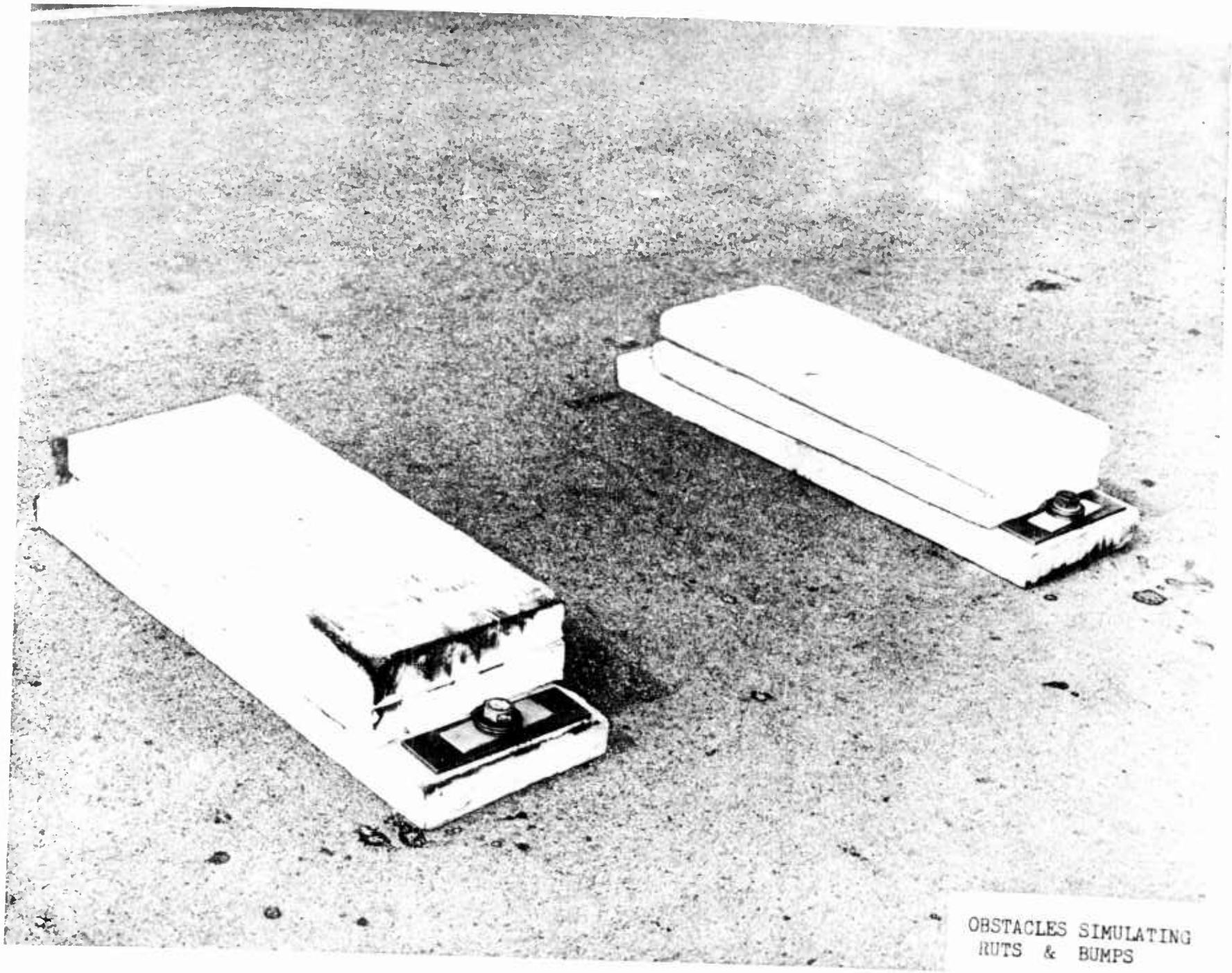

OBSTACLES SIMULATING
RUTS & BUMPS

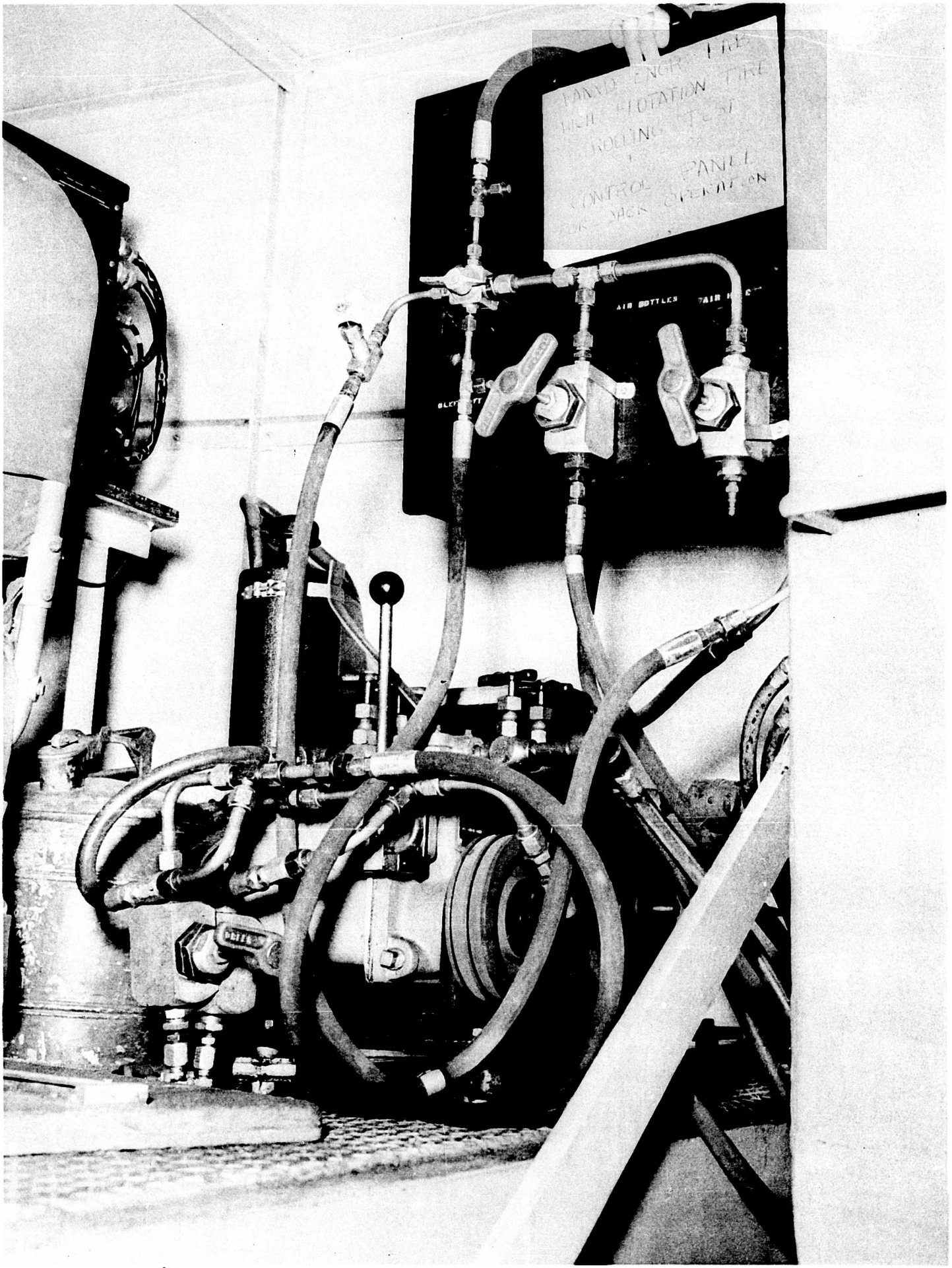
AIR BOTTLES

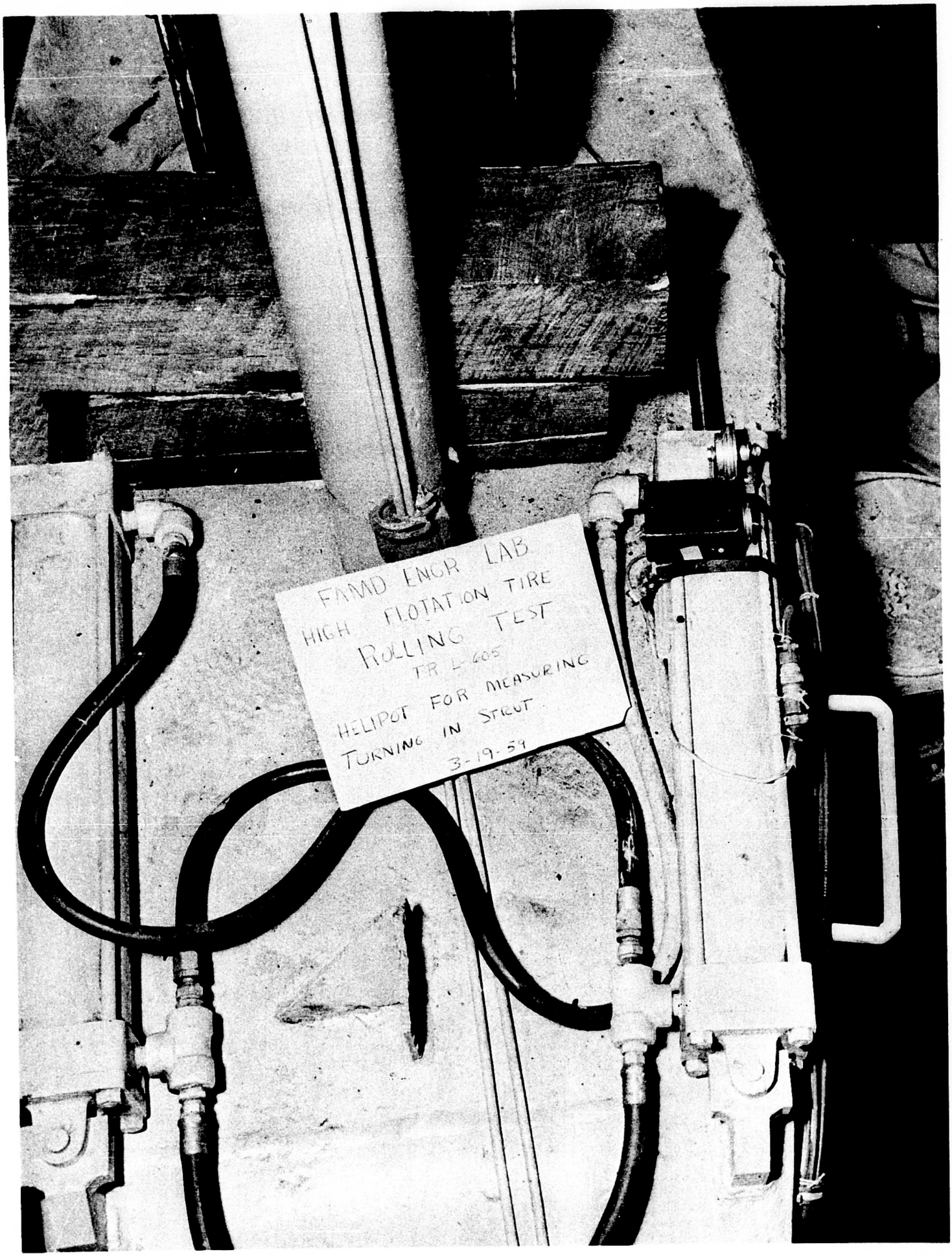
FAMD ENGR LAB
HIGH FLOTATION TIRE
ROLLING TEST
TR L-605
HELIPOT FOR MEASURING
TURNING IN STRUT
3-19-59

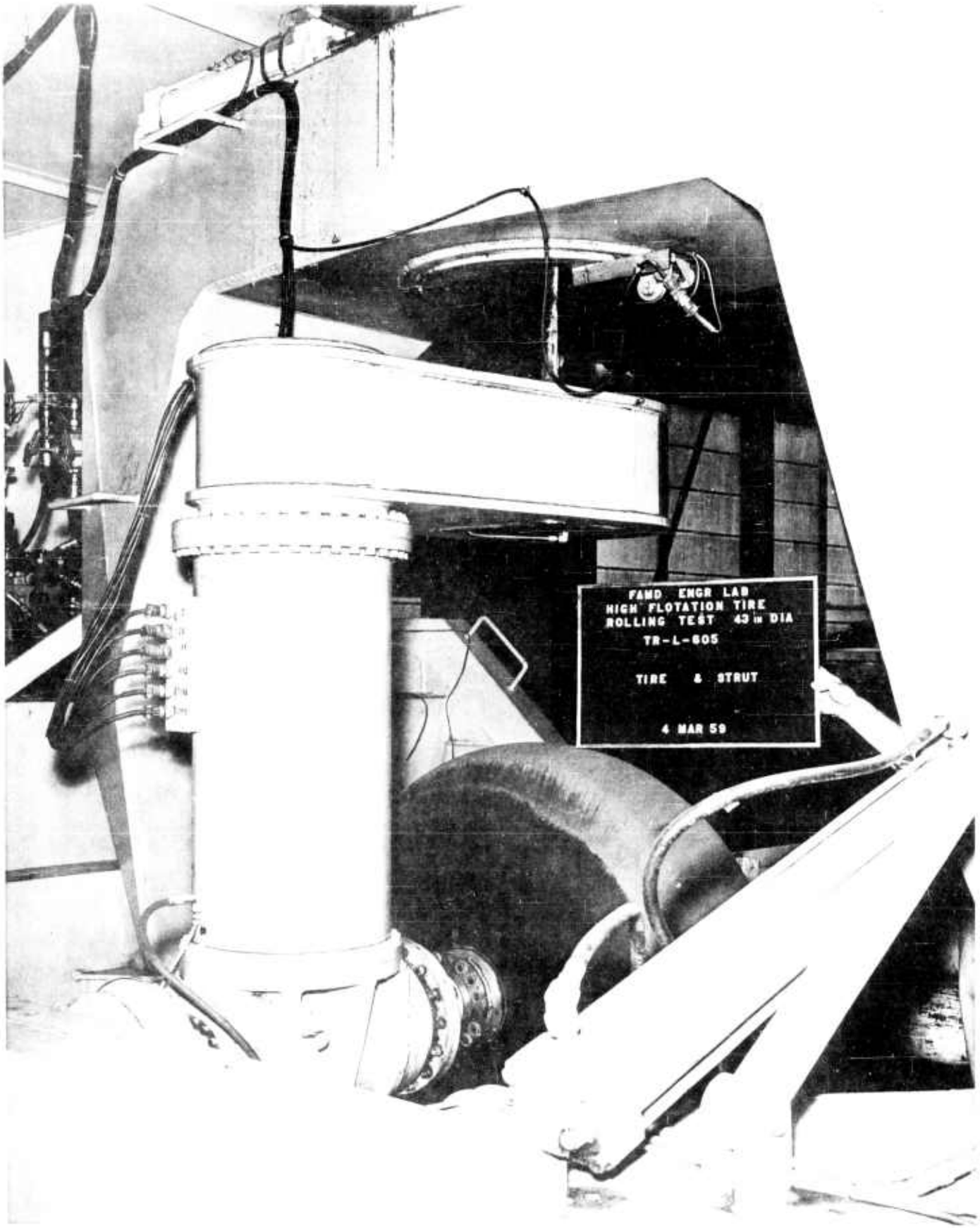
FAMD ENGR LAB
HIGH FLOTATION TIRE
ROLLING TEST 43 in DIA
TR-L-605
TIRE & STRUT
4 MAR 59

FAIRCHILD AIRCRAFT AND MISSILES DIVISION

HAGERSTOWN 10, MARYLAND

SUBJECT THE DESIGN AND DEVELOPMENT OF LABORATORY MODELS TO STUDY THE FEASIBILITY OF HIGH-FLOTATION TIRES FOR AIRCRAFT

PREPARED BY Battelle Memorial Institute Columbus, Ohio

CHECKED BY as per FAMD Purchase Order SC-85285

APPROVED BY

APPROVED BY

APPROVED BY

REPORT NO. R245.012

MODEL M-245B

COPY NO.

NO. OF PAGES

DATE August 1, 1958

REVISIONS

REVISION DATE	PAGES AFFECTED	APPROVED

NS-800-69B

PHASE REPORT

on

THE DESIGN AND DEVELOPMENT OF LABORATORY MODELS TO STUDY THE FEASIBILITY OF HIGH-FLOTATION TIRES FOR AIRCRAFT

to

FAIRCHILD AIRCRAFT DIVISION
FAIRCHILD ENGINE AND AIRPLANE CORPORATION

August 1, 1958

by

J. A. Hoess, W. F. Prien, J. H. Beck, C. W. Rodman, S. A. Gordon,
J. F. Voorhees, and R. J. McCrory

BATTELLE MEMORIAL INSTITUTE
505 King Avenue
Columbus 1, Ohio

TABLE OF CONTENTS

THE DESIGN AND DEVELOPMENT OF LABORATORY MODELS TO STUDY THE FEASIBILITY OF HIGH-FLOTATION TIRES FOR AIRCRAFT

by

J. A. Hoess, W. F. Prien, J. H. Beck, C. W. Rodman,
S. A. Gordon, J. E. Voorhees, and R. J. McCrory

During the period from June 27, 1956, through April 22, 1957, a research program entitled "An Analytical Study of High-Flotation Tires for Aircraft" was conducted at Battelle for the Fairchild Aircraft Division. Battelle's analysis in that research program indicated the feasibility of using high-flotation tires to dissipate the impact energy of landing aircraft. To demonstrate the validity of the conclusions drawn in this analytical program, the Fairchild Aircraft Division requested Battelle to submit a proposed research program on the construction of the associated equipment required for the mounting and laboratory testing of two high-flotation landing-gear systems. In response to this request, Battelle submitted a proposed research program, "The Design and Development of Laboratory Models to Study the Feasibility of High-Flotation Tires for Aircraft", dated March 15, 1957. An agreement was concluded between Battelle and Fairchild for this study. The present report covers the work on this program from its initiation on June 1, 1957, to June 1, 1958.

The objectives of the program listed in the proposed research program are:

(1) The development of two full-scale laboratory-model, high-flotation landing-gear systems meeting the specifications called for in the feasibility study. The static load ratings of the two units were to be 750 pounds and 1500 pounds.

(2) The design and construction of the equipment required for the mounting and laboratory testing of the two units.

(3) Laboratory testing of the high-flotation system components.

During the development of the first high-flotation landing-gear model, laboratory drop testing of the assembled unit was undertaken to provide insight into the actual operation of the complete high-flotation system. Because of the successful operation obtained with the first laboratory model, the design of the second unit was changed to make it adaptable to aircraft installation for flight evaluation.

This phase report covers the design, development, and testing of a high-flotation landing-gear system designed to carry a static load of 750 pounds.

SUMMARY

The high-flotation landing-gear concept embodies two basic objectives: (1) to provide a low-pressure tire capable of supporting the weight of an aircraft on soft soil or sand and capable of rolling over ruts and other obstructions without transmitting large forces to the airframe and (2) to dissipate the kinetic energy of the aircraft due to its vertical velocity, or sinking speed, by bleeding air out of the tire at the time of contact with the ground. The ability to dissipate energy would prevent excessive bouncing and eliminate the need for an oleo strut.

A third design requirement resulted from the large size of the high-flotation tires – the tires must be folded for retraction after take-off. This requirement and the necessity for light weight in aircraft components dictated a thin, flexible tire construction.

The function of energy dissipation required that a large, rapid-acting valve be designed to bleed a large volume of air out of the tire during the first fraction of a second after contact with the ground. Because of the speed of valve actuation required, it was first considered necessary to employ a power-operated valve mechanism. The use of powered-valve actuation with its associated controls has been discarded because of its complexity and because it is doubtful whether its response and reliability would be satisfactory. Valve actuation is being accomplished by a deflection between the tire hub and the strut under load.

The components of the high-flotation landing gear designed to carry a static load of 750 pounds have been designed to be extremely flexible for laboratory evaluation. Each component was tested to determine its characteristics before being assembled into the complete unit. This component testing proved to be especially valuable in the valve design, where the sleeve valve first proposed permitted excessive leakage and was replaced by a redesigned valve before actual testing of the complete landing gear was begun.

A pressure-sensing device which closes the valve at a given minimum tire pressure regardless of the load on the landing gear and which permits take-offs at elevated tire pressures without danger of valve actuation has been incorporated into the design. This function was not called for in the analytical specifications, but is considered to be necessary for successful operation of the system.

The helical bellows method proved to be the most successful method of tire folding. To induce the high-flotation tire to fold into a helical bellows, it is necessary to attach stiffening ribs to the tire and draw a vacuum of 12 inches of water inside the tire. This causes the tire to twist and collapse axially, forming a helical bellows without any external actuation other than the differential pressure across the walls of the tire.

A drop-test apparatus was constructed at Battelle to evaluate the dynamic characteristics of the assembled unit. Drop tests with this apparatus were made with various combinations of initial tire pressure, static load, sinking speed, and valve configuration. The results of these tests were highly satisfactory. The 34-inch-diameter high-flotation tire with a total load of 780 pounds was successfully tested at sinking speeds up to 8-1/4 feet per second with a maximum load factor of 3.8. Load factor is defined as the ratio of instantaneous vertical load to total static weight.

HIGH-FLOTATION LANDING-GEAR DESIGN

Design Specifications Determined in Analytical Study

The feasibility of using high-flotation landing-gear systems to dissipate the impact energy of landing aircraft was demonstrated, within the limits of accuracy of the analysis, in Battelle's research program, "An Analytical Study of High-Flotation Tires for Aircraft". This program resulted in a set of specifications for the operation of the air-bleeding system and for the geometry and fabrication of the high-flotation tires. Calculations showed that the orifices of the valves which bleed air from the tires during the landing impact must be 9, 14, 27, and 42 square inches in area for the 750, 1500, 4000, and 7500-pound static-load tire systems, respectively. The orifices must open wide in 5 milliseconds or less after the instantaneous load on the tire reaches 1.35 times the static weight. They must close completely in 25 milliseconds or less after the instantaneous load falls below 1.35 times the static weight. The tire diameters should be 34, 43, 60, and 74 inches for the 750, 1500, 4000, and 7500-pound static-load tire systems, respectively, and the initial tire pressure should be 17 psig for all four systems.

Early Design Concepts

To meet these specifications, a design study was conducted on various methods of load sensing and valve actuation. Most of the early concepts depended upon powered-valve actuation, either hydraulic or pneumatic, which was controlled by some type of independent load sensor such as an accelerometer. One typical system considered for valve actuation is shown in Figure 1. This system is a pneumatic or hydraulic servo-mechanism. The valve would be actuated by a power piston controlled by the load input and by an overriding pressure input which would close the valve when a given minimum tire pressure was reached. The sequence of operations for this system would be as follows:

(1) The load input is moved to the right with increasing load.

(2) A suitable linkage moves the spool valve to the right, and pressurized fluid enters the chamber on the backside of the power piston.

(3) The power piston moves to the left and opens the valve.

(4) As the valve opens, the spool valve is returned to its original position, thus halting the power piston. Therefore, a given position of the load-input rod would result in a given valve position.

(5) When a given minimum pressure is reached, the pressure-input rod is actuated and overrides the load input. The spool valve is thus moved to the left, allowing pressurized fluid to enter the chamber on the front side of the power piston.

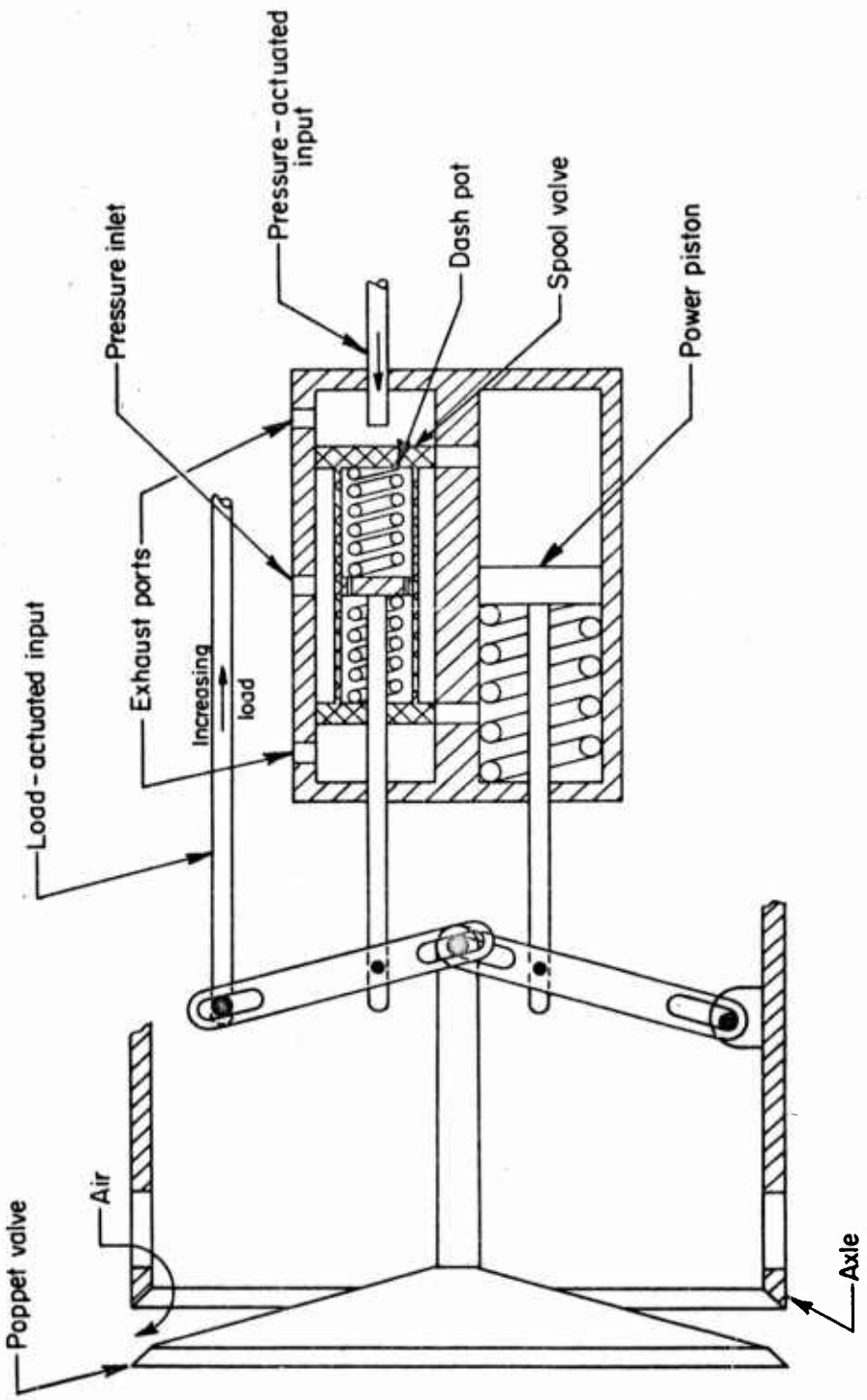

FIGURE 1. SCHEMATIC DIAGRAM OF PNEUMATIC OR HYDRAULIC SERVOMECHAMISM WITH LOAD AND OVER-RIDING PRESSURE CONTROLS FOR VALVE ACTUATION

(6) The power piston moves to the right, closing the valve. The spring on the front side of the power piston would close the valve in case of a failure in the fluid supply system.

Such systems presented many problems. They were fairly complex and required external power sources for valve actuation. It was also doubtful whether or not their response and reliability would be satisfactory. Because of these problems, an investigation was carried out to study the feasibility of using directly the force imposed on the landing gear for valve actuation.

Theoretical Basis for Direct Valve Actuation

A computer study was made of the dynamic response of the wheel-hub assembly during a landing to determine whether this response was fast enough to be used for valve actuation. The following system was considered in this study:

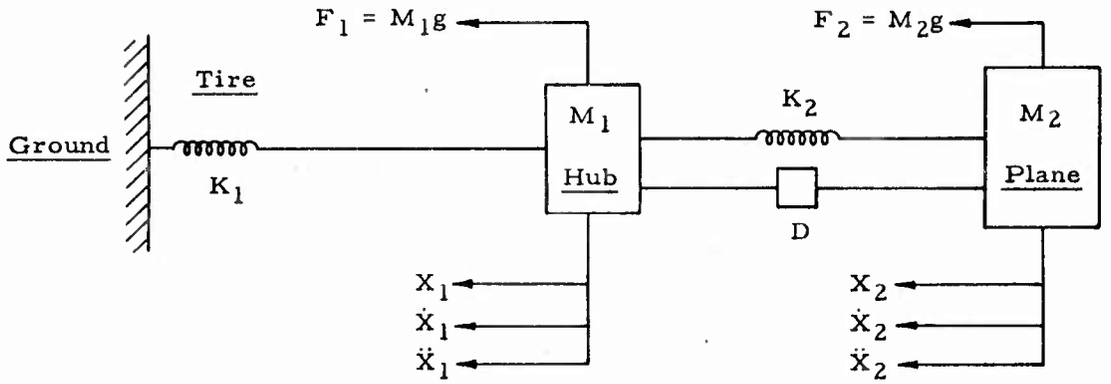

K_1 Undeflated tire spring rate, 12,000 lb/ft

K_2 Load-sensing spring rate, 18,000 lb/ft

M_1 Tire hub assembly mass, 1.16 slugs

M_2 Plane mass, 22.1 slugs

D Dashpot rate, 100 lb-sec/ft.

The basic dynamic equations for this system are:

$$K_1X_1 + M_1\ddot{X}_1 - K_2(X_2 - X_1) - D(\dot{X}_2 - \dot{X}_1) = F_1 = M_1g \qquad (1)$$

$$K_2(X_2 - X_1) + D(\dot{X}_2 - \dot{X}_1) + M_2\ddot{X}_2 = F_2 = M_2g \ . \qquad (2)$$

Figure 2 is a graph of the dynamic response results obtained for a landing of this system at a sinking speed of 8.4 ft/sec. In such a landing a relative movement of 3/8 inch between the wheel hub and the fixed strut would occur in about 0.015 second after touchdown. The force acting to produce this movement would reach over 900 pounds in that time. These results indicate that it is feasible to use the force and deflection between the tire hub assembly and the strut for valve actuation.

Design of Components of the 750-Pound Landing-Gear Unit

The high-flotation landing gear designed to carry a static load of 750 pounds was designed strictly as a laboratory test apparatus. Flexibility and adjustability were stressed throughout, to permit testing the 750-pound unit at conditions other than those specifically called for in the analytical study. This has necessarily resulted in a heavier unit than would be needed for aircraft applications.

Landing-Gear Linkage

Valve actuation in the 750-pound unit is accomplished by means of the deflection between the tire hub assembly and the strut. To obtain a deflection that would be sensitive only to the vertical load on the landing gear, it was first considered that a telescoping section should be provided in the main strut. The use of a telescoping main strut was discouraged, however, because it was thought that extremely heavy sections would be required to prevent deflections due to bending forces from detrimentally influencing the load-sensing function. Therefore, a linkage which would remove the major bending forces from the load sensor was devised.

Figure 3 is a picture of the landing-gear linkage. A telescoping load sensor is mounted in parallel with the main strut. The axle housing is connected to the main strut by means of a horizontal link, and the load sensor is fastened to the main strut by means of a ball joint which is free to move in a direction parallel to the center line of the axle. This type of mounting leaves the load sensor free of bending moments which might be imposed by tire loading, misalignments, or deflections of parts under load. The only bending moment carried through the load sensor is a small one which is imposed when the brakes are applied.

Axle, Axle Housing, and Brake

The air is bled from the tire through a tubular axle. Since the analytical study called for an orifice area of 9 square inches, it would be necessary to use a tubular axle with an internal diameter of about 3-3/8 inches. Because of tire geometry considerations, however, it was necessary to use an axle with a 2-11/16-inch internal diameter, which provides 5.67 square inches of flow area. This reduction in orifice area has a significant effect on the operating conditions of the high-flotation tire which was confirmed by the drop-test results.

Roller bearings are mounted in the stationary axle housing, and the axle is allowed to rotate with the tire. The axle is made of SAE 4135 steel hardened to 35 R_C,

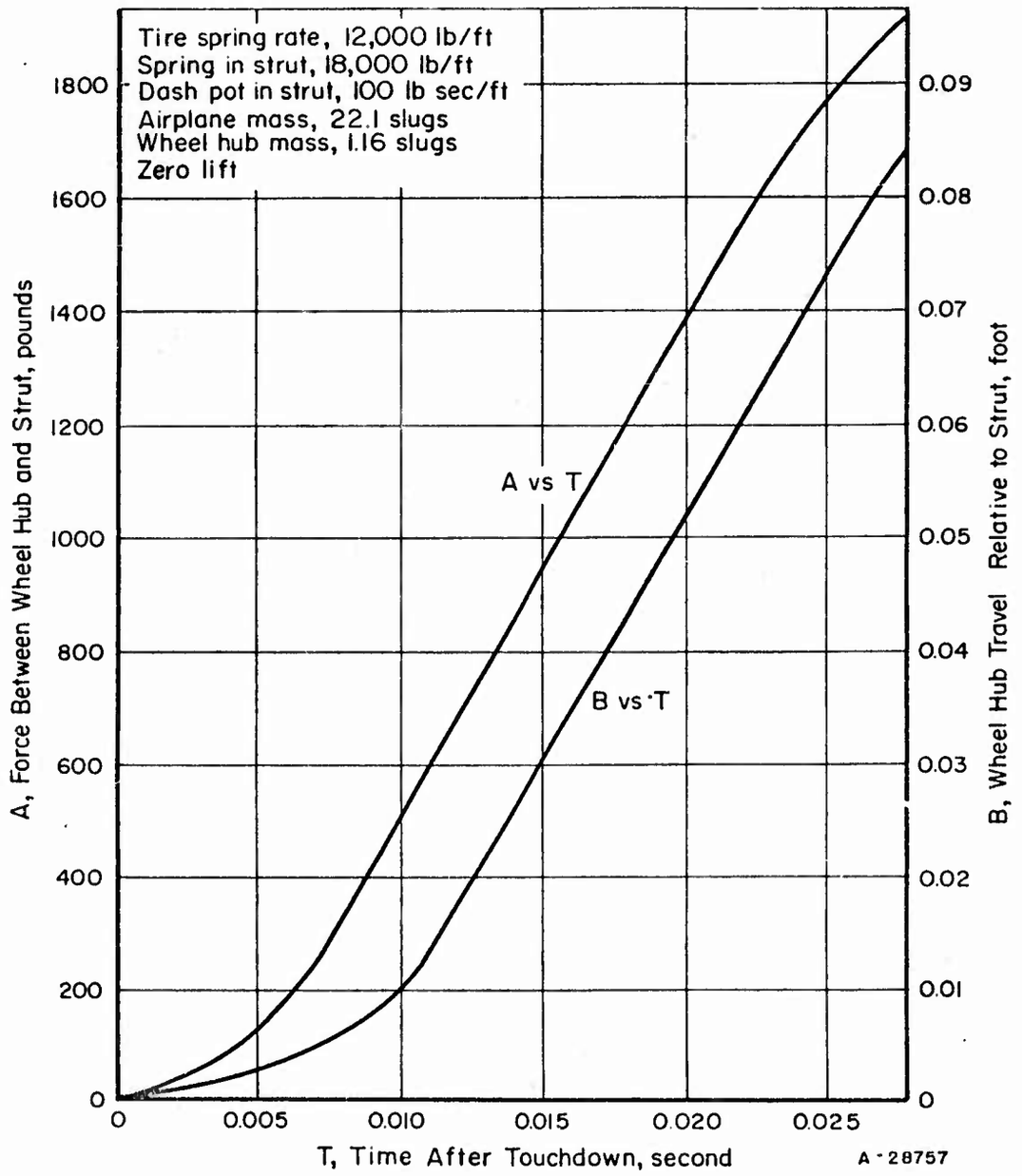

FIGURE 2. DYNAMIC RESPONSE OF WHEEL HUB DURING 8.4 FT/SEC LANDING

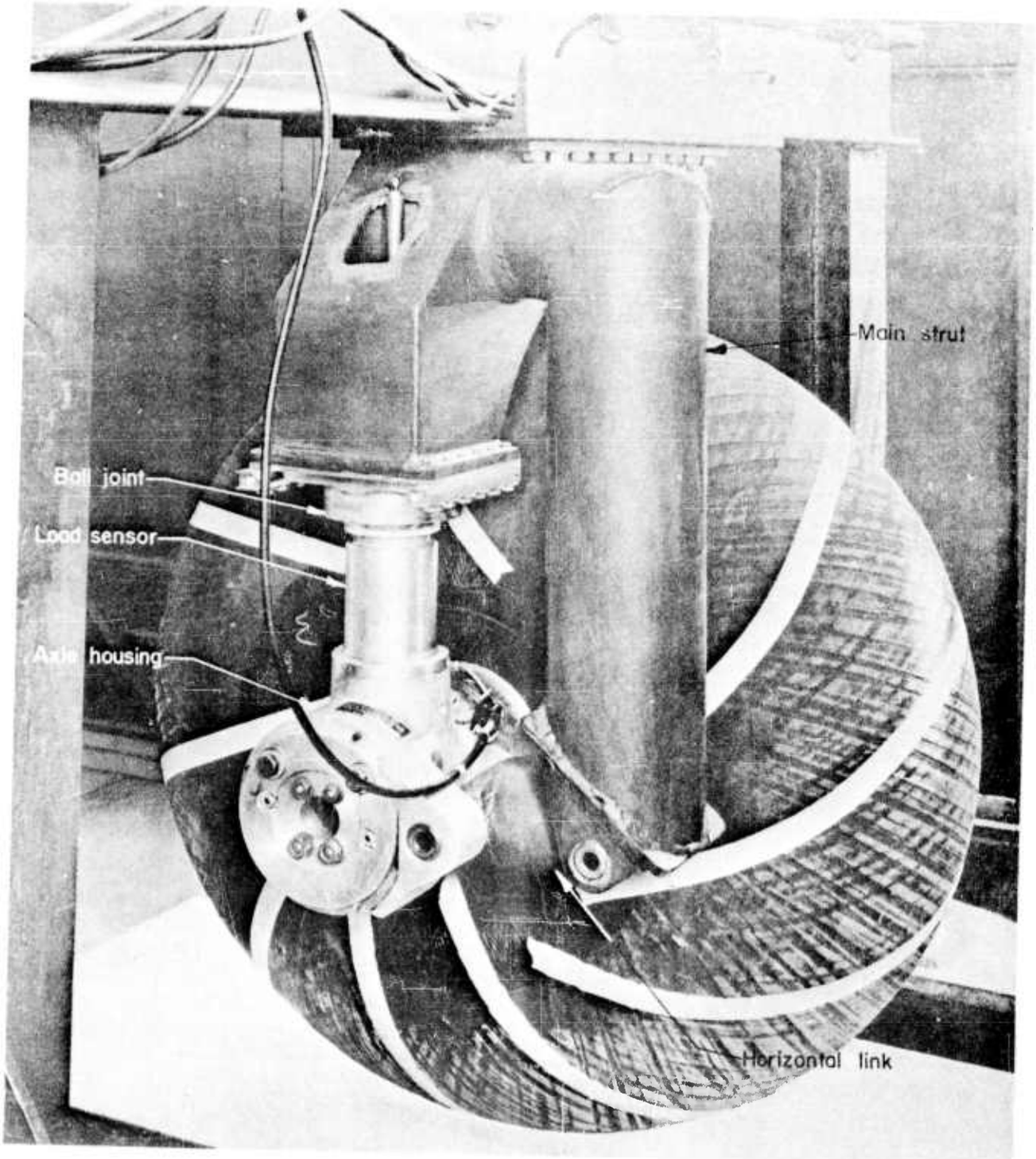

N50755

FIGURE 3. ASSEMBLED 750-POUND HIGH-FLOTATION LANDING GEAR SHOWING LINKAGE ARRANGEMENT

and the housing is an Almag 35 casting. The brake being used is an Auto Specialties 5 x 3-1/4 single-rotor brake which has been adapted to fit this particular installation.

Load Sensor

Figure 4 is a schematic sketch of the load-sensing strut which is being used in the 750-pound static load high-flotation landing-gear system. The unit has a stiff load-sensing spring mounted in series with a light energy-storage spring and an energy-absorbing dashpot which are mounted in parallel. Valve actuation is accomplished by means of a yoke-shaped bell crank which is mounted in the axle housing. A deflection of the load-sensing spring permits the bell-crank pushrod to move downward. This movement rotates the bell crank, which produces an axial movement of a ring that is mounted externally on the axle. This ring is connected to the valve pushrod by pins that pass through slots in the axle. The load-sensing strut functions in the following manner:

(1) The vertical load on the landing gear is transmitted from the axle housing through the load-sensing spring to the piston assembly.

(2) The deflection of the load-sensing spring under load actuates the yoke-shaped bell crank.

(3) The load between the piston assembly and the strut is shared by the energy-storage spring and the dashpot.

(4) After the dashpot reaches the end of its travel and bottoms, the major portion of the load is carried directly from the piston assembly to the strut. The energy-storage spring, however, continues to carry its portion of the load.

Since the load-sensing function is performed by the deflection of the load-sensing spring, this spring is the only component of the present load-sensing strut that is actually necessary for valve actuation. The energy-storage spring and the dashpot or "oleo" have been incorporated into the design, however, to obtain additional information as to how the high-flotation landing gear will function when installed in series with other forms of energy-storage or absorption devices. The first phase of the testing program was conducted with the energy-storage spring and the dashpot locked out of the system so that the energy dissipation characteristics of the high-flotation tire could be established. Tests are presently being conducted with the energy-storage spring and the dashpot installed, to determine their effect on the characteristics of the system.

Sleeve Valve

After an extensive investigation of possible valve configurations, it was decided that a sleeve valve would offer many advantages over other types of valves for bleeding air from the tire. It would not be loaded by the air pressure in the tire, and a small linear movement would permit several rows of ports to be opened, providing the characteristic of large valve area versus valve travel. By contouring the ports in the sleeves, it would be possible to experiment with various valve-area versus valve-stroke relationships.

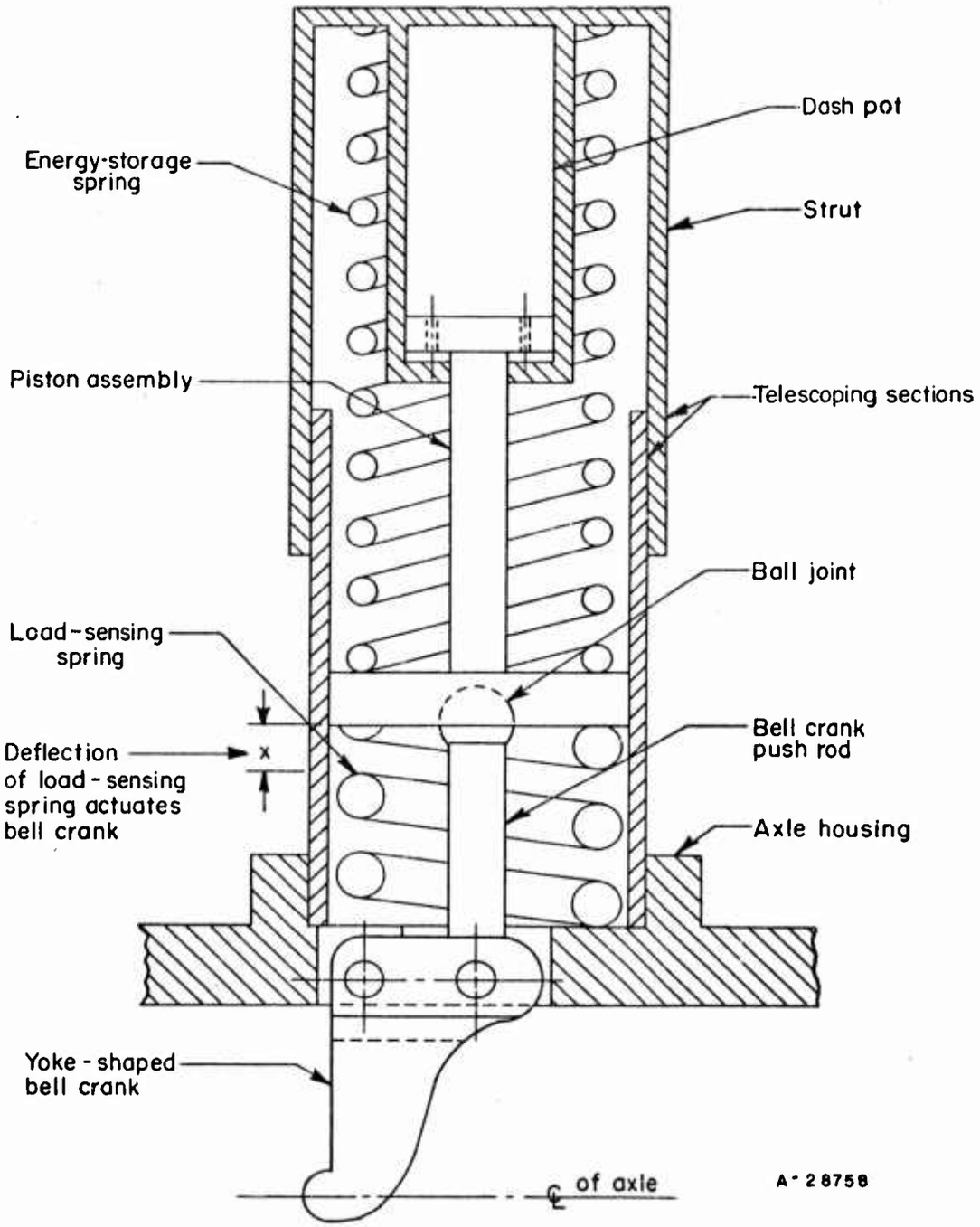

FIGURE 4. SCHEMATIC DRAWING OF LOAD-SENSING STRUT

The sleeve valve was designed to be internally mounted in the axle. Figure 5 is a photograph of the disassembled valve and a dummy axle. To prevent binding of the valve with axle deflections, the outer sleeve is flexibly supported by O-rings on the inside of the axle and, therefore, is not constrained to deflect with the axle. The inner sleeve is free to move axially in the flexibly supported outer sleeve. An analysis of the perforated cantilever axle showed that no prohibitive deflections should be encountered.

The total valve stroke from full open to full closed is 3/4 inch. After reaching the full-closed position, however, the valve is allowed to travel another 1/4 inch to aid in sealing. Thirty-four shaped ports are located in a double helix pattern on the sleeves. They have a total valve area of 6.7 square inches and the internal cross-sectional area of the internal sleeve is 4.4 square inches. The ports are so shaped that 30 per cent of the total valve area is exposed in the first 0.45 inch of valve travel. As the valve area then begins to increase much faster, the remaining 70 per cent of the valve area is exposed in the last 0.30 inch of valve travel.

Valve-Test Apparatus

To determine the characteristics of this sleeve valve, a laboratory test setup was constructed to measure the bleed-down rates of the valve as a function of port configuration, port area, and initial tire pressure. A 6.9 cubic foot tank, which has the same volume as the undeflected 34-inch-diameter tire, was used to simulate the tire. A dummy axle containing the sleeve valve was installed in the cover plate of the tank. Because of the high flow rates, steady static flow was not maintained. Instead, pressure-versus-time records were obtained while the air in the tank blew down through the sleeve valve.

Sleeve-Valve Characteristics

Table 1 shows the times required to bleed the test tank from 17 to 2 psig at various degrees of valve opening and closure. These results show that leakage is a major problem with the sleeve valve. It requires only 6 seconds to bleed the tank from 17 to 2 psig when the valve is in the closed position and only 11 seconds when the leakage path is increased by moving the valve 1/4 inch beyond the closed position. To reduce this high leakage rate, it would be necessary to hold extremely close tolerances on the sleeves and to make use of various coating techniques on the sealing surfaces. It was apparent, however, that even with extreme care in sleeve manufacture, the leakage rate would be excessive.

Redesigned Valve

To replace the original sleeve valve, a new valve configuration was conceived which is positively sealed in the closed position without the necessity of holding extremely close tolerances or using special valve-surface treatments. Figure 6 is a photograph of the disassembled valve and a dummy axle. Valve operation is as follows:

(1) Air passes from the tire to the axle through 8 large ports.

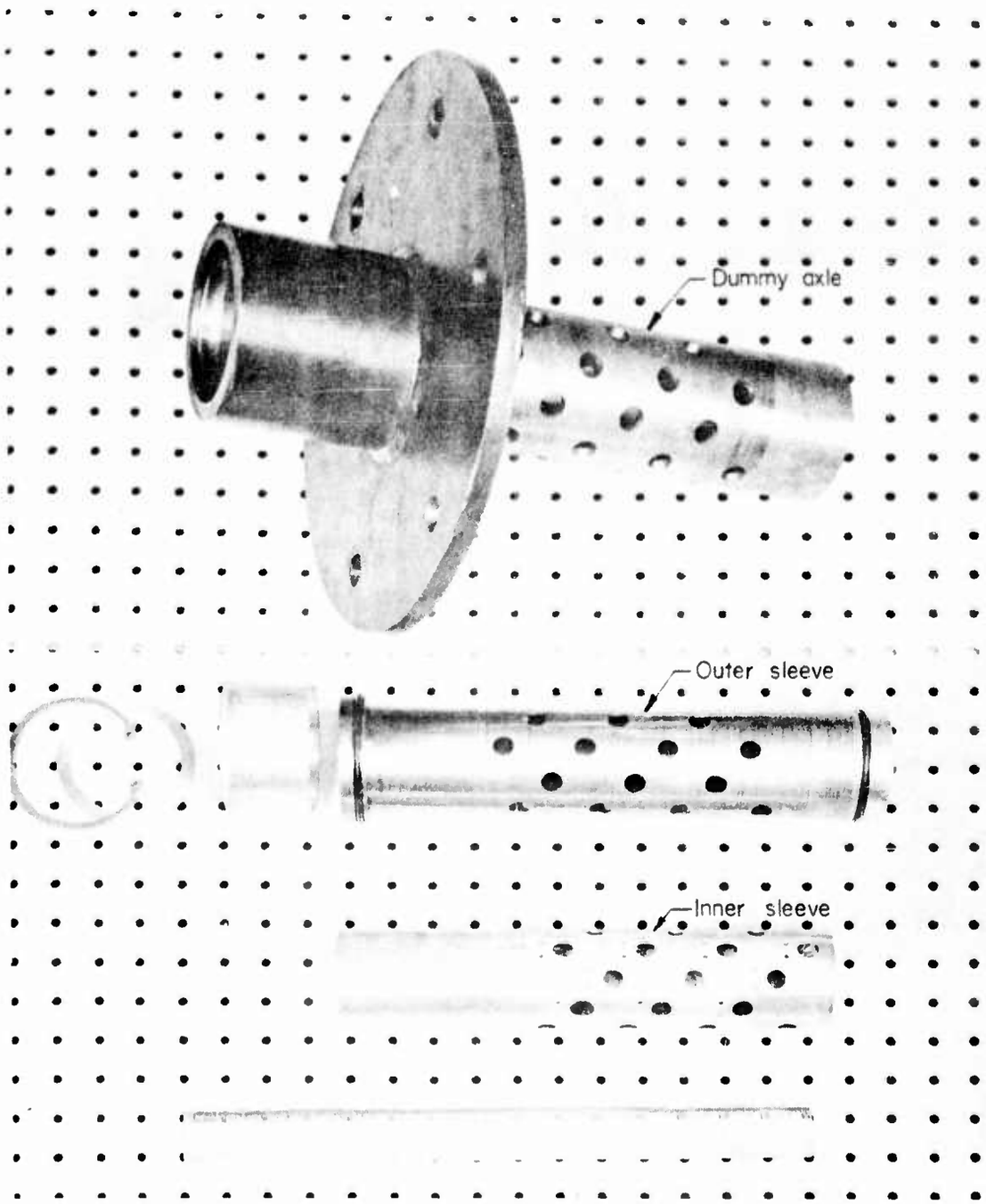

FIGURE 5. EXPERIMENTAL SLEEVE VALVE SHOWN DISASSEMBLED

TABLE 1. BLEED-DOWN RATES OF TIRE VALVES

Fraction of Full Valve Area[a], per cent	Fraction of Total Valve Stroke, per cent	Time Required to Bleed 6.9 Ft^3 Tank From 17 to 2 Psi, seconds
	Original Sleeve Valve	
100	100	0.25
67	83	0.30
33	62	0.45
0	0	6.00
0	-1/4-inch movement beyond port closure	11.00
	Present Valve Configuration	
100	100	0.25
67	67	0.28
33	33	0.40
0	0	∞

(a) Total valve areas for original and present valves are 5.7 and 10.8 square inches, respectively. Axle areas for original and and present configuration are 4.4 and 5.7 square inches, respectively.

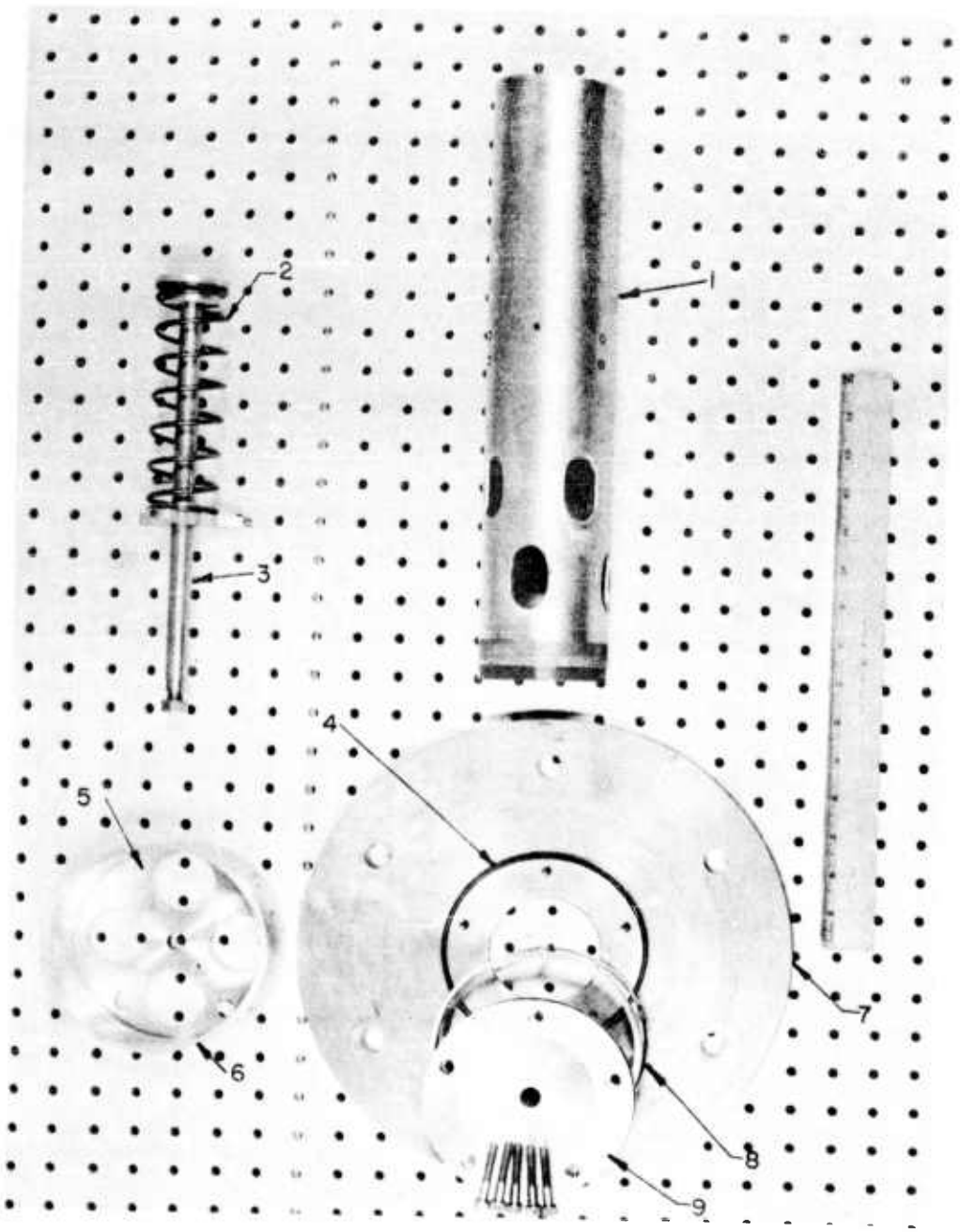

N50757

1. Dummy axle
2. Valve spring
3. Valve pushrod
4. Face-seal O-ring
5. Valve end plate
6. Outboard sleeve
7. Dummy outboard tire flange
8. Valve-port cylinder
9. Axle end plate

FIGURE 6. IMPROVED TIRE BLEED-DOWN VALVE SHOWN DISASSEMBLED

(2) An axle end plate, which is contoured to turn the air in a radial direction is mounted on the outboard tire flange.

(3) A replaceable programmed valve port cylinder is mounted between the axle end plate and the outboard tire flange.

(4) Valve area is controlled by an outboard sleeve which is mounted on the outside of the programmed valve port cylinder and which is sealed in the closed position by one reciprocating and one face-seal O-ring.

(5) The external sleeve is moved axially to uncover the valve ports by a pushrod which passes through the center of the axle end plate and which is sealed by a reciprocating O-ring. The pushrod is joined to the external sleeve by a light disk which is exposed to atmospheric pressure on both sides to prevent pressure loading of the valve.

(6) The valve is spring loaded in the closed position.

The eight axle ports have a total area of 8.0 square inches. Since the sleeve valve was removed from the inside of the axle, the effective internal axle area was increased from 4.4 to 5.7 square inches. The valve stroke from full open to full closed remained at 3/4 of an inch and the maximum valve area, without programming, is 10.8 square inches. A spring which applies a force of 66 pounds in the full-open position and 55 pounds in the closed position is used to close the valve and to hold it tightly against the face seal.

Redesigned Valve Characteristics

The bleed-down times for this valve are also shown in Table 1. They compare favorably with those of the original sleeve valve even though the air is required to mushroom out at a 90-degree angle at the end of the axle. The air-turning resistance has been compensated for by using larger port and axle areas in the new design. When the valve is in the full-open position, it requires 0.25 second to bleed the tire from 17 psig to 2 psig. No measurable leakage was encountered when the valve was in the closed position. During recent test runs, the valve has been closing from the full-open to the full-closed position in approximately 13 milliseconds.

Pressure Sensor

A feature that was not called for in the analytical study specifications, but which is believed to be essential for satisfactory tire performance, is an overriding pressure control. Such a pressure control would have two main purposes. The first would be to insure a given minimum tire pressure by closing the valve whenever this minimum pressure is reached regardless of the load on the landing gear. The second purpose would be to permit reinflation of the tire to some maximum take-off pressure without danger of actuating the valve during take-off.

A pressure-sensing unit has been built within the axle of the high-flotation landing gear to accomplish both of the pressure-control functions. The present pressure sensor is designed to close the valve at a minimum tire pressure of 2 psig during a landing and to permit the tire to be reinflated to 11 psig for take-off without danger of valve actuation. It controls valve actuation by means of a spacer block which is located between two sections of the valve pushrod. When the spacer block is located between the two sections of valve pushrod, the resulting assembly has sufficient length to actuate the valve, but when the spacer block is removed from between the two sections, the resulting assembly does not have sufficient length to actuate the valve.

The method by which the spacer block is engaged and disengaged from the valve pushrod is shown in Figure 7. Operation of the unit is as follows:

(1) The spacer block is guided by slots which are cut into a U-block, and is capable of moving axially with the valve pushrod assembly inside the axle.

(2) The U-block is mounted on guide pins and is free to move transversely with respect to the axle.

(3) The U-block is spring loaded to hold it in a position which will disengage the spacer block from the valve pushrod assembly.

(4) Cam straps, which are mounted between rollers on the U-block and balance rollers, move axially and control the transverse position of the U-block.

(5) The position of the cam straps is controlled by a piston which is loaded by tire pressure on one side and atmospheric pressure and a preset spring on the other side.

(6) When the tire pressure force on the piston is sufficient to overcome the piston spring force and the axial component of the force imposed on the cam straps by the U-block springs, the piston will move to the right thus moving the U-block down, and with it moving the spacer block to the engaged position.

(7) In the engaged position, the rollers on the U-block are seated on the horizontal section of the cam surface, and the U-block springs no longer impose an axial force on the cam straps.

(8) When the tire pressure force on the piston drops below the piston spring force, the piston moves to the left and allows the disengaging springs to lift the U-block and the spacer block to the disengaged position.

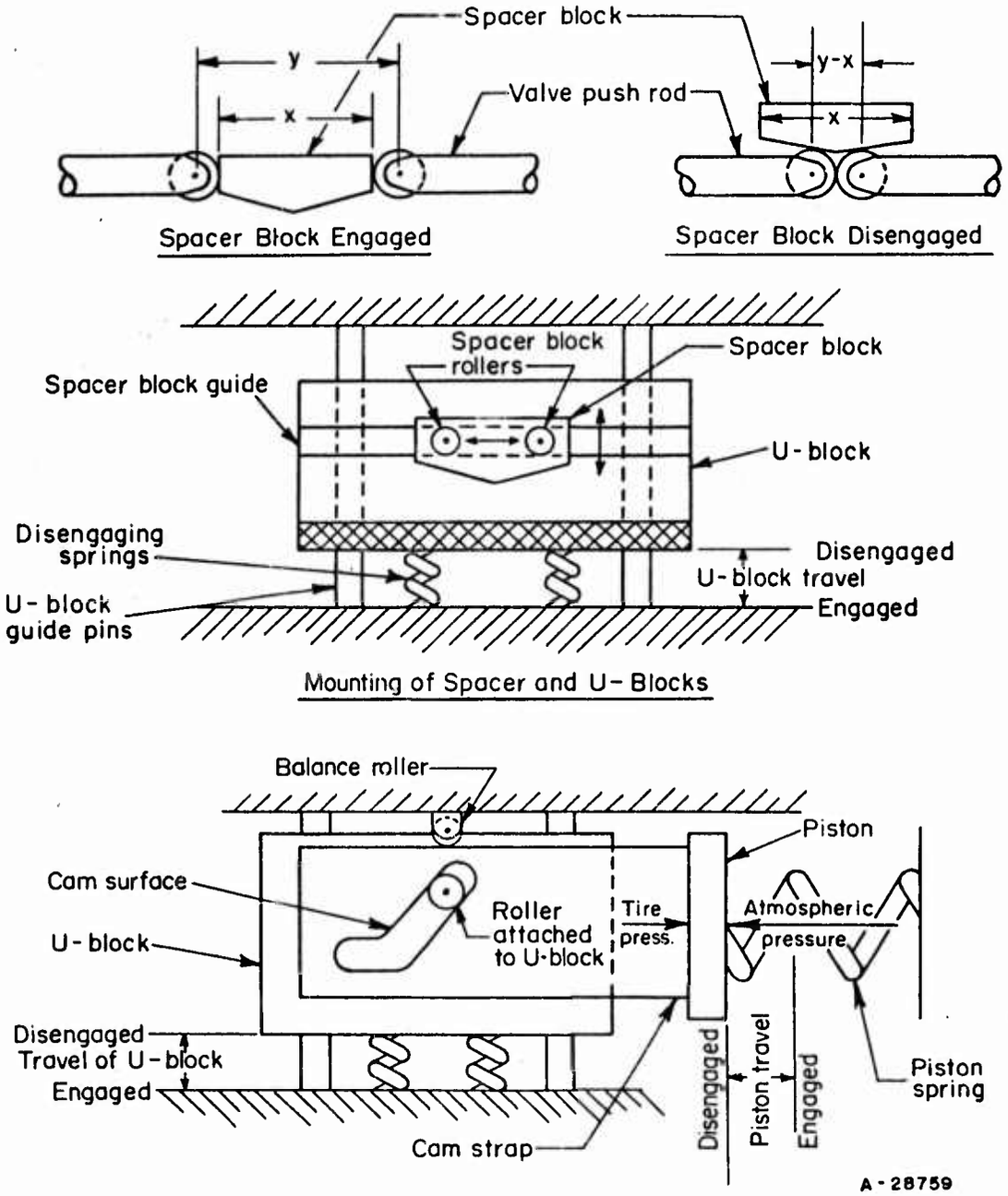

FIGURE 7. METHOD OF ENGAGING AND DISENGAGING SPACER BLOCK IN PRESSURE SENSOR

Pressure-Sensor Bench Testing and Characteristics

The pressure-sensing unit was extensively bench tested to determine its operating characteristics and reliability. It proved to be highly reliable under both static and dynamic conditions. The first series of tests were run under dynamic tire bleed-down conditions and static vibration conditions. These tests were conducted with the pressure-sensing unit connected to the valve test tank. Figure 8 is a picture of the test setup. Operation of the pressure-sensing unit was tested for all valve openings and pressure blow-down rates. The pressure at which the piston in the pressure-sensing unit began to move and the pressure at which the valve began to close were recorded. The pressure at which the piston began to move was extremely consistent. It remained between 2.75 and 3.0 psig at all blow-down rates. By the time the valve had started to close, the pressure had dropped to 2.2 psig for tests with full-valve opening, and to 2.4 psig for tests with the valve 1/3 open. Final tire pressure is dependent on the time required for valve closure. The engaging pressure during these tests varied from 11-1/2 to 12-1/2 psig.

To determine the effect of vibration on the sensitivity of the pressure-sensing unit, it was mounted on a M. B. Manufacturing Company Model C-3 vibrator table and allowed to bleed down from maximum tire pressure. Table 2 shows the effect of vibration loading on the pressure-sensor actuation pressure. The vibration loading was applied both axially and transversely. There was no appreciable change in the actuation pressure of the pressure-sensing unit when it was subjected to the various combinations of transverse loading, but axial vibrations did affect the actuation pressures slightly. An increase of 0.34 psig in actuation pressure was noted when an axial loading of 5 G's peak to peak at a frequency of 20 cps was applied to the pressure-sensing unit. Because of the low pressure of 2 to 3 psig, which would prevail during operation of the pressure sensor, it is doubtful that the soft tire will transmit axial loadings greater than those used in these tests.

TABLE 2. EFFECT OF VIBRATION ON PRESSURE-SENSOR ACTUATION PRESSURE

Acceleration Peak to Peak, G's	Frequency, cps	Actuation Pressure, psig
	Excitation Perpendicular to Axle Center Line	
0	0	3.09
10	20	3.00
10	100	3.00
	Excitation Parallel to Axle Center Line	
0	0	3.09
5	20	3.43
5	100	3.28

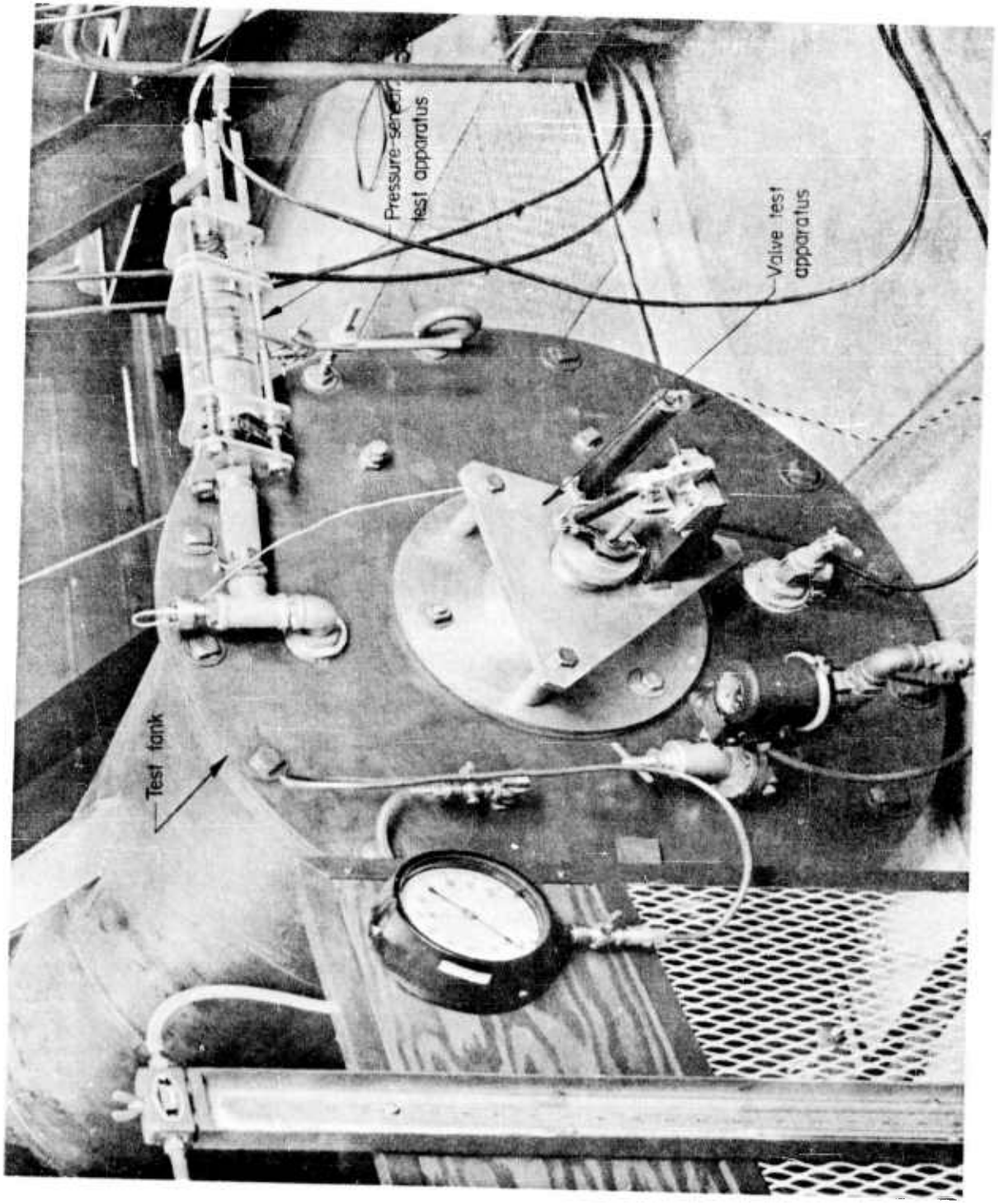

N48086

FIGURE 8. LABORATORY APPARATUS FOR EVALUATING TIRE BLEED-DOWN VALVE AND PRESSURE-SENSING UNIT

Rotary Seal

The air passage from the inflation-deflation system to the tire requires the use of two rotary seals between the rotary axle and the stationary axle housing. Because of space limitations, simplicity, and ease of application, large rotary O-ring seals are used. The rotary O-ring seals, which have a 1/16-inch-diameter cross section and a 90 durometer hardness, were installed according to the manufacturer's specifications. Before being incorporated into the design, however, they were laboratory tested under dynamic conditions.

During these tests two O-rings were mounted in a large stationary cylinder which represented the housing. A dummy axle, which was polished to 6 microinches rms, passed through the stationary cylinder and was rotated at speeds up to 1000 rpm. The section of the stationary cylinder between the two rotary O-rings was pressurized to 17 psig during the tests. To obtain satisfactory operation of the O-ring seals, it was found necessary to lubricate them with greases, such as Lubriplate No. 630AA, which are capable of operating at moderately elevated temperatures. Twenty 2-minute runs at an axle speed of 1000 rpm were completed with zero air leakage. The seals were allowed to cool between test runs. To reduce friction further and to decrease wear, the section of the axle in contact with the rotary seals has been chromium plated and polished to a 6-microinch rms finish.

Tire-Folding Provisions

Deflation and folding of the high-flotation tires after take-off are necessary that they will not require excessive space when they are retracted into the plane. Efforts to find the most satisfactory method of tire folding showed that the helical bellows method, which was recommended in the analytical study, offered the most promise. Early efforts to fold the tire into a helical bellows employed a mechanically applied torque, but the undistorted tire possesses extremely high torsional rigidity, and mechanical means of folding the tire would require excessively heavy equipment. It was found, however, that by drawing a vacuum in the tire, it could be induced to fold itself into a helical bellows.

Tire Modifications

Simply pulling a vacuum on the present tire geometry does not result in an acceptable folded tire package. Stiffening ribs must be applied to the tire to induce it to fold into a uniform symmetrical package. It is also necessary to start the tire folds mechanically at points midway between two adjoining ribs. Tests were conducted to determine the most satisfactory stiffening-rib pattern and to determine the necessary construction specifications to make a tire self-folding when a vacuum is drawn in it.

During the testing program, the stiffening ribs were cemented on the outer surface of a conventional 34-inch-diameter tire. Half-inch square, 50 durometer rubber strips were used as stiffening ribs, but they were not stiff enough to provide satisfactory tire folding. "B" size V-belts were used and produced satisfactory results. Experiments were carried out with variations in the stiffening-rib lead angle, the number of tire folds, and the distance between tire flanges. The helical stiffening

ribs were tested with lead angles of 0, 35, and 45 degrees. The most satisfactory results were obtained with a lead angle of 35 degrees. Six, seven, eight, ten, and fourteen stiffening ribs were used to determine the most desirable number of tire folds. With 10 and 14 ribs, it was found that the tire section between two adjoining ribs was too stiff to permit uniform creasing. The tire creased satisfactorily with eight ribs, although not quite so easily as with six or seven. Eight ribs permitted a slightly smaller final diameter than six or seven, however, and it was decided that this was the best number of ribs for this particular tire.

A more uniform outer diameter of the folded tire can be maintained by mounting circular stiffening ribs of a given diameter concentric with the axle on the side walls of the tire. The diameter of these stiffening ribs determines the final diameter of the folded tire. Tests indicate that the minimum diameter that can be successfully used for the side wall stiffening ribs in the 34-inch tire is 20 inches. The most satisfactory stiffening-rib configuration, therefore, consists of two circular ribs of 20-inch-diameter concentric with the axle and mounted on either side of the tire, and eight equally spaced helical ribs having a 35-degree lead angle. These ribs extend between the two circular side wall ribs. All ribs must be at least as stiff as a "B"-type V-belt. It is believed that such ribs could be molded into the tire during tire fabrication. Figure 9 shows pictures of the 34-inch-diameter tire in both the unfolded and folded conditions.

To start the creasing mechanically between the stiffening ribs, elastic cords were fastened to the interior of the tire midway between adjacent ribs. These cords were, in turn, fastened to a circular elastic cord, which was concentric with the axle, and thus provided a slight inward pull (4 pounds) on the section of the tire between the ribs. The elastic cords do not begin the creasing action until the tire pressure drops below 8 inches of water. It requires about 3 inches of water vacuum to start the folding action substantially and 12 inches of water vacuum to hold the tire in the completely folded position.

The tire-folding test axle was designed to hold the tire hubs out at their operational position until after the tire has been creased and one hub has started to rotate in relation to the other. By maintaining this distance between hubs, the initial tire creasing is substantially aided. After 10 degrees of rotation, the tire hubs are freed to move axially toward one another to further reduce the size of the folded tire. Total hub rotation during tire folding is about 90 degrees.

Tire-Flange Locking Mechanism

A positive lock on the inboard tire flange, which is allowed to move axially during the folding operation, is required to hold this flange in its operational position during a landing. Without such a locking mechanism, side loadings might unseat the flange during a landing with disastrous results. To accomplish this requirement, a method was devised to obtain positive locking of the inboard tire flange in its operational position during landings, but which will permit unlocking of the tire flange from the axle without any external actuation during the folding operation. This system, shown schematically in Figure 10, employs a pneumatic tube, inflated by tire pressure, to hold latches carried on the inboard tire flange in engagement with the axle. When the air pressure in the tire drops below a given value, the latches are disengaged by light springs and the tire is permitted to fold. The latches in the mechanism begin to disengage at 1-1/2 psig and are fully disengaged at 1/2 psig.

(a) N50753

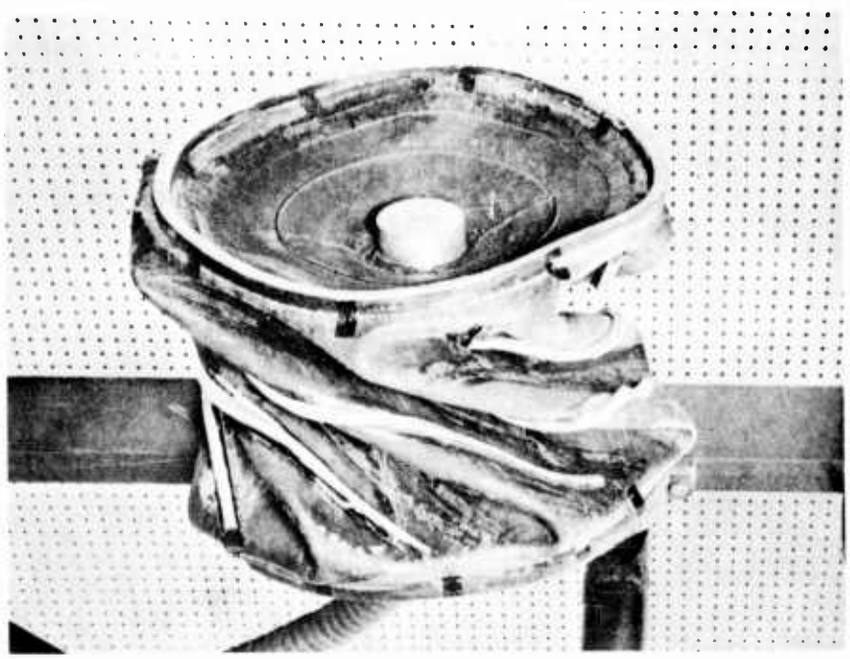

(b) N50754

FIGURE 9. HIGH-FLOTATION TIRE WITH STIFFENING RIBS SHOWN IN UNFOLDED AND FOLDED CONDITIONS

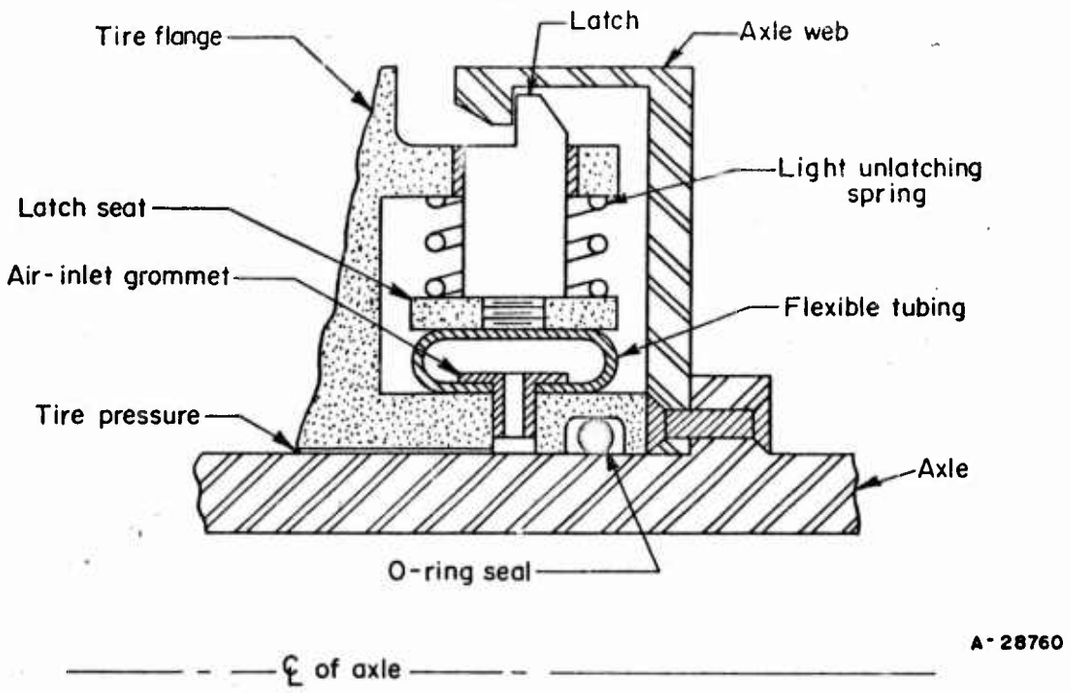

FIGURE 10. SCHEMATIC DRAWING OF TIRE-FLANGE LOCKING MECHANISM

Inflation-Deflation System

The use of the high-flotation tire necessitates an air-borne inflation-deflation system. This system must be capable of inflating the tire to its maximum initial inflation pressure (17 psig), making up for any possible tire leakage, and drawing a vacuum of 12 inches of water for tire folding. Fairly high capacity will be required to inflate and deflate the tire in short periods of time. The air-supply system used in the testing program is not designed for aircraft application. It is designed, however, to provide a minimum time for tire inflation. To inflate the tire, a solenoid valve, which is mounted between the tire and a large shop air line at 85 psig, is actuated for a given time interval. This time interval is sufficient to insure that the tire will reach, or slightly exceed, the desired initial tire pressure. In the event that the tire is slightly overinflated, it is bled down to the desired pressure. An adjustable pressure regulator is mounted in parallel with the timed solenoid valve. This regulator can be set to any desired pressure and furnishes air to replace losses due to any small amount of leakage. Tire deflation is accomplished by actuating a valve which connects the tire to a vacuum pump.

LANDING-GEAR DROP-TEST PROGRAM

Laboratory Drop-Test Apparatus

Component testing alone could not provide sufficient information to predict the operation of the complete high-flotation landing-gear system. Therefore, a drop-test apparatus was constructed at Battelle to perform preliminary tests on the assembled landing gear and to facilitate the acquisition of information on the necessary conditions for successful tire operation. During these preliminary tests, it was convenient to utilize the adjustability of the various components of the laboratory model high-flotation landing gear.

Drop-Tester Design

Figure 11 is a picture of the Battelle drop-test apparatus. It consists of a large four-bar linkage with a stationary vertical framework serving as one of the links. Two parallel arms are pinned to this frame one above the other. They guide the fourth link which is maintained in a vertical position. The distance between the pivot locations on the arms is 16 feet. To give the unit lateral stability, the arms are each constructed of two aluminum tubes which are spread 10 feet apart at the pivot location on the stationary frame. The high-flotation landing gear is mounted on the guided vertical link; in the remainder of this report this link will be referred to as the landing-gear carriage.

Landings can be made at any desired sinking speed by lifting the carriage to various heights with a crane and then dropping it. Since the guide arms cause the carriage to travel in an arc, the unit is designed to have the guide arms located in a horizontal position when the tire strikes the landing pad. This reduces to a minimum the effect of the circular path followed by the carriage.

The carriage has provisions for the attachment of additional weights. This makes it possible to carry out drop tests at various static loads. An emergency energy-absorption system is also provided for, in the event that the high-flotation tire fails to stop the vertical descent of the unit in the allowable tire deflection. The carriage has two outriggers mounted on either side of the high-flotation landing gear. These outriggers have pads on the bottom which strike piles of mounded sand when excessive tire deflections are encountered. Without this emergency stop serious damage could be done to the landing gear in the event of a blow-out or other serious malfunction. No such malfunction has yet occurred in the drop-testing program.

Drop-Tester Instrumentation

Evaluation of the landing-gear drop tests requires accurate knowledge of several important parameters. These parameters are:

(1) Tire deflection

(2) Acceleration

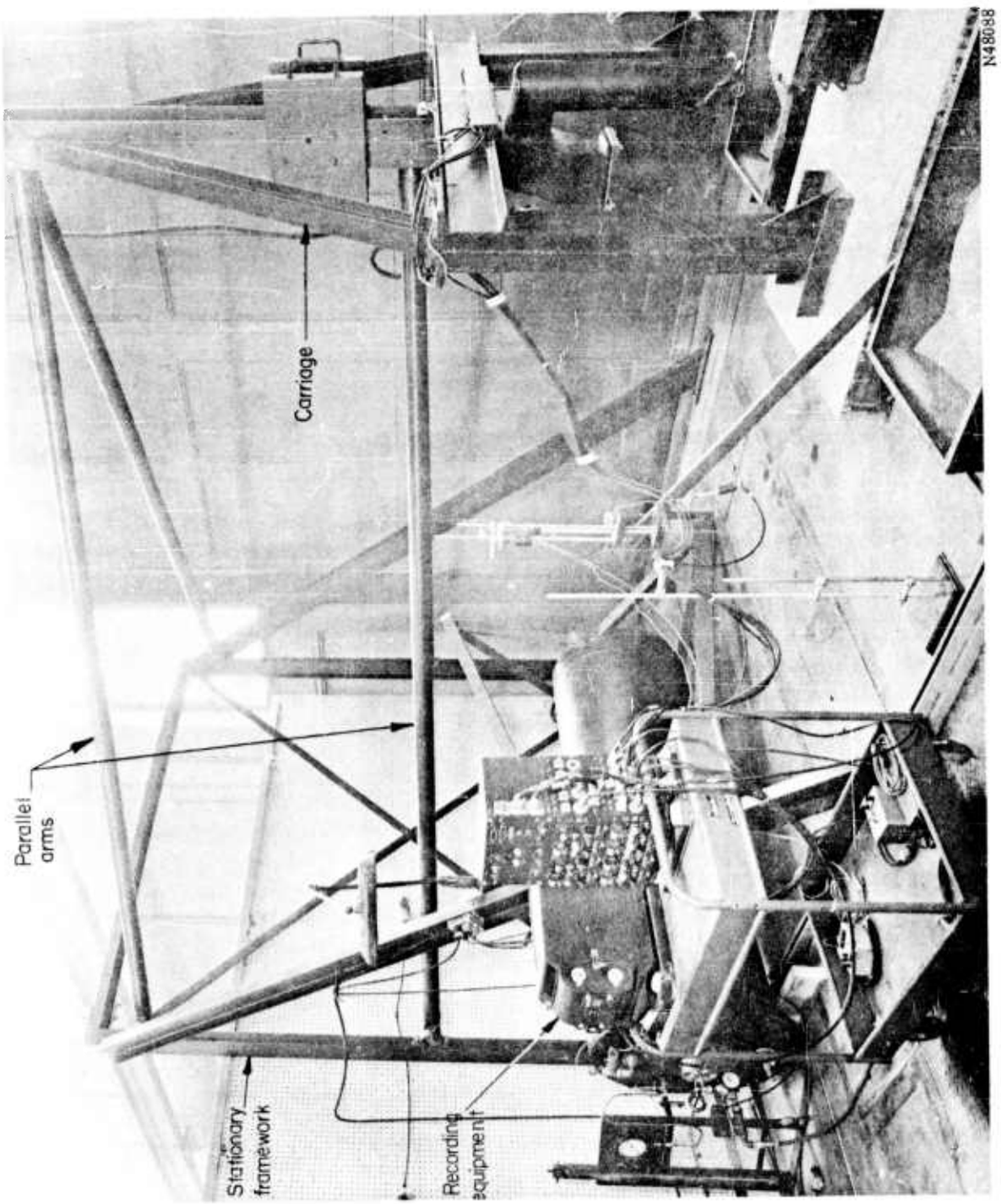

FIGURE 11. LANDING-GEAR DROP-TEST UNIT AND RECORDING INSTRUMENT

(3) Tire air pressure

(4) Valve position

(5) Sinking speed

(6) Time base.

A Consolidated 5-114 recording oscillograph was chosen to obtain the required information because of its excellent speed and sensitivity characteristics as well as on the basis of availability and adaptability. It is a high-speed, photographic, 18-channel recorder. Timing mark generation, automatic record numbering, and trace identification are self-contained features. A wide range of recording speeds and interchangeable galvanometers provide flexibility for special recording applications. A chart drive speed of 28.8 inches per second was selected for the landing-gear tests.

Because the travel of the landing-gear carriage is several times greater than the range of displacement transducers currently available, a lever system is used to scale down the carriage motion. This lever system consists of two links, one of which is pinned to the landing pad and the other of which is pinned to the carriage. The two links are then pinned together to form a scissors. The carriage displacement can be scaled down to any desired degree by mounting the pickup between the two links at various distances from the common pivot point. This scaled-down motion drives the slider of a linear potentiometer connected in a d-c bridge circuit to produce a signal proportional to carriage position.

Vertical acceleration forces encountered by the carriage are monitored by an accelerometer fastened to the carriage frame over the tire. Air pressure in the tire is measured by means of a variable-resistance pressure transducer. This pressure pickup is mounted inside the tire. Atmospheric reference pressure and lead wires pass through a tube which replaces one of the tire-flange retaining bolts. To provide an indication of valve position on the recording, a linear variable differential transformer (LVDT) is used to monitor the position of the valve. The recorder automatically provides a time base by marking the recording every one-hundredth second. Sinking speed is obtained by integrating the acceleration-time curve on the recording. Table 3 lists all the instrumentation equipment used along with information as to range, response, and sensitivity.

Drop-Test Conditions

Extensive drop testing of the assembled unit was carried out using the Battelle facility. During these tests the static load, initial tire pressure, sinking speed, and valve area were varied to determine their effects on the landing operation. Drop tests were carried out with static loads of 780 and 990 pounds. Sinking speeds ranging from 2-1/2 to 8-1/4 ft/sec were used in the 780-pound static load tests, and from 2-1/2 to 7-3/8 ft/sec in the 990-pound static load tests. Initial tire pressures were varied from 8 to 17 psig, and three different valve configurations were used. Valves A and B are similar in that they both have directly proportional valve area versus valve stroke characteristics. Valve A, however, has a larger magnitude of total area than Valve B.

TABLE 3. INSTRUMENTATION EQUIPMENT ON BATTELLE DROP TESTER

Function	Transducer	Range	Amplifier	Galvanometer
1. Displacement	Gianinni 8620-A Rectolinear potentiometer	4 inch	None	7-338
2. Acceleration	Statham C-15-350 Accelerometer	±15 G	1-113 B	7-323
3. Tire air pressure	CEC 4-311 Pressure pickup	0-100 psi	1-113 B	7-323
4. Valve position	Schaevitz 1000-SL LVDT	±1 inch	1-113 B	7-323

Amplifier – Power Supply

Consolidated Electrodynamics Corp.
Amplifier System D
Type 1-113 B Carrier amplifier

Carrier frequency: 3000 cps
Frequency response: ±2%, 0-600 cps
Maximum sensitivity: 1-mv input produces full-scale output
Linearity: ±2% between 0 and full scale, 0-600 cps

Recording Oscillograph

Consolidated Electrodynamics Corp. Type 5-114
Channels available: 18
Chart speed used: 28.8 in./sec
Timing marks: 0.01 sec

Galvanometers:	7-323	7-338
±5% Freq. range:	0-600 cps	0-125 cps
Sensitivity:	2.56 volts/inch	8.4 millivolts/inch
Application:	Acceleration Tire pressure Valve position	Tire displacement

Valve C is programmed so that the rate of valve-area opening is low during the first part, but high during the last part of the valve stroke. All three valves began to open when the load factor reached 0.75 and were full open when the load factor reached 1.5 for a static load of 780 pounds. A description of the three valves is as follows:

A. The area of Valve A increases at the rate of 14.4 $in.^2$/inch stroke and for a 3/4-inch stroke has a total area of 10.8 square inches.

B. The area of Valve B increases at the rate of 8.7 $in.^2$/inch stroke and for a 3/4-inch stroke has a total area of 6.5 square inches.

C. The area of Valve C increases at the rate of 5.8 $in.^2$/inch stroke for the first 5/16 inch of valve stroke and at the rate of 14.4 $in.^2$/inch stroke for the last 7/16 inch of valve stroke. The total area for a 3/4-inch stroke is 8.1 square inches.

Drop-Test Results

The first drop tests were made with the recommended initial tire pressure of 17 psig. The results of these tests were not satisfactory and indicated that the bleeding of air from the tire was not taking place fast enough to prevent the load factor from becoming excessive. With Valve A, the maximum load factor for a static load of 780 pounds and a sinking speed of 6-1/4 ft/sec reached 3.75. The impulse encountered during these early landings was so large that the tire often bounced back into the air.

Effect of Initial Tire Pressure on Maximum Load Factor

In an effort to reduce the magnitude of the maximum load factor and impulse, lower initial tire pressures were used. Figure 12 shows a graph of maximum load factors versus initial tire pressure obtained with Valve A for various combinations of sinking speed and static load. These results show that at the higher sinking speeds the maximum load factor was substantially reduced by employing lower initial tire pressures. In the case of the landing with a 780-pound static load and a sinking speed of 6-1/4 ft/sec, the maximum load factor was reduced from 3.75 to 2.80 when the initial tire pressure was reduced from 17 to 8 psig. The tire did not bounce in the 8-psig landing, and very little oscillation was observed in the system. A practical minimum pressure, in this case 8 psig, was reached, however, below which successful higher sinking speed landings were not possible because the tire was no longer capable of supplying a large enough impulse to stop the descent of the plane in the available tire deflection.

At the lower sinking speeds initial tire pressure had little effect on the maximum load factor because there was much more time available to bleed air from the tire. The graph shows that, for landings at a sinking speed of 2-1/2 ft/sec and a static load of 780 pounds, the maximum load factor remained fairly constant at 1.75. The maximum load factor for low-sinking-speed landings with a static load of 990 pounds was slightly reduced by a reduction in the initial tire pressure. By reducing the initial tire pressure from 17 to 11 psig in the landings made with Valve A at a sinking speed of 2-1/2 ft/sec and a static load of 990 pounds, the maximum load factor was reduced from 1.7 to 1.45.

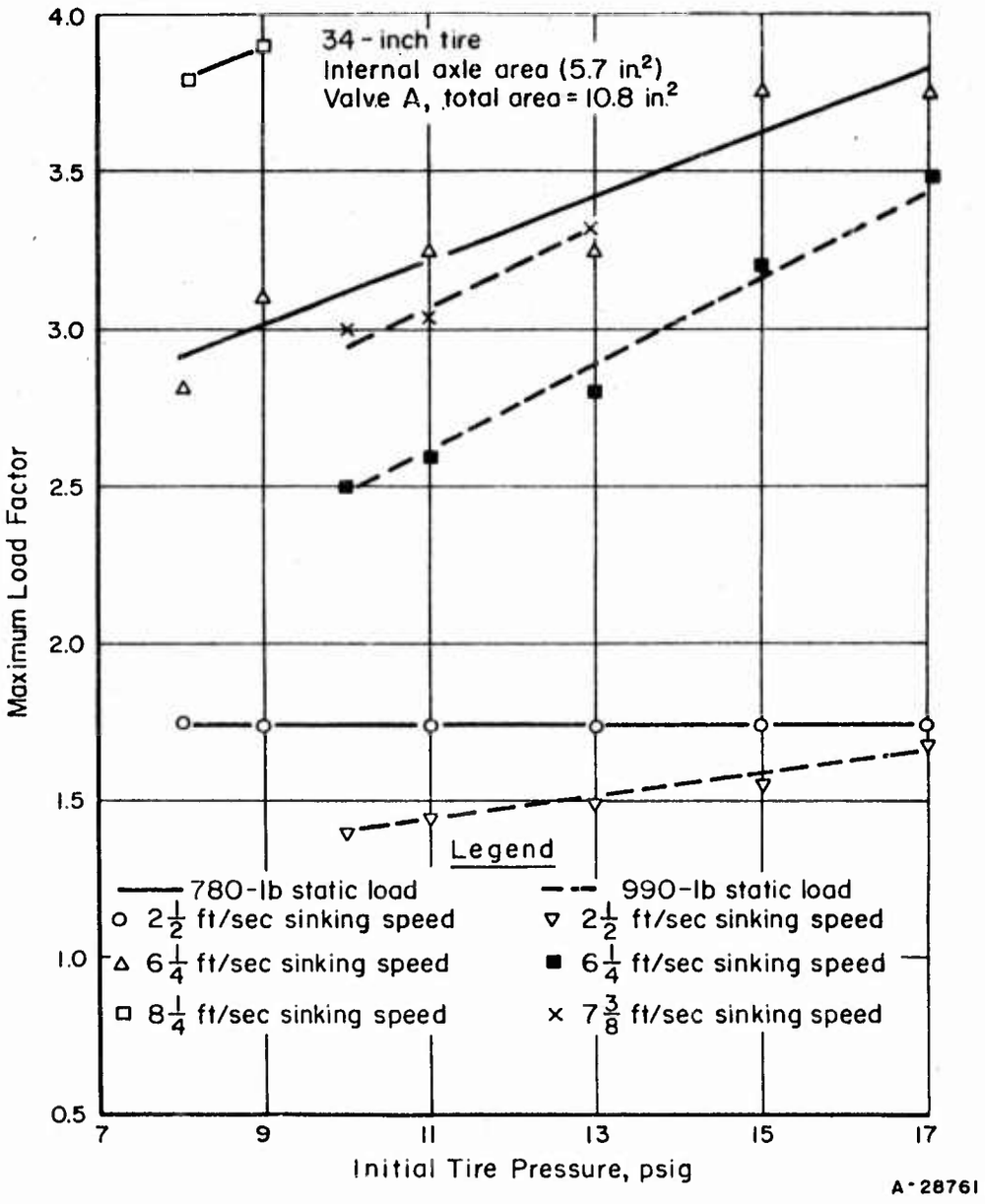

FIGURE 12. RELATION OF MAXIMUM LOAD FACTOR TO INITIAL TIRE PRESSURE

At any given initial tire pressure and sinking speed, the maximum load factor was less for the 990-pound static load than for the 780-pound static load landings. This was to be expected, since for any given load factor the 990-pound static load requires a higher force (and thus a larger tire deflection for any given tire pressure) than the 780-pound static load. This larger required tire deflection allows the tire more time to bleed down and thus reduces the maximum load factor.

Effect of Valve Area and Programming on Maximum Load Factor

Table 4 shows the effect of valve area and programming on the maximum load factor. The maximum load factor under any given conditions of static load, initial tire pressure, and sinking speed was slightly less for tests conducted with Valve A than for those conducted with Valve B. This difference varied from around 0.05 to 0.30 for sinking speeds of 2-1/2 and 7-3/8 ft/sec, respectively, in the 780-pound static-load tests. It was even smaller in the 990-pound static load tests varying from 0 in some cases to a maximum of 0.20 at an initial tire pressure of 11 psig and a sinking speed of 6-1/4 ft/sec. Since Valve A has a total area of 10.8 square inches and Valve B has a total area of only 6.5 square inches, it would seem that the difference in maximum load factors obtained with the two valves should have been larger than those which were recorded. The fact that the maximum load factor reached when using Valve B is only slightly larger than that reached when using Valve A indicates that the main limiting restriction to air flow from the tire is the internal axle area of 5.7 square inches, which is identical for both valves.

Programming of the valve area, as was done in Valve C, to have a slow rate of area increase during the first part and a fast rate of area increase during the last part of the valve stroke had a beneficial effect on the maximum load factor for tests with the 780-pound static load at low initial tire pressures and/or low sinking speeds. For 780-pound static load tests with an initial tire pressure of 17 psig, the maximum load factor obtained with Valve C was not lower than that obtained with Valve A at any sinking speed, but when the initial tire pressure was reduced to 9 psig the maximum load factor obtained with Valve C was less than that obtained with Valve A at sinking speeds up to 6-1/4 ft/sec. It is believed that this beneficial effect could be extended to the higher initial tire pressures and sinking speeds if the available axle area were larger.

At present the valve immediately opens to the full-open position for all tests at high initial pressure and/or high sinking speeds. Programming at these conditions has little effect since it merely reduces the amount of total valve area that could be exposed in the full-open position. At the lower initial tire pressures and/or sinking speeds, programming improves the tire performance because the valve is operating in the programmed portion of the stroke and can more closely regulate the flow of air from the tire.

The maximum load factor of landings conducted with a static load of 990 pounds did not vary substantially between tests made with Valves A and C. One reason for this is that it requires a larger change in force to result in a given change in load factor for landings made at higher static loads. Another reason is that in the 990-pound static-load tests the valve began to open at a load factor of 0.60 and was full open at a

TABLE 4. EFFECT OF VALVE AREA AND PROGRAMMING ON MAXIMUM LOAD FACTOR

Initial Tire Pressure, psig	Aircraft Sinking Speed, ft/sec	Maximum Load Factor		
		Valve A	Valve B	Valve C
	Static Load of 780 Pounds			
17	2-1/2	1.75	1.80	1.75
	4-3/4	3.05	3.15	3.10
	6-1/4	3.75	3.95	3.85
11	2-1/2	1.75	1.80	1.65
	6-1/4	3.30	3.40	3.15
	7-3/8	3.50	3.80	3.70
9	2-1/2	1.75	1.80	1.65
	6-1/4	3.10	3.20	2.85
	7-3/8	3.40	3.70	3.40
	Static Load of 990 Pounds			
17	2-1/2	1.70	1.70	1.75
	4-3/4	2.65	2.75	2.75
	6-1/4	3.35	3.35	3.35
11	2-1/2	1.45	1.60	1.50
	4-3/4	2.15	2.30	2.15
	6-1/4	2.60	2.80	2.70

Constant axle area of 5.7 $in.^2$, total valve stroke = 3/4 in.

Valve A - Valve area increases at rate of $\frac{14.4\ in.^2}{inch\ valve\ stroke}$

Valve B - Valve area increases at rate of $\frac{8.7\ in.^2}{inch\ valve\ stroke}$

Valve C - Valve area increases at rate of $\frac{5.8\ in.^2}{inch\ valve\ stroke}$

For first 5/16 inch of valve stroke and $\frac{14.4\ in.^2}{inch\ valve\ stroke}$ for last 7/16 inch of valve stroke.

load factor of 1.15. This reduced the time in which the valve was operating in the programmed portion of the stroke. Therefore, the maximum load factors of the landings made with the 990-pound static load were not so significantly affected by valve programming as those made with a 780-pound static load.

Optimum Operating Conditions and Range of Sinking Speeds

The highest sinking speed at which the unit was operated was 8-1/4 ft/sec. This sinking speed was attained in a series of drop tests that were made with a static load of 780 pounds, an initial tire pressure of 8 psig, and Valve A. Landings at all sinking speeds from 2-1/2 ft/sec to 8-1/4 ft/sec were successful under these conditions. Figures 13, 14, and 15 show the landing dynamic characteristics of the 34-inch-diameter high-flotation tire for these landings at sinking speeds of 2-1/2, 6-1/4, and 8-1/4 ft/sec, respectively. Figure 15 shows that the maximum load factor for the 8-1/4 ft/sec landing was 3.8, which is below the allowable design maximum of 4.0. The oscillation of the tire after valve operation, which is dependent on the energy remaining in the system, varied from around 1 inch peak-to-peak at the low sinking speeds to around 2 inches peak-to-peak at the higher sinking speeds.

Slightly higher initial tire pressure was required to give the best performance with the 990-pound static load. With an initial tire pressure of 10 psig, a static load of 990 pounds, and Valve A, the maximum load factor varied from 1.4 at a sinking speed of 2-1/2 ft/sec to 3.0 at a sinking speed of 7-3/8 ft/sec. The tire oscillation after these tests was around 1 inch peak-to-peak at all sinking speeds from 2-1/2 to 7-3/8 ft/sec.

Energy-Dissipation Capability of the High-Flotation Tire

Drop tests were made under identical conditions with and without valve actuation so that it would be possible to compare the two and determine the effectiveness of the high-flotation tire's energy dissipation capabilities. Figure 16 shows the dynamic characteristics of the 34-inch-diameter tire for a landing with a static load of 990 pounds, Valve A, an initial tire pressure of 10 psig, and a sinking speed of 7-3/8 ft/sec, but without valve actuation. Figure 17 shows the dynamic characteristics of a landing under the same conditions except that the valve is actuated.

By actuating the valve and bleeding air from the high-flotation tire, the maximum load factor was reduced from 4.55 in the landing with no valve actuation to 3.00. The landing made without valve actuation was unsuccessful: the tire bounced completely off the landing pad to a point just slightly below its original drop position. Almost zero energy was dissipated during the landing operation. The opposite was true, however, in the landing made with valve actuation. Almost all of the impact energy was dissipated by bleeding air from the high-flotation tire. It did not bounce, and only a 1-inch peak-to-peak oscillation remained in the system after valve actuation.

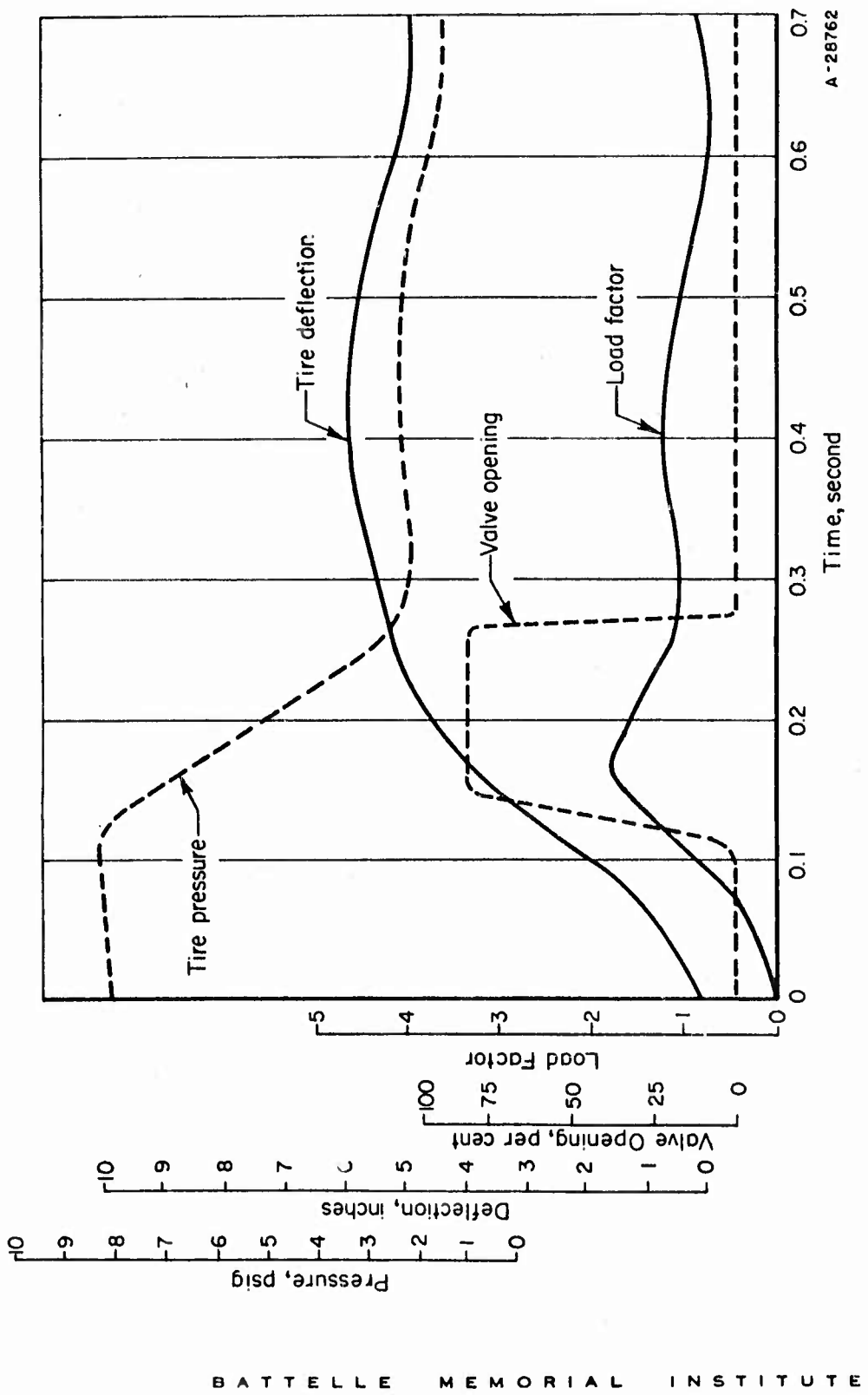

FIGURE 13. LANDING DYNAMICS OF A 34-INCH-DIAMETER HIGH-FLOTATION TIRE WITH AN INITIAL TIRE PRESSURE OF 8 PSIG, A STATIC LOAD OF 780 POUNDS, AND VALVE A AT SINKING SPEED OF 2-1/2 FT/SEC

Initial inflation pressure, 1152 lb/ft^2. Internal axle area, 0.04 ft^2 (5.7 in.^{2}).

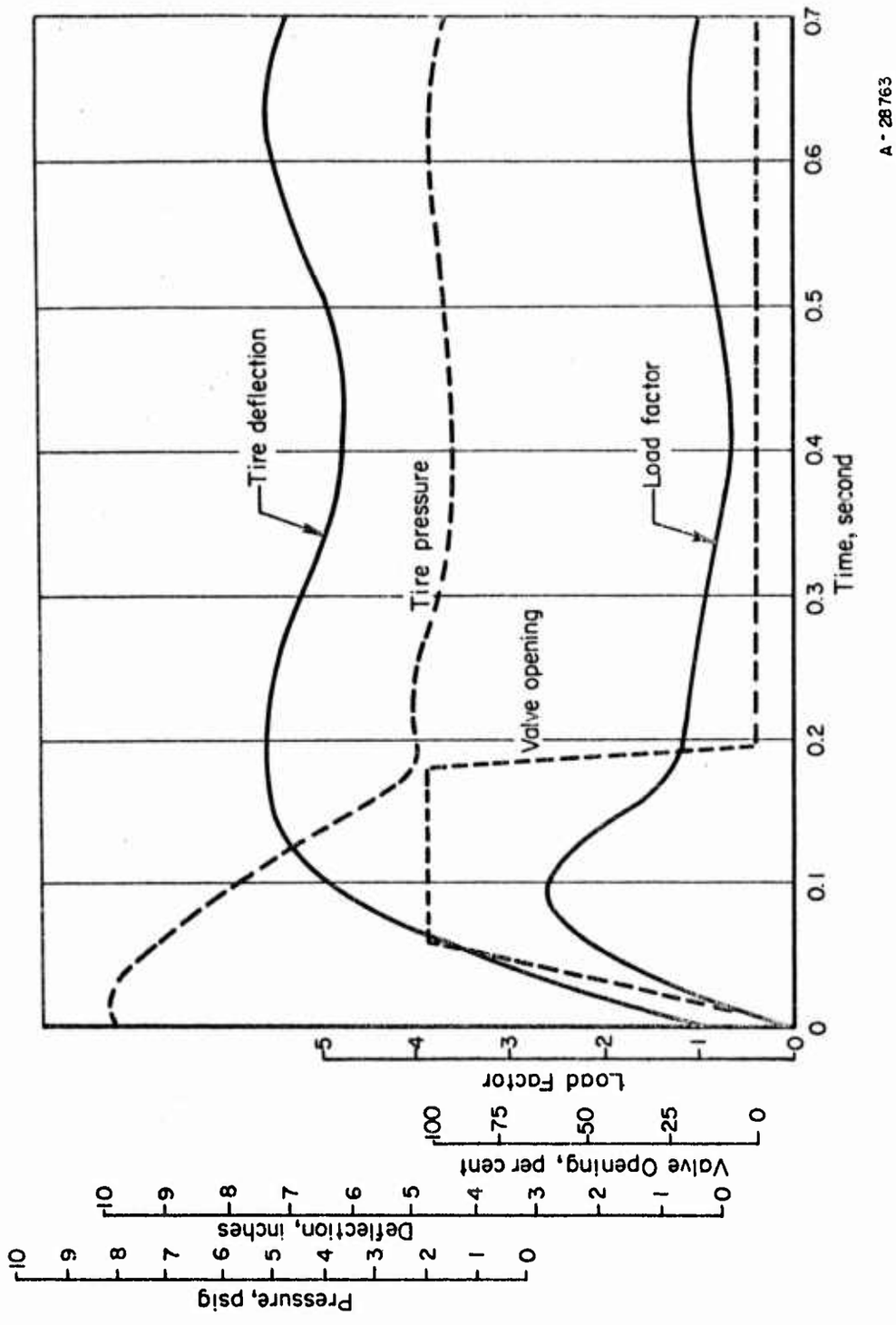

FIGURE 14. LANDING DYNAMICS OF A 34-INCH-DIAMETER HIGH-FLOTATION TIRE WITH AN INITIAL TIRE PRESSURE OF 8 PSIG, A STATIC LOAD OF 780 POUNDS, AND VALVE A AT A SINKING SPEED OF 6-1/4 FT/SEC

Initial inflation pressure, 1152 lb/ft^2. Internal axle area, 0.04 ft^2 (5.7 in.^{2}).

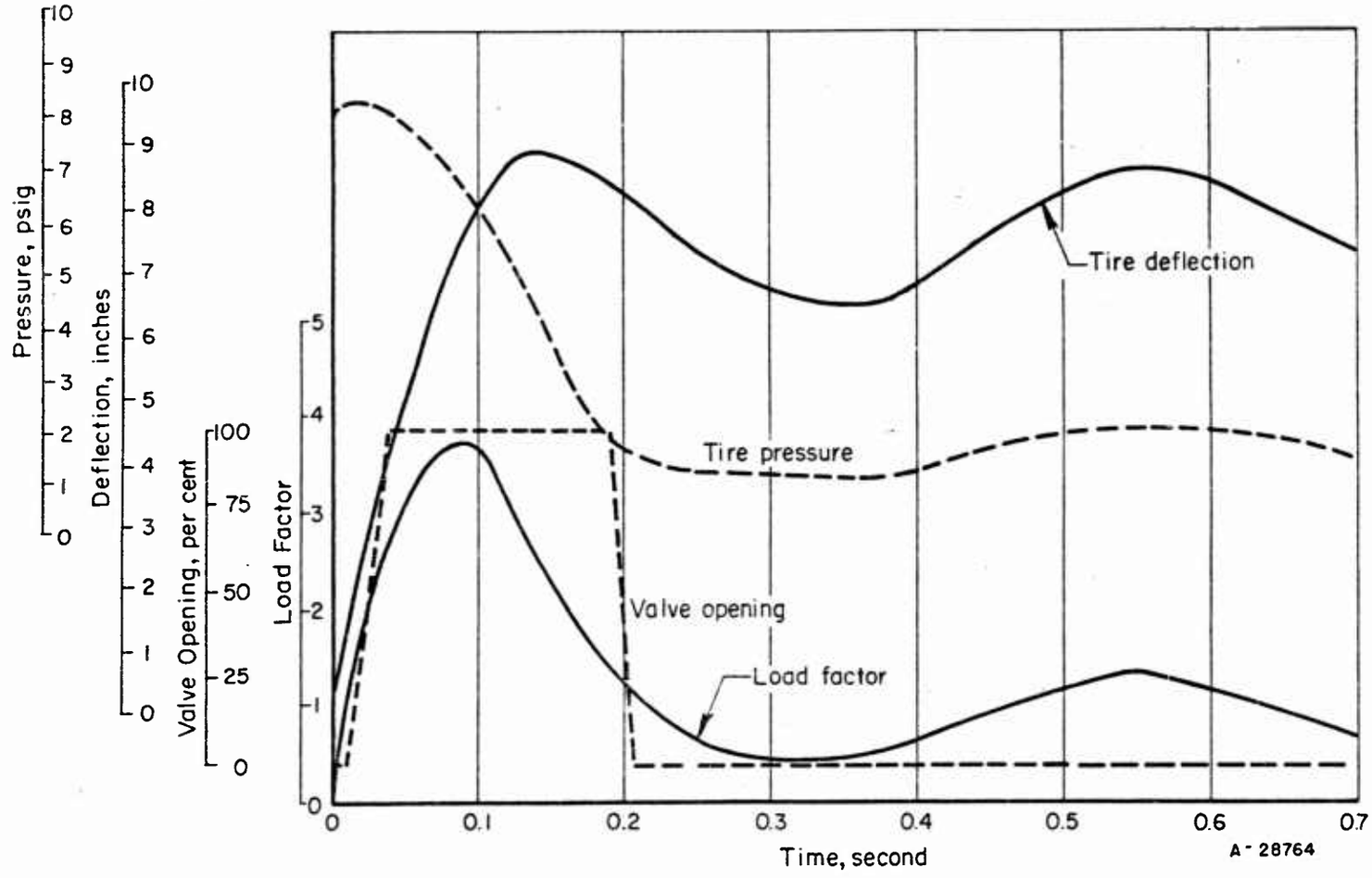

FIGURE 15. LANDING DYNAMIC OF A 34-INCH-DIAMETER HIGH-FLOTATION TIRE WITH AN INITIAL TIRE PRESSURE OF 8 PSIG, A STATIC LOAD OF 780 POUNDS, AND VALVE A AT A SINKING SPEED OF 8-1/4 FT/SEC

Initial inflation pressure, 1152 lb/ft^2. Internal axle area, 0.04 ft^2 (5.7 in.^{2}).

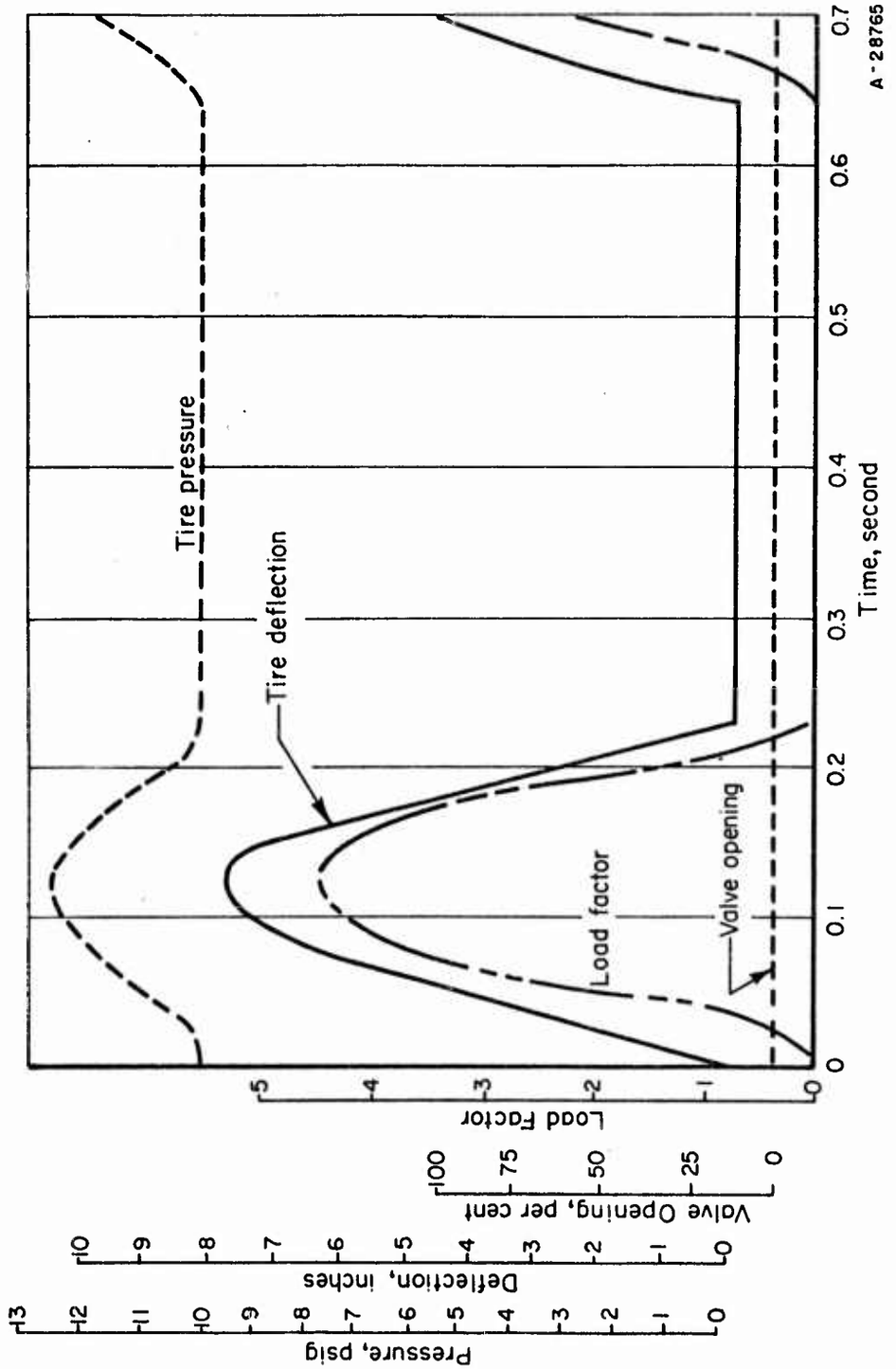

FIGURE 16. LANDING DYNAMICS OF A 34-INCH-DIAMETER HIGH-FLOTATION TIRE AT AN INITIAL TIRE PRESSURE OF 10 PSIG, A STATIC LOAD OF 990 POUNDS, AND A SINKING SPEED OF 7-3/8 FT/SEC WITHOUT VALVE ACTUATION

Internal axle area, 0.04 ft^2 (5.7 in.2).

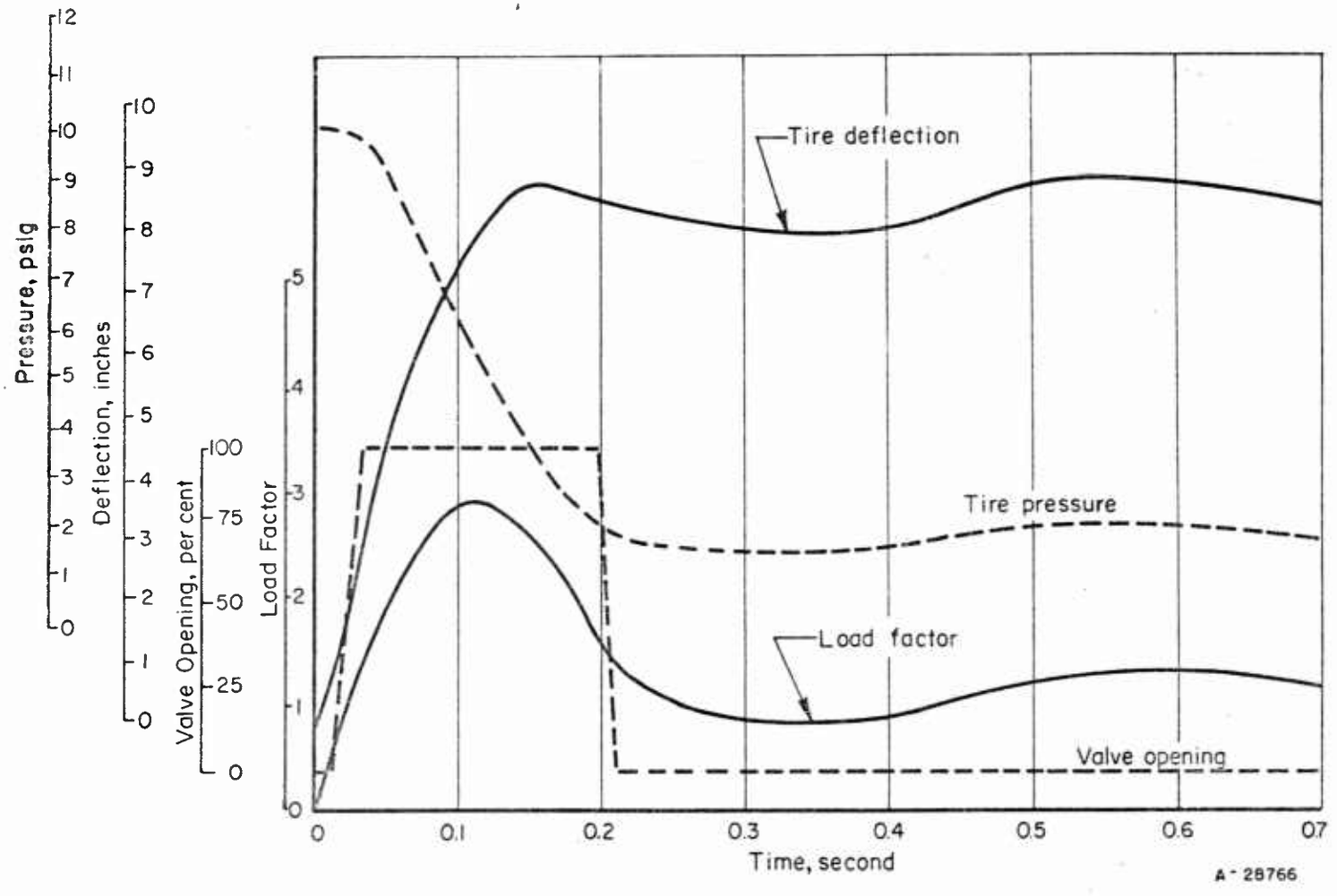

FIGURE 17. LANDING DYNAMICS OF A 34-INCH-DIAMETER HIGH-FLOTATION TIRE AT AN INITIAL TIRE PRESSURE OF 10 PSIG, A STATIC LOAD OF 990 POUNDS, AND A SINKING SPEED OF 7-3/8 FT/SEC WITH VALVE (A) ACTUATION

Internal axle area, 0.04 ft^2 (5.7 $in.^2$).

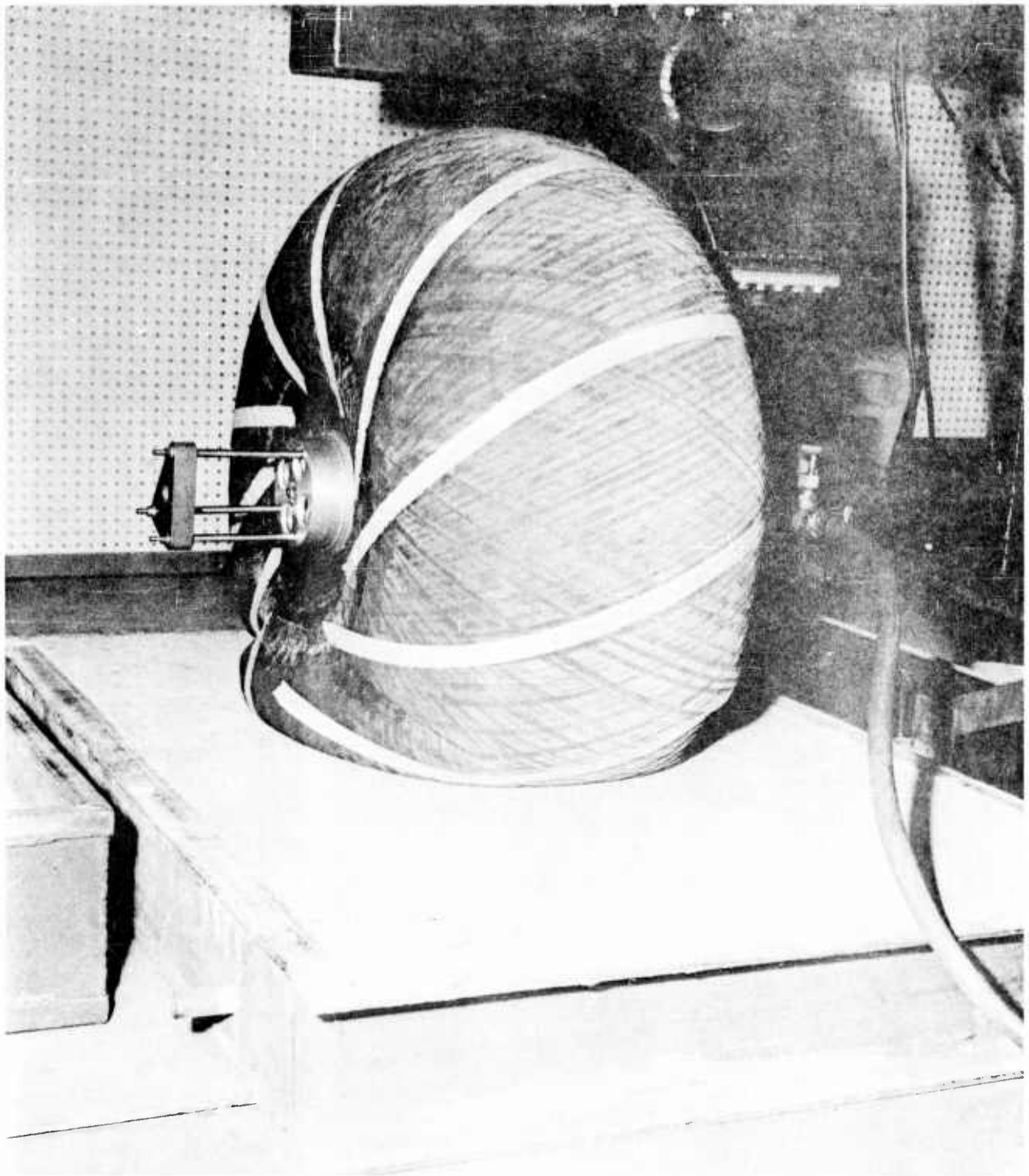

N50752

FIGURE 18. THIRTY-FOUR-INCH HIGH-FLOTATION TIRE INFLATED TO 2 PSIG AND SUPPORTING LOAD OF 750 POUNDS, SHOWING CREASING OF SIDEWALL OF TIRE AT EXTREMELY LOW PRESSURES

Final Tire Pressure

The final tire pressure achieved during the testing program ranged from 2 to 3 psig. It was evident, however, that the present 34-inch-diameter high-flotation tire would probably have difficulty in operating at the design final tire pressure of 2 psig when it is carrying a static load of 750 pounds.. Under these conditions the tire is significantly creased near the region in contact with the ground. Figure 18 is a picture of the 34-inch-diameter high-flotation tire with a static load of 750 pounds and a pressure of 2 psig. The clearly observable folds in the tire would undoubtedly cause excessive heating of the tire during ground operation. To avoid these tire creases it is necessary to inflate the tire to around 3-1/4 psig. If the 34-inch-diameter high-flotation tire is to operate successfully with a static load of 750 pounds, it may be necessary to either limit the final tire pressure to 3-1/4 psig or to reinflate the tire to this pressure immediately after touchdown.

CONCLUSIONS

The conclusions that can be drawn from the test results are:

(1) A deflection between the tire hub and the strut can be used for direct, mechanical valve actuation.

(2) It is possible to fold the 34-inch-diameter high-flotation tire into a helical bellows by mounting stiffening ribs on it and drawing a vacuum of 12 inches of water in it.

(3) The high-flotation landing-gear system is capable of successfully dissipating the landing impact energy of aircraft under laboratory drop-test conditions.

(4) The present 34-inch-diameter tire unit functions with load factors less than four at sinking speeds as high as 8-1/4 ft/sec with an initial tire pressure of 8 psig, a static load of 780 pounds, and Valve A. This maximum sinking speed could be increased slightly by increasing the axle area available for air flow.

FUTURE WORK

In the immediate future it is planned to carry out more extensive testing of the present 750-pound unit. These tests shall be conducted with the dashpot operating in the system to determine its effect on the high-flotation tire's characteristics. Tests will also be conducted at static loads lighter than 780 pounds.

On April 11, 1958, Battelle recommended to Fairchild an expansion of the present research program. This expanded program specifies that Battelle shall design, supervise construction, and perform laboratory tests on a pair of high-flotation landing gears designed to carry a static load of 1500 pounds. These units shall be used for flight testing of the high-flotation tire system on an L-19 aircraft. The laboratory testing of both the 750-pound laboratory model unit and the pair of 1500-pound flight test units shall include drop testing with spinup before drop to an equivalent of 75 knots. The design of the flight test 1500-pound pair of gears shall include the necessary struts for suitable attachment to an L-19 type aircraft. An inflation-deflation system shall be designed including all valves, controls, and mechanisms necessary for air-borne inflation-deflation and tire folding. The expanded program also calls for the design of the necessary brackets to mount the 1500-pound gears on the N.A.C.A. drop tester at Langley Field, Virginia, and a mechanism to extend the flight test system into the slip stream from the lowered ramp of a C-123 type aircraft while in flight to evaluate tire folding in a high-velocity air stream.

The design of the 1500-pound landing-gear system is now in progress. A number of weight-saving innovations have been devised and are being incorporated into the design. A wing-lift device for the Battelle drop tester shall also be designed in addition to the various apparatus called for in the expanded research program.

A record of all technical work performed on this project appears in Laboratory Record Books 13510, 13511, and 14103.

JAH:WFP:JHB:CWR:SAG:JEV:RJM/bjw

FAIRCHILD AIRCRAFT AND MISSILES DIVISION

HAGERSTOWN 10, MARYLAND

SUBJECT DESIGN AND DEVELOPMENT OF LABORATORY AND FLIGHT-TEST MODELS OF LANDING GEAR FOR AIRCRAFT TO BE OPERATED FROM ROUGH UNPREPARED FIELDS

PREPARED BY Battelle Memorial Institute, Columbus, Ohio. as per FAMD Purchase Order SC-85285

REPORT NO. R245.014

CHECKED BY

MODEL M-245B

APPROVED BY

COPY NO.

APPROVED BY

NO. OF PAGES

APPROVED BY

DATE 15 August 1959

REVISIONS

REVISION DATE	PAGES AFFECTED	APPROVED

NS-800-69B

FINAL REPORT

on

THE DESIGN AND DEVELOPMENT OF LABORATORY AND FLIGHT-TEST MODELS OF LANDING GEAR FOR AIRCRAFT TO BE OPERATED FROM ROUGH UNPREPARED FIELDS

to

FAIRCHILD AIRCRAFT AND MISSILES DIVISION
FAIRCHILD ENGINE AND AIRPLANE CORPORATION

August 15, 1959

by

W. F. Prien, R. D. Fannon, J. H. Beck, C. W. Rodman, J. A. Hoess,
J. E. Voorhees, and R. J. McCrory

BATTELLE MEMORIAL INSTITUTE
505 King Avenue
Columbus 1, Ohio

TABLE OF CONTENTS

TABLE OF CONTENTS
(Continued)

THE DESIGN AND DEVELOPMENT OF LABORATORY AND FLIGHT-TEST MODELS OF LANDING GEAR FOR AIRCRAFT TO BE OPERATED FROM ROUGH UNPREPARED FIELDS

by

W. F. Prien, R. D. Fannon, J. H. Beck, C. W. Rodman,
J. A. Hoess, J. E. Voorhees, and R. J. McCrory

During the first phase of this research program, which was entitled "The Design and Development of Laboratory Models to Study the Feasibility of High-Flotation Tires for Aircraft", the high-flotation landing gear designed to carry a static load of 750 pounds was successfully tested in the laboratory, demonstrating the feasibility of the high-flotation landing-gear system under laboratory conditions. The results obtained during the testing of the 750-pound landing-gear unit encouraged Battelle to recommend to the Fairchild Aircraft and Missiles Division an expansion of the research program to include the design and development of a high-flotation landing-gear system for flight testing. In response to a request by Fairchild, Battelle submitted a proposed expanded research program dated April 11, 1958. An agreement dated June 25, 1958, was concluded between Battelle and Fairchild authorizing this program and changing the title to "The Design and Development of Laboratory and Flight-Test Models of Landing Gear for Aircraft to be Operated From Rough Unprepared Fields".

The objectives of the program were expanded to include the following items:

(1) The design, supervision of construction, and laboratory testing of a pair of high-flotation landing gears designed to carry a static load of 1500 pounds. These units shall be used for flight testing of the high-flotation tire system on an L-19 aircraft.

(2) The laboratory testing of both the 750-pound laboratory-model unit and the pair of 1500-pound flight-test units. This testing shall include drop test with tire spin-up before touchdown to an equivalent of 75 knots.

(3) The design of the necessary struts for suitable attachment of the 1500-pound landing-gear units to an L-19 aircraft.

(4) The design of an airborne inflation-deflation system.

(5) The design of the necessary brackets to mount the 1500-pound gears on the N.A.S.A. drop tester at Langley Field, Virginia.

(6) The design of a dynamic tire-folding test apparatus to be mounted in a C-123 aircraft to evaluate tire folding in a high-velocity air stream.

The research program was further expanded by an agreement between Battelle and Fairchild on March 18, 1959. This expanded research program provided additional funds and time to complete all of the objectives called for in the June 25, 1958, agreement plus a number of additional objectives. These additional objectives included the following items:

(1) The construction and laboratory testing of the dynamic tire-folding test apparatus.

(2) The installation of a safety device in the high-flotation landing gear to operate a warning light in the cockpit when the gear is ready to land.

(3) The disassembly, inspection, modification, weather protection, and retesting after reassembly of the 1500-pound landing-gear units.

(4) The preparation of two new tires for mounting on the high-flotation landing gear.

(5) The provision of technical assistance to Fairchild during the flight testing of the high-flotation landing gear and the dynamic folding tests of the high-flotation tire.

During the laboratory testing of the 750- and 1500-pound landing-gear units, drop tests were conducted with wing lift as well as with tire spin-up. Both size units operated successfully under laboratory conditions, and the pair of 1500-pound units has been sent to Fairchild for flight testing.

This final report covers the work on the project from June 1, 1958, to its completion on August 15, 1959. It includes the testing of the 750-pound unit with tire spin-up and wing lift, the design of the 1500-pound unit and of its associated apparatus, and the laboratory testing of the 1500-pound unit.

SUMMARY

As a result of the successful operation obtained with the laboratory-model high-flotation landing gear designed to carry a static load of 750 pounds, the 1500-pound landing-gear unit has been designed to be adaptable to aircraft installation for flight testing. Its design embodies the same concepts and objectives as the design of the 750-pound unit, but a number of weight-saving innovations have been devised and are incorporated into its design.

Tire bleed-valve actuation in both designs is accomplished by a deflection between the tire hub and the strut when a vertical load is applied to the high-flotation tire. The heavy-load sensor that was used in the 750-pound landing-gear unit has been replaced by a much lighter closed hydraulic cylinder mounted in the axle. This cylinder has two pistons entering it; the pistons are at right angles to one another. The first of these pistons is fastened to a vertical load-carrying link and is larger in area than the second piston which is used to actuate the tire bleed valve. A high vertical load and a small deflection imposed on the first piston results in a lower axial load and larger deflection of the second piston.

Except for changes in geometry, the design of the pressure sensor and tire bleed valve for the 1500-pound landing-gear unit has remained essentially unchanged from that of the 750-pound unit. One additional feature, however, has been added to the

pressure sensor. A microswitch, which would be connected to a warning light in the plane, has been installed on the pressure sensor and is actuated when the pressure sensor cocks. This warning light would inform the pilot whether the pressure sensor was cocked.

The helical-bellows method of tire folding is used to fold the 43-inch-diameter tire. The same tire modifications used to induce the 34-inch-diameter tire to fold into a helical bellows are used on the 43-inch-diameter tire. A tire-folding apparatus, which is to be mounted in a C-123 aircraft and which will extend a 43-inch-diameter tire into the slip stream while in flight to test tire folding under dynamic conditions, has been designed, constructed, and successfully operated in the laboratory.

Struts to mount the 1500-pound landing-gear units on an L-19 aircraft, an inflation system to control the tire pressure of these units during flight testing, and a linkage to mount the high-flotation landing gear on the N.A.S.A. drop-test facility at Langley Field, Virginia, have been designed. The Battelle drop-test facility has been strengthened for drop tests with tire spin-up, and tire spin-up and wing lift devices have been designed and constructed.

Drop tests have been conducted with the 750- and 1500-pound landing-gear units. During these tests the initial tire pressure, static load, sinking speed, valve configuration, tire spin-up speed, and percentage wing lift were varied to determine their effect on the operation of the system. The results of these tests were highly satisfactory. The 43-inch-diameter high-flotation tire was successfully tested at sinking speeds ranging from 2-1/2 to 10-1/2 ft/sec.

DESIGN OF THE HIGH-FLOTATION LANDING GEAR AND ITS ASSOCIATED APPARATUS

Design of Components of the 1500-Pound Landing-Gear Unit

The basic method of operation of the 1500-pound high-flotation landing gear is patterned after its successfully performing 750-pound predecessor. While there are no basic changes in the method of operation of the 1500-pound unit from that of the 750-pound unit, there are a number of significant weight-saving design changes in some of the components. Weight considerations were necessitated by the fact that the 1500-pound unit was to be mounted and flight tested on an L-19 aircraft after preliminary laboratory testing had established the effect of the many variable parameters on the operation of the unit. The results of these changes in component design can be seen in the reduction of weight from the 73 pounds of the 750-pound unit to the 50 pounds of the 1500-pound unit and in the simplification of the mounting linkage which makes the unit more applicable to mounting and testing on an aircraft.

Landing-Gear Linkage

Tire bleed-valve actuation in the 1500-pound unit, as in the 750-pound unit, is accomplished by means of a relative displacement between the axle and the strut. While

the linkage used to mount the 750-pound unit prevented braking loads from drastically affecting the vertical load carried by the vertical load sensor, it was decided that too heavy a penalty in both weight and complexity had to be paid for this feature. Therefore, the mounting linkage for the 1500-pound unit was considerably simplified and consists of a four-bar linkage. The only limitation imposed on the operation of the system by this simplification is that the brakes should not now be applied during the first instant after tire touchdown since braking will affect the axial load carried by the vertical load-carrying link.

Figure 1 is a schematic sketch of the mounting linkage of the 1500-pound unit. The axle is L-shaped and is mounted to the strut by means of a pin which is parallel to, but which is located off center from, the axle and tire center line. This arrangement permits the axle and tire center line to be pivoted about this mounting pin. A vertical load-carrying link has one of its ends pinned to the strut and the other pinned to a slider link, or piston, that is mounted in a hydraulic cylinder fixed to the axle. The deflection between the slider link, or piston, and the axle actuates the tire bleed valve.

Wheel, Axle, and Brake

The tire is mounted on a 7075-T6 aluminum cylinder which serves as a wheel for the 43-inch-diameter tire. The earlier analytical study conducted at Battelle specified a required air-bleed orifice area of 14.2 square inches for the 43-inch-diameter, 1500-pound static load, high-flotation tire. In the 1500-pound unit the air is bled from the tire through eight large ports, which have a total area of 21.5 square inches, in the outboard end of the wheel. The wheel has an internal diameter of 4.75 inches, which provides approximately 17.7 square inches of flow area.

The wheel is mounted on a nonrotating axle, which is made of SAE 4340 steel hardened to 35 R_C, by means of two Timken Roller Bearings. The outboard bearing is approximately located on the center line of the tire, and the center-to-center bearing distance is 10.75 inches. The L-shaped axle is essentially two cylinders intersecting at right angles. The wheel and tire are mounted on the longer leg of the axle, and the pivot pin, which fastens the axle to the strut, passes through the shorter leg. The distance between the weel and tire center line and the pivot-pin center line is 3.75 inches.

Figure 2 is a photograph of the inboard side of the right-hand 1500-pound unit as mounted on the Battelle drop tester. The axle mounting and brake components are clearly visible in this picture. A spot brake with two cylinders or spots and with a single rotating disk is used on the 1500-pound unit. The brake disk is driven on its external periphery by a toothed flange which is fastened to the rotating wheel, and the brake-cylinder housing is fastened to the nonrotating axle. Because of the increase in the rolling radius of the 43-inch-diameter high-flotation tire over that of the conventional L-19 tire, it is necessary approximately to double the braking torque available from the conventional L-19 brake system. This is accomplished by using two 2-inch-diameter brake cylinders in place of the conventional one 2-inch-diameter brake cylinder that is used on the L-19. These cylinders are located 3-1/2 inches from the axle center line, and for a cylinder pressure of 900 psig and a brake-lining coefficient of friction of 0.25 the torque developed is 10,000 inch-pounds. Two smaller brake cylinders are used in place of one larger cylinder because they permit the use of a smaller diameter brake disk and, thus, do not reduce the ground clearance as much as a single larger cylinder would.

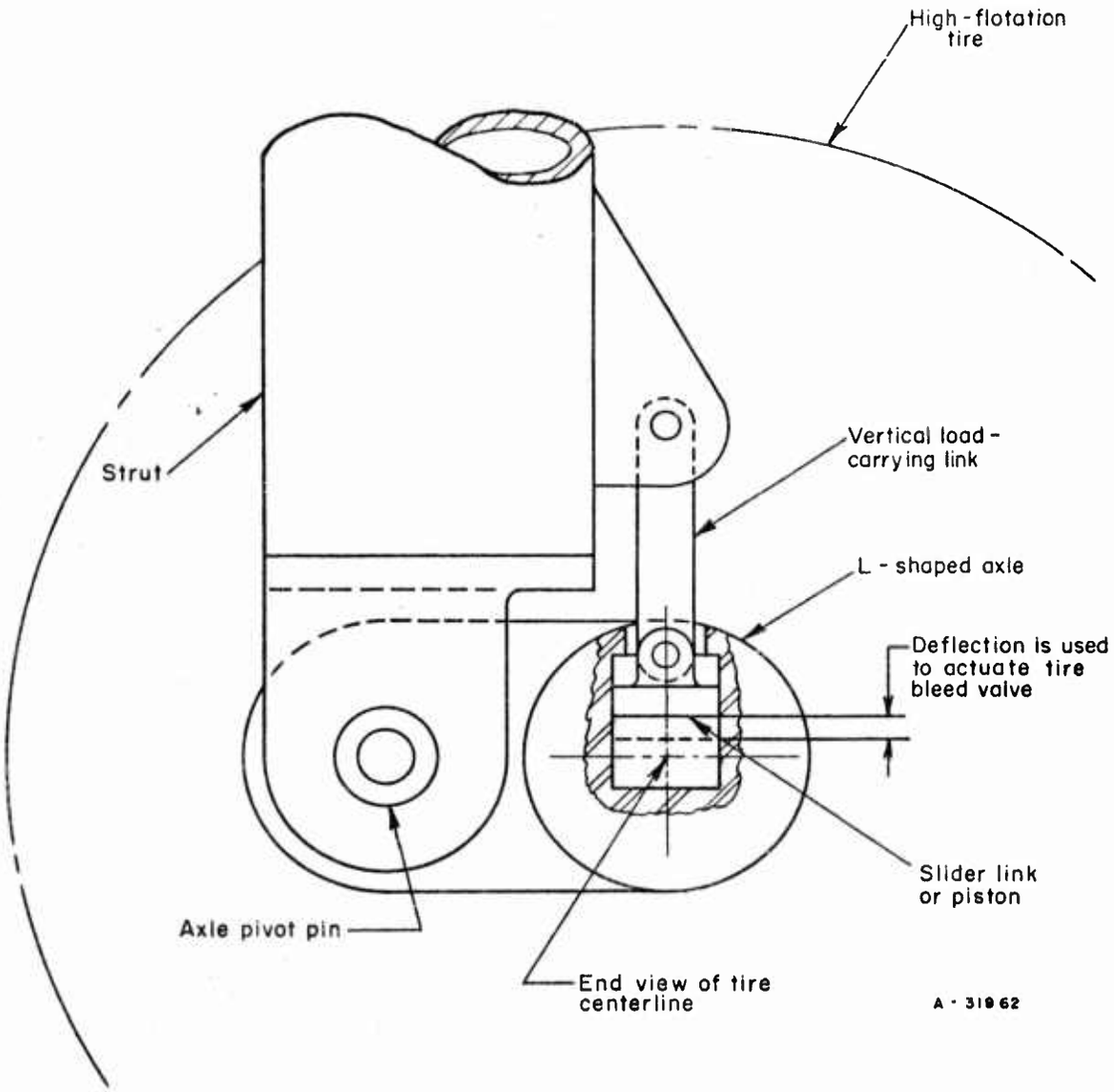

FIGURE 1. SCHEMATIC DRAWING OF THE MOUNTING LINKAGE OF THE 1500-POUND LANDING-GEAR UNIT

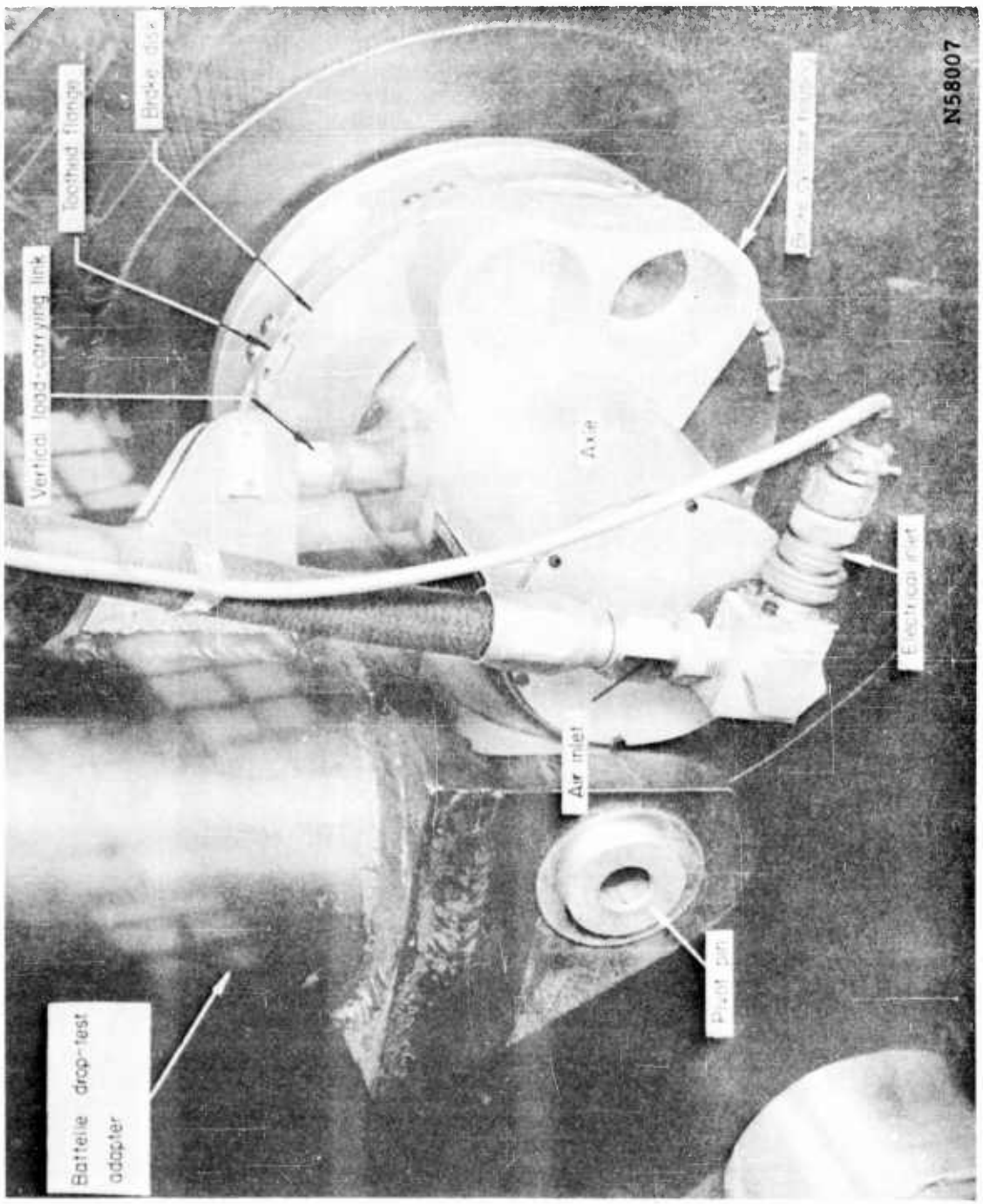

FIGURE 2. BRAKE AND MOUNTING ARRANGEMENT OF THE 1500-POUND HIGH-FLOTATION LANDING GEAR

Load-Sensing Cylinder

To reduce the weight and complexity of the load sensor used in the 750-pound unit, the energy-absorbing dashpot was not included in the design of the 1500-pound unit, and a method was devised to eliminate the large load-sensing spring that was formerly required. This method uses a small closed hydraulic cylinder which is mounted in the axle, and which has two pistons located at right angles to one another, entering it. Figure 3 is a schematic sketch of this load-sensing cylinder. One of the two pistons entering the load-sensing cylinder is larger in area than the other. The larger piston, which is mounted in the vertical direction and which is fastened to the ball-ended vertical load-carrying link, is 1-1/2 inches in diameter and has an area of 1.77 square inches. The smaller piston actuates the tire bleed valve and is formed by a stepped shaft which passes through the cylinder along the center line of the axle. This stepped shaft has diameters of 13/16 and 3/8 of an inch and has a differential area of 0.41 square inch. Therefore, the areas of the pistons are in the ratio of approximately 4.33 to 1, and the spring rates of the comparatively small valve and push-rod springs are increased 4.33 times relative to the larger piston.

When a vertical load of 4800 pounds is imposed on the larger piston by the vertical load-carrying link, the internal cylinder pressure rises to 2710 psig. The push-rod spring pulls the larger diameter portion of the stepped shaft back into the cylinder when the load on the larger piston is relieved. This spring has a preload of 15 pounds and a spring rate of 159 pounds per inch. Since the unit is located on the center line of the axle and since the pistons are located at right angles to one another, the bell-crank mechanism used to actuate the valve in the 750-pound unit has also been eliminated.

The load-sensing function is performed in the following manner:

(1) The vertical load on the tire is imposed on the vertical load-carrying link which applies this load to the larger piston in the load-sensing cylinder.

(2) A preload is applied to the stepped shaft, which passes through the load-sensing cylinder, by the valve and push-rod springs.

(3) As the load on the larger piston increases, the fluid pressure in the load-sensing cylinder increases.

(4) When the pressure in the cylinder reaches a value that applies a force on the stepped shaft sufficient to overcome the preload in the valve and push-rod springs, the stepped shaft is actuated and begins to open the tire bleed valve.

(5) The displacement of the stepped shaft is then directly proportional to the increase in load on the larger piston.

(6) The travel of the stepped shaft is limited to 1 inch by a rubber stop, and any further increase in the load on the larger piston increases the pressure in the load-sensing cylinder, but does not result in any further displacement of the stepped shaft.

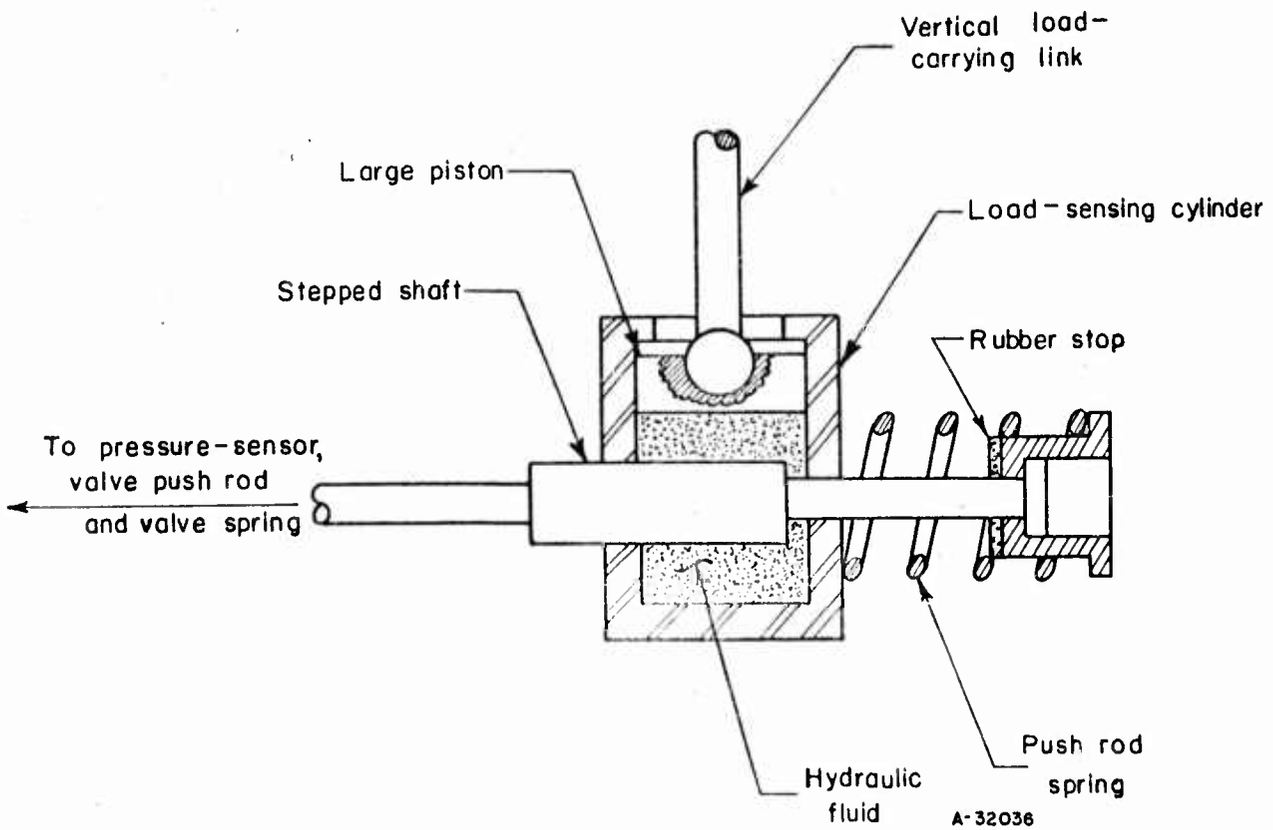

FIGURE 3. SCHEMATIC DRAWING OF LOAD-SENSING CYLINDER

Pressure Sensor

Because of the satisfactory operation of the pressure sensor in the 750-pound unit, the method of operation of the pressure sensor used in the 1500-pound unit is identical with that used in the 750-pound unit. The only major design changes were concerned with the geometry of the component. One additional feature, however, was added to the pressure sensor. Since the unit is to be flight tested, it was considered essential to provide some means of informing the pilot whether or not the pressure sensor is cocked before landing. To accomplish this, a microswitch is mounted on the pressure-sensor frame and is actuated when the pressure-sensor guide block is in the cocked position. The actuation of this switch turns on a light in the cockpit of the plane and lets the pilot know whether the pressure sensor is cocked. The electrical leads to this switch are brought out of the 1500-pound unit through the air passage. The pressure sensor, as installed on the L-19 aircraft, is set to disengage at a pressure of 2-1/2 psig and to engage or cock at a pressure of approximately 7-1/2 psig. Figure 4 is a photograph of the vertical load-carrying link, load-sensing cylinder, pressure sensor, and the air- and electrical-inlet assembly.

Tire Bleed Valve

The design of the tire bleed valve for the 1500-pound unit remained essentially the same as that for the 750-pound unit except for changes in geometry. The available valve stroke from the full open to the full closed position in the 1500-pound unit is 1 inch. The programmed valve-port cylinder has eight ports, an internal diameter of 8-3/4 inches, and a maximum available area of 24.4 square inches. To reduce the O-ring friction on the outboard sleeve, the large reciprocating O-ring seal has a hardness of 40 durometer. The valve spring is preloaded to 95 pounds and has a spring rate of 43 pounds per inch. This preload is sufficient to hold the outboard sleeve tightly against the O-ring face seal, and no leakage of either the O-ring reciprocating or face seal was noted at tire pressures as high as 25 psig. A vertical load of approximately 1050 pounds is required to start valve actuation, and the valve is full open at a vertical load of approximately 1950 pounds. As the tire bleed valve and the valve rod rotate with the tire and as the pressure sensor and valve push rod, which are mounted in the axle, do not rotate, a rotary thrust bearing is located between the valve rod and the valve push rod.

Folding of the 43-Inch-Diameter High-Flotation Tire

The 43-inch-diameter high-flotation tire is folded into a helical bellows in the same manner as the 34-inch-diameter tire. The same tire-folding provisions are necessary for both tires, and the same method of locking the inboard tire flange to the axle is employed in both units. These tire-folding provisions and the reasons for each and the design of the tire-flange locking mechanism are explained in detail in the Phase Report on this project, dated August 1, 1958.

Tire Modifications

To determine the most satisfactory stiffening-rib configuration for inducing the 43-inch-diameter high-flotation tire to fold into a helical bellows, tests were conducted

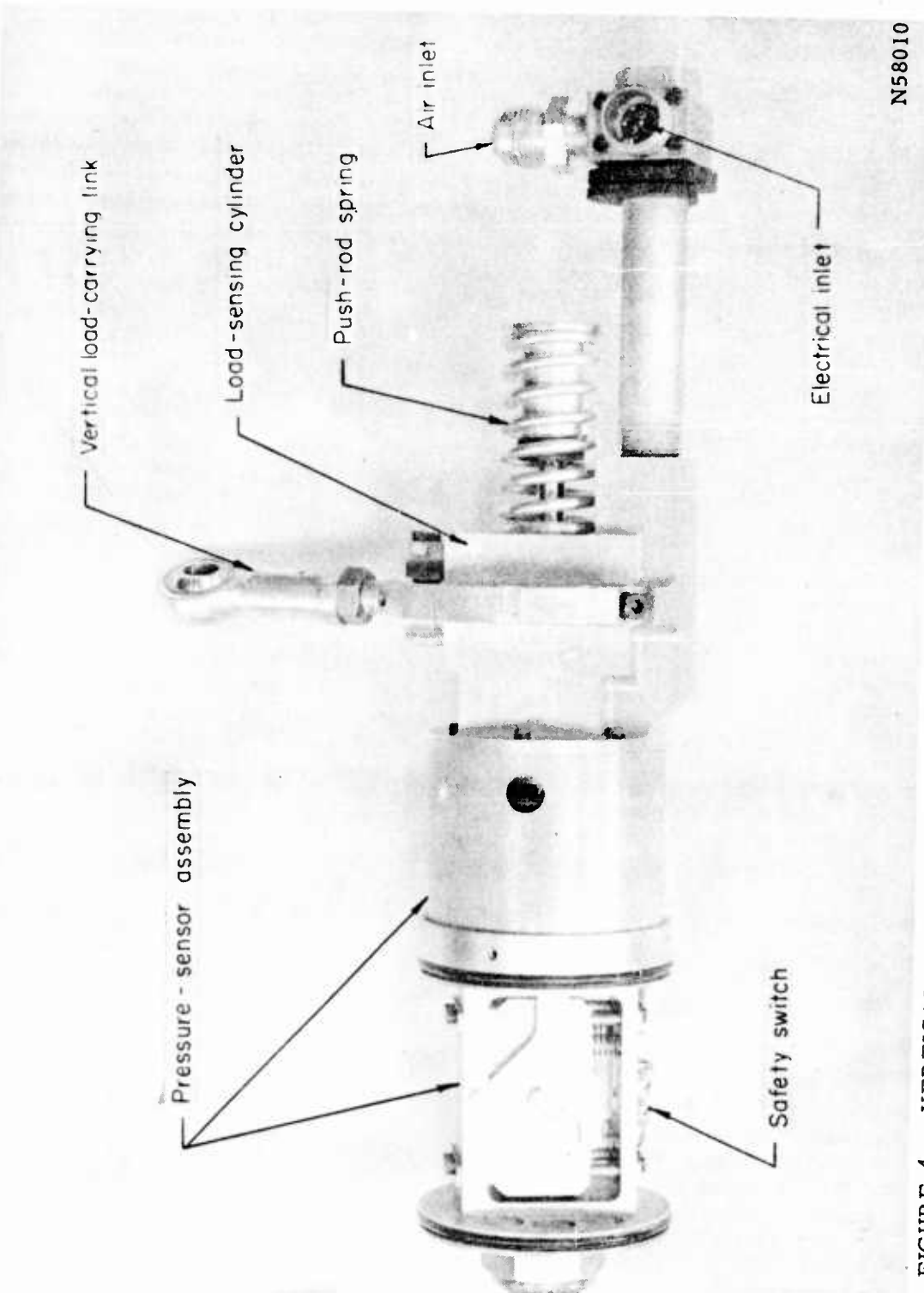

FIGURE 4. VERTICAL LOAD-CARRYING LINK, LOAD-SENSING CYLINDER, PRESSURE-SENSOR, AND AIR AND ELECTRICAL INLET ASSEMBLY

with various combinations of the number of ribs and the rib lead angle. Type "B" V-belts were cemented to the tire as stiffening ribs and performed satisfactorily. Lead angles of 10, 25, and 45 degrees were employed; a lead angle of 10 degrees gave the best results. Eight and ten stiffening ribs were used to determine the most desirable number of tire folds. The tire creased more easily with eight than ten folds, but ten folds permitted a slightly smaller folded diameter than eight, and it was decided that ten is the best number for this tire. The smallest diameter of the circular concentric stiffening ribs on the side walls of the tire that will insure a uniform outer diameter of the folded tire package is 24 inches. It was found that a vacuum of only 8 inches of water was required to hold the tire in the completely folded position.

To insure the proper folding of the tire that was used in the above tests, it was necessary to hold the tire hubs axially in their operational position until after the tire had been creased and one hub had rotated approximately 11 degrees with respect to the other. The inboard hub was then released and allowed to move axially toward the outboard hub. However, to fold successfully tire Number 16, the tire that will be used in the dynamic tire-folding tests, it was found to be necessary to hold the hubs axially in their operational position until they have rotated approximately 30 degrees with respect to one another. This variation in the folding requirements for the two tires indicates that, for tires of different stiffness or cord angle, it will be necessary to perform folding tests to determine what tire modifications are necessary to give optimum folding performance for that particular tire construction. Figure 5 is a sequence of photographs of the 43-inch-diameter high-flotation tire taken at various stages during the folding cycle.

Dynamic Tire-Folding Apparatus

To test the folding of the tire under dynamic conditions such as will be encountered during operation, a tire-folding apparatus which is to be installed in a C-123 aircraft was designed, constructed, and operated in the laboratory. Figure 6 is a schematic diagram showing the manner in which the 43-inch-diameter high-flotation tire will be extended and retracted from the C-123 during the dynamic folding tests. The apparatus will be rigidly fastened to the cargo ramp of the C-123, and the tire will be extended into the slip stream by rotating the extension arm 180 degrees. The extension arm is positioned by a chain that is driven by a powered screw jack.

The tire is connected to a three-way solenoid valve which is actuated to either inflate or deflate the tire. When this valve is in the inflate position, the tire is open to an accumulator which has been preinflated to a pressure that is sufficient to inflate the tire quickly from the folded condition. When the valve is in the deflate position, the tire is open to the vacuum side of an industrial-type vacuum-cleaner blower, and folds as it is evacuated.

Design of the L-19 Struts and Inflation System

Calculations showed that the spin-up and spring-back loads that would be applied to the high-flotation tire during landing would be larger than the maximum allowable spin-up or spring-back load that can be safely carried by the front-strut attachment fittings on the L-19. To permit landings at comparatively high sinking speeds with the

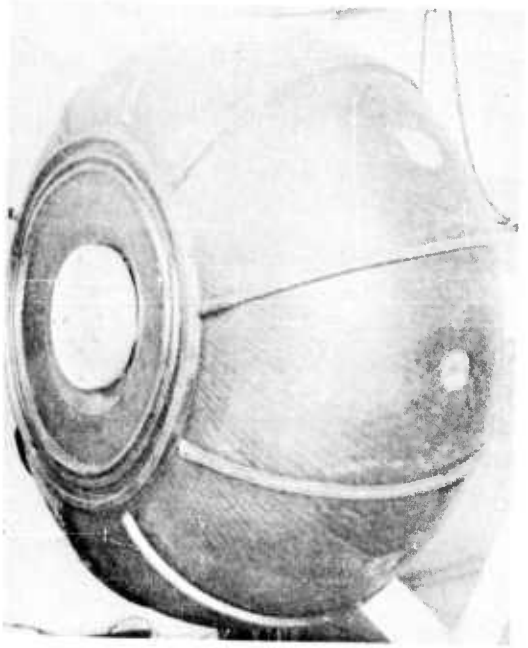

N59889
Tire Inflated

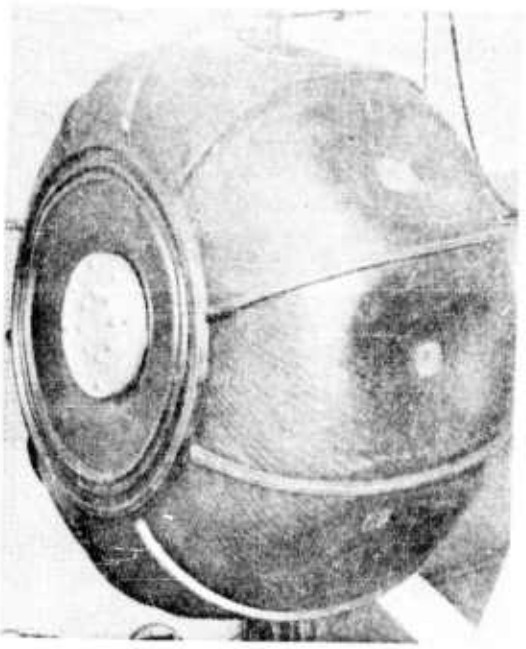

N59890
Tire at Atmospheric Pressure

N59891
Tire During Folding Operation

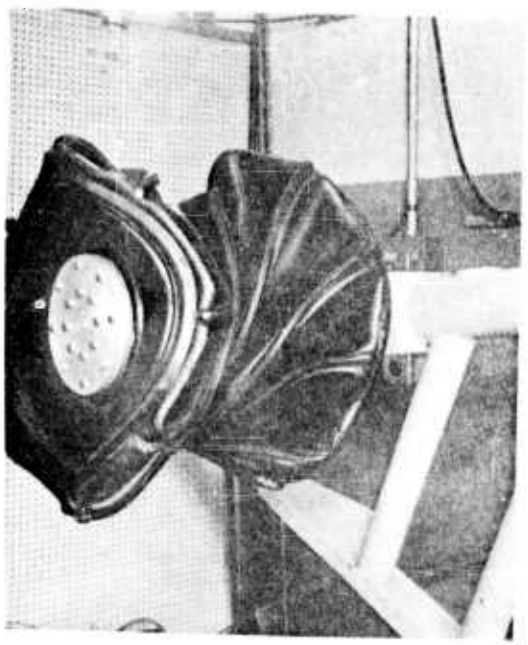

N59892
Tire Folded

FIGURE 5. FOLDING SEQUENCE OF THE 43-INCH-DIAMETER, HIGH-FLOTATION TIRE

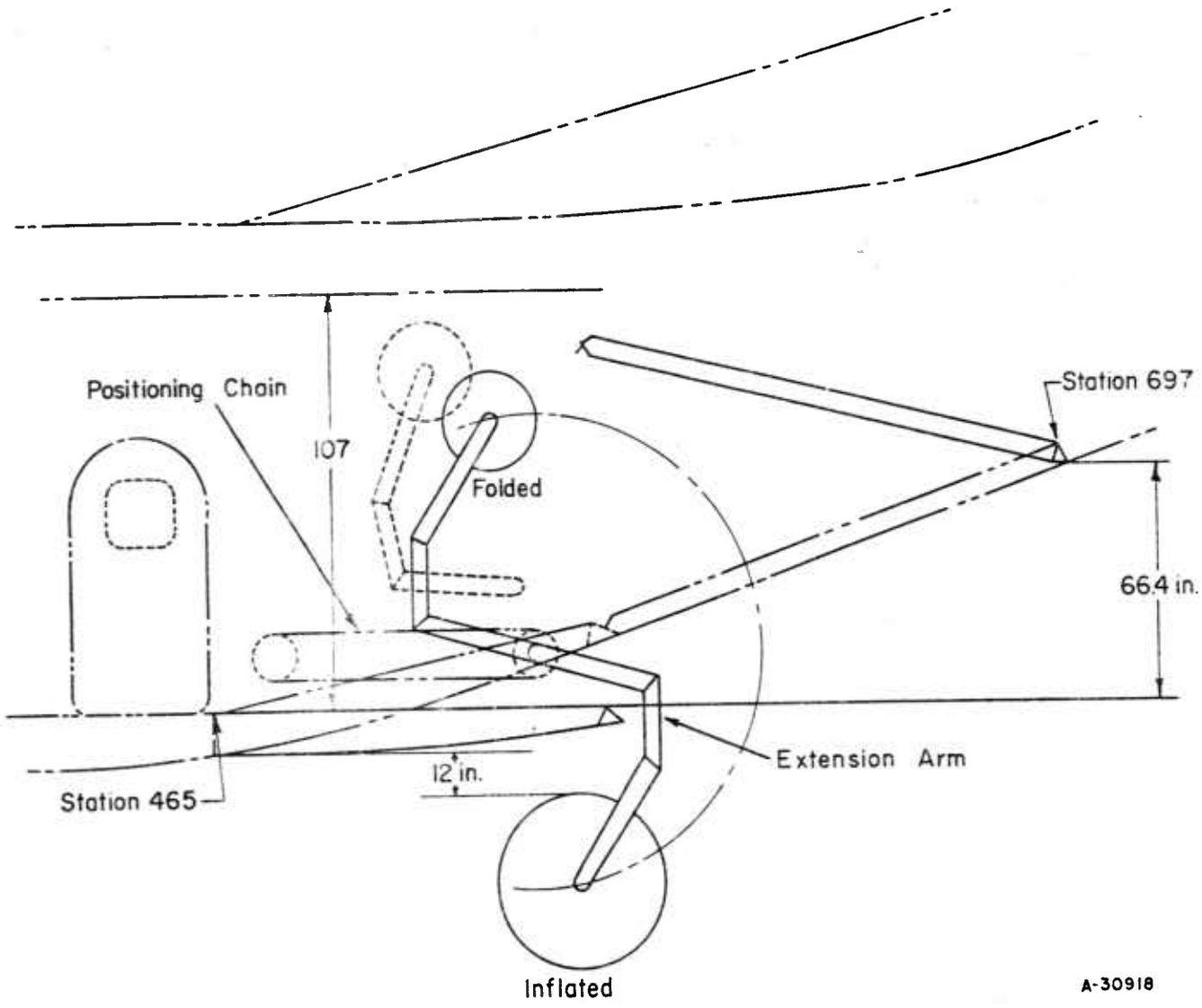

FIGURE 6. SCHEMATIC DIAGRAM SHOWING 43-INCH-DIAMETER HIGH-FLOTATION TIRE IN EXTENDED AND RETRACTED POSITIONS FOR FOLDING TEST ON C-123

high-flotation landing gear mounted on this aircraft, it was necessary to mount the landing gear on the L-19 by means of a structure which is fastened to the rear pontoon fittings as well as to the front-strut fittings.

Both of the high-flotation landing gears are mounted on a common front-strut weldment which is fastened to the L-19 by means of adapters that are mounted in the conventional L-19 front-strut fittings. The front-strut weldment is pinned to these adapters and is free to pivot in a fore-aft direction. It is held in place by two ball-ended rear struts which are fastened to it at the points where the landing-gear units are attached and which extend rearward to the rear pontoon-attachment fittings. The major reaction forces due to tire spin-up and spring back are carried by these rear struts.

Since the tires to be mounted on the L-19 for flight testing will not be folded, an inflation system has been designed without provisions for tire deflation. This sytem consists of a 3000-psig air-storage accumulator that is supplied by a 2-cfm compressor. Each tire is independently inflated through its own adjustable lever-operated pressure regulator. The system has provisions for automatic quick reinflation of the tires by a predetermined amount after tire bleed down so that the tire run-out pressure can be increased to a sufficient value to reduce tire wear and heating during the flight-test program. This quick reinflation is accomplished by connecting a second accumulator to the tires immediately after both tire bleed valves have closed. This second accumulator is preinflated to an adjustable pressure that is sufficient to raise the pressure in the two tires by the desired amount.

Design of the Langley Field Drop-Test Linkage

The minimum load that can be dropped in the N.A.S.A. drop-test facility at Langley Field, Virginia, is larger than 1500 pounds. This makes it impossible to conduct drop tests with the high-flotation landing gear designed to carry a static load of 1500 pounds mounted directly to the present drop-test carriage. Therefore, a linkage similar to the four-bar linkage used for drop testing at Battelle was designed to be fastened to the drop-test carriage at Langley Field. The high-flotation landing gear would be mounted on this linkage during the drop testing. The drop-test carriage would be fixed at a given vertical position, and the vertical motion of the high-flotation landing gear would be accomplished by raising and dropping the four-bar linkage in the same manner as is done with the Battelle drop tester. The horizontal motion of the unit would be provided by the N.A.S.A. drop tester. Adapters were designed to permit the testing of the landing gear with both yaw and roll. A safety stop was designed to limit the downward travel of the four-bar linkage. This safety stop would prevent the damaging of the high-flotation landing gear in the event of a tire failure.

LANDING-GEAR DROP-TEST PROGRAM

Laboratory Drop-Test Apparatus

Both the 750- and 1500-pound static-load high-flotation landing gears were drop tested under laboratory conditions at Battelle to determine the necessary conditions for successful system operation and to gain some insight into the possible effect that tire spin-up and wing lift will have on the operation of the system. To conduct drop tests with tire spin-up before touchdown and with wing-lift, it was necessary to make a number of alterations to the Battelle drop tester and to construct some additional components. The existing drop tester, which was described in the Phase Report, was strengthened and more rigidly mounted to the floor to permit drop tests with tire spin-up before touchdown, and tire spin-up and wing lift devices were designed and constructed. Figure 7 is a photograph of the Battelle drop-test apparatus showing the installation of the tire spin-up and wing-lift devices.

Tire Spin-Up Device

The tire spin-up device is capable of spinning up either the 34- or 43-inch-diameter high-flotation tire at speeds up to over 75 knots. An 8-1/2-inch-diameter aluminum roller, which is belt driven by a 2-horsepower motor, spins the tire up to speed when the roller and tire are brought into contact with one another. Both the roller and motor are mounted on an arm which is pivoted on a stationary frame. The arm is approximately 6 feet long and is pivoted at its mid-point. The roller is located at one end of the arm and can, therefore, be positioned to any location on an arc having a 3-foot radius. The unit is so positioned that this arc always intersects the circumference of the tire being tested, regardless of the drop height. To pivot the arm into position, a force is applied to the end of the arm on the opposite side of the pivot from the roller. Before the tire is dropped the arm is pivoted to a clear position.

Wing-Lift Device

Two air springs, which are located on either side of the landing pad and which engage the drop-tester carriage, are used to provide wing lift on the Battelle drop tester. They each consist of a cylinder so mounted in a tank that the combination has a low ratio of cylinder displacement to total volume. The total volume of a tank is 5700 cubic inches. Each cylinder is 3-5/8 inches in diameter, and each wing-lift piston has a maximum stroke of 18 inches. This results in a maximum displacement of 186 cubic inches and a maximum pressure increase of approximately 3.5 per cent. Since the pressure increase is small, the force on the piston remains essentially constant throughout the piston stroke. The drop-tester carriage does not engage the pistons until after it is dropped a given distance to obtain the desired sinking speed. By varying the pressure in the tanks, the per cent of wing lift can be controlled.

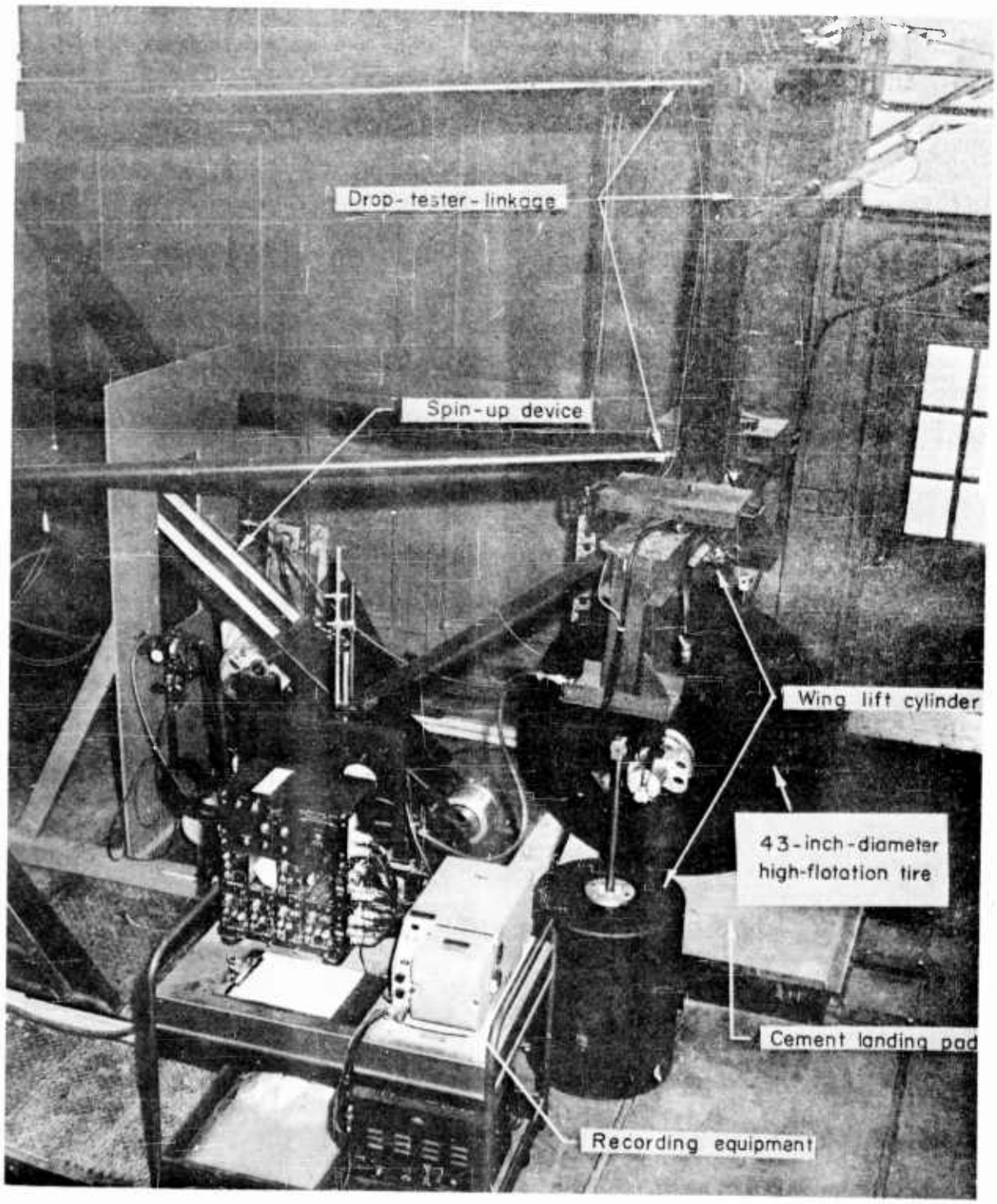

N58001

FIGURE 7. LANDING-GEAR DROP-TEST APPARATUS AND RECORDING INSTRUMENTATION

Drop-Tester Instrumentation

In drop tests of the high-flotation landing gear conducted after the Phase Report, the following information was recorded:

(1) Vertical tire deflection

(2) Vertical acceleration

(3) Valve position

(4) Sinking speed

(5) Rotational velocity of the tire

(6) Horizontal spin-up force

(7) Time base.

A Consolidated 5-116 fourteen-channel recording oscillograph was used to record the required information in place of the Consolidated 5-114 eighteen-channel unit that was used earlier in the project. The chart speed used was 32 inches per second.

Vertical tire deflection, vertical acceleration, valve position, sinking speed, and time base were obtained in the same manner as described in the Phase Report. Because valve position was measured with a transducer attached to a rotating member, a slip-ring system would have been necessary for completing the circuit between the transducer and the recorder in drop tests with tire spin-up. For this reason, valve position was recorded in zero spin-up speed tests only. The rotational velocity of the tire was obtained in two manners. In drop tests with the 750-pound unit, the rotational velocity of the tire was monitored by a tach-generator. The armature of the tach-generator was coupled to and driven by the rotating axle, and the case was mounted on the stationary-axle housing. In drop tests with the 1500-pound unit, as no means was readily available to mount the tach-generator between the rotating and nonrotating components of the unit, the tire rotational speed was monitored with a magnetic pickup. This magnetic pickup was mounted on the stationary brake housing and so located that the teeth on the rotating flange that drives the brake disk interrupted the magnetic field and induced a signal in the pickup coil. By recording these interruptions with respect to time, the average rotational speed of the tire over a given time interval was determined. Horizontal spin-up force was obtained in drop tests with both the 750- and 1500-pound units by cementing strain gages on the adapters used to mount these units to the Battelle drop tester.

Drop-Test Conditions

Since the publication of the Phase Report, extensive drop testing of both the 750- and the 1500-pound landing-gear units has been carried out on the Battelle drop-test facility. Drop tests with the 750-pound unit were conducted to determine what effects lower static load, tire spin-up before touchdown, wing lift, and dash-pot operation have on the performance of the unit. During drop testing of the 1500-pound unit, the static

load, initial tire pressure, sinking speed, valve area, tire spin-up speed, and percentage wing lift were varied to determine their effect on the landing operation and to establish an envelope of variable conditions in which successful landings could be made.

750-Pound Unit

All of the tests with the 750-pound unit were conducted with a total valve area of 10.8 square inches. Static loads of 710, 788, and 988 pounds were used, and the initial tire pressure ranged from 7 to 11 psig. The sinking speed was varied from 2-1/2 to 8-1/4 ft/sec in the 710- and 788-pound static-load tests and from 2-1/2 to 7-3/8 ft/sec in the 988-pound static load tests. Tire spin-up speeds before touchdown of 0, 32, 63, and 80 knots were used, and drop tests were conducted with 0, 50, and 100 per cent wing lift. Drop tests with the dash pot installed were conducted only with zero tire spin-up speed and zero per cent wing lift.

1500-Pound Unit

During the drop testing of the 1500-pound landing-gear unit, drop tests were carried out with static loads of 920, 1200, and 1500 pounds. Sinking speeds ranging from 2-1/2 to 10-1/2 ft/sec were used. Initial tire pressure was varied from 21 to 8 psig, and three different valve configurations were used. Valves A and B are similar in that they both have directly proportional valve-area versus valve-stroke characteristics. Valve A, however, has a larger magnitude of total area than Valve B. Valve C is so programmed that the rate of valve-area opening is low during the first part, but high during the last part of the valve stroke. A description of the three valves follows:

(A) The area of Valve A increases at the rate of 24.4 $in.^2$/in. valve stroke and for a 1-in. valve stroke has a total area of 24.4 $in.^2$.

(B) The area of Valve B increases at the rate of 14.6 $in.^2$/in. valve stroke and for a 1-in. valve stroke has a total area of 14.6 $in.^2$.

(C) The area of Valve C increases at the rate of 9.2 $in.^2$/in. valve stroke for the first 3/8-in. valve stroke and 24.4 $in.^2$/in. valve stroke for the last 5/8 in. of valve stroke. The total area for a 1-in. stroke is 18.7 $in.^2$.

Tire spin-up speeds before touchdown of 0, 61, and 78 knots were used, and percentage wing lift was varied from zero to 100 per cent.

750-Pound-Unit Drop-Test Results

710-Pound Static Load

As indicated by the increase in the maximum vertical-load factor when the static load was reduced from 990 to 780 pounds in earlier tests, the maximum vertical-load factor obtained in the drop tests with a static load of 710 pounds was higher for a given sinking speed than that obtained in drop tests conducted with a static load of 780 pounds.

Vertical-load factor is defined as the ratio of instantaneous vertical load to total static weight. An initial tire pressure of 8 psig resulted in the best over-all performance of the unit with a static load of 710 pounds. Table 1 is a listing of the maximum vertical-load factors obtained in drop tests without tire spin-up and wing lift over the full range of static loads and sinking speeds used during the drop testing of the 750-pound unit. The maximum vertical-load factor varied from 1.5 in the test with a static load of 990 pounds, an initial tire pressure of 11 psig and a sinking speed of 2-1/2 ft/sec to 4.2 in the test with a static load of 710 pounds, an initial tire pressure of 8 psig, and a sinking speed of 8-1/4 ft/sec.

TABLE 1. MAXIMUM VERTICAL-LOAD FACTORS OBTAINED IN DROP TESTS WITH THE 750-POUND LANDING GEAR

Aircraft Sinking Speed, ft/sec	Maximum Vertical-Load Factor(a)		
	990 Pounds+	780 Pounds*	710 Pounds*
2-1/2	1.5	1.8	1.8
4-3/4	2.2	2.4	2.5
6-1/4	2.5	2.8	3.1
7-3/8	3.0	3.3	3.6
8-1/4	--	3.8	4.2

Note: Constant axle area of 5.7 in.^{2}; total valve area of 10.8 in.^{2}; and zero spin-up speed, zero per cent wing lift.

(a) + - Initial tire pressure of 11 psig for 2-1/2 and 4-3/4 ft/sec sinking-speed tests and of 10 psig for 6-1/4 and 7-3/8 ft/sec sinking-speed tests.

* - Initial tire pressure of 8 psig for all sinking-speed tests.

Dash Pot Installed in Series With the High-Flotation Landing Gear

In the drop tests that were conducted with the dash pot installed in series with the high-flotation landing gear, a high shock load was imposed on the unit by the bottoming of the piston in the dash-pot cylinder. After the first series of drop tests with the dash pot installed, this shock load damaged the miniature ball bearings on the ends of the valve push rods in the pressure sensor. These bearings were replaced with plain rollers, and the dash-pot rate was increased to reduce the bottoming velocity of the piston. A second series of low-sinking-speed drop tests was then conducted with the dash pot installed. Although the performance of the unit appeared to be improved over that of the first series of tests with the dash pot installed, it was evident that to gain a more complete and reliable insight into the functioning of a dash pot in series with the high-flotation landing gear, it would be necessary to construct a more refined dash pot or "oleo" strut and to conduct a comparatively extensive drop-test program. It was considered that this course of action should not be followed at that particular time in the research program since it would seriously delay the achieving of the project objectives, the design, development, and determination of the operating characteristics and energy-dissipation capabilities of the high-flotation-tire venting system. It is not to be inferred from the above discussion that satisfactory operation cannot be obtained with the use of a dash pot or oleo strut in series with the high-flotation landing gear.

Drop Tests Conducted With Tire Spin-Up

Table 2 shows the values obtained for the maximum vertical-load factor and maximum spin-up load at various combinations of sinking speed and tire rotational speed for the drop tests conducted at static loads of 788 and 988 pounds and initial tire pressures of 8 and 10 psig, respectively. In the drop tests conducted with a static load of 788 pounds and an initial tire pressure of 8 psig, the maximum vertical-load factors ranged from 1.8 at a sinking speed of 2-1/2 ft/sec and tire rotational speeds of 32 and 63 knots, to 4.1 at a sinking speed of 8-1/4 ft/sec and a tire rotational speed of 63 knots. The maximum spin-up load of 1400 pounds occurred at a sinking speed of 8-1/4 ft/sec and a tire rotational speed of 63 knots. The maximum vertical-load factor attained in the drop tests conducted with a static load of 988 pounds and an initial tire pressure of 10 psig ranged from 1.6 at a sinking speed of 2-1/2 ft/sec and a tire rotational speed of 32 and 63 knots to 3.3 at a sinking speed of 7-3/8 ft/sec and a tire rotational speed of 32 knots. The maximum spin-up load of 1340 pounds occurred at a sinking speed of 6-1/4 ft/sec and tire rotational speeds of 63 and 80 knots.

The maximum spin-up load attained in the drop tests with a tire rotational speed of 63 knots was higher than that attained at a tire rotational speed of 32 knots. In most cases there was little difference between the maximum spin-up load attained at 63 knots and that attained at 80 knots. It is interesting to note that, in the drop test with a static load of 988 pounds, an initial tire pressure of 10 psig, and a sinking speed of 4-3/4 ft/sec, the maximum recorded spin-up load at a tire rotational speed of 63 knots was 1250 pounds while the spin-up load was only 1070 pounds at a tire rotational speed of 80 knots. The reason for this behavior is not known.

Drop Tests Conducted With Wing Lift

Table 3 shows the effect of initial tire pressure and wing lift on the maximum vertical-load factor. The maximum load factors listed are the total load factors applied to the drop-tester carriage and are equal to the sum of the wing lift and tire loads. In the tests with wing lift, the maximum load factor attained at the lower initial tire pressures was, in all cases, slightly lower than that attained at higher pressures. It is not practical, however, to reduce the initial tire pressure below the test values, because the small reduction in the maximum load factor that is realized is more than offset by the greater tire deflection required to arrest the vertical velocity.

The maximum load factor did not vary appreciably between the tests conducted at 50 and 100 per cent wing lift. The drop tests with 0 per cent wing lift were conducted at an earlier date than those with 50 and 100 per cent wing lift and have different sinking speeds than the drop tests with wing lift. The maximum load factor attained in the tests with wing lift was greater than that attained in tests at comparable sinking speeds without wing lift. However, the maximum load carried by the high-flotation tire was smaller in the tests with wing lift than in the tests without wing lift.

The wing-lift cylinders continued to apply wing lift to the unit after the landing impact. This continued application of the wing-lift force after the energy-dissipation cycle caused the tire to leave the ground in the tests with 100 per cent wing lift. The highest such bounce was 3 inches and occurred at a static load of 788 pounds, an initial tire pressure of 10 psig, and a sinking speed of 8 ft/sec.

TABLE 2. MAXIMUM VERTICAL-LOAD FACTOR AND SPIN-UP LOAD FOR DROP TESTS OF THE 750-POUND UNIT CONDUCTED WITH TIRE SPIN-UP

Aircraft Sinking Speed, ft/sec	Maximum Vertical-Load Factor at Indicated Spin-Up Speed				Maximum Spin-Up Load, lb, at Indicated Spin-Up Speed		
	0 Knots	32 Knots	63 Knots	80 Knots	32 Knots	63 Knots	80 Knots
Static Load of 788 Pounds, Initial Tire Pressure of 8 Psig							
2-1/2	1.8	1.8	1.8	--	500	800	--
3-3/4	--	--	2.0	1.9	--	1100	1100
4-3/4	2.4	2.4	2.3	2.4	900	1100	1200
6-1/4	2.8	2.9	2.9	2.9	930	1310	1300
7-3/8	3.3	3.3	3.4	3.5	1010	1300	1250
8-1/4	3.8	4.0	4.1	3.8	1200	1400	1370
Static Load of 988 Pounds, Initial Tire Pressure of 10 Psig							
2-1/2	1.45[a]	1.6	1.6	--	650	900	--
3-3/4	--	--	2.0	2.0	--	1075	1100
4-3/4	2.15[a]	2.3	2.2	2.1	890	1250	1070
6-1/4	2.5	2.8	2.8	2.9	1000	1340	1340
7-3/8	3.0	3.3	3.2	3.1	1180	1310	1300

Note: Constant axle area of 5.7 in.^{2}; total valve area of 10.8 in.^{2}; and zero per cent wing lift.
(a) Eleven psig.

TABLE 3. EFFECT OF INITIAL TIRE PRESSURE AND PERCENTAGE WING LIFT ON MAXIMUM VERTICAL-LOAD FACTOR MEASURED IN DROP TESTS OF THE 750-POUND UNIT

Initial Tire Pressure, psig	100 Per Cent Wing Lift		50 Per Cent Wing Lift		0 Per Cent Wing Lift[a]	
	Sinking Speed, ft/sec	Maximum Vertical-Load Factor	Sinking Speed, ft/sec	Maximum Vertical-Load Factor	Sinking Speed, ft/sec	Maximum Vertical-Load Factor[b]
Static Load of 788 Pounds						
7	--	--	1-5/8	1.8	2-1/2	--
8	--	--	1-5/8	1.8	2-1/2	1.8
10	--	--	1-5/8	2.0	2-1/2	1.8*
7	4-5/8	2.6	4-7/8	2.5	4-3/4	--
8	4-5/8	2.8	4-7/8	2.6	4-3/4	2.4
10	4-5/8	2.8	4-7/8	2.8	4-3/4	2.4*
7	6-1/2	3.1	6-5/8	3.1	7-3/8	--
8	6-1/2	3.3	6-5/8	3.2	7-3/8	3.3
10	6-1/2	3.5	6-5/8	3.5	7-3/8	3.5*
7	8	3.7	8-1/8	3.7	8-1/4	--
8	8	3.9	8-1/8	3.8	8-1/4	3.8
10	8	4.3	8-1/8	4.2	8-1/4	3.9*
Static Load of 988 Pounds						
8	--	--	1-5/8	2.0	2-1/2	--
10	--	--	1-5/8	2.2	2-1/2	1.5+
11	--	--	1-5/8	2.2	2-1/2	1.45
8	4-5/8	2.4	4-7/8	2.2	4-3/4	--
10	4-5/8	2.6	4-7/8	2.5	4-3/4	2.1+
11	4-5/8	2.6	4-7/8	2.6	4-3/4	2.15
8	6-1/2	3.0	6-5/8	2.9	7-3/8	--
10	6-1/2	3.2	6-5/8	3.2	7-3/8	3.00
11	6-1/2	3.4	6-5/8	3.2	7-3/8	3.05

Note: Constant axle area of 5.7 in.^{2}; total valve area of 10.8 in.^{2}; and zero spin-up speed.

(a) Tests at zero wing lift were carried out at different drop heights than those with wing lift and are listed as a reference to results previously obtained.

(b) * - 9 psig.
+ - 9 psig, modified valve reported as Valve B in Phase Report dated August 1, 1958.

1500-Pound-Unit Drop-Test Results

As in the drop testing of the 750-pound unit, the initial drop tests of the 1500-pound unit were made at the recommended initial tire pressure of 17 psig. During these tests the impact energy was effectively dissipated, and even though there was some oscillation of the landing gear present after the landing, the unit did not oscillate severely or bounce off of the landing pad as was encountered in the early drop tests with the 750-pound unit. Upon examination of the recorded data, however, it was found that the maximum vertical-load factor obtained in these tests was higher than anticipated.

Effect of Initial Tire Pressure on Maximum Vertical-Load Factor

To reduce the magnitude of the maximum vertical-load factor, drop tests were conducted with lower initial tire pressures. Figure 8 is a graph of maximum vertical-load factor versus initial tire pressure obtained with Valve A for various combinations of sinking speed and static load. These results show that, at the higher sinking speeds, the maximum vertical-load factor was substantially reduced by employing lower initial tire pressure. In the case of the landing with a 920-pound static load and a sinking speed of 7-1/4 ft/sec, the maximum vertical-load factor was reduced from 5.0 to 3.7 when the initial tire pressure was reduced from 21 to 9 psig. As in the case with the 750-pound unit, however, a practical minimum pressure was reached, below which successful higher sinking-speed landings were not possible because the tire was no longer capable of supplying enough impulse to stop the descent of the carriage in the available tire deflection.

The effect of initial tire pressure was not so noticeable at the lower sinking speeds. In the drop tests conducted with a static load of 920 pounds and a sinking speed of 2-1/2 ft/sec, there was essentially no change in the maximum vertical-load factor as the initial tire pressure was varied from 21 to 9 psig. It is interesting to note that, in the drop tests conducted with a static load of 1520 pounds, the maximum vertical-load factor obtained in the lower-sinking-speed landings actually began to increase again as the initial tire pressure was lowered below 13 psig. This resulted from the fact that, in the drop tests conducted with a high static load and with low sinking speed and initial tire pressure, a sufficient impulse was not applied to the unit to bring it to a stop before the tire bleed valve closed. The maximum vertical-load factor in these drop tests occurred after the valve had closed and was higher than the highest load that occurred while the valve was open.

Effect of Valve Area and Programming on Maximum Vertical-Load Factor

The results obtained in drop tests with the three tire bleed valves were fairly similar. There was a small increase in maximum vertical-load factor as the total valve area was reduced, but this increase was not as great as might have been expected. When the valve area was reduced 5.7 square inches from the 24.4 square inches of Valve A to the 18.7 square inches of Valve C, the maximum vertical-load factor obtained in drop tests conducted under the same conditions increased by only one to two tenths. Further reduction in valve area, however, caused the maximum vertical-load

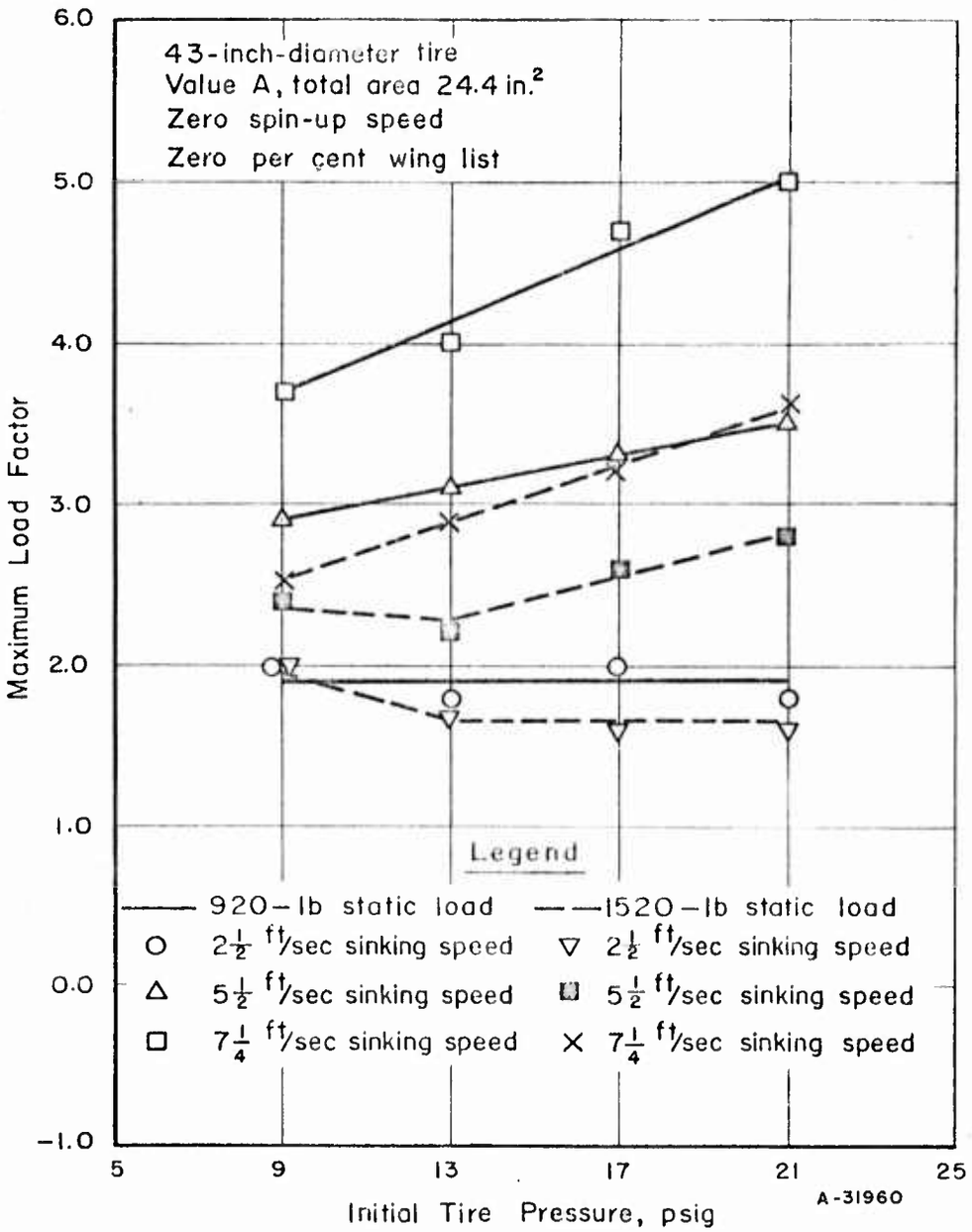

FIGURE 8. EFFECT OF INITIAL TIRE PRESSURE ON MAXIMUM VERTICAL LOAD FACTOR

factor to increase at a slightly faster rate. When the valve area was reduced an additional 4.1 square inches by replacing Valve C with Valve B, which had a total of 14.6 square inches, the maximum vertical-load factor increased by one to three tenths. This seems to indicate that the internal axle area of 17.4 square inches, which is the same for all three valves, and the resistance to air flow encountered in turning the air 90 degrees at the end of the axle limit the flow of air from the tire sufficiently to reduce the effectiveness of valve programming on the 1500-pound unit.

Valve B was eliminated from the testing program after the first sequence of tests because of the higher maximum vertical-load factors achieved with it. Continued testing with Valves A and C indicated that the best over-all performance of the unit with Valve A installed was obtained with an initial tire pressure of 12 psig for a static load of 1500 pounds and 10 psig for a static load of 1200 pounds. With Valve C installed, the best over-all performance was obtained with an initial tire pressure of 11 psig for a static load of 1500 pounds and 9 psig for a static load of 1200 pounds. Since the initial tire pressure used with Valve C was lower than that used with Valve A, the maximum vertical-load factor obtained in drop tests with the two was almost identical, even though Valve A had a larger area. Valve C was chosen to be installed in the unit during the flight tests because its smaller area would probably result in slightly better performance than that achieved with Valve A at sinking speeds below 2-1/2 ft/sec.

Drop Tests Conducted With Tire Spin-Up

The results obtained in the tests conducted with tire spin-up to 61 and 78 knots were in good agreement with those obtained with zero spin-up speed. Table 4 shows the values obtained for the maximum vertical-load factor and maximum spin-up load at various combinations of sinking speed and tire rotational speed for the drop tests conducted at static loads of 1200 and 1500 pounds and initial tire pressures of 9 and 11 psig, respectively. The maximum vertical-load factor obtained at the higher sinking speeds was slightly greater in the tests conducted with tire spin-up than in the tests conducted without tire spin-up. In the drop tests conducted with a static load of 1500 pounds, an initial tire pressure of 11 psig, and a sinking speed of 7-1/4 ft/sec, the maximum vertical-load factor increased from 2.7 in the drop test with zero spin-up speed to 3.1 in the drop test with a spin-up speed of 61 knots. At the lower sinking speeds, however, there was no noticeable difference in the maximum vertical-load factor attained in the tests with and without tire spin-up.

The maximum spin-up load obtained in the drop tests with tire spin-up was 2400 pounds. It occurred in the test conducted with a static load of 1500 pounds, an initial tire pressure of 11 psig, a sinking speed of 10-1/2 ft/sec, and a tire spin-up speed of 78 knots. There was little difference in the maximum spin-up load obtained in tests conducted at spin-up speeds of 61 and 78 knots.

Drop Tests Conducted With Wing Lift

Table 5 shows the effect of wing lift on the maximum vertical-load factor obtained in drop tests conducted at various sinking speeds and tire spin-up speeds. As in the case of the results listed for the drop tests of the 750-pound unit with wing lift, the maximum vertical-load factors listed are the total-load factors applied to the drop-tester carriage and are equal to the sum of the wing lift and tire loads. The maximum

TABLE 4. MAXIMUM VERTICAL-LOAD FACTOR AND MAXIMUM SPIN-UP LOAD OBTAINED IN DROP TESTS OF THE 1500-POUND UNIT CONDUCTED WITH TIRE SPIN-UP

Aircraft Sinking Speed, ft/sec	Maximum Vertical-Load Factor at Indicated Spin-Up Speed			Maximum Spin-Up Load, lb, at Indicated Spin-Up Speed	
	0 Knots	61 Knots	78 Knots	61 Knots	78 Knots
Static Load of 1200 Pounds, Initial Tire Pressure of 9 Psig					
2-1/2	1.7	--	--	--	--
3-1/4	--	1.8	1.8	1100	1050
7-1/4	3.1	3.1	3.0	2000	1900
10-1/2	4.2	4.4	4.4	2200	2300
Static Load of 1500 Pounds, Initial Tire Pressure of 11 Psig					
2-1/2	1.8	--	--	--	--
3-1/4	--	1.7	1.8	1350	1350
7-1/4	2.7	3.1	2.9	1900	1900
10-1/2	4.0	4.1	4.0	2350	2400

Note: Constant axle area of 17.4 in.^{2}; Valve C, total area 18.7 in.^{2}; and zero per cent wing lift.

TABLE 5. EFFECT OF WING LIFT AND TIRE SPIN-UP ON MAXIMUM VERTICAL-LOAD FACTOR OBTAINED IN DROP TESTS OF THE 1500-POUND UNIT

Aircraft Sinking Speed, ft/sec	Tire Spin-Up Speed, knots	Wing Lift, per cent	Maximum Vertical-Load Factor	
		Static Load, lb:	1200	1500
		Initial Pressure, psig:	9	11
2-1/2	0	0	1.7	1.8
		50-40(a)	1.9	1.7
		100-80(a)	1.7	1.7
3-1/4	61	0	1.8	1.7
		50-40	2.0	2.4
		100-80	2.0	2.1
7-1/4	0	0	3.1	2.7
		50-40	3.2	2.9
		100-80	3.2	3.0
	61	0	3.1	3.1
		50-40	--	3.1
		100-80	3.1	3.0
10-1/2	0	0	4.2	4.0
		50-40	4.3	4.0
		100-80	4.4	4.1
	61	0	4.4	4.1
		50-40	4.3	4.5
		100-80	4.2	4.2

Note: Constant axle area of 17.4 in.^{2} and Valve C, total area 18.7 in.^{2}

(a) The 1200-pound static-load tests were conducted with 50 and 100 per cent wing lift, and the 1500-pound static-load tests were conducted with 40 and 80 per cent wind lift.

vertical-load factor for the tests conducted at constant sinking speed and static weight was not substantially affected by varying the percentage wing lift or spin-up speed.

In some instances the total maximum vertical-load factor was less in the tests conducted with wing lift than in the tests conducted without wing lift. In the tests conducted at a sinking speed of 10-1/2 ft/sec, a static load of 1200 pounds, and a tire spin-up speed of 61 knots, the maximum vertical-load factor obtained with zero per cent wing lift was 4.4, and that obtained with 100 per cent wing lift was 4.2. Even in the tests in which the maximum vertical-load factor obtained with wing lift was higher than that obtained without wing lift, the maximum load carried by the high-flotation tire was less in the tests with wing lift than in the tests without wing lift.

The continued application of the wing-lift force by the wing-lift cylinders after the energy-dissipation cycle, in addition to the vertical load carried by the high-flotation tire, caused the drop-tester carriage to be accelerated upward after the landing impact. In the drop tests conducted with a static load of 1200 pounds and 100 per cent wing lift, the upward impulse applied to the carriage was sufficient to cause the tire to lose contact with the landing pad and the carriage to lose contact with the wing-lift cylinders. The carriage rose to a maximum height of 2-1/2 inches above the wing-lift-cylinder contact point in the test conducted at a sinking speed of 10-1/2 ft/sec. The carriage did not lose contact with the wing-lift cylinders in any of the tests conducted with a static load of 1200 pounds and 50 per cent wing lift. Except for the test conducted at a sinking speed of 10-1/2 ft/sec and 80 per cent wing lift, the carriage did not lose contact with the wing-lift cylinders in any of the tests conducted with a static load of 1500 pounds.

Optimum Operating Conditions and Range of Sinking Speeds for the 1500-Pound Unit

The best performance of the 1500-pound unit over the full range of sinking speeds was obtained with Valve C and an initial tire pressure of 9 psig for a static load of 1200 pounds and an initial tire pressure of 11 psig for a static load of 1500 pounds. Landings at all sinking speeds from 2-1/2 to 10-1/2 ft/sec were successful under these conditions. Figure 9 shows a graph of the maximum vertical-load factor versus sinking speed for drop tests conducted under these conditions without tire spin-up and wing lift. Except for the tests at extremely low sinking speeds, the maximum vertical-load factor was slightly less in the tests conducted with a static load of 1500 pounds than in those with a static load of 1200 pounds.

Figures 10, 11, and 12 show the landing dynamic characteristics of the 43-inch-diameter high-flotation tire for drop tests conducted with an initial tire pressure of 11 psig, a static load of 1500 pounds, Valve C, zero tire spin-up speed, and zero per cent wing lift at sinking speeds of 2-1/2, 7-1/4, and 10-1/2 ft/sec, respectively. The oscillation of the tire after valve operation, which is dependent on the energy remaining in the system, varied from around 4 inches peak to peak at a sinking speed of 2-1/2 ft/sec to around 1-5/8 inch peak to peak at a sinking speed of 10-1/2 ft/sec. A maximum vertical-load factor of 4.0, which was the allowable design maximum for the gear, was achieved in the 10-1/2 ft/sec landing.

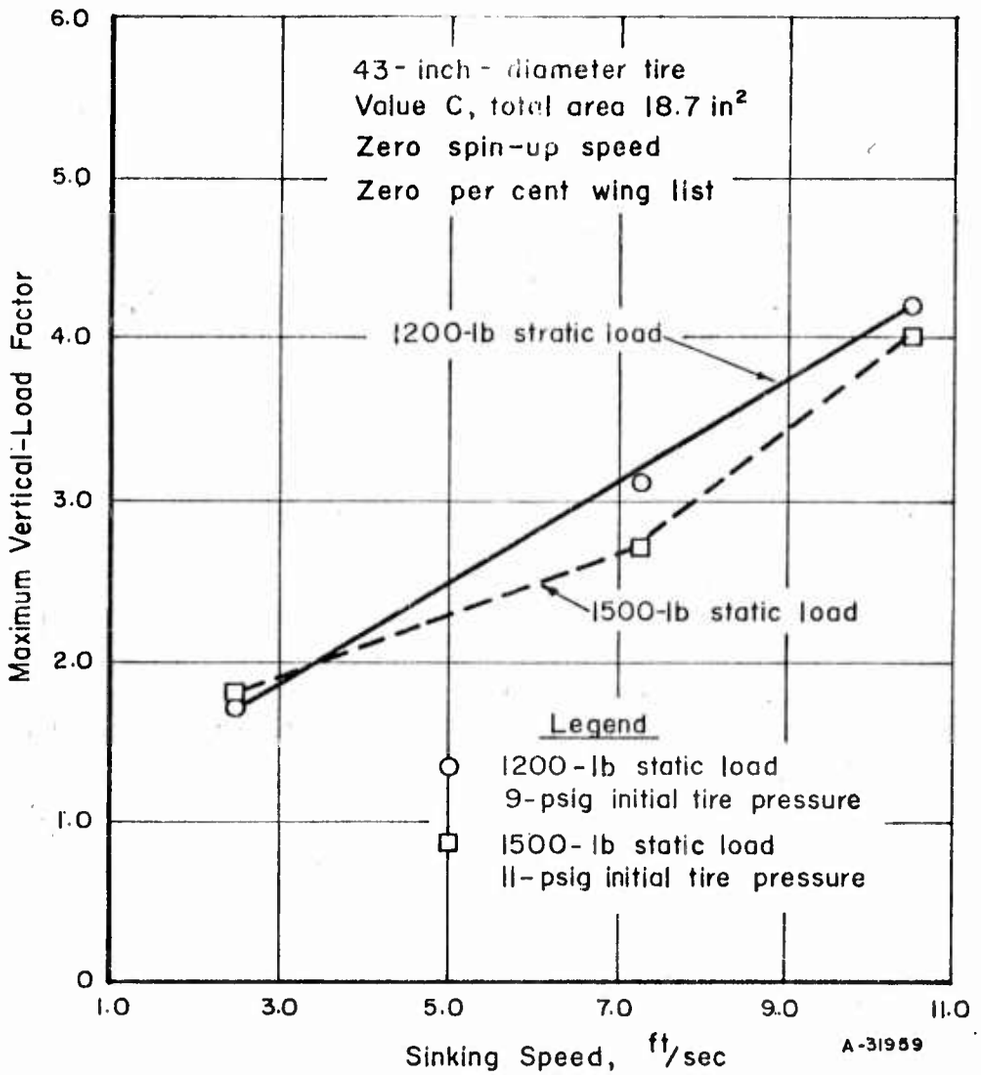

FIGURE 9. RELATION OF MAXIMUM VERTICAL-LOAD FACTOR TO SINKING SPEED

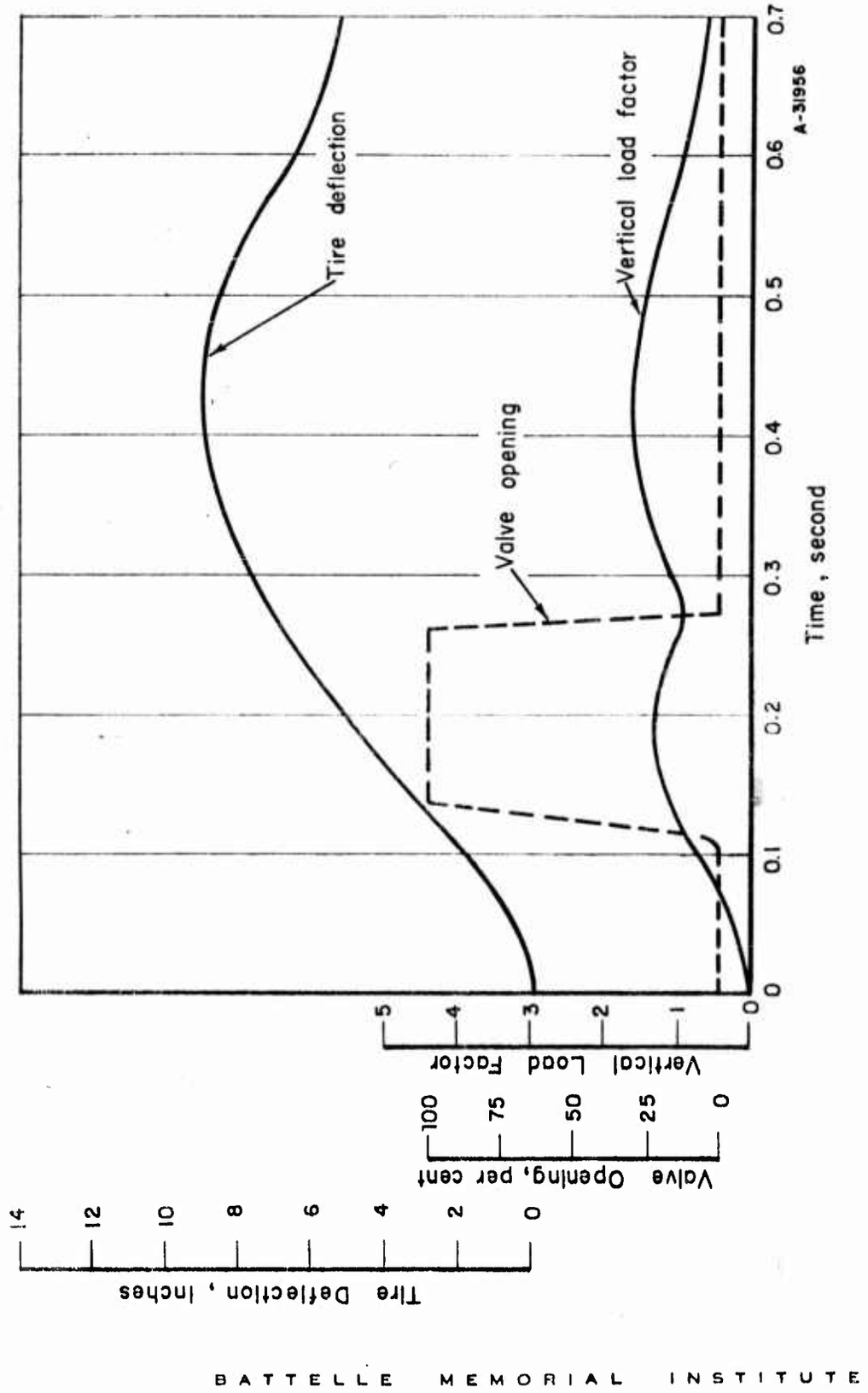

FIGURE 10. LANDING DYNAMICS OF A 43-INCH-DIAMETER, HIGH-FLOTATION TIRE WITH AN INITIAL TIRE PRESSURE OF 11 PSIG, A STATIC LOAD OF 1500 POUNDS, AND VALVE C AT A SINKING SPEED OF 2-1/2 FEET/SECOND

Zero spin-up speed. Zero per cent wing lift. Internal axle area, 17.7 in.^{2}.

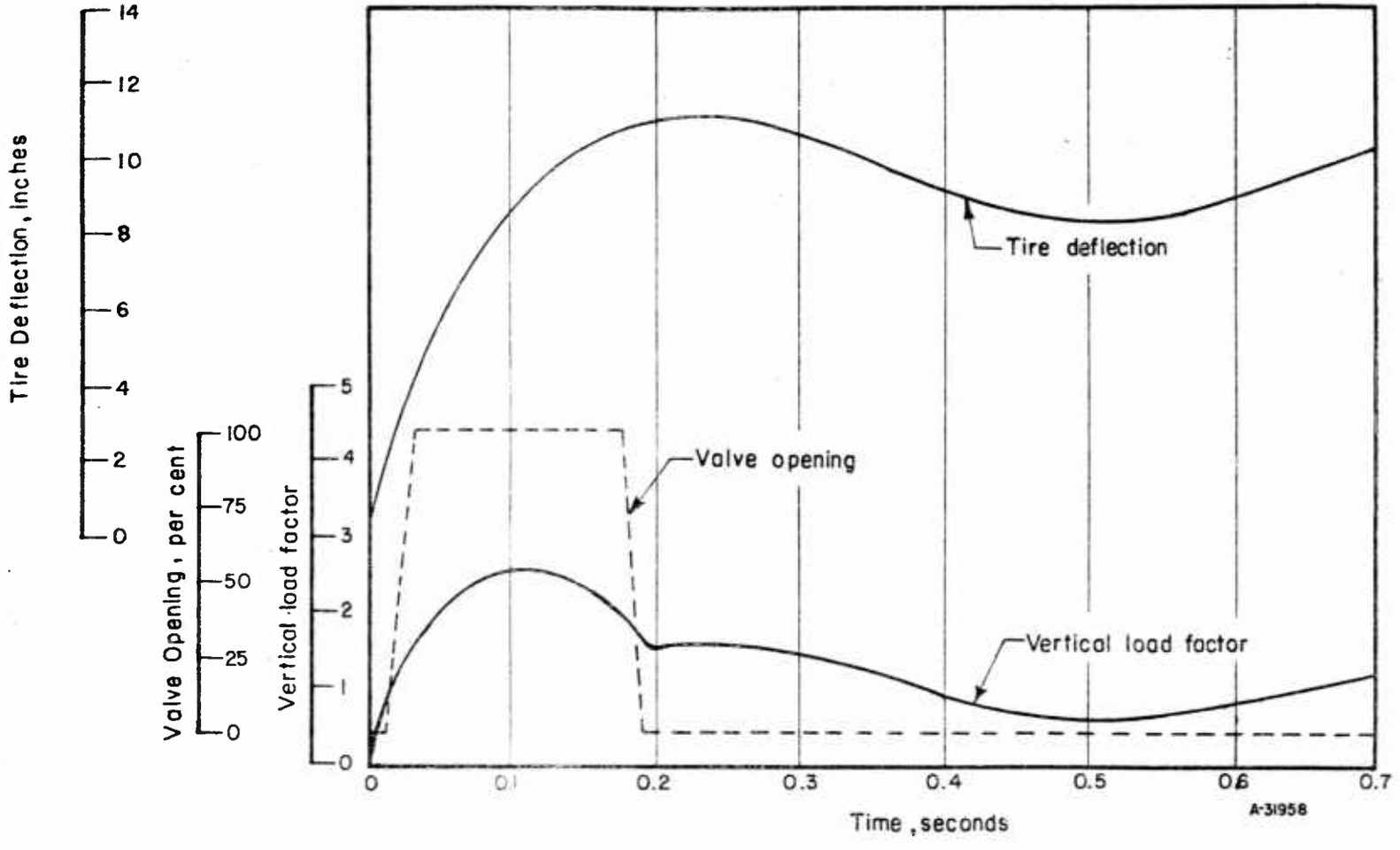

FIGURE 11. LANDING DYNAMICS OF A 43-INCH-DIAMETER, HIGH-FLOTATION TIRE WITH AN INITIAL TIRE PRESSURE OF 11 PSIG, A STATIC LOAD OF 1500 POUNDS AND VALVE C AT A SINKING SPEED OF 7-1/4 FEET/SECOND

Zero spin-up speed. Zero per cent wing lift. Internal axle area, 17.7 in.^{2}.

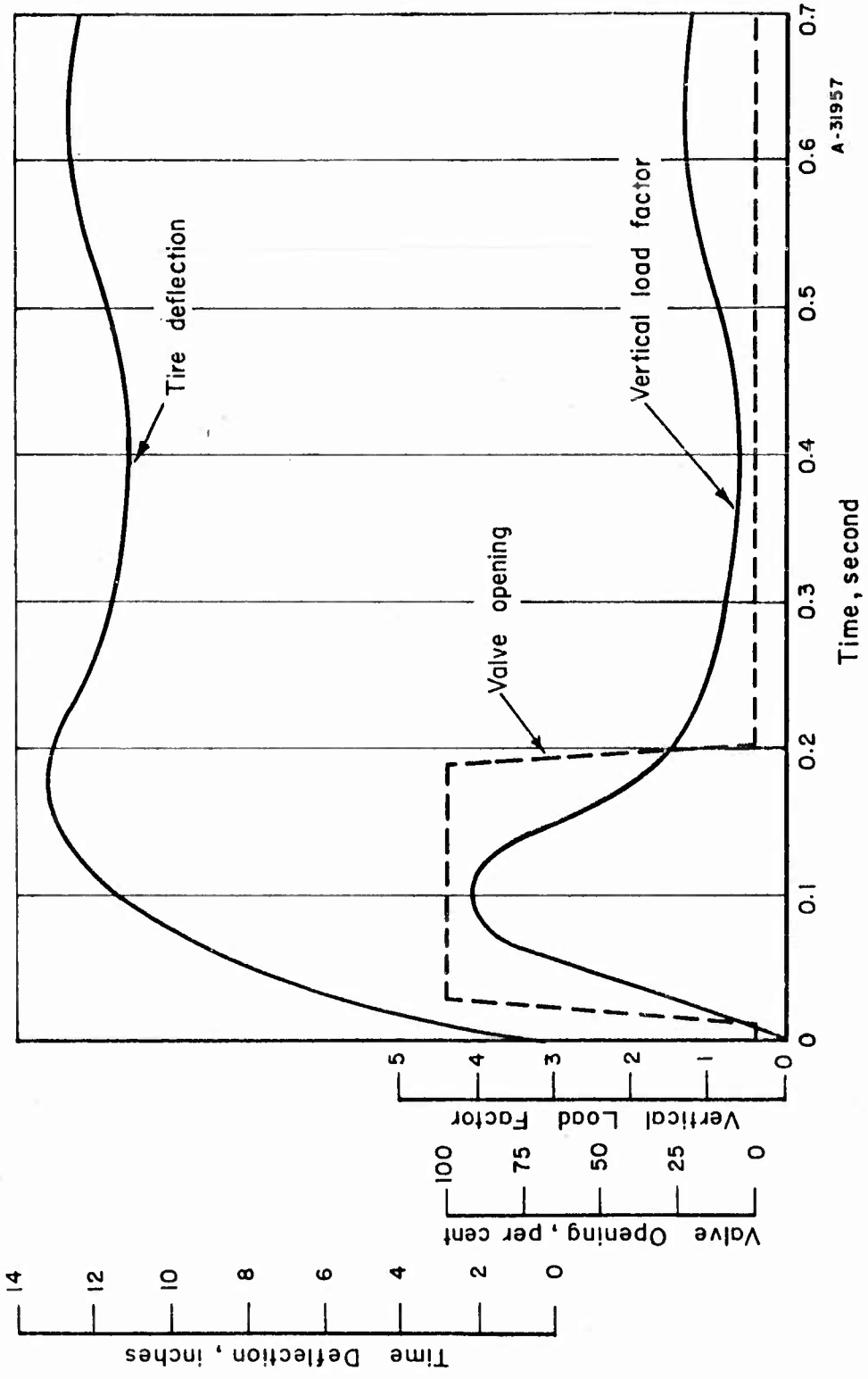

FIGURE 12. LANDING DYNAMICS OF A 43-INCH-DIAMETER, HIGH-FLOTATION TIRE WITH AN INITIAL TIRE PRESSURE OF 11 PSIG, A STATIC LOAD OF 1500 POUNDS, AND VALVE C AT A SINKING SPEED OF 10-1/2 FEET/SECOND

Zero spin-up speed. Zero per cent wing lift. Internal axle area, 17.7 $in.^2$.

Final Tire Pressure

The final tire pressure obtained in drop tests with the 1500-pound unit was affected by sinking speed and by tire spin-up. Final tire pressure decreased with increasing sinking speed and was approximately 1/2 psig higher in the low-sinking-speed drop tests with tire spin-up than in the drop tests without tire spin-up. The increase of final tire pressure with tire spin-up became less significant as the sinking speed increased. In the drop tests conducted with a static load of 1200 pounds, a tire spin-up speed of 61 knots, and sinking speeds ranging from 2-1/4 to 7-1/4 ft/sec, the final tire pressure ranged from 2.5 to 3.9 psig with the final tire pressure increasing with decreasing sinking speed. In drop tests conducted under the same conditions without tire spin-up, the final tire pressure ranged from 2.2 to 3.4 psig.

One of the reasons for this variation in final tire pressure is the difference in tire deflection at the instant of valve closure. As the tire deflection at the instant of valve closure increases, the mass of air retained in the tire decreases and the final equilibrium pressure decreases. Figure 13 is a sequence of photographs of the 43-inch-diameter high-flotation tire with various combinations of static load and tire pressure. At a tire pressure of 3 psig, the tire is still creased when supporting a load of 1500 pounds, but is not creased when supporting a load of 1200 pounds. It requires a tire pressure of approximately 3-1/2 psig to prevent creasing of the 43-inch-diameter high-flotation tire when it is supporting a static load of 1500 pounds.

CONCLUSIONS

The conclusions that can be drawn from the test results are:

(1) Both the 750- and 1500-pound static-load high-flotation landing gears are capable of successfully dissipating the landing-impact energy of aircraft under laboratory drop-test conditions.

(2) The high-flotation landing-gear system is capable of successful laboratory operation with both tire spin-up and wing lift and is not substantially affected by either.

(3) The present 43-inch-diameter tire unit functions with a maximum vertical-load factor of four or less at sinking speeds as high as 10-1/2 ft/sec with an initial tire pressure of 11 psig, a static load of 1500 pounds, Valve C, zero tire spin-up speed, and zero per cent wing lift.

(4) It is possible to fold the 43-inch-diameter high-flotation tire into a helical bellows in the manner in which the 34-inch-diameter tire has been folded.

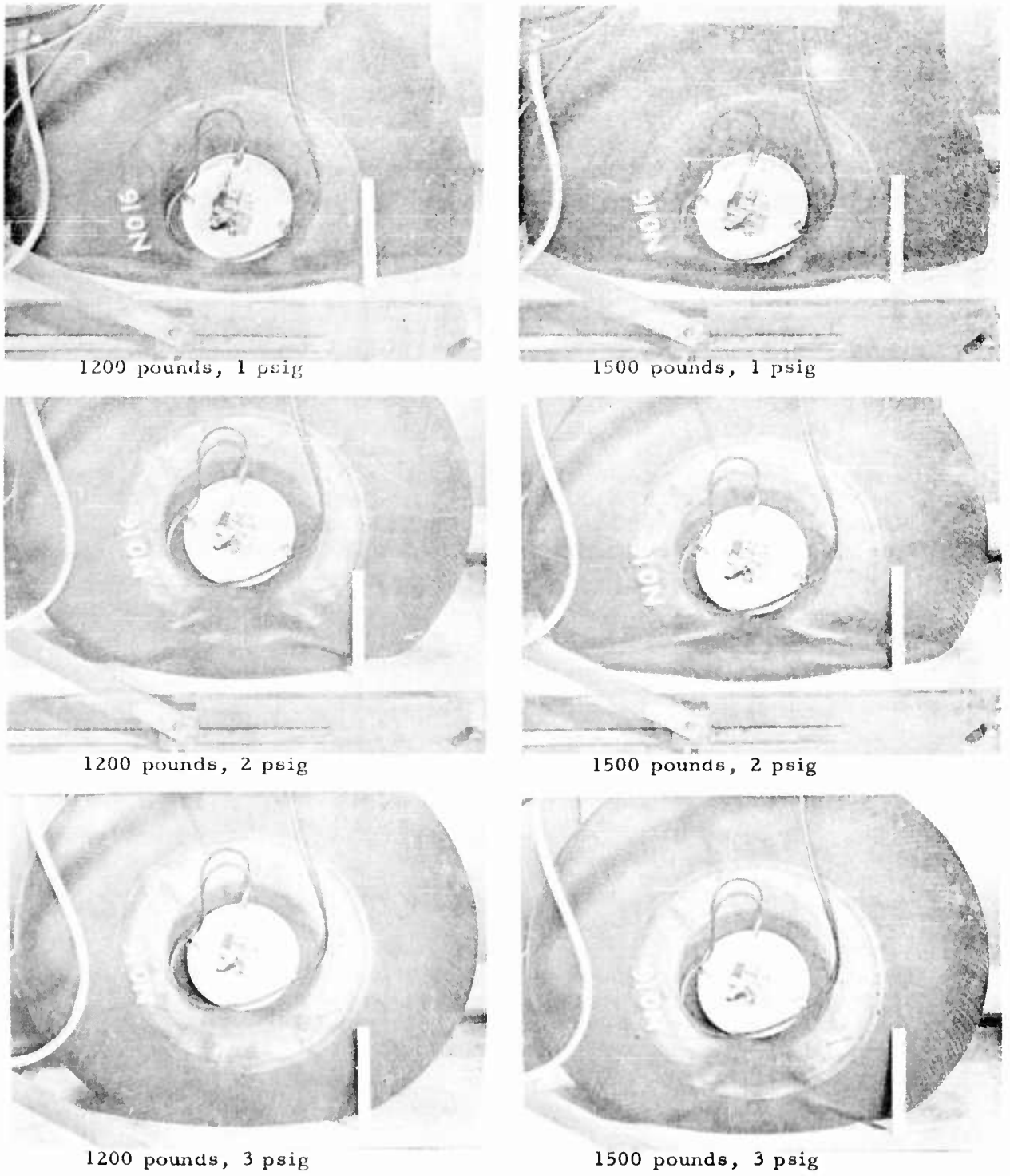

1200 pounds, 1 psig

1500 pounds, 1 psig

1200 pounds, 2 psig

1500 pounds, 2 psig

1200 pounds, 3 psig

1500 pounds, 3 psig

FIGURE 13. 43-INCH-DIAMETER HIGH-FLOTATION TIRE WITH VARIOUS COMBINATIONS OF STATIC LOAD AND TIRE PRESSURE

FUTURE WORK

Immediate Future

At the present time and in the immediate future, Fairchild will conduct flight testing of the 1500-pound static-load high-flotation landing gear mounted on the L-19 aircraft. Fairchild should consult with Battelle on any problems that occur during this flight-test program. To make this possible, Battelle has submitted to Fairchild, at their request, a proposal for an expansion of the present research program. Under this expanded program, Battelle would be authorized to provide technical assistance to Fairchild during the flight testing and demonstrations of the high-flotation landing gear for the period July 31 through December 31, 1959.

During the testing of the 1500-pound landing-gear unit, full advantage could not be taken of valve programming because the air flow seemed to be limited by the internal axle area of 17.4 square inches and by the resistance to air flow encountered in turning the air 90 degrees at the end of the axle. A better insight as to how the unit might operate with less resistance to air flow could be obtained with the present unit by reducing the volume of air to be bled from the tire during a landing. This could be accomplished by installing a flexible torus, capable of withstanding an inflation pressure of about 25 psig with negligible volume change, inside of the high-flotation tire. The inflated torus would retain the air inside of it and would reduce, by its volume, the volume of air that must be bled down during the landing. Such a torus has already been obtained by Fairchild, and drop testing to determine its performance capabilities could be conducted on the Battelle drop tester.

Future Component Design

The next logical step in the high-flotation landing-gear program is the design and development of an operational unit for use on a specific aircraft. While an operational unit will have to perform the same functions as the present laboratory and flight test unit, it will be necessary to make extensive component changes to simplify their design and to make the unit more applicable to operation under field conditions. The following component-design suggestions are made with this consideration in mind.

Bleed-Valve Design

In an operational unit, it would probably be desirable to have the tire bleed valve located internally rather than externally as it is in the present unit. This would reduce the possibility of the valve being damaged by striking an object during landing or take-off and would decrease the resistance to air flow by eliminating the necessity of turning the air at the outboard end of the axle. The valve configuration itself could take many forms. A sleeve valve similar to the one presently being used could be located internally by mounting the valve sleeves on the inboard side of the tire flange before the tire is wound on it. A pressure-balanced poppet-type valve appears to be attractive, especially if actuated in an inboard rather than an outboard direction.

Component Alterations Necessary for Inboard Valve Actuation

To actuate the tire-bleed valve in the inboard direction, minor changes would be required in the design of the load-sensing cylinder and pressure sensor. The only change necessary in the design of the load-sensing cylinder would be the reversal of the stepped shaft. If the larger diameter of the stepped shaft entered the load-sensing cylinder on the inboard, rather than the outboard side, the stepped shaft would be actuated in the inboard direction when a load was applied to the large piston.

Except for the design of the spacer block, the design and actuation of the pressure sensor could remain essentially as it is. Figure 14 shows the variation in the design of the pressure-sensor spacer block for use with a tire bleed valve actuated in either the outboard or inboard direction. For a valve actuated in the outboard direction, the spacer block holds the valve "push" rods apart during valve actuation and reduces their effective length by a distance, x, when the pressure sensor disengages. For a valve actuated in the inboard direction, the spacer block would hold the valve "pull" rods together during valve actuaion and would increase their effective length by a distance, x, when the pressure sensor disengaged.

Load- and Pressure-Sensor Cylinder

In the present unit, the closing of the tire bleed valve when a given minimum tire pressure is reached is accomplished by the removal of a spacer block from the valve push-rod assembly to shorten the effective length of the assembly. This spacer block could be eliminated and the same method of valve closing could be retained by the removal of the hydraulic link in the load-sensing cylinder from the valve push-rod assembly. Figure 15 is a schematic sketch of a proposed load- and pressure-sensor cylinder. The operation of the cylinder would be as follows:

(1) With the landing gear in the extended position, the weight of the tire and axle would pull the large piston to the top of the cylinder.

(2) The gas, which would be separated from the hydraulic fluid by a bladder or membrane in the lower accumulator chamber, would expand and force the hydraulic fluid through the control spool valve into the upper chamber.

(3) When the tire pressure reached the pressure-sensor cocking pressure, the control valve would be actuated to the engaged position and would close off the upper chamber from the lower accumulator chamber.

(4) Upon landing, the closed-off upper chamber would perform in the same manner that the present load-sensing cylinder does and the tire bleed valve would be actuated.

(5) When the tire pressure dropped to the pressure-sensor disengaging pressure, the control valve would be actuated to the disengaged position, as shown in Figure 15, and the upper chamber would again be open to the lower accumulator chamber.

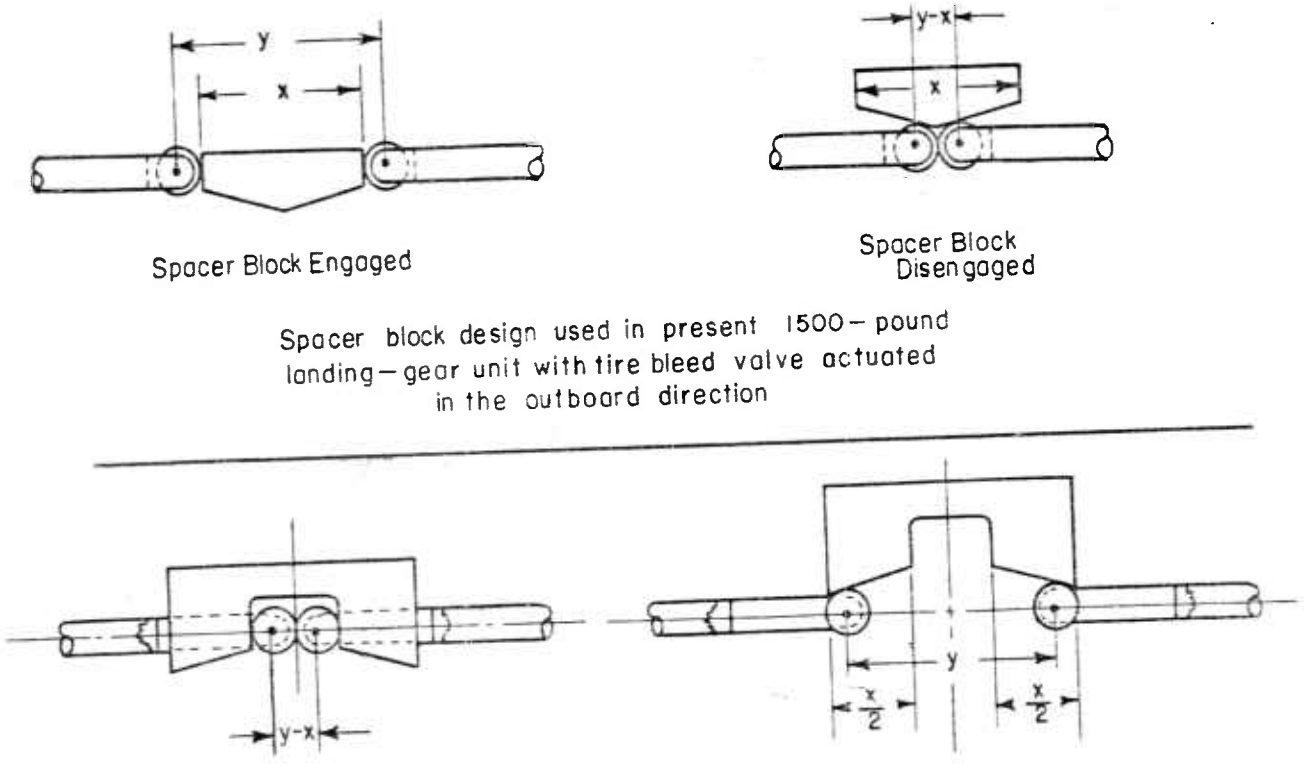

FIGURE 14. VARIATION IN THE DESIGN OF THE PRESSURE-SENSOR SPACER BLOCK FOR USE WITH A TIRE BLEED VALVE ACTUATED IN EITHER THE OUTBOARD OR INBOARD DIRECTION

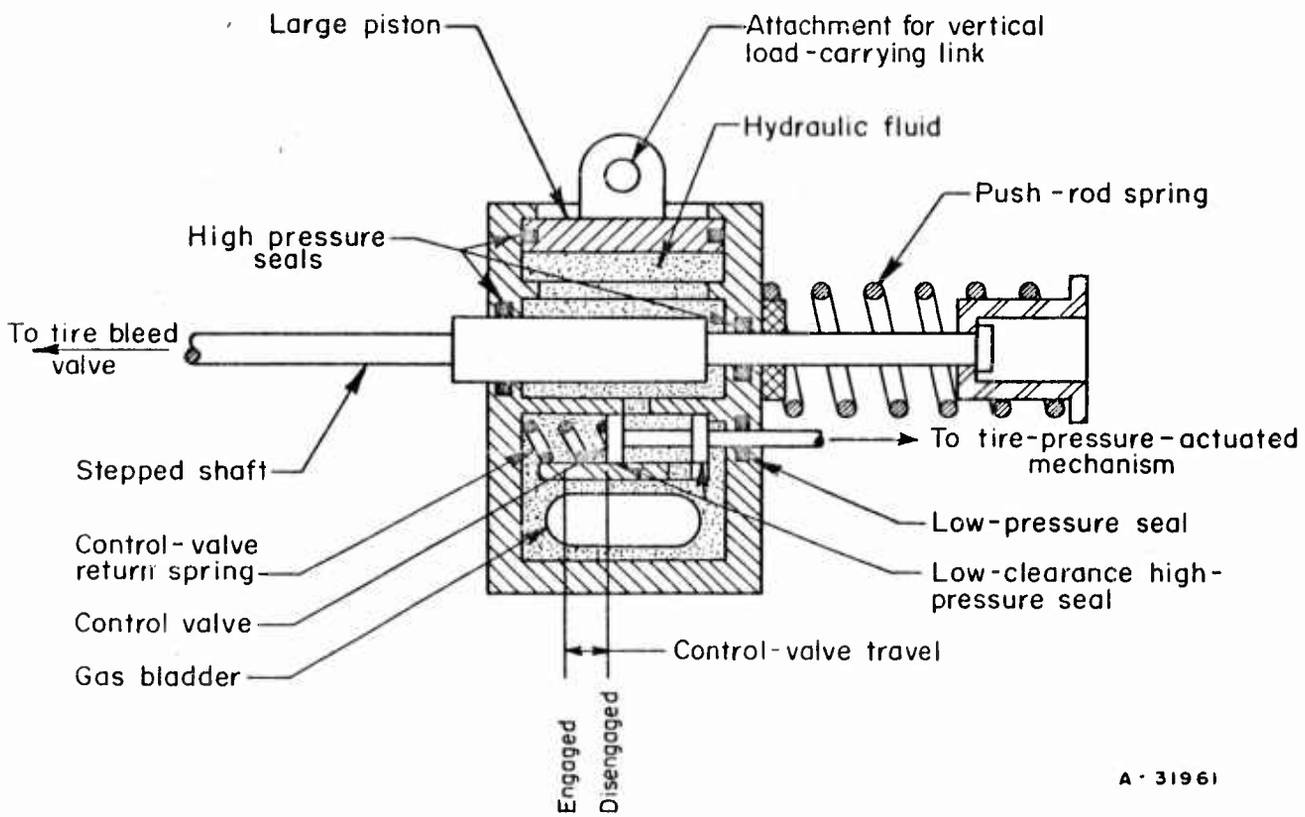

FIGURE 15. PROPOSED LOAD- AND PRESSURE-SENSOR CYLINDER

(6) The hydraulic fluid in the upper chamber would be forced into the accumulator chamber, compressing the gas bladder. The larger diameter portion of the stepped shaft would be pulled back into the cylinder by the push-rod spring, thus closing the tire bleed valve, and the vertical load on the large piston would force it into the cylinder until it bottomed on a stop.

The area of the control valve would have to be large enough to permit the hydraulic fluid displaced in the upper cylinder by the bottoming of the large piston and by the reentrance of the larger portion of the stepped shaft to flow into the accumulator chamber in from 0.01 to 0.02 of a second. To reduce and to maintain at a fairly constant value the force required to actuate the control valve, it would probably be beneficial to use an extremely low clearance, metal-to-metal fit on the sealing surfaces of the control valve. Such an arrangement would permit a small amount of leakage, but since the upper cylinder would be pressurized for only a fraction of a second during valve actuation, a small amount of leakage could be tolerated. At the point where the control-valve shaft emerges from the accumulator chamber a low-pressure, low-friction, zero-leakage seal could be used.

The control valve could be actuated in a number of ways. One method would employ the bellofram-piston and cam straps that are presently used. In this system the control valve could simply replace the U-shaped, pressure-sensing guide block and could be actuated by the cam strap in the same manner that this block presently is. Another method would be to actuate the control valve by a small solenoid which could be energized by a pressure switch or switches located in the tire.

In the design of any future load-sensing cylinders, attention should be given to the cushioning of the stepped shaft and large piston when they bottom on their respective stops. A neoprene seat is provided on the stepped shaft stop of the present unit, but a shock load is still applied in both the axial and vertical directions when the stepped shaft bottoms on this stop.

****

A record of all technical work performed on this project appears in Battelle Memorial Institute Laboratory Record Books 13510, 13511, 14103, and 15296.

WFP:RDF:JHB:CWR:JAH:JEV:RJM/mmk

FAIRCHILD AIRCRAFT AND MISSILES DIVISION

HAGERSTOWN 10, MARYLAND

SUBJECT INITIAL FLIGHT TESTS
HIGH FLOTATION LANDING GEAR

PREPARED BY A. J. Atkinson — REPORT NO. FT245-1

CHECKED BY J. A. Clopper — MODEL M-245B

APPROVED BY R. V. Ford — COPY NO.

APPROVED BY D. F. Weller — NO. OF PAGES 96

APPROVED BY R. A. Henson — DATE January 22, 1960

REVISIONS

REVISION DATE	PAGES AFFECTED	APPROVED
April 14, 1960	i, vii, viii, 1, 2, 3, 5, 6, 12, 23, 95; added 6a, 83a, 96.	
	Revised prior to release to include additional data.	

NS-800-69B

SUBJECT:- INITIAL FLIGHT TESTS, HIGH FLOTATION LANDING GEAR

DATE January 22, 1960
REVISED April 14, 1960

TABLE OF CONTENTS

LIST OF FIGURES

LIST OF FIGURES - continued

LIST OF FIGURES - continued

LIST OF FIGURES - continued

LIST OF FIGURES - continued

LIST OF FIGURES - continued

LIST OF TABLES

LIST OF PHOTOGRAPHS

DATE January 22, 1960
REVISED April 14, 1960

SUBJECT:- INITIAL FLIGHT TESTS, HIGH FLOTATION LANDING GEAR

I. INTRODUCTION

The purpose of these tests was to evaluate the functional and aerodynamic characteristics of the Fairchild High-Flotation Landing Gear, Model M-245B, as outlined in the test program.

The test program was completed in two phases. The initial testing was terminated on 4 August 1959 due to the contract funds being expended. A continuation of the contract was received which authorized the completion of testing and expanded the landing program to include sinking speeds of up to 10 fps in place of a maximum of 7.25 fps previously agreed upon.

II. SUMMARY AND CONCLUSIONS

A. General Conclusions

1. Test data presented in this report show that the M-245B landing gear has exceptional capability in absorbing obstacle and landing loads. These qualities, together with the high-flotation capabilities evaluated briefly in soft soil and mud, indicate that the operating conditions of military support aircraft can be greatly expanded by adaptations of this landing gear.

2. Further tests are recommended to obtain sufficient data for design of satisfactory struts to adapt this gear to operational aircraft and explore the rough field characteristics with additional gear damping provisions. It is unlikely that these tests, including landing and take-off across an array of obstacles, can be made on the present L-19 test bed because of aircraft structural limitations and the rigid strut installation.

3. The flight tests outlined in Reference (a) program were completed within the safety and structural limits of the gear and airplane with the exception of the highest rate of descent landings which exceeded by 0.15 g the airplane design load factor of 4.0 g. No damage was sustained by the gear or the airplane during these tests. The most significant conclusions from flight tests are as follows:

II. SUMMARY AND CONCLUSIONS

A. 3. - continued

a. The limiting obstacle height for the 43-inch tire (1500 lb capacity) is approximately 6 inches for low speed or STOL aircraft operating at ground speeds in the range up to 40 or 45 mph. Obstacles 8 inches high could be satisfactorily crossed at low taxi speeds. Tests were limited by drag strut springback obstacle loads although the 8-inch obstacle loads indicate a considerable increase in strut strength would be required to make a take-off or landing over this size obstacle. (Refer to Figure 9.)

NOTE: The loads presented in graphs of this report are referenced as noted in the Background section of this report, Paragraph 7.

b. Venting tire pressure at touchdown to absorb landing shock and loads is feasible although some revision of the valving is considered desirable for improvement of gear efficiency.

c. An operational installation of the gear should include some provisions for damping of rebound noted in high rate of descent landings and when taxiing through wide ditches.

d. Taxiing through mud, in which a 4-wheel drive jeep stalled, was satisfactory. However, operation under these conditions resulted in mud being thrown into the propeller by the tires and subsequently being blown over the aircraft, including the windshield. In an operational concept for propeller driven aircraft some provision would have to be made to eliminate or minimize this problem.

e. Tire folding in flight was successfully accomplished following the installation of an internal tube arrangement to assist in the dynamic folding of the tire.

SUBJECT:- INITIAL FLIGHT TESTS, HIGH FLOTATION LANDING GEAR

DATE January 22, 1960
REVISED April 14, 1960

II. SUMMARY AND CONCLUSIONS

B. Detailed Test Results

1. The M-245B landing gear with 43-inch tire operated satisfactorily and without malfunction in tests which included the following maximum conditions:

   a. Taxiing over rectangular 2 1/8 inch obstacle at 41 mph.

   b. Taxiing over rectangular 4 1/4 inch obstacle at 37 mph.

   c. Taxiing over rectangular 6 3/8 inch obstacle at 38 mph (Photo 35-390).

   d. Taxiing over rectangular 8 inch obstacle at 8 mph (Photo 35-388).

   e. Taxiing across 24 x 4 inch ditch at 36 mph.

   f. Taxiing across 24 x 6 inch ditch at 30 mph.

   g. Taxiing across 24 x 8 inch ditch at 15 mph (Photo 35-182).

   h. Landing at 10.25 fps rate of descent.

   i. Taxiing on mud approximately 6 inches deep (soil bearing strength too low to support a man's weight).

   j. Taxiing on soft soil.

   k. Landing and taking off from rough sod.

2. Normal accelerations obtained in taxi tests were well within the 4 g aircraft limits in tests over obstacles up to 6 3/8 inches at the highest speeds tested. This is shown in Figures 21, 22 and 23. Figure 23, for example, shows 2.3 g acceleration at 22 mph and 2.1 g acceleration at 37 mph in 6 3/8 inch obstacle tests.

SUBJECT:- INITIAL FLIGHT TESTS, HIGH FLOTATION LANDING GEAR

II. SUMMARY AND CONCLUSIONS

B. 2. - continued

Lateral and longitudinal accelerations are presented in the same plots. Acceleration data for 8-inch obstacle tests, presented in Figure 24, indicate no problem to 8 mph, (maximum 1.6 g, vertical) the speed at which tests were limited by drag strut loads. Time history plots of aircraft accelerations are presented for tests over obstacles in Figures 25 through 34, taxiing across ditches in Figures 44 through 53, and landings in Figures 59 and 60A. Vertical load factor versus sinking speed in landing tests verifies drop-test data as shown in Figure 54.

3. Gear vertical loads in taxi tests over obstacles of varying size at incremental tire pressures and speeds are presented in Figures 17 through 20. These plots show total vertical load, (rolling plus vertical component due to drag), and vertical load prior to obstacle contact is also shown for reference. Total vertical loads only are shown in the time history plots (figures referenced in paragraph 2). Vertical motion of the hub when taxiing over 6 3/8 inch obstacles at 2.7 psi tire pressure was negligible as recorded by motion picture. Photo 35-390 shows the obstacle enveloped by the tire with negligible vertical displacement of the hub. Obstacle absorption is also shown in Photo 35-388 - left gear on 8-inch obstacle, right gear on 6 3/8-inch obstacle.

4. Drag strut incremental loads for obstacle runs are presented in Figures 10 through 13 with drag load due to main gear reaction also shown for reference. Effect of tire pressure on incremental drag loads is shown in Figures 14, 15 and 16 which are crossplots of drag load data. Drag strut springback loads, which were the limiting factor in taxi tests, are presented in Figures 8 and 9. The drag strut loads in the time history plots referenced in paragraph 2 are total axial loads. In designing struts for an operational use of this gear, the drag strut loads of this report should be considered and total drag loads resulting from simultaneous obstacle contact and touchdown (not tested in this program) will also be a factor in determining structural strength. For initial drag loads at touchdown, see Figure 55.

II. SUMMARY AND CONCLUSIONS

B. Detailed Test Results - continued

5. In landing tests the gear absorbed vertical loads at touchdown with about the same efficiency as demonstrated in drop tests. Figure 54 compares drop test and landing test data, showing a c.g. load factor of 4.15 with a landing at 10.25 feet per second. This landing is also plotted as a time history (Figure 60A) which shows the need for damping of rebound after initial touchdown. (Note vertical loads and c.g. load factor on time history plots, Figures 59, 60 and 60A). Additional vertical load data on landing is presented in Figures 56, 57 and 58.

6. The quick-reinflation system used in these tests (description on Page 17) apparently is needed only for high rate of descent landings when pressure after tire venting at touchdown is less than 2.5 psi. Several landings were made without quick reinflation at rates of descent approximating 5 fps. The landing bounce tendency was not noticeably changed. Since the quick-reinflation system may increase tire pressure to as much as 4 psi after a light landing (3.0 or 3.5 residual pressure plus 1.0 or 0.5 psi reinflation) it could result in pressure at which obstacle absorption is considerably lessened. In Figures 59, 60 and 60A the tire pressures during quick reinflation are presented to show time of operation. Gage location is such that only stabilized pressure readings are accurate.

7. Taxiing over obstacles of 6 to 8 inch height on level terrain the tire deflects at low pressures to absorb the obstacles satisfactorily. For satisfactory operation over wide ditches (4 or 5 ft width) or rolling ground, additional damping would appear necessary on aircraft with one wheel on each main gear.

II. SUMMARY AND CONCLUSIONS

B. Detailed Test Results - continued

8. In-flight folding of the tire was satisfactory at 95 knots following modification of the folding system. The modification consisted mainly of the addition of an inflated internal diagonal tube arrangement to prevent premature collapse of the leading surface of the tire during the first stage of the folding cycle.

   In the original configuration diagonal ribs (fastened to the outside of the tire for economy purposes on the test article) produced satisfactory folding on the ground. However, when the tire was suspended in the airstream at 85 knots the ribs on the leading surface collapsed, destroying the diagonal convolutions required for proper folding. By removing the external ribs and adding an inflated internal rib system satisfactory results could be obtained.

9. Control of the airplane in flight with the M-245 gear installed was qualitatively satisfactory in take-off, climb, cruise and stall configurations. Longitudinal controllability was marginal immediately following high rate of descent landing impact. This was due to tail wheel bounce and the undamped oscillation of the tires following touchdown and was corrected by adding a small amount of engine power. Ground handling was satisfactory although maneuvering on pavement is slightly more difficult than the original gear especially when a pivoting turn is attempted.

10. A speed-power check was made and data presented in Figure 61 indicates that the gear and struts reduced airspeed at cruise power (approximately 2200 rpm, 130 BHP) by 23 mph, from 112 to 89 mph. This is applicable only to the test-bed which included fixed gear with heavy struts and strut fairings (reference Photo 35-388).

SUBJECT:- INITIAL FLIGHT TESTS, HIGH FLOTATION LANDING GEAR

II. SUMMARY AND CONCLUSIONS

B. Detailed Test Results - continued

11. Take-off performance data analysis presented in Table I shows that the figures presented in the L-19 pilot's manual for take-off and climb over 50 ft obstacle were matched within the limits of measuring accuracy. The test data plots are Figures 62 through 66.

12. Leakage through the tires and around hub seals will require much improvement for a production type or the aircraft will need a built-in set of jacks. With pressure from the reservoir shut-off, the test tires lost pressure completely in several hours. It was not possible to determine whether there was leakage through the rotary seals of the pressure-sensing element because of the other leaks noted above.

13. Extensive landing gear load data, for both the normal and high-flotation gear, appears in tabulated form in Appendix I of this report.

III. DISCUSSION

A. Background

1. The M-245B High-Flotation Landing Gear with 43 inch tire (1500 lb rated capacity) was tested by the Fairchild Structural Test Laboratory as reported in reference b, (static tests) and reference c (rolling tests). Drop tests were conducted by Batelle Memorial Institute, Columbus, Ohio, as reported in reference d.

2. In order to obtain comparative data the L-19A furnished for gear tests was instrumented and tested briefly before installing the M-245B landing gear. Gross weight was 2400 lb for all tests, ±30 lb of fuel, and c.g. was 33.5% m.a.c.

3. As a result of drop test findings and pre-test conference on operating procedures it was considered necessary to redesign part of the inflation system. This redesign, made for the reasons listed below, delayed the program only slightly since it was found that a simplified inflation system, adequate for taxi tests, could be installed and that refinements of the system for flight could be made later when design and drawings were completed. The changes from original plans required were as follows:

   a. Interconnection of tires was considered unacceptable because it would permit air from one tire to flow to the other tire in cross-wind taxiing or with other lateral load differences. To eliminate interconnection and still retain the feature of post-landing bleed-down to a preset roll-out pressure it was necessary to duplicate the system from the tire to the pilot's adjustable regulator (including the regulator).

III. DISCUSSION

A. 3. - continued

b. Drop tests indicated that a roll-out problem could be anticipated because of the variation of post-landing tire pressure with rate of descent which is illustrated as follows:

Rate of descent	Residual tire pressure
2.25 fps	3.6 psi
7.25 "	2.6 "
10.5 "	1.8 "

It appeared that with less than 3 psi and a 1200 lb load the tire would wrinkle excessively for roll-out. To correct this problem a smaller reservoir (650 cu. in) was added to the system. This "quick-reinflation" reservoir charged to approximately 200 psi, would discharge into the tires immediately after touch-down, raising tire pressure by approximately 1 psi. This reinflation value could be varied by the charge of the quick-reinflation reservoir. Pressure would then bleed down, through bleeds in the adjustable regulators, to the pressure selected by the pilot for roll-out.

c. The system as originally designed was considered unsafe for flight tests since it required a pilot, upon landing and during roll-out, to adjust two regulators (from 9 psi to roll-out pressure of approximately 3 psi) and push a button to reactivate the inflation system. In order to correct this and permit the pilot to select the roll-out pressure while on base leg or final approach two solenoid valves were added between the tires and regulators. These valves closed when the pilot selected the "Land" position on the gear control box and the pilot could then adjust the regulators to the roll-out tire pressure. After landing, the valves

III. DISCUSSION

A. 3. c. - continued

were reopened by a pressure-operated time delay switch. The solenoid valves also prevented back pressure during quick-re-inflation from damaging the regulators.

4. The M-245B system as installed on the L-19A did not include the tire deflation and folding provisions since these tests were programmed for completion on a large airplane. The initial in-flight folding tests were conducted on a C-119 airplane S/N 53-3136, using a specially constructed rig to lower the tire into the airstream through the paratainer door opening.

5. The weight of the control components on the test-bed installation was not representative of a possible production model. These parts such as regulators, solenoid valves and pressure piloted valve were off-the-shelf items selected for quick availability and a low cost test installation.

6. In order to obtain comparable weight with the various test configurations the c.g. of the airplane was practically dictated by the gear installation and the ballast space available. For determination of weight and c.g. the airplane, with instrumentation installed, was weighed in the level attitude (levelling on the control torque tube) in the original configuration, after installing the M-245B gear and again after installing the quick-reinflation system with flight control panel.

   a. Tests of the original gear configuration were made with a full fuel load but with instrumentation recording equipment installed at the observer's station and ballasted with 25 lb on the battery, 133 lb around the legs of the pilot's seat and 70 lb aft of the seat (horizontal arm 144.0). The airplane with pilot weighed

III. DISCUSSION

A. 6. a. - continued

2400 lb with c.g. 33.6% m.a.c. The highest weight listed for L-19 aircraft in T.O. 1L-19A-5 is 2100 lb at 30.5% m.a.c. and the same T.O. lists the aft c.g. limit of the L-19E as 31.0% m.a.c. at 2400 lb. The aircraft manufacturer was contacted and approval was obtained to use 33.6% m.a.c. as a test loading providing no spin maneuvers were planned and vertical load on the gear should be limited on landing to 7300 lb, (2100 lb x 3.47 g).

b. The installation of the M-245B gear with simplified inflation system and instrumentation allowed only 7 gallons of fuel for 2400 lbs, c.g. 27.5% m.a.c. Fuel was considered adequate for taxi operations.

c. When the final system was installed the airplane was overweight. The air compressor, chemical air dryer and related tubing were removed and the accumulator was charged from an external compressor unit before each flight. Instrumentation was changed to use a small dry-cell bridge battery. With 11 gallons of fuel the aircraft loading was 2429 lbs, c.g. 29.8% m.a.c. Limited by space and structure for mounting instrumentation and inflation equipment, this was considered the optimum obtainable with a reasonably safe fuel supply.

7. The zero references for load data presented in Figures 1 through 7 for the original gear were taken in flight. The high flotation gear zero references were obtained before and after test by jacking the airplane and disconnecting the drag struts for Ground runs 1 through 12. After installation of the flight system the zero references were recorded in flight immediately prior to landing or, in the case of obstacle tests, during a lift-off from the runway. An exception is the tire pressure which was obtained with the aircraft on jacks and tire pressure bled to zero.

III. DISCUSSION - continued

B. Test Comments

1. Original L-19A Configuration with Standard Gear

a. All tests listed in the program were conducted except the turning radius test which was discontinued when it was found that the steerable tail wheel controlled the radius of turn for approximately a 20° turn, then swivelled to permit practically a pivot at low speed and an incipient ground-loop. Thus it appeared that significant turn data could not be obtained.

b. Obstacle tests were carried to a maximum of 23 mph over a 2 x 6 inch plank. (Reference Figures 1 through 5.) These standard-gear loads were considerably higher than those of reference (e). It is noted that the tests of reference (e) were conducted at 2135 lb gross weight while Fairchild tests were at 2400 lb. The wide variation of gear load prior to obstacle contact is considered a result of changes in wing lift and in thrust vectors due to necessary throttle adjustments in obtaining the desired speeds (reference Figures 1, 2, 4 and 5).

c. Landings were made to a maximum rate of descent of 4.3 fps which were adjudged by the pilot as limiting by reason of gear deflection (reference Figures 6 and 7). Vertical loads on the gear were higher than those of comparable descent rate in the reference (e) report, probably due to weight difference. Longitudinal accelerations were practically identical to reference (e) while vertical accelerations for given descent rates were approximately 0.25 g lower.

SUBJECT:- INITIAL FLIGHT TESTS, HIGH FLOTATION LANDING GEAR

III. DISCUSSION

B. 1. Original L-19A Configuration with Standard Gear - continued

d. Data for comparison with the M-245B gear were also obtained for the remaining items of the test program which included speed-power (Figure 61), performance take-off and landing (Figures 62, 63 and 64 and Table I) and pivoting turns on sod and concrete. The latter data was not plotted since the high-flotation gear was not instrumented for side loads and torsion loads.

2. M-245 Landing Gear (simplified inflation system)

a. Tests with the simplified system (excluding parts required for flight test) were made over obstacles and ditches of varying sizes as reported in the summary and conclusions. Gross weight was 2400 lb with c.g. 27.5% m.a.c. When it became evident that maximum obstacle runs scheduled would result in exceeding the 2300 lb limit in the aft drag strut fitting, it was necessary to monitor loads and approach the high speed runs in cautious increments, with resulting delay in the program.

b. The tire pressure originally desired for test was 3.5 psi, a pressure which reduced wrinkling of the tire. This is also the pressure which remains in the tire after a light landing, consequently that at which obstacle contact can be anticipated. As seen in Figures 8 and 9, this pressure severly limited the speed at which obstacles could be negotiated within drag springback load limits of the drag strut fitting (originally 2300 lb). This total drag load results from the geometry of the gear which, in 3-point attitude positions the main strut forward of the strut attachment and introduces a 400 lb tension component in the drag strut due to 950 lb vertical static load.

III. DISCUSSION

B. 2. b. - continued

The vertical load increased dynamically when the airplane crossed an obstacle and spring-back loads of the fixed strut were additive. Drag strut incremental loads are presented in Figures 10 through 13 independent of vertical load reaction in the drag strut.

c. Obstacle tests were continued using a tire pressure of 2.7 psi after a brief exploration showed that rolling characteristics at this pressure would be acceptable although wrinkling was more than desired and the greater deflection of the tire resulted in premature wear. The anticipated tread width of the tire had been reinforced with a sheet of tread-stock neoprene approximately .060 inch thick. The sidewall area, where wear was encountered at low pressure, was covered only with .020 inch of relatively soft carcass-stock neoprene. On a production type tire of this size, if operation at pressure as low as 2.7 psi is desired, the tread width should be increased approximately 5 inches on each side of the tire.

d. Taxi tests over obstacles higher than 2 1/4 inches were limited to one obstacle (reference Photo 35390) in accordance with the test program provision covering danger to the airplane. It became obvious that in the repeated runs between two obstacles the tail wheel would eventually be damaged. On one occasion the tail wheel struck a 2-inch obstacle when using paired obstacles. In later demonstrations at slow speed a 6 inch and 8 inch obstacle were negotiated simultaneously without difficulty to demonstrate that no longitudinal control problem resulted. (Photo 35-388.) The obstacles used for tests were rectangular, as shown in the referenced photo, and no ramp was used.

III. DISCUSSION

B. 2. M-245 Landing Gear (simplified inflation system) - cont'd

e. The considerable scatter in gear vertical load data appears characteristic of low pressure tires when compared with data of reference (e). The vertical load data of Figures 17 through 20 is total load and the rolling load, also plotted, may be subtracted to obtain incremental loads due to obstacles.

f. Taxi tests across a ditch were made over a 2 ft by 4 ft box buried flush with the ground and filled with planks to vary the depth and width of the ditch. The 4 ft dimension (length) remained constant and the taxi path was across the 2 ft dimension (width) which was varied to 18 inches and 12 inches (Photo 35-182). The taxi tests across the ditch were conducted to limits of safe operation or to speeds at which loads recorded had reached maximums. As seen in Figures 35 through 43 the ditches 12 inches or 18 inches wide presented no problem at depths up to 6 inches. The ditch 24 inches wide and 8 inches deep resulted in sharply increased springback drag loads (Figure 37), vertical loads (Figure 40) and aircraft accelerations (Figure 43). Time history plots of vertical loads, drag loads and aircraft accelerations are presented for evaluation of dynamic characteristics in Figures 44-53.

3. M-245 Landing Gear, Complete Inflation System

a. Tests with the complete inflation system, including quick-reinflation but without folding provisions, were made in accordance with the program. Gross weight was 2400 lb ($\pm$30 lb fuel) with c.g. 29.8% m.a.c. Increments of descent rate were obtained for landing tests by increasing the height of the landing

SUBJECT:- INITIAL FLIGHT TESTS, HIGH FLOTATION LANDING GEAR

III DISCUSSION

B. 3. a. Continued

flare and stall. Attempts were also made to increase rate of descent by using forward stick at the time of the stall. The best results were obtained by use of 60° flaps, setting up a nose high, power-on approach and varying the height at which the engine was cut to control sinking speed.

b. After five flights with the quick-reinflation accumulator charged to 100 psi (resulting in 1 psi quick reinflation) the regulator for this accumulator was set to a minimum (60 psi) for approximately 0.7 psi quick reinflation. No significant change in gear or aircraft reaction was noted. However, this explains the lower pressure of Figure 60 compared with Figure 59 during the quick-reinflation period.

c. Initial landing tests were complicated by reason of the original tail wheel spring. At 2400 lbs gross weight a hard landing bent the original spring on several occasions. The first of two series of landing tests was terminated at a maximum sinking speed of 6.4 fps to preclude damage to the airplane through failure of the tail wheel spring.

A new tail wheel spring was supplied by TRECOM and installed on the airplane prior to the final landing tests. This spring was made of a slightly heavier gauge material than the original and held up well at the maximum attained sinking speed of 10.25 fps.

d. During the landing tests it was decided to reinforce the aft drag strut attachments. This change was simply a bracket attaching to the skin and an additional rib, increasing the limit for drag springback (tension) load from 2300 to 3500 lb. With this configuration it

III. DISCUSSION

B. 3. d.- continued

was possible to increase speed over obstacles as indicated by flagged test points on various plots. There was also noted a tendency to reduced springback loads for a given speed and tire pressure after stiffening the drag strut attachment. This may be seen, for example, on Figure 9.

e. Landing tests for recorded data were made on a macadam runway. Two landings were made for qualitative evaluation of characteristics on a rough sod field. No problems of control or rolling characteristics on rough sod were noted but the undamped bouncing when taxiing at 15-20 mph through a ditch about 6 inches deep and 5 feet wide was quite pronounced. Bouncing was also noted when taxiing on a "washboard" macadam surface.

f. Take-off was made from a macadam runway except one case when a take-off was made from a rolling stretch of rough sod. In the latter case the absence of damping was also notable on the test bed installation. No recording was made of load or acceleration data during the rough field take-off because of generator trouble at the time. Further tests were anticipated under more strenuous conditions but contract funds were expended before this could be accomplished.

g. It will be noted that side loads and torsion loads on the gear strut were not obtained. The gear structure was too heavy to obtain measurable deflections with the weight of the L-19 aircraft. This also eliminated measurement of turning loads on the gear and restricted such tests to qualitative evaluations.

III. DISCUSSION

B. 3. M-245 Landing Gear, Complete Inflation System - cont'd

h. Several drops were made from a crane in order to determine that the quick-reinflation system and valves were functioning satisfactorily before making a landing. Data is presented in Figure 54. During one of these drops the rudder of the aircraft was damaged and a replacement was obtained from TRECOM.

C. Description of Test System

1. Original Landing Gear

The original landing gear was unchanged from the standard L-19A configuration. Strain gages were installed for measurement of loads.

2. M-245B Landing Gear (Simplified Inflation System)

Pending engineering changes considered necessary for the flight tests a simplified inflation system was installed for the early phase of taxi tests. This system included a main reservoir (capacity 870 cu. in., 3000 psi) with regulators for individual tire pressure selection. The tires and hubs were in final configuration as related to ground operation.

3. M-245B Landing Gear (Flight Test System)

As finally installed the gear included, in addition to the above reservoir and regulators, the following:

a. Quick reinflation system consisting of a reservoir (capacity 650 cu. in.) which filled to an adjustable pressure (for early tests, 100 psi) when a pressure sensor cocked. It discharged into the tires when both pressure sensors uncocked after touchdown.

III. DISCUSSION

C. 3. M-245B Landing Gear (Flight Test System) - continued

b. Indicators

(1) Red warning light indicating that a pressure sensor was not cocked and ready for landing, light extinguished when both were cocked.

(2) Green indicator lights, one for each tire indicating when the tire pressure sensor was cocked and ready for landing.

c. Selectors

(1) Pressure regulators for selecting touchdown tire pressure or taxi pressure. These had adjustable stops set for 9 psi touchdown and approximately 3 psi for taxiing over obstacles. A mid-point selection for approximately 5 psi was used for taxiing on smooth surface and for take-off to avoid excessive tire wear.

(2) Control panel with electrical switch set for "cruise" position during in-flight tire inflation for landing. The switch was set to "Land, Taxi and T.O." position just prior to landing and this closed solenoid valves between the tires and the regulators so that the regulators could be set to 3 psi before landing. Without these valves the tire pressure would begin bleeding back through the regulators when they were set to roll-out pressure before landing. The solenoid valves also protected the regulators from the higher line pressures during quick-reinflation. The solenoid valves were automatically opened approximately 5 seconds after touchdown by an adjustable time-delay switch.

III. DISCUSSION

C. 3. M-245B Landing Gear (Flight Test System) - continued

d. Compressor

A compressor provided for the system was installed but it was found that with the instrumentation recording equipment the airplane would exceed 2400 lbs. Since a 2500 psi charge in the main reservoir was adequate for approximately 4 inflations of the tires, the compressor was removed and the reservoir was charged from a ground compressor unit prior to tests. This unit incorporated filters and chemical dryers. For a production system using 43-inch tires, it is believed that a compressor with 1500 psi or less capacity would prove adequate.

4. Operation of the Flight Test System, Typical

a. Prior to take-off the pilot adjusts the regulators to 5 psi, places the control switch to "Land, Taxi and T.O.". Since sensors are not cocked the solenoid valves remain open and the tires inflate to 5 psi.

b. After take-off the pilot places the control switch to "Cruise" position and pushes the regulators to the forward stops (preset to 9 psi). Red light indicates, and green lights do not, while tires inflate. When one tire reaches cocking pressure (approximately 7.5 psi) a green light comes on, red light remains on, the quick reinflation system reservoir (solenoid controlled) fills to preset pressure, and pressure continues to the tires. When the other tire reaches cocking pressure the corresponding green light comes on and the red light is extinguished. Pressure to the tires continues to increase to 9 psi and is maintained at that pressure.

III. DISCUSSION

C. 4. Operation of the Flight Test System, Typical - cont'd

c. On final approach, the pilot places the control switch to "Land, Taxi and T.O.", pushes regulator controls full aft to the stops and is ready for landing. Solenoid valves are now closed to prevent pressure bleeding through regulators from the tires.

d. At touch-down the tires exhaust to between 3.5 and 2.1 psi, depending on rate of descent, pressure sensors uncock individually when pressure sensor senses 2.5 psi inside the hub. (The variation in actual tire pressure results from the difference in volume of air exhausted from the tire when deflection at touchdown is large or small.) When the second pressure sensor uncocks the quick re-inflation system discharges the quantity of air in the 650 cu. in. reservoir into the tires (100 psi equals approximately 1 psi tire pressure increase) and triggers the time-delay relay. After the preset time-delay the solenoid valves are reopened between the tires and regulators and the pressure of the tires is increased or bled off to the value preset by the regulator low pressure stop (approximately 3 psi).

e. After roll-out the pilot places the regulators approximately mid-way between the stops for a 5-psi taxi pressure on smooth terrain or leaves the regulators on the low pressure stop for taxiing on rough, unprepared surface.

D. Instrumentation

Instrumentation was provided on the M-245B gear to record on an oscillograph as follows:

Drag loads of the gear, from strain gages on the eyebolt stem attaching the drag strut to the main strut assembly.

III. DISCUSSION

D. Instrumentation - continued

Vertical loads from strain gages on the vertical load links.

Vertical acceleration, from an accelerometer mounted on the floor and attaching to aircraft rib structure 22 inches aft of the firewall (over the main gear).

Longitudinal acceleration, from an accelerometer mounted adjacent to vertical accelerometer.

Lateral acceleration, from an accelerometer mounted on a board installed aft of the pilot's seat 49 inches aft of firewall, on centerline of the aircraft. This was directly below the mid-point of the wing root chord.

Tire pressure, from transducers installed in the inflation lines to the valves approximately 5 feet upstream of the tires. Thus, when measuring pressure during quick-reinflation of the tires (Figures 59 and 60) the measurement was actually line pressure until pressure stabilized. No completely satisfactory method could be found for measuring actual tire pressure since pressures inside the hub are also affected by air flow during tire inflation and venting. Comparison of vertical load and tire pressure in Figures 59 and 60 shows however that the lag in time between vertical load actuating the vent valve (approximately 1000 lb) and the drop in tire pressure (venting through hub) is approximately .02 second. Tire pressures stabilize about 2 seconds later upon completion of quick reinflation. This was satisfactory for determining proper functioning of the inflatioh system.

Ground speed, from a microswitch mounted on tail wheel to indicate each revolution of the wheel, with time correlation on oscillograph for rpm.

SUBJECT:- INITIAL FLIGHT TESTS, HIGH FLOTATION LANDING GEAR

DATE January 22, 1960
REVISED April 14, 1960

III. DISCUSSION

D. Instrumentation

Rate of descent was measured by equipment utilizing the reflection from the runway surface of a continuous audio tone projected from the aircraft. The principle of operation is as follows: Dependent on the distance traveled, the reflected sound will either tend to reinforce or cancel the projected sound as picked up by a microphone located near the source. The relative output level of the microphone is recorded on an oscillograph and, with the frequency used in these tests, peaks occur at approximately every two inches as the aircraft approaches the runway. Since time is also on the oscillograph record, rate is easily computed. Correction is made in the calculations for the effect of variation of the speed of sound with temperature.

Instrumentation for visual recording was as follows:

RPM, Free Air Temperature, Cylinder Head Temperature, Airspeed and Oil Temperature from standard aircraft instruments.

Manifold Pressure, Ranco, Inc. gauge, S/N AF 43-107717, calibrated for operating range. Pressure tap was in the line between the primer and the engine (primer inoperative).

Tire Pressure downstream of regulators, calibrated gauges.

Reservoir Pressure of main inflation system, gauge in outlet line reading to 3000 psi for the 870 cu. in. reservoir.

Regulated Air Pressure (to 200 psi) gauge in line between reservoir outlet regulator and tire inlet regulators.

III. DISCUSSION

D. Instrumentation - continued

Reservoir Pressure (to 200 psi) quick-reinflation system, gauge between reservoir outlet and solenoid valve controlling release of air to the tire.

Regulated Air Pressure (to 160 psi) gauge on regulated controlling air to the quick-reinflation reservoir.

E. Tire Folding Test Apparatus

Ground and in-flight folding and reinflation tests of the high flotation tire were conducted by means of a portable test rig. This rig contained the necessary supply of compressed gas, a vacuum pump, a means of raising and lowering the tire in the slipstream when airborne, and necessary controls. The test rig was so designed that it could be installed in the cargo hold of a C-119 airplane and the tire could be lowered into the airstream through the paratainer doors in the bottom of the fuselage.

Initial attempts to fold the tire in flight failed when the original configuration (external diagonal ribs) collapsed at its leading surface when lowered into the slipstream. The external ribs were removed and an internal tube arrangement was installed which assisted the dynamic folding of the tire.

The inner tube arrangement consisted of two tubes having a 3 1/2 inch diameter cross section and 21 inch outside diameter mounted inside the tire carcass, concentric with the axle. Ten inflatable internal ribs of 2 1/4 inch diameter cross-section were installed diagonally between the two inner tubes. Air lines connected the tube arrangement to the supply and evacuating sources.

SUBJECT:- INITIAL FLIGHT TESTS, HIGH FLOTATION LANDING GEAR

III. DISCUSSION

E. Tire Folding Test Apparatus - cont'd

The tire and the internal tube arrangement were inflated separately. During the folding sequence the tire was deflated and the internal ribs held the tire as the inner hub began its rotation. As the hub rotation continued, the internal ribs propagated the diagonal convolutions required for proper folding. Once the diagonal folds were initiated the internal tube was deflated and the hub completed its rotation to complete the sequence. Refer to Photos 36-918 through 36-921.

IV. REFERENCES

a. Fairchild Report No. FTE-201A, Flight Test Program, High Flotation Gear System (M-245) 18 April 1958, Revision C, 25 February 1959, as amended by letter TREC-AA9-89-02-000 ST 140 AV from Lt. Col. Steinkrauss to FAMD, March 25, 1959.

b. Fairchild Engineering Report No. R245-010, Static Test - High Flotation Tire, 19 February 1959.

c. Fairchild Engineering Report No. R245-011, Rolling Tests - High Flotation Tire.

d. Batelle Memorial Institute, Summary Report, The Design and Development of Laboratory and Flight-Test Models of Landing Gear for Aircraft to be Operated from Rough Unprepared Fields, August 15, 1959.

e. Goodyear Aircraft Report GER 9061, Rough Terrain Landing Gear Evaluation Program, 31 October 1958.

Figure 1

EFFECT OF GROUND SPEED ON VERTICAL LOAD

Over 2 1/8" Obstacle

L-19A Flight No. L-19-2 S/N 51-7441 April 29, 1959

Original Tire and Landing Gear

Tire Pressure 21 PSI

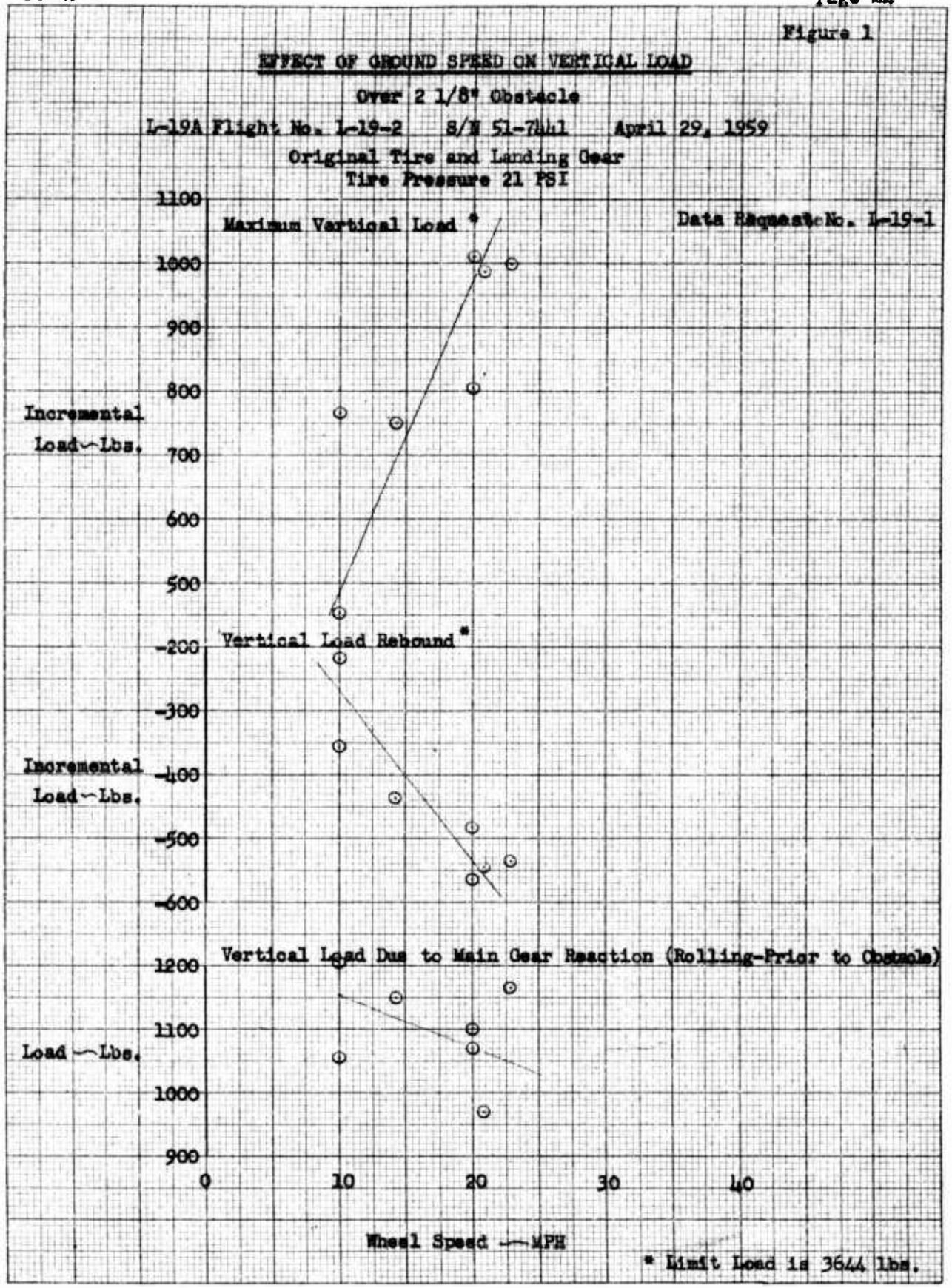

Figure 1

EFFECT OF GROUND SPEED ON VERTICAL LOAD

Over 2 1/8" Obstacle

L-19A Flight No. L-19-2 S/N 51-7041 April 29, 1959

Original Tire and Landing Gear
Tire Pressure 21 PSI

Data Request No. L-19-1

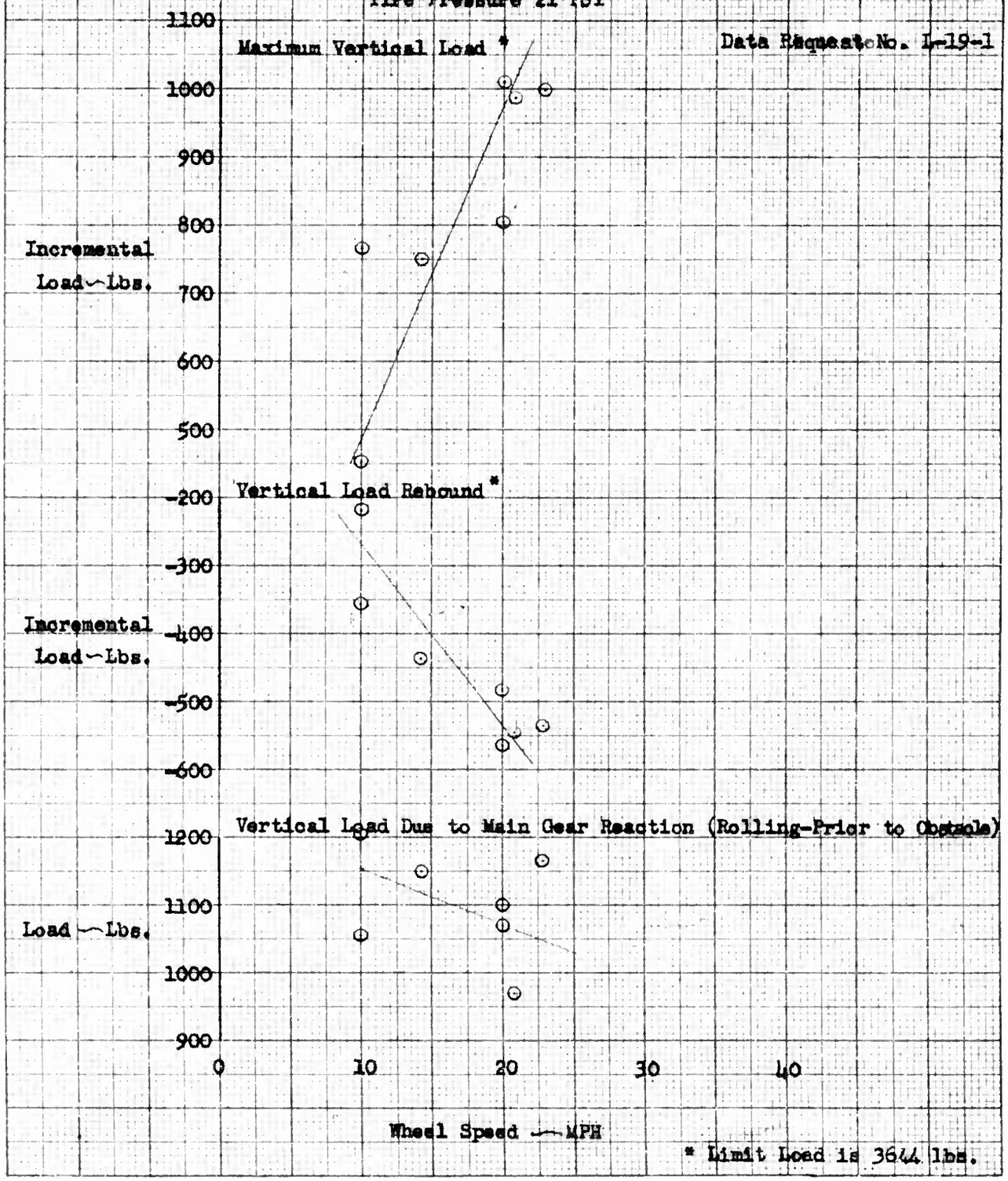

* Limit Load is 3644 lbs.

Figure 2

EFFECT OF GROUND SPEED ON DRAG LOAD

Over 2 1/8" Obstacle

L-19A Flight No. L-19-2 S/N 51-7141 April 29, 1959

Original Tire and Landing Gear

Tire Pressure 21 PSI

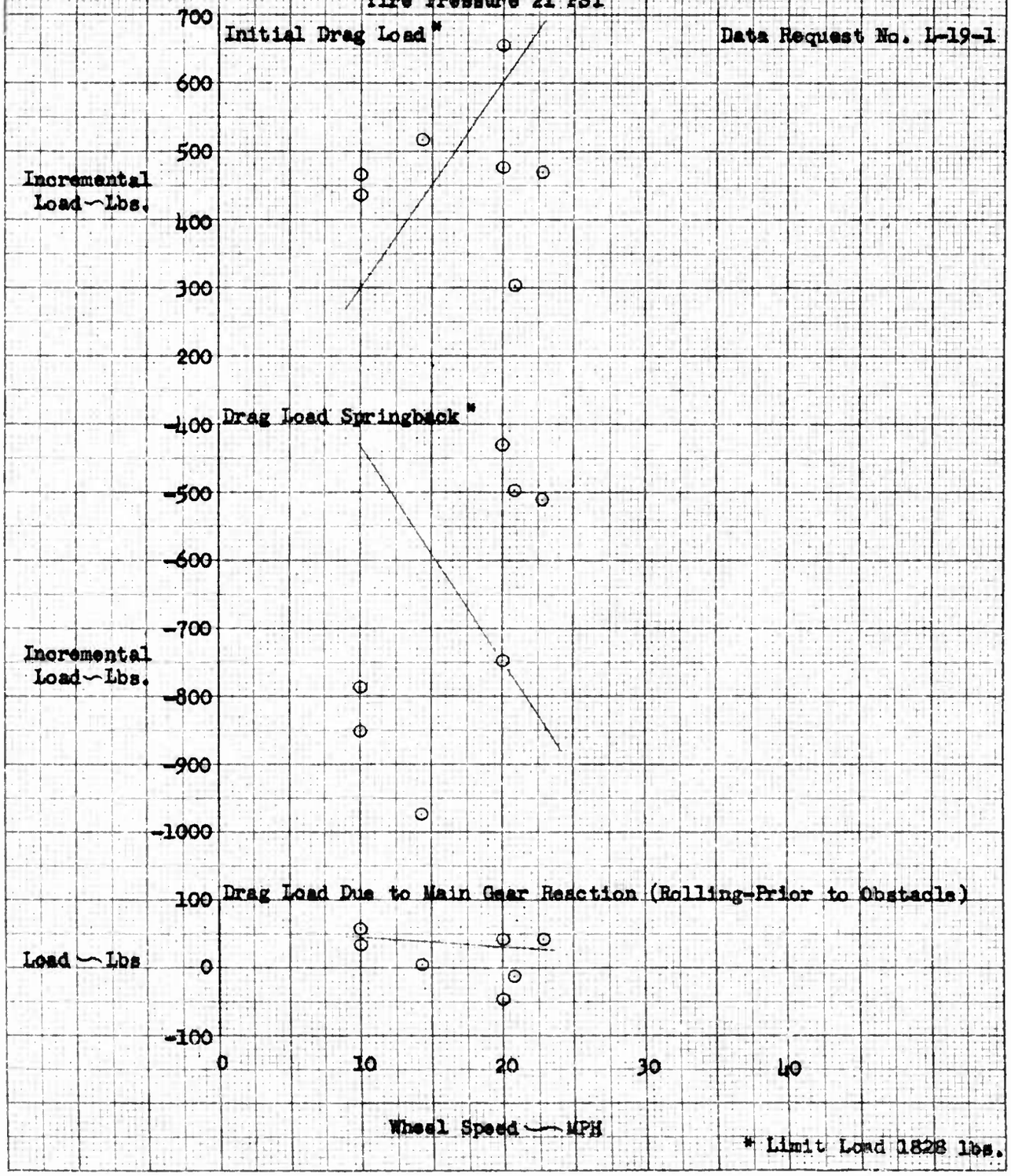

Figure 3

EFFECT OF GROUND SPEED ON AIRCRAFT ACCELERATIONS

Over 2 1/8" Obstacle

L-19A Flight No. L-19-2 S/N 51-7441 April 29, 1959

Original Tire and Landing Gear

Tire Pressure 21 PSI

Data Request No. L-19-1

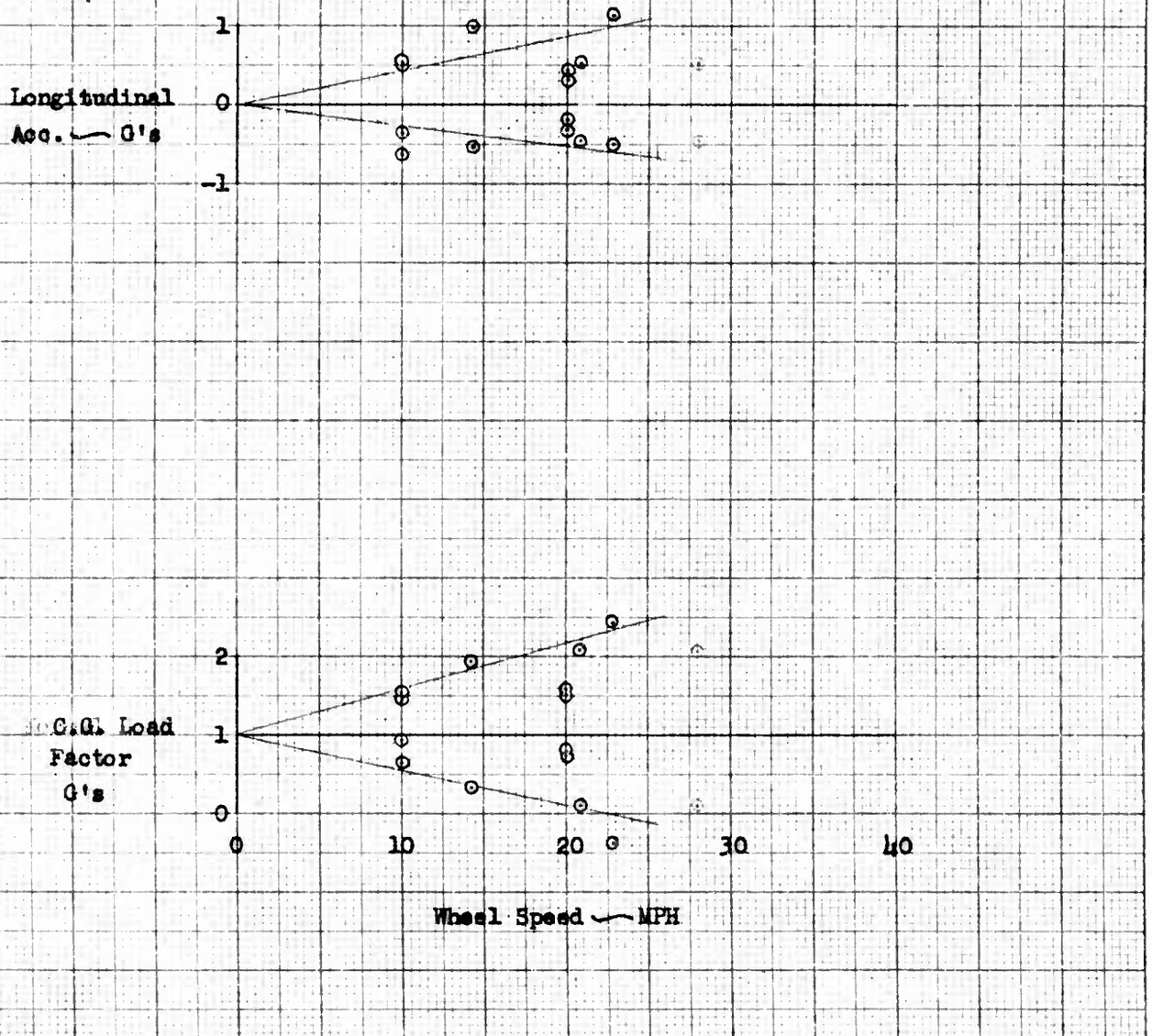

Figure 4

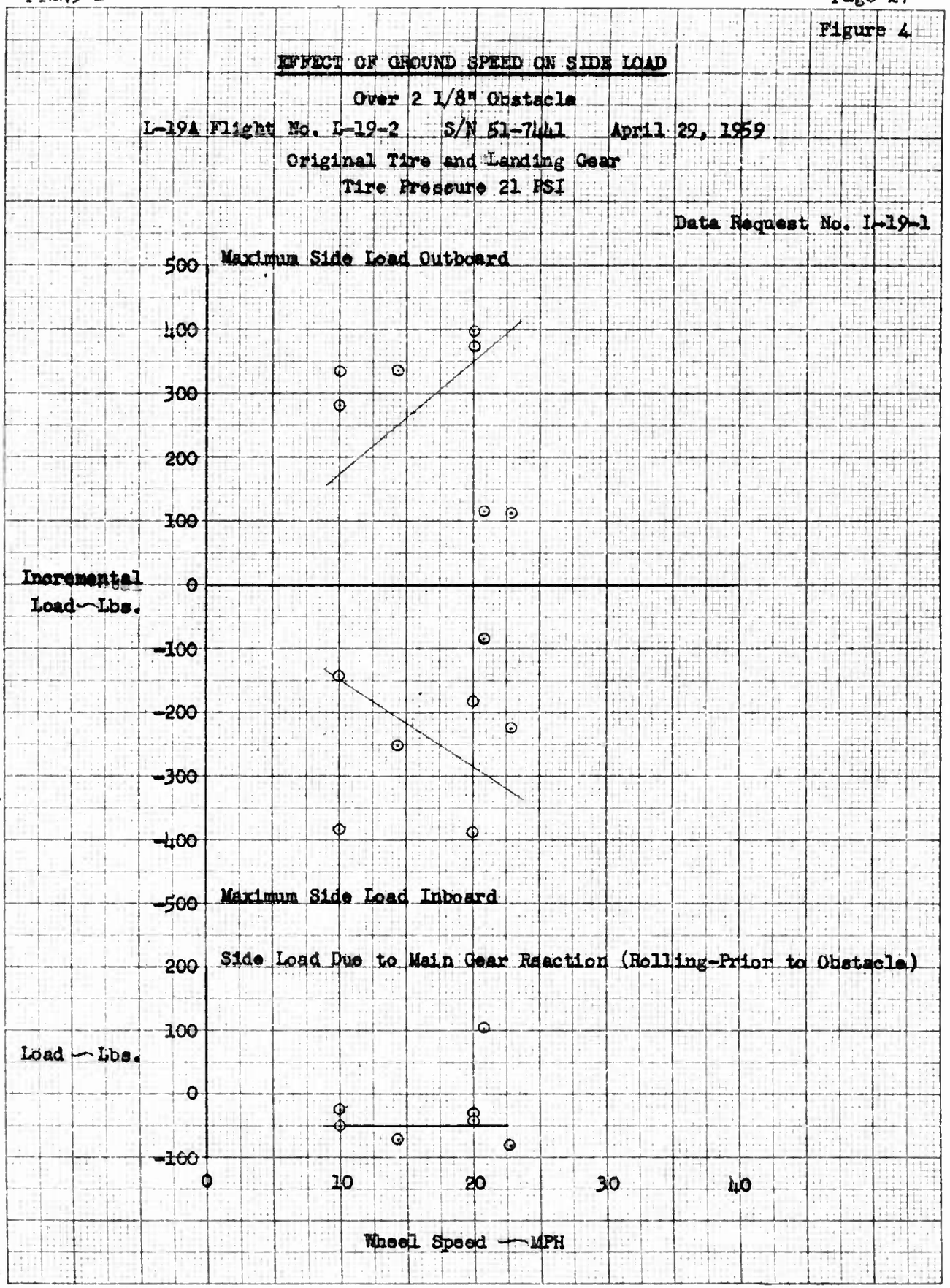

Figure 5

EFFECT OF GROUND SPEED ON TORSION (DRAG) LOAD

Over 2 1/8" Obstacle

L-19A Flight No. L-19-2 S/N 51-7141 April 29, 1959

Original Tire and Landing Gear

Tire Pressure 21 PSI

Data Request No. L-19-1

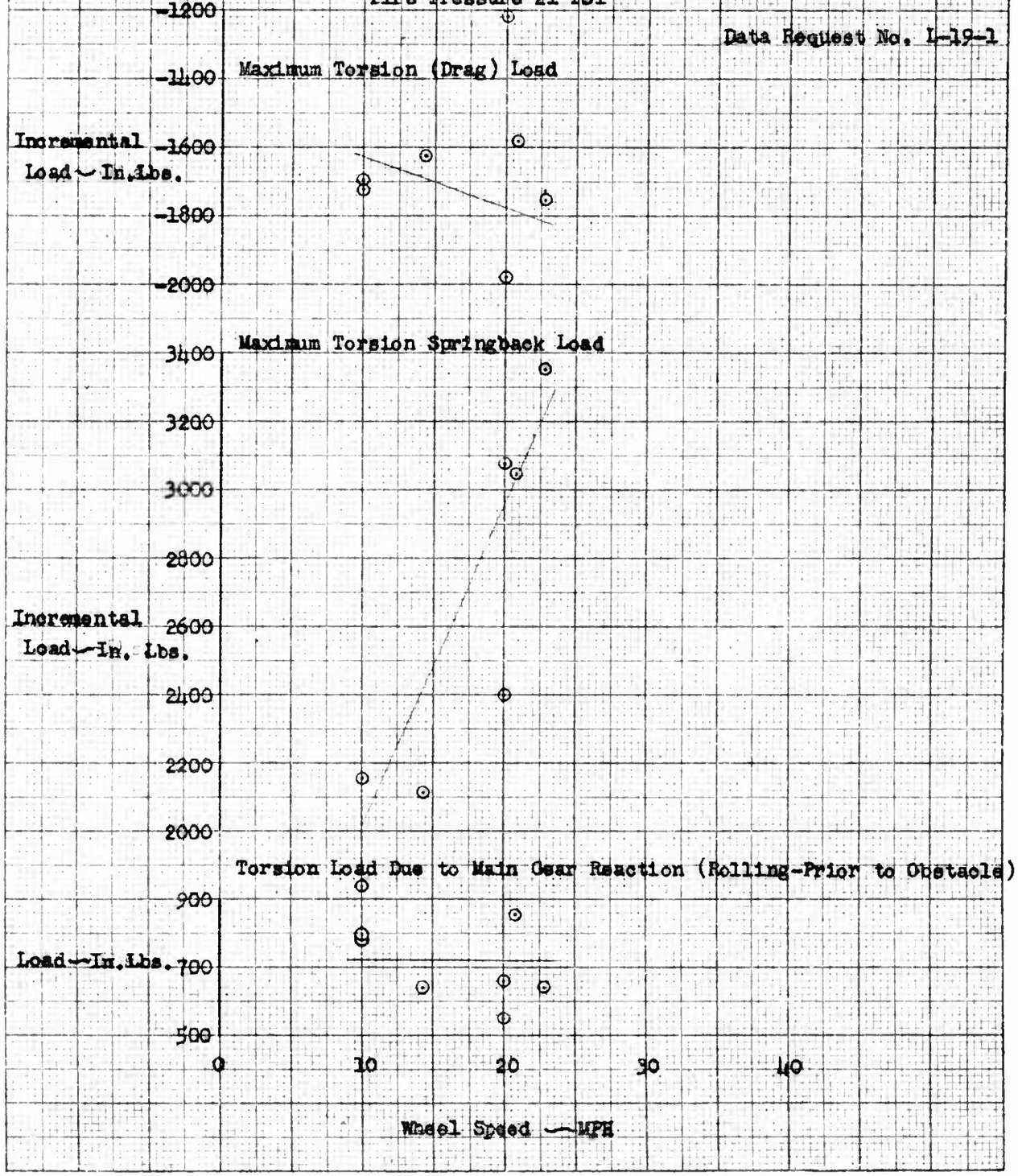

Figure 6

L-19A LANDING TESTS - ORIGINAL TIRE AND LANDING GEAR

Sinking Speed Vs. C.G. Load Factor, L. Gear Initial Drag and Vertical Loads

Flight No. L-19-1 S/N 51-7441 April 22, 1959

Tire Pressure 21 PSI

Data Request L-19-2

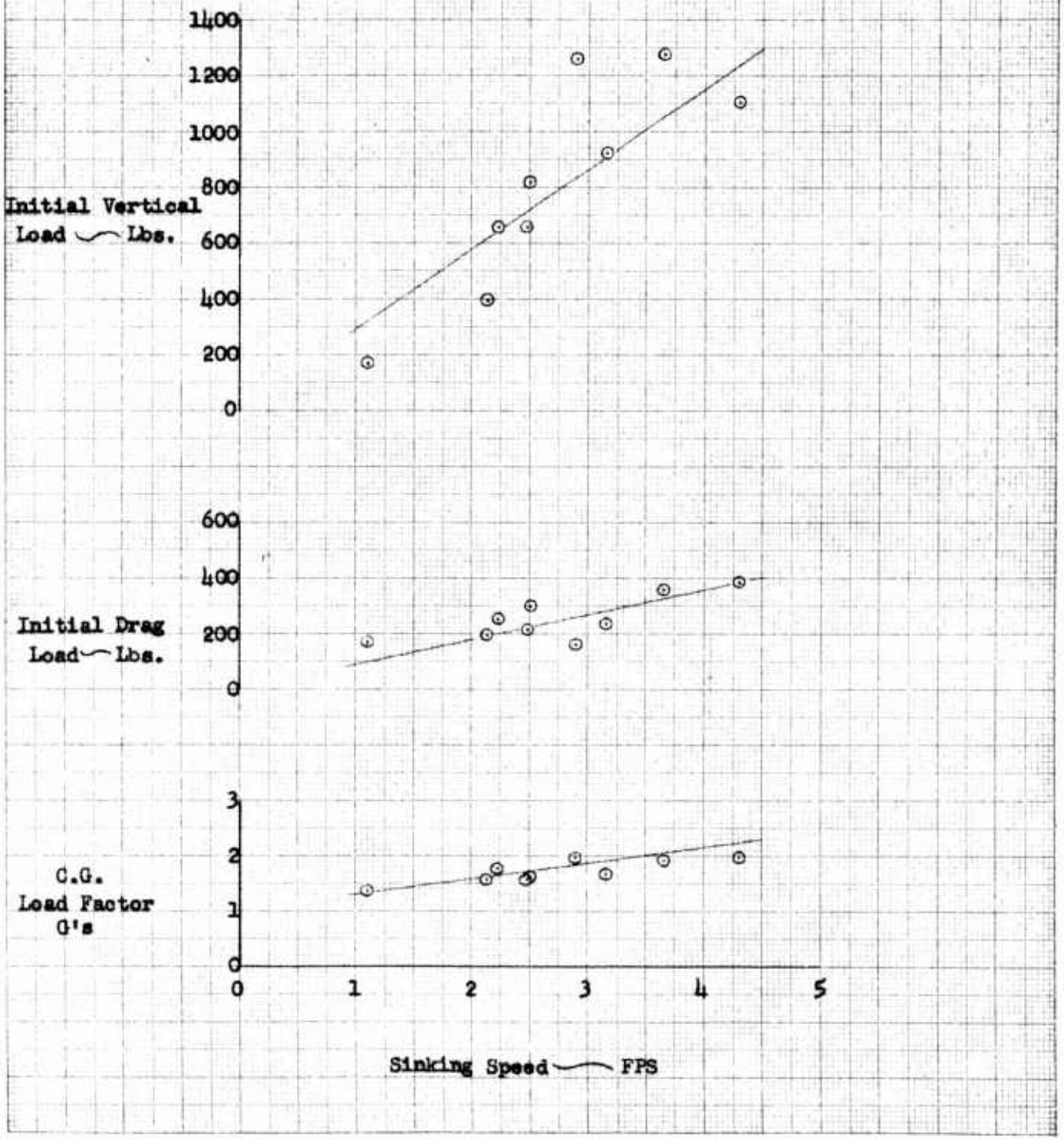

Figure 7

ORIGINAL TIRE AND GEAR LANDING LOAD TIME HISTORY

L-19A Flight No. 19-1 S/N 51-7441 June 22, 1959

Sinking Speed 4.3 fps FAT 57° F Data Request No. L-19-2

Oscillograph Record No. 24301

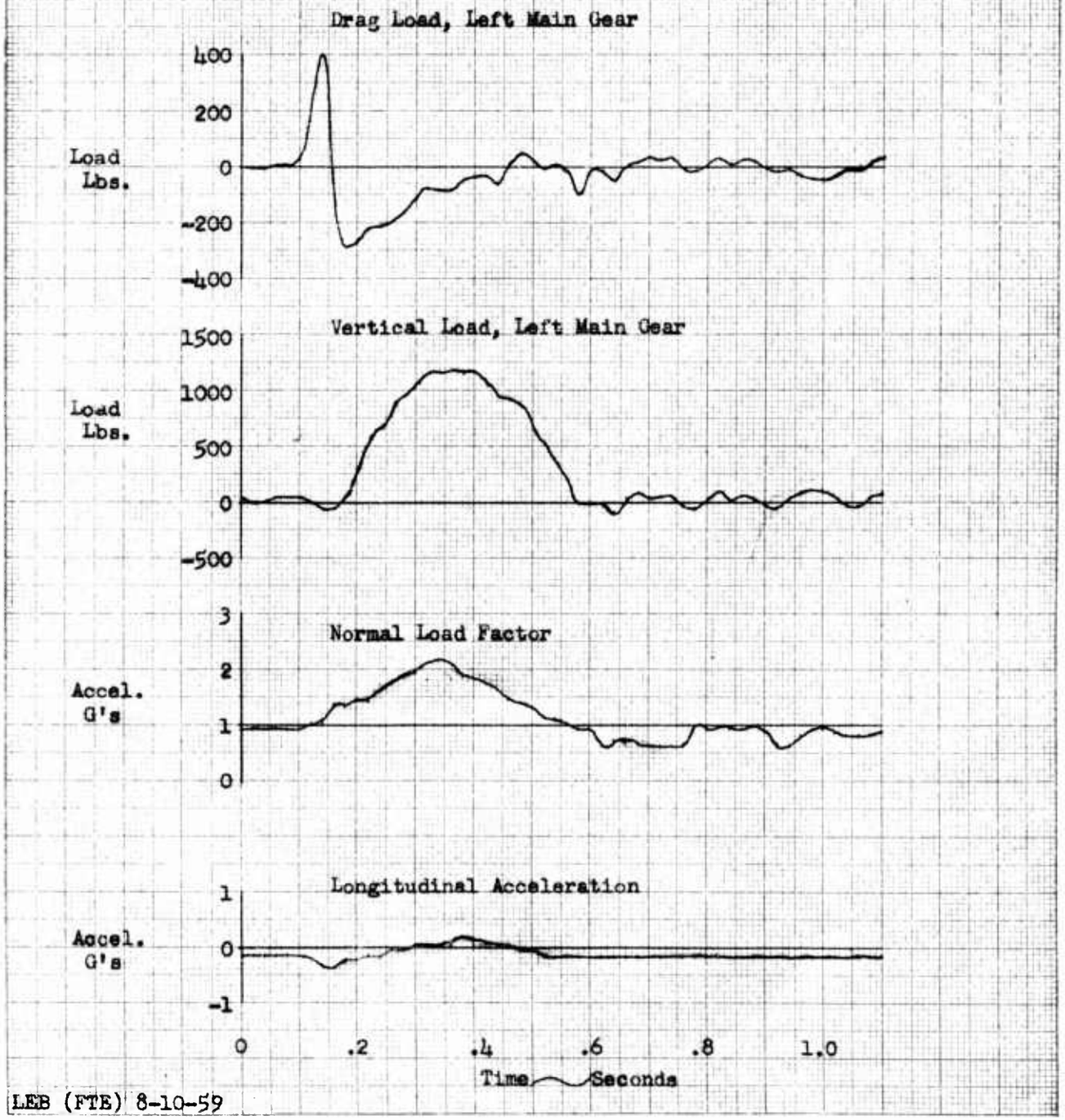

LEB (FTE) 8-10-59

Figure 8

EFFECT OF OBSTACLE HEIGHT, GROUND SPEED AND TIRE PRESSURE ON SPRINGBACK DRAG LOADS

L-19A Ground Tests S/N 51-7441 (M245B Landing Gear)

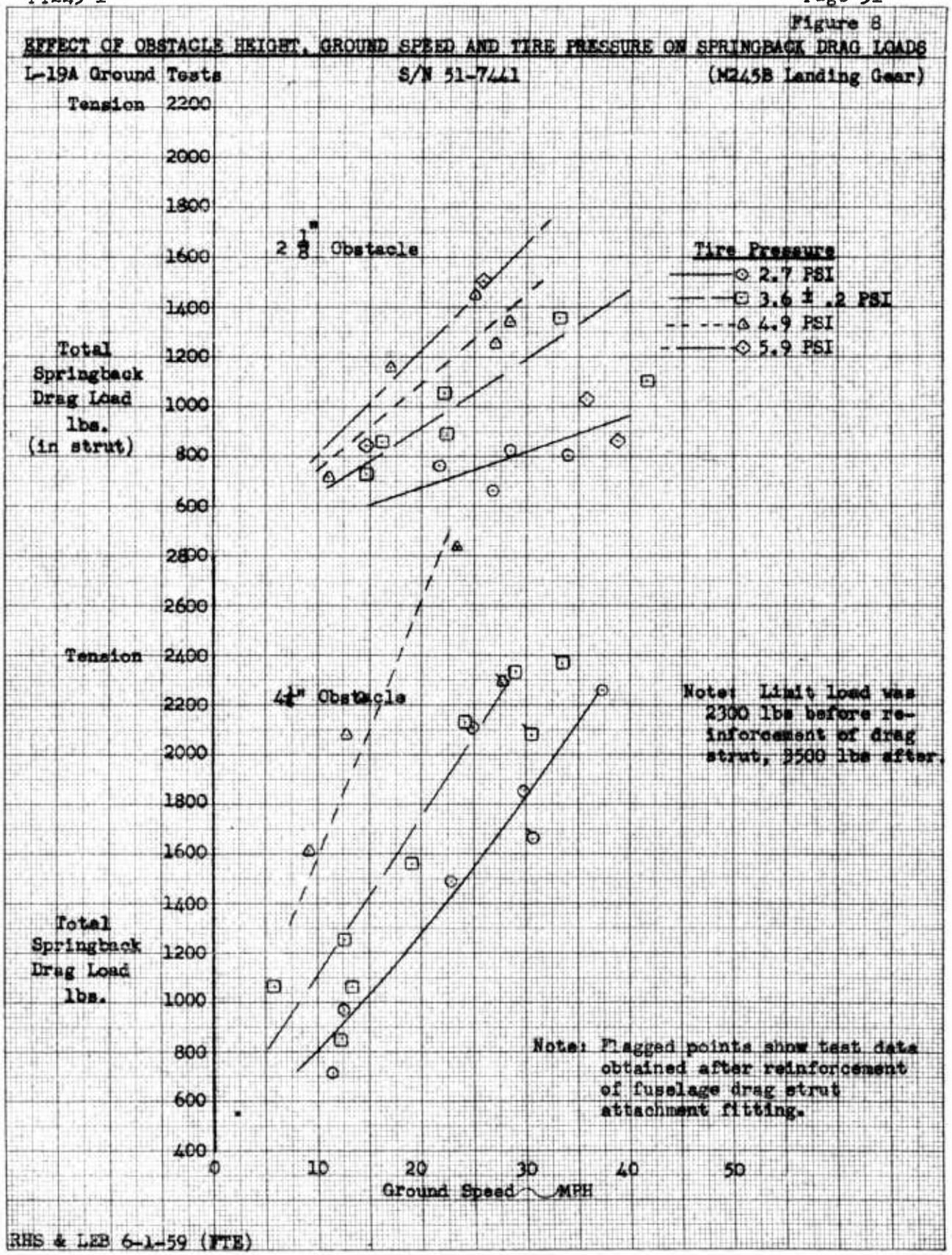

RHS & LEB 6-1-59 (FTE)

Figure 9

EFFECT OF OBSTACLE HEIGHT, GROUND SPEED AND TIRE PRESSURE ON SPRINGBACK DRAG LOADS

L-19A Ground Tests S/N 51-7441 (M245B Landing Gear)

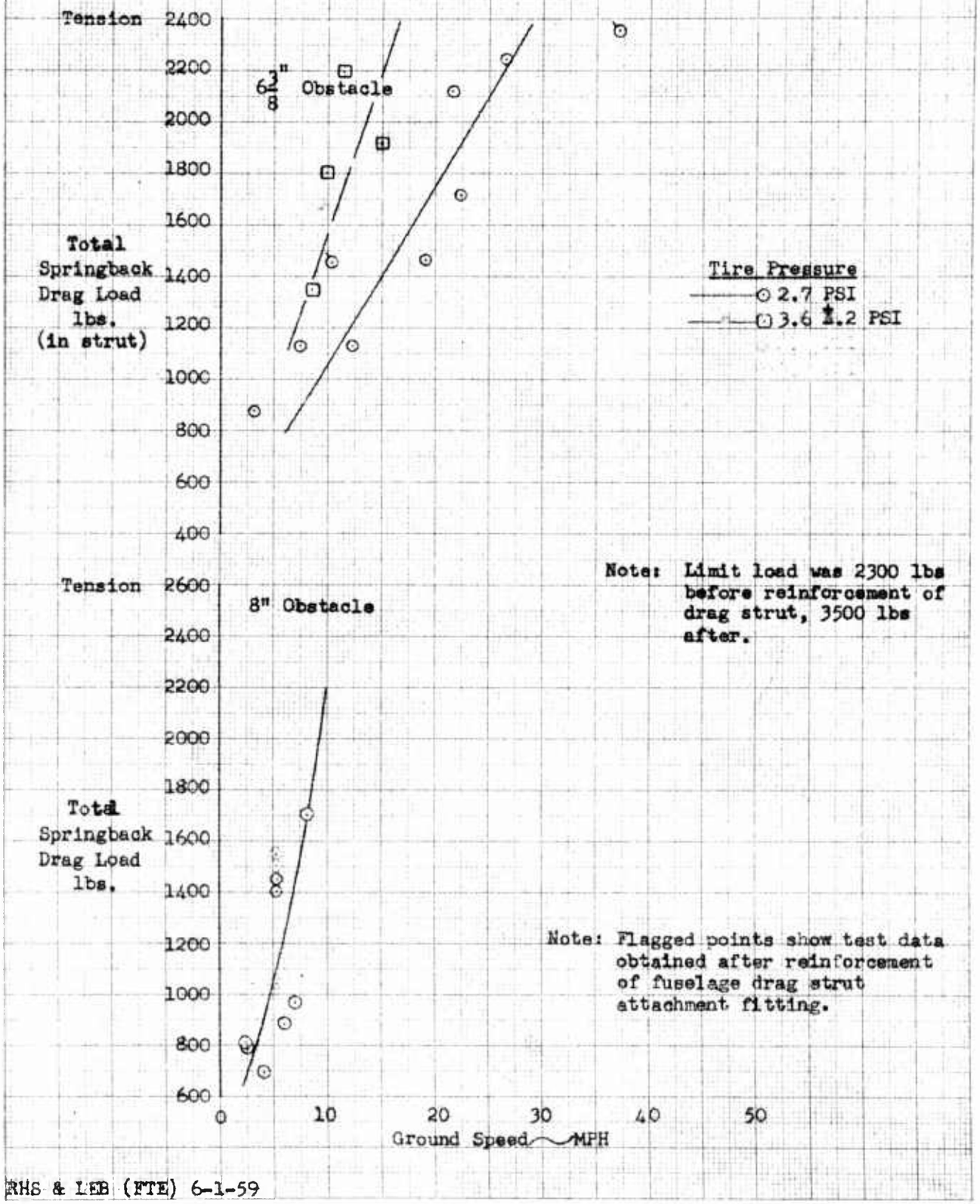

RHS & LEB (FTE) 6-1-59

Figure 10

EFFECT OF GROUND SPEED AND TIRE PRESSURE ON
DRAG STRUT AXIAL LOAD OVER 2½ INCH OBSTACLE

M245B Landing Gear — Data Request No. L-19-5

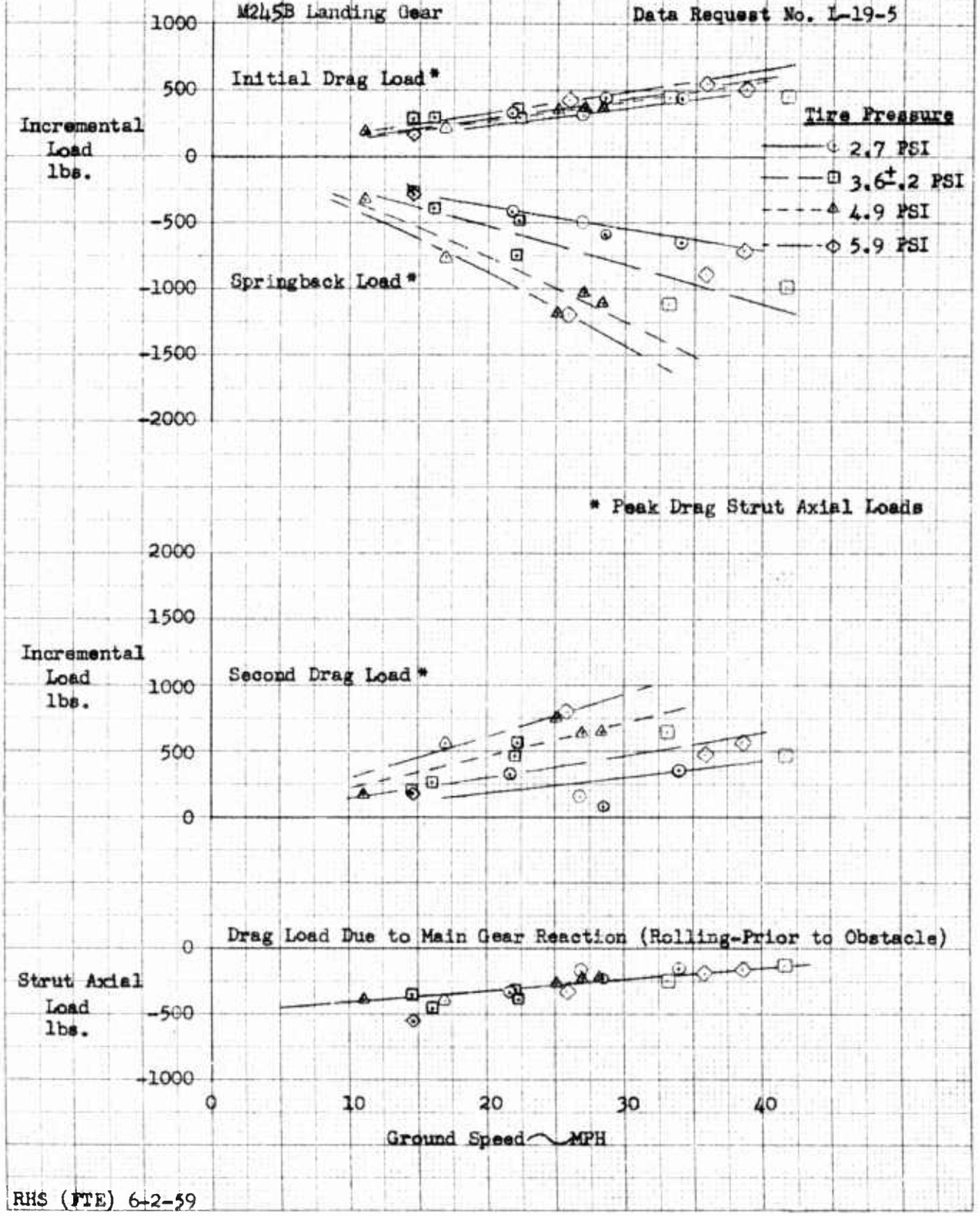

RHS (FTE) 6-2-59

Figure 11

EFFECT OF GROUND SPEED AND TIRE PRESSURE ON DRAG STRUT AXIAL LOAD OVER 4½ INCH OBSTACLE

M245B Landing Gear Data Request No. L-19-5

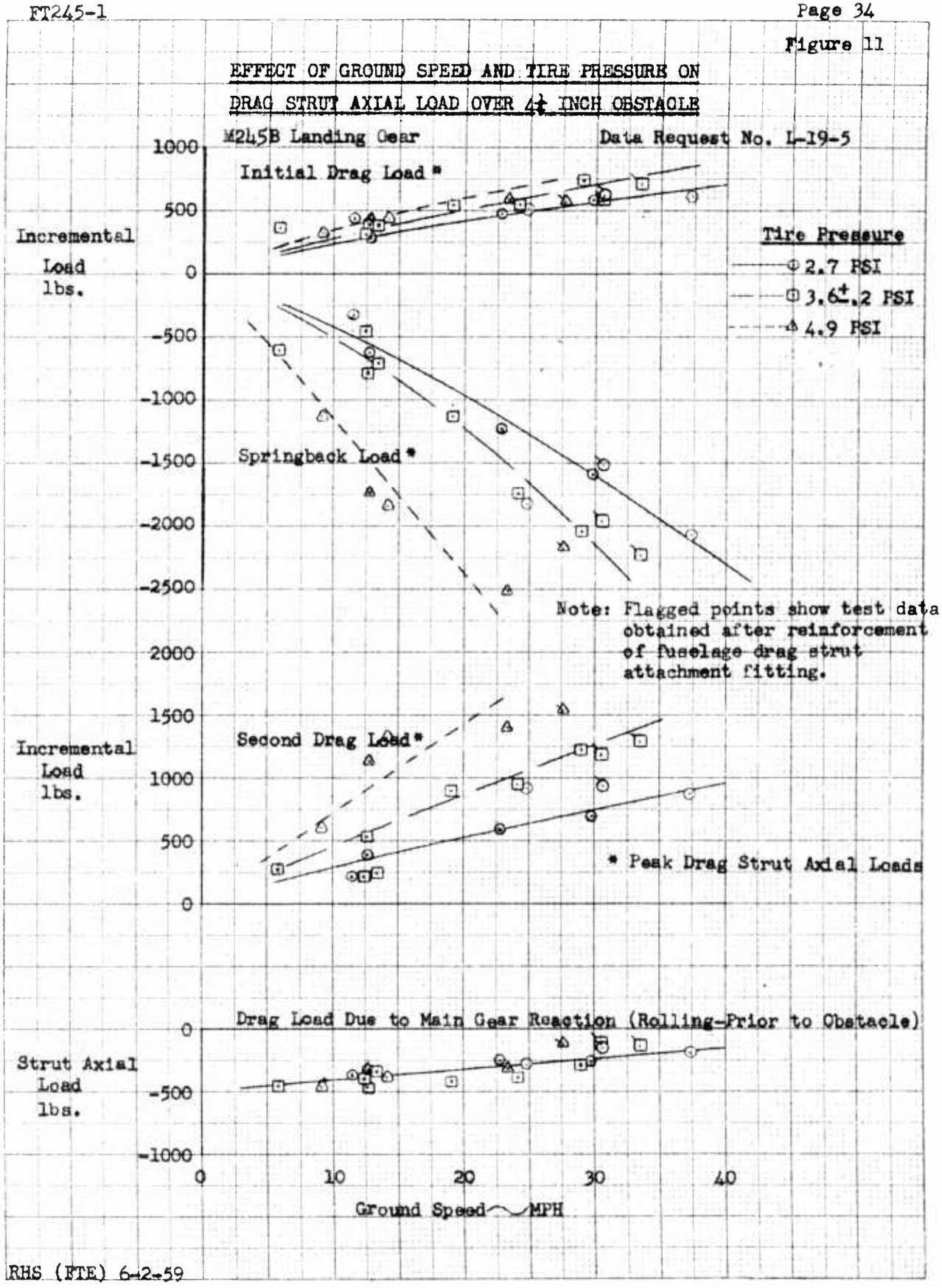

RHS (FTE) 6-12-59

Figure 12

EFFECT OF GROUND SPEED AND TIRE PRESSURE ON
DRAG STRUT AXIAL LOAD OVER 6⅜ INCH OBSTACLE
M245B Landing Gear

Data Request No. L-19-5

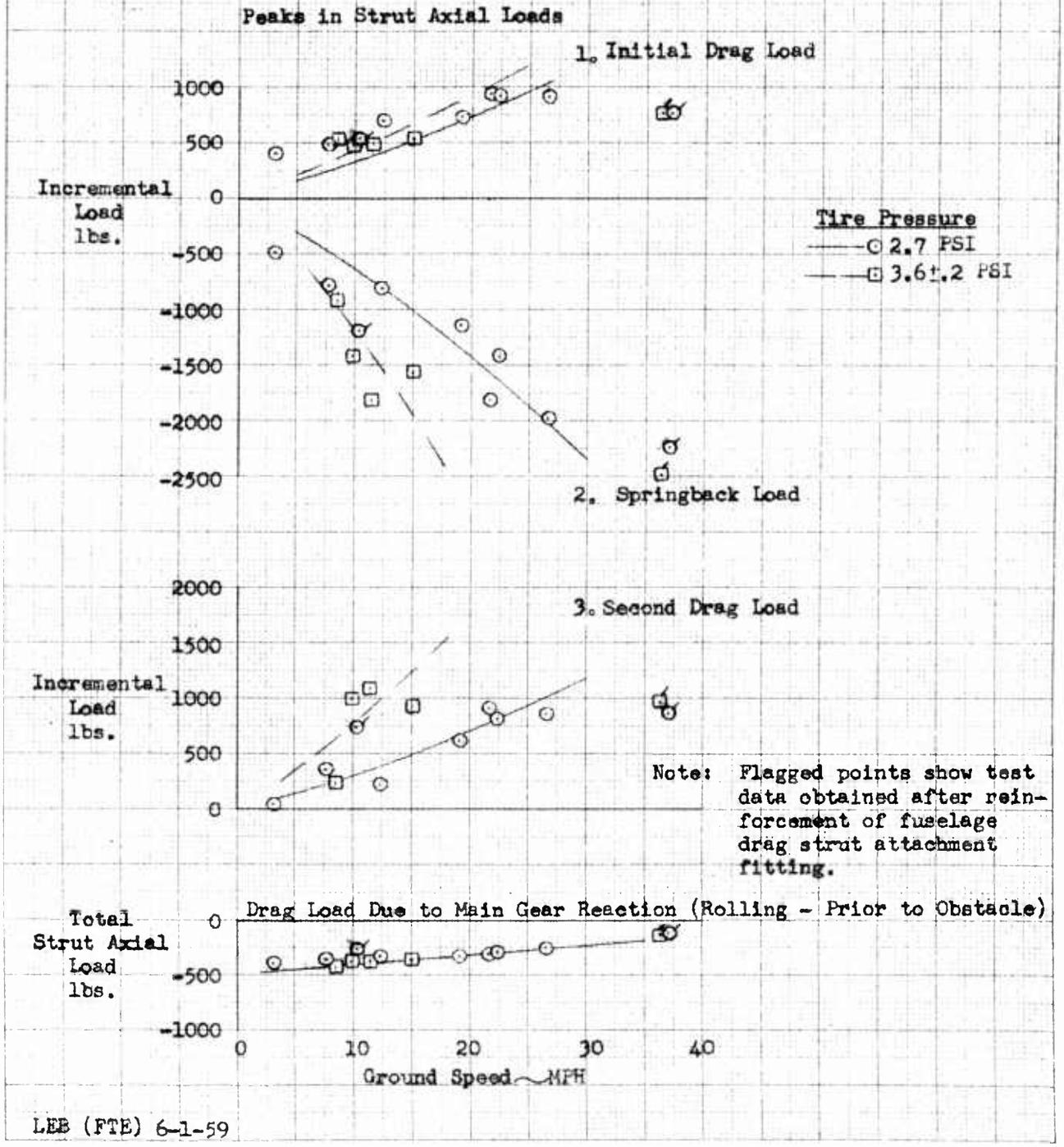

LEB (FTE) 6-1-59

Figure 13

EFFECT OF GROUND SPEED AND TIRE PRESSURE ON
DRAG STRUT AXIAL LOAD OVER 8 INCH OBSTACLE
M245B Landing Gear

Data Request No. L-19-5

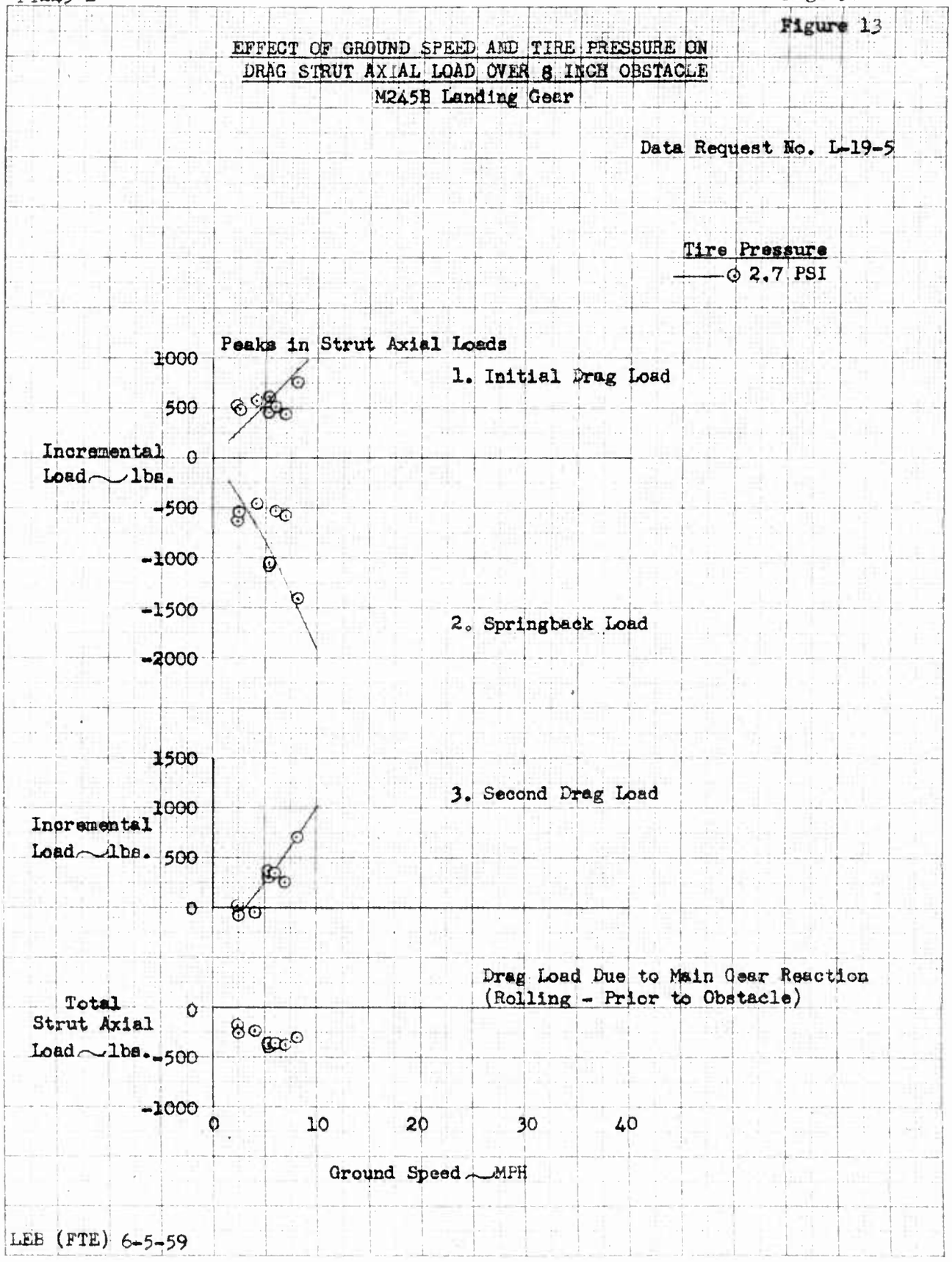

LEB (FTE) 6-5-59

Figure 14

INCREMENTAL DRAG STRUT AXIAL LOAD Vs TIRE PRESSURE
AT VARIOUS GROUND SPEEDS OVER 2½ INCH OBSTACLE
M-245B Landing Gear On L-19A Airplane

Data Request No. L-19-5

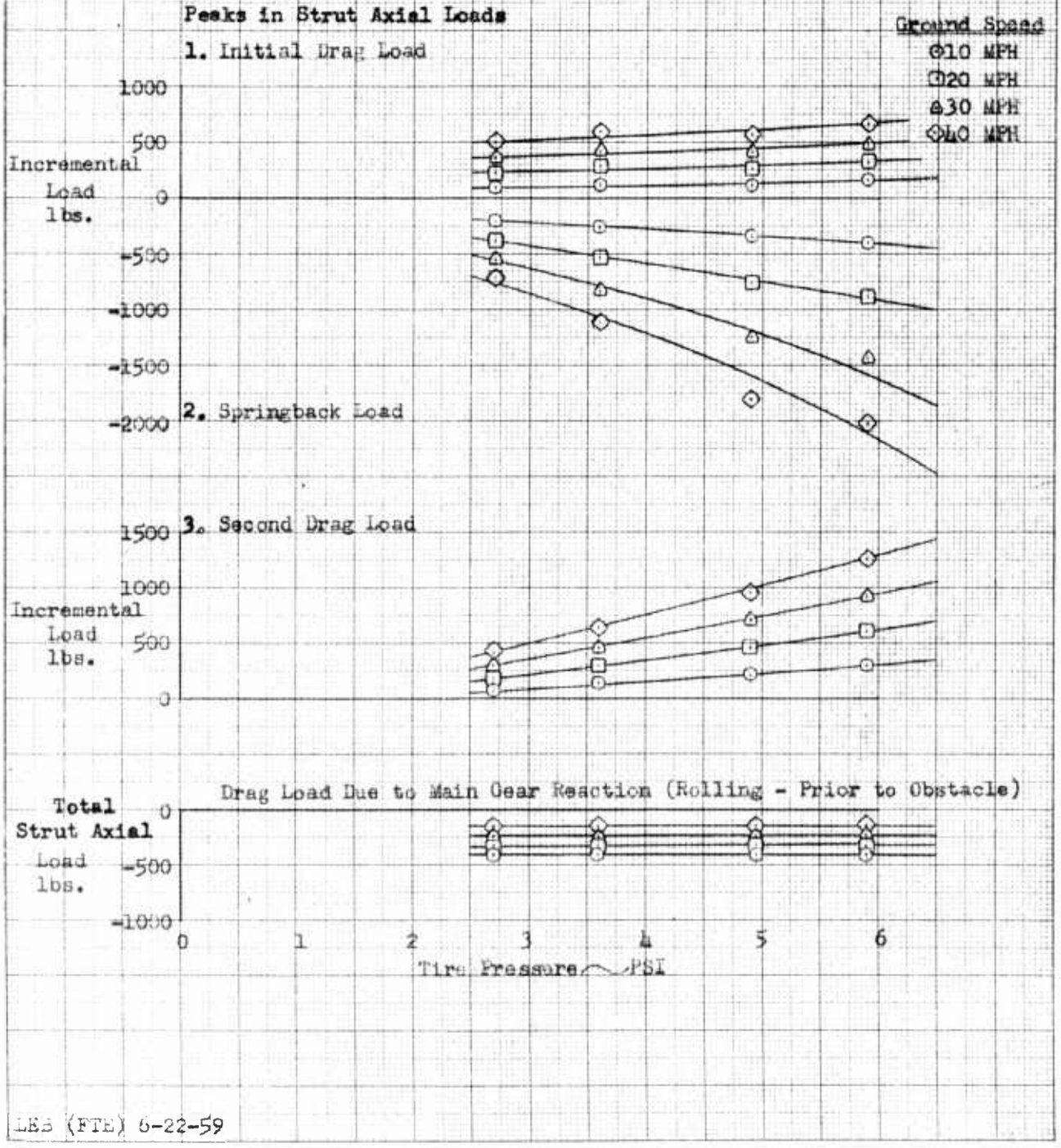

Figure 14

INCREMENTAL DRAG STRUT AXIAL LOAD Vs TIRE PRESSURE
AT VARIOUS GROUND SPEEDS OVER 2½ INCH OBSTACLE
M-245B Landing Gear On L-19A Airplane

Data Request No. L-19-5

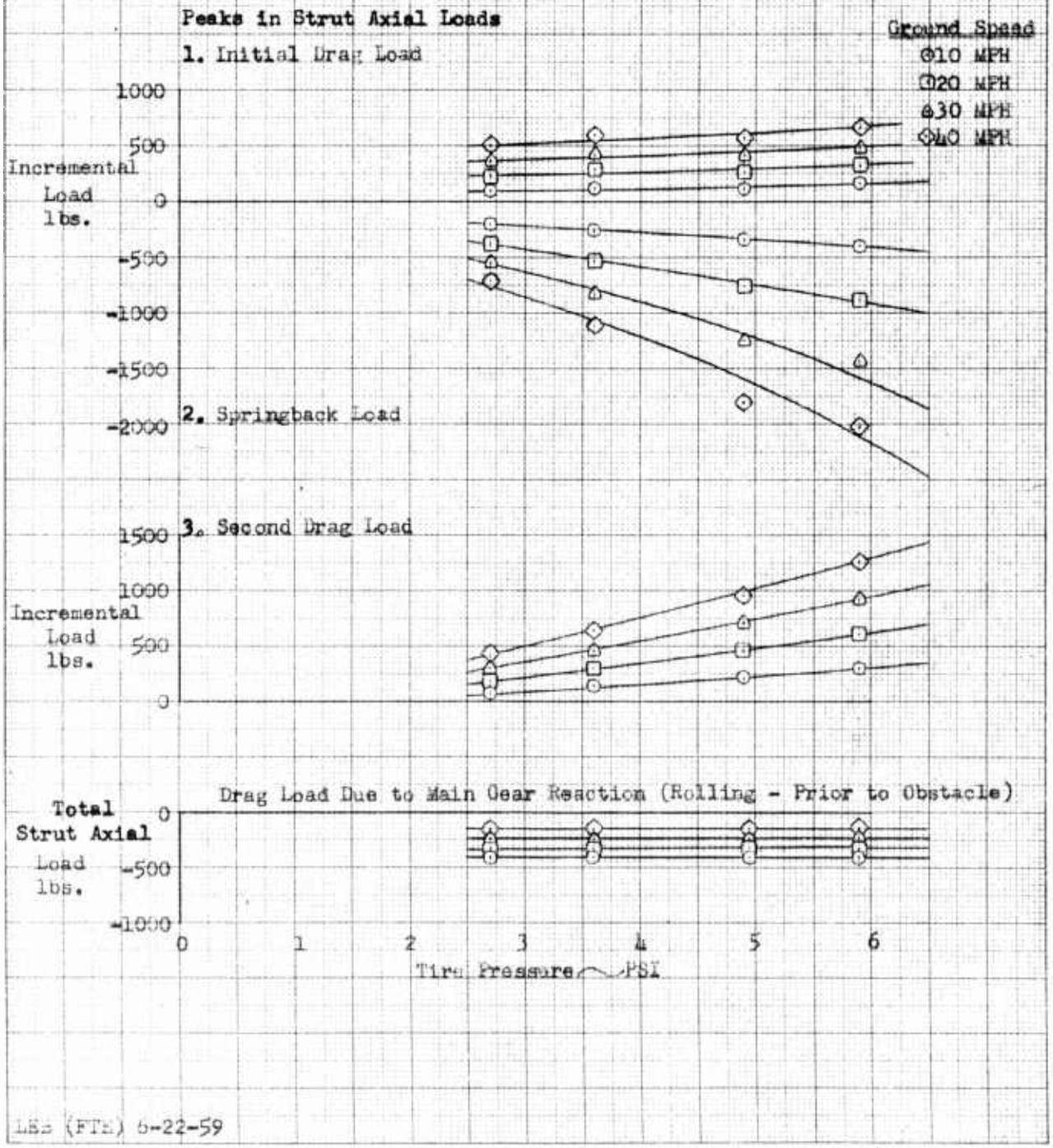

LBS (FTS) 6-22-59

Figure 15

INCREMENTAL DRAG STRUT AXIAL LOAD Vs TIRE PRESSURE
AT VARIOUS GROUND SPEEDS OVER 4½ INCH OBSTACLE
M-245B Landing Gear On L-19A Airplane

Data Request No. L-19-5

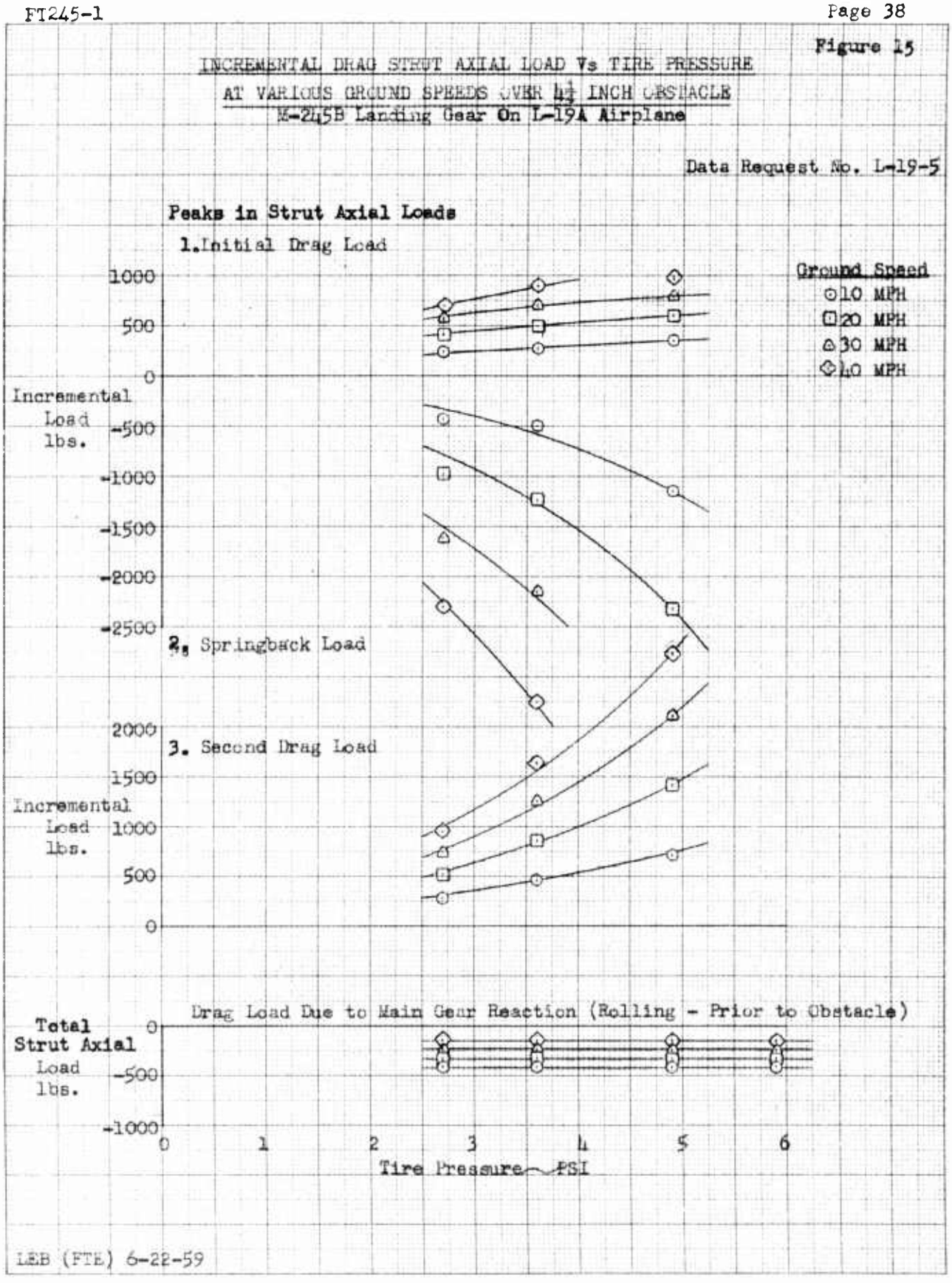

LEB (FTE) 6-22-59

Figure 16

INCREMENTAL DRAG STRUT AXIAL LOAD Vs TIRE PRESSURE
AT VARIOUS GROUND SPEEDS OVER 6⅜ INCH OBSTACLE
M-245B Landing Gear On L-19A Airplane

Data Request No. L-19-5

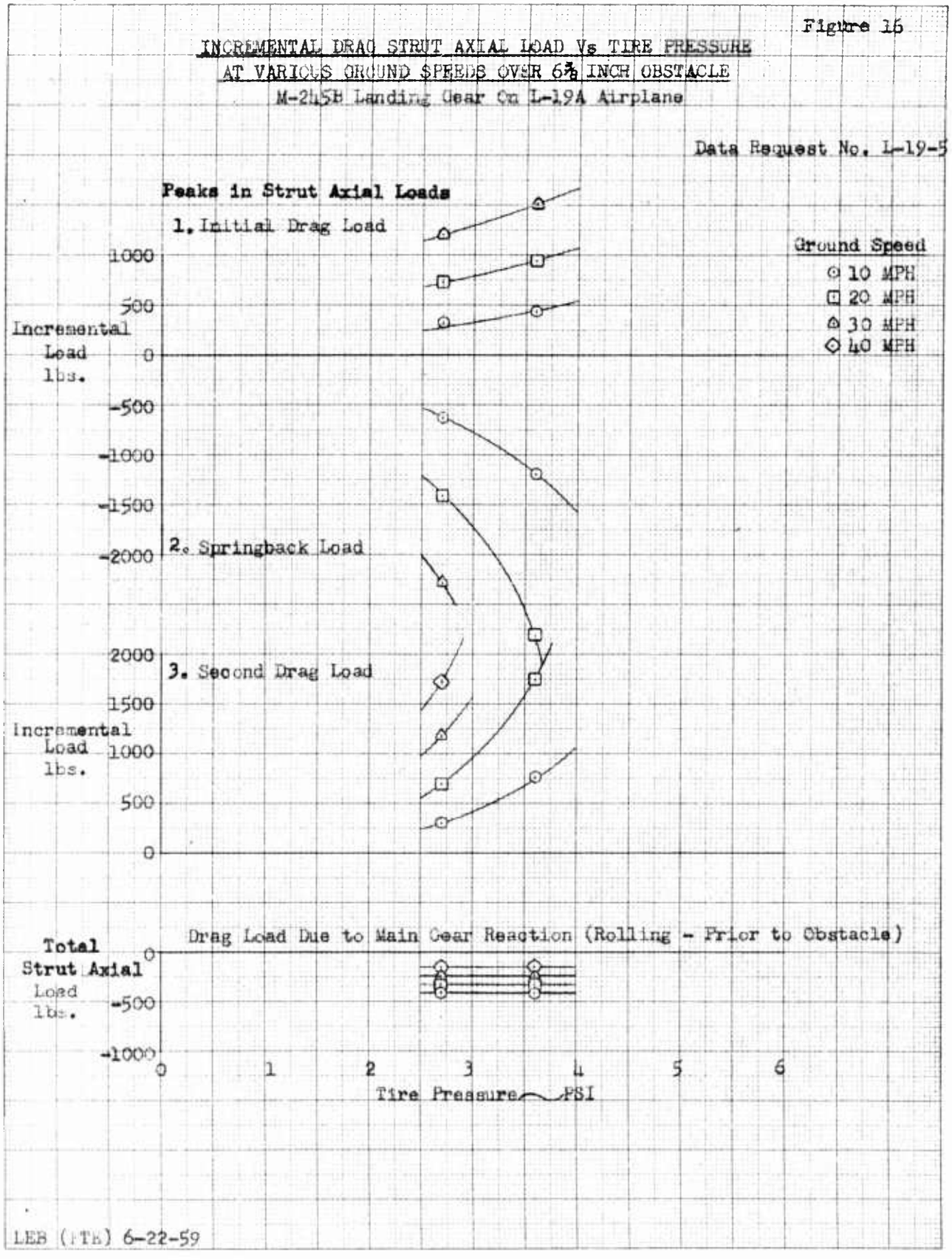

LEB (FTE) 6-22-59

Figure 17

EFFECT OF GROUND SPEED AND TIRE PRESSURE ON
VERTICAL LINK AXIAL LOAD OVER @ $\frac{1}{8}$ INCH OBSTACLE

M-245B Landing Gear Data Request No. L-19-5

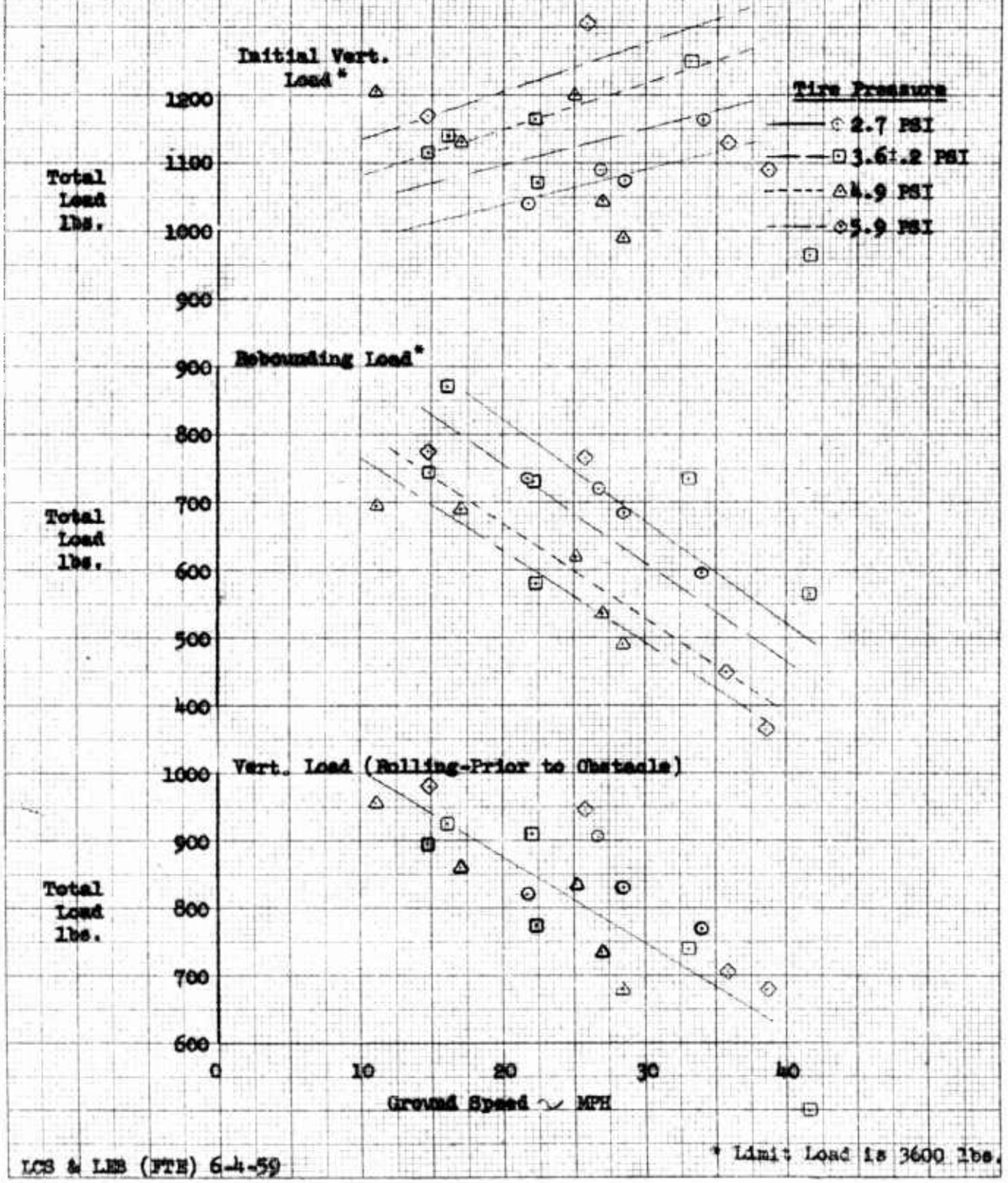

LCS & LEB (FTE) 6-4-59

* Limit Load is 3600 lbs.

Figure 18

EFFECT OF GROUND SPEED AND TIRE PRESSURE ON
VERTICAL LINK AXIAL LOAD OVER 4½ INCH OBSTACLE
M245B Landing Gear

Data Request No. L-19-5

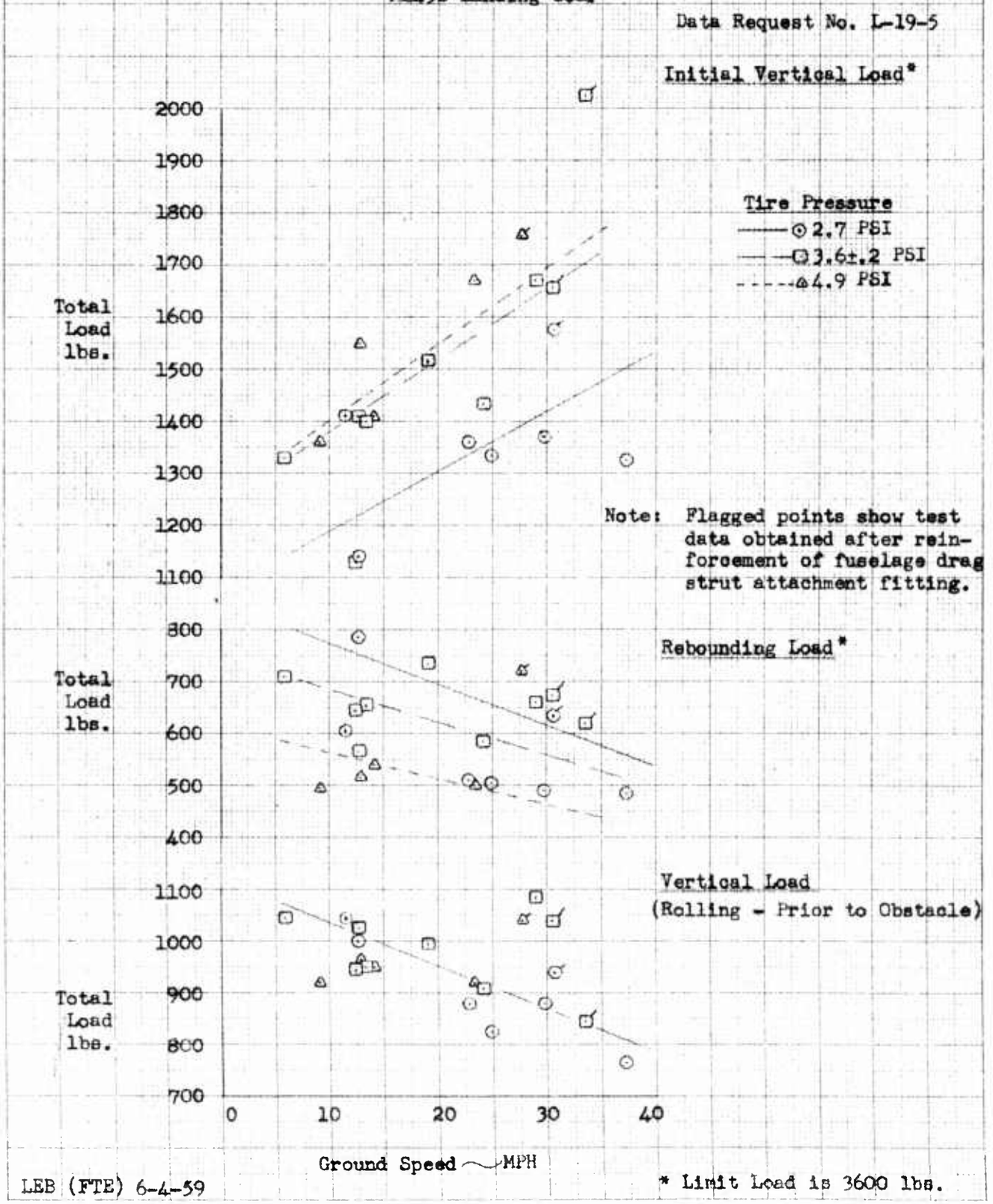

LEB (FTE) 6-4-59

* Limit Load is 3600 lbs.

Figure 19

EFFECT OF GROUND SPEED AND TIRE PRESSURE ON VERTICAL LINK AXIAL LOAD OVER 6 1/8 INCH OBSTACLE

M-245B Landing Gear Data Request No. L-19-5

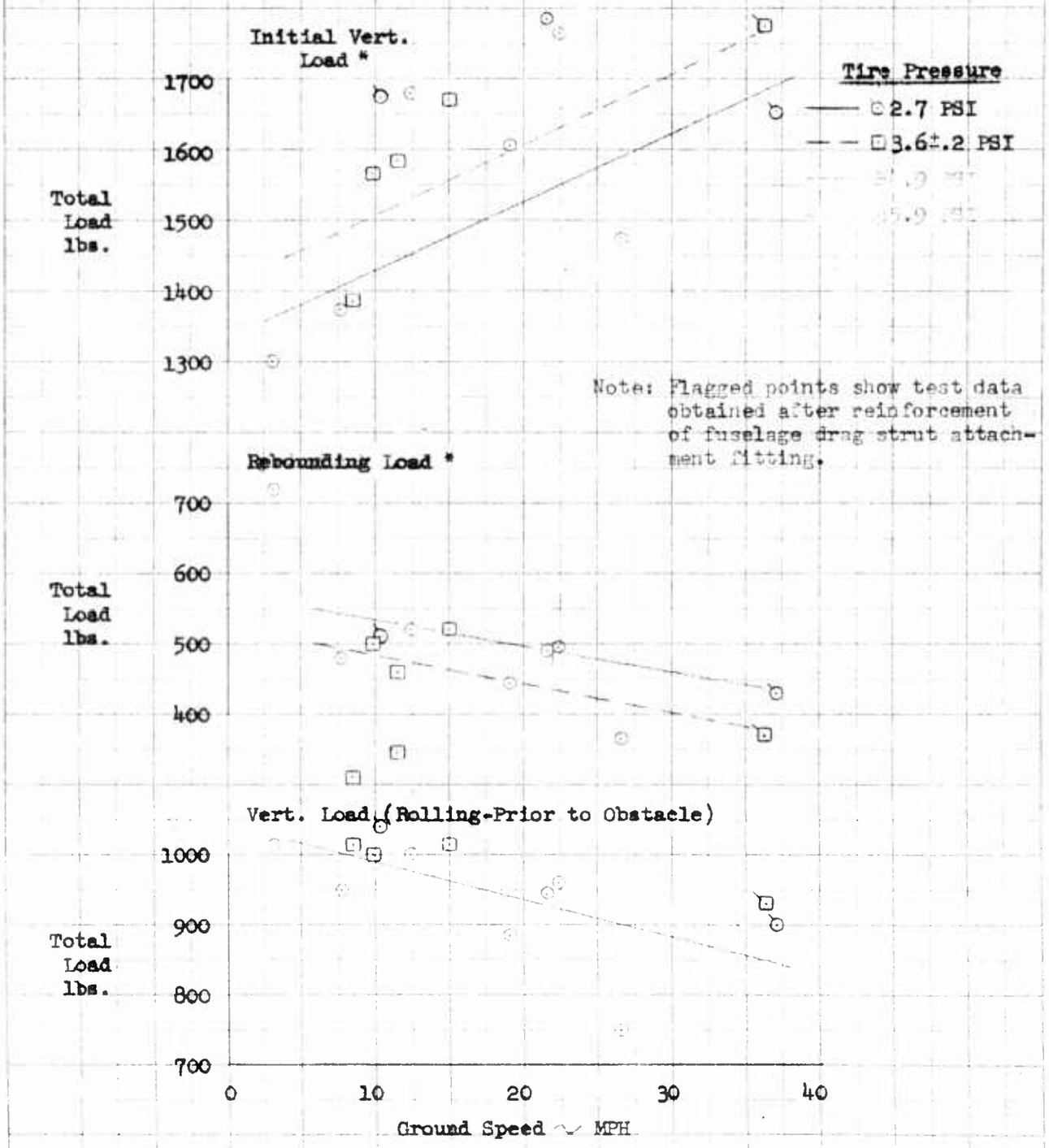

* Limit Load is 3600 lbs.

LCS & LEE (FTE) 6-4-59

Figure 20

EFFECT OF GROUND SPEED AND TIRE PRESSURE ON
VERTICAL LINK AXIAL LOAD OVER 8 INCH OBSTACLE
M245B Landing Gear

Data Request No. L-19-5

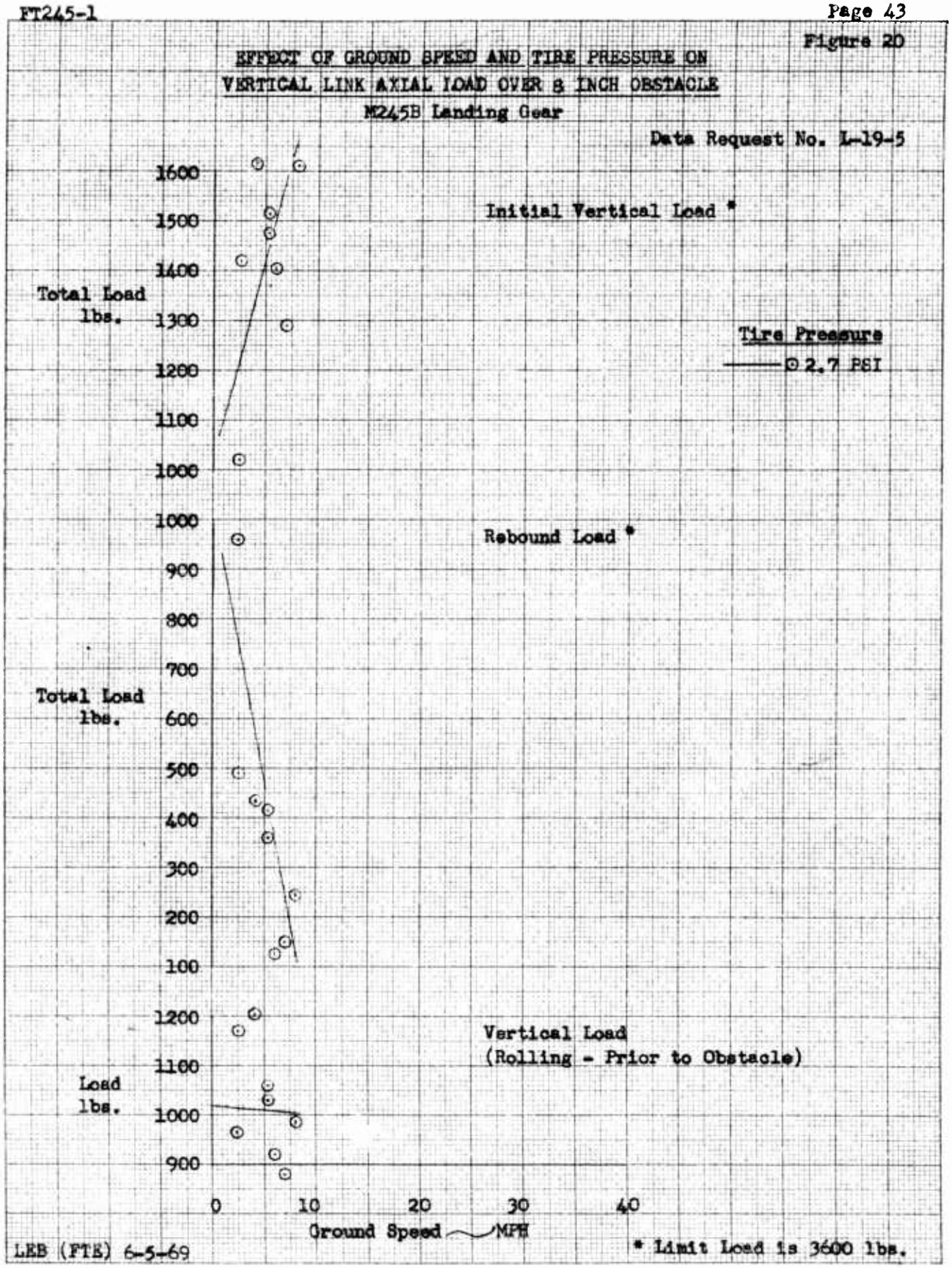

LEB (FTE) 6-5-69

* Limit Load is 3600 lbs.

Figure 21

EFFECT OF GROUND SPEED AND TIRE PRESSURE ON AIRCRAFT ACCELERATIONS OVER 2½ INCH OBSTACLE

M245B Landing Gear

Data Request No. L-19-5

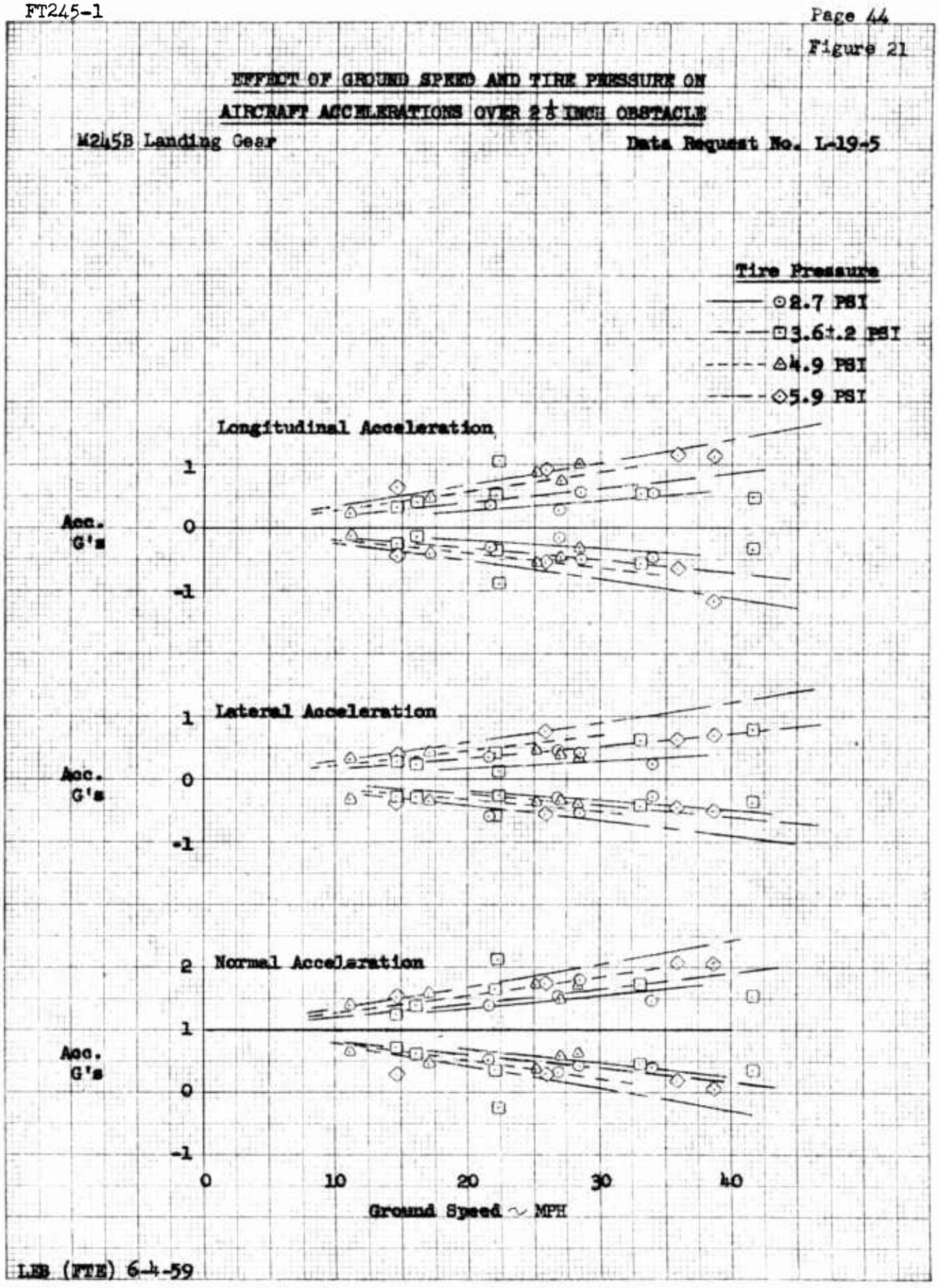

LEB (FTE) 6-4-59

Figure 22

EFFECT OF GROUND SPEED AND TIRE PRESSURE ON AIRCRAFT ACCELERATIONS OVER 4" TEETH OBSTACLE

M24SB Landing Gear

Data Request No. L-19-5

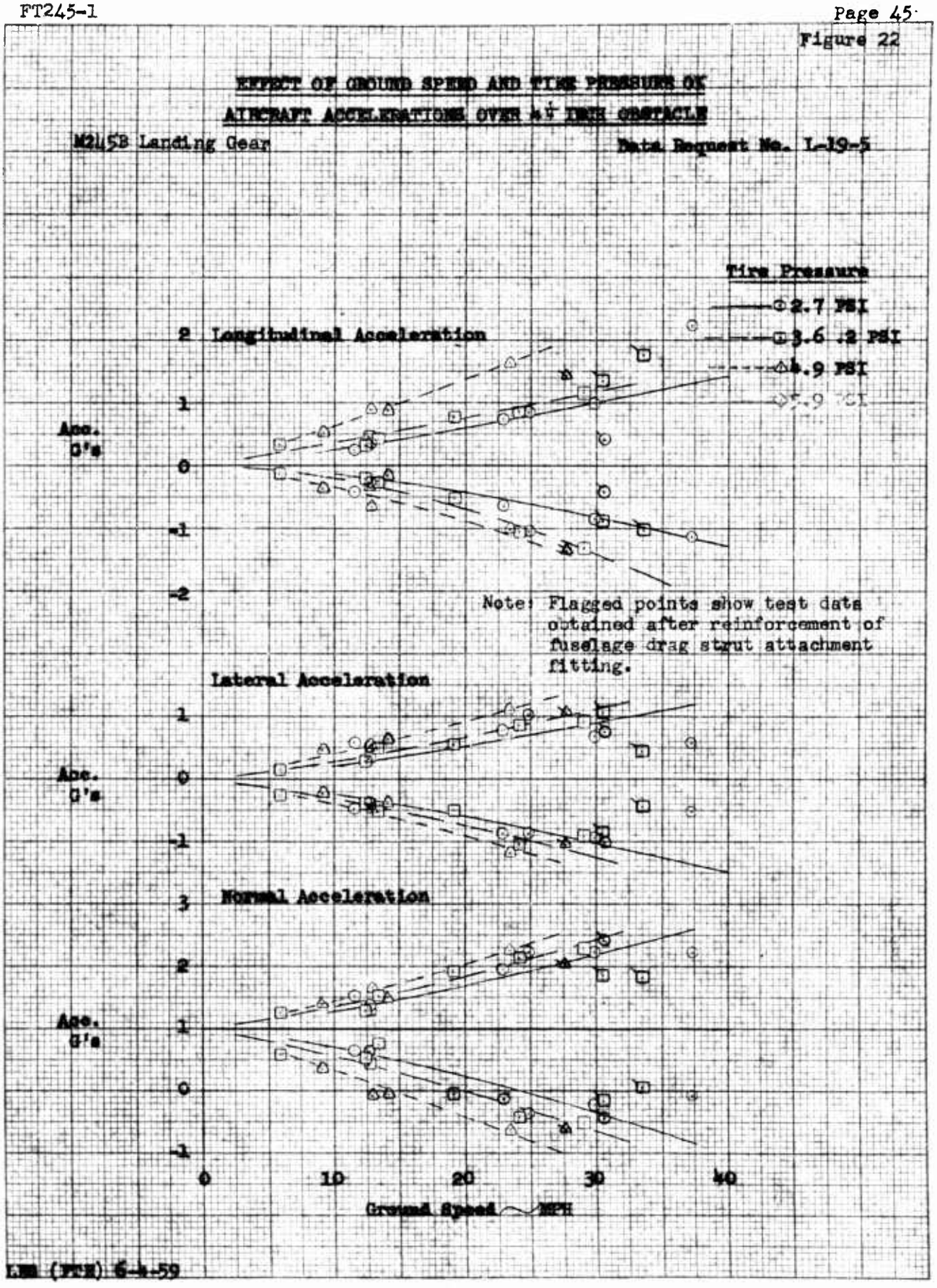

LMM (FTR) 6-4-59

Figure 23

EFFECT OF GROUND SPEED AND TIRE PRESSURE ON AIRCRAFT ACCELERATIONS OVER 6½ INCH OBSTACLE

M245B Landing Gear Data Request No. L-19-5

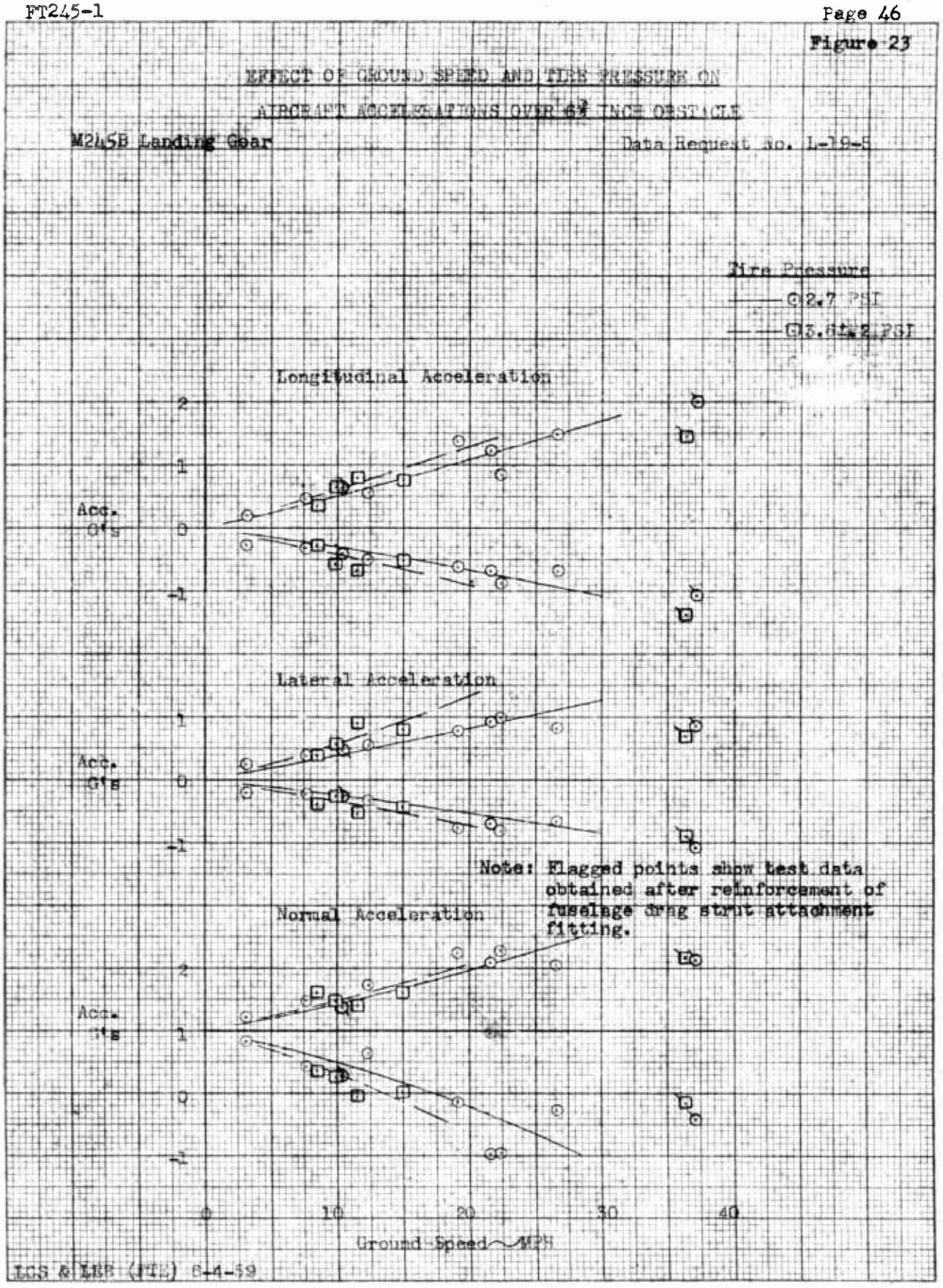

Note: Flagged points show test data obtained after reinforcement of fuselage drag strut attachment fitting.

LCS & LBP (FTE) 6-4-59

Figure 24

EFFECT OF GROUND SPEED AND TIRE PRESSURE ON AIRCRAFT ACCELERATIONS OVER 8 INCH OBSTACLE

M245B Landing Gear Data Request No. L-19-5

Tire Pressure
——⊙ 2.7 PSI

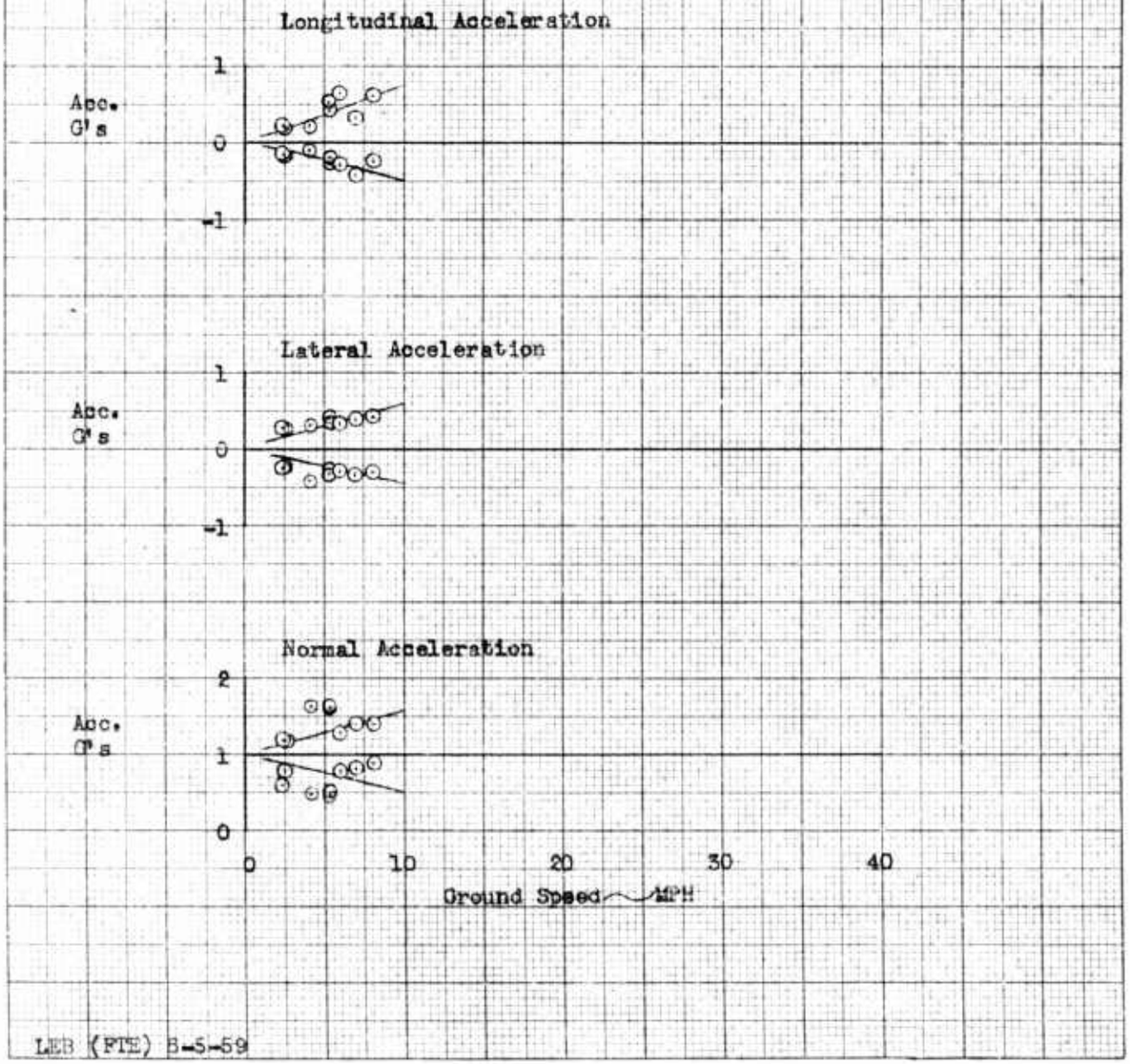

LEB (FTE) 8-5-59

Figure 25

TIME HISTORY OF TYPICAL TAXI OVER OBSTACLE

M245B Landing Gear

Obstacle Height 2 1/8" Tire Pressure 2.7 PSI Wheel Speed 34.0 MPH

Record No. 24597 May 27, 1959

Data Req. No. L19-5

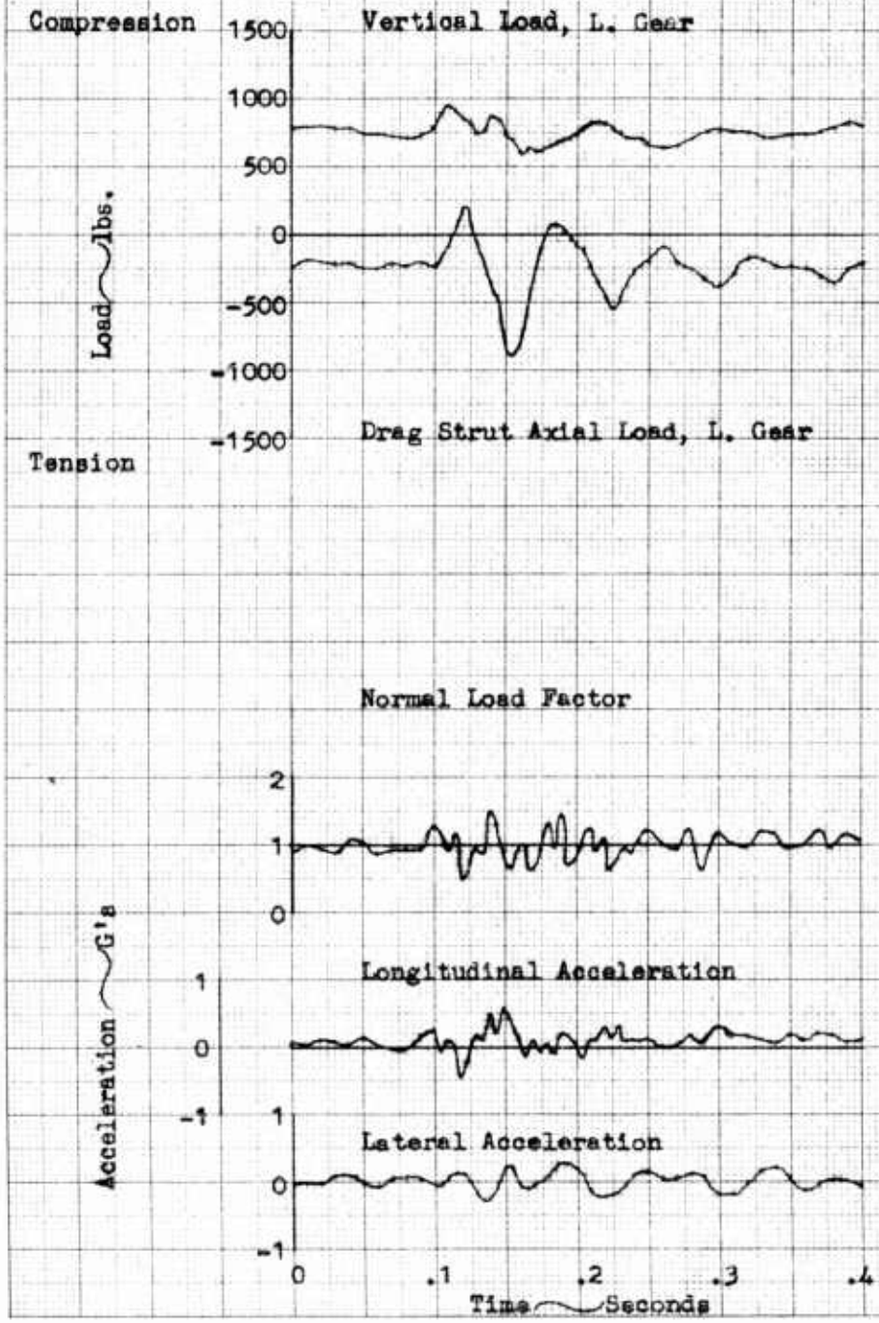

Figure 26

TIME HISTORY OF TYPICAL TAXI OVER OBSTACLE

M245B Landing Gear

Obstacle Height 2 1/8" Tire Pressure 3.6±.2 PSI Wheel Speed 33.1 MPH

Record No. 24722

June 5,1959

Data Req. No. L19-5

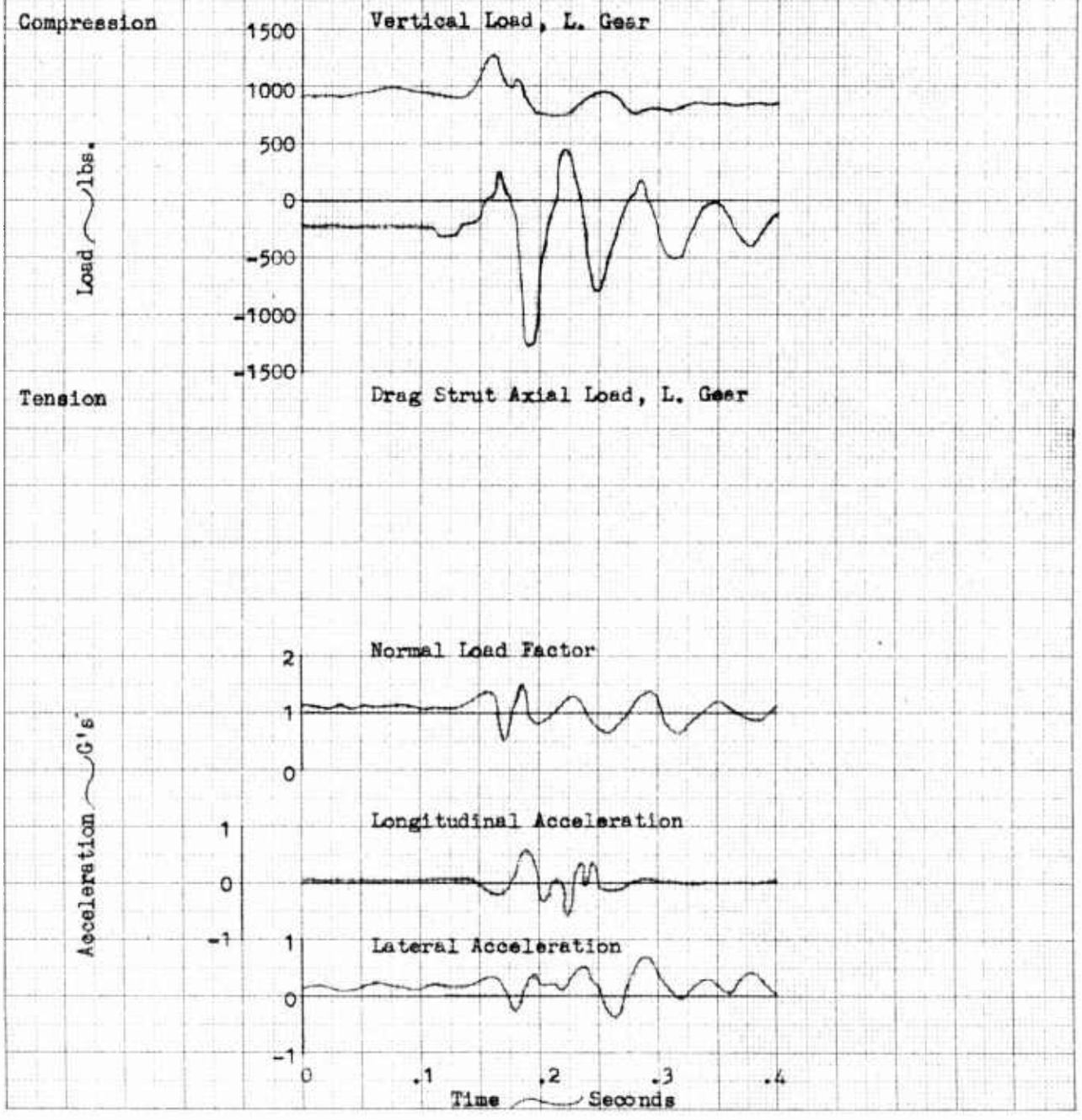

Figure 27

TIME HISTORY OF TYPICAL TAXI OVER OBSTACLE

M245B Landing Gear

Obstacle Height 2 1/8" Tire Pressure 4.9 PSI Wheel Speed 25.1 MPH

Record No. 24543 May 25, 1959

Data Req. No. L19-5

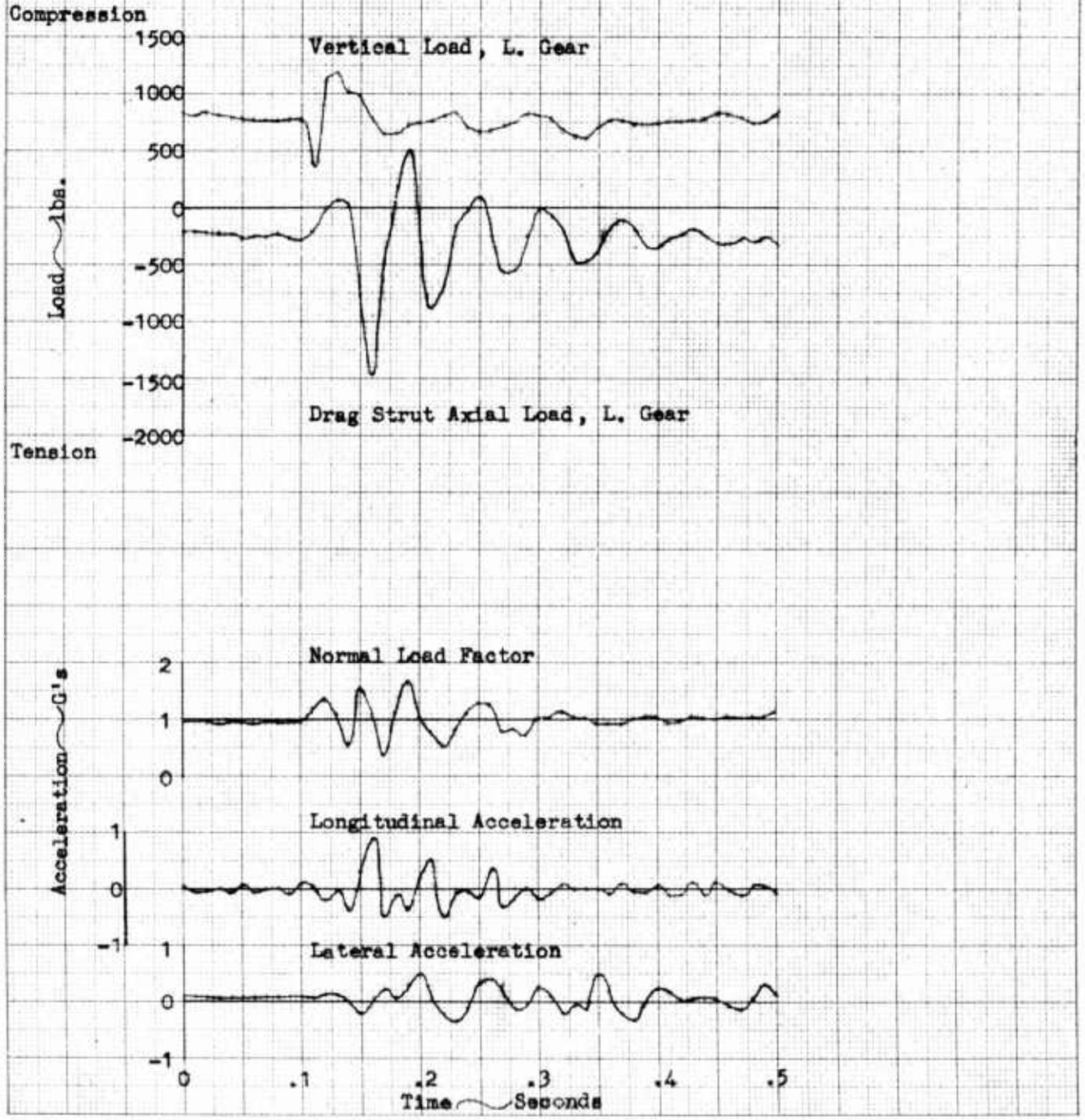

Figure 28

TIME HISTORY OF TYPICAL TAXI OVER OBSTACLE

M245B Landing Gear

Obstacle Height 2 1/8" Tire Pressure 5.9 PSI Wheel Speed 25.9 MPH

Record No. 24726 June 5, 1959

Data Req. No. L19-5

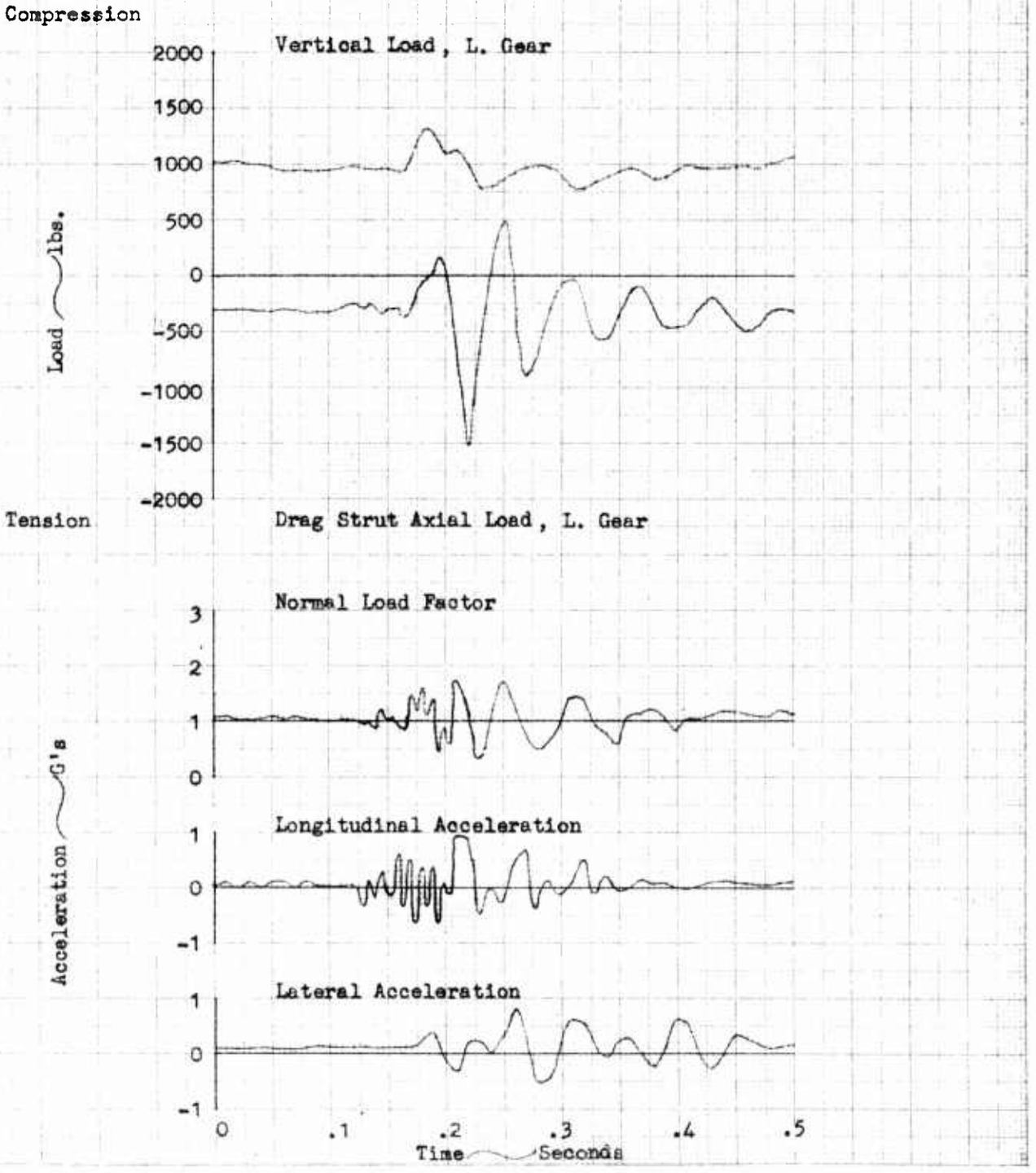

Figure 29

TIME HISTORY OF TYPICAL TAXI OVER OBSTACLE

M245B Landing Gear

Obstacle Height 4½" Tire Pressure 2.7 PSI Wheel Speed 37.3 MPH

Record No. 24733 June 5, 1959

Data Req. No. L19-5

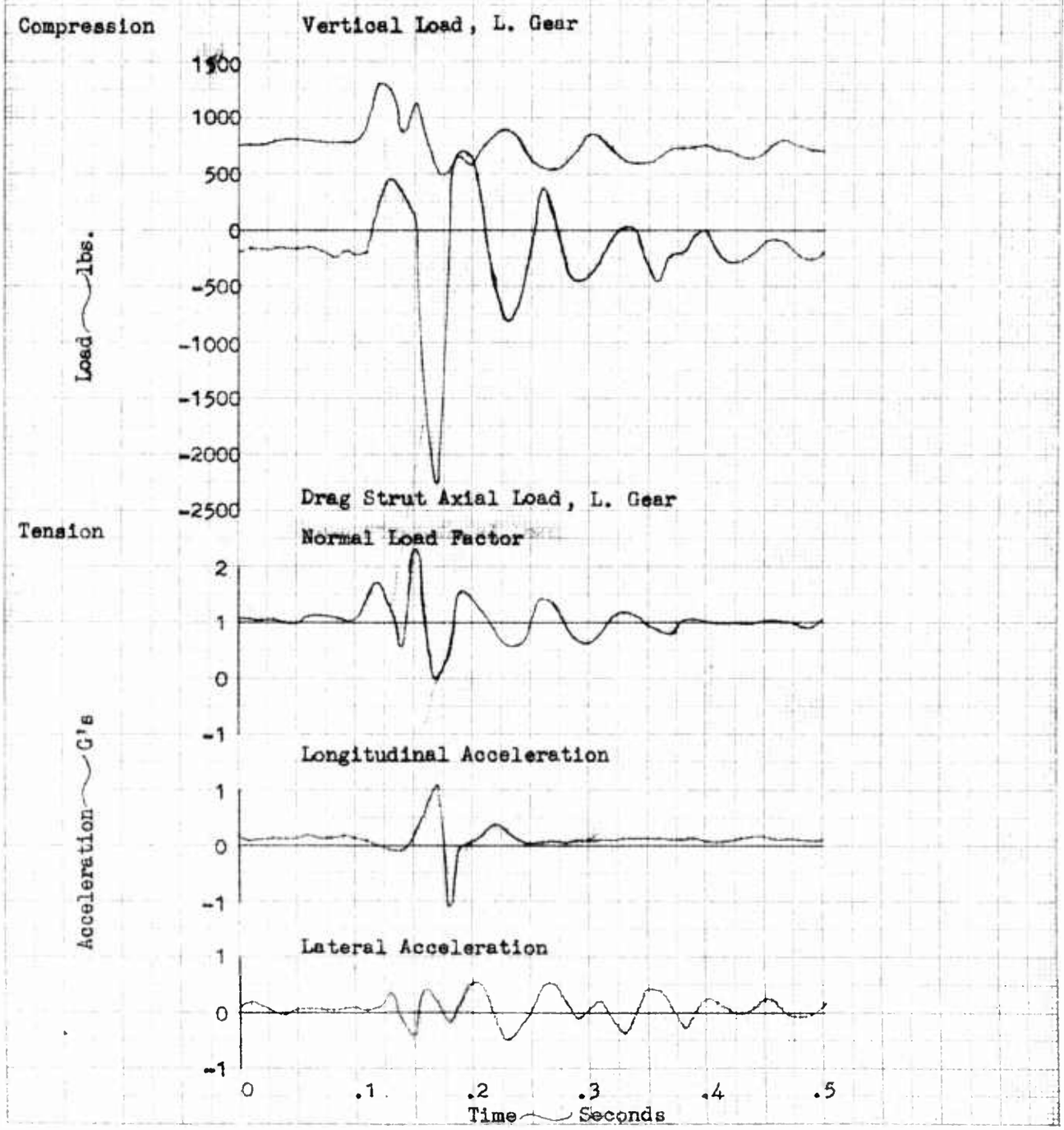

Figure 30

TIME HISTORY OF TYPICAL TAXI OVER OBSTACLE

M245B Landing Gear

Obstacle Height 4½" Tire Pressure 3.6±.2 PSI Wheel Speed 29.0 MPH

Record No. 24540

May 25, 1959

Data Req. No. L19-5

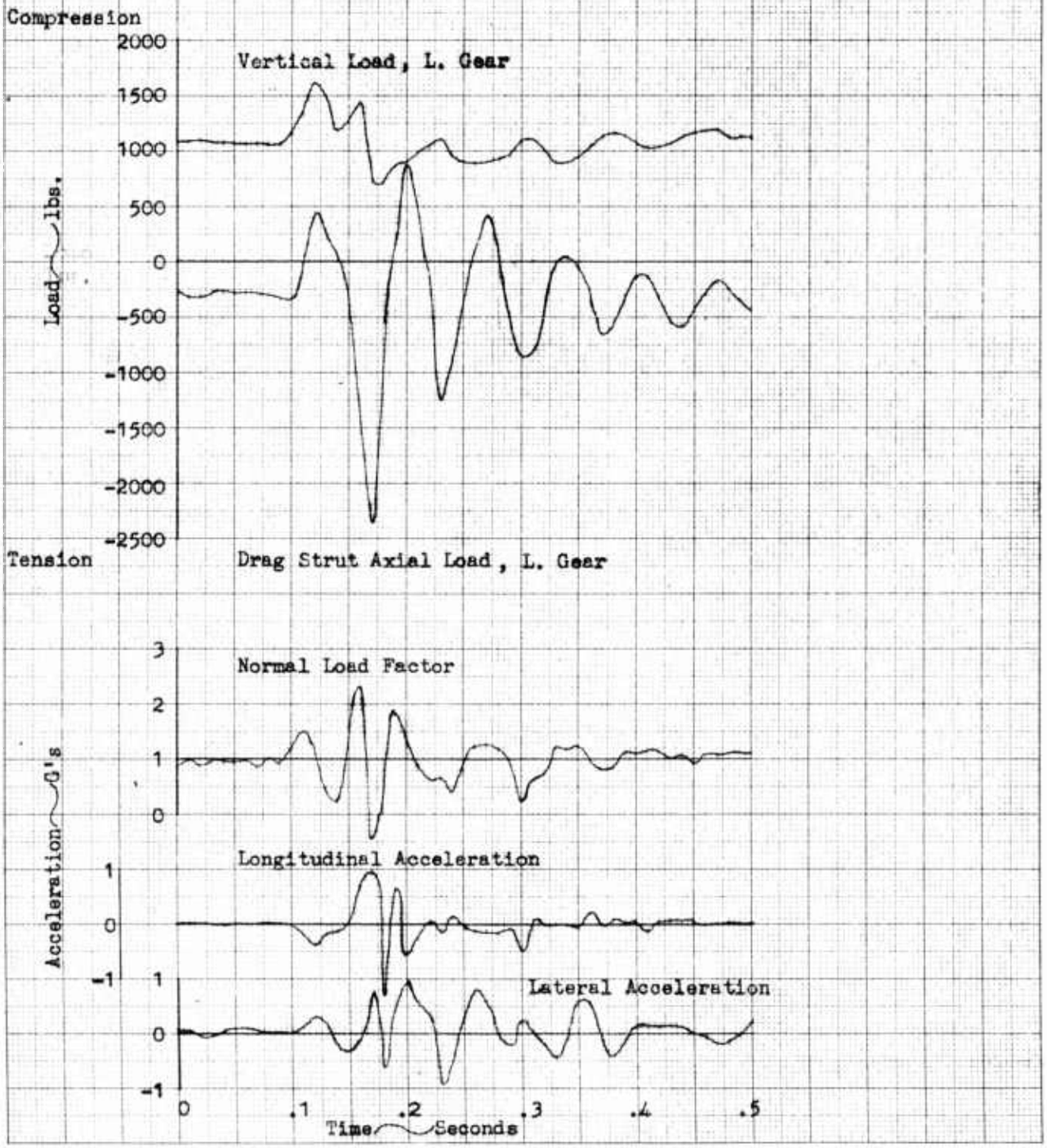

Figure 31

TIME HISTORY OF TYPICAL TAXI OVER OBSTACLE

M245B Landing Gear

Obstacle Height 4½"
Record No. 24579

Tire Pressure 4.9 PSI

Wheel Speed 23.4 MPH
May 27, 1959
Data Req. No. L19-5

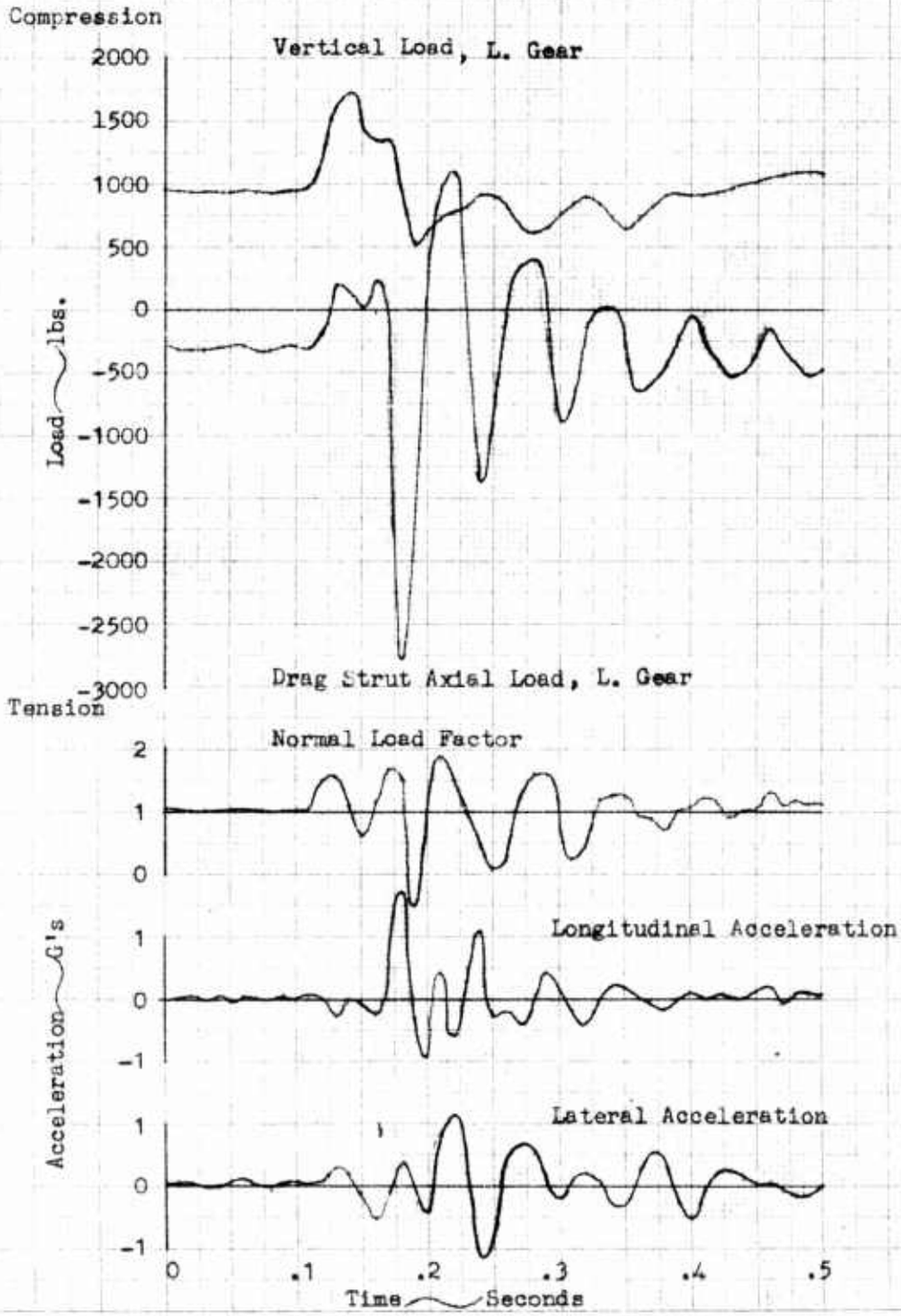

Figure 32

TIME HISTORY OF TYPICAL TAXI OVER OBSTACLE

M245B Landing Gear

Obstacle Height 6 3/8" Tire Pressure 2.7 PSI Wheel Speed 22.4 MPH

Record No. 24617 May 28, 1959

Data Req. No. L19-5

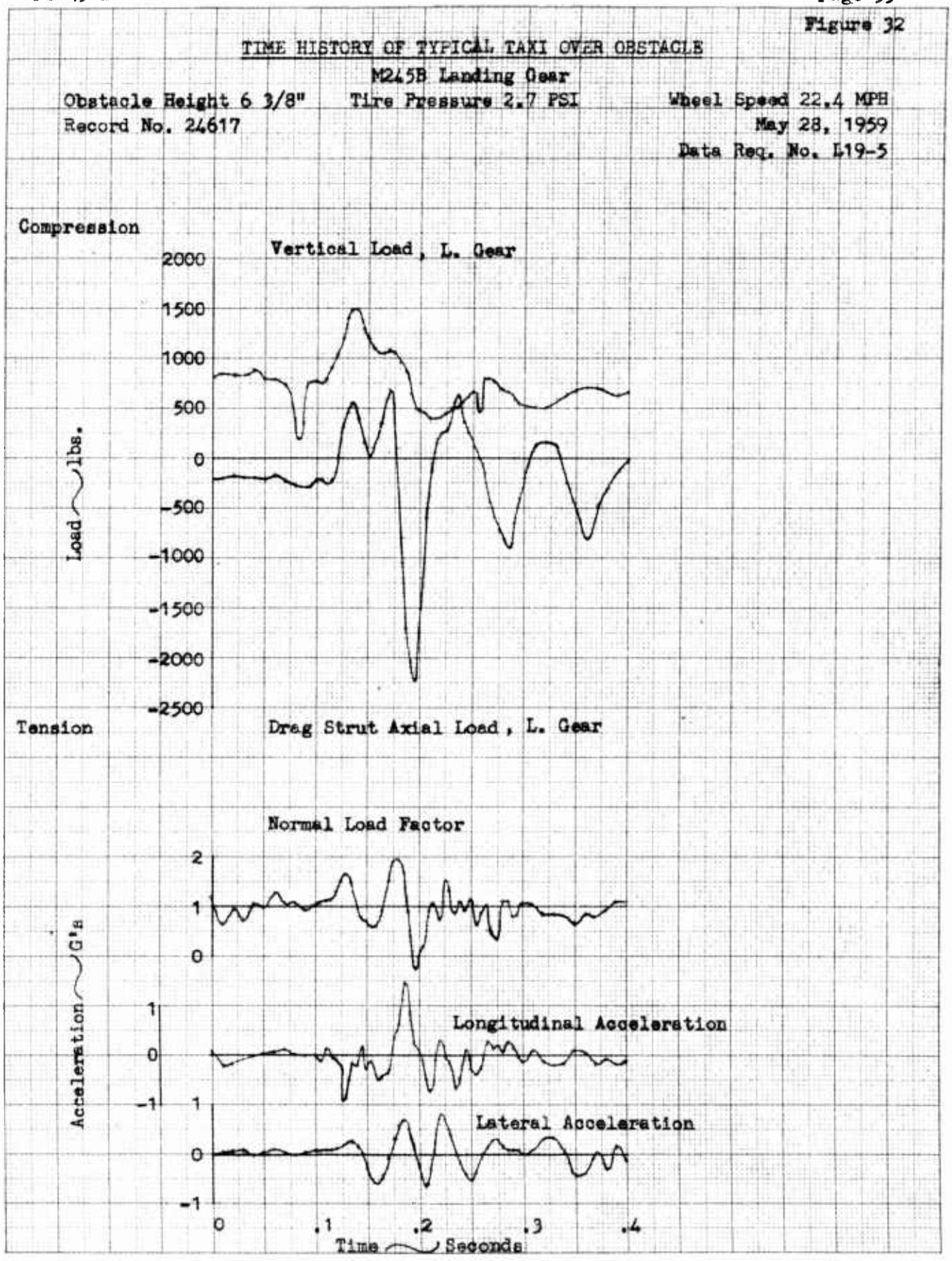

Figure 33

TIME HISTORY OF TYPICAL TAXI OVER OBSTACLE

M245B Landing Gear

Obstacle Height 6 3/8" Tire Pressure 3.7 PSI Wheel Speed 36.4 MPH

Record No. 25179 Data Req. No. L19-5

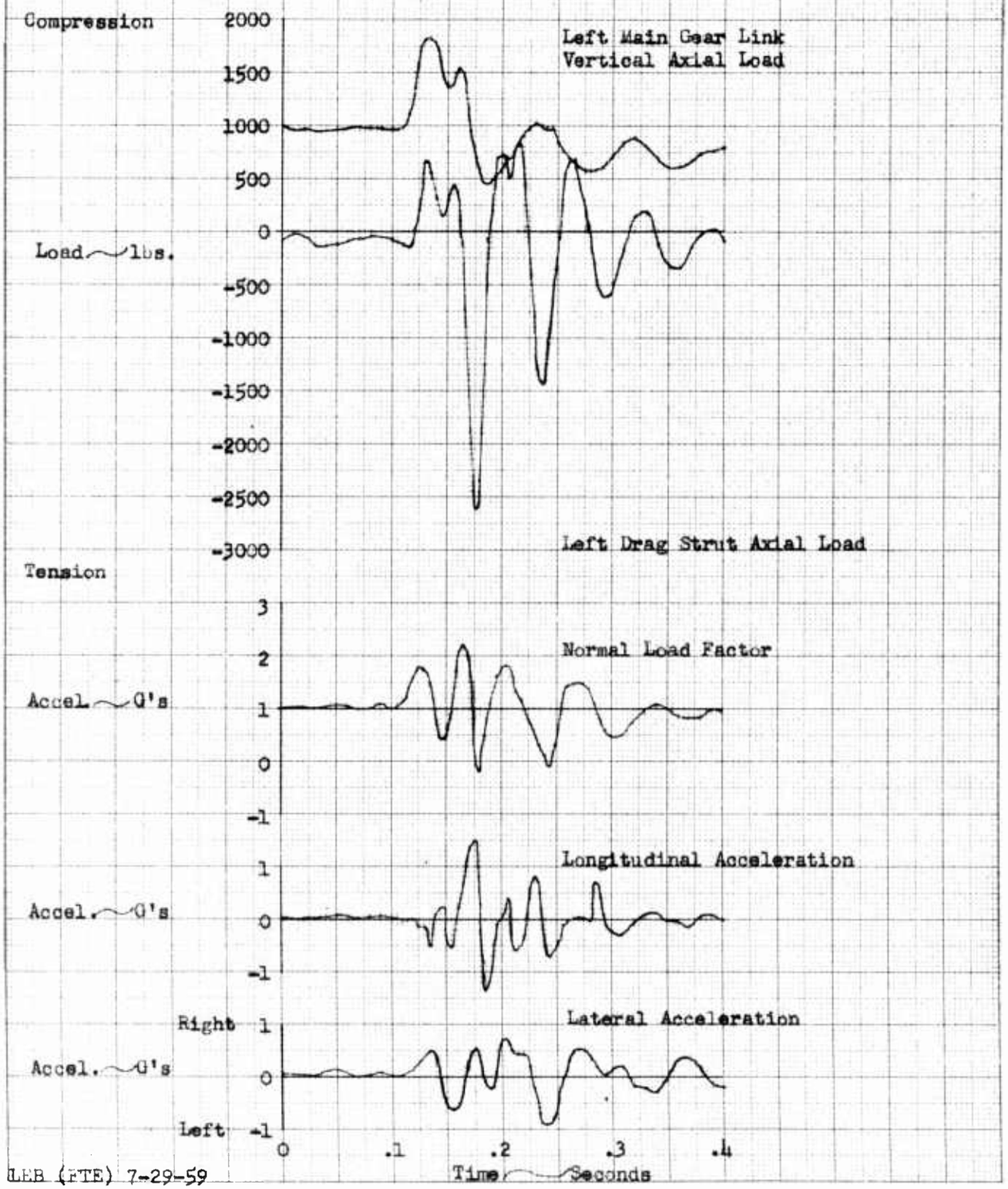

LEB (FTE) 7-29-59

Figure 34

TIME HISTORY OF TYPICAL TAXI OVER OBSTACLE

M245B Landing Gear

Obstacle Height 8" Tire Pressure 2.7 PSI Wheel Speed 8.1 MPH

Record No. 24638 June 2, 1959

Data Req. No. L19-5

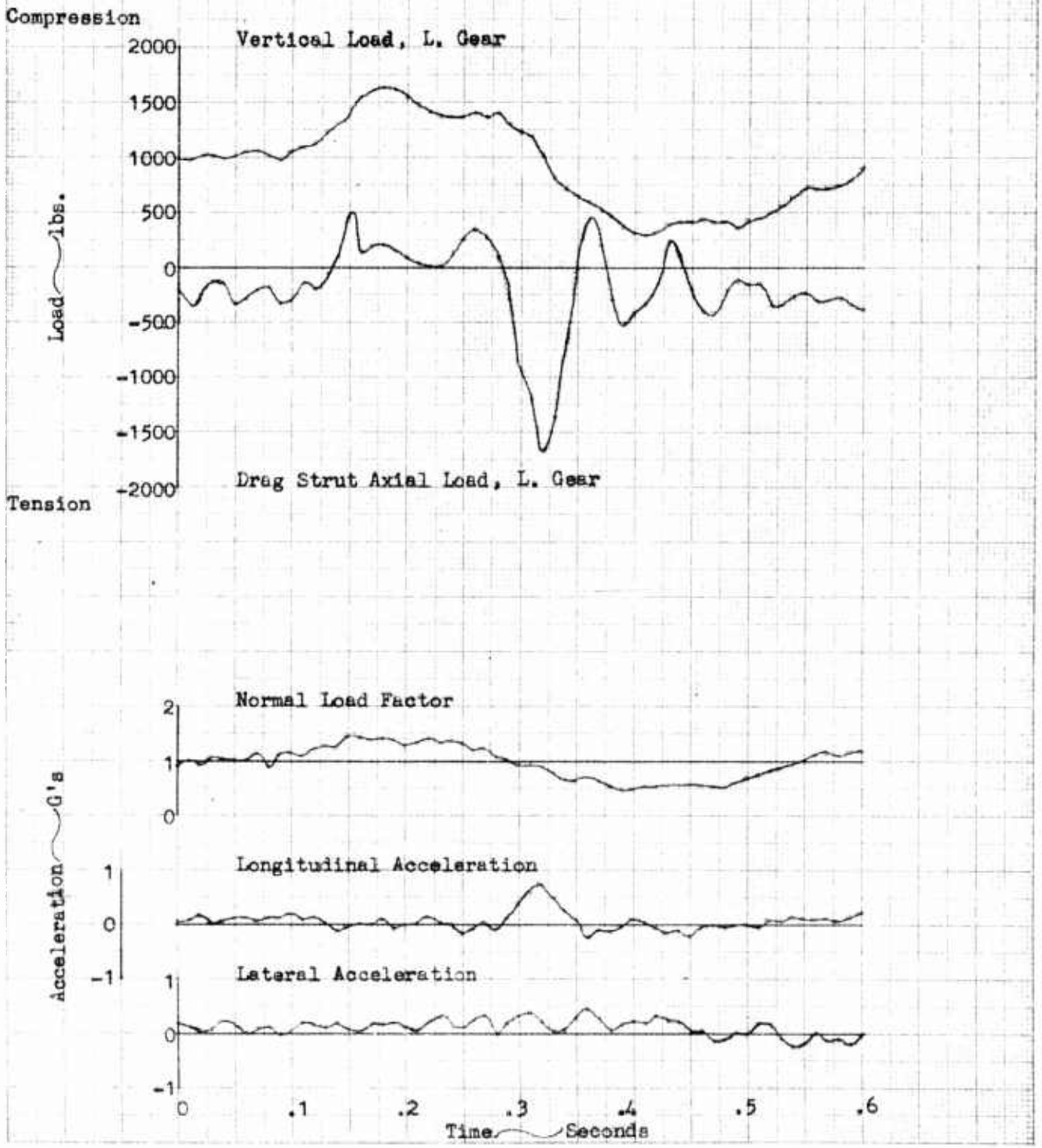

Figure 35

EFFECT OF GROUND SPEED ON DRAG STRUT AXIAL LOAD THROUGH 4 INCH DEEP DITCHES

M245B Landing Gear on L-19A Airplane

Data Request No. L-19-5

Ditch Width

- 12 In. (2.7 PSI Tire Press.)
- 18 In. (2.7 PSI Tire Press.)
- 24 In. (2.7 PSI Tire Press.)
- 24 In. (3.6 PSI Tire Press.)

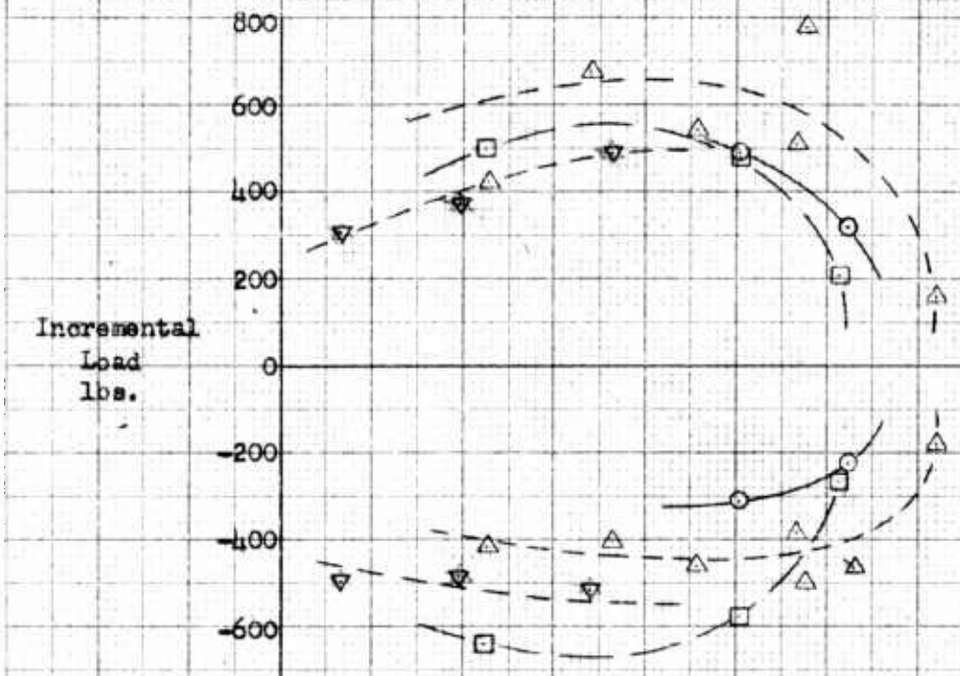

Note: Flagged points show test data obtained after reinforcement of fuselage drag strut attachment fitting.

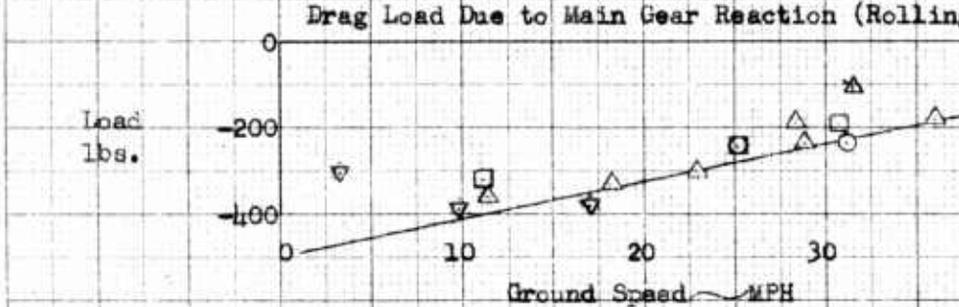

LEB (FTE) 6-25-59

Figure 36

EFFECT OF GROUND SPEED ON DRAG STRUT AXIAL LOAD THROUGH 6 INCH DEEP DITCHES

#245B Landing Gear on L-19A Airplane

Data Request No. L-19-5

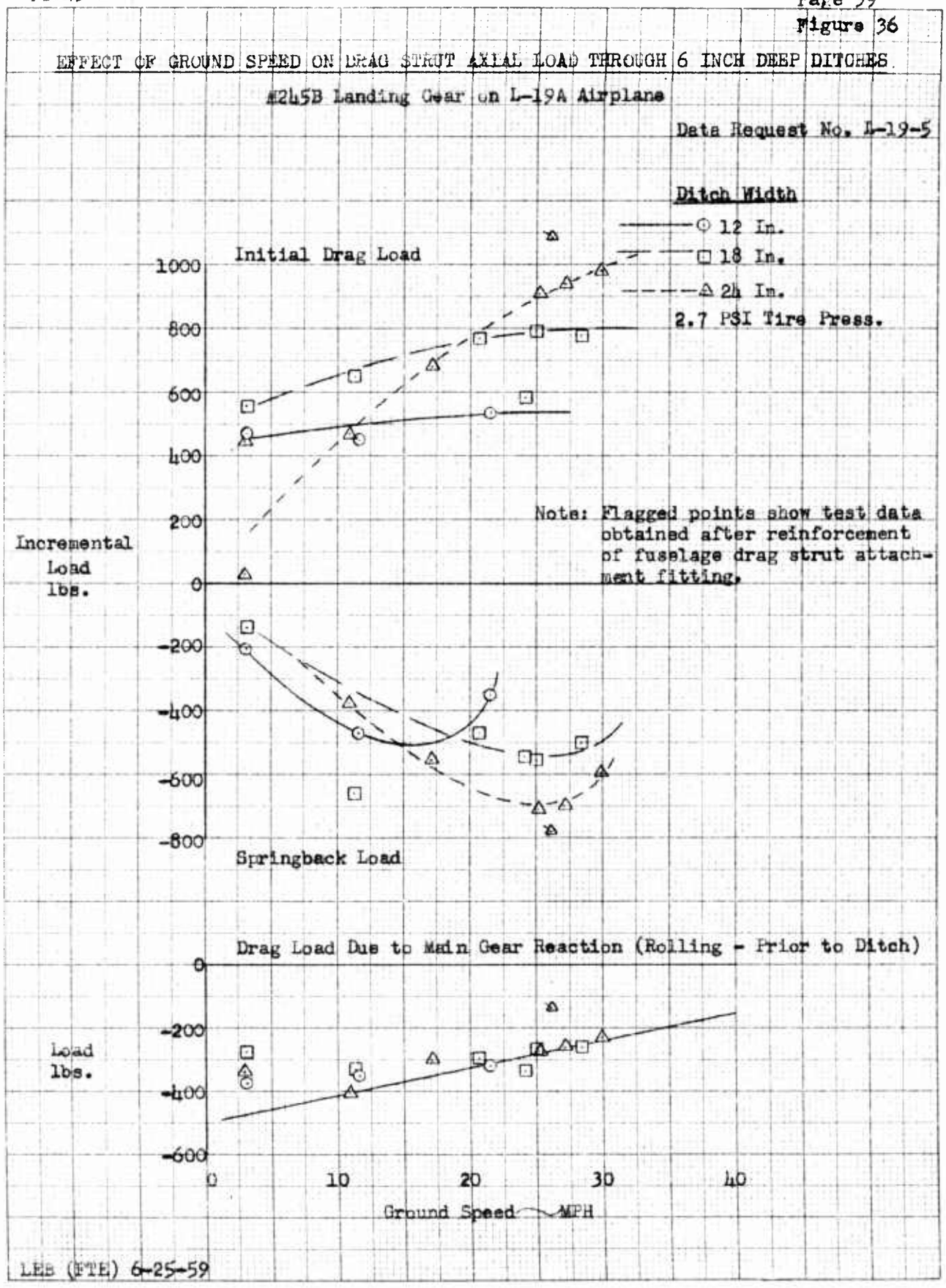

LEB (FTE) 6-25-59

Figure 37

EFFECT OF GROUND SPEED ON DRAG STRUT AXIAL LOAD THROUGH 8 INCH DEEP DITCHES

M245B Landing Gear on L-19A Airplane

Data Request No. L-19-5

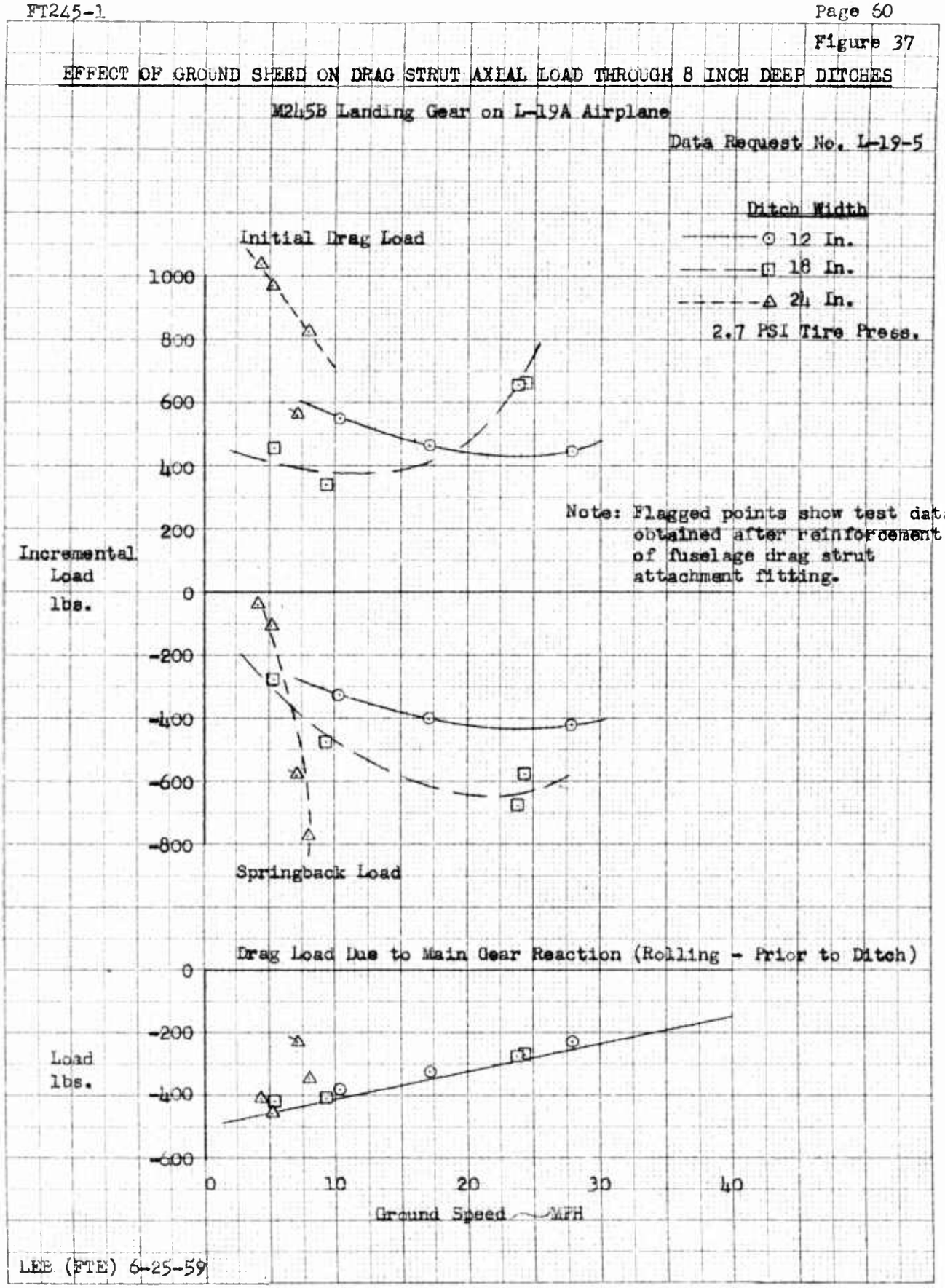

LEE (FTE) 6-25-59

Figure 38

EFFECT OF GROUND SPEED ON VERTICAL LINK AXIAL LOAD THROUGH 4 INCH DEEP DITCH

M245B Landing Gear on L-19A Airplane

Data Request No. L-19-5

Ditch Width

- ⊙ 12 In. (2.7 PSI Tire Press.)
- ⊡ 18 In. (2.7 PSI Tire Press.)
- △ 24 In. (2.7 PSI Tire Press.)
- ▽ 24 In. (3.6 PSI Tire Press.)

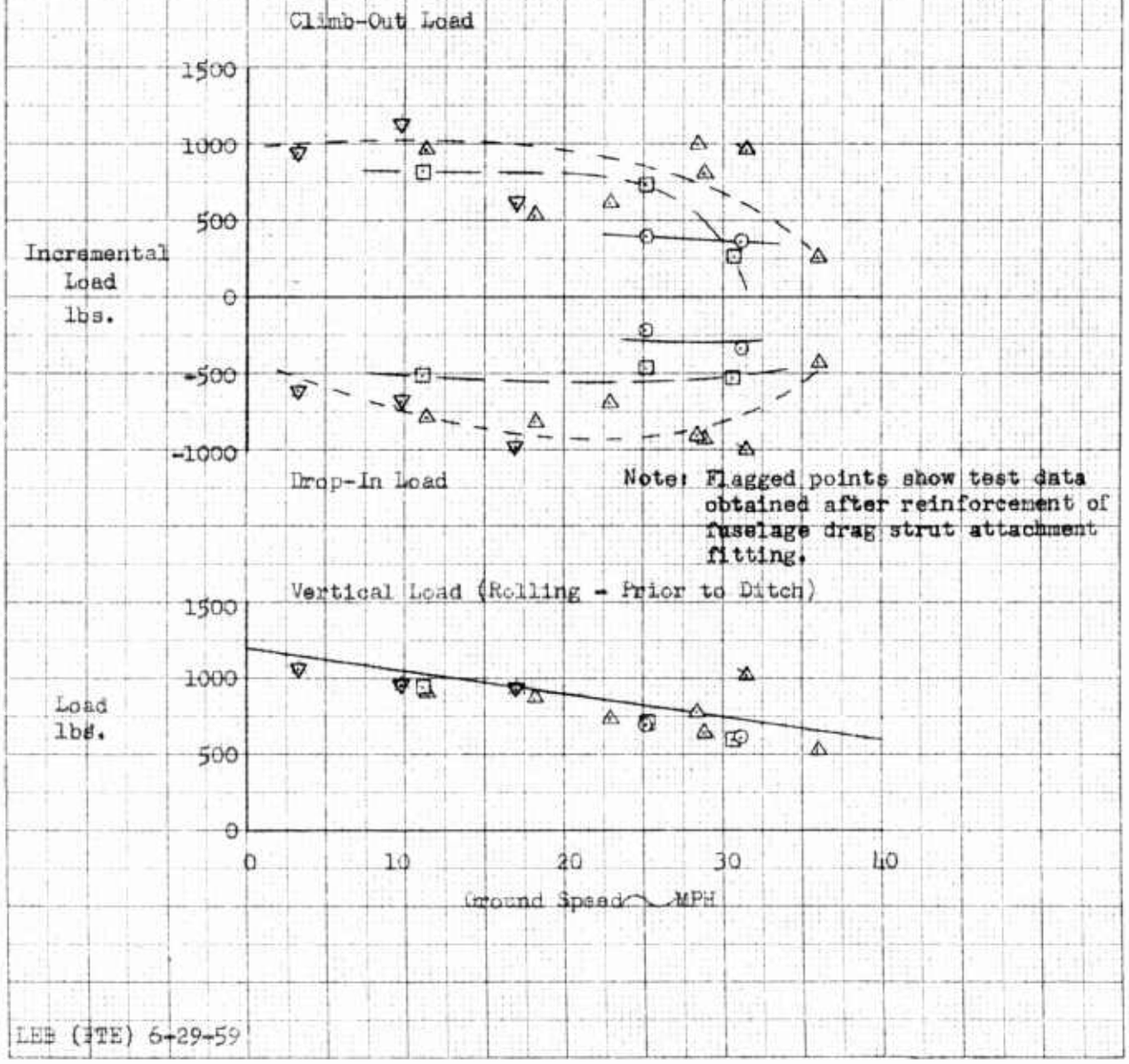

LEE (FTE) 6-29-59

Figure 39

EFFECT OF GROUND SPEED ON VERTICAL LINK AXIAL LOAD THROUGH 6 INCH DEEP DITCH

M245B Landing Gear on L-19A Airplane

Data Request No. L-19-5

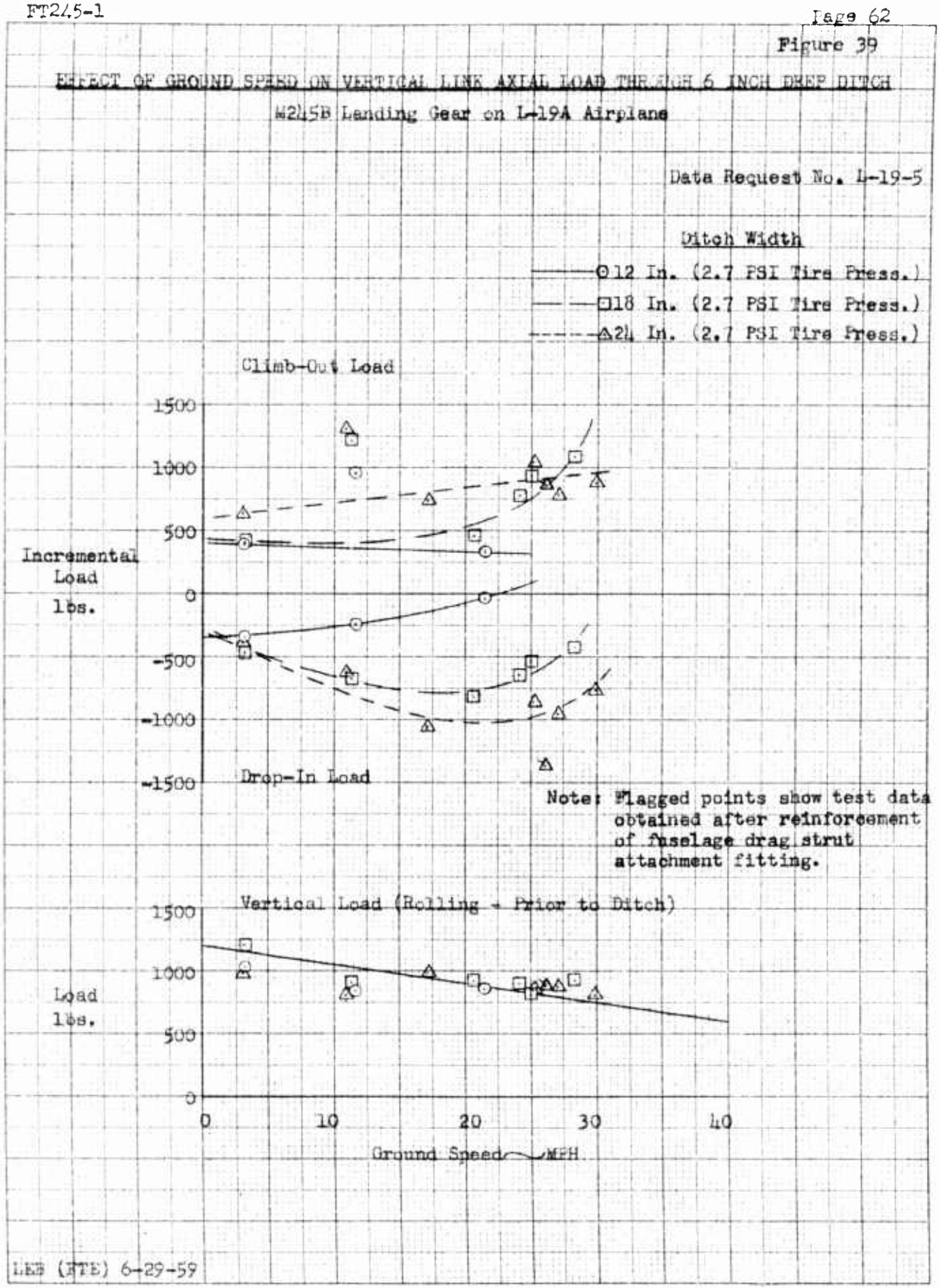

LEB (ETE) 6-29-59

Figure 40

EFFECT OF GROUND SPEED ON VERTICAL LINK AXIAL LOAD THROUGH 8 INCH DEEP DITCH

M245B Landing Gear on L-19A Airplane

Data Request No. L-19-5

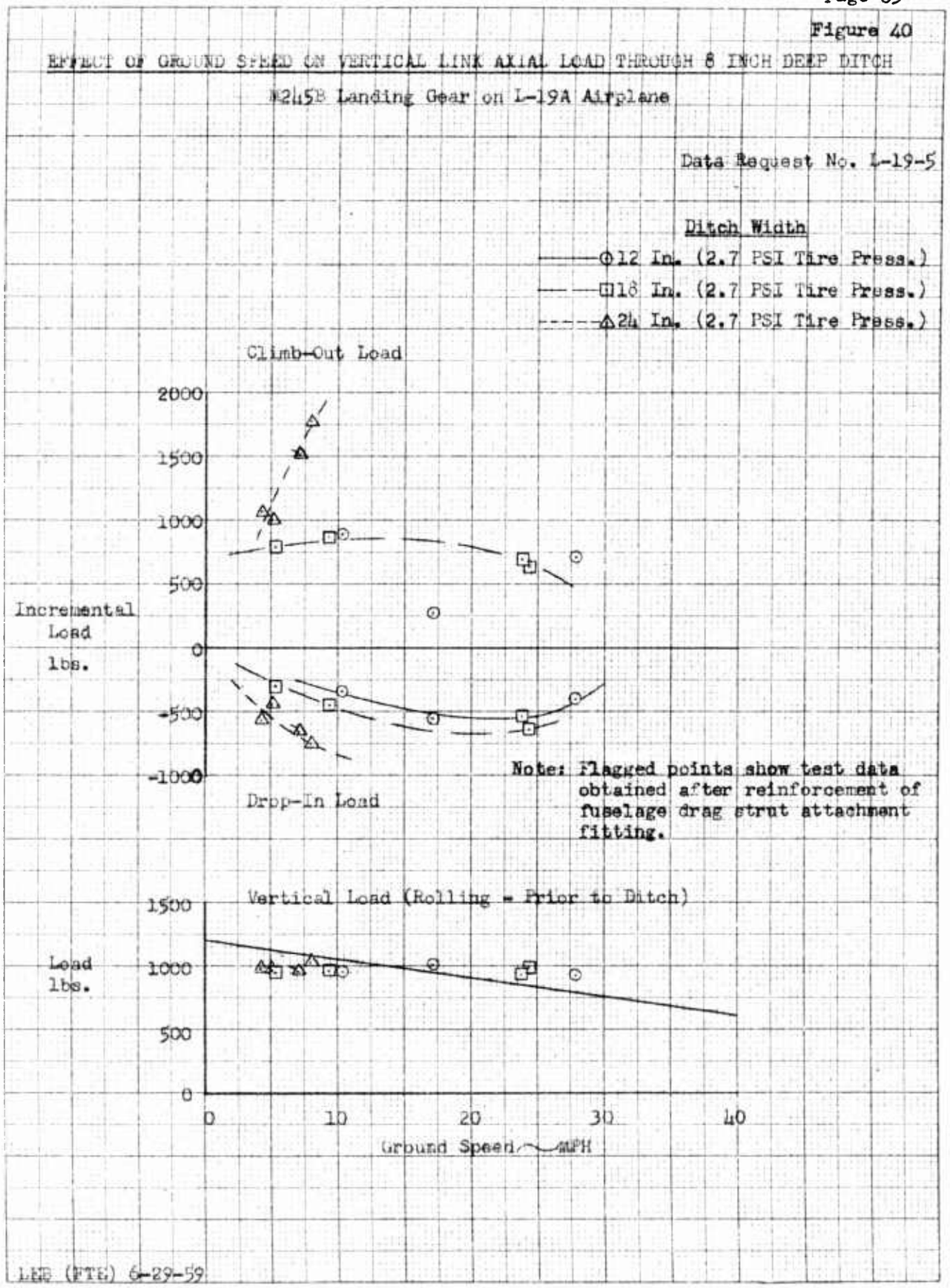

LRB (FTE) 6-29-59

Figure 41

EFFECT OF GROUND SPEED ON AIRPLANE ACCELERATIONS THROUGH 4 INCH DEEP DITCH

M245B Landing Gear on L-19A Airplane

Data Request No. L-19-5

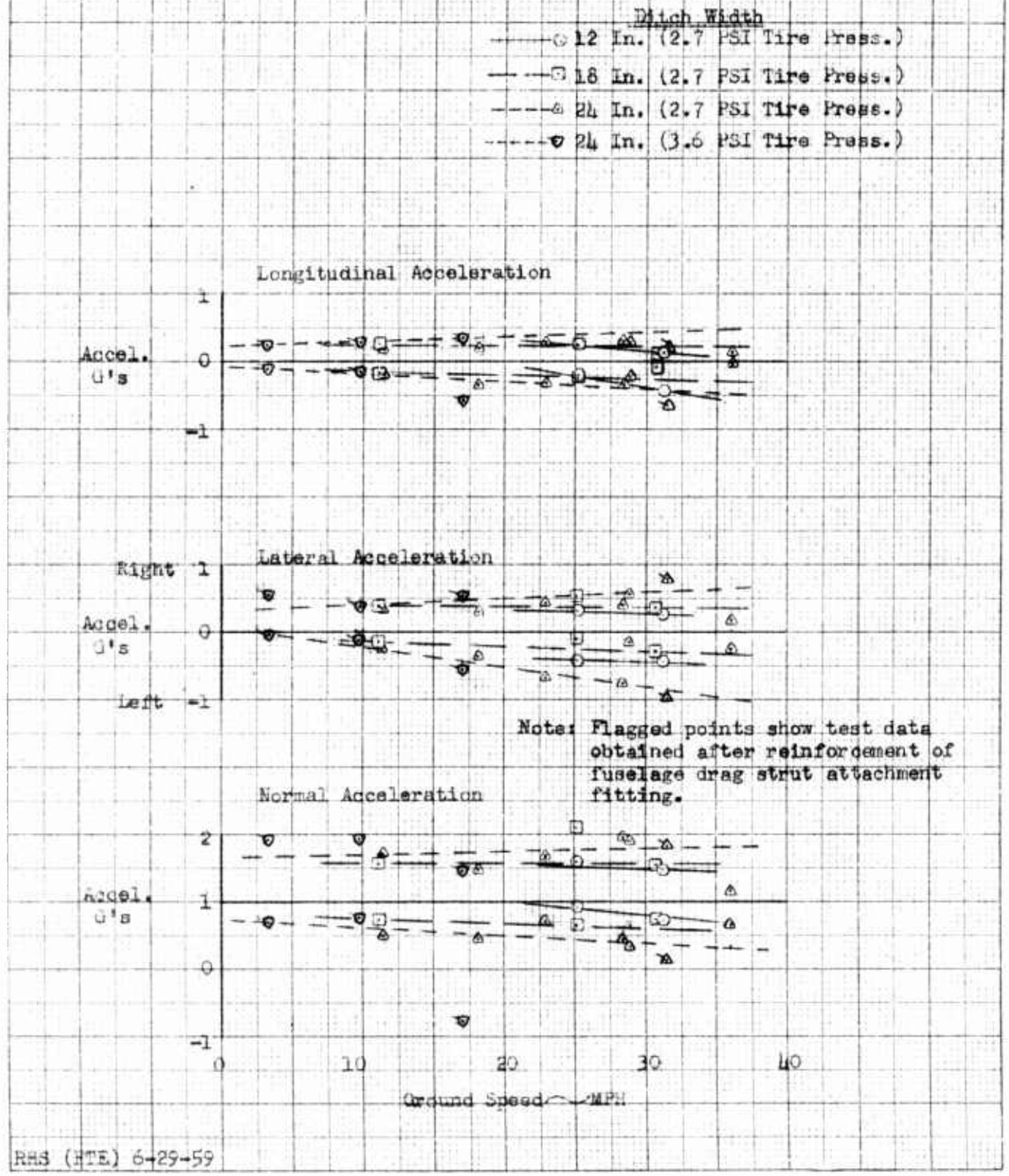

Note: Flagged points show test data obtained after reinforcement of fuselage drag strut attachment fitting.

RHS (HTE) 6-29-59

Figure 42

EFFECT OF GROUND SPEED ON AIRPLANE ACCELERATIONS THROUGH 6 INCH DEEP DITCH

M24.5B Landing Gear on L-19A Airplane

Data Request No. L-19-5

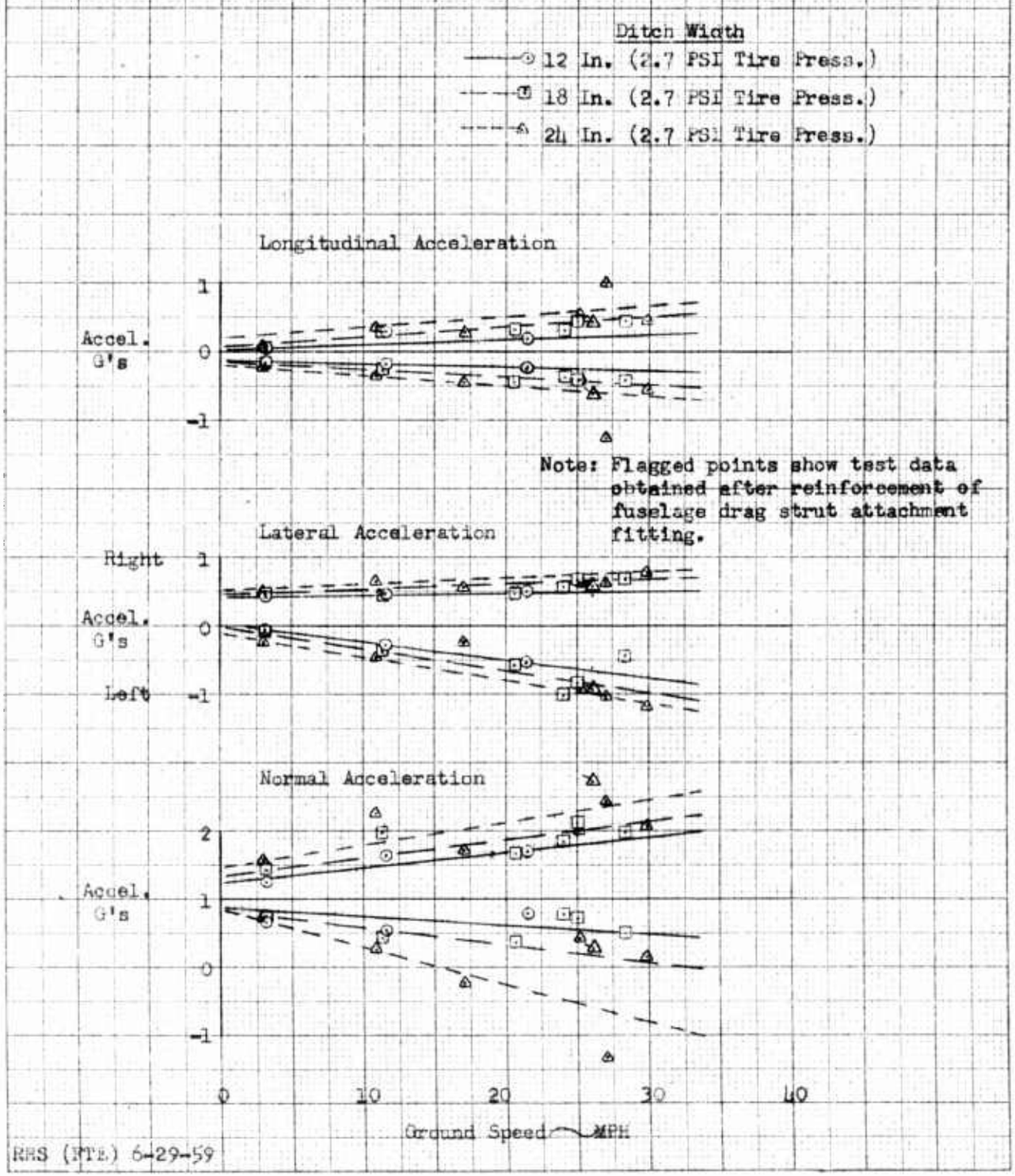

RRS (FTE) 6-29-59

Figure 43

EFFECT OF GROUND SPEED ON AIRPLANE ACCELERATIONS THROUGH 8 INCH DEEP DITCH

M245B Landing Gear on L-19A Airplane

Data Request No. L-19-5

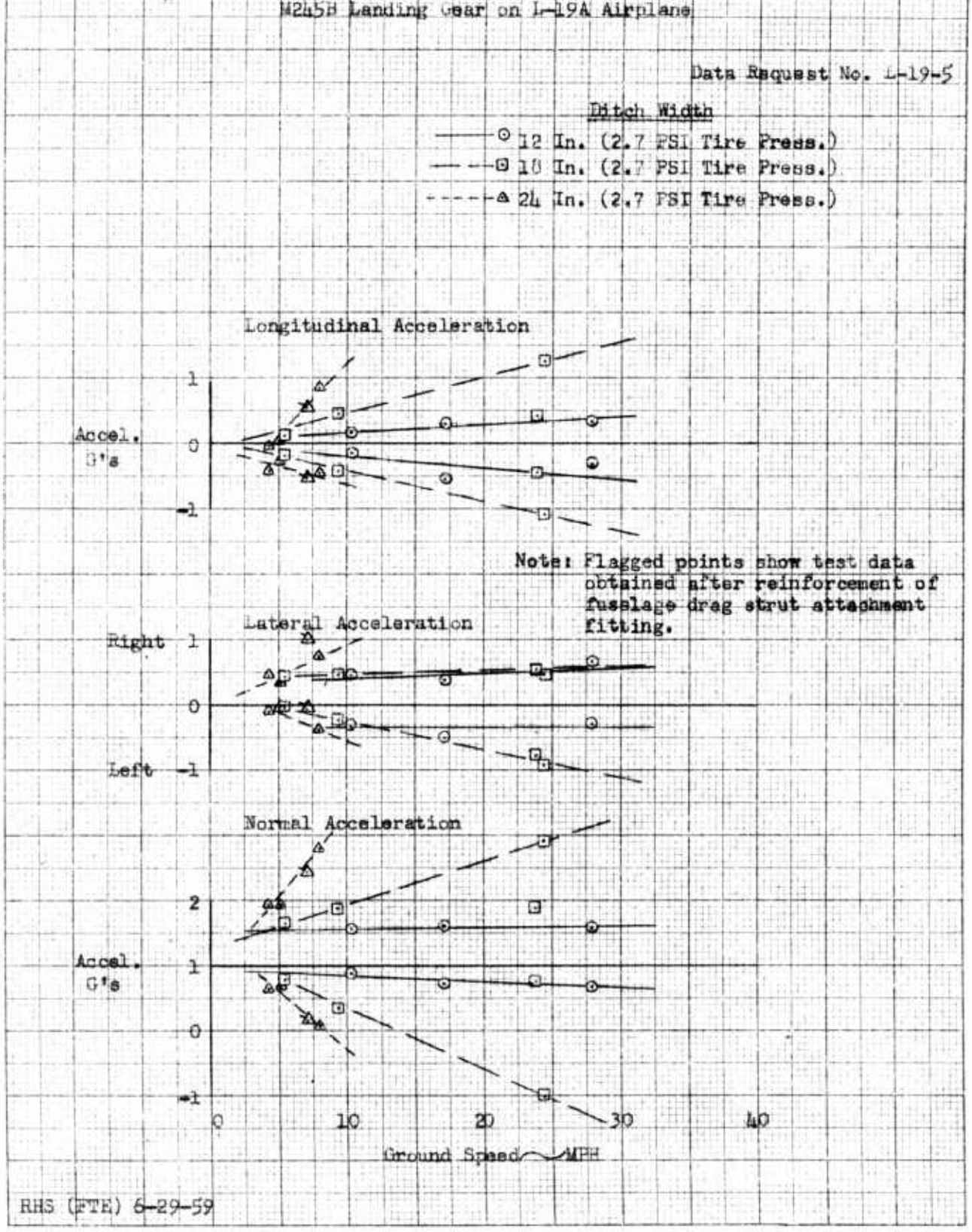

RHS (FTE) 6-29-59

Figure 44

TIME HISTORY OF TYPICAL TAXI THROUGH DITCH

M245B Landing Gear

Ditch Size 12"W x 4"D Tire Pressure 2.7 PSI Wheel Speed 25.2 MPH

Record No. 24641 June 2, 1959

Data Req. No. L19-5

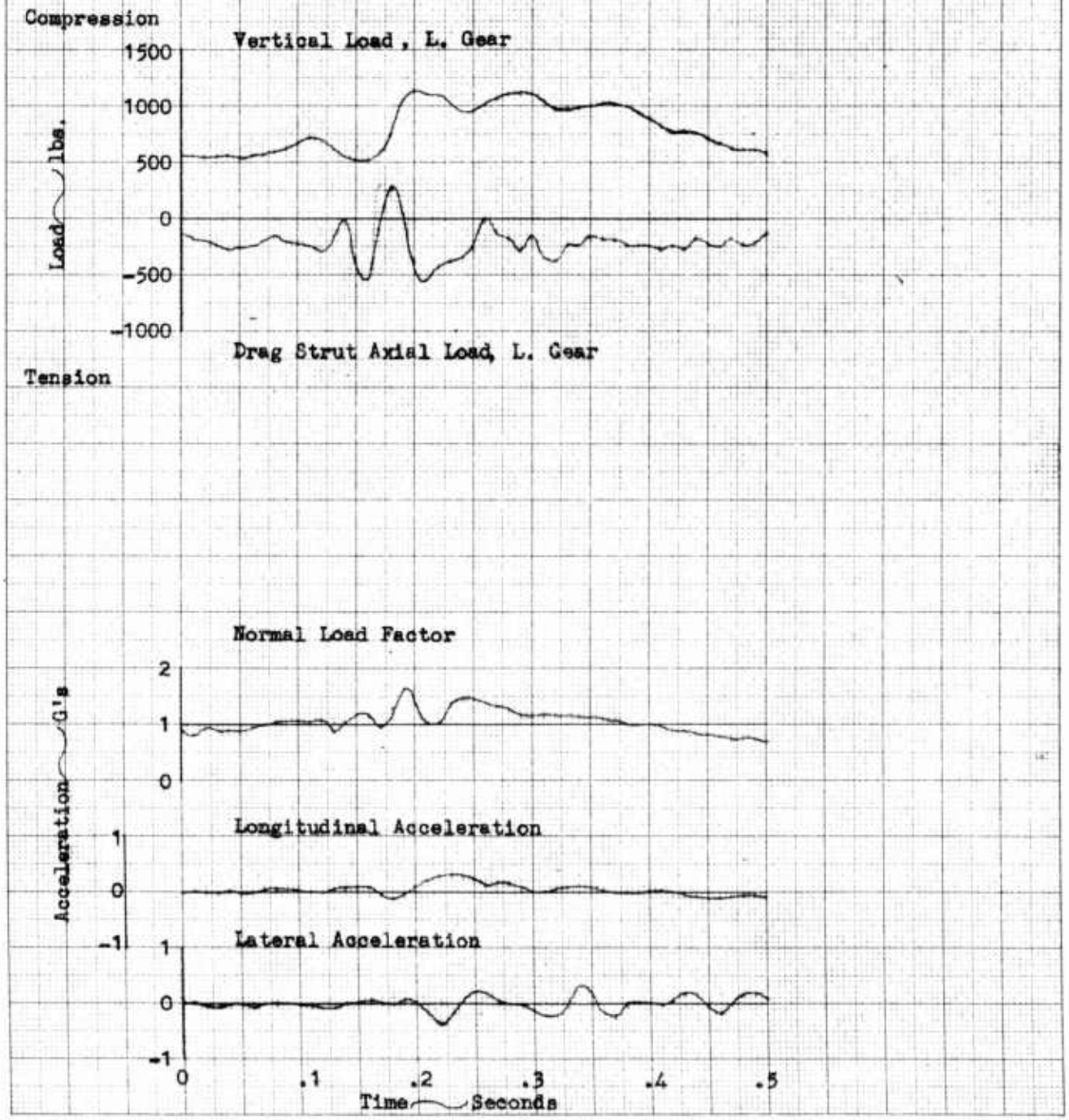

Figure 45

TIME HISTORY OF TYPICAL TAXI THROUGH DITCH

M245B Landing Gear

Ditch Size 18"W x 4"D Tire Pressure 2.7 PSI Wheel Speed 11.1 MPH

Record No. 24643 June 2, 1959

Data Req. No. L19-5

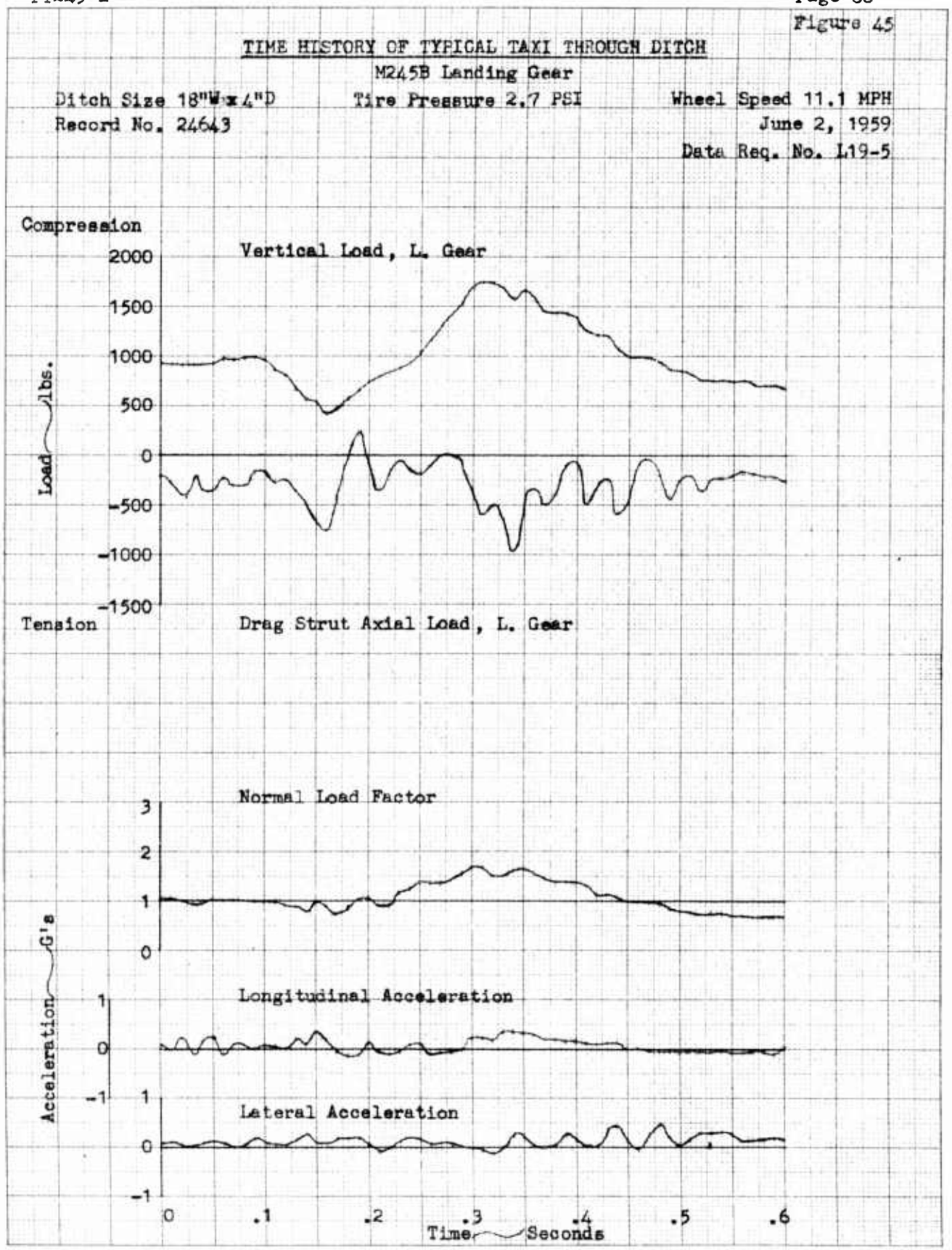

Figure 46

TIME HISTORY OF TYPICAL TAXI THROUGH DITCH

M245B Landing Gear

Ditch Size 24"W x 4"D Tire Pressure 2.7 PSI Wheel Speed 11.3 MPH

Record No. 24646 June 2, 1959

Data Req. No. L19-5

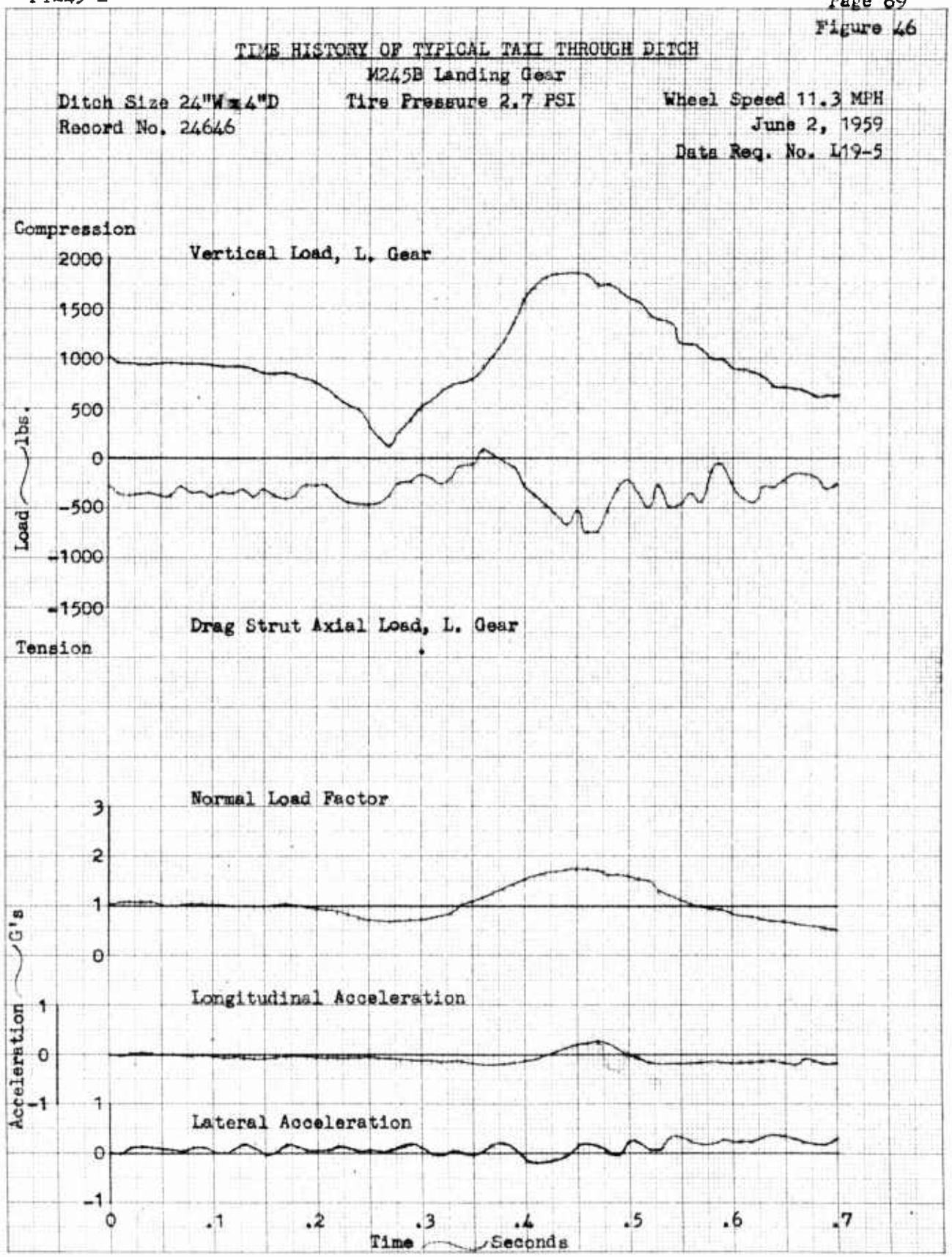

Figure 47

TIME HISTORY OF TYPICAL TAXI THROUGH DITCH

M245B Landing Gear

Ditch Size 12"W x 6"D Tire Pressure 2.7 PSI Wheel Speed 11.6 MPH

Record No. 24663 June 3, 1959

Data Req. No. 119-5

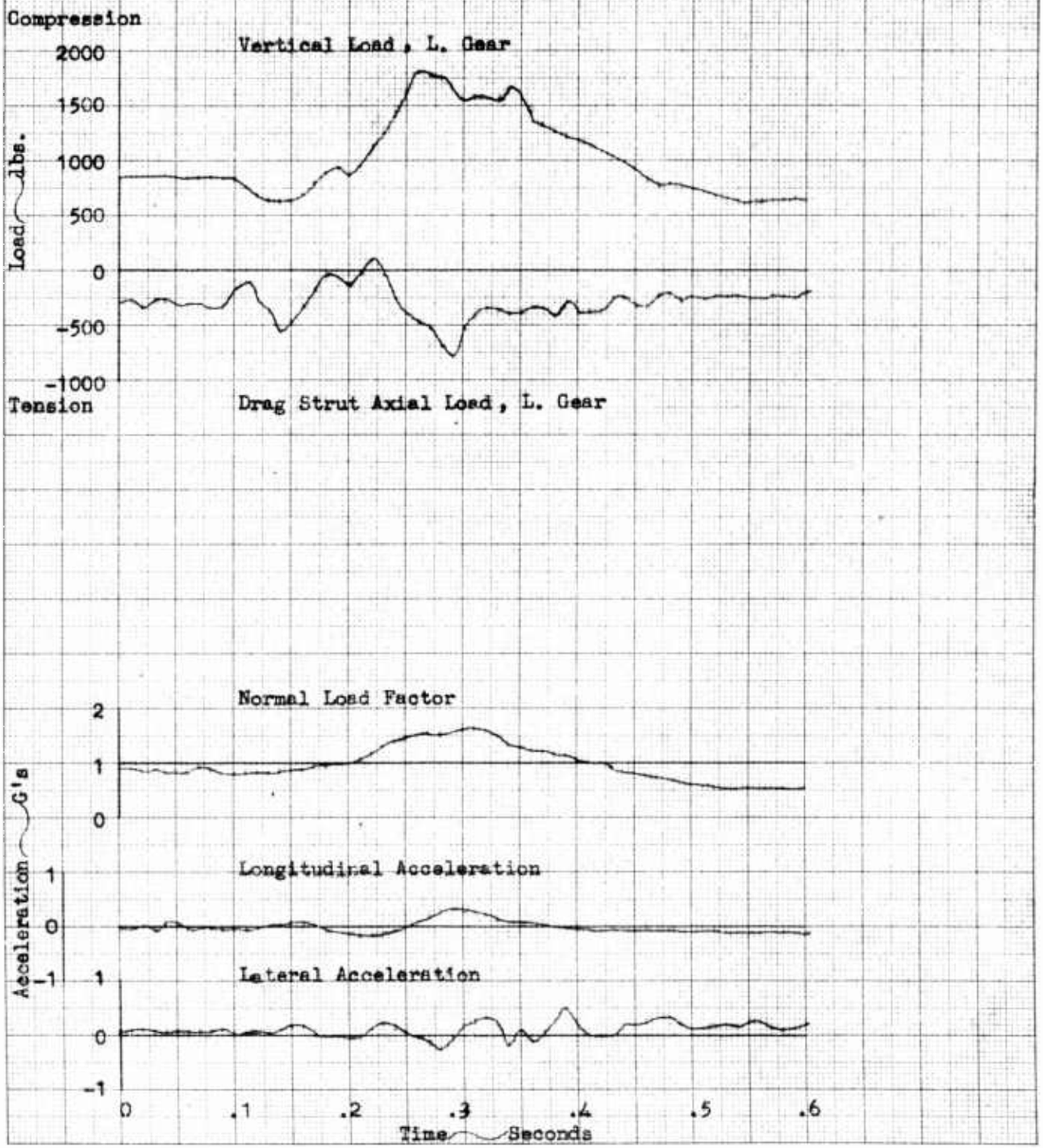

Figure 48

TIME HISTORY OF TYPICAL TAXI THROUGH DITCH

M245E Landing Gear

Ditch Size 18"W x 6"D Tire Pressure 2.7 PSI Wheel Speed 11.3 MPH

Record No. 24666

June 3, 1959

Data Req. No. L19-5

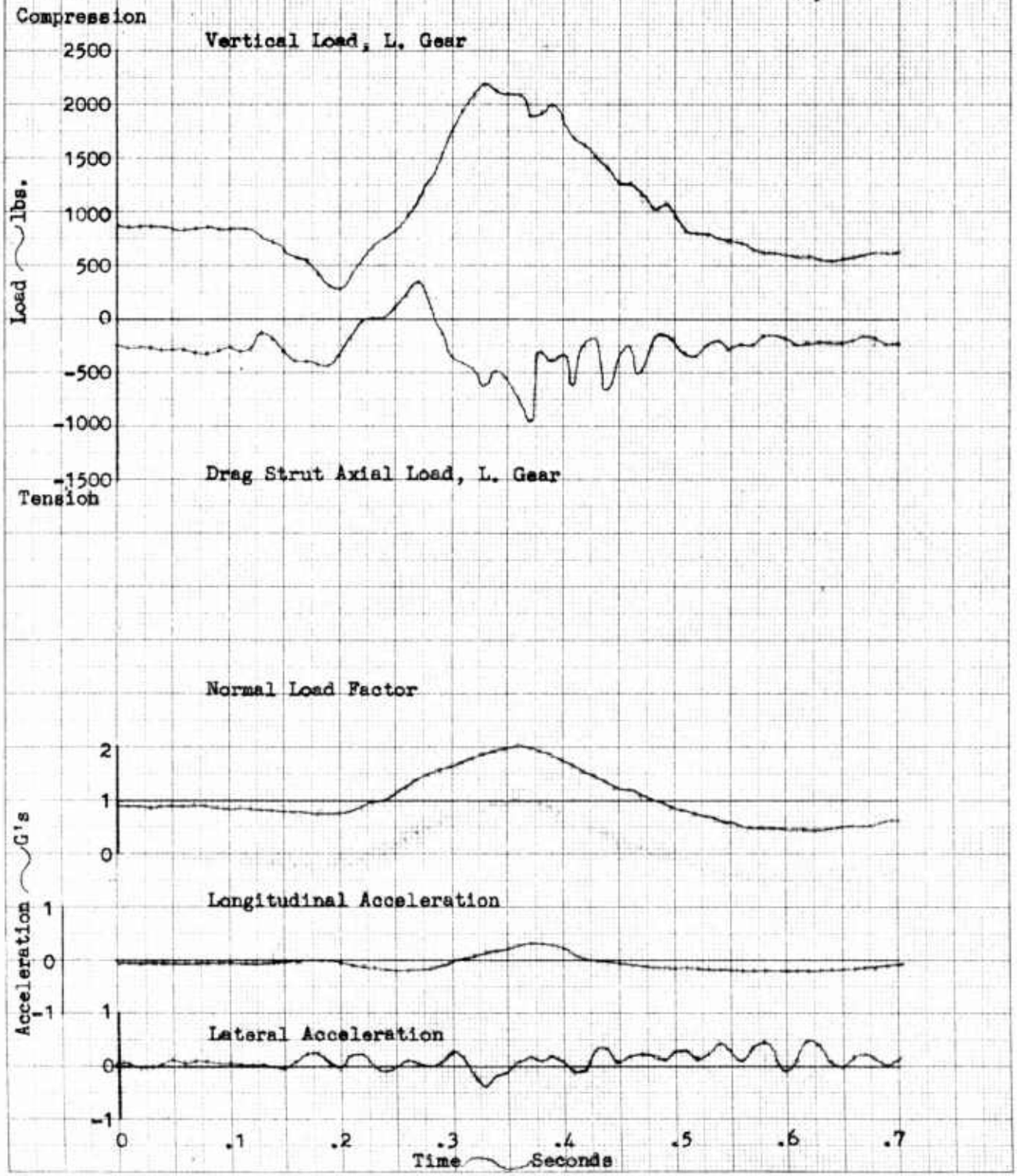

Figure 49

TIME HISTORY OF TYPICAL TAXI THROUGH DITCH

M245B Landing Gear

Ditch Size 24"W x 6"D Tire Pressure 2.7 PSI Wheel Speed 10.9 MPH

Record No. 24681 June 4, 1959

Data Req. No. L19-5

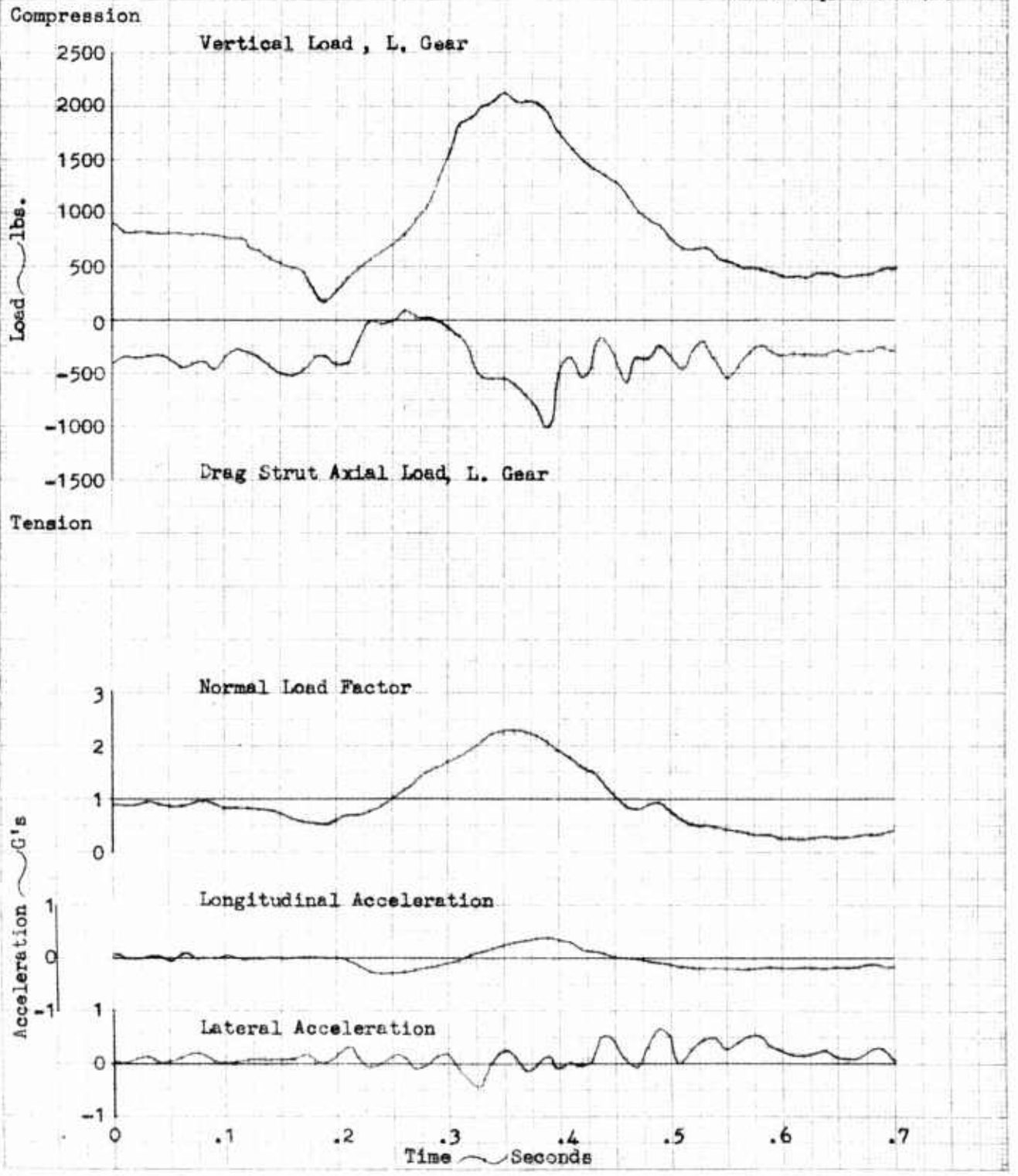

Figure 50

TIME HISTORY OF TYPICAL TAXI THROUGH DITCH

M245B Landing Gear

Ditch Size 12"W x 8"D Tire Pressure 2.7 PSI Wheel Speed 10.3 MPH

Record No. 24712 June 5, 1959

Data Req. No. L19-5

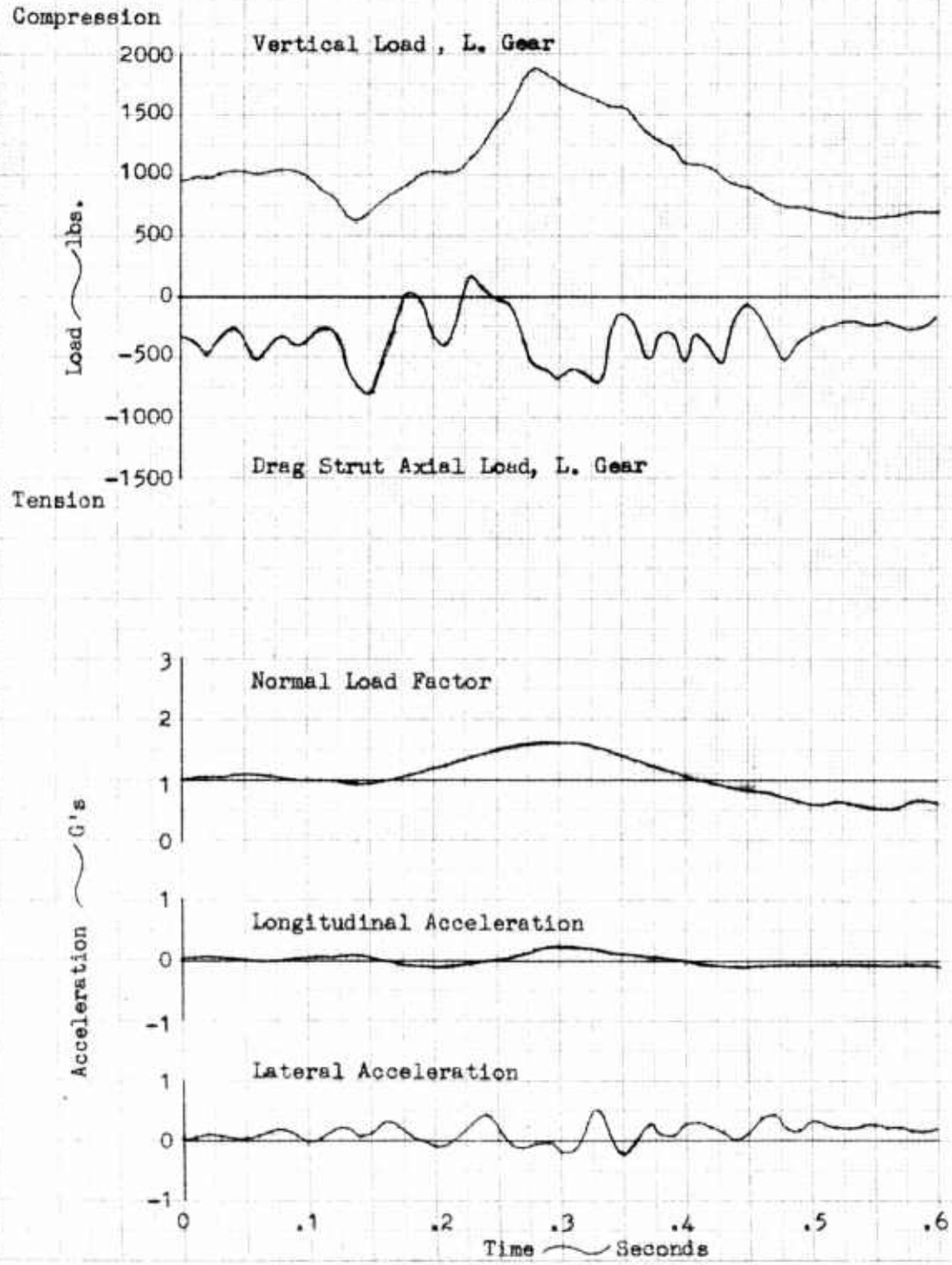

Figure 51

TIME HISTORY OF TYPICAL TAXI THROUGH DITCH

M245B Landing Gear

Ditch Size 18"W x 8"D Tire Pressure 2.7 PSI Wheel Speed 9.4 MPH

Record No. 24716 June 5, 1959

Data Req. No. L19-5

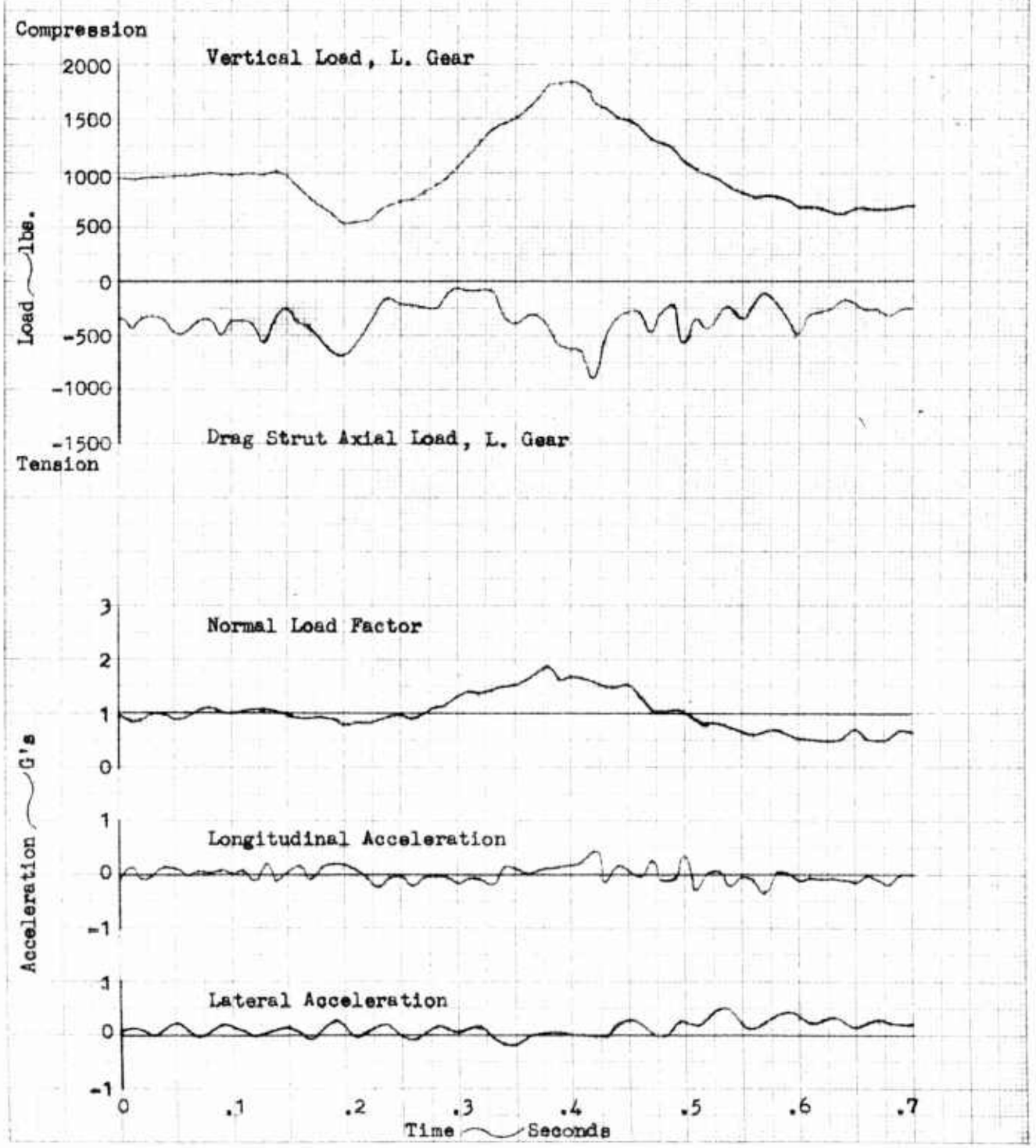

Figure 52

TIME HISTORY OF TYPICAL TAXI THROUGH DITCH

M245B Landing Gear

Ditch Size 24"W x 8"D Tire Pressure 2.7 PSI Wheel Speed 8.0 MPH

Record No. 24750 June 8, 1959

Data Req. No. L19-5

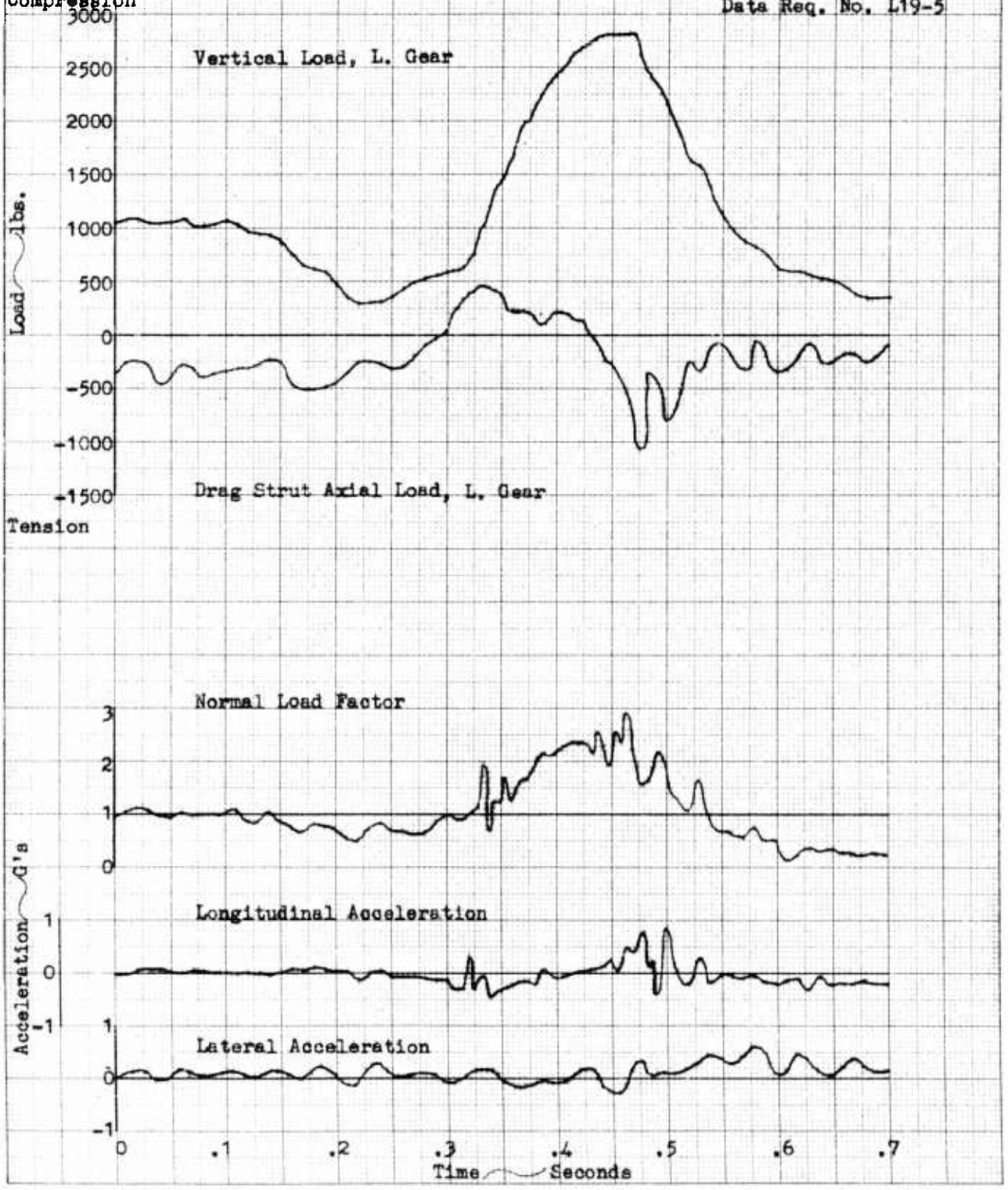

Figure 52

TIME HISTORY OF TYPICAL TAXI THROUGH DITCH

M245B Landing Gear

Ditch Size 24"W x 8"D Tire Pressure 2.7 PSI Wheel Speed 8.0 MPH

Record No. 24750 June 8, 1959

Data Req. No. L19-5

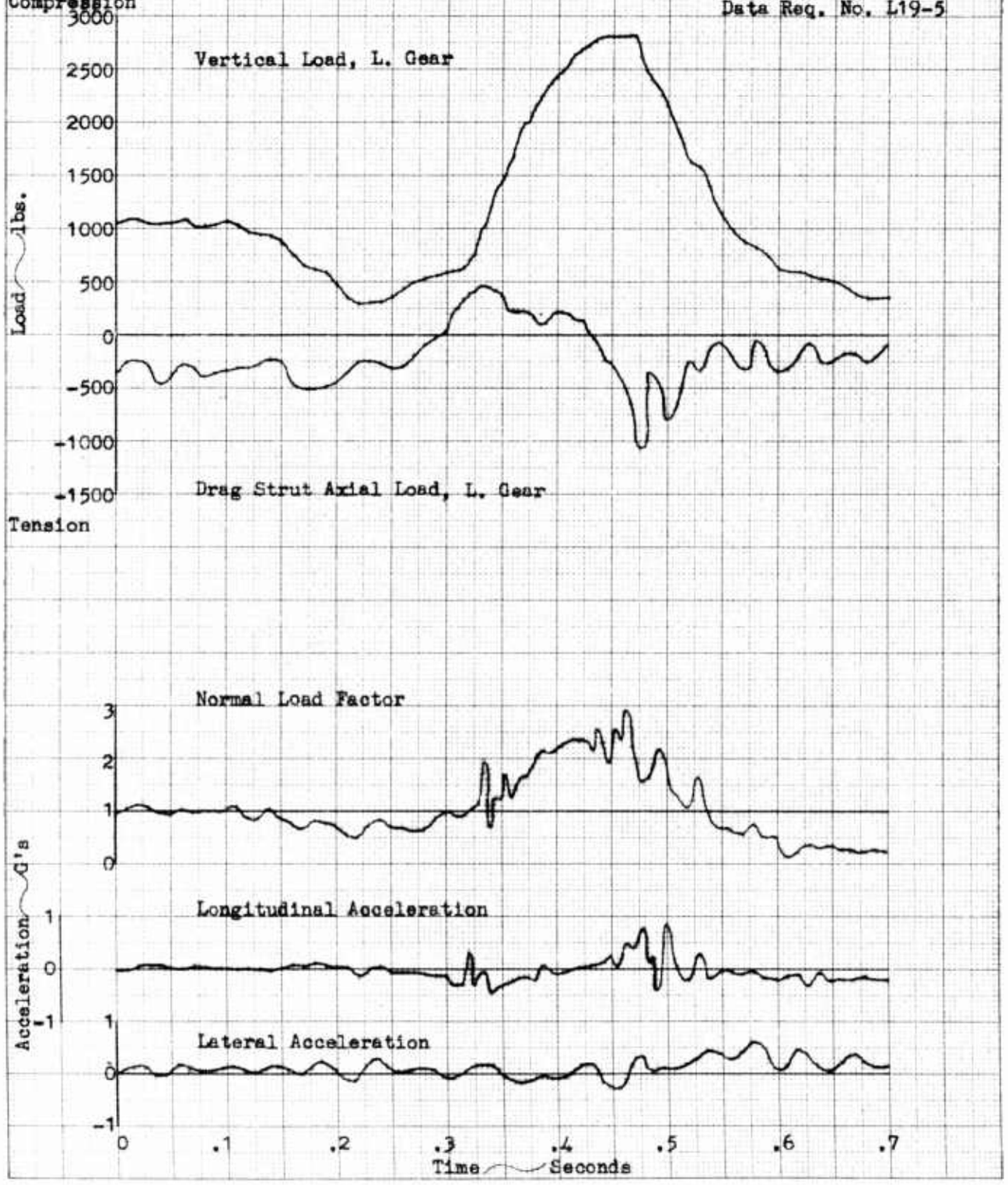

Figure 53

TIME HISTORY OF TYPICAL TAXI THROUOH DITCH

M245B Landing Gear

Ditch Size 24"Wx4"D Tire Pressure 3.6±.2 PSI Wheel Speed 9.8 MPH

Record No. 24729 June 5, 1959

Data Req. No. L19-5

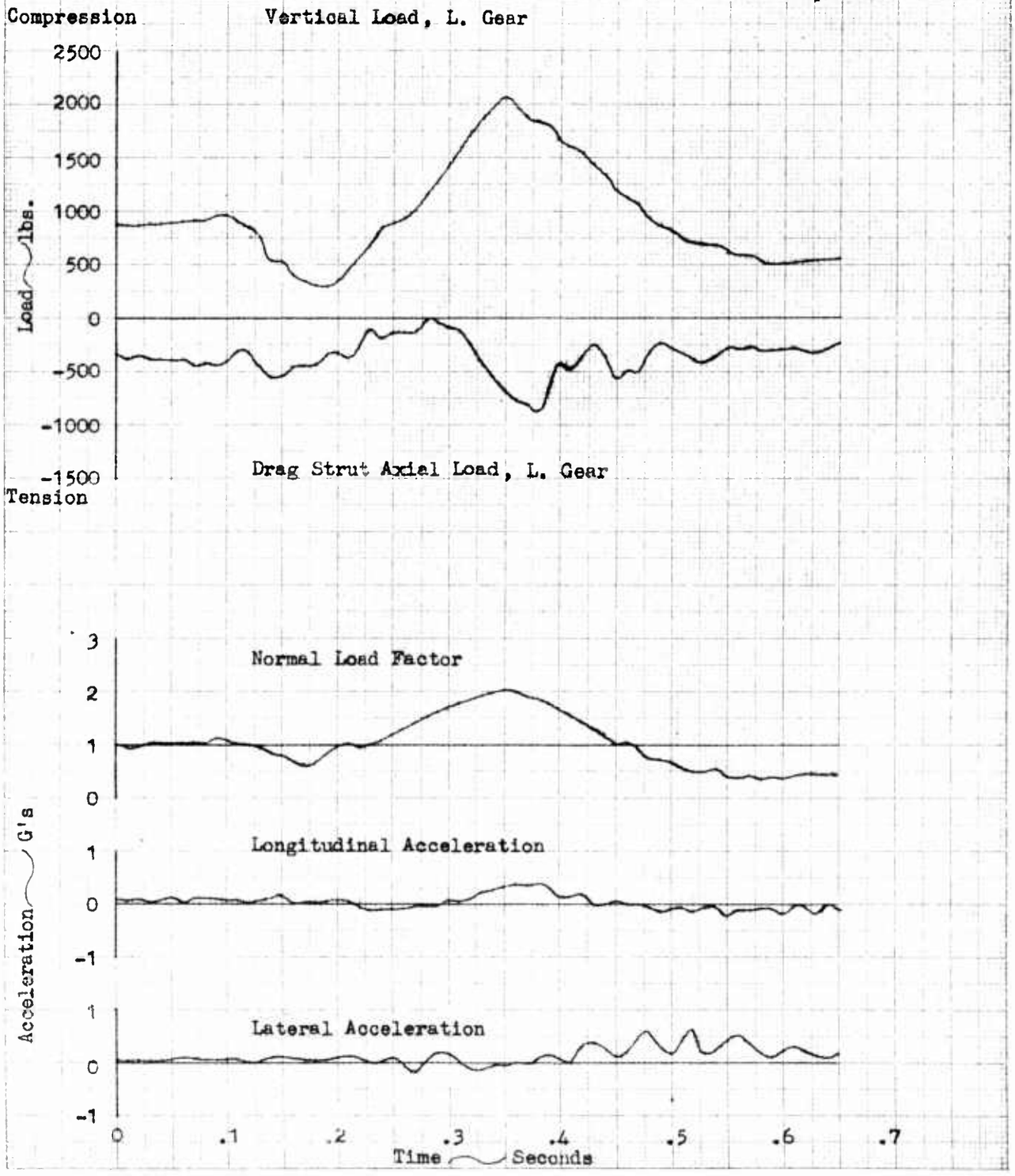

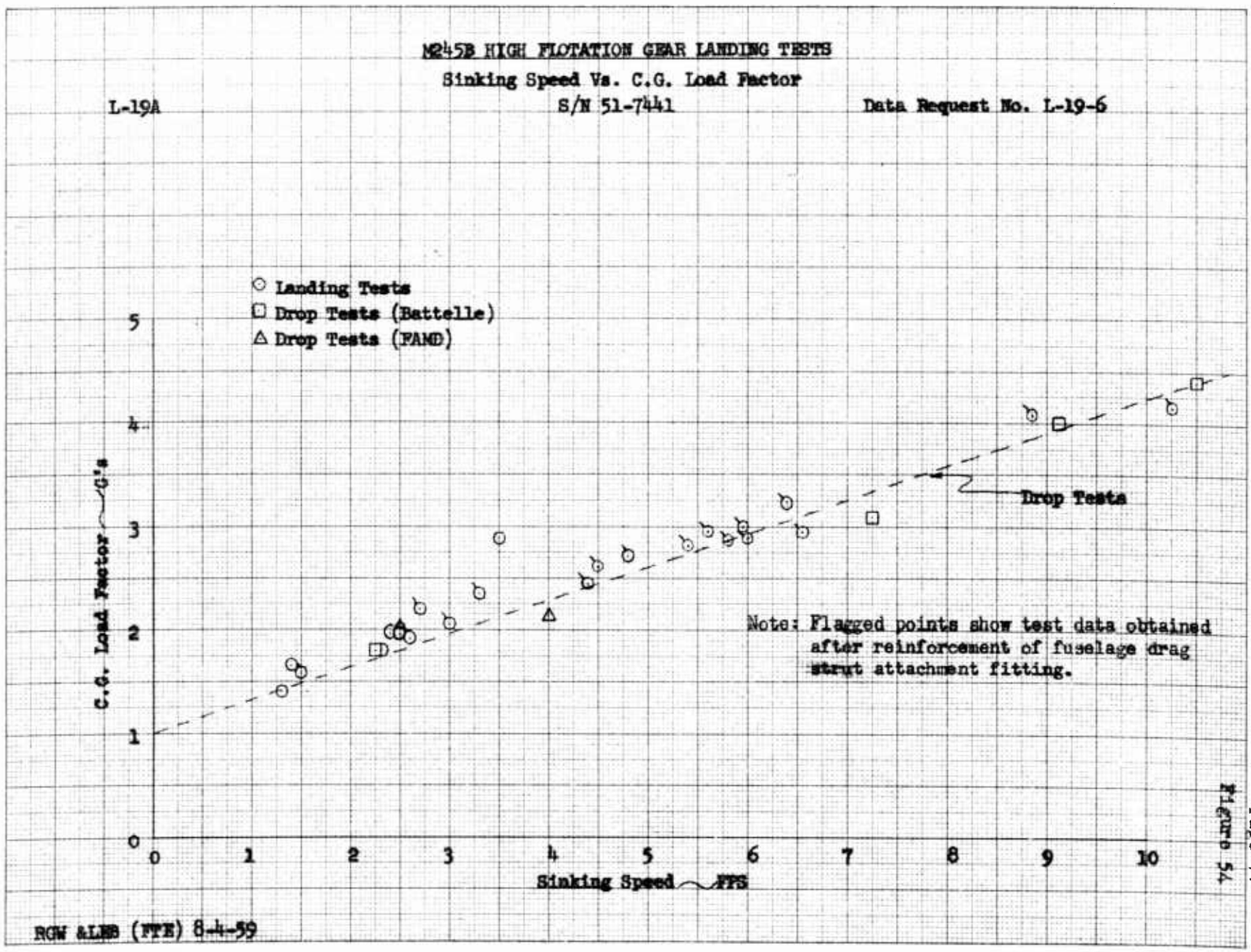

Figure 54

FT245-1

Figure 55

M-245B HIGH FLOTATION GEAR LANDING TESTS

Sinking Speed Vs. Initial Drag Strut Axial Load

S/N 51-7441 Data Request No. L-19-6B

L-19A

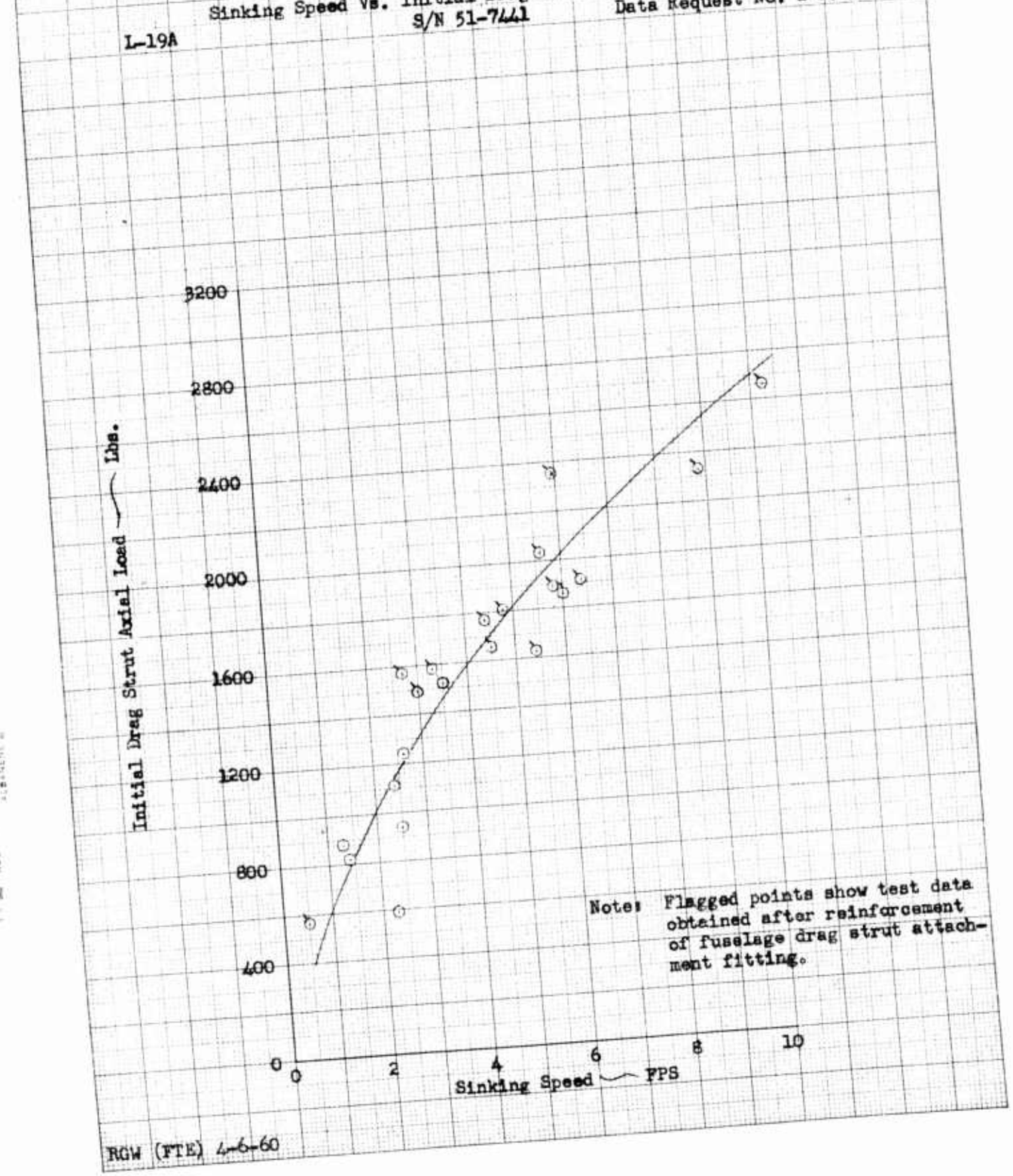

Note: Flagged points show test data obtained after reinforcement of fuselage drag strut attachment fitting.

RGW (FTE) 4-6-60

Figure 56

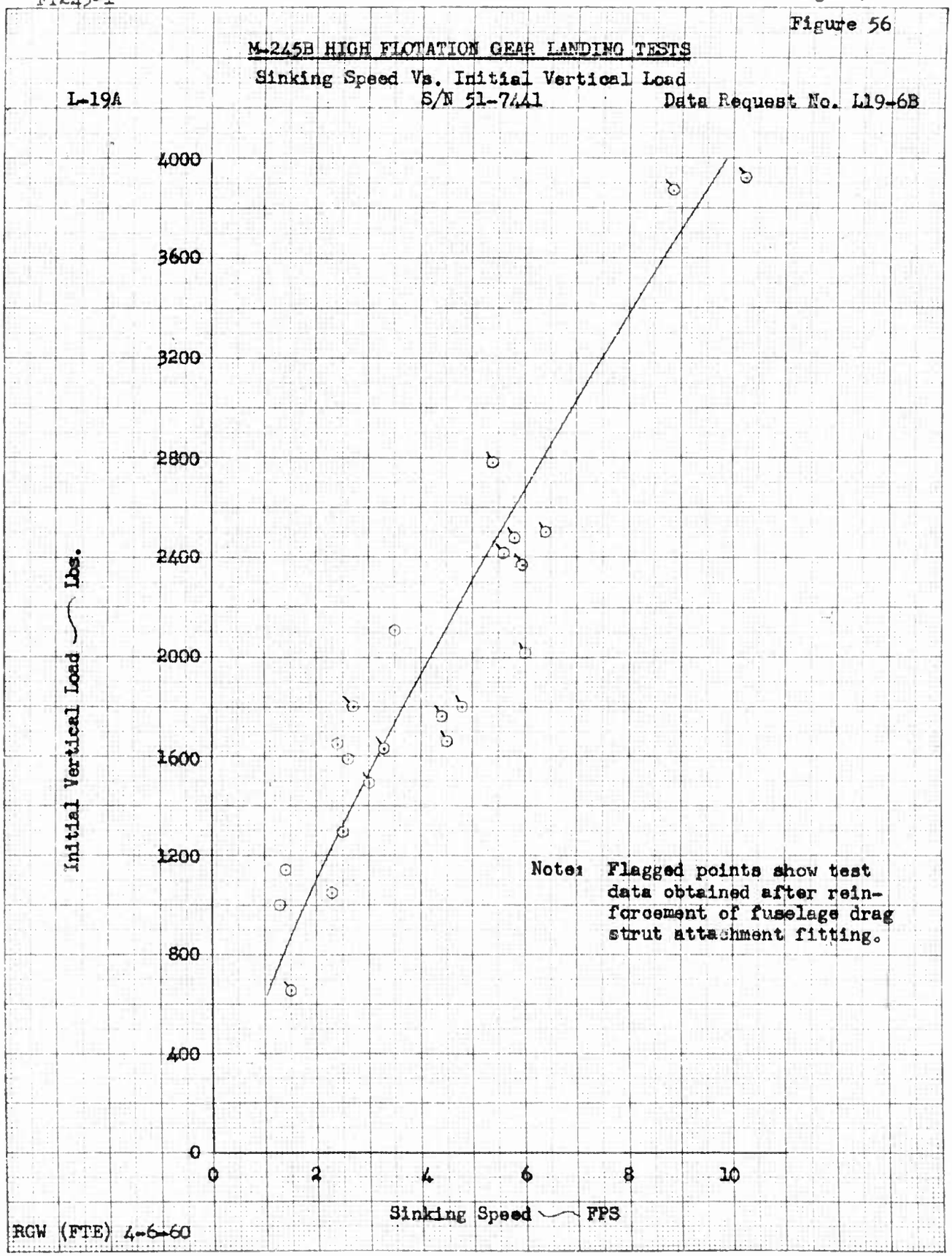

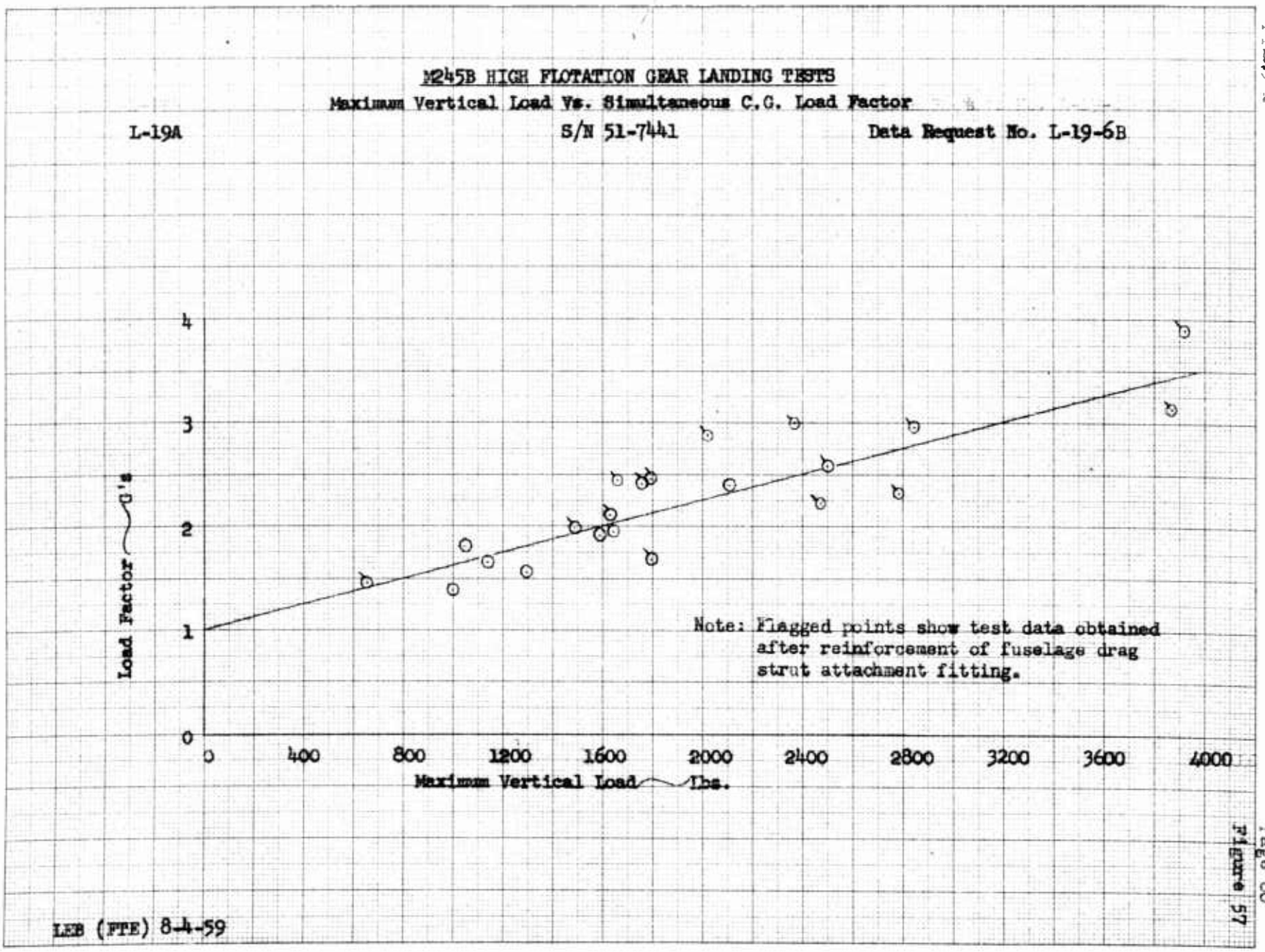

Figure 58

M245B HIGH FLOTATION GEAR LANDING TESTS

Maximum C.G. Load Factor Vs. Simultaneous Vertical Load

L-19A S/N 51-7441 Data Request No. L-19-6 B

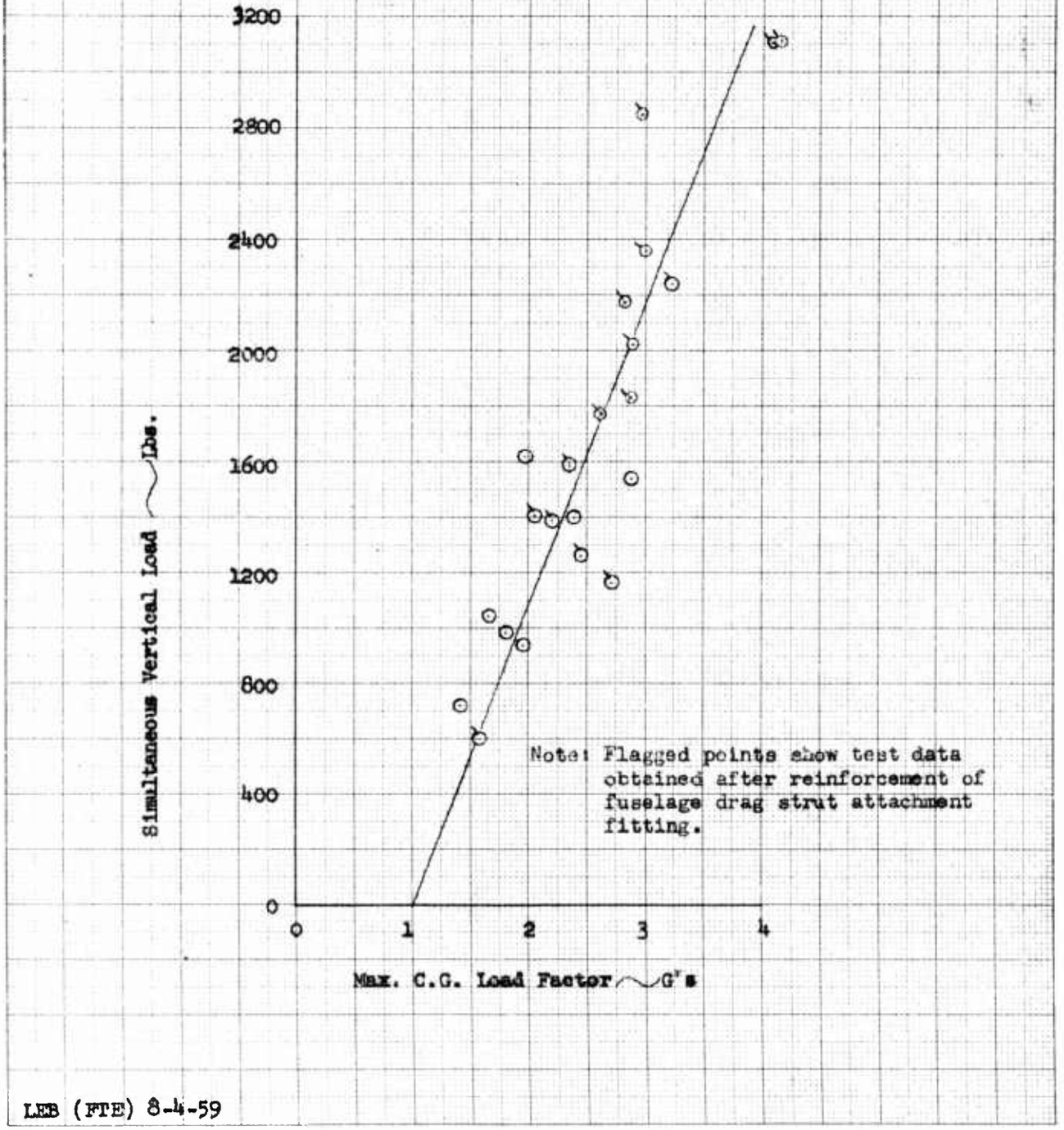

LEB (FTE) 8-4-59

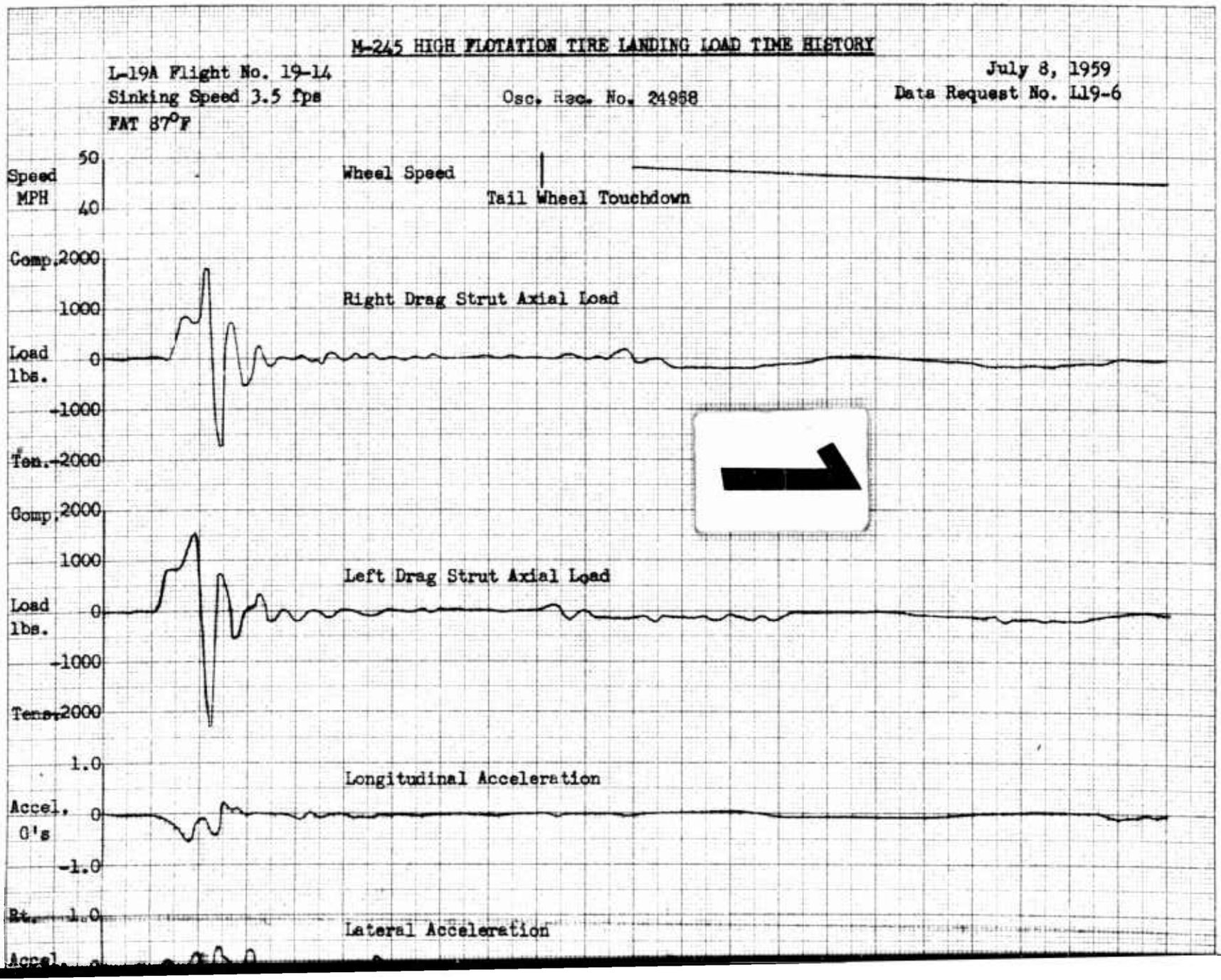

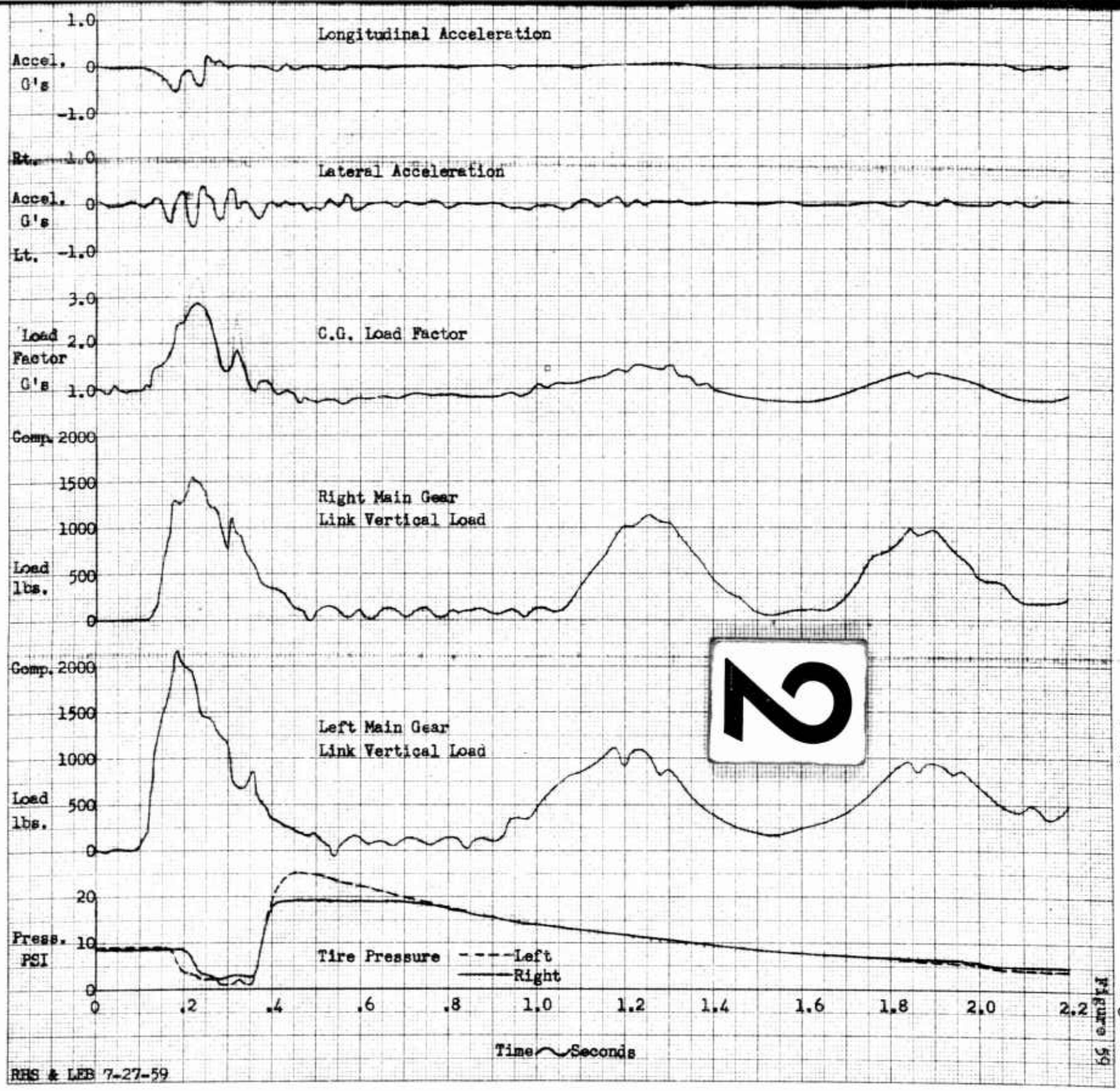

FT275-1

Page 82

Figure 59

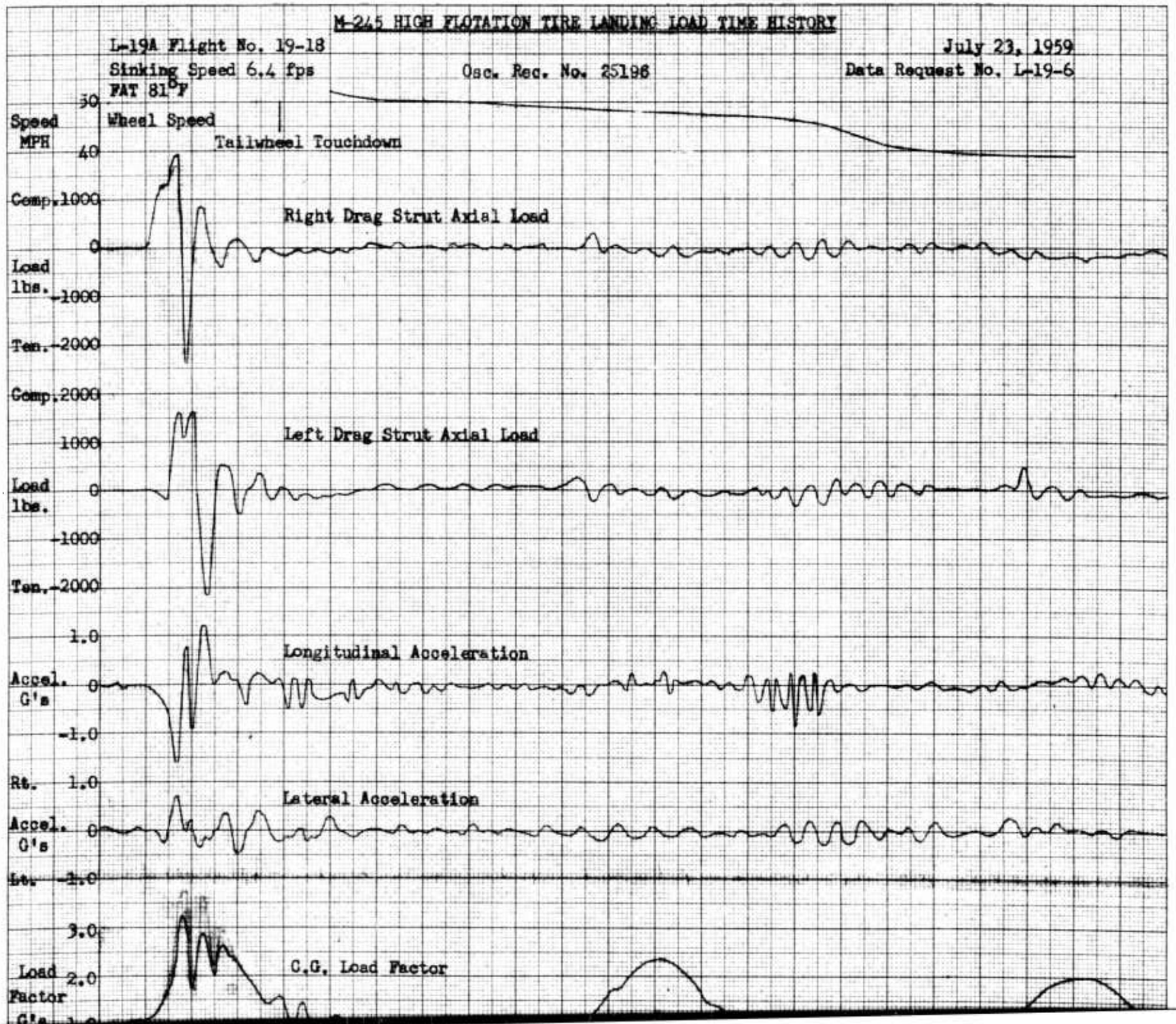

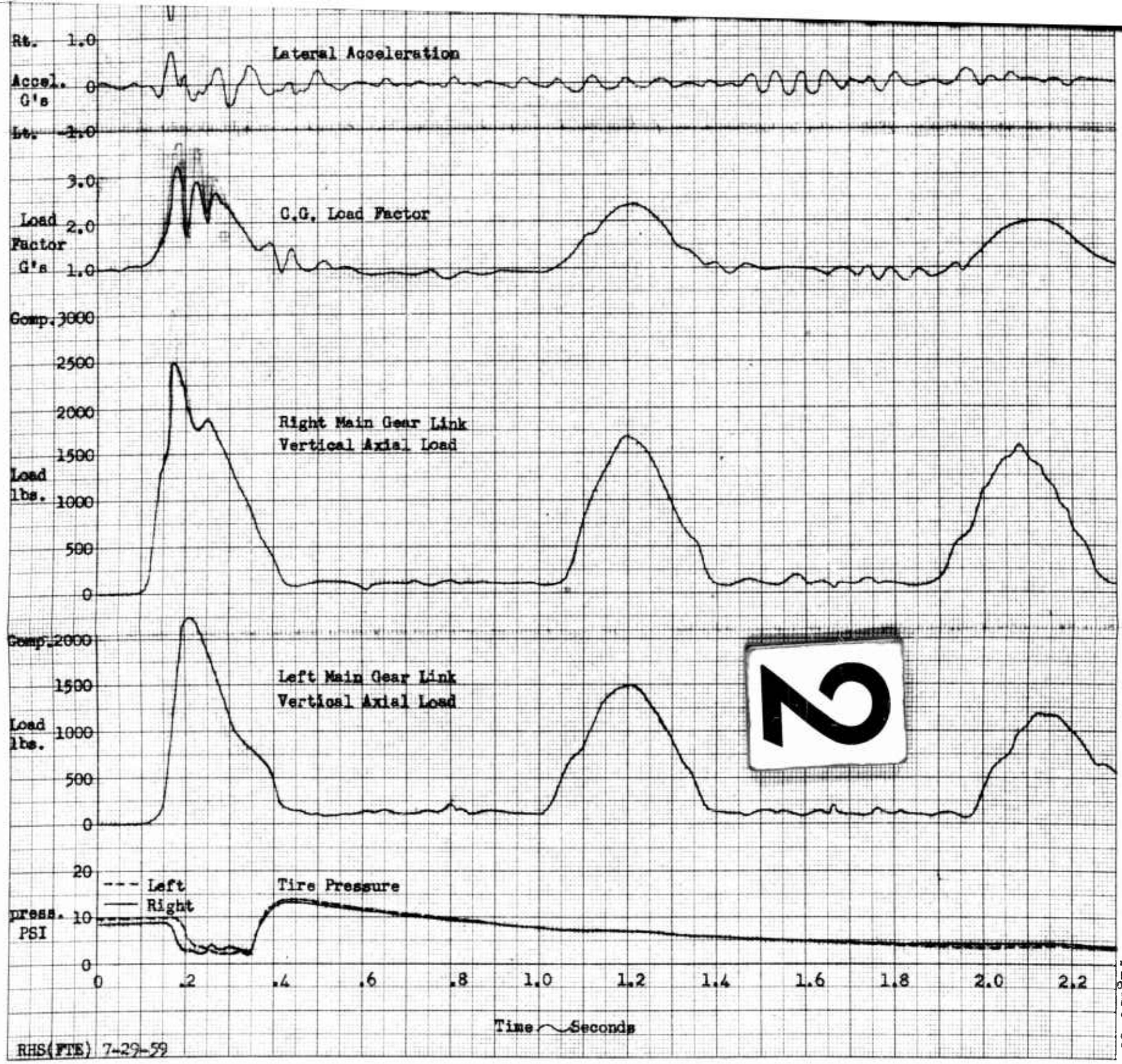

FT245-1

Page 83
Figure 60

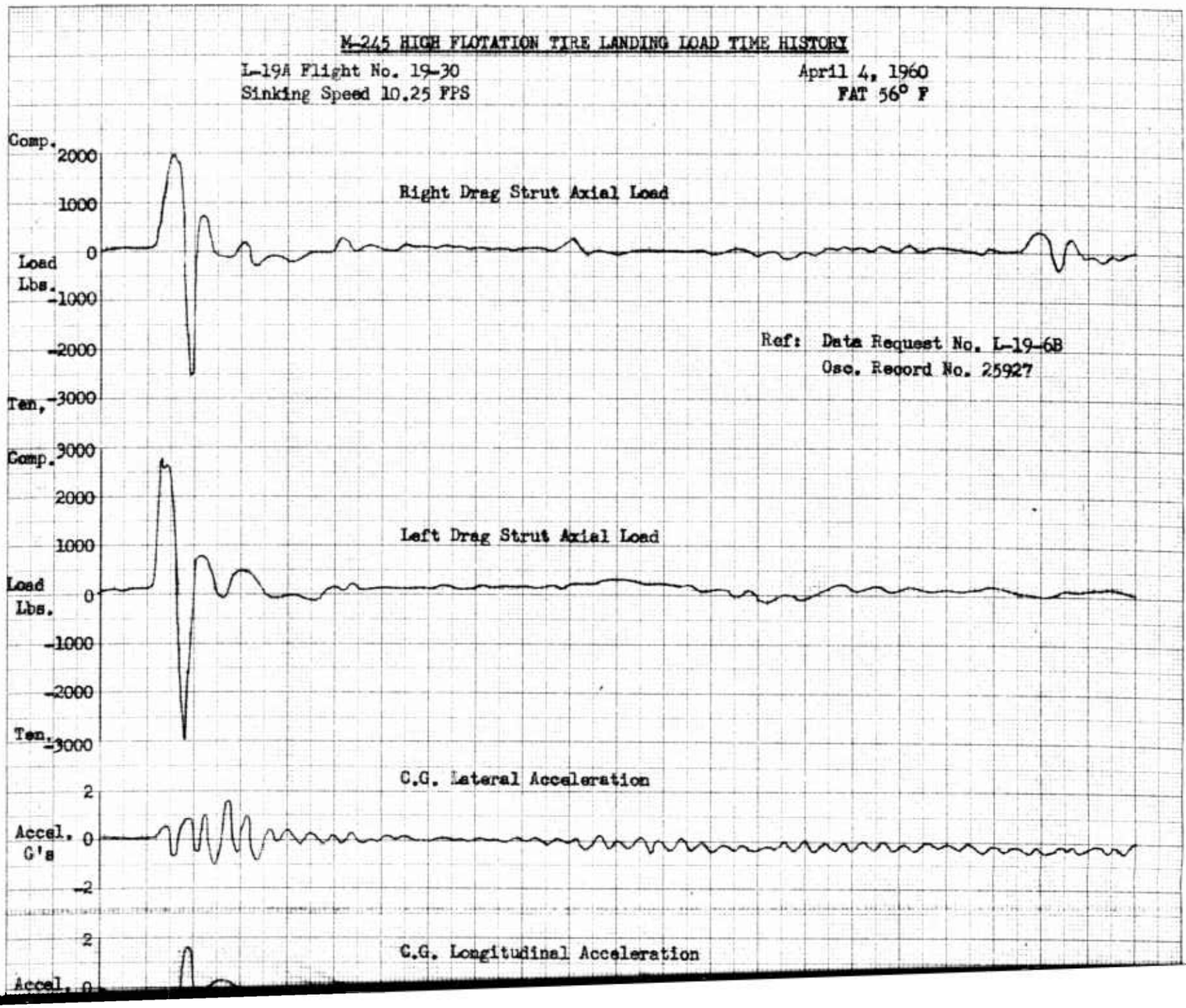

Figure 60A

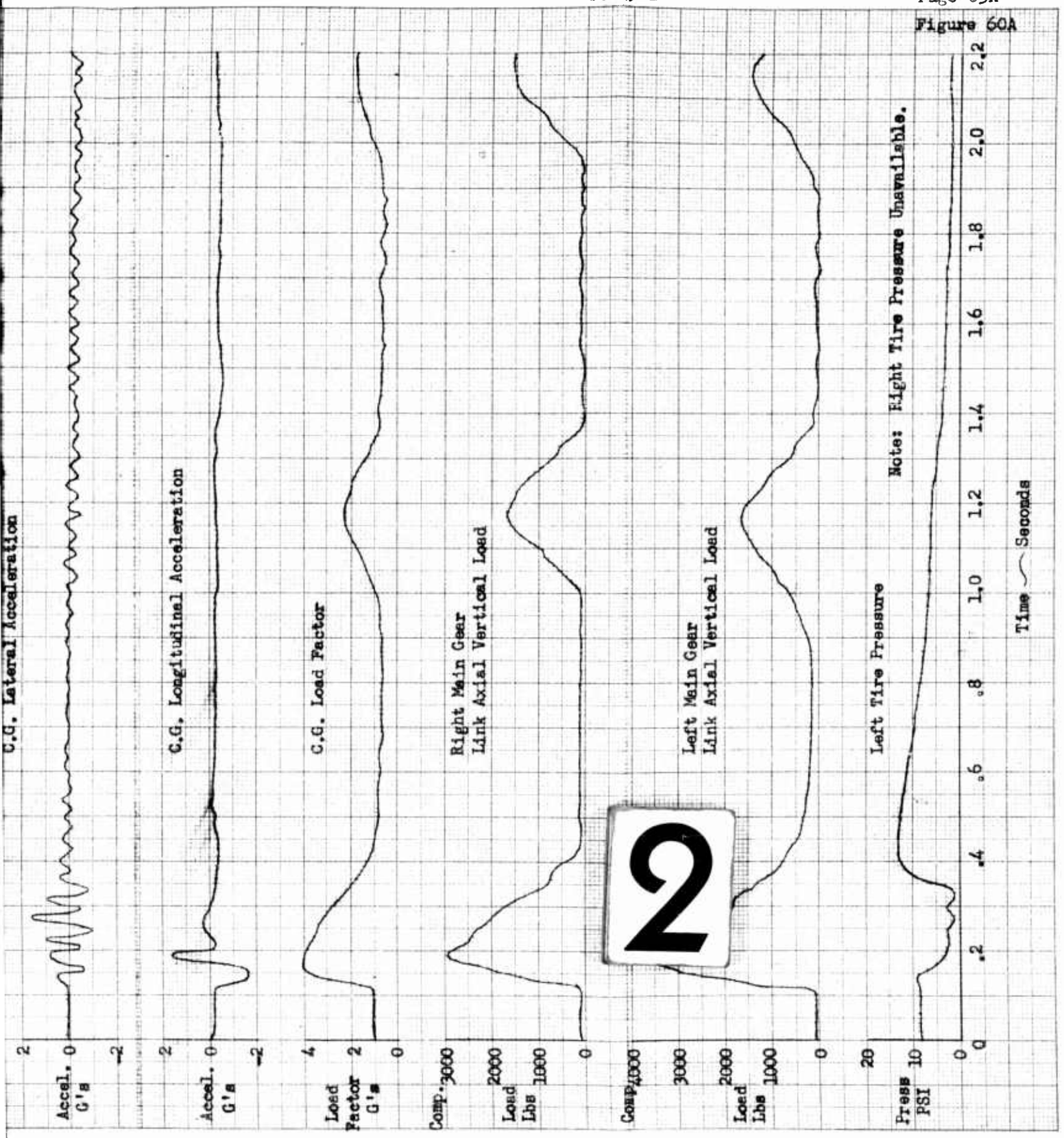
C.G. Lateral Acceleration
Accel. G's
2
0
-2
C.G. Longitudinal Acceleration
Accel. G's
2
0
-2
C.G. Load Factor
Load Factor G's
4
2
0
Right Main Gear
Link Axial Vertical Load
Comp.
3000
2000
1000
0
Load Lbs
Left Main Gear
Link Axial Vertical Load
Comp.
3000
2000
1000
0
Load Lbs
Left Tire Pressure
Note: Right Tire Pressure Unavailable.
Press PSI
20
10
0
0
.2
.4
.6
.8
1.0
1.2
1.4
1.6
1.8
2.0
2.2
Time — Seconds

Figure 61

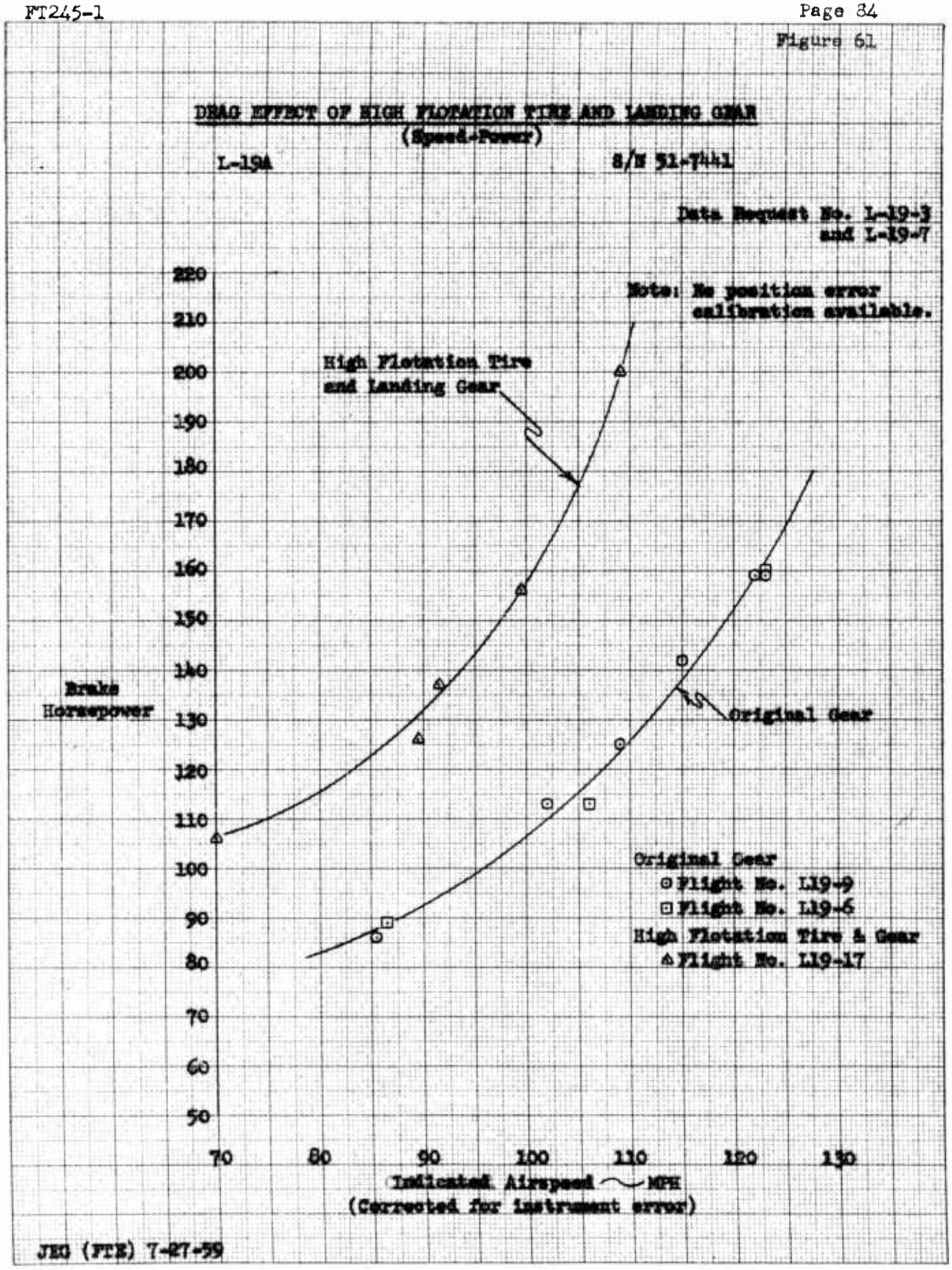

L-19A TAKE-OFF PERFORMANCE - ORIGINAL GEAR

Flight No. L-19-7, L-19-8 S/N 51-7441 May 4, 1959

Data Source: Photo Theodolite Data Request L-19-4

BHP 184

Run No. 9

Gr. Wt. 2400 lbs Flaps 30°

Wind Calm F.A.T. 22° C

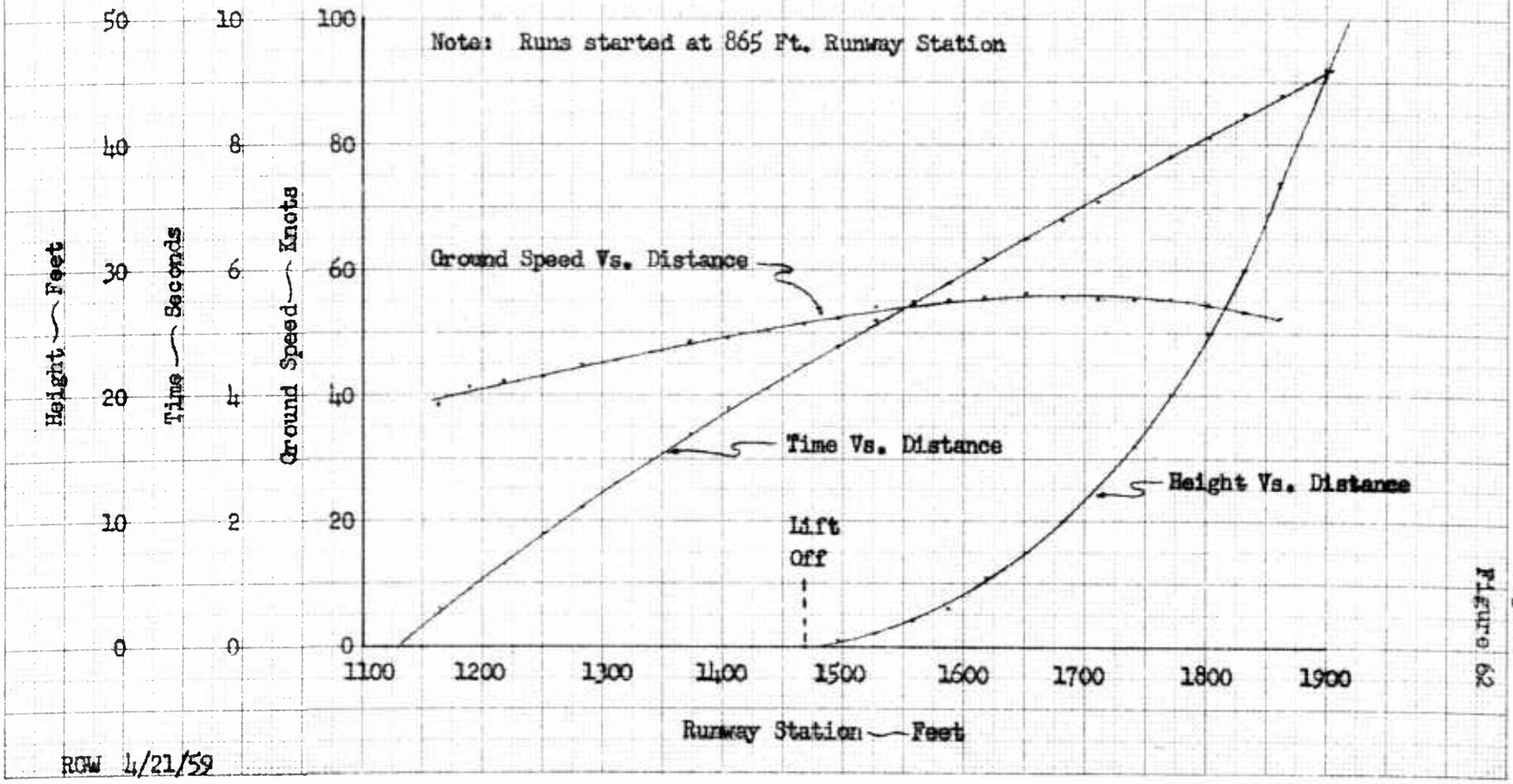

RGW 4/21/59

Figure 62

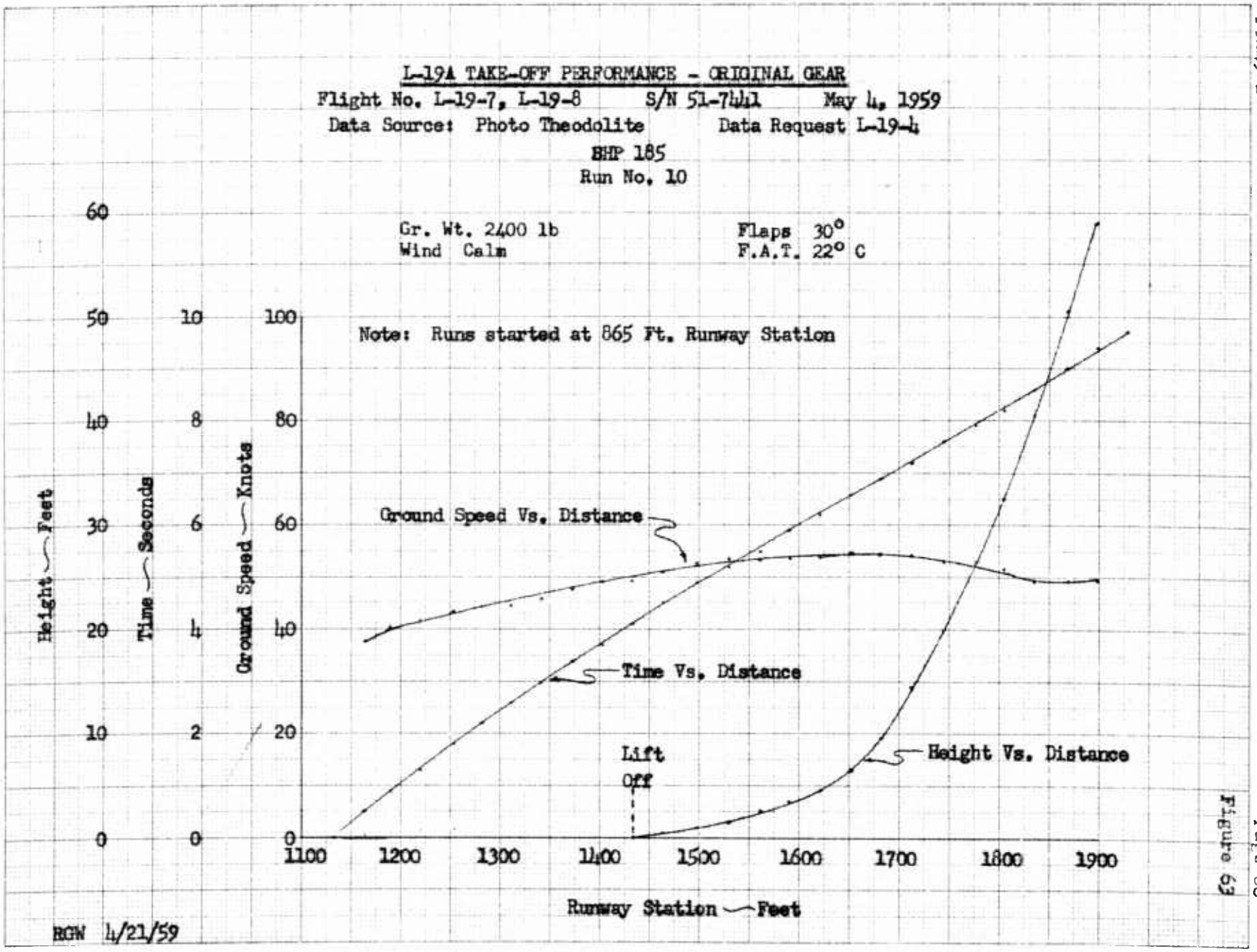

Figure 63

L-19A TAKE-OFF PERFORMANCE - ORIGINAL GEAR

Flight No. L-19-7, L-19-8 S/N 51-7441 May 4, 1959
Data Source: Photo Theodolite Data Request L-19-4
Run No. 11

Gr. Wt. 2400 lb
Wind 2 MPH

Flaps 30°
F.A.T. 22° C

Note: Runs started at 865 Ft. Runway Station

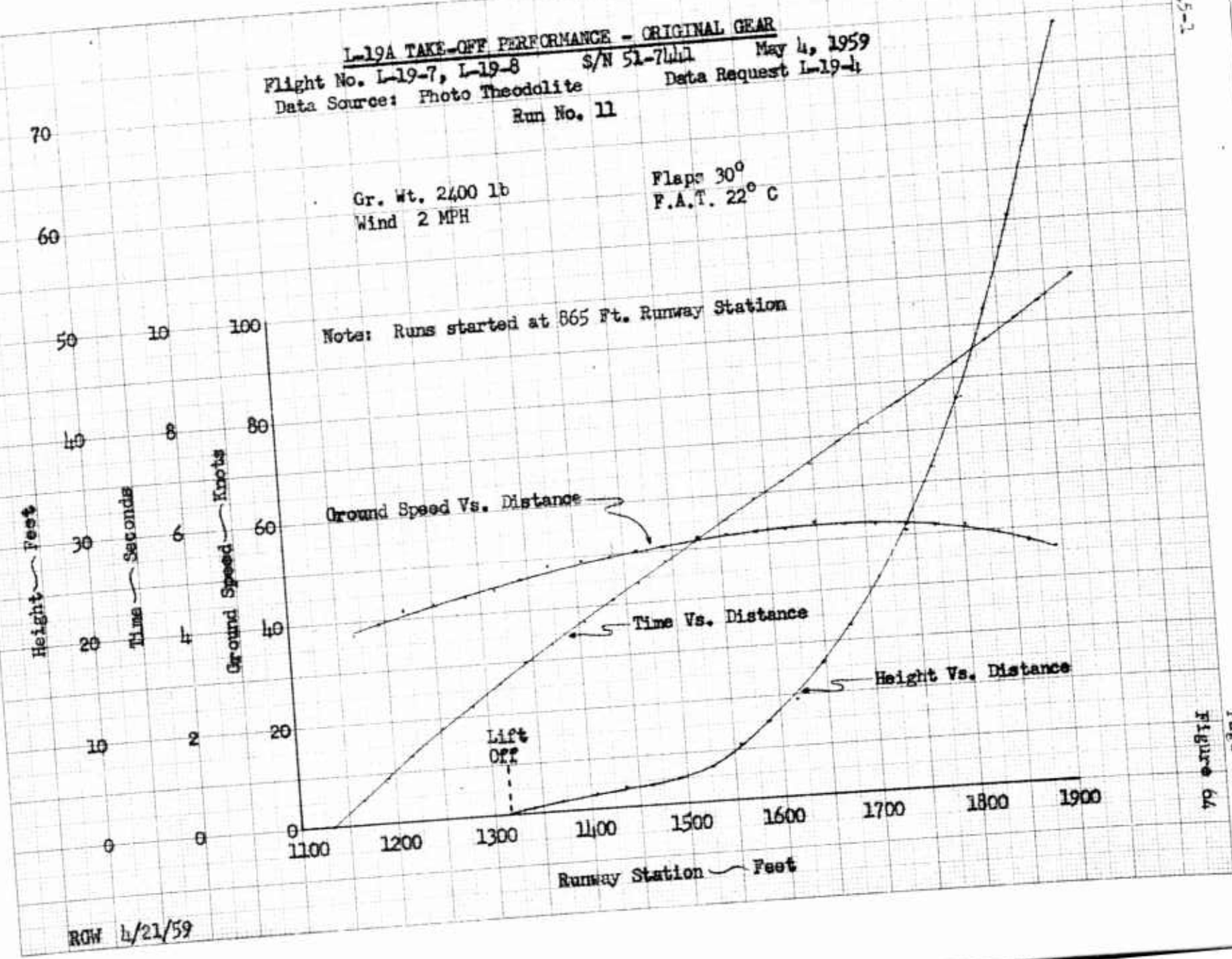

RGW 4/21/59

Figure 64

FT247-1

L-19A TAKE-OFF PERFORMANCE - HIGH FLOTATION GEAR

Flight No. L-19-18 S/N 51-7441 July 23, 1959

Data Source: Photo Theodolite Data Request L-19-8

Run No. 1

Gr. Wt. 2400 lbs Flaps 30°

Wind 1.4 mph F.A.T. 27° C

Note: Runs started at 970 Ft. Runway Station

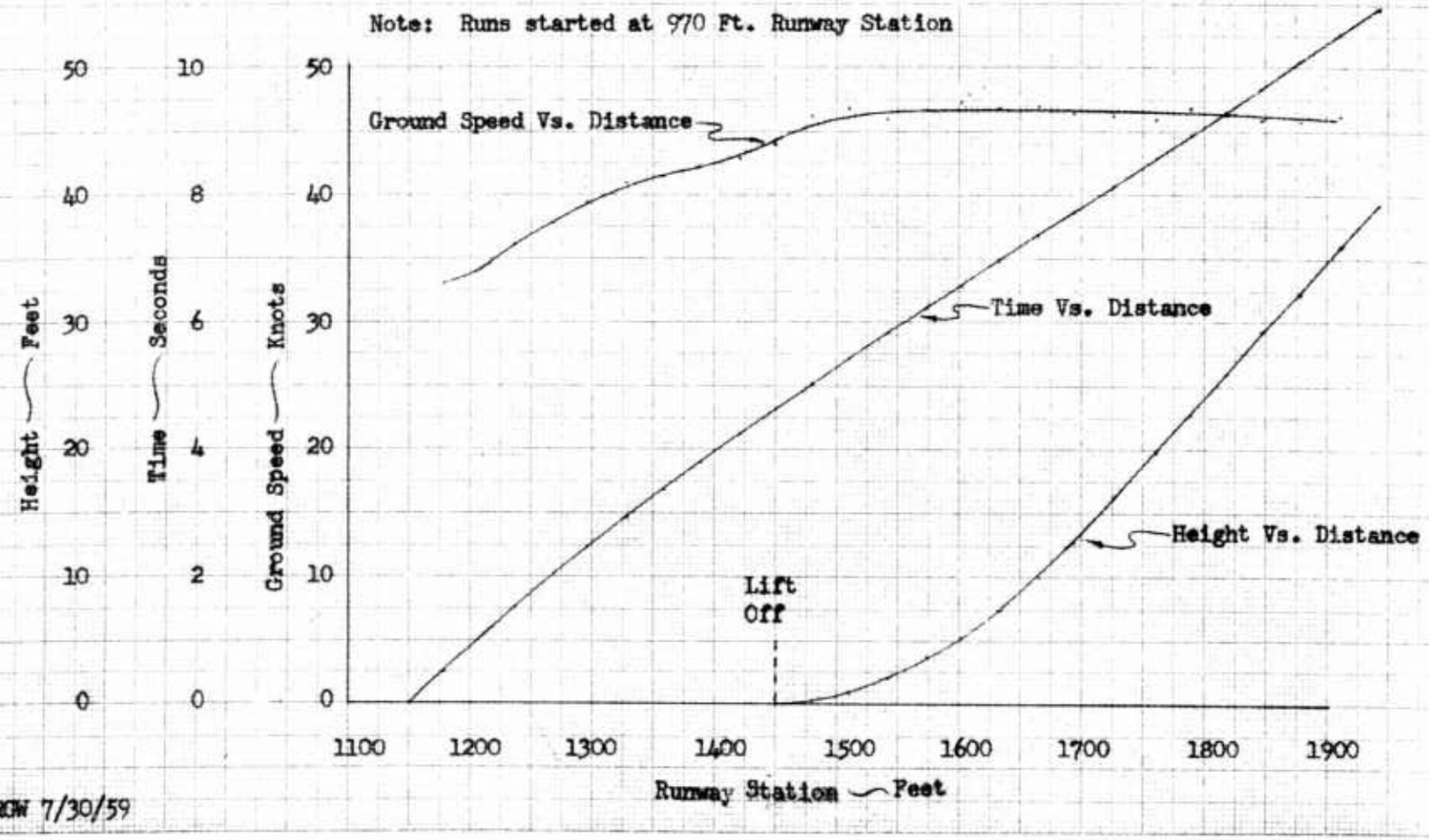

HGW 7/30/59

Figure 65

L-19A TAKE-OFF PERFORMANCE - HIGH FLOTATION GEAR

Flight No. L-19-18 S/N 51-7441 July 23, 1959
Data Source: Photo Theodolite Data Request L-19-8
Run No. 5

Gr. Wt. 2400 lbs Flaps 30°
Wind 1.8 mph F.A.T. 28° C

Note: Runs started at 970 Ft. Runway Station

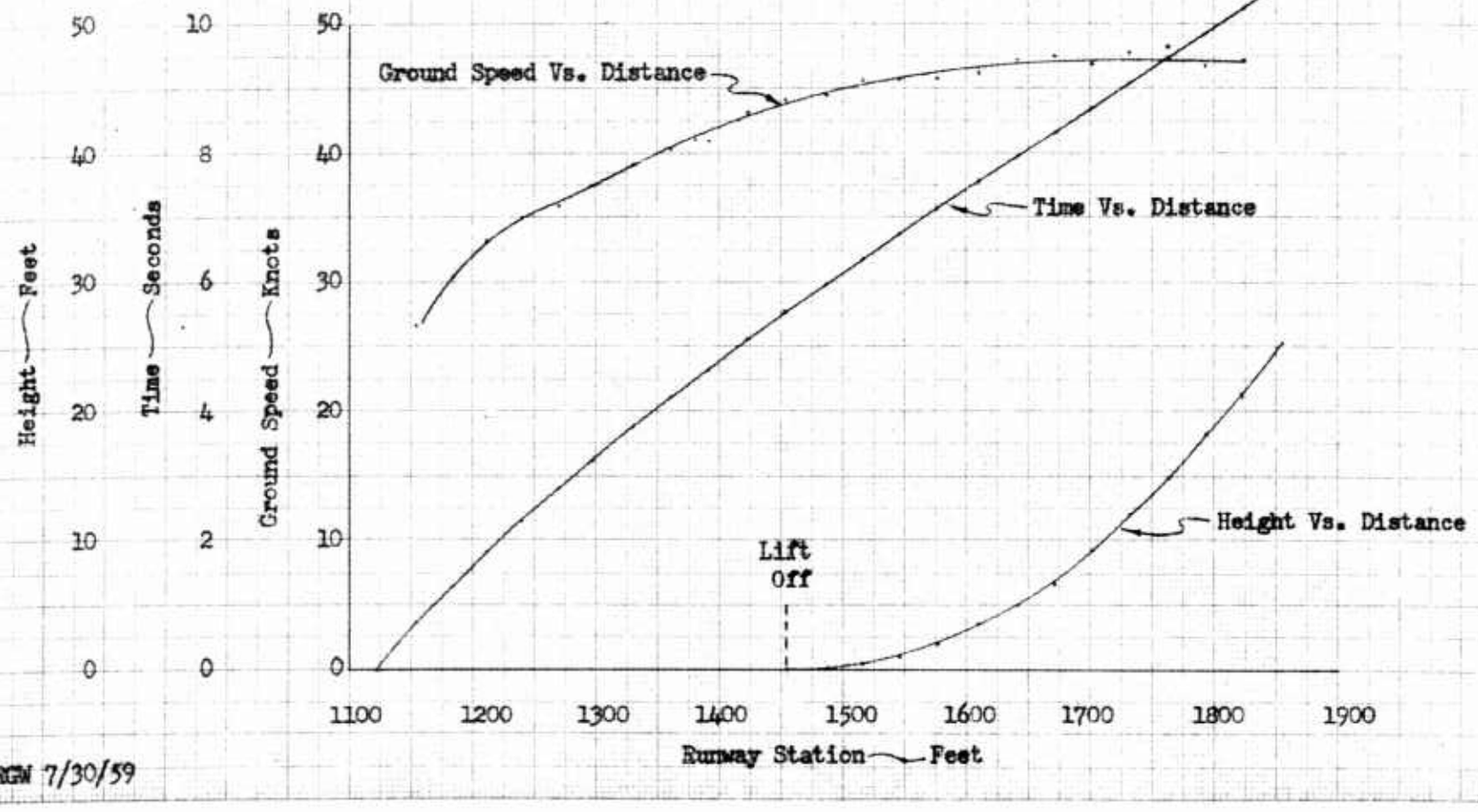

RGW 7/30/59

Figure 66

SUBJECT:- INITIAL FLIGHT TESTS, HIGH FLOTATION LANDING GEAR

TABLE I

L-19A COMPARATIVE PERFORMANCE DATA

Take-off

Data Request No. L19-8

ITEM	RUN NO.				
	Original Landing Gear 30° Flaps			High Flotation Gear 30° Flaps	
	9	10	11	1	5
Gross Weight (lbs)	2400	2400	2400	2400	2400
C.G. Location (% m.a.c.)	33.6	33.6	33.6	29.8	29.8
Head-wind (mph)	0	0	2.0	1.4	1.8
F.A.T. (°C)	22.0	22.0	22.0	27.5	28.5
Pressure Altitude (feet)	510	510	510	490	490
Ground Speed at lift-off (mph)	58.1	56.4	52.6	50.9	50.8
Lift-off Speed (kts, V_c)	56.7	55.0	53.4	50.5	51.0
Observed Ground Dist. (feet)	605	570	450	480	485
Observed Air Dist. to 50' (feet)	450	435	535	595	595
Observed Total Dist. (feet)	1055	1005	985	1075	1080
Manual Scheduled Lift-off Vc	53	53	53	53	53
Manual Ground Dist. (feet)	610	610	580	650	660
Manual Air Dist to 50' (feet)	410	410	420	450	460
Manual Total Dist (feet)	1020	1020	1000	1100	1120
Observed Total Dist/Man. Total Dist	1.034	0.985	0.985	0.977	0.964
Reference Figure No.	62	63	64	65	66

SUBJECT:- INITIAL FLIGHT TESTS, HIGH FLOTATION LANDING GEAR

TABLE IIA

LOG OF TESTS

Original L-19 Landing Gear

L-19A Serial No. Army 51-7441

Gross Weight 2400 lb, c.g. 33.6% m.a.c. at Take-off

Flight No. Date and Duration	Purpose	Remarks
1 4-22-59 10 min.	Comparative acceleration and gear load data during landings. Runs over 2-inch obstacle.	Tube stem of tail tire damaged.
2 4-29-59 5 min.	Same as Flight 1.	Satisfactory landing and obstacle run data obtained.
3 4-29-59 25 min.	Speed-power	Power determination not satisfactory due to instrumentation.
4 4-29-59 5 min.	Runs over 2-inch obstacle with sand ramp. Gear loads turning on concrete.	Turning radius tests dropped because of steerable tail wheel. Gear loads satisfactory.
5 5-1-59 5 min.	Runs over 2-inch obstacle at increased speed. Gear loads turning on sod.	Satisfactory data.
6 5-4-59 20 min.	Speed-power	Rough plot of data indicated results not satisfactorily comparable with power curve.
7 5-4-59 25 min.	Performance take-off and landings.	Camera runway coverage was inadequate for complete run to 50 ft over obstacle at the test weight.
8 5-4-59 25 min.	Repeat of Flight 7.	Satisfactory data obtained by starting runs nearer the downwind end of the runway.
9 5-5-59 25 min.	Speed-power.	Satisfactory data. Tests with original gear completed.

Total flight time L-19A with original gear, 2 hours 25 minutes.

TABLE IIB

LOG OF TESTS (cont'd)

M-245B High Flotation Landing Gear Installed with Simplified Inflation System

L-19A

Serial No. Army 51-7441
Pilot: R. V. Ford

Ground Test No. and Date	Purpose	Remarks
- 5-21-59	Functional checks of inflation system.	Inflation system adequate for ground tests. No data.
1 5-22-59	2-inch obstacles at 10-40 mph tire pressure 4 and 6.5 psi.	Satisfactory data obtained. Twin obstacles endanger tailwheel.
2 5-25-59	2-inch obstacle, 10-30 mph at 3.7 and 5.0 psi tire pressure.	Data indicated that obstacle tests at 5.0 psi may exceed drag load limits at higher speeds.
3 5-25-59	Rechecks of above with reduced attenuation.	Satisfactory data obtained. Drag loads near limits.
4 5-27-59	Rolling characteristics over ditch at 5-25 mph and 4.9 psi tire pressure. Taxi check at 2.7 psi tire pressure.	No heat buildup. Some wrinkles at slow speeds. No wrinkles observed at 35 mph.
5 5-27-59	Obstacles 4" and 2", 10-25 mph 2.7 psi tire pressure.	Data satisfactory.
6 5-28-59	Taxi runs. 6" obstacles. 2.7 psi tire pressure. Up to 27 mph calibrated wheel speed.	" "
7 6-3-59	8 inch obstacles; 4" deep ditch 2.7 psi tire press, 10-30 mph	" "
8 6-3-59	8" obstacles; slow speeds, 6" deep ditch, 2.7 psi	" "
9 6-4-59	6 3/8" and 8" obstacles; 4" and 6" deep ditches. Up to 36.0 mph	" "
10 6-4-59	Obstacles 4 1/4", 6 3/8". 8-10 mph and 6" deep ditch 25-30 mph	" "

TABLE IIB - continued

LOG OF TESTS (continued)

M-245B High Flotation Landing Gear Installed
with Simplified Inflation System

L-19A

Serial No. Army 51-7441
Pilot: R. V. Ford

Ground Test No. and Date	Purpose	Remarks
11 6-5-59	Ditch 4" and 8" deep; 2.7 psi tire pressure. Obstacles 2 1/8" and 4 1/4".	Data satisfactory.
12 6-8-59	4 1/4" obstacle at 2.7 and 3.7 psi tire pressure. Ditch 6" and 8" deep; 2.7 psi tire pressure.	" "

TABLE IIC
LOG OF TESTS
M-245B HIGH FLOTATION LANDING GEAR

L-19A

Serial No. Army 51-7441
Pilot: R. V. Ford

Flight No. Date and Duration	Purpose	Remarks
10* 7-1-59 15 min.	Functional tests of flight inflation system with quick reinflation.	Power-off stalls normal with T.O. and landing flap. On landing good shock absorption and quick reinflation gave smooth roll-out. Oil temperature reached limits.
11 7-6-59 15 min.	Landing tests. Quick reinflation to 5 psi.	Control satisfactory on lift-off and landings. Power-on stalls (2300 rpm) normal.
12 7-7-59 10 min.	Landing tests.	Late exhaust on right gear. Some directional difficulty believed due to tail wheel shimmy.
13 7-7-59 5 min.	Demonstration landing. Wing camera installed.	Tail wheel assembly bolts tightened and improvement resulted in tail wheel shimmy.
14 7-8-59 20 min.	Heavy landing for directional check and tire characteristics.	Satisfactory data obtained. No difficulty with tail.
15 7-21-59 10 min.	Demonstration. Increased speeds on obstacles and ditch.	Drag strut reinforcement installed. Tail spring satisfactory. Left tire wearing considerably where sidewalls contact ground at low pressure.
16 7-22-59 10 min.	Demonstration for AF and Army. Landings, ditch and obstacles. Increased landing loads.	Time history of one landing made. Approximately 4-inch bounce with 3 fps sinking speed.
17 7-23-59 25 min.	Speed power	Five speed power points obtained. Oil temperature 7° C over the 108° limit.
18 7-23-59 45 min.	Performance take-off Taxi in soft soil and mud.	Time history of one landing, 6-4 fps. (Figure 60)

* Note that first nine flights were with standard L-19 landing gear (Table IIA)

SUBJECT:- INITIAL FLIGHT TESTS, HIGH FLOTATION LANDING GEAR

TABLE IIC - continued

LOG OF TESTS

M-245B HIGH FLOTATION LANDING GEAR

Flight No. Date and Duration	Purpose	Remarks
19 7-24-59 5 min.	Demonstration landing on runway.	
20 7-24-59 5 min.	Taxi on soft soil and mud.	Tires throw mud into propeller. No problem in soft dry soil. Taxiied over mud where 4-wheel drive jeep stalled.
21 7-27-59 25 min.	Improved technique in landing. Check landing without quick-reinflation.	Nose high power approach with 60° flaps gives better rate of descent control.
22 7-28-59 10 min.	Landing checks without quick reinflation.	No notable change in bounce even with 3 point landing.
23 7-28-59 10 min.	Demonstration for Marines.	Landing, obstacles 6 3/8 and 8 inch, ditches 24 x 6 and 24 x 8 inch.
24 7-28-59 20 min.	Rough sod landing.	No problem with minor obstacles but wide ditch produced bad bounce during taxi, 15-20 mph.
25 7-29-59 15 min.	Demonstration.	Quick reinflation disconnected. (Same as Flight 23.)
26 3-29-60 5 min.	Post periodic inspection test flight.	Flight terminated early due to smoke in cockpit. Attributed to hot oil in windshield de-froster duct.
27 3-29-60 10 min.	Instrumentation check-out. High rate of descent landings.	Quick reinflation connected. Noticeable bounce on each of two landings.

SUBJECT:- INITIAL FLIGHT TESTS, HIGH FLOTATION LANDING GEAR

DATE January 22, 1960
REVISED April 14, 1960

TABLE IIC - continued

LOG OF TESTS

M-245B HIGH FLOTATION LANDING GEAR

Flight No. Date and Duration	Purpose	Remarks
28 4-1-60 30 min.	High rate of descent landings.	Quick reinflation connected. Four landings accomplished. 8.85 fps max. sinking speed. Airplane inspected - no damage.
29 4-1-60 15 min.	High rate of descent landings.	Quick reinflation connected. Three landings accomplished. 5.95 fps max. sinking speed.
30 4-4-60 10 min.	High rate of descent landings.	Quick reinflation connected. Two landings accomplished. 10.25 fps max. sinking speed. Airplane inspected - no damage.

Total flight time of L-19A with M-245B gear = 5 hours 15 minutes.

Note: In addition to these tests, three flights were made for in-flight folding tests of the tire using a C-119G airplane, AF S/N 53-3136.

July 31, 1959 1135-1210 (0+45)
August 3, 1959 1425-1455 (0+30)
March 23, 1960 1440-1520 (0+40)

On the first flight a tire patch over an internal bungee attachment point blistered severely at altitude and tests with the tire lowered into the slipstream were not considered advisable. The patch was replaced and a second flight was flown during which an attempt to fold the tire at 85 knots was unsuccessful. The tire was modified and successful folding was achieved on the third flight.

Photo 35-182

M-245B gear crossing ditch 24 inches wide, 8 inches deep, at 10-15 mph. Tire pressure is 3 psi.

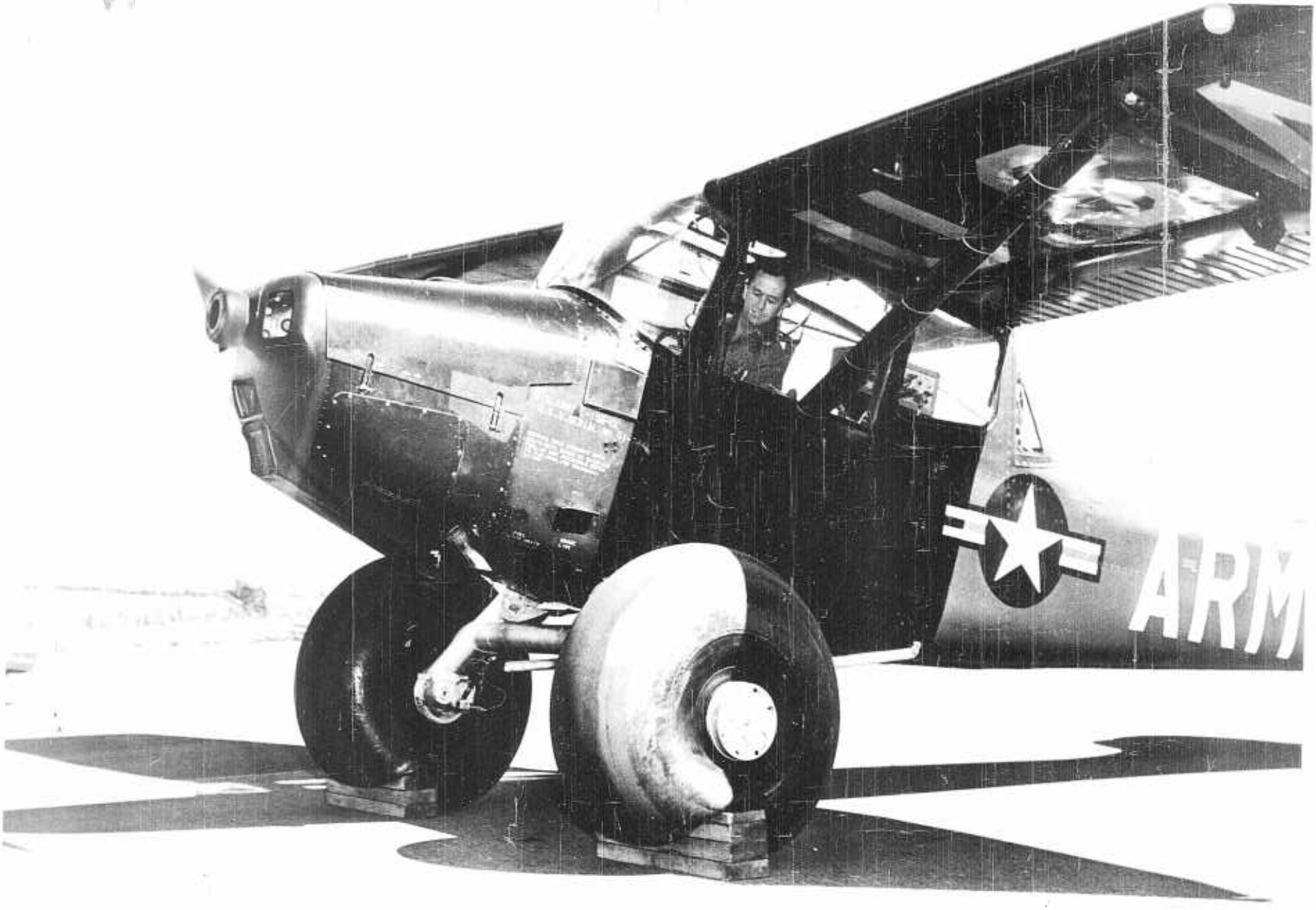

Photo 35-388

M-245B gear crossing 6 3/8 inch and 8 inch obstacles at approximately 8 mph. Tire pressure 2.7 psi.

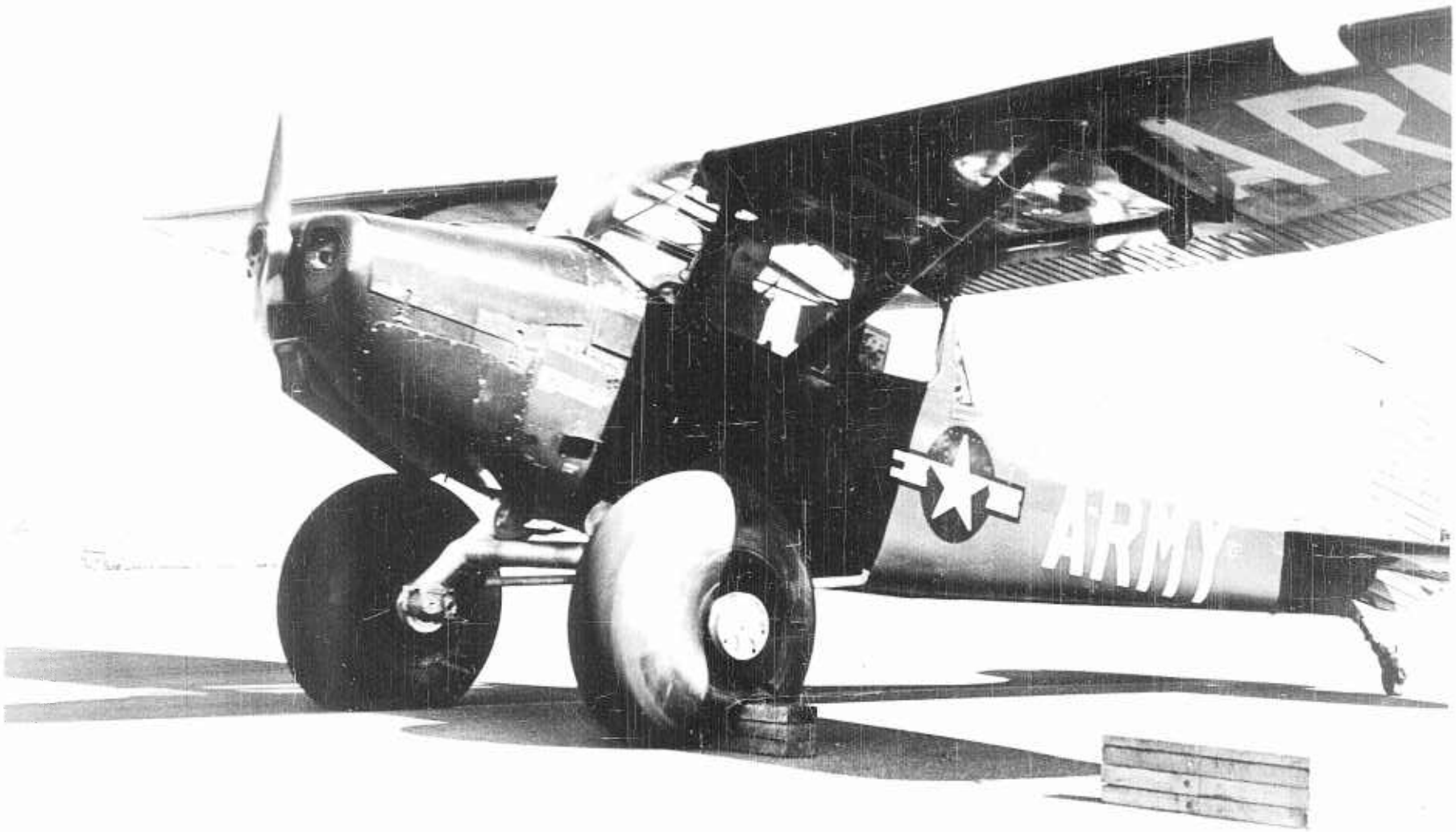

Photo 35-390

M-245B gear crossing 6-3/8 inch obstacle. With 2.7 psi tire pressure this obstacle was negotiated at speeds to 38 mph.

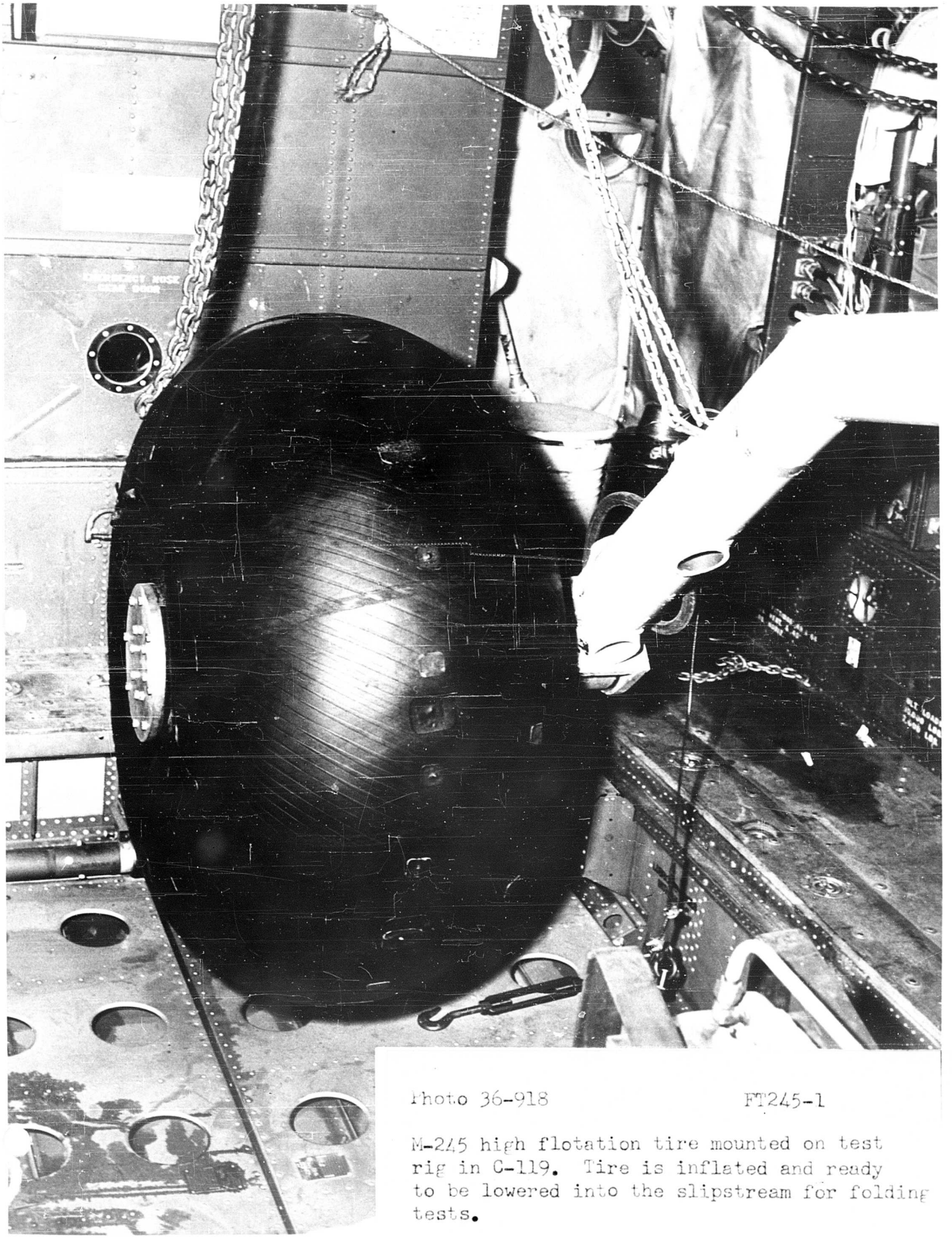

Photo 36-918 FT245-1

M-245 high flotation tire mounted on test rig in C-119. Tire is inflated and ready to be lowered into the slipstream for folding tests.

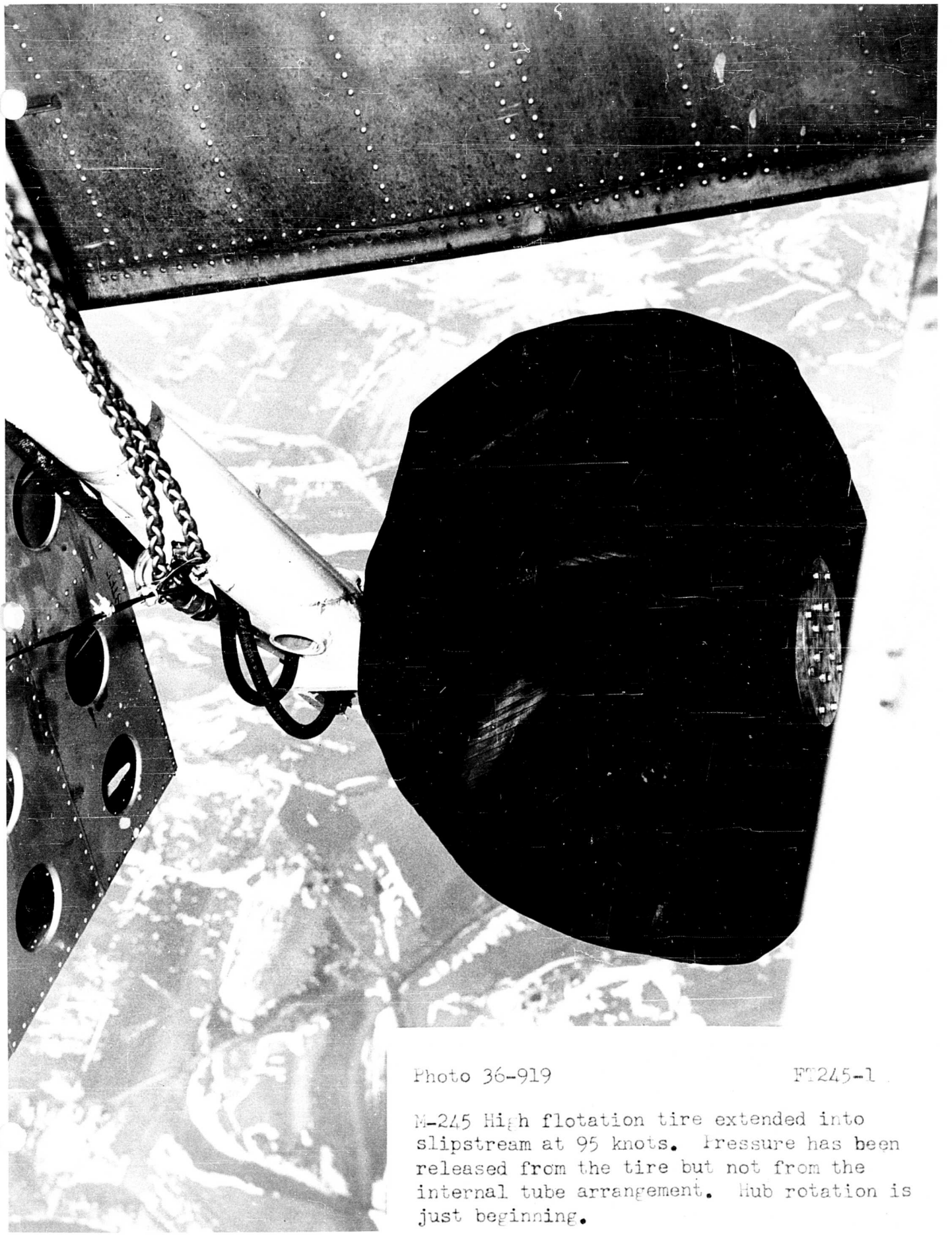

Photo 36-919 FT245-1

M-245 High flotation tire extended into slipstream at 95 knots. Pressure has been released from the tire but not from the internal tube arrangement. Hub rotation is just beginning.

Photo 36-920 FT245-1

M-245 high flotation tire during folding cycle. Hub rotation has begun. Tire pressure is depleted and pressure remains in the internal diagonal tubes.

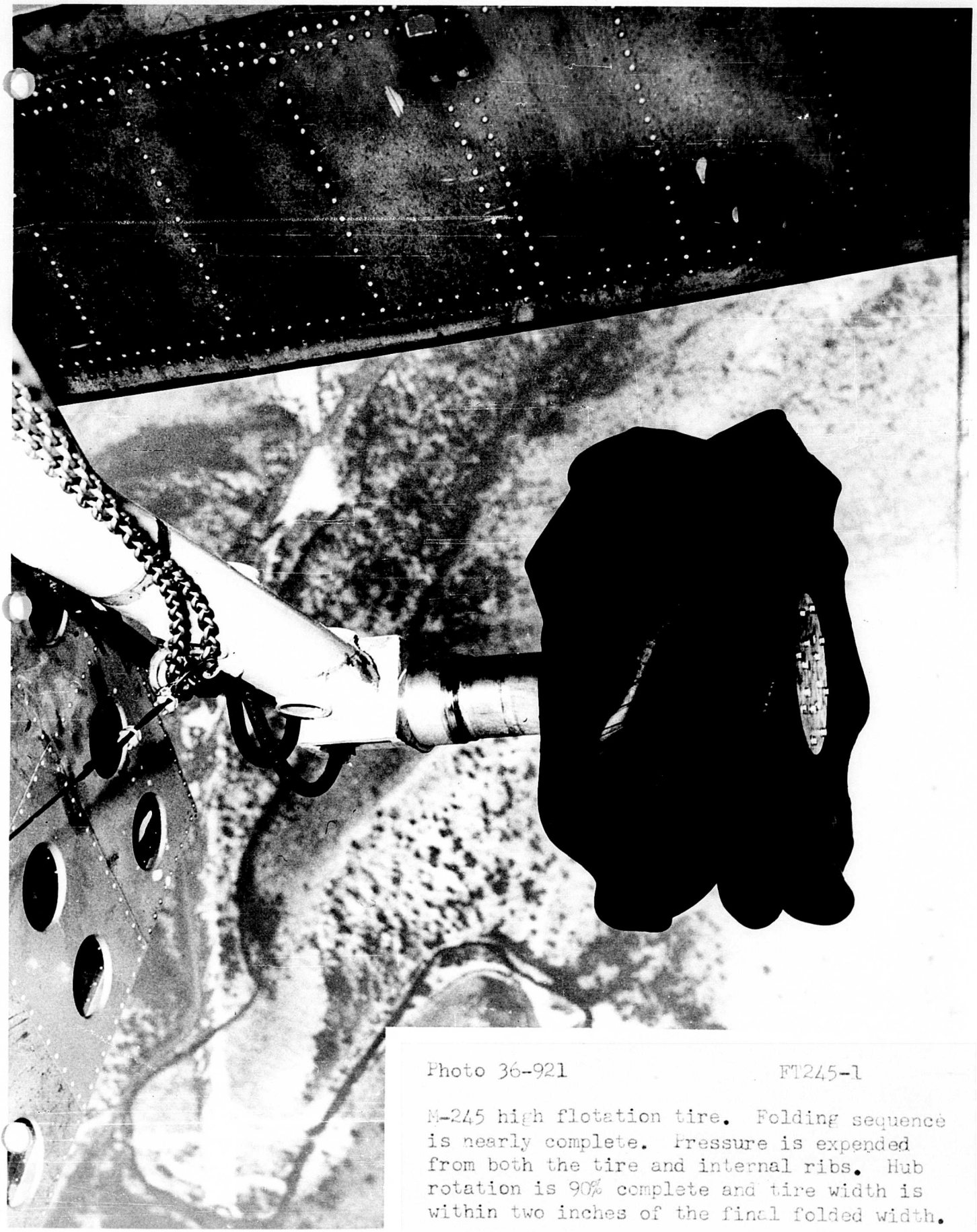

Photo 36-921 FT245-1

M-245 high flotation tire. Folding sequence is nearly complete. Pressure is expended from both the tire and internal ribs. Hub rotation is 90% complete and tire width is within two inches of the final folded width.

FAIRCHILD AIRCRAFT AND MISSILES DIVISION

HAGERSTOWN 10, MARYLAND

SUBJECT LANDING GEAR TEST DATA, M-245 B

PREPARED BY A. J. Atkinson — REPORT NO. FT245-1, Appendix I

CHECKED BY J. A. Clopper — MODEL M-245B

APPROVED BY R. V. Ford — COPY NO.

APPROVED BY D. W. Weller — NO. OF PAGES 90 + i

APPROVED BY R. A. Henson — DATE January 22, 1960

REVISIONS

REVISION DATE	PAGES AFFECTED	APPROVED

NS-800-69B

SUBJECT:- APPENDIX I
LANDING GEAR TEST DATA, M-245B

DATE January 22, 1960
REVISED

LIST OF TABLES

APPENDIX I

SUBJECT:- LANDING GEAR TEST DATA, M-245B

DATE January 22, 1960

REVISED

PURPOSE

To present data obtained in the initial ground and flight tests of the M-245B High Flotation Landing Gear installed on an L-19A aircraft.

REMARKS

The data presented in Tables I through VI is a detailed tabulation of data discussed in Report No. FT245-1. Its publication by this report is for reference and record purposes only.

Details of instrumentation and test configuration are also covered by the above report.

The zero time referenced in these tables is the instant prior to obstacle contact or landing touchdown.

TABLE I

L-19A ORIGINAL TIRE AND LANDING GEAR OBSTACLE LOADS

L-19A Flight No. L-19-2 S/N 51-7441
Test Conditions: Gross Wt. 2390 lbs, C.G. 33.5% m.a.c. Tire Press. 21 psi
2 1/8" Obstacle Data Request No. L-19-1

Item (Event)	Time (Sec)	Vertical Load (Lbs)	Torsional Load (In.Lbs.)	Side Load (Lbs)	Drag Load (Lbs)	C.G. Load Factor (g's)	Long. Acc. (g's)	Forward Velocity (MPH)
Oscillograph Record No. 24343								
Prior to Obstacle	0	1055	795	-51	33			10.0
Initial Drag Load	.025	-138			465			
Drag Load Springback	.050	-193			-851			
Initial Longitudinal Accel.	.025						-.37	
Longitudinal Accel. Rebound	.045						.49	
Maximum C.G. Load Factor (Pos.)	.067					1.40		
Maximum C.G. Load Factor (Neg.)	.200					.92		
Maximum Vertical Load	.045	766						
Vertical Load Rebound	.067	-357						
Maximum Side Load (Outbd.)	.029	- 69		280	268			
Maximum Side Load (Inbd.)	.067	-357		-386	-213			
Maximum Torsion (Drag)	.045		-1695					
Maximum Torsion Springback	.067		2156					
Oscillograph Record No. 24344								
Prior to Obstacle	0	1100	660	-41	41			20.0
Initial Drag Load	.030	-128			476			
Drag Load Springback	.050	-142			-748			
Initial Longitudinal Accel.	.030						-.31	
Longitudinal Accel. Rebound	.050						.42	
Maximum C.G. Load Factor (Pos.)	.070					1.59		
Maximum C.G. Load Factor (Neg.)	.220					.80		
Maximum Vertical Load	.040	803						
Vertical Load Rebound	.070	-484						
Maximum Side Load (Outbd.)	.030	-128		372	476			
Maximum Side Load (Inbd.)	.070	611		-183	310			
Maximum Torsion (Drag)	.040		-1980					
Maximum Torsion Springback	.070		2398					

TABLE I - continued

L-19A ORIGINAL TIRE AND LANDING GEAR OBSTACLE LOADS

L-19A Flight No. L-19-2 S/N 51-7441
Test Conditions: Gross Weight 2390 lbs, C.G. 33.5% m.a.c. Tire Pressure 21 psi
2 1/8" Obstacle Data Request No. L-19-1

Item (Evant)	Time (Sec)	Vertical Load (lbs)	Torsional Load (In Lbs)	Side Load (Lbs)	Drag Load (Lbs)	C.G. Load Factor (g's)	Long. Acc. (g's)	Forward Velocity (MPH)
Oscillograph Record No. 24345								
Prior to Obstacle	0	1205	780	-26	58			10.0
Initial Drag Load	.030	-124			436			
Drag Load Springback	.060	123			-788			
Initial Longitudinal Accel.	.032						-.63	
Longitudinal Accel. Rebound	.080						.52	
Maximum C.G. Load Factor (Pos.)	.090					1.53		
Maximum C.G. Load Factor (Neg.)	.200					.64		
Maximum Vertical Load	.040	451						
Vertical Load Rebound	.095	-219						
Maximum Side Load (Outbd.)	.032	-138		332	427			
Maximum Side Load (Inbd.)	.080	397		-143	- 7			
Maximum Torsion (Drag)	.058		-1723					
Maximum Torsion Springback	.085		1835					
Oscillograph Record No. 24346								
Prior to Obstacle	0	1070	550	-30	-46			20.0
Initial Drag Load	.035	25			654			
Drag Load Springback	.055	176			-431			
Initial Longitudinal Accel.	.010						-.19	
Longitudinal Accel. Rebound	.140						.31	
Maximum C.G. Load Factor (Pos.)	.070					1.51		
Maximum C.G. Load Factor (Neg.)	.180					.76		
Maximum Vertical Load	.075	1010						
Vertical Load Rebound	.180	-563						
Maximum Side Load (Outbd.)	.025	11		398	623			
Maximum Side Load (Inbd.)	.070	185		-390	171			
Maximum Torsion (Drag)	.040		-1217					
Maximum Torsion Springback	.057		3074					

TABLE I - continued

L-19A ORIGINAL TIRE AND LANDING GEAR OBSTACLE LOADS

L-19A Flight No. L-19-4 S/N 51-7441
Test Conditions: Gross Wt. 2365 Lbs, C.G. 33.5% m.a.c. Tire Pressure 21 psi
2 1/8" Obstacle Data Request No. L-19-1

Item (Event)	Time (Sec)	Vertical Load (Lbs)	Torsional Load (In Lbs)	Side Load (Lbs)	Drag Load (Lbs)	C.G. Load Factor (g's)	Long. Acc. (g's)	Forward Velocity (MPH)
Oscillograph Record No. 24361								
Prior to Obstacle	0	970	855	101	-12			20.8
Initial Drag Load	.020	-327			302			
Drag Load Springback	.043	-244			-498			
Initial Longitudinal Accel.	.015						-.46	
Longitudinal Accel. Rebound	.043						.51	
Maximum C.G. Load Factor (Pos.)	.076					2.08		
Maximum C.G. Load Factor (Neg.)	.050					.10		
Maximum Vertical Load	.064	988						
Vertical Load Rebound	.076	-546						
Maximum Side Load (Outbd.)	.052	2		115	-396			
Maximum Side Load (Inbd.)	.076	796		-85	279			
Maximum Torsion (Drag)	.040		-1581					
Maximum Torsion Springback	.066		3044					

TABLE I - continued

L-19A ORIGINAL TIRE AND LANDING GEAR OBSTACLE LOADS

L-19A Flight No. L-19-5 S/N 51-7441
Test Conditions: Gross Wt. 2400 lbs, C.G. 33.5% m.a.c. Tire Pressure 21 psi
2-1/8" Obstacle Data Request No. L-19-1

Item (Event)	Time (Sec)	Vertical Load (Lbs)	Torsional Load (In Lbs)	Side Load (Lbs)	Drag Load (Lbs)	C.G. Load Factor (g's)	Long. Acc. (g's)	Forward Velocity (MPH)
Oscillograph Record No. 24372								
Prior to Obstacle	0	1150	640	-71	4			14.3
Initial Drag Load	.030	-145			516			
Drag Load Springback	.060	-201			-974			
Initial Longitudinal Accel.	.030						-.53	
Longitudinal Accel. Rebound	.060						.99	
Maximum C.G. Load Factor (Pos.)	.090					1.95		
Maximum C.G. Load Factor (Neg.)	.110					.33		
Maximum Vertical Load	.080	750						
Vertical Load Rebound	.100	-438						
Maximum Side Load (Outbd.)	.030	-145		336	516			
Maximum Side Load (Inbd.)	.080	750		-251	154			
Maximum Torsion (Drag)	.060		-1626					
Maximum Torsion Springback	.080		2114					
Oscillograph Record No. 24373								
Prior to Obstacle	0	1165	640	-81	41			22.8
Initial Drag Load	.030	-188			469			
Drag Load Springback	.050	87			-511			
Initial Longitudinal Accel.	.030						-.50	
Longitudinal Accel. Rebound	.055						1.13	
Maximum C.G. Load Factor (Pos.)	.085					2.41		
Maximum C.G. Load Factor (Neg.)	.100					-.39		
Maximum Vertical Load	.075	999						
Vertical Load Rebound	.090	-537						
Maximum Side Load (Outbd.)	.040	-481		111	-46			
Maximum Side Load (Inbd.)	.060	971		-224	447			
Maximum Torsion (Drag)	.040		-1757					
Maximum Torsion Springback	.075		3350					

TABLE II

L-19A LANDING LOAD DATA, ORIGINAL TIRE AND LANDING GEAR

L-19A Flight No. L-19-1 S/N 51-7441
Test Conditions: Gr. Wt. 2580 lbs, C.G. 33.5% m.a.c. Tire Pressure 21 psi
Data Request No. L-19-2

Item (Event)	Time (Sec)	Vertical Load (Lbs)	Torsional Load (Lbs)	Side Load (Lbs)	Drag Load (Lbs)	C.G. Load Factor (g's)	Long. Acc. (g's)	Sink Speed (FPS)
Oscillograph Record No. 24301								
Touchdown	0							4.30
Initial Drag Load	0.03	- 67			383			
Drag Load Springback	0.23	1088			-103			
Initial Longitudinal Accel.	0.04						-0.40	
Longitudinal Accel., Rebound	0.27						0.07	
Maximum C.G. Load Factor (Pos.)	0.23					1.97		
Maximum C.G. Load Factor (Neg.)	0.56					0.68		
Maximum Vertical Load	0.26	1101						
Vertical Load Rebound	0.51	-175						
Maximum Side Load (Outbd.)	0.07	- 27		149	-176			
Maximum Side Load (Inbd.)	0.33	1007		-140	- 41			
Maximum Torsion (Drag)	0.09		-1480					
Maximum Torsion Springback	0.29		465					
Oscillograph Record No. 24302								
Touchdown	0							3.66
Initial Drag Load	0.03	- 40			358			
Drag Load Springback	0.19	1155			- 76			
Initial Longitudinal Accel.	0.03						-0.53	
Longitudinal Accel., Rebound	0.26						0.20	
Maximum C.G. Load Factor (Pos.)	0.25					1.92		
Maximum C.G. Load Factor (Neg.)	0.56					0.68		
Maximum Vertical Load	0.23	1276						
Vertical Load Rebound	0.54	-121						
Maximum Side Load (Outbd.)	0.06	40		137	35			
Maximum Side Load (Inbd.)	0.40	806		-147	47			
Maximum Torsion (Drag)	0.09		-1096					
Maximum Torsion Springback	0.25		1170					

FA-800-23A

TABLE II - continued

L-19A LANDING LOAD DATA, ORIGINAL TIRE AND LANDING GEAR

L-19A Flight No. L-19-1 S/N 51-7441
Test Conditions: Gross Wt. 2580 lbs, C.G. 33.5% m.a.c. Tire Pressure 21 psi
Data Request No. L-19-2

Item (Event)	Time (Sec)	Vertical Load (Lbs)	Torsional Load (Lbs)	Side Load (Lbs)	Drag Load (Lbs)	C.G. Load Factor (g's)	Long. Acc. (g's)	Sink Speed (FPS)
Oscillograph Record No. 24304								
Touchdown	0							2.50
Initial Drag Load	0.08	282			298			
Drag Load Springback	0.13	457			-750			
Initial Longitudinal Accel.	0.07						-0.35	
Longitudinal Accel. Rebound	0.26						0.07	
Maximum C.G. Load Factor (Pos.)	0.20					1.61		
Maximum C.G. Load Factor (Neg.)	0.73					0.82		
Maximum Vertical Load	0.25	819						
Vertical Load Rebound	0.55	-148						
Maximum Side Load (Outbd.)	0.12	389		343	-588			
Maximum Side Load (Inbd.)	0.36	685		91	36			
Maximum Torsion (Drag)	0.12		-1420					
Maximum Torsion Springback	0.29		585					

TABLE II - continued

L-19A LANDING LOAD DATA, ORIGINAL TIRE AND LANDING GEAR

L-19A Flight No. L-19-1 S/N 51-7441

Test Conditions: Gross Wt. 2390 lbs, C.G. 33.5% m.a.c. Tire Pressure 21 psi

Data Request No. L-19-2

Item (Event)	Time (Sec)	Vertical Load (Lbs)	Torsional Load (In.Lbs)	Side Load (Lbs)	Drag Load (Lbs)	C.G. Load Factor (g's)	Long. Acc. (g's)	Sink Speed (FPS)
Oscillograph Record No. 24347								
Touchdown	0							2.90
Initial Drag Load	.050	137			160			
Drag Load Springback	.125	685			-202			
Initial Longitudinal Accel.	.027						-.46	
Longitudinal Accel. Rebound	.170						.22	
Maximum C.G. Load Factor (Pos.)	.180					1.99		
Maximum C.G. Load Factor (Neg.)	.520					.76		
Maximum Vertical Load	.275	1259						
Vertical Load Rebound	.520	-191						
Maximum Side Load (Outbd.)	.027	41		155	114			
Maximum Side Load (Inbd.)	.355	1013		-189	45			
Maximum Torsion (Drag)	.100		-508					
Maximum Torsion Springback	.270		1204					

APPENDIX I

LANDING GEAR TEST DATA, M-245B

SUBJECT:-

REPORT NO. FT245-1 FAIRCHILD Aircraft and Missiles Div.

OF FAIRCHILD ENGINE & AIRPLANE CORPORATION

MODEL M-245B | PREPARED BY | CHECKED BY | APPROVED BY | PAGES | PAGE 8

DATE January 22, 1960

REVISED

TABLE II - continued

L-19A LANDING LOAD DATA, ORIGINAL TIRE AND LANDING GEAR

L-19A Flight No. L-19-2 S/N 51-7441
Test Conditions: Gross Wt. 2390 lbs, C.G. 33.5% m.a.c. Tire Pressure 21 psi
Data Request No. L-19-2

Item (Event)	Time (Sec)	Vertical Load (Lbs)	Torsional Load (In.Lbs)	Side Load (Lbs)	Drag Load (Lbs)	C.G. Load Factor (g's)	Long. Acc. (g's)	Sink Speed (FPS)
Oscillograph Record No. 24342								
Touchdown	0							2.48
Initial Drag Load	.065	178			213			
Drag Load Springback	.110	233			-219			
Initial Longitudinal Accel.	.060						-.35	
Longitudinal Accel. Rebound	.165						.18	
Maximum C.G. Load Factor (Pos.)	.150					1.59		
Maximum C.G. Load Factor (Neg.)	.570					.68		
Maximum Vertical Load	.255	657						
Vertical Load Rebound	.510	-301						
Maximum Side Load (Outbd.)	.120	260		96	-197			
Maximum Side Load (Inbd.)	.275	630		-60	- 64			
Maximum Torsion (Drag)	.120		-687					
Maximum Torsion Springback	.295		-160					

FA-800-23A

TABLE II - continued

L-19A LANDING LOAD DATA, ORIGINAL TIRE AND LANDING GEAR

L-19A Flight No. L-19-4 S/N 51-7441

Test Conditions: Gross Wt. 2365 lbs, C.G. 33.5% m.a.c. Tire Pressure 21 psi

Data Request No. L-19-2

Item (Event)	Time (Sec.)	Vertical Load (Lbs)	Torsional Load (In. Lbs)	Side Load (Lbs)	Drag Load (Lbs)	C.G. Load Factor (g's)	Long. Acc. (g's)	Sink Speed (FPS)
Oscillograph Record No. 24353								
Touchdown	0							2.14
Initial Drag Load	.052	137			197			
Drag Load Springback	.114	178			-383			
Initial Longitudinal Accel.	.028						-.43	
Longitudinal Accel. Rebound	.140						.10	
Maximum C.G. Load Factor (Pos.)	.140					1.57		
Maximum C.G. Load Factor (Neg.)	.680					.76		
Maximum Vertical Load	.250	397						
Vertical Load Rebound	.515	-287						
Maximum Side Load (Outbd.)	.120	178		19	-327			
Maximum Side Load (Inbd.)	.310	315		-22	- 79			
Maximum Torsion (Drag)	.132		-958					
Maximum Torsion Springback	.310		-363					

TABLE II - continued

L-19A LANDING LOAD DATA, ORIGINAL TIRE AND LANDING GEAR

L-19A Flight No. L-19-4 S/N 51-7441
Test Conditions: Gross Wt. 2365 lbs, C.G. 33.5% m.a.c. Tire Pressure 21 psi
Data Request No. L-19-2

Item (Event)	Time (Sec.)	Vertical Load (Lbs)	Torsional Load (In. Lbs)	Side Load (Lbs)	Drag Load (Lbs)	C.G. Load Factor (g's)	Long. Acc. (g's)	Sink Speed (FPS)
Oscillograph Record No. 24362								
Touchdown	0							2.23
Initial Drag Load	.075	164			249			
Drag Load Springback	.112	287			-294			
Initial Longitudinal Accel.	.035						-.34	
Longitudinal Accel. Rebound	.135						.12	
Maximum C.G. Load Factor (Pos.)	.177					1.77		
Maximum C.G. Load Factor (Neg.)	.645					.78		
Maximum Vertical Load	.248	685						
Vertical Load Rebound	.490	- 54						
Maximum Side Load (Outbd.)	.290	589		-105	-10			
Maximum Side Load (Inbd.)	.490	- 54		5	-27			
Maximum Torsion (Drag)	.122		-334					
Maximum Torsion Springback	.255		352					

FA-800-23A

TABLE II - continued

L-19A LANDING LOAD DATA, ORIGINAL TIRE AND LANDING GEAR

L-19A Flight No. L-19-5 S/N 51-7441
Test Conditions: Gross Weight 2400 lbs, C.G. 33.5% m.a.c. Tire Pressure 21 psi
Data Request No. L-19-2

Item (Event)	Time (Sec)	Vertical Load (Lbs)	Torsional Load (In. Lbs)	Side Load (Lbs)	Drag Load (Lbs)	C.G. Load Factor (g's)	Long. Acc. (g's)	Sink Speed (FPS)
Oscillograph Record No. 24371								
Touchdown	0							3.15
Initial Drag Load	.060	223			235			
Drag Load Springback	.105	447			-77			
Initial Longitudinal Accel.	.080						-.46	
Longitudinal Accel. Rebound	.120						.26	
Maximum C.G. Load Factor (Pos.)	.180					1.67		
Maximum C.G. Load Factor (Neg.)	.600					.74		
Maximum Vertical Load	.240	921						
Vertical Load Rebound	.510	-70						
Maximum Side Load (Outbd.)	.300	824		-179	150			
Maximum Side Load (Inbd.)	.525	-28		- 18	- 2			
Maximum Torsion (Drag)	.260		1056					
Maximum Torsion Springback	.495		- 87					

TABLE II - continued

L-19A LANDING LOAD DATA, ORIGINAL TIRE AND LANDING GEAR

L-19A Flight No. L-19-5 S/N 51-7441
Test Conditions: Gross Wt. 2400 lbs, C.G. 33.5% m.a.c. Tire Pressure 21 psi
Data Request No. L-19-2

Item (Event)	Time (Sec)	Vertical Load (Lbs)	Torsional Load (In. Lbs)	Side Load (Lbs)	Drag Load (Lbs)	C.G. Load Factor (g's)	Long. Acc. (g's)	Sink Speed (FPS)
Oscillograph Record No. 24374								
Touchdown	0							1.1
Initial Drag Load	.085	126			170			
Drag Load Springback	.145	98			-128			
Initial Longitudinal Accel.	.105						-.27	
Longitudinal Accel. Rebound	.195						-.07	
Maximum C.G. Load Factor (Pos.)	.230					1.36		
Maximum C.G. Load Factor (Neg.)	.640					.82		
Maximum Vertical Load	.270	168						
Vertical Load Rebound	.465	-195						
Maximum Side Load (Outbd.)	.190	126		50	-170			
Maximum Side Load (Inbd.)	-	-		-	-			
Maximum Torsion (Drag)	.210		-609					
Maximum Torsion Springback	-		-					

FA-800-23A

FA-800-23A

TABLE III

L-19A HIGH FLOTATION TIRE OBSTACLE LOADS

L-19A Ground Tests . S/N 51-7441 May 27, 1959
Obstacle Height 2 1/8" Tire Pressure 2.7 psi Data Request No. L-19-5

ITEM (Event) Oscillograph Record No. 24591	TIME (Sec)	Vertical Load (Lbs.)	Drag Strut Axial Load (Lbs.)	Normal Acc. (g's)	Long. Acc. (g's)	Lat. Acc. (g's)	Speed (MPH)
Prior to obstacle	0	820	-340				21.7
Initial Drag Strut Axial Load	.036	140	330		-.17		
Drag Strut Axial Load, Springback	.060	20	-425		.23		
Drag Strut Axial Load, 2nd cycle	.107	40	310		-.05		
Maximum Vertical Load	.075	220	-50	.29			
Vertical Load Rebound	.094	-85	-155	-.47			
Maximum Normal Acceleration (Pos.)	.113	45		.39			
Maximum Normal Acceleration (Neg.)	.083	-5		-.49			
Maximum Longitudinal Acc. (Positive)	.082	160	-155		.35		
Maximum Longitudinal Acc. (Negative)	.099	-55	115		-.31		
Maximum Lateral Acc. (Pos., to Right)	.160	20	-115			.37	
Maximum Lateral Acc. (Neg., to Left)	.139	-45	10			-.59	
Oscillograph Record No. 24720							
Prior to obstacle	0	985	-170				26.8
Initial Drag Strut Axial Load	.023	105	305		-.07		
Drag Strut Axial Load, Springback	.073	-160	-495		.18		
Drag Strut Axial Load, 2nd cycle	.092	- 35	160		.00		
Maximum Vertical Load	.059	185	-115	.32			
Vertical Load Rebound	.075	-185	-380	-.68			
Maximum Normal Acc. (Positive)	.055	135		.51			
Maximum Normal Acc. (Negative)	.075	-185		-.68			
Maximum Longitudinal Acc. (Positive)	.059	185	-115		.29		
Maximum Longitudinal Acc. (Negative)	.119	-135	160		-.16		
Maximum Lateral Acc. (Pos., to Right)	.100	-55	115			.47	
Maximum Lateral Acc. (Neg., to Left)	.125	-115	75			-.41	

Note: All Vertical and Drag Strut Axial Loads tabulated above are incremental. To obtain total loads, add calibrated loads prior to contact with obstacle to incremental values. All G values are also incremental.

FA-800-23A

TABLE III - continued

L-19A HIGH FLOTATION TIRE OBSTACLE LOADS

L-19A Ground Tests S/N 51-7441
Obstacle Height 2 1/8" Tire Pressure 2.7 psi Data Request No. L-19-5

ITEM Oscillograph Record No. 24593 (Event)	TIME (Sec)	Vertical Load (Lbs.)	Drag Strut Axial Load (Lbs.)	Normal Acc. (g's)	Long. Acc. (g's)	Lat. Acc. (g's)	Speed (MPH)
Prior to obstacle	0	830	-230				28.5
Initial Drag Strut Axial Load	.033	185	445		-.50		
Drag Strut Axial Load, Springback	.072	-100	-590		.57		
Drag Strut Axial Load, 2nd cycle	.109	-25	70		-.09		
Maximum Vertical Load	.027	245	240	-.08			
Vertical Load Rebound	.078	-145	-455	-.52			
Maximum Normal Acc. (Positive)	.060	245		.80			
Maximum Normal Acc. (Negative)	.076	-135		-.58			
Maximum Longitudinal Acc. (Positive)	.072	-100	-590		.57		
Maximum Longitudinal Acc. (Negative)	.033	185	445		-.50		
Maximum Lateral Acc. (Pos., to Right)	.107	-35	260			.42	
Maximum Lateral Acc. (Neg., to Left)	.130	25	-155			-.53	
Oscillograph Record No. 24597							
Prior to obstacle	0	770	-155				34.0
Initial Drag Strut Axial Load	.019	125	435		-.24		
Drag Strut Axial Load, Springback	.054	-80	-650		.45		
Drag Strut Axial Load, 2nd cycle	.083	-80	350		-.01		
Maximum Vertical Load	.011	395	-165	.35			
Vertical Load Rebound	.068	-175	-155	-.25			
Maximum Normal Acc. (Positive)	.042	95		.47			
Maximum Normal Acc. (Negative)	.020	95		-.60			
Maximum Longitudinal Acc. (Positive)	.051	-40	-590		.55		
Maximum Longitudinal Acc. (Negative)	.020	95	425		-.45		
Maximum Lateral Acc. (Pos., to Right)	.093	-85	260			.25	
Maximum Lateral Acc. (Neg., to Left)	.035	5	70			-.29	

Note: All Vertical and Drag Strut Axial Loads tabulated above are incremental. To obtain total loads, add calibrated loads prior to contact with obstacle to incremental values. All G values are also incremental.

TABLE III - continued

L-19A HIGH FLOTATION TIRE OBSTACLE LOADS

L-19A Ground Tests — S/N 51-7441 — Data Request No. L-19-5
Obstacle Height 2 1/8" — Tire Pressure 3.6±.2 psi

Item (Event)	Time (Sec)	Vertical Load (Lbs.)	Drag Strut Axial Load (Lbs.)	Normal Acc. (g's)	Long. Acc. (g's)	Lat. Acc. (g's)	Speed (MPH)
Oscillograph Record No. 24531							
Prior to obstacle	0	895	-350				14.7
Initial Drag Strut Axial Load	.043	210	285		-.12		
Drag Strut Axial Load, Springback	.075	-60	-380		.21		
Drag Strut Axial Load, 2nd cycle	.132	-35	190		-.11		
Maximum Vertical Load	.033	220	390	.04			
Vertical Load Rebound	.150	-150	40	-.03			
Maximum Normal Acc. (Positive)	.083	85		.25			
Maximum Normal Acc. (Negative)	.110	35		-.29			
Maximum Longitudinal Acc. (Positive)	.070	-75	-325		.32		
Maximum Longitudinal Acc. (Negative)	.022	175	180		-.25		
Maximum Lateral Acc. (Pos., to Right)	.175	-55	10			.23	
Maximum Lateral Acc. (Neg., to Left)	.204	-25	75			-.23	
Oscillograph Record No. 24486							
Prior to obstacle	0	925	-460				16.1
Initial Drag Strut Axial Load	.039	175	295		-.06		
Drag Strut Axial Load, Springback	.065	-20	-400		.15		
Drag Strut Axial Load, 2nd cycle	.120	-5	260		-.02		
Maximum Vertical Load	.028	215	240	.12			
Vertical Load Rebound	.059	-55	-310	.00			
Maximum Normal Acc. (Positive)	.075	125		.39			
Maximum Normal Acc. (Negative)	.093	25		-.37			
Maximum Longitudinal Acc. (Positive)	.061	-45	-360		.40		
Maximum Longitudinal Acc. (Negative)	.100	20	-20		-.14		
Maximum Lateral Acc. (Pos., to Right)	.165	-35	80			.23	
Maximum Lateral Acc. (Neg., to Left)	.200	-70	5			-.23	

Note: All Vertical and Drag Strut Axial Loads tabulated above are incremental. To obtain total loads, add calibrated loads prior to contact with obstacle to incremental values. All G values are also incremental.

SUBJECT:- APPENDIX I LANDING GEAR TEST DATA, M-245B

REPORT NO. M-245-1 — FAIRCHILD Aircraft and Missiles Div.
MODEL M-245B — PREPARED BY — OF FAIRCHILD ENGINE & AIRPLANE CORPORATION
CHECKED BY — APPROVED BY
DATE January 22, 1960 — REVISED — PAGES — PAGE 16

TABLE III - continued

L-19A HIGH FLOTATION TIRE OBSTACLE LOADS

L-19A Ground Tests — S/N 51-7441 — Data Request No. L-19-5
Obstacle Height 2 1/8" — Tire Pressure 3.6±.2 psi

Item (Event)	Time (Sec)	Vertical Load (Lbs.)	Drag Strut Axial Load (Lbs.)	Normal Acc. (g's)	Long. Acc. (g's)	Lat. Acc. (g's)	Speed (MPH)
Oscillograph Record No. 24533							
Prior to obstacle	0	910	-305				22.1
Initial Drag Strut Axial Load	.039	130	350		.03		
Drag Strut Axial Load, Springback	.074	0	-750		.27		
Drag Strut Axial Load, 2nd cycle	.096	-60	465		-.21		
Maximum Vertical Load	.025	255	245	.25			
Vertical Load Rebound	.084	-180	-245	-.52			
Maximum Normal Acc. (Positive)	.060	110		.66			
Maximum Normal Acc. (Negative)	.082	-155		-.64			
Maximum Longitudinal Acc. (Positive)	.050	-45	-245		.52		
Maximum Longitudinal Acc. (Negative)	.090	-115	295		-.44		
Maximum Lateral Acc. (Pos., to Right)	.160	-140	95			.43	
Maximum Lateral Acc. (Neg., to Left)	.132	-55	-380			-.53	
Oscillograph Record No. 24487							
Prior to obstacle	0	775	-395				22.3
Initial Drag Strut Axial Load	.031	60	295		-.29		
Drag Strut Axial Load, Springback	.065	-15	-900		.95		
Drag Strut Axial Load, 2nd cycle	.087	25	655		-.46		
Maximum Vertical Load	.020	295	220	.37			
Vertical Load Rebound	.078	-195	25	-1.16			
Maximum Normal Acc. (Positive)	.053	195		1.12			
Maximum Normal Acc. (Negative)	.075	-315		-1.24			
Maximum Longitudinal Acc. (Positive)	.060	125	-700		1.07		
Maximum Longitudinal Acc. (Negative)	.079	-175	200		-.89		
Maximum Lateral Acc. (Pos.,to Right)	.162	-45	285			.12	
Maximum Lateral Acc. (Neg.,to Left)	.137	-80	-220			-.25	

Note: All Vertical and Drag Strut Axial Loads tabulated above are incremental. To obtain total loads,add calibrated loads prior to contact with obstacle to incremental values.
All G values are also incremental.

REPORT NO. [illegible] FAIRCHILD Aircraft and Missiles Div.
MODEL M-245B — PREPARED BY — OF FAIRCHILD ENGINE & AIRPLANE CORPORATION — CHECKED BY — PAGES — PAGE 17
SUBJECT:- APPENDIX I LANDING GEAR TEST DATA, M-245B — DATE January 22, 1960 — REVISED — APPROVED BY

FA-800-23A

TABLE III - continued

L-19A HIGH FLOTATION TIRE OBSTACLE LOADS

L-19A Ground Tests S/N 51-7441
Obstacle Height 2 1/8" Tire Pressure 3.6±.2 psi Data Request No. L-19-5

Item (Event) Oscillograph Record No. 24722	Time (Sec.)	Vertical Load (Lbs.)	Drag Strut Axial Load (Lbs.)	Normal Acc. (g's)	Long. Acc. (g's)	Lat. Acc. (g's)	Speed (MPH)
Prior to obstacle	0	740	-245				33.1
Initial Drag Strut Axial Load	.065	405	445		-.27		
Drag Strut Axial Load, Springback	.092	45	-1110		.52		
Drag Strut Axial Load, 2nd cycle	.121	15	645		-.57		
Maximum Vertical Load	.053	510	275	.32			
Vertical Load Rebound	.116	-5	340	.13			
Maximum Normal Acc. (Positive)	.082	300		.72			
Maximum Normal Acc. (Negative)	.070	280		-.53			
Maximum Longitudinal Acc. (Positive)	.089	120	-940		.53		
Maximum Longitudinal Acc. (Negative)	.121	15	645		-.57		
Maximum Lateral Acc. (Pos., to Right)	.139	45	315			.61	
Maximum Lateral Acc. (Neg., to Left)	.164	155	-125			-.42	
Oscillograph Record No. 24721							
Prior to Obstacle	0	500	-125				41.6
Initial Drag Strut Axial Load	.023	465	455		-.33		
Drag Strut Axial Load, Springback	.042	85	-980		.49		
Drag Strut Axial Load, 2nd cycle	.073	65	475		.03		
Maximum Vertical Load	.023	465	455	.40			
Vertical Load Rebound	.073	65	475	.25			
Maximum Normal Acc. (Positive)	.020	460		.53			
Maximum Normal Acc. (Negative)	.110	260		-.64			
Maximum Longitudinal Acc. (Positive)	.042	85	-980		.49		
Maximum Longitudinal Acc. (Negative)	.023	465	455		-.33		
Maximum Lateral Acc. (Pos., to Right)	.151	145	-10			.79	
Maximum Lateral Acc. (Neg., to Left)	.128	125	65			-.38	

Note: All Vertical and Drag Strut Axial Loads tabulated above are incremental. To obtain total loads, add calibrated loads prior to contact with obstacle to incremental values. All G values are also incremental.

FA-800-23A

TABLE III - continued

L-19A HIGH FLOTATION TIRE OBSTACLE LOADS

L-19A Ground Tests S/N 51-7441 Data Request No. L-19-5
Obstacle Height 2 1/8" Tire Pressure 4.9 psi

Item (Event)	Time (Sec.)	Vertical Load (Lbs.)	Drag Strut Axial Load (Lbs.)	Normal Acc. (g's)	Long. Acc. (g's)	Lat. Acc. (g's)	Speed (MPH)
Oscillograph Record No. 24541							
Prior to obstacle	0	955	-390				11.1
Initial Drag Strut Axial Load	.035	230	190		-.05		
Drag Strut Axial Load, Springback	.119	120	-325		.15		
Drag Strut Axial Load, 2nd cycle	.150	150	170		.05		
Maximum Vertical Load	.045	250	135	.12			
Vertical Load Rebound	.170	-260	-75	.08			
Maximum Normal Acc. (Positive)	.099	40		.39			
Maximum Normal Acc. (Negative)	.128	80		-.35			
Maximum Longitudinal Acc. (Positive)	.089	-55	-125		.23		
Maximum Longitudinal Acc. (Negative)	.021	190	160		-.12		
Maximum Lateral Acc. (Pos., to Right)	.105	110	-295			.31	
Maximum Lateral Acc. (Neg., to Left)	.222	-140	55			-.32	
Oscillograph Record No. 24542							
Prior to obstacle	0	860	-400				17.0
Initial Drag Strut Axial Load	.040	230	220		-.04		
Drag Strut Axial Load, Springback	.078	35	-760		.29		
Drag Strut Axial Load, 2nd cycle	.103	-110	560		-.37		
Maximum Vertical Load	.030	270	190	.10			
Vertical Load Rebound	.156	-170	125	-.21			
Maximum Normal Acc. (Positive)	.111	-110		.53			
Maximum Normal Acc. (Negative)	.088	-60		-.54			
Maximum Longitudinal Acc. (Positive)	.063	75	-445		.47		
Maximum Longitudinal Acc. (Negative)	.105	-95	530		-.41		
Maximum Lateral Acc. (Pos., to Right)	.165	-150	230			.42	
Maximum Lateral Acc. (Neg., to Left)	.192	-130	-150			-.35	

Note: All Vertical and Drag Strut Axial Loads tabulated above are incremental. To obtain total loads, add calibrated loads prior to contact with obstacle to incremental values. All G values are also incremental.

SUBJECT:- APPENDIX I LANDING GEAR TEST DATA, M-245B

DATE January 22, 1960 REVISED

FA-800-23A

TABLE III - continued

L-19A HIGH FLOTATION TIRE OBSTACLE LOADS

L-19A Ground Tests S/N 51-7441 Data Request No. L-19-5
Obstacle Height 2 1/8" Tire Pressure 4.9 psi

Item (Event)	Time (Sec.)	Vertical Load (Lbs.)	Drag Strut Axial Load (Lbs.)	Normal Acc. (g's)	Long. Acc. (g's)	Lat. Acc. (g's)	Speed (MPH)
Oscillograph Record No. 24543							
Prior to obstacle	0	835	-255				25.1
Initial Drag Strut Axial Load	.032	235	350		-.33		
Drag Strut Axial Load, Springback	.059	-80	-1195		.27		
Drag Strut Axial Load, 2nd cycle	.083	-80	750		-.23		
Maximum Vertical Load	.022	365	265	.35			
Vertical Load Rebound	.230	-215	-210	.06			
Maximum Normal Acc. (Positive)	.090	-60		.72			
Maximum Normal Acc. (Negative)	.067	-155		-.63			
Maximum Longitudinal Acc. (Positive)	.051	190	-590		.88		
Maximum Longitudinal Acc. (Negative)	.072	-160	200		-.56		
Maximum Lateral Acc. (Pos., to Right)	.093	-75	275			.47	
Maximum Lateral Acc. (Neg., to Left)	.127	5	-105			-.36	
Oscillograph Record No. 24544							
Prior to obstacle	0	735	-230				27.0
Initial Drag Strut Axial Load	.027	335	360		-.27		
Drag Strut Axial Load, Springback	.050	-95	-1025		.32		
Drag Strut Axial Load, 2nd cycle	.080	-130	645		-.48		
Maximum Vertical Load	.017	310	245	.25			
Vertical Load Rebound	.072	-200	315	.16			
Maximum Normal Acc. (Positive)	.042	150		.49			
Maximum Normal Acc. (Negative)	.060	-150		-.41			
Maximum Longitudinal Acc. (Positive)	.044	75	-825		.76		
Maximum Longitudinal Acc. (Negative)	.080	-130	645		-.47		
Maximum Lateral Acc. (Pos., to Right)	.083	-60	420			.39	
Maximum Lateral Acc. (Neg., to Left)	.121	75	-65			-.34	

Note: All Vertical and Drag Strut Axial Loads tabulated above are incremental. To obtain total loads, add calibrated loads prior to contact with obstacle to incremental values. All G values are also incremental.

SUBJECT:- APPENDIX I
LANDING GEAR TEST DATA, M-245B

DATE January 22, 1960
REVISED

TABLE III - continued

L-19A HIGH FLOTATION TIRE OBSTACLE LOADS

L-19A Ground Tests
Obstacle Height 2 1/8"

S/N 51-7441
Tire Pressure 4.9 psi

Data Request No. L-19-5

Item (Event) Oscillograph Record No. 24545	Time (Sec)	Vertical Load (Lbs)	Drag Strut Axial Load (Lbs)	Normal Acc. (g's)	Long. Acc. (g's)	Lat. Acc. (g's)	Speed (MPH)
Prior to obstacle	0	630	-230				23.4
Initial Drag Strut Axial Load	.023	270	360		-.05		
Drag Strut Axial Load, Springback	.049	-60	-1110		.64		
Drag Strut Axial Load, 2nd cycle	.078	-175	645		-.11		
Maximum Vertical Load	.018	310	245	.25			
Vertical Load Rebound	.053	-190	-610	-.37			
Maximum Normal Acc. (Positive)	.071	-170		.70			
Maximum Normal Acc. (Negative)	.053	-130		-.39			
Maximum Longitudinal Acc. (Positive)	.045	60	-760		1.01		
Maximum Longitudinal Acc. (Negative)	.061	-180	-190		-.31		
Maximum Lateral Acc. (Pos., to Right)	.085	-155	505			.37	
Maximum Lateral Acc. (Neg., to Left)	.215	-95	105			-.40	

Note: All Vertical and Drag Strut Axial Loads Tabulated above are incremental. To obtain total loads, add calibrated loads prior to contact with obstacle to incremental values. All G values are also incremental.

APPENDIX I
SUBJECT:- LANDING GEAR TEST DATA, M-245B

DATE January 22, 1960
REVISED

FA-800-23A

TABLE III - continued

L-19A HIGH FLOTATION TIRE OBSTACLE LOADS

L-19A Ground Tests — S/N 51-7441 — Data Request No. L-19-5
Obstacle Height 2 1/8" — Tire Pressure 5.9 psi

Item (Event) Oscillograph Record No. 24491	Time (Sec)	Vertical Load (Lbs)	Drag Strut Axial Load (Lbs)	Normal Acc. (g's)	Long. Acc. (g's)	Lat. Acc. (g's)	Speed (MPH)
Prior to obstacle	0	930	-555				14.7
Initial Drag Strut Axial Load	.035	190	160		-.09		
Drag Strut Axial Load, Springback	.100	130	-290		.28		
Drag Strut Axial Load, 2nd cycle	.130	-35	170		.03		
Maximum Vertical Load	.035	190	160	.33			
Vertical Load Rebound	.153	-205	-115	.16			
Maximum Normal Acc. (Positive)	.090	45		.53			
Maximum Normal Acc. (Negative)	.182	-90		-.71			
Maximum Longitudinal Acc. (Positive)	.110	110	-250		.65		
Maximum Longitudinal Acc. (Negative)	.146	-190	85		-.45		
Maximum Lateral Acc. (Pos., to Right)	.098	105	-230			.39	
Maximum Lateral Acc. (Neg., to Left)	.123	-5	115			-.37	
Oscillograph Record No. 24726							
Prior to obstacle	0	945	-325				25.9
Initial Drag Strut Axial Load	.093	235	435		-.08		
Drag Strut Axial Load, Springback	.120	0	-1190		.69		
Drag Strut Axial Load, 2nd cycle	.150	-80	800		-.20		
Maximum Vertical Load	.085	360	295	.17			
Vertical Load Rebound	.130	-180	-160	-.70			
Maximum Normal Acc. (Positive)	.112	155		.74			
Maximum Normal Acc. (Negative)	.130	-180		-.70			
Maximum Longitudinal Acc. (Positive)	.112	155	-705		.91		
Maximum Longitudinal Acc. (Negative)	.137	-165	305		-.54		
Maximum Lateral Acc. (Pos., to Right)	.160	-20	200			.77	
Maximum Lateral Acc. (Neg., to Left)	.134	20	-275			-.56	

Note: All Vertical and Drag Strut Axial Loads tabulated above are incremental. To obtain total loads, add calibrated loads prior to contact with obstacle to incremental values. All G values are also incremental.

FA-800-23A

TABLE III - continued

L-19A HIGH FLOTATION TIRE OBSTACLE LOADS

L-19A Ground Tests S/N 51-7441 Data Request No. L-19-5
Obstacle Height 2 1/8" Tire Pressure 5.9 psi

Item (Event)	Time (Sec)	Vertical Load (lbs)	Drag Strut Axial Load (lbs)	Normal Acc. (g's)	Long. Acc. (g's)	Lat. Acc. (g's)	Speed (MPH)
Oscillograph Record No. 24727							
Prior to obstacle	0	705	-190				35.8
Initial Drag Strut Axial Load	.064	360	550		-.04		
Drag Strut Axial Load, Springback	.080	-125	-885		.79		
Drag Strut Axial Load, 2nd Cycle	.110	-255	475		-.10		
Maximum Vertical Load	.056	425	220	.25			
Vertical Load Rebound	.110	-255	475	.25			
Maximum Normal Acc. (Positive)	.060	335		1.08			
Maximum Normal Acc. (Negative)	.080	-125		-.81			
Maximum Longitudinal Acc. (Positive)	.073	-95	-800		1.16		
Maximum Longitudinal Acc. (Negative)	.062	365	540		-.64		
Maximum Lateral Acc. (Pos., to Right)	.110	-255	475			.62	
Maximum Lateral Acc. (Neg., to Left)	.086	-175	-540			-.45	
Oscillograph Record No. 24725							
Prior to obstacle	0	630	-160				38.7
Initial Drag Strut Axial Load	.031	260	515		-.26		
Drag Strut Axial Load, Springback	.047	-85	-705		1.13		
Drag Strut Axial Load, 2nd cycle	.080	-285	530		-.33		
Maximum Vertical Load	.029	410	455	.11			
Vertical Load Rebound	.070	-315	380	.74			
Maximum Normal Acc. (Positive)	.031	260		1.08			
Maximum Normal Acc. (Negative)	.049	-100		-.95			
Maximum Longitudinal Acc. (Positive)	.047	-85	-705		1.13		
Maximum Longitudinal Acc. (Negative)	.036	320	315		-1.17		
Maximum Lateral Acc. (Pos., to Right)	.080	-285	530			.70	
Maximum Lateral Acc. (Neg., to Left)	.057	-180	-590			-.50	

Note: All Vertical and Drag Strut Axial Loads tabulated above are incremental. To obtain total loads, add calibrated loads prior to contact with obstacle to incremental values. All G values are also incremental.

TABLE III - continued

L-19A HIGH FLOTATION TIRE OBSTACLE LOADS

L-19A Ground Tests — S/N 51-7441 — Data Request No. L-19-5
Obstacle Height 4 1/4" — Tire Pressure 2.7 psi

Item (Event) Oscillograph Record No. 24594	Time (Sec)	Vertical Load (lbs.)	Drag Strut Axial Load (lbs.)	Normal Acc. (g's)	Long. Acc. (g's)	Lat. Acc. (g's)	Speed (MPH)
Prior to obstacle	0	1045	-385				11.5
Initial Drag Strut Axial Load	.038	265	445		-.08		
Drag Strut Axial Load, Springback	.109	-155	-330		.20		
Drag Strut Axial Load, 2nd cycle	.148	125	210		-.17		
Maximum Vertical Load	.050	365	375	.21			
Vertical Load Rebound	.188	-440	-50	-.25			
Maximum Normal Acc. (Positive)	.115	0		.52			
Maximum Normal Acc. (Negative)	.133	45		-.35			
Maximum Longitudinal Acc. (Positive)	.153	35	-95		.25		
Maximum Longitudinal Acc. (Negative)	.222	-255	280		-.41		
Maximum Lateral Acc. (Pos., to Right)	.203	-340	155			.59	
Maximum Lateral Acc. (Neg., to Left)	.232	-215	280			-.49	
Oscillograph Record No. 24590							
Prior to obstacle	0	1000	-340				12.7
Initial Drag Strut Axial Load	.038	140	290		-.21		
Drag Strut Axial Load, Springback	.079	-120	-630		.37		
Drag Strut Axial Load, 2nd cycle	.113	20	385		-.05		
Maximum Vertical Load	.040	140	280	-.12			
Vertical Load Rebound	.173	-215	0	.00			
Maximum Normal Acc. (Positive)	.166	-185		.33			
Maximum Normal Acc. (Negative)	.146	-135		-.37			
Maximum Longitudinal Acc. (Positive)	.079	-120	-630		.37		
Maximum Longitudinal Acc. (Negative)	.102	-25	270		-.29		
Maximum Lateral Acc. (Pos., to Right)	.177	-185	70			51	
Maximum Lateral Acc. (Neg., to Left	.293	-40	60			-.43	

Note: All Vertical and Drag Strut Axial Loads tabulated above are incremental. To obtain total loads, add calibrated loads prior to contact with obstacle to incremental values. All G values are also incremental.

FA-800-23A

TABLE III - continued

L-19A HIGH FLOTATION TIRE OBSTACLE LOADS

L-19A Ground Tests S/N 51-7441 Data Request No. L-19-5
Obstacle Height 4 1/4" Tire Pressure 2.7 psi

Item (Event) Oscillograph Record No. 24595	Time (Sec.)	Vertical Load (lbs.)	Drag Strut Axial Load (lbs.)	Normal Acc. (g's)	Long. Acc. (g's)	Lat. Acc. (g's)	Speed (MPH)
Prior to obstacle	0	880	-250				22.8
Initial Drag Strut Axial Load	.038	480	475		-.24		
Drag Strut Axial Load, Springback	.098	-245	-1240		.61		
Drag Strut Axial Load, 2nd cycle	.139	-145	590		-.64		
Maximum Vertical Load	.038	480	475	.33			
Vertical Load Rebound	.102	-370	-870	-.99			
Maximum Normal Acc. (Positive)	.077	135		.95			
Maximum Normal Acc. (Negative)	.104	-365		-1.13			
Maximum Longitudinal Acc. (Positive)	.095	-175	-1200		.74		
Maximum Longitudinal Acc. (Negative)	.110	-245	105		-.65		
Maximum Lateral Acc. (Pos., to Right)	.127	-95	330			.78	
Maximum Lateral Acc. (Neg., to Left	.150	-80	260			-.86	
Oscillograph Record No. 24732							
Prior to obstacle	0	825	-285				24.9
Initial Drag Strut Axial Load	.044	510	515		-.31		
Drag Strut Axial Load, Springback	.095	-180	-1825		.86		
Drag Strut Axial Load, 2nd cycle	.132	-85	920		-.50		
Maximum Vertical Load	.044	510	515	.17			
Vertical Load Rebound	.100	-320	-1255	-1.27			
Maximum Normal Acc. (Positive)	.084	285		1.21			
Maximum Normal Acc. (Negative)	.101	-305		-1.38			
Maximum Longitudinal Acc. (Positive)	.095	-180	-1825		.86		
Maximum Longitudinal Acc. (Negative)	.109	-235	0		-1.03		
Maximum Lateral Acc. (Pos., to Right)	.128	-95	845			1.02	
Maximum Lateral Acc. (Neg., to Left)	.151	-15	-420			-.89	

Note: All Vertical and Drag Strut Axial Loads tabulated above are incremental. To obtain total loads, add calibrated loads prior to contact with obstacle to incremental values.
All G values are also incremental.

TABLE III - continued

L-19A HIGH FLOTATION TIRE OBSTACLE LOADS

L-19A Ground Tests — S/N 51-7441 — Data Request No. L-19-5
Obstacle Height 4 1/4" — Tire Pressure 2.7 psi

Item (Event) Oscillograph Record No. 24596	Time (Sec.)	Vertical Load (lbs.)	Drag Strut Axial Load (lbs.)	Normal Acc. (g's)	Long. Acc. (g's)	Lat. Acc. (g's)	Speed (MPH)
Prior to obstacle	0	880	-260				29.8
Initial Drag Strut Axial Load	.028	485	580		-.37		
Drag Strut Axial Load, Springback	.077	-240	-1595		.96		
Drag Strut Axial Load, 2nd cycle	.116	-165	695		-.35		
Maximum Vertical Load	.023	490	455	.49			
Vertical Load Rebound	.082	-390	-1045	-1.11			
Maximum Normal Acc. (Positive)	.068	255		1.22			
Maximum Normal Acc. (Negative)	.083	-370		-1.22			
Maximum Longitudinal Acc. (Positive)	.072	-65	-1375		1.00		
Maximum Longitudinal Acc. (Negative)	.088	-320	-240		-.84		
Maximum Lateral Acc. (Pos., to Right)	.109	-135	495			.69	
Maximum Lateral Acc. (Neg., to Left)	.133	-20	215			-.95	
Oscillograph Record No. 24733							
Prior to obstacle	0	765	-190				37.3
Initial Drag Strut Axial Load	.030	440	620		-.10		
Drag Strut Axial Load, Springback	.067	-200	-2070		1.55		
Drag Strut Axial Load, 2nd cycle	.090	-120	875		-.07		
Maximum Vertical Load	.022	560	465	.55			
Vertical Load Rebound	.069	-280	-1825	-.38			
Maximum Normal Acc. (Positive)	.055	370		1.21			
Maximum Normal Acc. (Negative)	.072	-235		-1.08			
Maximum Longitudinal Acc. (Positive)	.064	-155	-2035		2.23		
Maximum Longitudinal Acc. (Negative)	.079	-240	0		-1.12		
Maximum Lateral Acc. (Pos., to Right)	.102	-125	715			.58	
Maximum Lateral Acc. (Neg., to Left)	.047	195	465			-.52	

Note: All Vertical and Drag Strut Axial Loads tabulated above are incremental. To obtain total loads, add calibrated loads prior to contact with obstacle to incremental values. All G values are also incremental.

FA-800-23A

TABLE III - continued

L-19A HIGH FLOTATION TIRE OBSTACLE LOADS

L-19A Flight No. 19-15 S/N 51-7441
Obstacle Size 4¼" Tire Pressure 2.7 psi Data Request No. L-19-5

Item (Event)	Time (Sec)	Vertical Load (Lbs)	Drag Strut Axial Load (Lbs)	Normal Acc. (g's)	Long. Acc. (g's)	Lat. Acc. (g's)	Speed (MPH)
Oscillograph Record No. 25152							
Prior to obstacle	0	940	-150				30.6
Initial Drag Strut Axial Load	.020	635	620		-.22		
Drag Strut Axial Load, Springback	.068	-265	-1510		.30		
Drag Strut Axial Load, 2nd Cycle	.104	- 20	940		-.28		
Maximum Vertical Load	.020	635	620	.41			
Vertical Load Rebound	.075	-305	-1055	-1.43			
Maximum Normal Acc. (Positive)	.058	410		1.41			
Maximum Normal Acc. (Negative)	.075	-305		-1.43			
Maximum Longitudinal Acc. (Positive)	.064	20	-1000		.42		
Maximum Longitudinal Acc. (Negative)	.090	-100	295		-.42		
Maximum Lateral Acc. (Pos., to Right)	.068	-265	-1510			.75	
Maximum Lateral Acc. (Neg., to Left)	.131	80	-665			-1.02	

Note: All Vertical and Drag Strut Axial Loads tabulated above are incremental. To obtain loads, add calibrated loads prior to contact with obstacle to incremental values. All G values are also incremental.

REPORT NO. [illegible] Div. of Fairchild Engine & Airplane Corporation
MODEL M-245B
PREPARED BY
CHECKED BY
APPROVED BY
SUBJECT:- APPENDIX I FLIGHT TEST DATA, M-245B
DATE January 22, 1960
REVISED
PAGES
PAGE 27

TABLE III - continued

L-19A HIGH FLOTATION TIRE OBSTACLE LOADS

L-19A Flight No. 19-16 S/N 51-7441
Obstacle Size 4-1/4" Tire Pressure 3.1 psi Data Request No. L-19-5

Item (Event)	Time (Sec)	Vertical Load (Lbs)	Drag Strut Axial Load (Lbs)	Normal Acc. (g's)	Long. Acc. (g's)	Lat. Acc. (g's)	Forward Velocity (MPH)
Oscillograph Record No. 25178							
Prior to obstacle	0	845	-140				33.5
Initial Drag Strut Axial Load	.055	225	710		-.37		
Drag Strut Axial Load, Springback	.073	1095	-2230		1.77		
Drag Strut Axial Load, 2nd Cycle	.105	-40	1280		-.14		
Maximum Vertical Load	.078	1180	-1840	-.85			
Vertical Load Rebound	.175	-225	160	+.22			
Maximum Normal Acc. (Positive)	.067	660		+.81			
Maximum Normal Acc. (Negative)	.080	1010		-.94			
Maximum Longitudinal Acc. (Positive)	.073	1095	-2230		1.77		
Maximum Longitudinal Acc. (Negative)	.085	745	-170		-1.01		
Maximum Lateral Acc. (Pos. to Right)	.180	-185	-335			.44	
Maximum Lateral Acc. (Neg. to Left)	.149	-60	130			-.44	

Note: All Vertical and Drag Strut Axial Loads tabulated above are incremental. To obtain loads, add calibrated loads prior to contact with obstacle to incremental values. All G values are also incremental.

TABLE III - continued

L-19A HIGH FLOTATION TIRE OBSTACLE LOADS

L-19A Flight No. 19-15 S/N 51-7441 Data Request No. L-19-5
Obstacle Size 4-1/4 " Tire Pressure 3.7 psi

Item (Event)	Time (Sec)	Vertical Load (Lbs)	Drag Strut Axial Load (Lbs)	Normal Acc. (g's)	Long. Acc. (g's)	Lat. Acc. (g's)	Forward Velocity (MPH)
Oscillograph Record No. 25164							
Prior to obstacle	0	1040	-115				30.5
Initial Drag Strut Axial Load	.024	615	600		-.65		
Drag Strut Axial Load, Springback	.070	-345	-1965		1.17		
Drag Strut Axial Load, 2nd Cycle	.104	-165	1190		-.40		
Maximum Vertical Load	.024	615	600	.45			
Vertical Load Rebound	.074	-365	-1605	-.58			
Maximum Normal Acc. (Positive)	.062	100		.86			
Maximum Normal Acc. (Negative)	.079	-305		-1.16			
Maximum Longitudinal Acc. (Positive)	.067	-205	-1455		1.35		
Maximum Longitudinal Acc. (Negative)	.082	-285	-125		-.89		
Maximum Lateral Acc. (Pos., to Right)	.071	-365	-1785			1.07	
Maximum Lateral Acc. (Neg., to Left)	.138	-125	-715			-.89	

Note: All Vertical and Drag Strut Axial Loads tabulated above are incremental. To obtain loads, add calibrated loads prior to contact with obstacle to incremental values. All G values are also incremental.

REPORT NO. 12445-1 FAIRCHILD AIRCRAFT AND MISSILES DIV. OF FAIRCHILD ENGINE & AIRPLANE CORPORATION
MODEL M-245B
PREPARED BY
CHECKED BY
APPROVED BY
PAGES PAGE 20
SUBJECT:- APPENDIX I LANDING GEAR TEST DATA, M-245B
DATE January 22, 1960
REVISED

TABLE III - continued

L-19A HIGH FLOTATION TIRE OBSTACLE LOADS

L-19A Ground Tests — S/N 51-7441 — Data Request No. L-19-5
Obstacle Height 4 1/4" — Tire Pressure 3.6 ±.2 psi

Item (Event) Oscillograph Record No. 24534	Time (Sec.)	Vertical Load (lbs.)	Drag Strut Axial Load (lbs.)	Normal Acc. (g's)	Long. Acc. (g's)	Lat. Acc. (g's)	Speed (MPH)
Prior to obstacle	0	1045	-445				5.8
Initial Drag Strut Axial Load	.106	240	360		-.09		
Drag Strut Axial Load, Springback	.239	-60	-610		.19		
Drag Strut Axial Load, 2nd cycle	.338	-290	265		-.05		
Maximum Vertical Load	.088	285	255	.16			
Vertical Load Rebound	.358	-335	-30	-.27			
Maximum Normal Acc. (Positive)	.055	230		.25			
Maximum Normal Acc. (Negative)	.313	-295		-.41			
Maximum Longitudinal Acc. (Positive)	.233	-80	-540		.33		
Maximum Longitudinal Acc. (Negative)	.100	260	340		-.13		
Maximum Lateral Acc. (Pos., to Right)	.115	215	255			.15	
Maximum Lateral Acc. (Neg., to Left)	.362	-305	-55			-.25	
Oscillograph Record No. 24510							
Prior to obstacle	0	945	-400				12.4
Initial Drag Strut Axial Load	.030	185	315		.07		
Drag Strut Axial Load, Springback	.113	60	-455		.20		
Drag Strut Axial Load, 2nd cycle	.164	-300	205		-.16		
Maximum Vertical Load	.030	185	315	.02			
Vertical Load Rebound	.164	-300	205	-.23			
Maximum Normal Acc. (Positive)	.102	60		.29			
Maximum Normal Acc. (Negative)	.190	-180		-.47			
Maximum Longitudinal Acc. (Positive)	.110	60	-405		.31		
Maximum Longitudinal Acc. (Negative)	.015	165	265		-.21		
Maximum Lateral Acc. (Pos., to Right)	.254	-220	5			.29	
Maximum Lateral Acc. (Neg., to Left)	.128	45	-165			-.39	

Note: All Vertical and Drag Strut Axial Loads tabulated above are incremental. To obtain total loads, add calibrated loads prior to contact with obstacle to incremental values. All G values are also incremental.

REPORT NO. FT245-1 — FAIRCHILD AIRCRAFT AND MISSILES DIV. OF FAIRCHILD ENGINE & AIRPLANE CORPORATION
MODEL M-245B — PREPARED BY — CHECKED BY — APPROVED BY
SUBJECT:- APPENDIX I LANDING GEAR TEST DATA, M-245B
DATE January 22, 1960 — REVISED

FA-800-23A

TABLE III - continued

L-19A HIGH FLOTATION TIRE OBSTACLE LOADS

L-19A Ground Tests S/N 51-7441 Data Request No. L-19-5
Obstacle Height 4 1/4" Tire Pressure 3.6±.2 psi

Item (Event) Oscillograph Record No. 24536	Time (Sec.)	Vertical Load (lbs.)	Drag Strut Axial Load (lbs.)	Normal Acc. (g's)	Long. Acc. (g's)	Lat. Acc. (g's)	Speed (MPH)
Prior to obstacle	0	1025	-465				12.7
Initial Drag Strut Axial Load	.035	345	380		-.19		
Drag Strut Axial Load, Springback	.116	150	-790		.19		
Drag Strut Axial Load, 2nd cycle	.148	-255	530		-.85		
Maximum Vertical Load	.040	385	370	.16			
Vertical Load Rebound	.165	-460	190	.02			
Maximum Normal Acc. (Positive)	.100	15		.29			
Maximum Normal Acc. (Negative)	.128	25		-.58			
Maximum Longitudinal Acc. (Positive)	.107	85	-695		.45		
Maximum Longitudinal Acc. (Negative)	.140	-120	190		-.31		
Maximum Lateral Acc. (Pos., to Right)	.102	40	-505			.31	
Maximum Lateral Acc. (Neg., to Left	.136	-55	-85			-.39	
Oscillograph Record No. 24511							
Prior to obstacle	0	950	-345				13.4
Initial Drag Strut Axial Load	.042	450	375		.07		
Drag Strut Axial Load, Springback	.110	285	-720		.23		
Drag Strut Axial Load, 2nd cycle	.153	-160	245		-.06		
Maximum Vertical Load	.042	450	375	.16			
Vertical Load Rebound	.165	-295	165	.21			
Maximum Normal Acc. (Positive)	.100	140		.52			
Maximum Normal Acc. (Negative)	.130	275		-.27			
Maximum Longitudinal Acc. (Positive)	.098	85	-370		.41		
Maximum Longitudinal Acc. (Negative)	.022	295	305		-.24		
Maximum Lateral Acc. (Pos., to Right)	.107	215	-655			.49	
Maximum Lateral Acc. (Neg., to Left)	.141	55	-95			-.51	

Note: All Vertical and Drag Strut Axial Loads tabulated above are incremental. To obtain total loads, add calibrated loads prior to contact with obstacle to incremental values. All G values are also incremental.

SUBJECT:- APPENDIX I
LANDING GEAR TEST DATA, M-245B

TABLE III - continued

L-19A HIGH FLOTATION TIRE OBSTACLE LOADS

L-19A Ground Tests
Obstacle Height 4 1/4"

S/N 51-7441
Tire Pressure 3.6±.2 psi

Data Request No. L-19-5

Item (Event)	Time (Sec.)	Vertical Load (lbs.)	Drag Strut Axial Load (lbs.)	Normal Acc. (g's)	Long. Acc. (g's)	Lat. Acc. (g's)	Speed (MPH)
Oscillograph Record No. 24539							
Prior to obstacle	0	995	-420				19.1
Initial Drag Strut Axial Load	.038	480	540		-.19		
Drag Strut Axial Load, Springback	.090	-15	-1140		.29		
Drag Strut Axial Load, 2nd cycle	.116	-55	900		-.51		
Maximum Vertical Load	.030	520	435	.31			
Vertical Load Rebound	.142	-260	-10	-.35			
Maximum Normal Acc. (Positive)	.075	180		.93			
Maximum Normal Acc. (Negative)	.099	-155		-1.05			
Maximum Longitudinal Acc. (Positive)	.075	130	-720		.78		
Maximum Longitudinal Acc. (Negative)	.116	-55	900		-.51		
Maximum Lateral Acc. (Pos., to Right)	.170	-195	-40			.56	
Maximum Lateral Acc. (Neg., to Left	.146	-215	-315			-.50	
Oscillograph Record No. 24538							
Prior to obstacle	0	910	-390				24.2
Initial Drag Strut Axial Load	.020	525	550		-.35		
Drag Strut Axial Load, Springback	.073	-240	-1740		.82		
Drag Strut Axial Load, 2nd cycle	.102	-80	950		.05		
Maximum Vertical Load	.020	525	550	.37			
Vertical Load Rebound	.081	-325	-920	-1.42			
Maximum Normal Acc. (Positive)	.061	250		1.13			
Maximum Normal Acc. (Negative)	.081	-325		-1.42			
Maximum Longitudinal Acc. (Positive)	.065	195	-1170		.86		
Maximum Longitudinal Acc. (Negative)	.083	-275	75		-1.04		
Maximum Lateral Acc. (Pos., to Right)	.106	85	940			.87	
Maximum Lateral Acc. (Neg., to Left)	.132	-15	-815			-1.04	

Note: All Vertical and Drag Strut Axial Loads tabulated above are incremental. To obtain total loads, add calibrated loads prior to contact with obstacle to incremental values. All G Values are also incremental.

FA-800-23A

TABLE III - continued

L-19A HIGH FLOTATION TIRE OBSTACLE LOADS

L-19A Ground Tests S/N 51-7441 Data Request No. L-19-5
Obstacle Height 4 1/4" Tire Pressure 3.6±.2 psi

Item (Event) Oscillograph Record No. 24540	Time (Sec.)	Vertical Load (lbs.)	Drag Strut Axial Load (lbs.)	Normal Acc. (g's)	Long. Acc. (g's)	Lat. Acc. (g's)	Speed (MPH)
Prior to obstacle	0	1085	-295				29.0
Initial Drag Strut Axial Load	.020	585	740		-.45		
Drag Strut Axial Load, Springback	.057	-230	-2040		1.34		
Drag Strut Axial Load, 2nd cycle	.103	-155	1225		-.51		
Maximum Vertical Load	.019	585	720	.27			
Vertical Load Rebound	.072	-425	-970	-1.34			
Maximum Normal Acc. (Positive)	.053	345		1.29			
Maximum Normal Acc. (Negative)	.074	-395		-1.52			
Maximum Longitudinal Acc. (Positive)	.055	-20	-1565		1.16		
Maximum Longitudinal Acc. (Negative)	.080	-275	125		-1.32		
Maximum Lateral Acc. (Pos., to Right)	.103	-155	1225			.92	
Maximum LateralAcc. (Neg., to Left	.129	40	-845			-.92	

Note: All Vertical and Drag Strut Axial Loads tabulated above are incremental. To obtain total loads, add calibrated loads prior to contact with obstacle to incremental values. All G values are also incremental.

FA-800-23A

TABLE III - continued

L-19A HIGH FLOTATION TIRE OBSTACLE LOADS

L-19A Ground Tests — S/N 51-7441 — Data Request No. L-19-5
Obstacle Height 4 1/4" — Tire Pressure 4.9 psi

Item (Event) Oscillograph Record No. 24693	Time (Sec.)	Vertical Load (lbs.)	Drag Strut Axial Load (lbs.)	Normal Acc. (g's)	Long. Acc. (g's)	Lat. Acc. (g's)	Speed (MPH)
Prior to obstacle	0	920	-470				9.1
Initial Drag Strut Axial Load	.040	365	325		-.14		
Drag Strut Axial Load, Springback	.164	-100	-1140		.42		
Drag Strut Axial Load, 2nd cycle	.192	-275	605		-.36		
Maximum Vertical Load	.060	440	230	.25			
Vertical Load Rebound	.250	-425	325	-.17			
Maximum Normal Acc. (Positive)	.500	215		.40			
Maximum Normal Acc. (Negative)	.229	-380		-.65			
Maximum Longitudinal Acc. (Positive)	.160	-35	-1120		.53		
Maximum Longitudinal Acc. (Negative)	.192	-275	605		-.36		
Maximum Lateral Acc. (Pos., to Right)	.198	-295	535			.47	
Maximum Lateral Acc. (Neg., to Left)	.219	-390	-325			-.22	
Oscillograph Record No. 24575							
Prior to obstacle	0	965	-335				12.8
Initial Drag Strut Axial Load	.045	545	430		-.03		
Drag Strut Axial Load, Springback	.128	-45	-1745		.58		
Drag Strut Axial Load, 2nd cycle	.155	-335	1130		-.67		
Maximum Vertical Load	.055	585	365	.25			
Vertical Load Rebound	.236	-450	10	-.16			
Maximum Normal Acc. (Positive)	.161	-400		.66			
Maximum Normal Acc. (Negative)	.192	-315		-1.09			
Maximum Longitudinal Acc. (Positive)	.121	185	-1390		.89		
Maximum Longitudinal Acc. (Negative)	.155	-335	1130		-.67		
Maximum Lateral Acc. (Pos., to Right)	.162	-410	910			.54	
Maximum Lateral Acc. (Neg., to Left)	.285	-235	365			-.42	

Note: All Vertical and Drag Strut Axial Loads tabulated above are incremental. To obtain total loads, add cllibrated loads prior to contact with obstacle to incremental values. All G values are also incremental.

TABLE III - continued
L-19A HIGH FLOTATION TIRE OBSTACLE LOADS

L-19A Ground Tests
Obstacle Height 4 1/4"

S/N 51-7441
Tire Pressure 4.9 psi

Data Request No. L-19-5

Item (Event)	Time (Sec.)	Vertical Load (lbs.)	Drag Strut Axial Load (lbs.)	Normal Acc. (g's)	Long. Acc. (g's)	Lat. Acc. (g's)	Speed (MPH)
Oscillograph Record No. 24697							
Prior to obstacle	0	950	-385				14.1
Initial Drag Strut Axial Load	.085	185	430		-.09		
Drag Strut Axial Load, Springback	.116	-205	-1839		.80		
Drag Strut Axial Load, 2nd cycle	.148	-385	1325		-.26		
Maximum Vertical Load	.050	460	325	.02			
Vertical Load Rebound	.165	-410	-345	-.40			
Maximum Normal Acc. (Positive)	.148	-385		.50			
Maximum Normal Acc. (Negative)	.122	-325		-1.07			
Maximum Longitudinal Acc. (Positive)	.112	-105	-1715		.88		
Maximum Longitudinal Acc. (Negative)	.143	-370	1275		-.66		
Maximum Lateral Acc. (Pos., to Right)	.151	-390	1140			.64	
Maximum Lateral Acc. (Neg., to Left)	.173	-260	-865			-.39	
Oscillograph Record No. 24579							
Prior to obstacle	0	920	-315				23.4
Initial Drag Strut Axial Load	.063	410	585		-.20		
Drag Strut Axial Load, Springback	.085	-300	-2520		1.44		
Drag Strut Axial Load, 2nd cycle	.116	-185	1400		-.26		
Maximum Vertical Load	.035	750	510	.49			
Vertical Load Rebound	.090	-420	-1725	-1.44			
Maximum Normal Acc. (Positive)	.075	275		1.24			
Maximum Normal Acc. (Negative)	.092	-385		-1.63			
Maximum Longitudinal Acc. (Positive)	.082	-65	-2245		1.65		
Maximum Longitudinal Acc. (Negative)	.098	-340	155		-1.02		
Maximum Lateral Acc. (Pos., to Right)	.118	-175	1350			1.10	
Maximum Lateral Acc. (Neg., to Left)	.140	-25	-1090			-1.19	

Note: All Vertical and Drag Strut Axial Loads tabulated above are incremental. To obtain total loads, add calibrated loads prior to contact with obstacle to incremental values. All G values are also incremental.

TABLE III - continued

L-19A HIGH FLOTATION TIRE OBSTACLE LOADS

L-19A Ground Tests — S/N 51-7441 — Data Request No. L-19-5
Obstacle Height 6 3/8" — Tire Pressure 2.7 psi

Item (Event) Oscillograph Record No. 24610	Time (Sec.)	Vertical Load (Lbs.)	Drag Strut Axial Load (lbs.)	Normal Acc. (g's)	Long. Acc. (g's)	Lat. Acc. (g's)	Speed (MPH)
Prior to obstacle	0	1015	-395				3.2
Initial Drag Strut Axial Load	.175	265	410		-.15		
Drag Strut Axial Load, Springback	.488	-105	-480		.19		
Drag Strut Axial Load, 2nd cycle	.792	-295	50		-.05		
Maximum Vertical Load	.147	285	315	.12			
Vertical Load Rebound	.792	-295	50	-.04			
Maximum Normal Acc. (Positive)	.102	185		.21			
Maximum Normal Acc. (Negative)	.507	- 80		-.17			
Maximum Longitudinal Acc. (Positive)	.579	-105	210		.20		
Maximum Longitudinal Acc. (Negative)	.085	160	335		-.27		
Maximum Lateral Acc. (Pos., to Right)	.255	155	365			.25	
Maximum Lateral Acc. (Neg., to Left)	.857	-145	-20			-.20	
Oscillograph Record No. 24611							
Prior to obstacle	0	950	-355				7.7
Initial Drag Strut Axial Load	.042	195	480		-.27		
Drag Strut Axial Load, Springback	.212	100	-775		.24		
Drag Strut Axial Load, 2nd cycle	.263	-340	355		-.09		
Maximum Vertical Load	.063	425	305	.37			
Vertical Load Rebound	.325	-470	125	-.29			
Maximum Normal Acc. (Positive)	.059	380		.48			
Maximum Normal Acc. (Negative)	.306	-440		-.56			
Maximum Longitudinal Acc. (Positive)	.201	95	-545		.45		
Maximum Longitudinal Acc. (Negative)	.044	215	470		-.31		
Maximum Lateral Acc. (Pos., to Right)	.253	-260	270			.38	
Maximum Lateral Acc. (Neg., to Left)	.229	-75	-510			-.23	

Note: All Vertical and Drag Strut Axial Loads tabulated above are incremental. To obtain total loads, add calibrated loads prior to contact with obstacle to incremental values. All G values are also incremental.

FA-800-23A

TABLE III - continued

L-19A HIGH FLOTATION TIRE OBSTACLE LOADS

L-19A Ground Tests S/N 51-7441 Data Request No. L-19-5
Obstacle Height 6 3/8" Tire Pressure 2.7 psi

Item (Event) Oscillograph Record No. 24613	Time (Sec.)	Vertical Load (lbs.)	Drag Strut Axial Load (lbs.)	Normal Acc. (g's)	Long. Acc. (g's)	Lat. Acc. (g's)	Speed (MPH)
Prior to obstacle	0	1000	-325				12.3
Initial Drag Strut Axial Load	.053	605	700		-.12		
Drag Strut Axial Load, Springback	.142	280	-805		.39		
Drag Strut Axial Load, 2nd cycle	.219	-425	220		-.18		
Maximum Vertical Load	.080	680	620	.27			
Vertical Load Rebound	.215	-480	180	-.29			
Maximum Normal Acc. (Positive)	.130	305		.73			
Maximum Normal Acc. (Negative)	.144	280		-.37			
Maximum Longitudinal Acc. (Positive)	.099	315	-200		.55		
Maximum Longitudinal Acc. (Negative)	.047	465	650		-.50		
Maximum Lateral Acc. (Pos., to Right)	.213	-470	180			.54	
Maximum Lateral Acc. (Neg., to Left)	.080	680	620			-.34	
Oscillograph Record No. 24615							
Prior to obstacle	0	885	-325				19.1
Initial Drag Strut Axial Load	.033	500	730		-.47		
Drag Strut Axial Load, Springback	.105	285	-1140		.24		
Drag Strut Axial Load, 2nd cycle	.172	-335	615		-.42		
Maximum Vertical Load	.049	720	680	.10			
Vertical Load Rebound	.160	-440	200	-.37			
Maximum Normal Acc. (Positive)	.092	275		1.25			
Maximum Normal Acc. (Negative)	.121	-275		-1.14			
Maximum Longitudinal Acc. (Positive)	.093	245	-740		1.38		
Maximum Longitudinal Acc. (Negative)	.132	-360	325		-.61		
Maximum Lateral Acc. (Pos., to Right)	.243	-275	295			.78	
Maximum Lateral Acc. (Neg., to Left)	.127	-365	75			-.77	

Note: All Vertical and Drag Strut Axial Loads tabulated above are incremental. To obtain total loads, add calibrated loads prior to contact with obstacle to incremental values. All G values are also incremental.

TABLE III - continued

L-19A HIGH FLOTATION TIRE OBSTACLE LOADS

L-19A Ground Tests — S/N 51-7441 — Data Request No. L-19-5
Obstacle Height 6 3/8" — Tire Pressure 2.7 psi

Item (Event)	Time (Sec.)	Vertical Load (lbs.)	Drag Strut Axial Load (lbs.)	Normal Acc. (g's)	Long. Acc. (g's)	Lat. Acc. (g's)	Speed (MPH)
Oscillograph Record No. 24683							
Prior to obstacle	0	945	-310				21.6
Initial Drag Strut Axial Load	.030	785	940		-.45		
Drag Strut Axial Load, Springback	.095	130	-1810		.69		
Drag Strut Axial Load, 2nd cycle	.120	-245	910		-.46		
Maximum Vertical Load	.035	840	820	.38			
Vertical Load Rebound	.108	-455	-490	-1.70			
Maximum Normal Acc. (Positive)	.077	250		1.09			
Maximum Normal Acc. (Negative)	.103	-295		-1.97			
Maximum Longitudinal Acc. (Positive)	.080	265	-950		1.23		
Maximum Longitudinal Acc. (Negative)	.141	-320	555		-.69		
Maximum Lateral Acc. (Pos., to Right)	.225	-320	310			.94	
Maximum Lateral Acc. (Neg., to Left)	.252	-185	-255			-.70	
Oscillograph Record No. 24616							
Prior to obstacle	0	960	-295				22.4
Initial Drag Strut Axial Load	.036	780	920		-.39		
Drag Strut Axial Load, Springback	.097	125	-1420		.57		
Drag Strut Axial Load, 2nd cycle	.153	-245	815		-.49		
Maximum Vertical Load	.037	805	890	.52			
Vertical Load Rebound	.108	-465	-920	-1.37			
Maximum Normal Acc. (Positive)	.082	255		1.29			
Maximum Normal Acc. (Negative)	.105	-400		-1.96			
Maximum Longitudinal Acc. (Positive)	.081	195	-545		.85		
Maximum Longitudinal Acc. (Negative)	.146	-335	595		-.88		
Maximum Lateral Acc. (Pos., to Right)	.227	-315	190			.98	
Maximum Lateral Acc. (Neg., to Left)	.155	-235	815			-.81	

Note: All Vertical and Drag Strut Axial Loads tabulated above are incremental. To obtain total loads, add calibrated loads prior to contact with obstacle to incremental values. All G values are also incremental.

FA-800-23A

TABLE III - continued

L-19A HIGH FLOTATION TIRE OBSTACLE LOADS

L-19A Ground Tests S/N 51-7441 Data Request No. L-19-5
Obstacle Height 6 3/8" Tire Pressure 27 psi

Item (Event) Oscillograph Record No. 24617	Time (Sec.)	Vertical Load (lbs.)	Drag Strut Axial Load (lbs.)	Normal Acc. (g's)	Long. Acc. (g's)	Lat. Acc. (g's)	Speed (MPH)
Prior to obstacle	0	750	-250				26.6
Initial Drag Strut Axial Load	.068	275	920		-.38		
Drag Strut Axial Load, Springback	.094	-245	-1975		.26		
Drag Strut Axial Load, 2nd cycle	.133	-260	855		-.53		
Maximum Vertical Load	.038	725	775	.33			
Vertical Load Rebound	.113	-385	250	.02			
Maximum Normal Acc. (Positive)	.077	320		1.05			
Maximum Normal Acc. (Negative)	.094	-255		-1.27			
Maximum Longitudinal Acc. (Positive)	.086	60	-1465		1.49		
Maximum Longitudinal Acc. (Negative)	.108	-345	-125		-.69		
Maximum Lateral Acc. (Pos., to Right)	.121	-340	440			.82	
Maximum Lateral Acc. (Neg., to Left)	.104	-325	-555			-.66	

Note: All Vertical and Drag Strut Axial Loads tabulated above are incremental. To obtain total loads, add calibrated loads prior to contact with obstacle to incremental values. All G values are also incremental.

FA-800-23A

TABLE III - continued

L-19A HIGH FLOTATION TIRE OBSTACLE LOADS

L-19A Flight No. 19-15 S/N 51-7441

Obstacle Size 6-3/8" Tire Pressure 2.7 psi Data Request No. L-19-5

Item (Event)	Time (Sec)	Vertical Load (Lbs)	Drag Strut Axial Load (lbs)	Normal Acc. (g's)	Long. Acc. (g's)	Lat. Acc. (g's)	Speed (MPH)
Oscillograph Record No. 25154							
Prior to obstacle	0	1040	-265				10.3
Initial Drag Strut Axial Load	.035	450	540		-.24		
Drag Strut Axial Load, Springback	.153	125	-1190		.57		
Drag Strut Axial Load, 2nd Cycle	.190	-345	740		-.36		
Maximum Vertical Load	.052	635	370	.32			
Vertical Load Rebound	.230	-530	-255	- .71			
Maximum Normal Acc. (Positive)	.119	225		.39			
Maximum Normal Acc. (Negative)	.230	-490		- .71			
Maximum Longitudinal Acc. (Positive)	.151	165	-1160		.63		
Maximum Longitudinal Acc. (Negative)	.190	-345	740		-.40		
Maximum Lateral Acc. (Pos., to Right)	.200	-470	475			.47	
Maximum Lateral Acc. (Neg., to Left)	.445	0	- 30			-.28	
Oscillograph Record No. 25156							
Prior to obstacle	0	900	-115				37.1
Initial Drag Strut Axial Load	.029	735	770		-.48		
Drag Strut Axial Load, Springback	.075	-325	-2245		.57		
Drag Strut Axial Load, 2nd Cycle	.109	-205	865		-.48		
Maximum Vertical Load	.031	755	760	.41			
Vertical Load Rebound	.095	-470	485	.15			
Maximum Normal Acc. (Positive)	.068	205		1.13			
Maximum Normal Acc. (Negative)	.075	-325		-1.41			
Maximum Longitudinal Acc. (Positive)	.070	60	-1835		2.00		
Maximum Longitudinal Acc. (Negative)	.068	-350	-465		-1.07		
Maximum Lateral Acc. (Pos., to Right)	.118	- 40	590			.85	
Maximum Lateral Acc. (Neg., to Left)	.147	- 40	-485			-1.08	

Note: All Vertical and Drag Strut Axial Loads tabulated are incremental. To obtain loads, add calibrated loads prior to contact with obstacle to incremental values. All G values are also incremental.

FA-800-23A

TABLE III - continued

L-19A HIGH FLOTATION TIRE OBSTACLE LOADS

L-19A Flight No. 19-16 S/N 51-7441
Obstacle Size 6-3/8" Tire Pressure 3.2 psi Data Request No. L-19-5

Item (Event)	Time (Sec)	Vertical Load (Lbs)	Drag Strut Axial Load (Lbs)	Normal Acc. (g's)	Long. Acc. (g's)	Lat. Acc. (g's)	Forward Velocity (MPH)
Oscillograph Record No. 25179							
Prior to obstacle	0	930	-140				36.4
Initial Drag Strut Axial Load	.031	825	775		-.21		
Drag Strut Axial Load, Springback	.075	-310	-2490		1.46		
Drag Strut Axial Load, 2nd Cycle	.115	-145	960		-.58		
Maximum Vertical Load	.035	845	735	.52			
Vertical Load Rebound	.088	-560	130	-.28			
Maximum Normal Acc. (Positive)	.066	-475		1.18			
Maximum Normal Acc. (Negative)	.080	-455		-1.16			
Maximum Longitudinal Acc. (Pos.)	.075	-310	-2490		1.46		
Maximum Longitudinal Acc. (Neg.)	.088	-560	130		-1.38		
Maximum Lateral Acc.(Pos. to Right)	.102	-290	605			.70	
Maximum Lateral Acc.(Neg. to Left)	.140	0	-1055			-.90	

Note: All Vertical and Drag Strut Axial Loads tabulated above are incremental. To obtain loads, add calibrated loads prior to contact with obstacle to incremental values. All G values are also incremental.

TABLE III - continued
L-19A HIGH FLOTATION TIRE OBSTACLE LOADS

L-19A Ground Tests — S/N 51-7441 — Data Request No. L-19-5
Obstacle Heights 6 3/8" — Tire Pressure 3.6±.2 psi

Item (Event) Oscillograph Record No. 24694	Time (Sec.)	Vertical Load (lbs.)	Drag Strut Axial Load (lbs.)	Normal Acc. (g's)	Long. Acc. (g's)	Lat. Acc. (g's)	Speed (MPH)
Prior to obstacle	0	1015	-430				8.5
Initial Drag Strut Axial Load	.107	370	535		-.18		
Drag Strut Axial Load, Springback	.260	-385	-920		.35		
Drag Strut Axial Load, 2nd cycle	.288	-365	230		-.14		
Maximum Vertical Load	.095	370	470	.15			
Vertical Load Rebound	.358	-705	180	-.55			
Maximum Normal Acc. (Positive)	.610	235		.61			
Maximum Normal Acc. (Negative)	.320	-460		-.65			
Maximum Longitudinal Acc. (Positive)	.260	-385	-920		.35		
Maximum Longitudinal Acc. (Negative)	.182	145	500		-.28		
Maximum Lateral Acc. (Pos., to Right)	.271	-380	-395			.40	
Maximum Lateral Acc. (Neg., to Left)	.419	-360	95			-.38	
Oscillograph Record No. 24693							
Prior to obstacle	0	1000	-385				9.9
Initial Drag Strut Axial Load	.040	380	490		-.31		
Drag Strut Axial Load, Springback	.174	-115	-1420		.51		
Drag Strut Axial Load, 2nd cycle	.207	-440	995		-.57		
Maximum Vertical Load	.067	565	440	.19			
Vertical Load Rebound	.275	-500	545	-.21			
Maximum Normal Acc. (Positive)	.546	260		.48			
Maximum Normal Acc. (Negative)	.230	-430		-.74			
Maximum Longitudinal Acc. (Positive)	.170	-5	-1380		.65		
Maximum Longitudinal Acc. (Negative)	.207	-440	995		-.57		
Maximum Lateral Acc. (Pos., to Right)	.210	-450	845			.58	
Maximum Lateral Acc. (Neg., to Left)	.310	-400	-250			-.27	

Note: All Vertical and Drag Strut Axial Loads tabulated above are incremental. To obtain total loads, add calibrated loads prior to contact with obstacle to incremental values. All G values are also incremental.

TABLE III - continued

L-19A HIGH FLOTATION TIRE OBSTACLE LOADS

L-19A Ground Tests
Obstacle Height 6 3/8"

S/N 51-7441
Tire Pressure 3.6±.2 psi

Data Request No. L-19-5

Item (Event)	Time (Sec.)	Vertical Load (lbs.)	Drag Strut Axial Load (lbs.)	Normal Acc. (g's)	Long. Acc. (g's)	Lat. Acc. (g's)	Speed (MPH)
Oscillograph Record No. 24696							
Prior to obstacle	0	1145	-375				11.5
Initial Drag Strut Axial Load	.035	360	490		-.14		
Drag Strut Axial Load, Springback	.142	-215	-1820		.62		
Drag Strut Axial Load, 2nd cycle	.172	-570	1085		-.68		
Maximum Vertical Load	.050	440	385	.27			
Vertical Load Rebound	.255	-685	280	-.08			
Maximum Normal Acc. (Positive)	.078	-625		.40			
Maximum Normal Acc. (Negative)	.150	-465		-1.05			
Maximum Longitudinal Acc. (Positive)	.132	45	-1380		.80		
Maximum Longitudinal Acc. (Negative)	.172	-570	1085		-.68		
Maximum Lateral Acc. (Pos., to Right)	.078	-625	900			.90	
Maximum Lateral Acc. (Neg., to Left)	.205	-550	-845			-.51	
Oscillograph Record No. 24684							
Prior to obstacle	0	1015	-360				15.0
Initial Drag Strut Axial Load	.030	550	545		-.20		
Drag Strut Axial Load, Springback	.113	250	-1555		.58		
Drag Strut Axial Load, 2nd cycle	.137	-285	925		-.51		
Maximum Vertical Load	.040	655	510	.35			
Vertical Load Rebound	.147	-495	470	.27			
Maximum Normal Acc. (Positive)	.140	-340		.61			
Maximum Normal Acc. (Negative)	.175	-300		-.99			
Maximum Longitudinal Acc. (Positive)	.103	320	-1345		.76		
Maximum Longitudinal Acc. (Negative)	.137	-285	925		-.51		
Maximum Lateral Acc. (Pos., to Right)	.147	35	470			.80	
Maximum Lateral Acc. (Neg., to Left)	.127	-200	-130			-.43	

Note: All Vertical and Drag Strut Axial Loads tabulated above are incremental. To obtain total loads, add calibrated loads prior to contact with obstacle to incremental values. All G values are also incremental.

SUBJECT:- APPENDIX I
LANDING GEAR TEST DATA, M-245B

DATE January 22, 1960
REVISED

TABLE III - continued

L-19A HIGH FLOTATION TIRE OBSTACLE LOADS

S/N 51-7441

L-19A Ground Tests
Obstacle Height 8"

Tire Pressure 2.7 psi

Data Request No. L-19-5

Item (Event)	Time (Sec.)	Vertical Load (lbs.)	Drag Strut Axial Load (lbs.)	Normal Acc. (g's)	Long. Acc. (g's)	Lat. Acc. (g's)	Speed (MPH)
Oscillograph Record No. 24636							
Prior to obstacle	0	965	-180				2.4
Initial Drag Strut Axial Load	.245	55	510		-.11		
Drag Strut Axial Load, Springback	.840	-355	-630		.20		
Drag Strut Axial Load, 2nd cycle	1.000	75	21		.00		
Maximum Vertical Load	.245	55	510	.15			
Vertical Load Rebound	.940	5	-190	-.37			
Maximum Normal Acc. (Positive)	.215	40		.17			
Maximum Normal Acc. (Negative)	.955	-635		-.40			
Maximum Longitudinal Acc. (Positive)	.730	90	-435		.23		
Maximum Longitudinal Acc. (Negative)	.290	15	470		-.14		
Maximum Lateral Acc. (Pos., to Right)	.405	290	435			.28	
Maximum Lateral Acc. (Neg., to Left)	.980	-635	-160			-.26	
Oscillograph Record No. 24637							
Prior to obstacle	0	1170	-255				2.5
Initial Drag Strut Axial Load	.196	210	490		-.14		
Drag Strut Axial Load, Springback	.635	-445	-535		.18		
Drag Strut Axial Load, 2nd cycle	.905	-435	-75		.04		
Maximum Vertical Load	.165	250	415	.15			
Vertical Load Rebound	.770	-680	-330	-.19			
Maximum Normal Acc. (Positive)	.150	190		.17			
Maximum Normal Acc. (Negative)	.710	-620		-.21			
Maximum Longitudinal Acc. (Positive)	.645	-470	-500		.20		
Maximum Longitudinal Acc. (Negative)	.305	35	445		-.18		
Maximum Lateral Acc. (Pos., to Right)	.245	145	385			.27	
Maximum Lateral Acc. (Neg., to Left)	.815	-640	-275			-.23	

Note: All Vertical and Drag Strut Axial Loads tabulated above are incremental. To obtain total loads, add calibrated loads prior to contact with obstacle to incremental values. All G values are also incremental.

FA-800-23A

TABLE III - continued

L-19A HIGH FLOTATION TIRE OBSTACLE LOADS

L-19A Ground Tests — S/N 51-7441 — Data Request No. L-19-5
Obstacle Height 8" — Tire Pressure 2.7 psi

Item (Event) Oscillograph Record No. 24660	Time (Sec.)	Vertical Load (lbs.)	Drag Strut Axial Load (lbs.)	Normal Acc. (g's)	Long. Acc. (g's)	Lat. Acc. (g's)	Speed (MPH)
Prior to obstacle	0	1205	-235				4.1
Initial Drag Strut Axial Load	.185	380	585		-.09		
Drag Strut Axial Load, Springback	.415	-615	-460		.09		
Drag Strut Axial Load, 2nd cycle	.472	-735	-45		.00		
Maximum Vertical Load	.165	410	490	.27			
Vertical Load Rebound	.505	-770	-235	-.49			
Maximum Normal Acc. (Positive)	.750	340		.64			
Maximum Normal Acc. (Negative)	.460	-770		-.52			
Maximum Longitudinal Acc. (Positive)	.750	340	-320		.23		
Maximum Longitudinal Acc. (Negative)	.185	380	585		-.09		
Maximum Lateral Acc. (Pos., to Right)	.320	-90	-130			.31	
Maximum Lateral Acc. (Neg., to Left)	.655	-95	-225			-.41	
Oscillograph Record No. 24677							
Prior to obstacle	0	1062	-360				5.3
Initial Drag Strut Axial Load	.067	315	460		-.14		
Drag Strut Axial Load, Springback	.315	-345	-1045		.31		
Drag Strut Axial Load, 2nd cycle	.350	-345	375		-.19		
Maximum Vertical Load	.120	455	395	.27			
Vertical Load Rebound	.410	-700	1270	-.48			
Maximum Normal Acc. (Positive)	.660	280		.63			
Maximum Normal Acc.(Negative)	.395	-625		-.50			
Maximum Longitudinal Acc. (Positive)	.305	-280	75		.41		
Maximum Longitudinal Acc. (Negative)	.350	-345	375		-.19		
Maximum Lateral Acc. (Pos., to Right)	.402	-680	55			.41	
Maximum Lateral Acc. (Neg., to Left)	.680	340	340			-.27	

Note: All Vertical and Drag Strut Axial Loads tabulated above are incremental. To obtain total loads, add calibrated loads prior to contact with obstacle to incremental values. All G values are also incremental.

TABLE III - continued

L-19A HIGH FLOTATION TIRE OBSTACLE LOADS

L-19A Ground Tests
Obstacle Height 8"

S/N 51-7441
Tire Pressure 2.7 psi

Data Request No. L-19-5

Item (Event) Oscillograph Record No. 24678	Time (Sec.)	Vertical Load (lbs.)	Drag Strut Axial Load (lbs.)	Normal Acc. (g's)	Long. Acc. (g's)	Lat. Acc. (g's)	Speed (MPH)
Prior to obstacle	0	1030	-395				5.3
Initial Drag Strut Axial Load	.230	80	610		-.15		
Drag Strut Axial Load, Springback	.312	-275	-1055		.42		
Drag Strut Axial Load, 2nd cycle	.350	-320	300		-.22		
Maximum Vertical Load	.120	445	460	.25			
Vertical Load Rebound	.412	-615	140	-.48			
Maximum Normal Acc. (Positive)	.670	350		.61			
Maximum Normal Acc. (Negative)	.440	-510		-.53			
Maximum Longitudinal Acc. (Positive)	.305	450	-930		.53		
Maximum Longitudinal Acc. (Negative)	.345	-315	225		-.24		
Maximum Lateral Acc. (Pos., to Right)	.162	300	310			.36	
Maximum Lateral Acc. (Neg., to Left)	.675	335	-170			-.31	
Oscillograph Record No. 24661							
Prior to obstacle	0	920	-360				6.0
Initial Drag Strut Axial Load	.050	285	510		-.28		
Drag Strut Axial Load, Springback	.265	25	-525		.25		
Drag Strut Axial Load, 2nd cycle	.390	-655	350		-.17		
Maximum Vertical Load	.100	485	340	.27			
Vertical Load Rebound	.375	-795	235	-.69			
Maximum Normal Acc. (Positive)	.110	475		.29			
Maximum Normal Acc. (Negative)	.400	-580		-.71			
Maximum Longitudinal Acc. (Positive)	.265	25	-525		.65		
Maximum Longitudinal Acc. (Negative)	.045	265	500		-.29		
Maximum Lateral Acc. (Pos., to Right)	.295	-145	-415			.35	
Maximum Lateral Acc. (Neg., to Left)	.510	-205	000			-.29	

Note: All Vertical and Drag Strut Axial Loads tabulated above are incremental. To obtain total loads, add calibrated loads prior to contact with obstacle to incremental values. All G values are also incremental.

FA-800-23A

TABLE III - continued

L-19A HIGH FLOTATION TIRE OBSTACLE LOADS

L-19A Ground Tests S/N 51-7441 Data Request No. L-19-5
Obstacle Heights 8" Tire Pressure 2.7 psi

Item (Event) Oscillograph Record No. 24650	Time (Sec.)	Vertical Load (lbs.)	Drag Strut Axial Load (lbs.)	Normal Acc. (g's)	Long. Acc. (g's)	Lat. Acc. (g's)	Speed (MPH)
Prior to obstacle	0	880	-335				7.0
Initial Drag Strut Axial Load	.048	295	445		-.30		
Drag Strut Axial Load, Springback	.255	-150	-585		.28		
Drag Strut Axial Load, 2nd cycle	.352	-680	255		-.14		
Maximum Vertical Load	.090	410	265	.35			
Vertical Load Rebound	.340	-730	140	-.58			
Maximum Normal Acc. (Positive)	.058	355		.40			
Maximum Normal Acc. (Negative)	.385	-485		-.69			
Maximum Longitudinal Acc. (Positive)	.230	125	-460		.34		
Maximum Longitudinal Acc. (Negative)	.043	230	435		-.42		
Maximum Lateral Acc. (Pos., to Right)	.275	-195	-310			.39	
Maximum Lateral Acc. (Neg., to Left)	.385	-485	-30			-.33	
Oscillograph Record No. 24638							
Prior to obstacle	0	985	-300				8.1
Initial Drag Strut Axial Load	.055	420	755		-.09		
Drag Strut Axial Load, Springback	.222	-90	-1405		.54		
Drag Strut Axial Load, 2nd cycle	.263	-470	705		-.23		
Maximum Vertical Load	.085	625	470	.33			
Vertical Load Rebound	.315	-740	55	-.58			
Maximum Normal Acc. (Positive)	.070	530		.40			
Maximum Normal Acc. (Negative)	.305	-730		-.62			
Maximum Longitudinal Acc. (Positive)	.220	20	-1375		.62		
Maximum Longitudinal Acc. (Negative)	.260	-430	670		-.23		
Maximum Lateral Acc. (Pos., to Right)	.260	-430	670			.41	
Maximum Lateral Acc. (Neg., to Left)	.440	-390	20			-.30	

Note: All Vertical Loads and Drag Strut Axial Loads tabulated above are incremental. To obtain total loads, add calibrated loads prior to contact with obstacle to incremental values.
All G values are also incremental.

FA-800-23A

TABLE IV

L-19A HIGH FLOTATION TIRE DITCH LOADS

L-19A Ground Tests
Ditch Size 12" wide
4" deep

S/N 51-7441
Tire Pressure 2.7 psi

Data Request No. L-19-5

Item (Event)	Time (Sec.)	Vertical Load (lbs.)	Drag Strut Axial Load (lbs.)	Normal Acc. (g's)	Long. acc. (g's)	Lat. Acc. (g's)	Speed (MPH)
Oscillograph Record No. 24641							
Prior to ditch	0	695	-245				25.2
Initial Drag Strut Axial Load	.080	40	490		-.19		
Drag Strut Axial Load, Springback	.108	390	-310		.12		
Maximum Vertical Load	.058	-220	-300	.15			
Vertical Load Rebound	.100	400	-205	.29			
Maximum Normal Acc. (Positive)	.095	390		.60			
Maximum Normal Acc. (Negative)	.115	390		-.08			
Maximum Longitudinal Acc (Positive)	.134	265	-235		.26		
Maximum Longitudinal Acc (Negative)	.075	-20	405		-.20		
Maximum Lateral Acc. (Pos., to Right)	.240	270	-10			.31	
Maximum Lateral Acc. (Neg., to Left)	.120	380	-205			-.42	
Oscillograph Record No. 24642							
Prior to ditch	0	605	-235				31.2
Initial Drag Strut Axial Load	.255	-80	320		-.43		
Drag Strut Axial Load, Springback	.285	240	-225		.07		
Maximum Vertical Load	.235	-340	30	-.08			
Vertical Load Rebound	.272	305	-20	.42			
Maximum Normal Acc. (Positive)	.275	225		.48			
Maximum Normal Acc. (Negative)	.290	205		-.27			
Maximum Longitudinal Acc. (Positive)	.315	95	45		.12		
Maximum Longitudinal Acc. (Negative)	.255	-80	320		-.43		
Maximum Lateral Acc. (Pos., to Right)	.415	175	-10			.26	
Maximum Lateral Acc. (Neg., to Left)	.297	165	-130			-.41	

Note: All Vertical and Drag Strut axial Loads tabulated above are incremental. To obtain total loads, add calibrated loads prior to contact with ditch to incremental values. All G values are also incremental.

FA-800-23A

TABLE IV - continued

L-19A HIGH FLOTATION TIRE DITCH LOADS

L-19A Ground Tests
Ditch Size 18" wide
4" deep

S/N 51-7441
Tire Pressure 2.7 psi

Data Request No. L-19-5

Item (Event)	Time (Sec.)	Vertical Load (lbs.)	Drag Strut Axial Load (lbs.)	Normal Acc. (g's)	Long. Acc. (g's)	Lat. Acc. (g's)	Speed (MPH)
Oscillograph Record No. 24643							
Prior to ditch	0	945	-320				11.1
Initial Drag Strut Axial Load	.085	-315	500		-.11		
Drag Strut Axial Load, Springback	.237	615	-640		.23		
Maximum Vertical Load	.065	-520	-340	-.27			
Vertical Load Rebound	.215	825	-300	.54			
Maximum Normal Acc. (Positive)	.225	785		.56			
Maximum Normal Acc. (Negative)	.065	-520		-.27			
Maximum Longitudinal Acc. (Positive)	.235	695	-555		.26		
Maximum Longitudinal Acc. (Negative)	.120	-110	140		-.18		
Maximum Lateral Acc. (Pos., to Right)	.335	195	-130			.39	
Maximum Lateral Acc. (Neg., to Left)	.220	785	-255			-.15	
Oscillograph Record No. 24644							
Prior to ditch	0	700	-225				25.2
Initial Drag Strut Axial Load	.072	445	480		-.16		
Drag Strut Axial Load, Springback	.098	570	-575		.09		
Maximum Vertical Load	.042	-470	-320	-.04			
Vertical Load Rebound	.085	730	105	-.02			
Maximum Normal Acc. (Positive)	.075	525		1.10			
Maximum Normal Acc. (Negative)	.095	550		-.35			
Maximum Longitudinal Acc. (Positive)	.035	-430	-510		.23		
Maximum Longitudinal Acc. (Negative)	.060	-185	385		-.23		
Maximum Lateral Acc. (Pos., to Right)	.127	325	-330			.52	
Maximum Lateral Acc. (Neg., to Left)	.106	595	-340			-.10	

Note: All Vertical and Drag Strut Axial Loads tabulated above are incremental. To obtain total loads, add calibrated loads prior to contact with ditch to incremental values.
All G values are also incremental.

TABLE IV - continued

L-19A HIGH FLOTATION TIRE DITCH LOADS

L-19A Ground Tests
Ditch Size 18" wide
4" deep

S/N 51-7441
Tire Pressure 2.7 psi

Data Request No. L-19-5

Item (Event) Oscillograph Record No. 24645	Time (Sec.)	Vertical Load (lbs.)	Drag Strut Axial Load (lbs.)	Normal Acc. (g's)	Long. Acc. (g's)	Lat. Acc. (g's)	Speed (MPH)
Prior to ditch	0	600	-190				30.7
Initial Drag Strut Axial Load	.270	-125	205		-.09		
Drag Strut Axial Load, Springback	.290	220	-265		-.01		
Maximum Vertical Load	.248	-525	10	-.15			
Vertical Load Rebound	.285	265	-160	.12			
Maximum Normal Acc. (Positive)	.335	50		.54			
Maximum Normal Acc. (Negative)	.300	205		-.25			
Maximum Longitudinal Acc. (Positive)	.344	50	000		.11		
Maximum Longitudinal Acc. (Negative)	.270	-125	205		-.09		
Maximum Lateral Acc. (Pos., to Right)	.425	260	-20			.36	
Maximum Lateral Acc. (Neg., to Left)	.310	145	-120			-.29	

Note: All Vertical and Drag Strut Axial Loads tabulated above are incremental. To obtain total loads, add calibrated loads prior to contact with ditch to incremental values.
All G values are also incremental.

TABLE IV - continued

L-19A HIGH FLOTATION TIRE DITCH LOADS

L-19A Ground Tests
Ditch Size 24" wide
4" deep

S/N 51-7441
Tire Pressure 2.7 psi

Data Request No. L-19-5

Item (Event)	Time (Sec)	Vertical Load (lbs.)	Drag Strut Axial Load (lbs.)	Normal Acc. (g's)	Long. Acc. (g's)	Lat. Acc. (g's)	Speed (MPH)
Oscillograph Record No. 24646							
Prior to ditch	0	905	-360				11.3
Initial Drag Strut Axial Load	.260	- 5	425		-.16		
Drag Strut Axial Load, Springback	.363	860	-415		+.18		
Maximum Vertical Load	.170	-790	- 10	-.37			
Vertical Load Rebound	.333	955	-275	+.67			
Maximum Normal Acc. (Positive)	.360	905		+.71			
Maximum Normal Acc. (Negative)	.615	-300		-.50			
Maximum Longitudinal Acc. (Positive)	.370	825	-360		+.20		
Maximum Longitudinal Acc. (Negative)	.425	440	- 10		-.19		
Maximum Lateral Acc. (Pos., to Right)	.537	-170	55			+.35	
Maximum Lateral Acc. (Neg., to Left	.304	720	20			-.25	
Oscillograph Record No. 24647							
Prior to ditch	0	870	-330				18.2
Initial Drag Strut Axial Load	.170	30	490		-.32		
Drag Strut Axial Load, Springback	.228	355	-405		+.15		
Maximum Vertical Load	.130	-820	45	-.40			
Vertical Load Rebound	.283	525	120	+.46			
Maximum Normal Acc. (Positive)	.275	465		+.49			
Maximum Normal Acc. (Negative)	.115	-750		-.54			
Maximum Longitudinal Acc. (Positive)	.220	375	-330		+.20		
Maximum Longitudinal Acc. (Negative)	.175	200	470		-.34		
Maximum Lateral Acc. (Pos., to Right)	.143	-680	280			+.30	
Maximum Lateral Acc. (Neg., to Left)	.201	370	- 95			-.36	

Note: All Vertical and Drag Strut Axial Loads tabulated above are incremental. To obtain total loads, add calibrated loads prior to contact with ditch to incremental values. All G values are also incremental.

FA-800-23A

TABLE IV - continued

L-19A HIGH FLOTATION TIRE DITCH LOADS

L-19A Ground Tests
Ditch Size 24" wide
4" deep

S/N 51-7441
Tire Pressure 2.7 psi

Data Request No. L-19-5

Item (Event)	Time (Sec)	Vertical Load (lbs.)	Drag Strut Axial Load (lbs.)	Normal Acc. (g's)	Long. Acc. (g's)	Lat. Acc. (g's)	Speed (MPH)
Oscillograph Record No. 24648							
Prior to ditch	0	730	-300				22.9
Initial Drag Strut Axial Load	.117	355	545		-.31		
Drag Strut Axial Load, Springback	.150	485	-460		+.23		
Maximum Vertical Load	.080	-695	75	-.46			
Vertical Load Rebound	.130	605	300	+.29			
Maximum Normal Acc. (Positive)	.122	455		+.67			
Maximum Normal Acc. (Negative)	.125	530		-.29			
Maximum Longitudinal Acc. (Positive)	.063	355	-255		+.29		
Maximum Longitudinal Acc. (Negative)	.117	355	545		-.31		
Maximum Lateral Acc. (Pos., to Right)	.102	375	290			+.42	
Maximum Lateral Acc. (Neg., to Left)	.150	485	-460			-.68	
Oscillograph Record No. 24649							
Prior to ditch	0	775	-190				28.4
Initial Drag Strut Axial Load	.098	655	510		+.27		
Drag Strut Axial Load, Springback	.113	380	-385		+.22		
Maximum Vertical Load	.069	-905	30	-.37			
Vertical Load Rebound	.095	1000	395	+.94			
Maximum Normal Acc. (Positive)	.097	640		+.96			
Maximum Normal Acc. (Negative)	.117	375		-.56			
Maximum Longitudinal Acc. (Positive)	.108	505	85		+.30		
Maximum Longitudinal Acc. (Negative)	.121	340	-309		-.35		
Maximum Lateral Acc. (Pos., to Right)	.083	-585	140			+.40	
Maximum Lateral Acc. (Neg., to Left)	.128	305	-265			-.77	

Note: All Vertical and Drag Strut Axial Loads tabulated above are incremental. To obtain total loads, add calibrated loads prior to contact with ditch to incremental values.
All G values are also incremental.

FA-800-23A

TABLE IV - continued

L-19A HIGH FLOTATION TIRE DITCH LOADS

L-19A Ground Tests S/N 51-7441 Data Request No. L-19-5
Ditch Size 24" wide Tire Pressure 2.7 psi
4" deep

Item (Event)	Time (Sec.)	Vertical Load (lbs.)	Drag Strut Axial Load (lbs.)	Normal Acc. (g's)	Long. Acc. (g's)	Lat. Acc. (g's)	Speed (MPH)
Oscillograph Record No. 24675							
Prior to ditch	0	645	-235				28.8
Initial Drag Strut Axial Load	.092	620	780		-.15		
Drag Strut Axial Load, Springback	.119	580	-500		+.12		
Maximum Vertical Load	.061	-925	45	-.44			
Vertical Load Rebound	.105	805	- 65	-.15			
Maximum Normal Acc. (Positive)	.085	-130		+.90			
Maximum Normal Acc. (Negative)	.112	715		-.67			
Maximum Longitudinal Acc. (Positive)	.145	395	- 30		+.28		
Maximum Longitudinal Acc. (Negative)	.077	-565	140		-.22		
Maximum Lateral Acc. (Pos., to Right)	.082	-305	255			+.57	
Maximum Lateral Acc. (Neg., to Left)	.121	580	-470			-.15	
Oscillograph Record No. 24676							
Prior to ditch	0	525	-180				36.0
Initial Drag Strut Axial Load	.250	-435	160		+.03		
Drag Strut Axial Load, Springback	.560	145	-180		+.04		
Maximum Vertical Load	.250	-435	160	-.17			
Vertical Load Rebound	.610	260	- 10	+.12			
Maximum Normal Acc. (Positive)	.330	-150		+.17			
Maximum Normal Acc. (Negative)	.280	-400		-.34			
Maximum Longitudinal Acc. (Positive)	.350	- 45	45		+.14		
Maximum Longitudinal Acc. (Negative)	.150	-245	45		-.01		
Maximum Lateral Acc. (Pos. to Right)	.258	-320	85			+.18	
Maximum Lateral Acc. (Neg., to Left)	.382	50	- 65			-.25	

Note: All Vertical and Drag Strut Axial Loads tabulated above are incremental. To obtain total loads, add calibrated loads prior to contact with ditch to incremental values.
All G values are also incremental.

FA-800-23A

TABLE IV - continued

L-19A HIGH FLOTATION TIRE DITCH LOADS

L-19A Flight No. 19-15 S/N 51-7441
Ditch Size 24" wide Tire Pressure 2.7 psi Data Request No. L-19-5
4" deep

Item (Event)	Time (Sec)	Vertical Load (Lbs)	Drag Strut Axial Load (Lbs)	Normal Acc. (g's)	Long. Acc. (g's)	Lat. Acc. (g's)	Forward Velocity (MPH)
Oscillograph Record No. 25158							
Prior to obstacle	0	1020	-105				31.5
Initial Drag Strut Axial Load	.029	960	1055		-.65		
Drag Strut Axial Load, Springback	.052	410	-465		-.06		
Maximum Vertical Load	.010	-1000	-65	-.30			
Vertical Load Rebound	.029	960	1055	.66			
Maximum Normal Acc. (Positive)	.080	185		.83			
Maximum Normal Acc. (Negative)	.004	-695		-.88			
Maximum Longitudinal Acc. (Positive)	.010	-1000	-65		.18		
Maximum Longitudinal Acc. (Negative)	.029	960	1055		-.65		
Maximum Lateral Acc. (Pos. to Right)	.178	225	-55			.79	
Maximum Lateral Acc. (Neg. to Left)	.061	410	-255			-.99	

Note: All Vertical and Drag Strut Axial Loads tabulated above are incremental. To obtain loads, add calibrated loads prior to contact with obstacle to incremental values. All G values are also incremental.

TABLE IV - continued

L-19A HIGH FLOTATION TIRE DITCH LOADS

L-19A Ground Tests
Ditch Size 12" wide
6" deep

S/N 51-7441
Tire Pressure 2.7 psi

Data Request No. L-19-5

Item (Event)	Time (Sec.)	Vertical Load (lbs.)	Drag Strut Axial Load (lbs.)	Normal Acc. (g's)	Long. Acc. (g's)	Lat. Acc. (g's)	Speed (MPH)
Oscillograph Record No. 24662							
Prior to ditch	0	1030	-375				3.2
Initial Drag Strut Axial Load	.580	225	470		-.13		
Drag Strut Axial Load, Springback	.712	275	-205		.01		
Maximum Vertical Load	.310	-345	-75	-.19			
Vertical Load Rebound	.620	390	85	.21			
Maximum Normal Acc. (Positive)	.480	190		.25			
Maximum Normal Acc. (Negative)	.840	-100		-.33			
Maximum Longitudinal Acc. (Positive)	.730	230	20		.04		
Maximum Longitudinal Acc. (Negative)	.590	260	385		-.16		
Maximum Lateral Acc. (Pos., to Right)	.810	-40	75			.41	
Maximum Lateral Acc. (Neg., to Left)	.445	150	45			-.06	
Oscillograph Record No. 24663							
Prior to ditch	0	840	-350				11.6
Initial Drag Strut Axial Load	.115	240	450		-.17		
Drag Strut Axial Load, Springback	.192	735	-470		.29		
Maximum Vertical Load	.035	-240	-205	-.15			
Vertical Load Rebound	.160	960	-131	.54			
Maximum Normal Acc. (Positive)	.210	750		.64			
Maximum Normal Acc. (Negative)	.480	-190		-.46			
Maximum Longitudinal Acc. (Positive)	.192	735	-470		.29		
Maximum Longitudinal Acc. (Negative)	.110	125	330		-.19		
Maximum Lateral Acc. (Pos., to Right)	.290	345	65			.47	
Maximum Lateral Acc. (Neg., to Left)	.180	870	-350			-.29	

Note: All Vertical and Drag Strut Axial Loads tabulated above are incremental. To obtain total loads, add calibrated loads prior to contact with ditch to incremental values.
All G values are also incremental.

FA-800-23A

TABLE IV - continued

L-19A HIGH FLOTATION TIRE DITCH LOADS

L-19A Ground Tests
Ditch Size 12" wide
6" deep

S/N 51-7441
Tire Pressure 2.7 psi

Data Request No. L-19-5

Item (Event) Oscillograph Record No. 24664	Time (Sec.)	Vertical Load (lbs.)	Drag Strut Axial Load (lbs.)	Normal Acc. (g's)	Long. Acc. (g's)	Lat. Acc. (g's)	Speed (MPH)
Prior to ditch	0	860	-320				21.5
Initial Drag Strut Axial Load	.080	-40	535		-.21		
Drag Strut Axial Load, Springback	.115	315	-350		.07		
Maximum Vertical Load	.035	-340	85	-.06			
Vertical Load Rebound	.105	415	-140	-.02			
Maximum Normal Acc. (Positive)	.093	260		.70			
Maximum Normal Acc. (Negative)	.030	-320		-.21			
Maximum Longitudinal Acc. (Positive)	.135	245	-160		.19		
Maximum Longitudinal Acc. (Negative)	.075	-150	375		-.24		
Maximum Lateral Acc. (Pos., to Right)	.145	170	-160			.50	
Maximum Lateral Acc. (Neg., to Left)	.125	300	-310			-.53	

Note: All Vertical and Drag Strut Axial Loads tabulated above are incremental. To obtain total loads, add calibrated loads prior to contact with ditch to incremental values.
All G values are also incremental.

FA-800-23A

TABLE IV - continued

L-19 HIGH FLOTATION TIRE DITCH LOADS
S/N 51-7441

L-19A Ground Tests
Ditch Size 18" wide
6" deep

Tire Pressure 2.7 psi

Data Request No. L-19-5

Item (Event)	Time (Sec.)	Vertical Load (lbs.)	Drag Strut Axial Load (lbs.)	Normal Acc. (g's)	Long. Acc. (g's)	Lat. Acc. (g's)	Speed (MPH)
Oscillograph Record No. 24665							
Prior to ditch	0	1205	-275				3.2
Initial Drag Strut Axial Load	.555	250	555		-.16		
Drag Strut Axial Load, Springback	.710	- 15	-140		-.01		
Maximum Vertical Load	.220	-470	-160	-.21			
Vertical Load Rebound	.420	410	140	+.40			
Maximum Normal Acc. (Positive)	.410	380		+.42			
Maximum Normal Acc. (Negative)	.200	-455		-.25			
Maximum Longitudinal Acc. (Positive)	.210	-455	-140		+.03		
Maximum Longitudinal Acc. (Negative)	.495	340	480		-.19		
Maximum Lateral Acc. (Pos., to Right)	.710	- 15	-140			+.47	
Maximum Lateral Acc. (Neg., to Left)	.315	35	- 75			-.09	
Oscillograph Record No. 24666							
Prior to ditch	0	915	-330				11.3
Initial Drag Strut Axial Load	.168	165	650		-.23		
Drag Strut Axial Load, Springback	.265	965	-660		+.28		
Maximum Vertical Load	.098	-675	-105	-.31			
Vertical Load Rebound	.230	1220	-300	+.83			
Maximum Normal Acc. (Positive)	.060	1105		+.98			
Maximum Normal Acc. (Negative)	.500	-345		-.58			
Maximum Longitudinal Acc. (Positive)	.275	965	-190		+.29		
Maximum Longitudinal Acc. (Negative)	.160	5	520		-.28		
Maximum Lateral Acc. (Pos., to Right)	.522	-390	95			+.45	
Maximum Lateral Acc. (Neg., to Left)	.230	1220	-300			-.39	

Note: All Vertical and Drag Strut Axial Loads tabulated above are incremental. To obtain total loads, add calibrated loads prior to contact with ditch to incremental values. All G values are also incremental.

FA-800-23A

TABLE IV - continued

L-19 HIGH FLOTATION TIRE DITCH LOADS

L-19A Ground Tests
Ditch Size 18" wide
6" deep

S/N 51-7441
Tire Pressure 2.7 psi

Data Request No. L-19-5

Item (Event)	Time (Sec.)	Vertical Load (lbs.)	Drag Strut Axial Load (lbs.)	Normal Acc. (g's)	Long. Acc. (g's)	Lat. Acc. (g's)	Speed (MPH)
Oscillograph Record No. 24679							
Prior to ditch	0	925	-295				20.7
Initial Drag Strut Axial Load	.090	80	770		-.42		
Drag Strut Axial Load, Springback	.130	400	-470		+.31		
Maximum Vertical Load	.055	-820	-385	-.63			
Vertical Load Rebound	.112	470	85	-.19			
Maximum Normal Acc. (Positive)	.090	80		+.67			
Maximum Normal Acc. (Negative)	.055	-820		-.63			
Maximum Longitudinal Acc. (Positive)	.130	400	-470		+.31		
Maximum Longitudinal Acc. (Negative)	.100	280	735		-.45		
Maximum Lateral Acc. (Pos., to Right)	.085	-100	610			+.48	
Maximum Lateral Acc. (Neg., to Left)	.120	450	-160			-.58	
Oscillograph Record No. 24699							
Prior to ditch	0	900	-335				24.1
Initial Drag Strut Axial Load	.085	550	585		-.24		
Drag Strut Axial Load, Springback	.122	625	-545		+.23		
Maximum Vertical Load	.045	-645	-400	-.21			
Vertical Load Rebound	.105	780	- 85	+.02			
Maximum Normal Acc. (Positive)	.133	530		+.84			
Maximum Normal Acc. (Negative)	.045	-645		-.21			
Maximum Longitudinal Acc. (Positive)	.138	430	-385		+.30		
Maximum Longitudinal Acc. (Negative)	.060	-500	270		-.38		
Maximum Lateral Acc. (Pos., to Right)	.138	430	-385			+.56	
Maximum Lateral Acc. (Neg., to Left)	.110	885	-270			-1.01	

Note: All Vertical and Drag Strut Axial Loads tabulated above are incremental. To obtain total loads, add calibrated loads prior to contact with ditch to incremental values. All G values are also incremental.

TABLE IV - continued

L-19A HIGH FLOTATION TIRE DITCH LOADS

L-19A Ground Tests
Ditch Size 18" wide
6" deep

S/N 51-7441
Tire Pressure 2.7 psi

Data Request No. L-19-5

Item (Event)	Time (Sec.)	Vertical Load (lbs.)	Drag Strut Axial Load (lbs.)	Normal Acc. (g's)	Long. Acc. (g's)	Lat. Acc. (g's)	Speed (MPH)
Oscillograph Record No. 24680							
Prior to ditch	0	805	-265				25.0
Initial Drag Strut Axial Load	.075	670	790		-.39		
Drag Strut Axial Load, Springback	.105	850	-555		+.27		
Maximum Vertical Load	.038	-525	-545	-.27			
Vertical Load Rebound	.090	945	- 30	+.04			
Maximum Normal Acc. (Positive)	.072	730		+1.11			
Maximum Normal Acc. (Negative)	.042	-485		-.29			
Maximum Longitudinal Acc. (Positive)	.128	590	-425		+.43		
Maximum Longitudinal Acc. (Negative)	.072	730	715		-.41		
Maximum Lateral Acc. (Pos., to Right)	.128	590	-425			+.68	
Maximum Lateral Acc. (Neg., to Left)	.100	805	-480			-.83	
Oscillograph Record No. 24700							
Prior to ditch	0	925	-260				28.4
Initial Drag Strut Axial Load	.078	750	775		-.42		
Drag Strut Axial Load, Springback	.105	920	-500		+.09		
Maximum Vertical Load	.032	-425	50	-.48			
Vertical Load Rebound	.092	1035	180	+.83			
Maximum Normal Acc. (Positive)	.128	805		+.99			
Maximum Normal Acc. (Negative)	.025	-365		-.50			
Maximum Longitudinal Acc. (Positive)	.132	760	-270		+.45		
Maximum Longitudinal Acc. (Negative)	.078	750	775		-.42		
Maximum Lateral Acc. (Pos., to Right)	.042	720	-220			+.68	
Maximum Lateral Acc. (Neg., to Left)	.112	910	-135			-.43	

Note: All Vertical and Drag Strut Axial Loads tabulated above are incremental. To obtain total loads, add calibrated loads prior to contact with ditch to incremental values. All G values are also incremental.

TABLE IV - continued

L-19A HIGH FLOTATION TIRE DITCH LOADS

L-19A Ground Tests
Ditch Size 24" wide
6" deep

S/N 51-7441
Tire Pressure 2.7 psi

Data Request No. L-19-5

Item (Event)	Time (Sec.)	Vertical Load (lbs.)	Drag Strut Axial Load (lbs.)	Normal Acc. (g's)	Long. Acc. (g's)	Lat. Acc. (g's)	Speed (MPH)
Oscillograph Record No. 24667							
Prior to ditch	0	985	-340				3.0
Initial Drag Strut Axial Load	.560	280	445		-.21		
Drag Strut Axial Load, Springback	.905	333	30		-.03		
Maximum Vertical Load	.210	-380	-160	-.23			
Vertical Load Rebound	.485	640	290	+.40			
Maximum Normal Acc. (Positive)	.455	620		+.58			
Maximum Normal Acc. (Negative)	.740	230		-.29			
Maximum Longitudinal Acc. (Positive)	.255	-280	-150		+.07		
Maximum Longitudinal Acc. (Negative)	.560	280	445		-.21		
Maximum Lateral Acc. (Pos., to Right)	.655	205	235			+.50	
Maximum Lateral Acc. (Neg., to Left)	1.290	-300	45			-.22	
Oscillograph Record No. 24681							
Prior to ditch	0	810	-405				10.9
Initial Drag Strut Axial Load	.160	20	470		-.31		
Drag Strut Axial Load, Springback	.290	1040	-375		+.35		
Maximum Vertical Load	.085	-625	75	-.44			
Vertical Load Rebound	.250	1310	-140	+1.22			
Maximum Normal Acc. (Positive)	.260	1245		+1.26			
Maximum Normal Acc. (Negative)	.510	-400		-.74			
Maximum Longitudinal Acc. (Positive)	.290	1040	-375		+.35		
Maximum Longitudinal Acc. (Negative)	.145	-135	360		-.35		
Maximum Lateral Acc. (Pos., to Right)	.390	60	150			+.64	
Maximum Lateral Acc. (Neg., to Left)	.225	1150	- 45			-.47	

Note: All Vertical and Drag Strut Axial Loads tabulated above are incremental. To obtain total loads, add calibrated loads prior to contact with ditch to incremental values.
All G values are incremental.

FA-800-23A

TABLE IV - continued

L-19A HIGH FLOTATION TIRE DITCH LOADS

L-19A Ground Tests
Ditch Size 24" wide
6" deep

S/N 51-7441
Tire Pressure 2.7 psi

Data Request No. L-19-5

Item (Event)	Time (Sec.)	Vertical Load (lbs.)	Drag Strut Axial Load (lbs.)	Normal Acc. (g's)	Long. Acc. (g's)	Lat. Acc. (g's)	Speed (MPH)
Oscillograph Record No. 24682							
Prior to ditch	0	985	-300				17.1
Initial Drag Strut Axial Load	.168	75	680		-.34		
Drag Strut Axial Load, Springback	.305	600	-555		+.01		
Maximum Vertical Load	.107	-1055	- 20	-1.17			
Vertical Load Rebound	.238	740	-140	+.65			
Maximum Normal Acc. (Positive)	.195	510		+.71			
Maximum Normal Acc. (Negative)	.113	-1040		-1.22			
Maximum Longitudinal Acc. (Positive)	.220	625	-510		+.28		
Maximum Longitudinal Acc. (Negative)	.145	-305	300		-.46		
Maximum Lateral Acc. (Pos., to Right)	.130	-810	320			+.57	
Maximum Lateral Acc. (Neg., to Left)	.312	455	-170			-.24	
Oscillograph Record No. 24701							
Prior to ditch	0	850	-270				25.2
Initial Drag Strut Axial Load	.110	680	910		-.41		
Drag Strut Axial Load, Springback	.145	750	-710		+.47		
Maximum Vertical Load	.070	-860	-335	-.59			
Vertical Load Rebound	.138	1015	-210	+.63			
Maximum Normal Acc. (Positive)	.158	770		+1.00			
Maximum Normal Acc. (Negative)	.070	-860		-.59			
Maximum Longitudinal Acc. (Positive)	.158	770	-355		+.53		
Maximum Longitudinal Acc. (Negative)	.110	680	910		-.41		
Maximum Lateral Acc. (Pos., to Right)	.145	565	-270			+.65	
Maximum Lateral Acc. (Neg., to Left)	.132	920	- 85			-.91	

Note: All Vertical and Drag Strut Axial Loads tabulated above are incremental. To obtain total loads, add calibrated loads prior to contact with ditch to incremental values. All G values are also incremental.

TABLE IV - continued

L-19A HIGH FLOTATION TIRE DITCH LOADS

L-19A Ground Tests
Ditch Size 24" wide
6" deep

S/N 51-7441
Tire Pressure 2.7 psi

Data Request No. L-19-5

Item (Event)	Time (Sec.)	Vertical Load (lbs.)	Drag Strut Axial Load (lbs.)	Normal Acc. (g's)	Long. Acc. (g's)	Lat. Acc. (g's)	Speed (MPH)
Oscillograph Record No. 24753							
Prior to ditch	0	875	-260				27.1
Initial Drag Strut Axial Load	.090	335	940		+.24		
Drag Strut Axial Load, Springback	.120	600	-700		+.31		
Maximum Vertical Load	.060	-950	- 75	-.27			
Vertical Load Rebound	.190	785	240	+.34			
Maximum Normal Acc. (Positive)	.097	725		+1.43			
Maximum Normal Acc. (Negative)	.100	665		-2.31			
Maximum Longitudinal Acc. (Positive)	.093	690	835		+1.00		
Maximum Longitudinal Acc. (Negative)	.108	750	- 20		-1.26		
Maximum Lateral Acc. (Pos., to Right	.232	280	-325			+.64	
Maximum Lateral Acc. (Neg., to Left)	.202	610	-135			-1.02	
Oscillograph Record No. 24702							
Prior to ditch	0	810	-230				29.9
Initial Drag Strut Axial Load	.075	585	980		-.50		
Drag Strut Axial Load, Springback	.103	625	-595		+.05		
Maximum Vertical Load	.042	-760	-210	-.80			
Vertical Load Rebound	.090	880	165	-.15			
Maximum Normal Acc. (Positive)	.125	665		+1.07			
Maximum Normal Acc. (Negative)	.048	-740		-.84			
Maximum Longitudinal Acc. (Positive)	.130	525	-450		+.45		
Maximum Longitudinal Acc. (Negative)	.080	770	865		-.55		
Maximum Lateral Acc. (Pos. to Right)	.165	665	-345			+.79	
Maximum Lateral Acc. (Neg. to Left)	.108	665	-270			-1.19	

Note: All Vertical and Drag Strut Axial Loads tabulated above are incremental. To obtain total loads, add calibrated loads prior to contact with ditch to incremental values.
All G values are also incremental.

REPORT NO. T1245-1 FAIRCHILD Aircraft and Missiles Div.
MODEL M-245B PREPARED BY OF FAIRCHILD ENGINE & AIRPLANE CORPORATION
CHECKED BY APPROVED BY
SUBJECT:- APPENDIX I LANDING GEAR TEST DATA, M-245B
DATE January 22, 1960 PAGES PAGE 62
REVISED

TABLE IV - continued

L-19A HIGH FLOTATION TIRE DITCH LOADS

L-19A Flight No. 19-15
Ditch Size 24" wide
6" deep

S/N 51-7441
Tire Pressure 2.7 psi

Data Request No. L-19-5

Item (Event)	Time (Sec)	Vertical Load (Lbs)	Drag Strut Axial Load (Lbs)	Normal Acc. (g's)	Long. Acc. (g's)	Lat. Acc. (g's)	Forward Velocity (MPH)
Oscillograph Record No. 25160							
Prior to obstacle	0	1105	-135				26.1
Initial Drag Strut Axial Load	.040	100	1085		-.48		
Drag Strut Axial Load, Springback	.079	675	-780		+.44		
Maximum Vertical Load	.007	-1370	-170	-.62			
Vertical Load Rebound	.074	860	-570	-.04			
Maximum Normal Acc. (Positive)	.047	655		+1.71			
Maximum Normal Acc. (Negative)	.010	-1000		-.71			
Maximum Longitudinal Acc. (Positive)	.079	675	-780		+.44		
Maximum Longitudinal Acc. (Negative)	.046	715	855		-.61		
Maximum Lateral Acc. (Pos. to Right)	.035	-145	360			+.58	
Maximum Lateral Acc. (Neg. to Left)	.074	860	-570			-.93	

Note: All Vertical and Drag Strut Axial Loads tabulated above are incremental. To obtain loads, add calibrated loads prior to contact with obstacle to incremental values. All G values are also incremental.

TABLE IV - continued

L-19A HIGH FLOTATION TIRE DITCH LOADS

L-19A Flight No. 19-16 S/N 51-7441 Data Request No. L-19-5
Ditch Size 24" wide Tire Pressure 2.8 psi
7" deep

Item (Event)	Time (Sec)	Vertical Load (Lbs)	Drag Strut Load (Lbs)	Normal Acc. (g's)	Long. Acc. (g's)	Lat. Acc. (g's)	Forward Velocity (MPH)
Oscillograph Record No. 25181							
Prior to obstacle	0	1035	-120				30.3
Initial Drag Strut Axial Load	.097	125	950		-.04		
Drag Strut Axial Load, Springback	.118	515	-605		-.21		
Maximum Vertical Load	.066	-1035	-290	-.57			
Vertical Load Rebound	.104	845	250	.33			
Maximum Normal Acc. (Positive)	.150	185		.87			
Maximum Normal Acc. (Negative)	.061	-910		-.57			
Maximum Longitudinal Acc. (Positive)	.140	310	-95		.16		
Maximum Longitudinal Acc. (Negative)	.120	435	-560		-.23		
Maximum Lateral Acc. (Pos, to Right)	.241	250	-95			.75	
Maximum Lateral Acc. (Neg, to Left)	.125	395	-335			-1.01	

Note: All Vertical and Drag Strut Axial Loads tabulated above are incremental. To obtain loads, add calibrated loads prior to contact with obstacle to incremental values. All G values are also incremental.

TABLE IV - continued

L-19A HIGH FLOTATION TIRE DITCH LOADS

L-19A Flight No. 19-16 S/N 51-7441
Ditch Size 24" wide
7" deep Tire Pressure 2.8 psi Data Request No. L-19-5

Item (Event)	Time (Sec)	Vertical Load (Lbs)	Drag Strut Axial Load (Lbs)	Normal Acc. (g's)	Long. Acc. (g's)	Lat. Acc. (g's)	Forward Velocity (MPH)
Oscillograph Record No. 25180							
Prior to obstacle	0	930	-215				18.2
Initial Drag Strut Axial Load	.075	145	645		-.35		
Drag Strut Axial Load, Springback	.220	475	-505		.19		
Maximum Vertical Load	.142	-890	150	-1.11			
Vertical Load Rebound	.283	765	120	.41			
Maximum Normal Acc. (Positive)	.315	580		.59			
Maximum Normal Acc. (Negative)	.142	-890		-1.11			
Maximum Longitudinal Acc. (Positive)	.290	560	-440		.52		
Maximum Longitudinal Acc. (Nagative)	.295	580	-150		-.43		
Maximum Lateral Acc. (Pos. to Right)	.162	-455	345			.58	
Maximum Lateral Acc. (Neg. to Left)	.278	725	160			.44	

Note: All Vertical and Drag Strut Axial Loads tabulated above are incremental. To obtain loads, add calibrated loads prior to contact with obstacle to incremental values. All G values are also incremental.

FA-800-23A

TABLE IV - continued

L-19A HIGH FLOTATION TIRE DITCH LOADS

L-19A Ground Tests S/N 51-7441 Data Request No. L-19-5
Ditch Size 12" wide Tire Pressure 2.7 psi
8" deep

Item (Event) Oscillograph Record No. 24712	Time (Sec.)	Vertical Load (lbs.)	Drag Strut Axial Load (lbs.)	Normal Acc. (g's)	Long. Acc. (g's)	Lat. Acc. (g's)	Speed (MPH)
Prior to ditch	0	960	-330				10.3
Initial Drag Strut Axial Load	.132	220	550		-.10		
Drag Strut Axial Load, Springback	.230	645	-325		.10		
Maximum Vertical Load	.039	-345	-305	-.11			
Vertical Load Rebound	.185	890	-210	.55			
Maximum Normal Acc. (Positive)	.195	830		.57			
Maximum Normal Acc. (Negative)	.039	-345		-.11			
Maximum Longitudinal Acc. (Positive)	.195	830	-265		.18		
Maximum Longitudinal Acc. (Negative)	.096	80	125		-.16		
Maximum Lateral Acc. (Pos., to Right)	.227	670	-295			.46	
Maximum Lateral Acc. (Neg., to Left)	.203	745	-230			-.31	
Oscillograph Record No. 24713							
Prior to ditch	0	1005	-325				17.2
Initial Drag Strut Axial Load	.130	-275	465		-.53		
Drag Strut Axial Load, Springback	.170	60	-400		.10		
Maximum Vertical Load	.096	-550	-190	-.21			
Vertical Load Rebound	.240	275	-10	.34			
Maximum Normal Acc. (Positive)	.190	115		.61			
Maximum Normal Acc. (Negative)	.168	80		-.28			
Maximum Longitudinal Acc. (Positive)	.193	95	-285		.30		
Maximum Longitudinal Acc. (Negative)	.130	-275	465		-.53		
Maximum Lateral Acc. (Pos., to Right)	.282	105	-315			.38	
Maximum Lateral Acc. (Neg., to Left)	.173	60	-350			-.50	

Note: All Vertical and Drag Strut Axial Loads tabulated above are incremental. To obtain total loads, add calibrated loads prior to contact with ditch to incremental values.
All G values are also incremental.

TABLE IV - continued

L-19A HIGH FLOTATION TIRE DITCH LOADS

L-19A Ground Tests
Ditch Size 12" wide
8" deep

S/N 51-7441
Tire Pressure 2.7 psi

Data Request No. L-19-5

Item (Event) Oscillograph Record No. 24714	Time (Sec.)	Vertical Load (lbs.)	Drag Strut Axial Load (lbs.)	Normal Acc. (g's)	Long. Acc. (g's)	Lat. Acc. (g's)	Speed (MPH)
Prior to ditch	0	925	-230				27.9
Initial Drag Strut Axial Load	.088	295	445		-.24		
Drag Strut Axial Load, Springback	.120	630	-420		.12		
Maximum Vertical Load	.055	-400	180	-.21			
Vertical Load Rebound	.185	705	20	.45			
Maximum Normal Acc. (Positive)	.152	440		.59			
Maximum Normal Acc. (Negative)	.046	-335		-.32			
Maximum Longitudinal Acc. (Positive)	.062	-240	-245		.33		
Maximum Longitudinal Acc. (Negative)	.081	105	245		-.31		
Maximum Lateral Acc. (Pos., to Right)	.165	560	0			.65	
Maximum Lateral Acc. (Neg., to Left)	.196	630	-65			-.30	

Note: All Vertical and Drag Strut Axial Loads tabulated above are incremental. To obtain total loads, add calibrated loads prior to contact with ditch to incremental values.
All G values are also incremental.

FA-800-23A

TABLE IV - continued

L-19A HIGH FLOTATION TIRE DITCH LOADS

L-19A Ground Tests
Ditch Size 18" wide
8" deep

S/N 51-7441
Tire Pressure 2.7 psi

Data Request No. L-19-5

Item (Event)	Time (Sec)	Vertical Load (lbs.)	Drag Strut Axial Load (lbs.)	Normal Acc. (g's)	Long. Acc. (g's)	Lat. Acc. (g's)	Speed (MPH)
Oscillograph Record No. 24715							
Prior to ditch	0	950	-420				5.4
Initial Drag Strut Axial Load	.302	345	455		-.19		
Drag Strut Axial Load, Springback	.460	460	-275		+.12		
Maximum Vertical Load	.146	-300	10	-.21			
Vertical Load Rebound	.394	790	135	+.59			
Maximum Normal Acc. (Positive)	.375	720		+.64			
Maximum Normal Acc. (Negative)	.146	-300		-.21			
Maximum Longitudinal Acc. (Positive)	.460	460	-275		+.12		
Maximum Longitudinal Acc. (Negative)	.302	345	455		-.19		
Maximum Lateral Acc. (Pos., to Right)	.569	-205	125			+.43	
Maximum Lateral Acc. (Neg., to Left)	.350	710	315			+.02	
Oscillograph Record No. 24716							
Prior to ditch	0	965	-410				9.4
Initial Drag Strut Axial Load	.223	380	340		-.07		
Drag Strut Axial Load, Springback	.320	685	-475		+.41		
Maximum Vertical Load	.102	-450	-245	-.30			
Vertical Load Rebound	.303	870	-200	+.47			
Maximum Normal Acc. (Positive)	.272	765		+.89			
Maximum Normal Acc. (Negative)	.570	-315		-.64			
Maximum Longitudinal Acc. (Positive)	.317	730	-420		+.46		
Maximum Longitudinal Acc. (Negative)	.413	35	30		-.42		
Maximum Lateral Acc. (Pos., to Right)	.432	- 75	150			+.47	
Maximum Lateral Acc. (Neg., to Left)	.245	505	0			-.23	

Note: All Vertical and Drag Strut Axial Loads tabulated above are incremental. To obtain total loads, add calibrated loads prior to contact with ditch to incremental values. All G values are also incremental.

TABLE IV - continued

L-19A HIGH FLOTATION TIRE DITCH LOADS

L-19A Ground Tests
Ditch Size 18" wide
8" deep

S/N 51-7441
Tire Pressure 2.7 psi

Data Request No. L-19-5

Item (Event)	Time (Sec)	Vertical Load (lbs.)	Drag Strut Axial Load (lbs.)	Normal Acc. (g's)	Long. Acc. (g's)	Lat. Acc. (g's)	Speed (MPH)
Oscillograph Record No. 24717							
Prior to ditch	0	930	-275				23.8
Initial Drag Strut Axial Load	.071	-275	655		-.26		
Drag Strut Axial Load, Springback	.130	425	-675		+.41		
Maximum Vertical Load	.055	-540	-275	-.11			
Vertical Load Rebound	.105	690	-170	+.11			
Maximum Normal Acc. (Positive)	.089	-140		+.89			
Maximum Normal Acc. (Negative)	.058	-510		-.25			
Maximum Longitudinal Acc. (Positive)	.130	425	-675		+.41		
Maximum Longitudinal Acc. (Negative)	.063	-400	275		-.44		
Maximum Lateral Acc. (Pos., to Right)	.145	295	-475			+.55	
Maximum Lateral Acc. (Neg., to Left)	.118	610	-380			-.78	
Oscillograph Record No. 24749							
Prior to ditch	0	985	-270				24.4
Initial Drag Strut Axial Load	.089	-360	660		-.37		
Drag Strut Axial Load, Springback	.156	350	-575		+.83		
Maximum Vertical Load	.067	-640	-545	.00			
Vertical Load Rebound	.123	645	-345	-.06			
Maximum Normal Acc. (Positive)	.115	640		+1.91			
Maximum Normal Acc. (Negative)	.105	585		-2.00			
Maximum Longitudinal Acc. (Positive)	.105	585	430		+1.26		
Maximum Longitudinal Acc. (Negative)	.113	625	10		-1.09		
Maximum Lateral Acc. (Pos., to Right)	.161	255	-430			+.47	
Maximum Lateral Acc. (Neg., to Left)	.133	570	-395			-.92	

Note: All Vertical and Drag Strut Axial Loads tabulated above are incremental. To obtain total loads, add calibrated loads prior to contact with ditch to incremental values. All G values are also incremental.

TABLE IV - continued

L-19A HIGH FLOTATION TIRE DITCH LOADS

L-19A Ground Tests
Ditch Size 24" wide
8" deep

S/N 51-7441
Tire Pressure 2.7 psi

Data Request No. L-19-5

Item (Event)	Time (Sec.)	Vertical Load (lbs.)	Drag Strut Axial Load (lbs.)	Normal Acc. (g's)	Long. Acc. (g's)	Lat. Acc. (g's)	Speed (MPH)
Oscillograph Record No. 24718*							
Prior to ditch	0	970	-455				5.1
Initial Drag Strut Axial Load	.450	950	970		-.27		
Drag Strut Axial Load, Springback	.620	- 60	-105		-.07		
Maximum Vertical Load	.240	-445	- 20	-.25			
Vertical Load Rebound	.495	1000	590	+.85			
Maximum Normal Acc. (Positive)	.460	980		+.93			
Maximum Normal Acc. (Negative)	.230	-430		-.32			
Maximum Longitudinal Acc. (Positive)	.600	185	0		+.03		
Maximum Longitudinal Acc. (Negative)	.460	980	825		-.29		
Maximum Lateral Acc. (Pos., to Right)	.630	-120	160			+.34	
Maximum Lateral Acc. (Neg., to Left)	.287	- 95	275			-.01	
Oscillograph Record No. 24719							
Prior to ditch	0	980	-410				4.3
Initial Drag Strut Axial Load	.488	860	1035		-.41		
Drag Strut Axial Load, Springback	.680	-195	- 40		-.14		
Maximum Vertical Load	.215	-565	- 40	-.34			
Vertical Load Rebound	.433	1065	770	+.89			
Maximum Normal Acc. (Positive)	.429	1055		+.93			
Maximum Normal Acc. (Negative)	.200	-525		-.36			
Maximum Longitudinal Acc. (Positive)	.615	285	160		-.04		
Maximum Longitudinal Acc. (Negative)	.500	750	905		-.42		
Maximum Lateral Acc. (Pos., to Right)	.610	305	180			+.45	
Maximum Lateral Acc. (Neg., to Left)	.339	410	150			-.10	

Note: All Vertical and Drag Strut Axial Loads tabulated above are incremental. To obtain total loads, add calibrated loads prior to contact with ditch to incremental values. All G values are also incremental.

* Did not hit ditch squarely.

FA-800-23A

TABLE IV - continued

L-19A HIGH FLOTATION TIRE DITCH LOADS

L-19A Ground Tests
Ditch Size 24" wide
8" deep

S/N 51-7441
Tire Pressure 2.7 psi

Data Request No. L-19-5

Item (Event)	Time (Sec.)	Vertical Load (lbs.)	Drag Strut Axial Load (lbs.)	Normal Acc. (g's)	Long. Acc. (g's)	Lat. Acc. (g's)	Speed (MPH)
Oscillograph Record No. 24750							
Prior to ditch	0	1025	-345				8.0
Initial Drag Strut Axial Load	.232	- 75	825		-.35		
Drag Strut Axial Load, Springback	.378	1465	-775		+.67		
Maximum Vertical Load	.121	-750	75	-.44			
Vertical Load Rebound	.363	1775	-325	+1.80			
Maximum Normal Acc. (Positive)	.363	1775		+1.80			
Maximum Normal Acc. (Negative)	.512	-450		-.92			
Maximum Longitudinal Acc. (Positive)	.401	1030	-500		+.86		
Maximum Longitudinal Acc. (Negative)	.389	1295	- 85		-.46		
Maximum Lateral Acc. (Pos., to Right)	.482	-265	230			+.74	
Maximum Lateral Acc. (Neg., to Left)	.354	1755	-125			-.39	

Note: All Vertical and Drag Strut Axial Loads tabulated above are incremental. To obtain total loads, add calibrated loads prior to contact with ditch to incremental values. All G values are also incremental.

TABLE IV - continued

L-19A HIGH FLOTATION TIRE DITCH LOADS

L-19A Flight No. 19-15 S/N 51-7441 Data Request No. L-19-5
Ditch Size 24" wide Tire Pressure 2.7 psi
8" deep

Item (Event)	Time (Sec)	Vertical Load (Lbs)	Drag Strut Axial Load (Lbs)	Normal Acc. (g's)	Long. Acc. (g's)	Lat. Acc. (g's)	Forward Velocity (MPH)
Oscillograph Record No. 25162							
Prior to obstacle	0	960	-230				7.1
Initial Drag Strut Axial Load	.155	-305	560		-.28		
Drag Strut Axial Load, Springback	.330	1225	-580		.38		
Maximum Vertical Load	.088	-655	-10	-.41			
Vertical Load Rebound	.310	1510	-135	1.43			
Maximum Normal Acc. (Positive)	.310	1510		1.43			
Maximum Normal Acc. (Negative)	.553	-655		-.83			
Maximum Longitudinal Acc. (Positive)	.292	1490	-210		.55		
Maximum Longitudinal Acc. (Negative)	.394	165	190		-.51		
Maximum Lateral Acc. (Pos. to Right)	.415	-60	85			1.00	
Maximum Lateral Acc. (Neg. to Left)	.382	1510	230			-.08	

Note: All Vertical and Drag Strut Axial Loads tabulated above are incremental. To obtain loads, add calibrated loads prior to contact with obstacle to incremental values. All G values are also incremental.

TABLE IV - continued

L-19A HIGH FLOTATION TIRE DITCH LOADS

L-19A Ground Tests
Ditch Size 24" wide
4" deep

S/N 51-7441
Tire Pressure 3.6 ± 2 psi

Data Request No. L-19-5

Item (Event)	Time (Sec.)	Vertical Load (lbs.)	Drag Strut Axial Load (lbs.)	Normal Acc. (g's)	Long. Acc. (g's)	Lat. Acc. (g's)	Speed (MPH)
Oscillograph Record No. 24728							
Prior to ditch	0	1070	-305				3.3
Initial Drag Strut Axial Load	.375	820	305		-.07		
Drag Strut Axial Load, Springback	.452	465	-495		+.23		
Maximum Vertical Load	.185	-620	-105	-.23			
Vertical Load Rebound	.410	945	180	+.83			
Maximum Normal Acc. (Positive)	.390	845		+.91			
Maximum Normal Acc. (Negative)	.170	-570		-.30			
Maximum Longitudinal Acc. (Positive)	.452	465	-495		+.23		
Maximum Longitudinal Acc. (Negative)	.295	265	210		-.11		
Maximum Lateral Acc. (Pos., to Right)	.540	-195	-190			+.54	
Maximum Lateral Acc. (Neg., to Left)	.295	265	210			-.03	
Oscillograph Record No. 24729							
Prior to ditch	0	960	-390				9.8
Initial Drag Strut Axial Load	.182	235	370		-.10		
Drag Strut Axial Load, Springback	.282	900	-485		+.19		
Maximum Vertical Load	.089	-680	65	-.21			
Vertical Load Rebound	.250	1125	-265	+.93			
Maximum Normal Acc. (Positive)	.250	1125		+.93			
Maximum Normal Acc. (Negative)	.080	-645		-.23			
Maximum Longitudinal Acc. (Positive)	.265	1005	-410		+.29		
Maximum Longitudinal Acc. (Negative)	.150	- 45	265		-.15		
Maximum Lateral Acc. (Pos., to Right)	.418	-225	30			+.39	
Maximum Lateral Acc. (Neg., to Left)	.220	805	135			-.11	

Note: All Vertical and Drag Strut Axial Loads tabulated above are incremental. To obtain total loads, add calibrated loads prior to contact with ditch to incremental values. All G values are also incremental.

FA-800-23A

TABLE IV - continued

L-19A HIGH FLOTATION TIRE DITCH LOADS

L-19A Ground Tests
Ditch Size 24" wide
4" deep

S/N 51-7441
Tire Pressure 3.6 ±2 psi

Data Request No. L-19-5

Item (Event)	Time (Sec)	Vertical Load (lbs.)	Drag Strut Axial Load (lbs.)	Normal Acc. (g's)	Long. Acc. (g's)	Lat. Acc. (g's)	Speed (MPH)
Oscillograph Record No. 24730							
Prior to ditch	0	930	-380				17.0
Initial Drag Strut Axial Load	.160	- 40	675		-.56		
Drag Strut Axial Load, Springback	.200	410	-515		+.34		
Maximum Vertical Load	.125	-980	220	-1.55			
Vertical Load Rebound	.267	605	40	+.38			
Maximum Normal Acc. (Positive)	.163	-145		+.47			
Maximum Normal Acc. (Negative)	.123	-960		-1.78			
Maximum Longitudinal Acc. (Positive)	.200	410	-515		+.34		
Maximum Longitudinal Acc. (Negative)	.160	- 40	675		-.56		
Maximum Lateral Acc. (Pos., to Right)	.143	-720	285			+.53	
Maximum Lateral Acc. (Neg., to Left)	.261	585	170			-.54	

Note: All Vertical and Drag Strut Axial Loads tabulated above are incremental. To obtain total loads, add calibrated loads prior to contact with ditch to incremental values. All G values are also incremental.

TABLE V

L-19A HIGH FLOTATION TIRE LANDING LOADS

L-19A Flight No. L-19-12
Tire Pressure - L. 8.6 psi
R. 8.5 psi

S/N 51-7441
Sinking Speed 1.2 fps

Data Request No. L-19-6

Item (Event)	Time (Sec)	Vertical Load (lbs)		Drag Strut Axial Load (lbs)		C.G. Load Factor (g's)	Long. Acc. (g's)	Lat. Acc. (g's)	Speed (MPH)
		Right	Left	Right	Left				
Oscillograph Record No. 24939									
First Gear Contact (Right Main)	0								42.3*
Initial Left Drag Strut Axial Load	.210	470	655	- 330	700		-.59		
Left Drag Strut Axial Load, Springback	.245	125	545	110	- 480		.04		
Left Drag Strut Axial Load, 2nd Cycle	.280	50	485	110	200		-.22		
Maximum Left Gear Vertical Load	.183	720	745	280	260	+1.41			
Left Gear Vertical Load Rebound	.428	80	55	40	- 80	.89			
Initial Right Drag Strut Axial Load	.128	1000	445	880	320		-.57		
Right Drag Strut Axial Load, Springback	.150	805	440	-1140	410		.18		
Right Drag Strut Axial Load, 2nd Cycle	.183	720	745	280	260		-.22		
Maximum Right Gear Vertical Load	.130	1000	470	750	350	+1.39			
Right Gear Vertical Load Rebound	.298	- 35	420	110	- 150	1.02			
Maximum C.G. Load Factor (Positive)	.182	720	745			1.41			
Maximum C.G. Load Factor (Negative)	.422	70	55			.85			
Maximum Longitudinal Accel. (Positive)	.151	770	445	-1110	500		.42		
Maximum Longitudinal Accel. (Negative)	.210	470	655	- 330	700		-.59		
Maximum Lateral Accel. (Pos., to Right)	.154	770	510	- 840	600			.40	
Maximum Lateral Accel. (Neg., to Left)	.110	895	470	700	30			-.14	

* Wheel speed measured at instant of tail wheel touchdown.

TABLE V - continued

L-19A HIGH FLOTATION TIRE LANDING LOADS

L-19A Flight No. L-19-12 S/N 51-7441
Tire Pressure - L. 8.6 psi Sinking Speed 1.4 fps Data Request No. L-19-6
R. 8.6 psi

Item (Event)	Time (Sec)	Vertical Load (lbs)		Drag Strut Axial Load (lbs)		C.G. Load Factor (g's)	Long. Acc. (g's)	Lat. Acc. (g's)	Speed (MPH)
		Right	Left	Right	Left				
Oscillograph Record No. 24937									
First Gear Contact (Both)	0								—
Initial Left Drag Strut Axial Load	.130	1130	1030	770	860		.57		
Left Drag Strut Axial Load, Springback	.170	865	995	- 170	- 920		0		
Left Drag Strut Axial Load, 2nd Cycle	.205	730	710	- 220	280		.30		
Maximum Left Gear Vertical Load	.150	895	1070	- 520	800	1.66			
Left Gear Vertical Load Rebound	.295	145	10	100	10	.89			
Initial Right Drag Strut Axial Load	.112	1015	895	820	510		-.75		
Right Drag Strut Axial Load, Springback	.156	880	1015	- 000	480		.06		
Right Drag Strut Axial Load, 2nd Cycle	.188	935	940	570	- 220		-.38		
Maximum Right Gear Vertical Load	.135	1140	1030	780	860	1.66			
Right Gear Vertical Load Rebound	.341	- 40	115	80	20	.79			
Maximum C.G. Load Factor (Positive)	.140	1045	1050			1.66			
Maximum C.G. Load Factor (Negative)	.345	- 10	120			.79			
Maximum Longitudinal Accel. (Positive)	.160	900	995	- 790	40		.59		
Maximum Longitudinal Accel. (Negative)	.128	1100	1025	700	840		-.77		
Maximum Lateral Accel. (Pos., to Right)	.317	120	85	- 30	10			.20	
Maximum Lateral Accel. (Neg., to Left)	.173	855	985	- 50	- 890			-.32	

TABLE V - continued

L-19A HIGH FLOTATION TIRE LANDING LOADS

L-19A Flight No. L-19-15 S/N 51-7441 Data Request No. L-19-6
Tire Pressure - L. 8.8 psi Sinking Speed 1.5 fps
R. 8.5 psi

Item (Event)	Time (Sec)	Vertical Load (lbs)		Drag Strut Axial Load (lbs)		C.G. Load Factor (g's)	Long. Acc. (g's)	Lat. Acc. (g's)	Speed (MPH)
		Right	Left	Right	Left				
Oscillograph Record No. 25149									
First Gear Contact (Right Main)	0								46.1
Initial Left Drag Strut Axial Load	.189	410	590	-395	600		-.26		
Left Drag Strut Axial Load, Springback	.245	245	470	- 60	-464		-.18		
Left Drag Strut Axial Load, 2nd Cycle	.273	130	450	- 20	265		-.40		
Maximum Left Gear Vertical Load	.205	390	615	80	455	+1.43			
Left Gear Vertical Load Rebound	.538	95	0	- 20	- 10	+ .66			
Initial Right Drag Strut Axial Load	.129	655	410	565	285		-.48		
Right Drag Strut Axial Load, Spring back	.182	430	550	-555	390		-.26		
Right Drag Strut Axial Load, 2nd Cycle	.214	390	590	150	325		-.36		
Maximum Right Gear Vertical Load	.130	655	410	435	295	+1.47			
Right Gear Vertical Load Rebound	.333	- 35	205	- 80	65	+ .96			
Maximum C.G. Load Factor (Positive)	.100	600	390			+1.58			
Maximum C.G. Load Factor (Negative)	.634	35	80			+ .53			
Maximum Longitudinal Accel. (Positive)	.238	260	450	-180	-400		-.12		
Maximum Longitudinal Accel. (Negative)	.137	615	390	415	410		-.55		
Maximum Lateral Accel. (Pos., to Right)	.284	95	410	- 80	40			+.15	
Maximum Lateral Accel. (Neg., to Left)	.310	55	265	90	-135			-.20	

TABLE V - continued

L-19A HIGH FLOTATION TIRE LANDING LOADS

L-19A Flight No. L-19-11 S/N 51-7441 Data Request No. L-19-6
Tire Pressure - L. 4.1 psi Sinking Speed 1.9 fps
R. 4.3 psi

Item (Event)	Time (Sec)	Vertical Load (lbs)		Drag Strut Axial Load (lbs)		C.G. Load Factor (g's)	Long. Acc. (g's)	Lat. Acc. (g's)	Speed (MPH)
		Right	Left	Right	Left				
Oscillograph Record No. 24929									
First Gear Contact (Right Main)	0								52.9*
Initial Left Drag Strut Axial Load	.170	985	445	- 80	1060		- .10		
Left Drag Strut Axial Load, Springback	.198	895	1290	- 150	- 960		+ .23		
Left Drag Strut Axial Load, 2nd Cycle	.230	730	1170	- 330	360		- .06		
Maximum Left Gear Vertical Load	.175	1050	1400	- 430	850	1.81			
Left Gear Vertical Load Rebound	.405	120	-100	0	- 50	.91			
Initial Right Drag Strut Axial Load	.145	995	1120	590	470		- .45		
Right Drag Strut Axial Load, Springback	.182	975	445	- 960	190		+ .59		
Right Drag Strut Axial Load, 2nd Cycle	.213	895	1330	210	- 160		0		
Maximum Right Gear Vertical Load	.175	1050	1400	- 430	850	1.81			
Right Gear Vertical Load Rebound	.353	-110	305	- 170	- 110	.89			
Maximum C.G. Load Factor (Positive)	.180	985	1360			1.81			
Maximum C.G. Load Factor (Negative)	.395	180	70			.89			
Maximum Longitudinal Accel. (Positive)	.183	665	680	500	530		+ .61		
Maximum Longitudinal Accel. (Negative)	.095	975	955	- 520	110		- .59		
Maximum Lateral Accel. (Pos, to Right)	.295	130	905	- 70	- 80			.68	
Maximum Lateral Accel. (Neg., to Left)	.271	370	935	30	- 70			-.40	

* Ground speed measured at instant of tail wheel touchdown.

SUBJECT:- APPENDIX I LANDING GEAR TEST DATA, M-245B

REPORT NO. FT245-1 | FAIRCHILD Aircraft and Missiles Div. OF FAIRCHILD ENGINE & AIRPLANE CORPORATION | PAGES | PAGE 78
MODEL M-245B | PREPARED BY | CHECKED BY | APPROVED BY
DATE January 22, 1960
REVISED

TABLE V - continued

L-19A HIGH FLOTATION TIRE LANDING LOADS

L-19A Flight No. L-19-14 S/N 51-7441 Data Request No. L-19-6
Tire Pressure - L. 9.0 psi Sinking Speed 2.4 fps
R. 8.7 psi

Item (Event)	Time (Sec)	Vertical Load (lbs)		Drag Strut Axial Load (lbs)		C.G. Load Factor (g's)	Long. Acc. (g's)	Lat. Acc. (g's)	Speed (MPH)
		Right	Left	Right	Left				
Oscillograph Record No. 24967									
First Gear Contact (Both)	0								50.3*
Initial Left Drag Strut Axial Load	.109	1070	1620	650	1110		-.52		
Left Drag Strut Axial Load, Springback	.129	1210	1610	1330	-1880		.49		
Left Drag Strut Axial Load, 2nd Cycle	.161	1000	1220	-780	620		-.27		
Maximum Left Gear Vertical Load	.110	1080	1645	670	1050	1.95			
Left Gear Vertical Load Rebound	.320	20	10	- 80	-160	.72			
Initial Right Drag Strut Axial Load	.130	1235	1620	1350	-1840		.29		
Right Drag Strut Axial Load, Springback	.152	1055	1150	-1300	220		.34		
Right Drag Strut Axial Load, 2nd Cycle	.185	935	1045	550	-800		.11		
Maximum Right Gear Vertical Load	.134	1275	1620	1190	-1590	1.95			
Right Gear Vertical Load Rebound	.404	- 20	95	- 20	110	1.02			
Maximum C.G. Load Factor (Positive)	.130	1235	1620			1.97			
Maximum C.G. Load Factor (Negative)	.382	- 10	35			.35			
Maximum Longitudinal Accel. (Positive)	.128	1170	1540	1280	-1720		.53		
Maximum Longitudinal Accel. (Negative)	.110	1080	1645	670	1050		-.56		
Maximum Lateral Accel. (Pos, to Right)	.172	845	1190	- 50	110			.46	
Maximum Lateral Accel. (Neg., to Left)	.192	865	950	- 80	-610			-.62	

* Ground speed measured at instant of tail wheel touchdown.

FA-800-23A

TABLE V - continued

L-19A HIGH FLOTATION TIRE LANDING LOADS

L-19A Flight No. L-19-13 S/N 51-7441
Tire Pressure - L. 8.6 psi Sinking Speed 2.5 fps Data Request No. L-19-6
R. 8.6 psi

Item (Event)	Time	Vertical Load (lbs)		Drag Strut Axial Load (lbs)		C.G. Load Factor (g's)	Long. Acc. (g's)	Lat. Speed Acc. (g's)(MPH)
		Right	Left	Right	Left			
Oscillograph Record No. 24946								
First Gear Contact (Right Main)	0							35.1*
Initial Left Drag Strut Axial Load	.210	920	1435	- 590	1460		-.23	
Left Drag Strut Axial Load, Springback	.246	410	1210	90	-1320		.24	
Left Drag Strut Axial Load, 2nd Cycle	.277	355	750	- 160	480		-.12	
Maximum Left Gear Vertical Load	.228	855	1595	- 200	700	1.87		
Left Gear Vertical Load Rebound	.600	110	65	+ 40	- 30	1.33		
Initial Right Drag Strut Axial Load	.120	1250	140	940	- 10		-.35	
Right Drag Strut Axial Load, Springback	.154	1065	790	-1220	1000		.05	
Right Drag Strut Axial Load, 2nd Cycle	.188	1080	1315	80	520		-.12	
Maximum Right Gear Vertical Load	.130	1295	155	740	110	1.57		
Right Gear Vertical Load Rebound	.305	-165	890	- 10	- 540	1.24		
Maximum C.G. Load Factor (Positive)	.220	935	1505			1.96		
Maximum C.G. Load Factor (Negative)	.600	110	65			.80		
Maximum Longitudinal Accel. (Positive)	.244	445	1230	70	-1270		.34	
Maximum Longitudinal Accel. (Negative)	.165	1070	1130	- 530	860		-.42	
Maximum Lateral Accel. (Pos., to Right)	.158	1070	965	-1070	1070			.60
Maximum Lateral Accel (Neg., to Left)	.435	30	85	40	- 50			-.33

* Wheel speed measured at instant of tail wheel touchdown.

TABLE V - continued

L-19A HIGH FLOTATION TIRE LANDING LOADS

L-19A Flight No. L-19-11 S/N 51-7441 Data Request No. L-19-6
Tire Pressure - L. 8.5 psi Sinking Speed 2.6 fps
R. 8.3 psi

Item (Event)	Time (Sec)	Vertical Load (lbs)		Drag Strut Axial Load (lbs)		C.G. Load Factor (g's)	Long. Acc. (g's)	Lat. Acc. (g's)	Speed (MPH)
		Right	Left	Right	Left				
Oscillograph Record No. 24931									
First Gear Contact (Right Main)	0								51.1*
Initial Left Drag Strut Axial Load	.228	960	1540	-220	1410		- .27		
Left Drag Strut Axial Load, Springback	.256	690	1450	- 20	-1850		- .92		
Left Drag Strut Axial Load, 2nd Cycle	.285	760	1150	-200	370		+ .02		
Maximum Left Gear Vertical Load	.245	925	1950	-270	80	2.24			
Left Gear Vertical Load Rebound	.574	80	215	- 10	- 10	.76			
Initial Right Drag Strut Axial Load	.105	1490	0	+1240	-180		- .67		
Right Drag Strut Axial Load, Springback	.126	1390	-155	-1760	20		- .76		
Right Drag Strut Axial Load, 2nd Cycle	.150	1235	110	500	310		- .65		
Maximum Right Gear Vertical Load	.112	1590	55	310	-100	1.92			
Right Gear Vertical Load Rebound	.423	-25	445	20	-190	.94			
Maximum C.G. Load Factor (Positive)	.125	1400	-125			2.39			
Maximum C.G. Load Factor (Negative)	.590	120	245			.76			
Maximum Longitudinal Accel. (Positive)	.165	1280	695	30	330		.61		
Maximum Longitudinal Accel. (Negative)	.133	1290	-210	-1020	130		-1.68		
Maximum Lateral Accel. (Pos, to Right)	.133	1290	-210	-1020	130			.39	
Maximum Lateral Accel. (Neg., to Left)	.220	950	1415	-170	1330			-.28	

* Ground speed measured at instant of tail wheel touchdown.

TABLE V - continued

L-19A HIGH FLOTATION TIRE LANDING LOADS

L-19A Flight No. L-19-15 S/N 51-7441
Tire Pressure - L. 8.9 psi Sinking Speed 2.7 fps Data Request No. L-19-6
R. 8.5 psi

Item (Event)	Time (Sec)	Vertical Load (lbs)		Drag Strut Axial Load (lbs)		C.G. Load Factor (g's)	Long. Acc. (g's)	Lat. Acc. (g's)	Speed (MPH)
		Right	Left	Right	Left				
Oscillograph Record No. 25150									
First Gear Contact (Left Main)	0								47.6
Initial Left Drag Strut Axial Load	.072	- 35	1450	-130	1570		-.59		
Left Drag Strut Axial Load, Springback	.100	390	1570	860	-1845		-.22		
Left Drag Strut Axial Load, 2nd Cycle	.127	895	1430	180	540		-.42		
Maximum Left Gear Vertical Load	.089	110	1795	245	115	1.68			
Left Gear Vertical Load Rebound	.476	130	- 20	10	- 30	.85			
Initial Right Drag Strut Axial Load	.151	1085	1350	1640	-635		-.38		
Right Drag Strut Axial Load, Springback	.190	1030	980	-1285	65		.12		
Right Drag Strut Axial Load, 2nd Cycle	.210	935	1000	255	190		-.12		
Maximum Right Gear Vertical Load	.171	345	1245	655	-275	1.60			
Right Gear Vertical Load Rebound	.410	- 55	285	- 40	- 65	.89			
Maximum C.G. Load Factor (Positive)	.138	915	1390			2.20			
Maximum C.G. Load Factor (Negative)	.675	95	80			.79			
Maximum Longitudinal Accel. (Positive)	.190	1030	980	-1285	65		.12		
Maximum Longitudinal Accel. (Negative)	.080	- 35	450	-130	1570		-.65		
Maximum Lateral Accel. (Pos., to Right)	.200	1010	960	-535	220			+.86	
Maximum Lateral Accel. (Neg., to Left)	.167	1290	1245	780	-315			-.26	

TABLE V - continued

L-19A HIGH FLOTATION TIRE LANDING LOADS

L-19A Flight No. 19-16 S/N 51-7441 Data Request No. L-19-6
Tire Pressure - L. 8.8 psi Sinking Speed 3.0 fps
R. 8.0 psi

Item (Event)	Time (Sec)	Vertical Load (lbs) Right	Vertical Load (lbs) Left	Drag Strut Axial Load (lbs) Right	Drag Strut Axial Load (lbs) Left	C.G. Load Factor (g's)	Long. Acc. (g's)	Lat. Acc. (g's)	Speed (MPH)
Oscillograph Record No. 25176									
First Gear Contact (Left Gear)	0								50.3
Initial Left Drag Strut Axial Load	.093	840	1425	365	1495		-1.09		
Left Drag Strut Axial Load, Springback	.115	1105	1465	1285	-2045		.49		
Left Drag Strut Axial Load, 2nd Cycle	.140	1310	1385	900	400		- .31		
Maximum Left Gear Vertical Load	.110	1045	1490	980	-1830	1.98			
Left Gear Vertical Load Rebound	.520	55	20	- 30	0	.93			
Initial Right Drag Strut Axial Load	.125	1235	1425	1640	-830		-1.01		
Right Drag Strut Axial Load, Springback	.159	1270	1260	-1980	- 45		.76		
Right Drag Strut Axial Load, 2nd Cycle	.179	1120	1035	710	-315		- .45		
Maximum Right Gear Vertical Load	.133	1365	1385	1475	110	2.02			
Right Gear Vertical Load Rebound	.389	- 20	85	- 90	10	.76			
Maximum C.G. Load Factor (Positive)	.135	1325	1405			2.05			
Maximum C.G. Load Factor (Negative)	.410	75	105			.74			
Maximum Longitudinal Accel. (Positive)	.155	1270	1280	-1880	- 20		.93		
Maximum Longitudinal Accel. (Negative)	.093	840	1425	365	1495		-1.09		
Maximum Lateral Accel. (Pos., to Right)	.159	1270	1260	-1980	- 45			.40	
Maximum Lateral Accel. (Neg., to Left)	.090	785	1405	605	1435			-.30	

TABLE V - continued

L-19A HIGH FLOTATION TIRE LANDING LOADS

L-19A Flight No. 19-16 S/N 51-7441 Data Request No. L-19-6
Tire Pressure - L. 8.6 psi Sinking Speed 3.3 fps
R. 7.9 psi

Item (Event)	Time (Sec)	Vertical Load (lbs)		Drag Strut Axial Load (lbs)		C.G. Load Factor (g's)	Long. Acc. (g's)	Lat. Acc. (g's)	Speed (MPH)
		Right	Left	Right	Left				
Oscillograph Record No. 25177									
First Gear Contact (Left Gear)	0								44.7
Initial Left Drag Strut Axial Load	.075	1100	1445	680	1585		-1.13		
Left Drag Strut Axial Load, Springback	.099	1325	1630	1770	-2370		.41		
Left Drag Strut Axial Load, 2nd Cycle	.125	1310	1280	-1660	690		.93		
Maximum Left Gear Vertical Load	.100	1365	1630	1940	-2240	2.11			
Left Gear Vertical Load Rebound	.390	410	40	70	- 10	.80			
Initial Right Drag Strut Axial Load	.100	1365	1630	1940	-2240		- .27		
Right Drag Strut Axial Load, Springback	.129	1290	1280	-1790	690		.62		
Right Drag Strut Axial Load, 2nd Cycle	.154	1085	1260	1205	-765		.10		
Maximum Right Gear Vertical Load	.115	1515	1425	365	- 10	1.83			
Right Gear Vertical Load Rebound	.680	20	85	- 10	- 65	.85			
Maximum C.G. Load Factor (Positive)	.090	1235	1590			2.35			
Maximum C.G. Load Factor (Negative)	.510	185	85			.32			
Maximum Longitudinal Accel. (Positive)	.125	1310	1280	-1660	690		.93		
Maximum Longitudinal Accel. (Negative)	.070	1065	1425	730	1530		-1.42		
Maximum Lateral Accel. (Pos., to Right)	.136	1100	1260	-435	120			.32	
Maximum Lateral Accel. (Neg., to Left)	.115	1515	1425	365	- 10			- .51	

REPORT NO. FT245-1 FAIRCHILD AIRCRAFT AND MISSILES DIV.
OF FAIRCHILD ENGINE & AIRPLANE CORPORATION
MODEL M-245B PREPARED BY CHECKED BY APPROVED BY
PAGES PAGE 84
SUBJECT:- APPENDIX I LANDING GEAR TEST DATA, M-245B
DATE January 22, 1960
REVISED

FA-800-23A

TABLE V - continued

L-19A HIGH FLOTATION TIRE LANDING LOADS

L-19A Flight No. L-19-14 S/N 51-7441 Data Request No. L-19-6
Tire Pressure - L. 8.8 psi Sinking Speed 3.5 fps
R. 8.5 psi

Item (Event)	Time (Sec)	Vertical Load (lbs)		Drag Strut Axial Load (lbs)		C.G. Load Factor (g's)	Long. Acc. (g's)	Lat. Acc. (g's)	Speed (MPH)
		Right	Left	Right	Left				
Oscillograph Record No. 24968									
First Gear Contact (Left Main)	0								47.6*
Initial Left Drag Strut Axial Load	.087	1285	2100	670	1520		-.43		
Left Drag Strut Axial Load, Springback	.116	1515	1925	1440	-2260		-.29		
Left Drag Strut Axial Load, 2nd Cycle	.143	1435	1420	-990	740		-.41		
Maximum Left Gear Vertical Load	.086	1295	2110	660	1500	2.40			
Left Gear Vertical Load Rebound	.444	110	- 65	30	- 20	.76			
Initial Right Drag Strut Axial Load	.114	1500	1915	1740	-2110		-.20		
Right Drag Strut Axial Load, Springback	.135	1490	1535	-1730	140		-.46		
Right Drag Strut Axial Load, 2nd Cycle	.165	1225	1530	680	-240		.05		
Maximum Right Gear Vertical Load	.125	1550	1790	-220	-1330	2.84			
Right Gear Vertical Load Rebound	.386	- 40	155	- 30	40	.81			
Maximum C.G. Load Factor (Positive)	.137	1490	1540			2.87			
Maximum C.G. Load Factor (Negative)	.460	40	85			.74			
Maximum Longitudinal Accel. (Positive)	.154	1280	1405	130	330		.15		
Maximum Longitudinal Accel. (Negative)	.075	1145	1720	690	1300		-.60		
Maximum Lateral Accel. (Pos, to Right)	.140	1460	1435	-1400	650			.35	
Maximum Lateral Accel. (Neg., to Left)	.120	1530	1890	1090	-1890			-.49	

* Ground speed measured at instant of tail wheel touchdown.

TABLE V - continued

L-19A HIGH FLOTATION TIRE LANDING LOADS

L-19A Flight No. L-19-18 S/N 51-7441
Tire Pressure - L. 8.9 psi Sinking Speed 4.4 fps Data Request No. L-19-6
R. 8.0 psi

Item (Event)	Time (Sec.)	Vertical Load (lbs)		Drag Strut Axial Load (lbs)		C.G. Load Factor (g's)	Long. Acc. (g's)	Lat. Acc. (g's)	Speed (MPH)
		Right	Left	Right	Left				
Oscillograph Record No. 25198									
First Gear Contact (Right Main)	0								50.0
Initial Left Drag Strut Axial Load	.129	1165	1445	245	1770		- .59		
Left Drag Strut Axial Load, Springback	.164	945	1180	-100	-1580		+ .63		
Left Drag Strut Axial Load, 2nd Cycle	.197	870	970	-180	735		- .08		
Maximum Left Gear Vertical Load	.135	1260	1755	30	1685	2.45			
Left Gear Vertical Load Rebound	.400	130	- 85	- 40	- 30	.87			
Initial Right Drag Strut Axial Load	.077	1500	145	1770	415		-1.17		
Right Drag Strut Axial Load, Springback	.103	1350	1000	-1910	1160		+ .12		
Right Drag Strut Axial Load, 2nd Cycle	.129	1165	1445	245	1770		- .59		
Maximum Right Gear Vertical Load	.092	1760	890	-180	885	2.41			
Right Gear Vertical Load Rebound	.320	- 35	330	0	-105	1.15			
Maximum C.G. Load Factor (Positive)	.135	1260	1755	30	1685	2.45			
Maximum C.G. Load Factor (Negative)	.440	0	145	- 20	10	.78			
Maximum Longitudinal Accel. (Positive)	.160	905	1155	- 70	-1505		+ .77		
Maximum Longitudinal Accel. (Negative)	.120	1110	1280	-140	1470		- .75		
Maximum Lateral Accel. (Pos., to Right)	.105	1315	1055	-1820	1270			+.57	
Maximum Lateral Accel. (Neg., to Left)	.345	55	185	- 70	-235			-.35	

FA-800-23A

TABLE V - continued

L-19A HIGH FLOTATION TIRE LANDING LOADS

L-19A Flight No. L-19-18 S/N 51-7441
Tire Pressure - L. 9.2 psi Sinking Speed 4.8 fps Data Request No. L-19-6
R. 8.1 psi

Item (Event)	Time (Sec)	Vertical Load (lbs)		Drag Strut Axial Load (lbs)		C.G. Load Factor (g's)	Long. Acc. (g's)	Lat. Acc. (g's)	Speed (MPH)
		Right	Left	Right	Left				
Oscillograph Record No. 25197									
First Gear Contact (Right Main)	0								49.0
Initial Left Drag Strut Axial Load	.103	1740	1695	-2075	2475		- .02		
Left Drag Strut Axial Load, Springback	.129	1315	1675	1100	2290		- .16		
Left Drag Strut Axial Load, 2nd Cycle	.160	1260	1405	-475	950		- .18		
Maximum Left Gear Vertical Load	.113	1590	1860	-285	1120	2.69			
Left Gear Vertical Load Rebound	.370	55	20	20	- 30	1.0			
Initial Right Drag Strut Axial Load	.075	1500	1220	1810	1225		-1.03		
Right Drag Strut Axial Load, Springback	.100	1760	1590	-2145	2145		- .10		
Right Drag Strut Axial Load, 2nd Cycle	.130	1295	1630	1235	1920		- .24		
Maximum Right Gear Vertical Load	.090	1795	1465	-365	1375	2.47			
Right Gear Vertical Load Rebound	.310	35	85	100	-105	1.04			
Maximum C.G. Load Factor (Positive)	.115	1165	1840			2.72			
Maximum C.G. Load Factor (Negative)	.345	75	60			.96			
Maximum Longitudinal Accel. (Positive)	.115	1165	1840	-160	500		+ .10		
Maximum Longitudinal Accel. (Negative)	.065	1240	870	1375	1440		-1.23		
Maximum Lateral Accel. (Pos., to Right)	.172	1090	1200	-180	75			+.60	
Maximum Lateral Accel. (Neg., to Left)	.187	1075	910	60	-320			-.50	

TABLE V - continued

L-19A HIGH FLOTATION TIRE LANDING LOADS

L-19A Flight No. L-19-18 S/N 51-7441
Tire Pressure - L. 9.3 psi Sinking Speed 6.4 fps Data Request No. L-19-6
R. 8.1 psi

Item (Event)	Time (Sec)	Vertical Load (lbs)		Drag Strut Axial Load (lbs)		C.G. Load Factor (g's)	Long. Acc. (g's)	Lat. Acc. (g's)	Speed (MPH)
		Right	Left	Right	Left				
Oscillograph Record No. 25196									
First Gear Contact (Right Main)	0								51.6
Initial Left Drag Strut Axial Load	.067	2500	1180	1910	1590		-1.74		
Left Drag Strut Axial Load, Springback	.134	1760	2005	595	-2120		+1.09		
Left Drag Strut Axial Load, 2nd Cycle	.167	1685	1590	-405	500		+ .10		
Maximum Left Gear Vertical Load	.115	1850	2230	365	1175	2.43			
Left Gear Vertical Load Rebound	.400	95	40	-110	-150	.93			
Initial Right Drag Strut Axial Load	.067	2500	1180	1910	1590		-1.74		
Right Drag Strut Axial Load, Springback	.095	2185	1920	-2395	1430		+ .44		
Right Drag Strut Axial Load, 2nd Cycle	.126	1760	2085	840	-1740		+1.09		
Maximum Right Gear Vertical Load	.067	2500	1180	1910	1590	2.58			
Right Gear Vertical Load Rebound	.345	55	105	- 80	-150	1.11			
Maximum C.G. Load Factor (Positive)	.089	2240	1695			3.22			
Maximum C. G. Load Factor (Negative)	.320	75	125			.80			
Maximum Longitudinal Accel. (Positive)	.130	1760	2045	790	-2036		1.11		
Maximum Longitudinal Accel. (Negative)	.067	2500	1180	1910	1590		-1.74		
Maximum Lateral Accel. (Pos., to Right)	.069	2480	1200	1630	1565			+.65	
Maximum Lateral Accel. (Neg., to Left)	.203	1315	1075	150	-450			-.46	

APPENDIX I
SUBJECT:- LANDING GEAR TEST DATA, K-245B

REPORT NO. 245-1 FAIRCHILD Aircraft and Missile Div.
OF FAIRCHILD ENGINE & AIRPLANE CORPORATION
MODEL K-245B
PREPARED BY
CHECKED BY
APPROVED BY
PAGES
PAGE 88
DATE January 22, 1960
REVISED

TABLE VI - continued

L-19A HIGH FLOTATION TIRE LANDING LOADS

L-19A Flight No. L-19-28 S/N 51-7441 April 1, 1960
Tire Pressure - L. 8.2 psi** Sinking Speed 8.85 fps Data Request No. L-19-6B

Item (Event)	Time (Sec)	Vertical Load (lbs)		Drag Strut Axial Load (lbs)		C.G. Load Factor (g's)	Long. Acc. (g's)	Lat. Acc. (g's)	Speed (MPH)
		Right	Left	Right	Left				
Oscillograph Record No. 25908									
First Gear Contact (Left Main Gear)	0								***
Initial Left Drag Strut Axial Load	.029	50	1580	-175	2325				
Left Drag Strut Axial Load, Springback	.073	1330	3870	2370	-2585*				
Left Drag Strut Axial Load, 2nd Cycle	.120	2540	2820	-1250	1000				
Maximum Left Gear Vertical Load	.073	1330	3870	2370	-2585*	3.13			
Left Gear Vertical Load Rebound	.590	15	-75	90	115	.58			
Initial Right Drag Strut Axial Load	.075	1350	3715	2410	-2585*				
Right Drag Strut Axial Load, Springback	.115	2855	2725	-1680*	700				
Right Drag Strut Axial Load, 2nd Cycle	.139	2250	3090	1145	0				
Maximum Right Gear Vertical Load	.110	3110	2860	-1680*	600	4.08			
Right Gear Vertical Load Rebound	.425	-35	55	75	155	.60			
Maximum C.G. Load Factor (Positive)	.110	3110	2860			4.08			
Maximum C.G. Load Factor (Negative)	.650	-17	0			.58			
Maximum Longitudinal Accel. (Positive)	.110	3110	2860	-1680*	600		+1.24		
Maximum Longitudinal Accel. (Negative)	.029	50	1580	-175	2325		- .88		
Maximum Lateral Accel. (Pos. to Right)	.200	1850	1470	-165	185			1.10*	
Maximum Lateral Accel. (Neg. to Left)	.225	1175	1485	-35	-380			-1.50	

* Traces off oscillograph.
** Right Tire Pressure Unavailable.
*** Forward Velocity not recorded.

TABLE VI - continued

L-19A HIGH FLOTATION TIRE LANDING LOADS

L-19A Flight No. L-19-30 | S/N 51-7441 | April 4, 1960
Tire Pressure - L. 8.5 psi** | Sinking Speed 10.25 fps | Data Request No. L-19-6B

Item (Event)	Time (Sec)	Vertical Load (lbs)		Drag Strut Axial Load (lbs)		C.G. Load Factor (g's)	Long. Acc. (g's)	Lat. Acc. (g's)	Speed (MPH)
		Right	Left	Right	Left				
Oscillograph Record No. 25927									
First Gear Contact (Left Main Gear)	0								*
Initial Left Drag Strut Axial Load	.031	790	1590	800	2660		-1.47		
Left Drag Strut Axial Load, Springback	.081	2930	3780	-290	-2970		1.51		
Left Drag Strut Axial Load, 2nd Cycle	.116	2500	3450	660	780		-0.35		
Maximum Left Gear Vertical Load	.087	3000	3920	-1750	-1620	+3.90			
Left Gear Vertical Load Rebound	.657	100	30	80	110	+ .62			
Initial Right Drag Strut Axial Load	.055	1900	2910	1950	1880		-1.60		
Right Drag Strut Axial Load, Springback	.092	2970	3800	-2560	-840		+1.43		
Right Drag Strut Axial Load, 2nd Cycle	.124	2410	3340	770	690		-0.15		
Maximum Right Gear Vertical Load	.087	3000	3920	-1750	-1620	+3.90			
Right Gear Vertical Load Rebound	.350	-20	340	0	-170	+ .62			
Maximum C.G. Load Factor (Positive)	.060	2100	3110			4.15			
Maximum C.G. Load Factor (Negative)	.002	0	0			.96			
Maximum Longitudinal Accel. (Positive)	.087	3000	3920	-1750	-1620		+1.70		
Maximum Longitudinal Accel. (Negative)	.042	1410	2180	1420	2610		-1.84		
Maximum Lateral Accel. (Pos. to Right)	.173	1900	1890	-180	80			+1.61	
Maximum Lateral Accel. (Neg. to Left)	.144	2290	3130	-60	100			-1.09	

* Forward Velocity unavailable.
** Right Tire Pressure unavailable.

APPENDIX I
SUBJECT:- LANDING GEAR TEST DATA, M-245B

REPORT NO. FT245-1 | PREPARED BY Fairchild Aircraft and Missiles Div. OF FAIRCHILD ENGINE & AIRPLANE CORPORATION | CHECKED BY | APPROVED BY
MODEL M-245B | PAGES | PAGE 90
DATE January 22, 1960
REVISED

REPORT NO FT245-1 FAIRCHILD Aircraft and Missiles Div. OF FAIRCHILD ENGINE & AIRPLANE CORPORATION

MODEL M-245B | PREPARED BY | CHECKED BY | APPROVED BY | PAGES | PAGE 91

SUBJECT:- APPENDIX I
LANDING GEAR TEST DATA, M-245B

DATE January 22, 1960
REVISED

TABLE VI

L-19A HIGH FLOTATION TIRE DROP TEST LOADS

S/N 51-7441

L-19A Drop Test
Tire Pressure - Right 8.4
Left 8.3

Data Request No. L-19-6

Item (Event)	Time (Sec)	Vertical Load (Lbs)		Drag Strut Axial Load (Lbs)		C.G. Load Factor (g's)	Long. Acc. (g's)	Lat. Acc. (g's)	Sinking Speed (FPS)
		Right	Left	Right	Left				
Oscillograph Record No. 25137									
First Gear Contact Simultaneous									
Initial Left Drag Strut Axial Load	.027	115	105	-50	-65		1.65		
Left Drag Strut Axial Load, Springback	.119	1870	2140	-545	-990		2.50		
Left Drag Strut Axial Load, 2nd Cycle	.207	1255	1060	-455	-450		2.02		
Maximum Left Gear Vertical Load	.119	1870	2140	-545	-990	2.01			
Left Gear Vertical Load Rebound	.540	790	785	-300	-375	.81			
Initial Right Drag Strut Axial Load	.031	115	105	-50	-110		1.61		
Right Drag Strut Axial Load, Springback	.106	1890	1950	-735	-870		2.43		
Right Drag Strut Axial Load, 2nd Cycle	.188	1270	1145	-370	-540		1.98		
Maximum Right Gear Vertical Load	.119	1870	2140	-545	-990	1.98			
Right Gear Vertical Load Rebound	.550	770	785	-300	-384	.79			
Maximum C.G. Load Factor (Positive)	.115	1850	2115			2.01			
Maximum C.G. Load Factor (Negative)	.003	95	105			-1.42			
Maximum Longitudinal Accel. (Positive)	.119	1870	2140	-545	-990		2.48		
Maximum Longitudinal Accel. (Negative)	.058	95	85	-85	-110		1.55		
Maximum Lateral Accel. (Pos. to Right)	.129	1600	1925	-515	-825			.37	
Maximum Lateral Accel. (Neg. to Left)	.149	1485	1670	-580	-625			-.29	
Sinking Speed									2.5

TABLE VI - continued

L-19A HIGH FLOTATION TIRE DROP TEST LOADS

S/N 51-7441

L-19A Drop Test
Tire Pressure - Right 8.5
Left 8.5

Data Request No. L-19-6

Item (Event)	Time (Sec)	Vertical Load (Lbs)		Drag Strut Axial Load (Lbs)		C.G. Load Factor (g's)	Long. Acc. (g's)	Lat. Acc. (g's)	Sinking Speed (FPS)
		Right	Left	Right	Left				
Oscillograph Record No. 25138									
First Gear Contact Simultaneous									
Initial Left Drag Strut Axial Load	.056	95	65	-20	-35		1.57		
Left Drag Strut Axial Load, Springback	.215	2215	1820	-755	-1010		2.33		
Left Drag Strut Axial Load, 2nd Cycle	.295	1485	1315	-505	-595		2.10		
Maximum Left Gear Vertical Load	.215	2215	1820	-755	-1010	2.13			
Left Gear Vertical Load Rebound	.610	500	615	-205	-295	.51			
Initial Right Drag Strut Axial Load	.056	95	65	-20	-35		1.57		
Right Drag Strut Axial Load, Springback	.215	2215	1820	-755	-1010		2.33		
Right Drag Strut Axial Load, 2nd Cycle	.295	1485	1315	-505	-595		2.10		
Maximum Right Gear Vertical Load	.215	2215	1820	-755	-1010	2.13			
Right Gear Vertical Load Rebound	.630	480	635	-205	-295	.49			
Maximum C.G. Load Factor (Positive)	.215	2215	1820			2.13			
Maximum C.G. Load Factor (Negative)	.056	95	65			-.54			
Maximum Longitudinal Accel. (Positive)	.250	1925	1925	-715	-815		2.48		
Maximum Longitudinal Accel. (Negative)	.060	95	85	-95	-100		1.47		
Maximum Lateral Accel. (Pos. to Right)	.205	2025	1905	-700	-890			.18	
Maximum Lateral Accel. (Neg. to Left)	.220	210	[illegible]	[illegible]	[illegible]				